Analysis of nuclear exosome associated co-factors in *Saccharomyces cerevisiae*

A thesis submitted to the University of Sheffield for the degree of Doctor of Philosophy

by

William Garland

Department of Molecular Biology and Biotechnology
University of Sheffield
United Kingdom

January 2014

Abstract

The degradation of RNA is a ubiquitous phenomenon critical to many biological processes. The eukaryotic exosome complex is a major source of 3'-5' exoribonuclease activity and is required for multiple RNA processing and degradation pathways. To modulate the recognition and fate of RNA substrates, the exosome recruits a number of additional cofactors. This study focuses on the function and relationships between the proteins Rrp6, Rrp47, Rex1 and Mpp6 that function in nuclear RNA quality control mechanisms, 3'-end processing of stable RNAs and the degradation of cryptic unstable transcripts (CUTs). The function of Rrp6 is largely dependent on the physical interaction with Rrp47 and the expression levels of either protein are mutually dependent on this physical interaction. The function of Rrp6/Rrp47 is redundant with Mpp6-dependent or Rex1-dependent processes. This is supported by the synthetic lethal interactions between *rrp6Δ* and *rrp47Δ* mutants with loss of function *mpp6* or *rex1* mutant. However, the molecular basis of these interactions is not clear. To investigate if Rrp47 can function when physically divorced from Rrp6, a novel approach was used to separate the Rrp6/Rrp47 complex *in vivo* whilst maintaining stable expression of Rrp47. Segregated Rrp47 was shown to be functional when combined with *mpp6Δ* or *rex1Δ* mutants. However, segregating C-terminal truncated Rrp47 protein from Rrp6 caused a block in growth in *mpp6Δ* and *rex1Δ* mutants. RNA analysis reveals a block in 3' maturation of box C/D snoRNAs in conditional *rex1 rrp47* mutants and a strong accumulation of RNA surveillance targets in conditional *mpp6 rrp47* mutants. These findings provide insight into the basis of synthetic lethal interactions and highlight specific redundant pathways. Finally, whilst these studies validate the role of Mpp6 in RNA surveillance pathways, little is known about the protein itself. Mutational analysis is employed to identify and characterise the functional regions of the Mpp6 protein. This identifies crucial regions required for function *in vivo* including residues that may be required for association with the exosome and associated sub-complexes.

Acknowledgements

First and foremost I would like to thank Phil, my supervisor, not only for the opportunity of this studentship but providing constant advice, ideas and guidance. Without his continuous support and encouragement I would have found the past four years a lot more difficult.

I share my gratitude with the past and present members of the Mitchell lab, Becky, Martin, Eileen, Taib and Shler who have provided an amazing environment to work in. A particular mention goes to Moni, who has helped me through so much with constant support, encouragement, ideas and conversation. I would also like to thank my students, Alex, Brian, Catherine and Sam who contributed to my work and were a pleasure to supervise.

I'd also like to thank my advisors Ewald Hettema and Pete Sudbery for their critical advice and support during this time.

Many thanks are due to my mum for her constant support and guidance throughout everything I do. Her encouragement has helped me through good, bad and no doubt everything I have yet to face.

Finally, I would like to thank Bianca for being encouraging, understanding and generally amazing in all respects. Without her unwavering support, care and companionship I would not have made it through the past four years. Inn hobbbok hafna.

This work is dedicated to the memory of my dad who inspired me into the world of science at a young age. I would not be here today if it wasn't for him.

Index of Contents

Index of Figures

Index of Tables

Abbreviations, units and nomenclature

Abbreviations and units used throughout this study are listed below. The mention of yeast throughout the text refers to *Saccharomyces cerevisiae* unless otherwise stated. Nomenclature used in this study is compliant with guidelines for *S. cerevisiae* compiled by the Committee of Genetic Nomenclature ("Saccharomyces cerevisiae," 1998). Yeast wildtype genes are written in upper case and italicised (e.g. *MPP6*), mutant alleles are in lower case and italicised (e.g. *mpp6*) and proteins being with a capital letter followed by lower case (e.g. Mpp6).

Abbreviations used in this study.

5'FOA	5'fluoroorotic acid
ATP	adenosine triphosphate
CIP	calf-intestinal alkaline phosphatase
CTD	C-terminal domain
CUT	cryptic unstable transcript
DEPC	diethylpyrocarbonate
DMSO	dimethyl sulfoxide
dNTP	deoxyribonucleotide triphosphate
ds	double stranded
DTT	dithiothreitol
Endo	endonuclease
EPPCR	error-prone polymerase chain reaction
ETS	external transcribed spacer
Exo	exonuclease
gDNA	genomic DNA
GST	glutathione-S-transferase
GTC	guanidine thiocynate
HCl	hydrochloric acid
His	histidine
IPTG	isopropyl β-D-1-thigalactopyranoside

ITS	internal transcribed spacer
mRNA	messenger RNA
MW	molecular weight
ncRNA	non-coding RNA
NTD	N-terminal domain
OD	optical density
ORF	open reading frame
Ori	origin of replication
PCR	polymerase chain reaction
PEG	polyethyleneglycol
PMSF	phenylmethylsulphonylfluoride
PNK	polynucleotide kinase
poly(A)	polyadenylated
poly(U)	polyuridylated
RBD	RNA binding domain
RNA pol	DNA dependent RNA polymerase
RNase	ribonuclease
RNP	ribonucleoprotein
rDNA	ribosomal DNA
rRNA	ribosomal RNA
SD	synthetic dextrose medium
SDM	site directed mutagenesis
SDS	sodium dodecyl sulphate
SGal	synthetic galactose medium
snoRNA	small nucleolar RNA
snRNA	small nuclear RNA
ss	single stranded
SUT	stable uncharacterised transcript
TAP	tandem affinity purification
TCA	trichloroacetic acid
TEMED	*N*,*N*,*N*′,*N*′-Tetramethylethylenediamine
T_m	melting temperature
tRNA	transfer RNA

TS	temperature sensitive
UTR	untranslated region
UV	ultraviolet
v/v	percentage volume per volume
w/v	percentage weight per volume
WT	wildtype
XUT	Xrn1-sensitive unstable transcript
ZnK	zinc-knuckle
zz	protein A tag

Units used in this study

bp	base pair
CFU	colony forming units
cpm	counts per minute
Da	daltons
g	gram
g	g-force (relative centrifugal force)
kb	kilobase
kDa	kiladalton
l	litre
mg	milligram
ml	millilitre
mM	millimolar
ng	nanogram
nM	nanomolar
pmol	picomolar
rpm	revolutions per minute
S	Svedberg
U	units (of enzyme)
µg	microgram
µM	micromolar
µl	microlitre

Chapter 1: Introduction

1.1 RNA degradation in Eukaryotes

RNA degradation is a necessary activity, key to the maintenance of stable cellular transcriptomes and is ubiquitous to all kingdoms of life. As with all biomolecules, RNA transcripts exist in a constant state of flux and require a high level of dynamic control for all aspects of RNA metabolism. All characterised classes of RNA are transcribed as long precursor molecules and undergo processing reactions to generate mature transcripts. Surveillance and quality control mechanisms purge the cell of aberrant RNA molecules to prevent disruption to cellular processes. Furthermore, RNAs are degraded as part of natural turnover pathways and contributes to the recycling of nucleotides. For coding transcripts, RNA turnover acts as part of a number of mechanisms to control gene expression levels (Houseley and Tollervey, 2009; Jackowiak et al., 2011; Parker, 2012).
These productive and destructive degradation pathways require the function of three classes of cellular RNase enzymes: endonucleases that cleave RNA internally, 5'-3' exonucleases that degrade from the 5' end of RNA, and 3'-5' exonucleases that act on the 3' end. As with many biological systems, a large degree of redundancy exists between RNases and degradation pathways. With the advent of high-throughput technologies combined with classical techniques, it has become apparent that there is a large functional overlap between RNases. This suggests that multiple enzymes are synergistic in the recognition of the same target RNA (Houseley and Tollervey, 2009). Redundant pathways serve to make RNA degradation pathways more robust and fundamentally enhance the overall efficiency.

1.1.1. The eukaryotic exosome complex

A major source of 3'-5' exonuclease activity in eukaryotes is provided by the RNA exosome complex (Allmang et al., 1999b; Mitchell et al., 1997). The exosome

plays key roles in both processing and degradation pathways of all characterised RNA species in the cytoplasm and nucleus of eukaryotic and archeal cells (Chlebowski et al., 2013). The complex itself is composed of a non-catalytic barrel-like core of nine essential polypeptides (EXO9) that associates with Rrp44 and Rrp6 proteins to provide ribonuclease activity. Rrp44 provides both endonuclease and 3'-5' exonuclease activity and is found in both cytoplasmic and nuclear exosome complexes known together as EXO10 (Lorentzen et al., 2008; Mitchell et al., 1997). Rrp6 is related to bacterial RNaseD and provides additional exonuclease activity to the nuclear exosome in yeast (Allmang et al., 1999b; Briggs et al., 1998). The complex is ubiquitous in all eukaryotes studied so far and shows a large degree of homology to related structures in bacteria and archaea (Lykke-Andersen et al., 2009).

The exosome complex is a critical component of all eukaryotic cells with functions linked to roles ranging from ribosome biogenesis to gene silencing. Whilst a degree of functional redundancy exists within various components of the exosome and associated factors, all components of the EXO10 complex are essential for viability (Allmang et al., 1999b; Mitchell et al., 1997). A small number of diseases have been associated with the human exosome, namely the rare autoimmune disease polymyositis scleroderma in which patients develop antibodies against PM/Scl-75 and PM/Scl-100 (homologs of EXO10 components Rrp45 and Rrp6 respectively) (Allmang et al., 1999b; Gelpi et al., 1990). It was recently shown that germline mutations in the Rrp44-related *DIS3L2* are linked to Perlman syndrome of overgrowth and a predisposition Wilm's tumor development (Astuti et al., 2012). Additionally, whole-genome sequencing revealed a high frequency of mutations in the Rrp44-homolog *hDIS3* allele in patients with multiple myeloma (MM), a lethal neoplastic disease (Chapman et al., 2011).

In addition to processing and degradation of major classes of RNA transcripts, the exosome was shown to contribute to the rapid suppression of a hidden layer of intergenic pervasive transcription. Such non-coding RNAs were termed cryptic unstable transcripts (CUTs) and are shown to accumulate in exosome mutants (Arigo et al., 2006; Thiebaut et al., 2006; Wyers et al., 2005). Whilst the role of

CUTs is still relatively unknown, a few studies have recently reported possible functions in gene regulation (Camblong et al., 2007; Castelnuovo et al., 2013; Martens et al., 2005).

With multiple functions and a wide array of RNA substrates, the exosome complex requires a high level of modulation to control the fate of target transcripts. Multiple processing and degradation pathways are achieved through the physical and functional association with various co-factors and complexes. These auxiliary factors have been widely characterised and studied in relation to the activation of the exosome. However, the mechanisms that govern substrate recognition and targeting to various exosome-dependent pathways are yet to be fully understood.

1.1.2. Functions of the eukaryotic exosome

The catalytic activities of the nuclear and cytoplasmic exosome target all classes of RNA in eukaryotes and play key roles in multiple pathways involving RNA processing and degradation. The modulation of such activities is due to compartmentalization in the nucleolus, nucleoplasm and cytoplasm along with physical and function associations with a variety of co-factors and complexes. The eukaryotic exosome has been shown to be involved in 3' end processing of stable RNAs, cytoplasmic turnover of mRNAs, and in nuclear and cytoplasmic RNA surveillance pathways for coding and non-coding RNAs including CUTs.

All characterised classes of stable RNAs are generated from longer precursor transcripts that undergo exonuclease and/or endonuclease processing to generate mature RNA. The eukaryotic exosome was originally identified in yeast as a processing complex with 3'-5' exonuclease activity involved in the 3' end processing of the 5.8S rRNA component of mature ribosomes (Mitchell et al., 1997). Subsequent analyses reported that exosome activity was required for the 3' maturation of snRNA and snoRNAs (Allmang et al., 1999a; van Hoof et al., 2000a). Mature 5.8S rRNA is processed from the 7S pre-rRNA molecule which itself is derived from a 35S pre-rRNA polycistronic precursor transcribed by RNA

polymerase I. The exonuclease activity of Rrp44, a catalytic subunit of both nuclear and cytoplasmic exosomes, processes the 3' end of 7S rRNA to produce the 5.8S + 30 species (5.8S rRNA extended by 30nt at the 3' end) (Mitchell et al., 1996). The accumulation of extended 5.8S transcripts is characteristic of exosome and Rrp6 mutants (Briggs et al., 1998; Mitchell et al., 2003, 1997). The 5.8S + 30 rRNA is processed to 6S rRNA species by Rrp6 which is subsequently exported to the cytoplasm for final maturation steps involving the cytoplasmic nuclease Ngl2 (Thomson and Tollervey, 2010). The 3' +30 species is accumulated in *rrp6Δ* mutants. However, mature 5.8S rRNA is still generated, most likely due to redundant exonuclease pathways (Briggs et al., 1998). The Rex1, Rex2 and Rex3 exonucleases were shown to have redundant functions in 3'- end 5.8S maturation. Double *rex1Δ rex2Δ* and triple *rex1Δ rex2Δ rex3Δ* mutants exhibited an accumulation of the 6S pre-rRNA species (van Hoof et al., 2000b). This suggests that the 3' maturation of 5.8S rRNA could utilize multiple pathways involving various exonucleases to generate mature transcripts. Interestingly, loss of function *rex1* mutants are synthetic lethal with *rrp6Δ* alleles suggesting a level of functional redundancy in the processing of shared substrates (Peng et al., 2003; van Hoof et al., 2000b).

The 3' ends of pre-snRNAs and pre-snoRNAs were also shown to require the function of the exosome and associated co-factors (Allmang et al., 1999a; Costello et al., 2011; Mitchell et al., 2003; van Hoof et al., 2000a). Exosome and *rrp6Δ* mutants accumulate 3' extended pre-snRNA and pre-snoRNA transcripts that are polyadenylated (Allmang et al., 1999a; van Hoof et al., 2000a). Transcriptional termination of snoRNA genes occurs at a proximal Nrd1/Nab3/Sen1 (NNS) dependent site I and a distal, failsafe mRNA cleavage/polyadenylation site II (Steinmetz and Brow, 2003; Steinmetz et al., 2006). Normal productive snoRNA production proposed to be mediated by NNS-dependent termination at site I followed by polyadenylation and subsequent 3'-end trimming by Rrp6 (Grzechnik and Kufel, 2008). The function of Rrp6 in pre-rRNA processing and 3'-end formation of snRNA and snoRNAs is dependent on physical and function interactions with the exosome-associated cofactor Rrp47. Loss of Rrp47 in yeast resembles RNA processing and degradation phenotypes

observed in *rrp6Δ* strains. (Costello et al., 2011; Feigenbutz et al., 2013b; Mitchell et al., 2003; Stead et al., 2007).

In the cytoplasm the exosome complex has only been reported to act on mRNA transcripts, functioning in normal mRNA turnover and in the degradation of aberrant transcripts as part mRNA surveillance pathways.

The turnover of mRNAs in yeast can occur via two pathways, both involving an initial shortening of the poly(A) tail by deadenylases and followed by either 5'-3' or 3'-5' exonucleolytic degradation. The removal of the 5' cap by decapping enzymes Dcp1 and Dcp2 leaves the mRNA susceptible to 5'-3' degradation by the Xrn1 exonuclease (Beelman et al., 1996; Dunckley and Parker, 1999; Hsu and Stevens, 1993). Deadenylation can also lead to a 3'-5' degradation pathway involving the cytoplasmic exosome (Anderson and Parker, 1998; van Hoof et al., 2000c). In yeast, the former 5'-3' pathway is considered to be the major pathway in mRNA turnover whereas the later exosome-dependent pathway plays a minor role. The catalytic activity of the cytoplasmic exosome is provided by the essential protein, Rrp44 which possess both exo- and endonuclease activities (Dziembowski et al., 2007; Lebreton et al., 2008; Mitchell et al., 1997). A loss of Rrp44 exonuclease activity leads to the accumulation of mRNA decay intermediates and is synthetic lethal with the loss of Xrn1 (Dziembowski et al., 2007; Schneider et al., 2009).

The cytoplasmic exosome associates with the SKI (Superkiller) complex composed of the DExH-box helicase Ski2 along with Ski3 and Ski8 (Anderson and Parker, 1998; Synowsky and Heck, 2008). The SKI and cystoplasmic exosome complexes are physically coupled via the GTPase protein Ski7 via independent regions in the N-terminus (Araki et al., 2001). Defects in *SKI* genes inhibit mRNA 3'-5' decay pathways and are synthetic lethal with *xrn1Δ* mutants. These results suggest that that the SKI complex works in concert with the cytoplasmic exosome in 3'-5' mRNA decay pathways that are redundant with the 5'-3' decapping pathway (Johnson and Kolodner, 1995; Mitchell and Tollervey, 2003). The role of the SKI complex in cytoplasmic turnover is relatively unknown although a recent crystal structure of the complex suggests that RNA substrates are channeled

through the helicase domain of Ski2 into the central channel of EXO9 to reach the exonuclease site in Rrp44 (Halbach et al., 2013).

The removal of aberrant mRNA transcripts in RNA surveillance pathways is a critical process to maintain the integrity of protein-coding gene transcripts. Such aberrant mRNAs need to be distinguished from normal coding RNAs through surveillance mechanisms and target faulty transcripts for rapid degradation. The cytoplasmic exosome contributes to the degradation of aberrant mRNAs in nonsense-mediated decay (NMD), non-stop decay (NSG) and no-go decay (NGD) pathways (Doma and Parker, 2006; Mitchell and Tollervey, 2003; Takahashi et al., 2003; van Hoof et al., 2002). Transcripts that contain premature termination codons (PTCs), due to transcriptional errors or post-transcriptional processing, are targeted to NMD pathways. As with normal mRNA turnover, two NMD pathways exist in yeast. The major 5'-3' NMD pathway involves decapping followed by rapid 5'-end degradation involving Xrn1 (Muhlrad and Parker, 1994). The cytoplasmic exosome, in cooperation with the SKI complex, was also shown to be required for a secondary 3'-5' degradation pathway of PTC-containing transcripts (Mitchell and Tollervey, 2003). Exosome mutants have been shown to stabilise mRNA transcripts that lack stop codons (Frischmeyer et al., 2002; van Hoof et al., 2002). In such cases, translating ribosomes read through the mRNA and stalls at the 3' poly(A) tail of the transcript. Ski7 is proposed to recognize stalled ribosome and co-recruit the SKI complex and cytoplasmic exosome resulting in rapid degradation of the aberrant transcript. The C-terminal domain of Ski7 is homologous to translation factors eEF1A and eRF3 and it has been suggested that this domain interacts with the stalled ribosome (Araki et al., 2001; van Hoof et al., 2002). The no-go decay pathway is induced by stalling of the ribosome at structured elements within mRNAs during translation (Doma and Parker, 2006). The NGD model proposes that transcripts undergo endonucleolytic cleavage that releases 5' and 3' mRNA fragments. The 3'-fragment is degraded by the 5'-3' exonuclease Xrn1 whereas the 5'-fragment is degraded through co-operation between the SKI complex and the cytoplasmic exosome (Doma and Parker, 2006).

In addition to RNA surveillance and quality control of coding mRNAs in the cytoplasm, the exosome complex is responsible for targeted 3'-5' degradation of coding and non-coding pre-RNA species in the nucleus. Defective RNA precursors are the result of mutation or errors in RNA transcription and processing. The nuclear exosome recruits a plethora of co-factors and complexes to specifically target aberrant transcripts derived from RNA polymerase I, II and III in distinct pathways whilst allowing normal RNAs to undergo normal maturation. Analogous to redundant 3' and 5' degradation pathways in the cytoplasm, the exonuclease Rat1 functions in 5'-3' RNA surveillance pathways in the nucleus (Fang et al., 2005). Recent advances in high-throughput transcriptome and microarray analysis have revealed key factors in RNA surveillance and their target transcripts. However, the mechanisms that distinguish between normal and aberrant transcripts are still poorly understood.

The activity of the nuclear exosome is dependent on additional proteins and complexes including the Trf4/Air2/Mtr4 (TRAMP) polyadenylation complex, the Nrd1/Nab3/Sen1 (NNS) complex and the nuclear RNA binding proteins Rrp47 and Mpp6 (Chlebowski et al., 2013). The nuclear exosome possesses an additional catalytic component from the physical and functional association with Rrp6, a RNaseD-related 3'-5' exonuclease (Burkard and Butler, 2000).
The TRAMP complex plays a key role in targeting aberrant ncRNAs for degradation in yeast. TRAMP complexes are typically comprised of the poly(A) polymerase Trf4, either of two zinc-knuckle RNA binding proteins Air1 or Air2 and the putative RNA helicase Mtr4. (LaCava et al., 2005; Vanácová et al., 2005; Wyers et al., 2005). TRAMP adds short 3' oligo(A) tails to RNA substrates to target for degradation by the nuclear exosome complex and/or Rrp6. The addition of short single stranded RNA is suggested to present a more favorable substrate for the exosome-associated exonucleases Rrp44 and Rrp6. (LaCava et al., 2005). Targets of the TRAMP complex encompass transcripts from all three RNA polymerases including hypermodified pre-tRNA$_i^{Met}$, aberrant 23S pre-rRNA, 3' truncated 5S (5S*), unspliced pre-tRNAs, read-through snoRNAs and cryptic-unstable transcripts. All aforementioned transcripts are stabilised in both TRAMP and exosome mutants suggesting a functional coupling between the two

complexes in RNA surveillance and degradation pathways (Allmang et al., 1999a; Copela et al., 2008; Grzechnik and Kufel, 2008; Kadaba et al., 2006; LaCava et al., 2005; Neil et al., 2009; Wlotzka et al., 2011; Wyers et al., 2005).

A novel class of non-coding RNA species derived from pervasive Pol II transcription of intergenic regions was identified in a transcriptome-wide analysis of *rrp6Δ* cells (Wyers et al., 2005). These ncRNAs, termed cryptic unstable transcripts (CUTs), were shown to be virtually undetectable in wild-type cells suggesting that they are targeted for rapid degradation by the exosome. CUTs were shown to be 3' polyadenylated with a high level of heterogeneity and appear as a smear in northern blot hybridisation analysis (Arigo et al., 2006; Thiebaut et al., 2006; Wyers et al., 2005). It was demonstrated that CUTs are polyadenylated by Trf4 as part of the TRAMP complex, which targets transcripts for subsequent degradation by the exosome (Wyers et al., 2005). A detailed analysis of the model CUT *NEL025c* revealed that the Nrd1/Nab3/Sen1 (NNS) complex is involved in transcriptional termination of CUTs and triggers subsequent degradation involving TRAMP and the exosome. A depletion of Nrd1 or Nab3 results in the accumulation of 3'-extended read-through transcripts including snoRNAs and CUTs (Arigo et al., 2006; Thiebaut et al., 2006). The loss of exosome-associated cofactors Rrp47 and Mpp6 result in the stabilisation of *NEL025c* and other cryptic transcripts suggesting a role in ncRNA surveillance pathways in concert with the NNS complex, TRAMP, Rrp6 and EXO10 (Milligan et al., 2008).
Various genome-wide transcriptome analyses have reported pervasive intergenic transcription in many eukaryotes including humans, budding and fission yeast, fruit flies and plants (Bertone et al., 2004; David et al., 2006; Dutrow et al., 2008; Li et al., 2006; Stolc et al., 2004). High resolution mapping of the pervasive transcriptome revealed subclasses of intergenic transcripts (Neil et al., 2009; Xu et al., 2009). In addition to CUTs, stable-annotated transcripts (SUTs) are defined as intergenic transcripts that are observed in both wildtype and *rrp6Δ* cells. This suggests that SUTs are not ubiquitously degraded by the exosome. In addition to exosome-dependent degradation involving Rrp6 and Rrp47, SUTs are primarily degraded in the cytoplasm through NMD pathways involving decapping enzymes Dcp1/2 and the 5'-3' exonuclease Xrn1 (Marquardt et al., 2011). Transcriptome-

wide analysis of *rrp6Δ*, *rrp44*$^{exo-}$ and *rrp44*$^{endo-}$ mutants reported that both catalytic subunits of the nuclear exosome are involved in the degradation of previously annotated CUTs and SUTs and show a large degree of substrate overlap (David et al., 2006; Gudipati et al., 2012b; Neil et al., 2009; Xu et al., 2009). Inactivation of the endonuclease domain of Rrp44 did not significantly stabilise CUT and SUT transcripts however double *rrp44*$^{exo-endo-}$ mutants showed a greater accumulation in comparison to the single *rrp44*$^{exo-}$ mutant (Gudipati et al., 2012b).

The function(s) of CUTs and SUTs, if any, are still relatively unknown. A growing number of pervasive ncRNAs have been shown to have possible regulatory functions to control gene expression. The expression of *SER3*, a gene involved in serine and glycine biosynthesis, is modulated by the *SRG1* SUT transcribed from the intergenic regulatory region of the *SER3* allele. *SRG1* was initially identified in a transcriptome wide screen for CUTs but was subsequently shown to be primarily degraded in the cytoplasmic by Xrn1 (Davis and Ares, 2006; Martens et al., 2004; Thompson and Parker, 2007). A high level of transcription of the *SRG1* SUT was observed when cells were grown in rich medium. The constant transcription of *SRG1* was postulated to prevent the binding of transcription factors to initiate *SER3* transcription thereby repressing *SER3* (Martens et al., 2005, 2004). The transcription of the *PHO84* gene was shown to decrease in *rrp6Δ* cells and it was subsequently revealed that a CUT was generated in the antisense direction downstream of the *PHO84* ORF (Camblong et al., 2007). Instead of transcriptional silencing through RNAi-like mechanisms, it has been suggested that the act of antisense CUT/SUT transcription itself silences sense transcription. The antisense transcript recruits the Hda1/2/3 histone deacetylase complex resulting in *PHO84* silencing through chromatin rearrangement. Persistent antisense transcription may therefore act as a buffering system to prevent sense transcription until a threshold of sense activation signals is reached (Camblong et al., 2007; Castelnuovo et al., 2013).

The understanding of pervasive transcription and the reasoning behind this seemingly wasteful process is still in its infancy. The nuclear exosome complex plays a key role in the rapid turnover of unstable ncRNAs in concert with Rrp47,

Mpp6, the NNS complex and TRAMP. Whilst it is known that these protein complexes are required for CUT turnover, the mechanisms involved are yet to be elucidated.

1.1.3 Composition of the eukaryotic core-exosome complex

The eukaryotic exosome complex shares common functional and structural features with evolutionary related structures such as the archeal exosome and bacterial PNPase and RNase PH. These complexes are comprised of multiple subunits that oligomerize to form a ring-like structure with a central channel which can accommodate single-stranded RNA (Harlow et al., 2004; Ishii et al., 2003; Liu et al., 2006; Lorentzen et al., 2005; Shi et al., 2008).

Bacterial RNase PH is composed of a homohexamer of PH subunits that form a pseudo-ring structure with three-fold symmetry (Figure 1.1.A) (Harlow et al., 2004; Ishii et al., 2003). In a similar manner, PNPase forms a pseudo-hexameric ring through oligomerisation of three PNPase units comprised of two RNase PH-like domains, an S1 RNA binding domain and a KH domain (Figure 1.1.B) (Shi et al., 2008). Crystal structures of exosome complexes from archeal thermophiles *S. solfataricus, A. fulgidus* and *P. abyssi* reveal a pseudo-hexameric ring composed of three Rrp41/Rrp42 heterodimers which share sequence identity with RNase PH proteins. The ring-like structure is capped by three copies of Rrp4 and/or Csl4, which contain S1 domains. Rrp4 also contains a KH domain akin to PNPase domains (Figure 1.1.C) (Lorentzen et al., 2005).

The crystal structure of a reconstituted eukaryotic exosome (EXO9) revealed many similarities to the archeal exosome (Liu et al., 2006). The complex is composed of a six membered pseudo-ring structure composed three-heterodimeric pairs of RNase PH related proteins (Rrp41-Rrp45, Rrp43-Rrp46 and Mtr3-Rrp42). Three S1/KH containing proteins (Rrp4, Rrp40 and Csl4) form an asymmetric trimeric, capped structure on top of the PH ring (Figure 1.1.D). The complex forms a narrow channel of ~10-12 Å which allows unstructured ssRNA to thread through the complex (Liu et al., 2006; Makino et al., 2013a). Both PNPase and

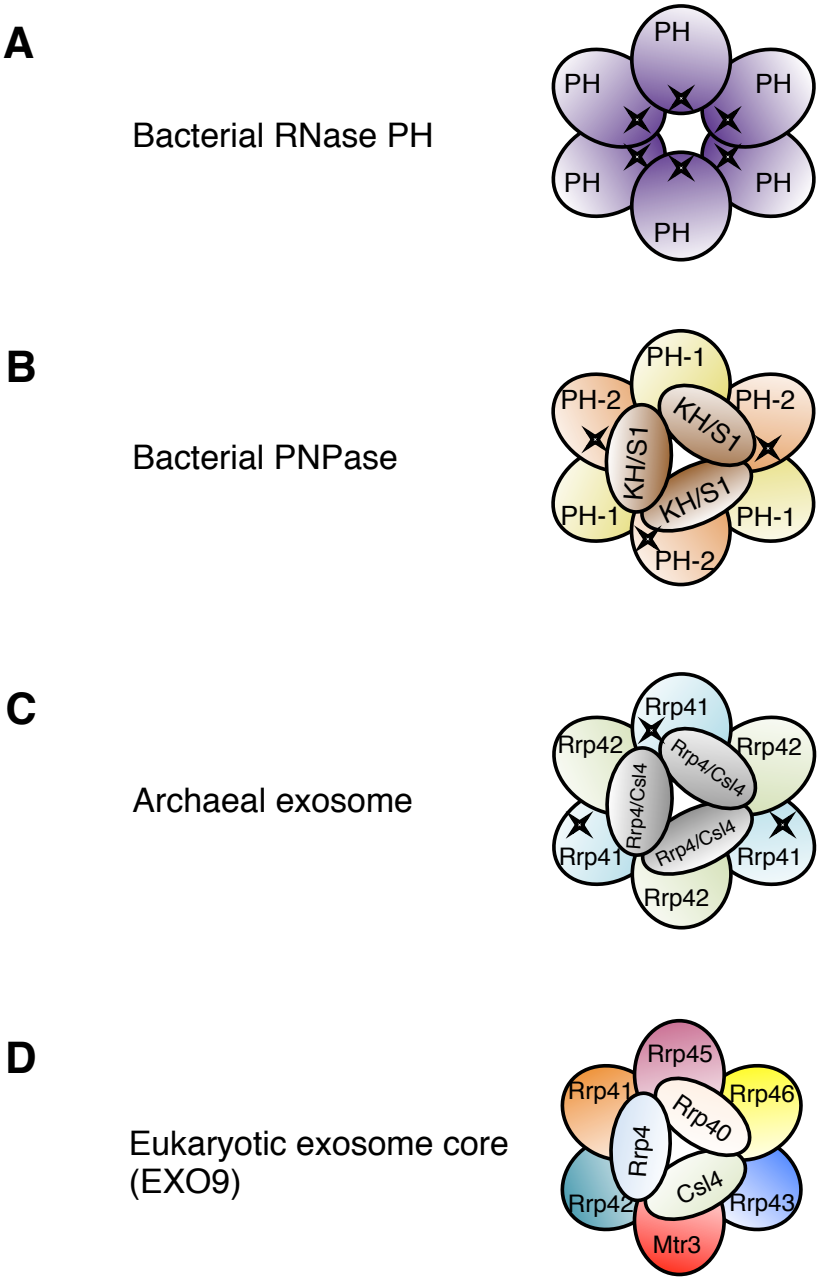

Figure 1.1. Conserved architecture of evolutionary related exonuclease complexes. Cartoon representation of bacterial RNase PH (A), bacterial PNPase (B), the archaeal exosome (C) and the eukaryotic exosome core (D). Subunits containing phosphorolytic and hydrolytic exoribonuclease active sites are marked with a cross.

the archeal exosome contain active sites in the central pore of the respective complexes that catalyse phosphorylytic 3'-5' exonuclease activity (Lorentzen et al., 2005; Nurmohamed et al., 2009). Surprisingly, the eukaryotic EXO9 complex does not possess any exonuclease activity. This is because most residues critical for RNA binding, phosphate and cation coordination have not been conserved over evolution (Dziembowski et al., 2007; Liu et al., 2006). Catalytic activity of the core-exosome is provided through physical and function association with Rrp44 (also known as Dis3) which possesses both 3'-5' exonuclease and endonuclease activities (Dziembowski et al., 2007; Lebreton et al., 2008; Liu et al., 2006; Schaeffer et al., 2009; Schneider et al., 2009).The N-terminal PIN domain of Rrp44 physically interacts with the bottom of EXO9 complex with PH-like proteins Rrp41 and Rrp45 to form the EXO10 complex (Figure 1.2.A,B) (Makino et al., 2013a; Schneider et al., 2009). The catalytically active EXO10 complex is ubiquitously found in both the nucleus and cytoplasm of all eukaryotes (Lorentzen et al., 2008; Mitchell et al., 1997). In addition, the nuclear exosome recruits Rrp6, a RNase D related protein which provides additional 3'-5' exonuclease activity (Briggs et al., 1998; Mitchell et al., 1997). A crystal structure of EXO10 in complex with a fragment of Rrp6 shows that the C-terminal region of the protein physical interacts with the cap region of the core-exosome complex (Makino et al., 2013a)

The barrel-like architecture of the exosome can also be likened to structure of the proteasome complex, which is comprised of four seven-membered stacked rings. Although both complexes are functionally unrelated and act on different substrates, it is interesting to recognize the exosome and proteasome complex as examples of convergent evolution to a common architecture. The similarities between bacterial PNPase, RNase PH, archeal and eukaryotic exosome are more likely due to divergent evolution (Groll et al., 1997; Lorentzen and Conti, 2006).

Various *in vitro* studies propose that single-stranded RNA is threaded through the S1/KH capped structure and down the channel of the PH ring to reach the exonuclease active site of Rrp44 docked on the bottom of the complex (Bonneau et al., 2009; Malet et al., 2010). A 2.8 Å resolution crystal structure of EXO10 plus

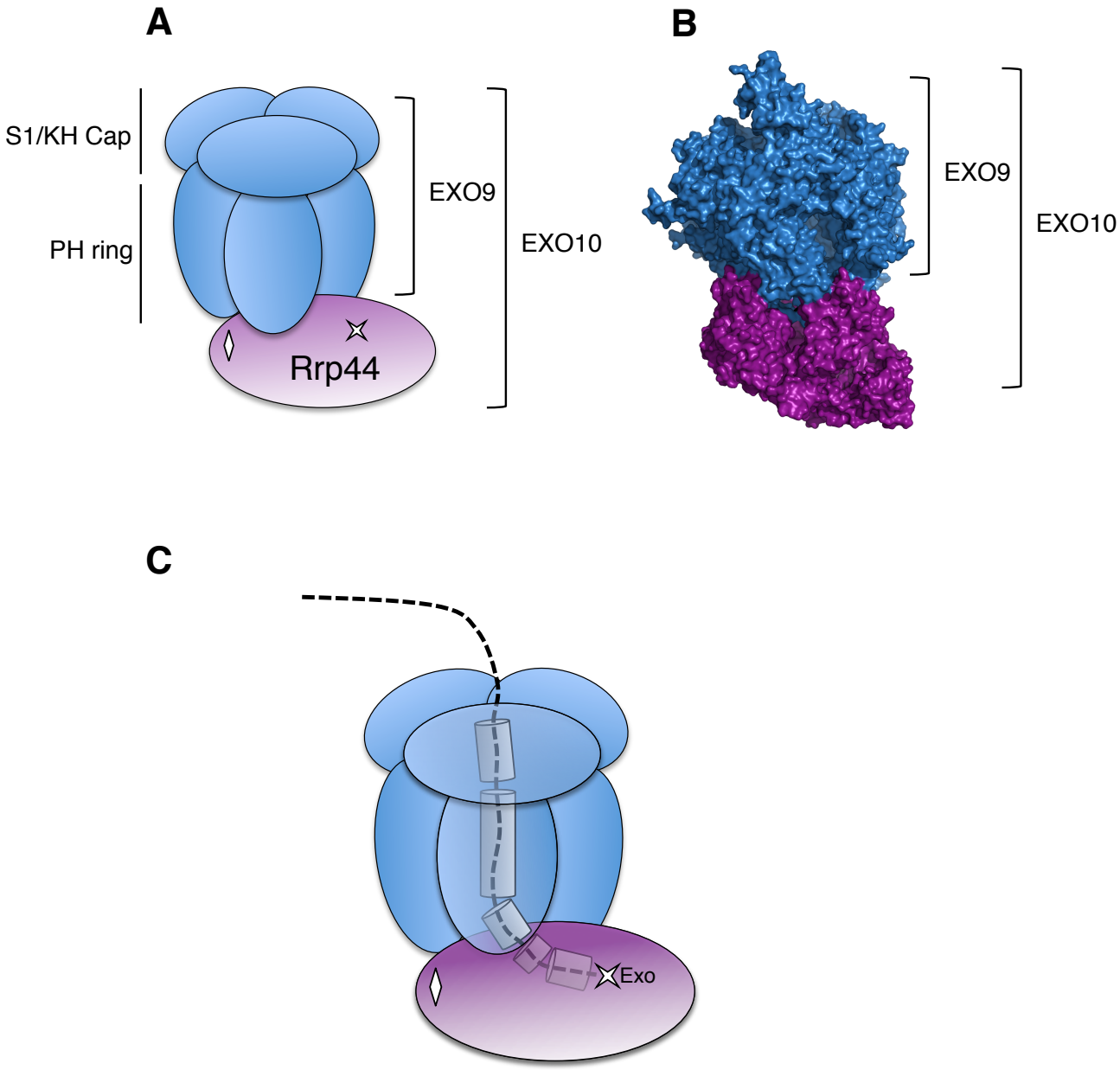

Figure 1.2. The eukaryotic EXO10 complex. (A) Structural arrangement of S1/KH and PH subunits (EXO9) plus Rrp44 (EXO10) to form the eukaryotic exosome core complex. The cartoon representation is based on the x-ray structure of the 11 subunit nuclear exosome complex shown in **(B)** and coloured respectively (Makino et al. 2013) (PDB=4IFD). **(C)** RNA is proposed to be channeled through the central channel of EXO9 to reach the exonuclease active site of Rrp44. Exonuclease and endonuclease sites are marked with a cross and diamond, respectively.

$Rrp6_{CT}$ in complex with RNA revealed the binding path of ssRNA through the channel of EXO9 (Makino et al., 2013a). The structure reveals that RNA is threaded into the channel after unwinding at the entry pore composed of the cap proteins Rrp4 and Rrp40. Subsequent base-stacking and base flipping mechanisms interact with the substrate to move the RNA though the capped structure into the internal channel and exit EXO9 to reach the exonuclease domain of Rrp44 (Figure 1.2.C). All components of EXO9 contribute to RNA binding through the complex to traverse a 110-Å path between the entrance pore and Rrp44 (Makino et al., 2013a)

All constituents of the EXO9 complex are essential for viability in yeast. However, catalytic subunits Rrp44 and Rrp6 are able to bind RNA and retain catalytic activity in the absence of EXO9 (Allmang et al., 1999b; Dziembowski et al., 2007; Januszyk et al., 2011; Liu et al., 2006; Mitchell et al., 1997). This raises questions regarding the functions of the core-exosome complex other than as a scaffold. The exonuclease activity of Rrp44 *in vitro* is decreased when in complex with EXO9 suggesting that the exosome core exerts a much needed layer of control (Bonneau et al., 2009; Liu et al., 2006; Wasmuth and Lima, 2012). It has long been proposed that the recruitment of various cofactors and complexes allows modulation of exosome activity to process a wide variety of RNA substrates. Two recent independent analyses propose that the central channel of EXO9 is important in the modulation of both exonuclease and endonuclease functions of cytoplasmic and nuclear exosomes (Karolina Drążkowska, Rafał Tomecki, Krystian Stoduś, Katarzyna Kowalska, Mariusz Czarnocki-Cieciura, 2013; Wasmuth and Lima, 2012). Mutants with occlusions in the PH central channel resulted in loss of catalytic function of Rrp44 and Rrp6 exonucleases *in vitro* and caused a loss of viability *in vivo*. Interestingly, occlusion mutants also caused an inhibition of Rrp44 endonuclease activity *in vitro* suggesting that the active site of the PIN domain is access via the central channel. This does not corroborate with recent structural studies which shows no access between the channel and the PIN domain which appears to be exposed to the solvent (Karolina Drążkowska, Rafał Tomecki, Krystian Stoduś, Katarzyna Kowalska, Mariusz Czarnocki-Cieciura, 2013; Makino et al., 2013a; Wasmuth and Lima, 2012). The channel occlusion data also

proposes that RNA substrates can pass through the EXO9 cap structure and exit through possible side channels between the S1/KH protein cap and the PH protein ring. However, the mechanism by which EXO9 can select a path for either exonuclease is yet to be resolve (Wasmuth and Lima, 2012) .

1.2. Catalytic components of the eukaryotic exosome

1.2.1 Rrp44 (Ribosomal RNA-processing protein 44)

The core structure of the yeast exosome contains 9 subunits, 6 of which share 20-30% identity with bacterial 3'-5' exonucleases. However, unlike bacterial and archeal homologs, the eukaryotic core-exosome does not process catalytic activity (Liu et al., 2006; Mitchell et al., 1997). Enzymatic activity is provided through the association with Rrp44 (also known as Dis3 or Mtr17). Rrp44 possesses both 3'-5' exonuclease and endonuclease activity and is present in both cytoplasmic and nuclear exosome complexes. (Dziembowski et al., 2007; Lebreton et al., 2008; Liu et al., 2006; Schneider et al., 2009). The catalytic activity of Rrp44 as part of the exosome complex has been implicated in processing and degradation pathways of all classes of RNAs (Section 1.1.2).

Rrp44 is an essential 113kDa protein that shares homology with members of the bacterial RNase II family of hydrolytic 3'-5' exonucleases (Mitchell et al., 1997). Similar to *E. coli* RNase II, Rrp44 contains two N-terminal cold shock RNA-binding domains (CSD1 and CSD2 respectively), a central exoribonuclease (RNB) domain and a C-terminal S1 RNA binding domain (Frazão et al., 2006; Schneider et al., 2007). Additionally, Rrp44 contains a N-terminal PIN (Pilus-forming N-terminus) domain that harbors endonuclease activity and is required to physically tether the protein to the core-exosome (Figure 1.3.) (Schneider et al., 2007). A conserved

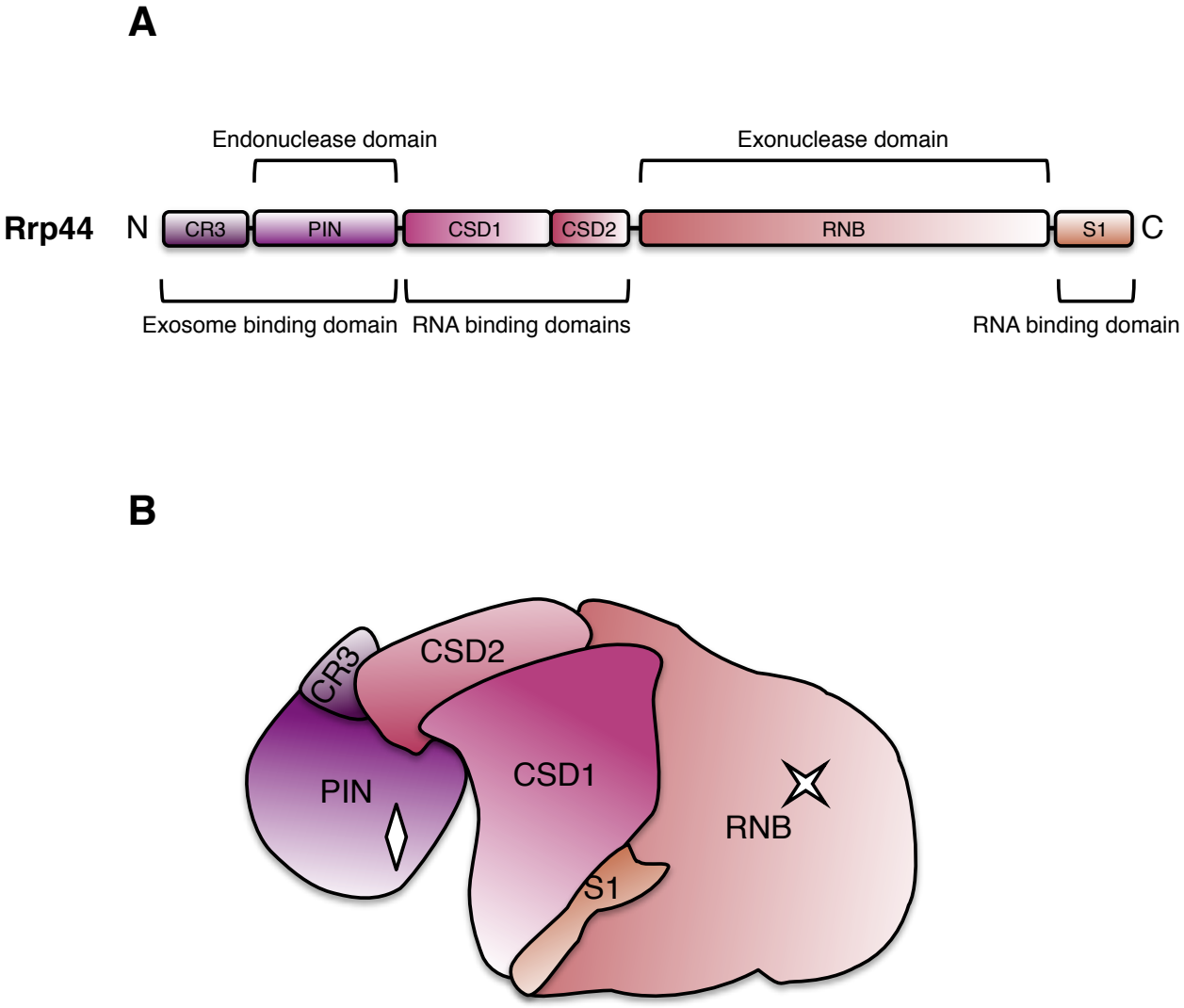

Figure 1.3 Domain organisation and structural arrangement of Rrp44. (A) Schematic representation of Rrp44 domain architecture as defined by Pfam (http://pfam.xfam.org/). Rrp44 contains an N-terminal CR3 domain (residues 1-84), a PIN catalytic domain harboring endonuclease activity (84-235), two cold shock RNA binding domains (CSD1 235-400, CSD2 400-474), a RNB catalytic domain harboring exonuclease activity (474-909) and a C-terminal S1 RNA binding domain (909-1001). **(B)** Structure representation of Rrp44 based on EM and X-ray crystallography data (Wang et al. 2007; Bonneau et al. 2009; Makino et al. 2013). Exonuclease and endonuclease containing domains are marked with a cross and diamond, respectively.

CR3 motif (cysteine-rich domain with three cysteines) N-terminal to the PIN domain is suggested to cluster with a conserved histidine residue and co-ordinate a divalent cation. Mutations in the CR3 motif leads to impaired catalytic activity and a reduced interaction with the core exosome suggesting that this region is important for structural integrity of Rrp44 (Schaeffer et al., 2012). The crystal structure of Rrp44 has been determined in three reports including co-complexes with RNA, a Rrp44-Rrp41-Rrp45 complex and more recently the structure of an 11-subunit exosome core containing EXO9, Rrp44 and the C-terminus of Rrp6 was solved (Bonneau et al., 2009; Lorentzen et al., 2008; Makino et al., 2013a). Combining results from structural and *in vitro* studies, it has been suggested that substrate RNA is threaded through the central channel of the core exosome to reach the exonuclease domain of Rrp44 (Bonneau et al., 2009; Malet et al., 2010).

The PIN domain is found in over 300 proteins from bacteria, archaea and eukarya domains. The endonuclease active site contains four highly conserved basic residues ($D_{91}E_{120}D_{171}D_{198}$) that co-ordinate two divalent cations that are essential for catalytic activity *in vitro* (Schneider et al., 2009). In addition to endonucleolytic activity, the PIN domain physically connects Rrp44 to the RNase PH proteins on the exosome core (Rrp41, Rrp45) (Bonneau et al., 2009; Makino et al., 2013a; Schneider et al., 2009). Yeast strains lacking either exonuclease or endonuclease activity (Rrp44^{exo-} or Rrp44^{endo-} respectively) are viable whereas double Rrp44$^{exo-, endo-}$ mutants are lethal (Dziembowski et al., 2007; Schneider et al., 2009, 2007). Structural studies have revealed that the endonuclease site in the PIN domain is exposed to outer solvent and does not require channeling through the exosome core. (Bonneau et al., 2009; Schneider et al., 2009). Whilst Rrp44 has a wide range of characterised substrate targets, those specific to endonuclease activity are relatively unknown. *In vivo* northern blot analysis of Rrp44^{endo-} mutants shows an accumulation of the 5'ETS fragment produced during 35S rRNA processing (Schneider et al., 2009). The endonuclease can cleave circular and linear ssRNA but is unable to process dsRNA substrates *in vitro* (Schaeffer et al., 2009).

The exoribonuclease (RNB) domain of Rrp44 shares many features with motifs in bacterial RNase II and RNase R and is responsible for the 3'-5' processive exonuclease activity of the core-exosome (Dziembowski et al., 2007; Frazão et al., 2006; Lorentzen et al., 2008; Mitchell et al., 1997). Catalytic activity is dependent on four highly conserved aspartate residues that co-ordinate two magnesium ions that hydrolytically cleave the backbone of RNA substrates. The loss of Rrp44 is lethal in yeast yet surprisingly mutations in the conserved Asp residues abolishes catalytic activity but are tolerated (Dziembowski et al., 2007; Liu et al., 2006; Schaeffer et al., 2009; Schneider et al., 2007). The exonuclease active site is buried within the protein and requires substrates with ssRNA overhangs of at least 7nt long to enter a narrow cavity formed by the CSD1, CSD2 and S1 RNA binding domains. This cavity forms a clamp structure similarly observed in bacterial RNase II. The clamp architecture holds substrates in place whilst the exonuclease attacks the 3' ends of ssRNA and degrades in a processive manner, releasing nucleoside 5'-monophosphates and leaving a short product of a few nucleotides long. (Lorentzen et al., 2008; Wang et al., 2007; Zuo et al., 2006). In contrast to RNaseII, Rrp44 is able to degrade structured substrates *in vitro* as long as there is a single-stranded 3' overhang of at least 4 nucleotides. Longer 3' overhangs are more efficiently degraded (Dziembowski et al., 2007; Lorentzen et al., 2008). This suggests that the processive nature of the enzyme is able to unwind structured RNA upon capture in the clamp channel prior to subsequent degradation.
Crystal structure analysis of the core-exosome plus Rrp44 reveal that the central channel formed by EXO9 feeds into the exoribonucleolytic channel of Rrp44 and RNA substrates are threaded through. This requires an unstructured ssRNA overhang of at least 31-33nt to be able to pass through the exosome core to reach the active site of Rrp44. (Bonneau et al., 2009; Makino et al., 2013a; Malet et al., 2010). An alternative, more direct, route has been proposed where RNA can bypass the core-exosome channel and access the exonuclease domain of Rrp44 directly. This secondary route is theorized to be accessible with much shorter 3' ssRNA overhangs and could possibly be a pathway for the degradation of highly structured substrates (Bonneau et al., 2009; Makino et al., 2013a; Wang et al., 2007)

The exosome complex has been shown to function in the degradation and processing of a multitude of coding and non-coding RNAs produced from all three RNA polymerases (Allmang et al., 2000; Kadaba et al., 2004; van Hoof et al., 2000a; Wlotzka et al., 2011). Catalytic activity can be attributed to three units; the endonuclease domain of Rrp44 and the exonuclease domains of both Rrp44 and Rrp6. Determining the specific targets of each catalytic unit is challenging due to levels of redundancy and co-operation within the exosome and other exonucleases.

Novel high-resolution, transcriptome-wide analyses of *rrp6Δ*, *rrp44*$^{exo-}$ and *rrp44*$^{endo-}$ mutants have recently identified a broad range of exosome substrates (Gudipati et al., 2012b). Both Rrp44 and Rrp6 appear to have overlapping targets yet distinct functions suggesting a level of co-operation between each catalytic unit. This dataset proposes that Rrp44 and Rrp6 both function in the degradation of CUTs and SUTs whereas Rrp44 has a more specific role in pre-tRNA degradation and the turnover of intro-containing mRNAs. In addition to the turnover of CUTs and SUTs, Rrp6 was proposed to play a specific role in pre-snRNA and snoRNA degradation. This is consistent with previous observations of accumulated 3'-extended pre-snRNA and snoRNA species in *rrp6Δ* strains (Allmang et al., 1999a; Gudipati et al., 2012b; van Hoof et al., 2000a).

In vivo protein-RNA crosslinking and analysis of cDNAs (CRAC) was applied to Rrp44 and Rrp6 along with catalytic mutants to identify target substrates (Schneider et al., 2012). Transcriptome-wide binding profiles identified associated substrates from all classes of RNA in accordance to previous analysis. Interestingly, disruption of the endonuclease domain (Rrp44^{endo-}) did not appear to alter substrate binding significantly. However, the Rrp44^{exo-} mutant showed a strong enrichment of characterised exosome substrates including CUTs, SUTs, snRNAs and snoRNAs. Strikingly, almost 40% of observed crosslinks in the Rrp44^{exo-} mutant were products of RNA Pol III transcription including 5S rRNA and U6 snRNA. A large amount of crosslinked transcripts were shown to be oligoadenylated, which implies that they had been targeted for degradation. Parallel CRAC analyses using Trf4, a component of the TRAMP complex, revealed strong overlaps in oligoadenylated substrates which corroborates previous studies suggesting co-operation between TRAMP-dependent polyadenylation and

exosome-degradation (Houseley and Tollervey, 2006; LaCava et al., 2005; Schneider et al., 2012; Vanácová et al., 2005; Wyers et al., 2005). CRAC analysis also revealed a strong overlap of substrates between Rrp6 and Rrp44. This level of functional redundancy may explain the synthetic lethality between *rrp6Δ* and *rrp44*$^{exo-}$ mutants. The Tollervey lab proposes a model for strong co-operation between the endonuclease domain of Rrp44 with the exonuclease domains of Rrp44 and Rrp6. Endonucleolytic cleavage events would provide favorable free 3' ends for Rrp6, Rrp44 or other cellular exonucleases such as Rex1. In *rrp44*$^{exo-}$ mutants, endonuclease activity would still provide substrates for degradation by Rrp6 or other exonucleases, albeit less efficiently (Schneider et al., 2012).

1.2.2 Rrp6 (Ribosomal RNA-processing protein 6)

Rrp6 is a member of the DEDD superfamily of 3'-5' exonucleases which also includes bacterial RNaseD (Zuo and Deutscher, 2001). In addition to Rrp44, Rrp6 provides catalytic activity to the exosome but differs in its exclusive association with the nuclear exosome (Allmang et al., 1999b). Deletion of RRP6 is not and cause slow growth phenotypes at 30°C and no growth at 37°C (Briggs et al., 1998). The loss of core exosome components is lethal; therefore *rrp6Δ* strains are a useful tool for the understanding of exosome-mediated processing and degradation of all classes of RNA. The characterisation of cryptic unstable transcripts (CUTs) was carried out in *rrp6Δ* strains as a tool to maintain stable expression of unstable intergenic transcripts (Wyers et al., 2005). Rrp6 interacts physically and functionally with a small nuclear RNA binding protein called Rrp47. The expression levels of either protein are mutually dependent on this physical interaction with Rrp47 being more sensitive to the loss of Rrp6 (Costello et al., 2011; Feigenbutz et al., 2013a, 2013b; Garland et al., 2013; Stead et al., 2007)

The human homolog or Rrp6, PM-Scl100, was initially identified as a protein for which antibodies were found in patients suffering from polymitosis, sclerderma or an overlap of the two diseases (Alderuccio, 1991; Ge et al., 1992). Immunoprecipitation experiments revealed PM-Scl100 to be associated with large

complexes of 11-16 proteins (Gelpi et al., 1990; Reimer et al., 1986). Rrp6 was initially identified in yeast through genetic screening where *rrp6* mutants showed suppression of a temperature sensitive *pap1-1* mutation. Subsequent cloning and sequencing of the *RRP6* locus revealed significant homology to Pm-Scl100 (Briggs et al., 1998).

Rrp6 comprises 733 amino acids and has a molecular weight of ~84kDa. The protein contains an N-terminal PMC2NT domain (Staub et al., 2004), an exonuclease domain, two HRDC (Helicase RNaseD C-terminal) domains (Midtgaard et al., 2006) and a bipartite nuclear localisation signal (NLS) at the C-terminus (Figure 1.4.A) (Briggs et al., 1998).

The N-terminal PMC2NT (N-terminal domain in 3'-5'-exonucleases like Polymyositis autoantigen 2) domain of Rrp6 ($Rrp6_{NT}$) interacts physically with the N-terminal Sas10/C1D domain of the RNA binding protein Rrp47, a small nuclear-specific exosome associated co-factor (Stead et al., 2007). Normal expression levels of Rrp47 are strongly dependent on the physical interaction with $Rrp6_{NT}$ with protein levels decreased by 90% in the absence of Rrp6 (Feigenbutz et al., 2013b; Stead et al., 2007). The PMC2NT domain is found in eukaryotic Rrp6 homologs but not in bacterial RNaseD (Carpousis, 2002). Although crystal structures of Rrp6 have been solved, these unfortunately do not include the N-terminal regions of the protein (Makino et al., 2013a; Midtgaard et al., 2006). Protein structure prediction programs suggest the N-terminus to be largely α-helical in nature. Partial crystal structures confirm four short α-helices between residues 132 and 210 (Kelley and Sternberg, 2009; Midtgaard et al., 2006; Stead et al., 2007). The PMC2NT domain alone is sufficient to bind Rrp47 *in vitro*, yet inclusion of the α-helices downstream of the PMC2NT domain increases the efficiency of the pulldown (Stead et al., 2007).

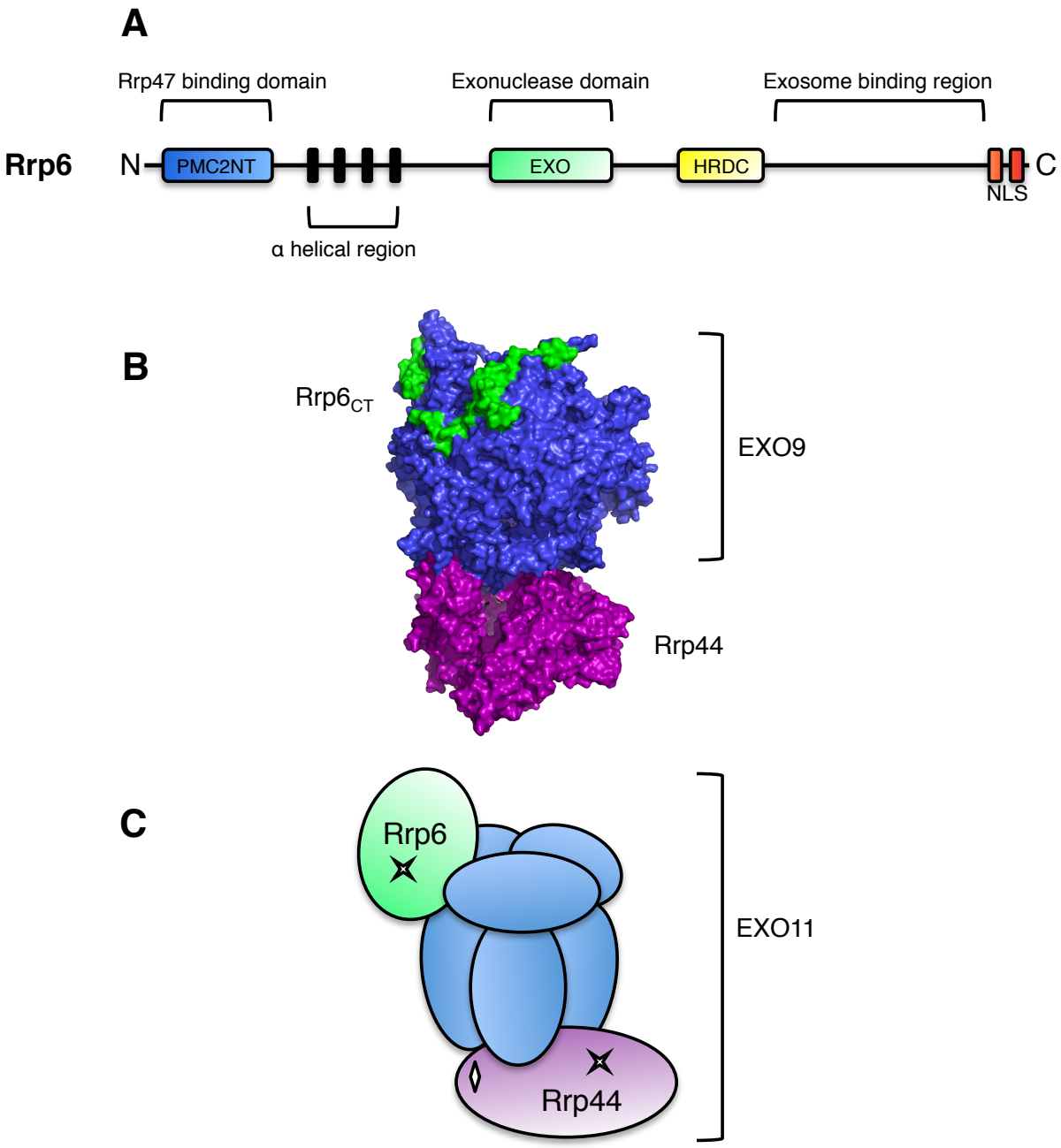

Figure 1.4. Domain structure of Rrp6 and organisation of EXO11 complex. (A) Schematic representation of Rrp6 domain architecture as defined by Pfam. Rrp6 contains an N-terminal PMC2NT domain (residues 13-102), four α-helices (132-210), a catalytic exonuclease (EXO) domain (283-381), a HRDC domain (438-505) and a C-terminal nuclear localisation signal (NLS). The exosome binding region of Rrp6 is defined between residues 518-693. **(B)** X-ray structure of the eukaryotic EXO9 complex plus Rrp44 and the C-terminal region of Rrp6 ($Rrp6_{CT}$) from Makino et al (2013) (PDB=4IFD). The C-terminus of Rrp6 (Green) physically interacts with Csl4, Mtr3 and Rrp43 of the core exosome complex (EXO9) **(C)** Cartoon representation of the EXO11 complex. Exonuclease and endonuclease containing domains are marked with a cross and diamond, respectively.

The exonuclease domain of Rrp6 contains three motifs conserved between homologs in model organisms termed ExoI, ExoII and ExoIII respectively (Burkard and Butler, 2000). The DEDD family of proteins are characterised by an Asp-Glu-Asp-Asp motif in the catalytic residues of the exonuclease active site. These residues co-ordinate two divalent cations that are involved in the activation of a water molecule to attack the terminal phosphodiester bond of the target nucleic acid (Steitz and Steitz, 1993). Rrp6 was shown to require both Mn^{2+} and Zn^{2+} cations to form protein-ribonucleotide complexes through systematic crystallographic analysis of cation binding (Midtgaard et al., 2006). Mutations in critical aspartate or glutamate residues lead to a loss of catalytic function. The *RRP6* gene was originally cloned by complementation of a catalytic *rrp6-1* allele that harbors a D238N mutation (Briggs et al., 1998; Burkard and Butler, 2000).

Rrp6 contains two HRDC (Helicase RNaseD C-terminal) domains that fold into characteristic 5-α-helical structures. First identified in the RecQ family of proteins, the HRDC domain was characterised as a putative nucleic acid binding domain (Morozov et al., 1997). Crystal structures of Rrp6 peptides have only included the N-terminal-end HRDC1 domain which folds almost undistinguishable to the homologous domain found in bacterial RNaseD (Midtgaard et al., 2006; Zuo et al., 2005). The RNA binding properties of the HRDC domains in Rrp6 have not been demonstrated experimentally. Crystal structures revealed the position of the HRDC1 domain to be stabilised by a conserved aspartic acid residue (D457) in concordance with a homologous D232 in RNaseD. RNA analysis in a D457A mutant shows a retarded function for 3'-maturation of 5.8S rRNA and snoRNA yet the turnover of 5'ETS and polyadenylated snoRNAs was not affected. This suggests that the position of the HRDC1 domain is important for the 3'-end processing function of Rrp6 but is not important for RNA degradation most likely in concert with the core exosome and Rrp44 (Midtgaard et al., 2006; Phillips and Butler, 2003). Deletion of either or both HRDC domains in Rrp6 results in the loss of association with the core-exosome complex. HRDC2, but not HRDC1 deletions in Rrp6 allow normal 3'-end processing of pre-5.8S rRNA and pre-snoRNAs but are unable to degrade 5'ETS. This demonstrated that Rrp6 functions independently of the core-exosome in 3'-end processing but still requires the core

exosome and co-operative activity with Rrp44 for the turnover of degradation substrates (Callahan and Butler, 2008). Rrp6 has since been shown to allosterically stimulate the function of Rrp44 (Wasmuth and Lima, 2012) and will be discussed below.

The C-terminal region of Rrp6 contains two putative nuclear localisation signals (NLS). Biofractionation experiments initially revealed Rrp6 to be associated with only the nuclear fraction of exosome complexes. This was corroborated by immunofluorescence analysis revealing Rrp6 was localized to the nucleus (Allmang et al., 1999b; Briggs et al., 1998). Deletion of the NLS region of Rrp6 results in mis-localisation to the cytoplasm (Phillips and Butler, 2003). More recently it has been shown that Rrp6 is imported into the nucleus via the importin complex involving the Srp1/Kap95 heterodimer (the yeast homologs of importins α and β) (Feigenbutz et al., 2013b). Mass spec analysis of Rrp6 pulldowns were shown to contain Srp1 and Kap95 proteins and corroborated in a later study (Feigenbutz et al., 2013b; Synowsky et al., 2009). Interestingly, the Rrp6-associated co-factor Rrp47 was not found to be associated with the Rrp6/Srp1 complex suggesting that Rrp47 is localised to the nucleus independent of Rrp6 before the assembly of the Rrp6/Rrp47 homodimer (Feigenbutz et al., 2013b). Additionally, the C-terminus of Rrp6 ($Rrp6_{CT}$) is required for contact with the core exosome complex. A recent crystal structure of EXO10 in complex with $Rrp6_{CT}$ shows that this region interacts with the Csl4 subunit of the S1/KH cap along with Mtr3 and Rrp43 subunits that make up the PH ring of EXO9 (Figure 1.4.B-C) (Makino et al., 2013a)

1.2.3. Specific functions of Rrp6 in RNA maturation and degradation

The initial identification and characterisation of yeast Rrp6 showed that catalytic *rrp6-1* mutants resulted in the accumulation of a 5.8S rRNA species extended at the 3' end by 30 nucleotides dubbed 5.8S + 30. This phenotype correlated with a 20 fold decrease in mature levels of 5.8S compared to wildtype levels suggesting a block in 3'-end processing (Briggs et al., 1998). However, the majority of pre-5.8S rRNA molecules are correctly processed to mature 5.8S suggesting a level of redundancy via alternative pathways. Rrp6 trims the 5.8S + 30 rRNA species,

generated from the 7S rRNA by exosome-dependent processing, to 6S rRNA which undergoes final 3'-end maturation by Ngl2 after export to the cytoplasm (Briggs et al., 1998; Mitchell et al., 1997, 1996; Thomson and Tollervey, 2010). The 3' extended 5.8S + 30 rRNA is also accumulated in yeast cells lacking Rrp47 and a similar phenotype was observed in mammalian cells depleted of the human homolog C1D (Mitchell et al., 2003; Schilders et al., 2007; Stead et al., 2007). This suggests a key requirement of Rrp47 is to aid Rrp6 in efficient 3'-end processing rRNA precursors. The mechanism by which Rrp47 promotes Rrp6 catalytic activity is still poorly understood.

In addition to the maturation of ribosomal RNA, Rrp6 function has been ascribed to the 3'-end processing of snoRNAs and snRNA precursor transcripts. Northern blot analysis of snoRNAs and snRNAs in *rrp6Δ* cells showed a slowed migration suggesting a block in the final steps of processing. Pre-snoRNA and some snRNAs are transcribed as 3' extended precursors that undergo initial 3'-5' trimming by Rrp44 as part of the core-exosome before release and undergoing the final precise 3'-maturation by Rrp6 (Allmang et al., 1999a; van Hoof et al., 2000a). Rrp6 is still able to function in 3'-end processing of 5.8S, snoRNAs and snRNAs independently of association with the core exosome complex but is dependent on the physical interaction with Rrp47 (Callahan and Butler, 2008; Mitchell et al., 2003; Stead et al., 2007).

The surveillance and degradation of aberrant ncRNAs, rRNA processing intermediates and products of pervasive intergenic transcription is key in maintaining a stable transcriptome in eukaryotes. Rrp6 and the core-exosome have been shown to be major contributors in many surveillance and degradation pathways in concert with additional co-factors and complexes. As Rrp6 is a non-essential component of the nuclear exosome, *rrp6Δ* strains have allowed the identification and characterisation of a myriad of RNA degradation substrates.

In the absence of Rrp6, cells not only show rRNA processing defects but also accumulate byproducts of processing such as the excised spacer fragment extending from the 5' end to the A_0 cleavage site of the 35S polycistronic pre-

rRNA transcript (5' external transcribed spacer, 5'ETS). The 5'ETS processing byproduct is also accumulated in core exosome mutants suggesting a co-operative or redundant pathway for 5'ETS degradation (Allmang et al., 1999a, 1999b; de la Cruz et al., 1998).

As mentioned above, Rrp6 is required for the final steps of 3'-end maturation of snoRNA and some snRNAs. A block in the processing of snRNA and snoRNAs results in the accumulation of short 3' extended transcripts as observed in *rrp6Δ* mutants (Allmang et al., 1999a). Additionally, *rrp6, rrp47* and core exosome mutants were shown to accumulate a smaller amount of longer 3'-polyadenylated snoRNA and snRNAs. This phenotype was also observed upon the loss of an ATP-dependent RNA helicase, Mtr4 (Allmang et al., 1999a; de la Cruz et al., 1998; Mitchell et al., 2003; van Hoof et al., 2000a). Polyadenylation of other ncRNAs were reported such as pre-rRNA, rRNA and a hypermodified aberrant pre-$tRNA_i^{Met}$ (Kadaba et al., 2004; Kuai et al., 2004). The stabilisation of defective $tRNA_i^{Met}$ was observed in mutations in a putative poly(A) polymerase, Trf4. Likewise, $tRNA_i^{Met}$ was stabilised in the absence of Rrp6 or conditional *rrp44* mutants (Kadaba et al., 2004). This suggested that Trf4-dependent polyadenylation of ncRNAs leads to degradation by the exosome and Rrp6. Both Trf4 and Mtr4 were identified to be components of the nuclear polyadenylation TRAMP complex comprised of the poly(A) polymerase Trf4, zinc knuckle RNA binding protein Air2 and the RNA helicase Mtr4. (LaCava et al., 2005; Vanácová et al., 2005). The components of the TRAMP complex will be discussed further below. Rrp6, Rrp44 and TRAMP complexes work in concert to play an essential role in the turnover of non-coding RNAs.

Transcriptome-wide analysis of yeast strains lacking Rrp6 identified polyadenylated non-coding RNAs in agreement with previous observations. Additionally, a novel class of polyadenylated RNA pol II transcripts derived from intergenic regions was identified and later termed as cryptic unstable transcripts (CUTs). Polyadenylation of CUTs is almost completely dependent on the activity of Trf4 as part of the TRAMP complex (Wyers et al., 2005). The use of *rrp6Δ* and TRAMP mutant strains has been widely reported as a tool to stabilise and

characterise cryptic unstable transcripts (Camblong et al., 2007; Davis and Ares, 2006; Uhler et al., 2007; Wyers et al., 2005; Xu et al., 2009).

Whilst the role of Trf4 and Rrp6 in polyadenylation and subsequent degradation of CUTs was clear, the mechanism for initial targeting was relatively unknown. Through ChIP analysis it was revealed that Nrd1 and Nab3 proteins are localised to chromosomal regions expressing CUTs (Arigo et al., 2006). Nrd1 and Nab3 have previously been shown to be involved in 3'-end formation of snRNAs and snoRNAs coupled to transcriptional termination in concert with RNA Pol II and the RNA helicase Sen1 collectively known as the NNS (Nrd1/Nab3/Sen1) complex (Conrad et al., 2000; Steinmetz and Brow, 1996; Steinmetz et al., 2001). In *nrd1* and *nab3* mutants, 3'-extended snoRNA transcripts are accumulated due to errors in transcriptional termination. The resulting transcripts read through the normal Nrd1-dependent termination point and extend into neighboring coding regions before termination at an mRNA cleavage/polyadenylation site. In addition to sn- and snoRNAs, 3'-extended read-through transcripts that arise from the well characterised *NEL025c* CUT locus were accumulated in conditional *nrd1* and *nab3* mutants (Arigo et al., 2006; Thiebaut et al., 2006). Two classes of *NEL025c* transcript were characterised in the Libri and Corden labs; a series of short, polyadenylated *NEL025c*$_S$ transcripts and a longer *NEL025c*$_L$ transcript. The shorter species were shown to be polyadenylated by Trf4 as part of the TRAMP complex and are stabilised in exosome mutants including *rrp6Δ* strains. The *NEL025c*$_L$ species accumulates in conditional *nrd1* and *nab3* mutants and is polyadenylated by Pap1. This supports a model of alternative transcription termination of CUTs where shorter RNAs from Nrd1/Nab3-dependent termination are polyadenylated by Trf4 as targets for exosome-dependent degradation. Longer transcripts are generated from a loss of Nrd1/Nab3-dependent termination and read through into downstream genes before terminated at the canonical mRNA cleavage/polyadenylation site (Arigo et al., 2006; Thiebaut et al., 2006; Wyers et al., 2005). This model along with other data suggests that the exosome/Rrp6/TRAMP and NNS complexes couple transcriptional termination, polyadenylation and rapid turnover of CUTs as part of a major RNA surveillance complex. However, the mechanisms that govern substrate recognition for either

productive or destructive generation of RNA PolII transcripts are still relatively unknown.

It has been suggested that exosome-associated cofactors that possess RNA binding activity such as Rrp47, Mpp6 and the Air1/2 proteins may function to differentiate substrate recognition to target transcripts for processing or degradation pathways coupled with TRAMP, Nrd1/Nab3 and the core-exosome or Rrp6 (Milligan et al., 2008; Mitchell et al., 2003; Schmidt et al., 2012). The mechanisms underlying this putative substrate recognition are poorly characterised and further investigation is required.

1.3. Exosome associated co-factors

The nuclear exosome complex must distinguish a wide array of RNA substrates for a number of separable functions *in vivo*. The nuclease activities of Rrp44 and Rrp6 require regulation to prevent ubiquitous RNA degradation. The physical association of Rrp44 to the catalytically inert EXO9 significantly decreases enzymatic activity (Liu et al., 2006; Wasmuth and Lima, 2012). Further modulation of Rrp6 and Rrp44 is achieved through the association with small nuclear proteins Rrp47 and Mpp6 in addition to larger complexes such as Trf4/Air2/Mtr4 (TRAMP) and Nrd1/Nab3/Sen1 (NNS). These co-factors are proposed to be required for recognition of substrates in order to recruit the exosome for productive or degradative functions. A summary of exosome components and cofactors is detailed in Figure 1.5 and Table 1.1.

1.3.1 Rrp47 (Ribosomal RNA-processing protein 47)

The yeast protein Rrp47 (also known as Lrp1 and yC1D) is a nuclear-specific exosome-associated co-factor that can bind RNA and DNA (Kumar et al., 2002; Mitchell et al., 2003; Stead et al., 2007). Along with its putative human homolog C1D, Rrp47 was implicated as a DNA binding protein involved in double strand

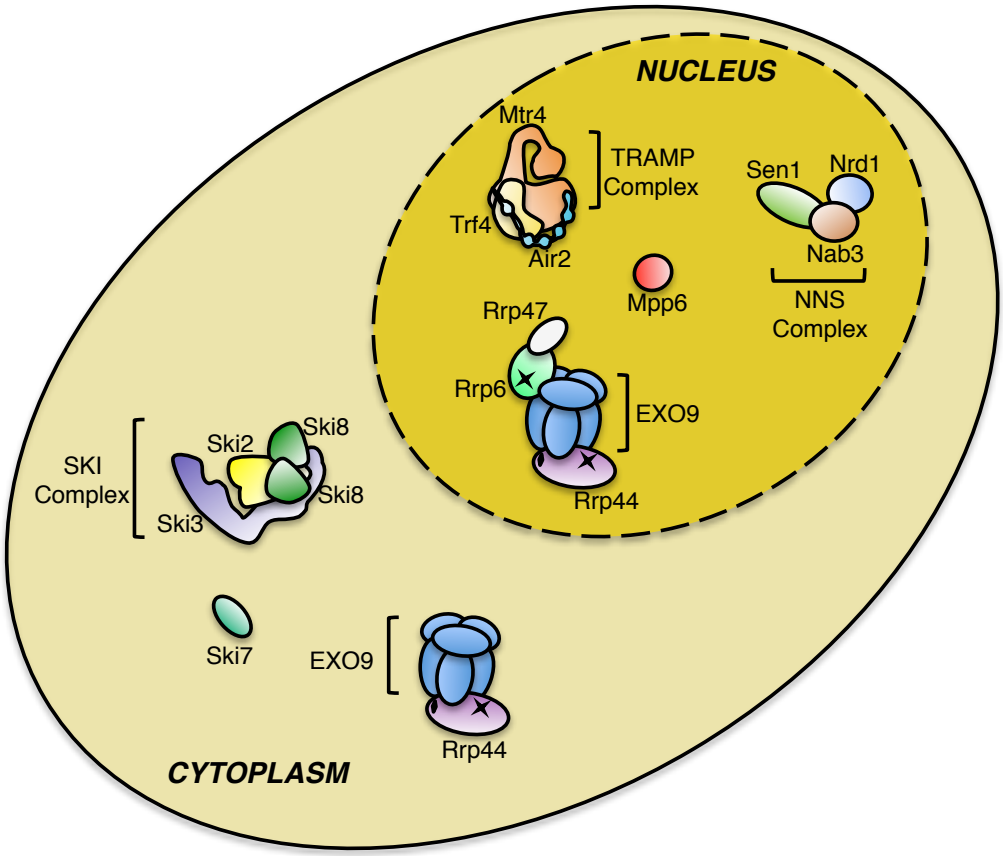

Figure 1.5. Summary of exosome associated co-factors in *S. cerevisiae*.
The yeast core exosome (EXO9) associates with a number of distinct co-factors and complexes in both the nucleus and cytoplasm. Co-factors depicted have been identified to be functionally and/or physically associated with EXO9.

Complex/co-factors	Yeast protein	Location	Human homolog	Description/role
Core Exosome (EXO9)	Rrp41	n + c	hRrp41	RNasePH domain, non-catalytic core exosome component
	Rrp42	n + c	hRrp42	RNasePH domain, non-catalytic core exosome component
	Mtr3	n + c	hMtr3	RNasePH domain, non-catalytic core exosome component
	Rrp43	n + c	hRrp43	RNasePH domain, non-catalytic core exosome component
	Rrp45	n + c	hRrp45	RNasePH domain, non-catalytic core exosome component
	Rrp46	n + c	hRrp46	RNasePH domain, non-catalytic core exosome component
	Rrp4	n + c	hRrp4	S1/KH domain, non-catalytic core exosome component
	Rrp40	n + c	hRrp40	S1/KH domain, non-catalytic core exosome component
	Csl4	n + c	hCsl4	S1/KH domain, non-catalytic core exosome component
Catalytic subunits	Rrp44	n + c	Dis3, Dis3L, Dis3L2	RNaseII-related 3'-5' exonuclease, putative endonuclease
	Rrp6	n	PM/Scl-100	RNaseD-related 3'-5' exonuclease
TRAMP complex	Trf4	n	?PAPD5 + POLS	Non-canonical poly(A) polymerase
	Trf5	n	?PAPD5 + POLS	Non-canonical poly(A) polymerase
	Air1	n	?ZCCHC7	ZnK RNA binding protein
	Air2	n	?ZCCHC7	ZnK RNA binding protein
	Mtr4	n	hMtr4 (SKIV2L2)	DExH RNA helicase
NNS complex	Nrd1	n	?	RNA binding and RNA pol II CTD binding
	Nab3	n	?	RNA binding
	Sen1	n	Senataxin	Type I 5'-3' ATP-dependent DNA/RNA helicase
SKI complex	Ski2	c	hMtr4 (SKIV2L2)	DExH RNA helicase
	Ski3	c	hSki3	Ski complex component
	Ski8	c	hSki8	Ski complex component
Co-factors	Rrp47	n	C1D	RNA/DNA binding protein
	Mpp6	n	MPP6	RNA binding protein
	Ski7	c	?	Bridges SKI and exosome complexes, putative GTPase

Table 1.1. Summary of Exosome components and associated proteins in yeast. Proteins are subcategorized into known complexes. Characterised human homologs are shown.'?' indicates that sequence homologs have not been identified or have not been confirmed. Location refers to subcellular localisation of proteins, either in the nucleus (n) and/or the cytoplasm (c).

break repair of DNA (Erdemir et al., 2002; Nehls et al., 1998; Yavuzer et al., 1998). Rrp47 was identified as an exosome-associated protein through pulldown experiments using Rrp44 and subsequent mass spectrometry (Mitchell et al., 2003). Both Rrp47 and C1D associate physically and functionally with the nuclear exosome component Rrp6 (PM-Scl-100 in humans) and the stability of Rrp47 expression is dependent on the physical interaction with Rrp6 (Feigenbutz et al., 2013b; Schilders et al., 2007; Stead et al., 2007). Loss-of function *rrp47* mutants exhibit RNA phenotypes similar to observations in *rrp6Δ* mutants suggesting a requirement for the processing of 5.8S rRNA, snoRNAs, snRNAs and the degradation of cryptic unstable transcripts (CUTS) (Arigo et al., 2006; Costello et al., 2011; Milligan et al., 2008; Mitchell et al., 2003). Yeast strains lacking Rrp47 are synthetic lethal with a loss of the exosome co-factor Mpp6 (Milligan et al., 2008) or the 3'-5' exonuclease Rex1 (Peng et al., 2003).

Rrp47 is a small basic protein with a molecular weight of 21kDa. With a lack of published structural information, secondary structure prediction analysis suggests that the first ~120 residues of the protein are to be generally α-helical in nature whereas the C-terminus is thought to be highly disordered and unstructured (Kelley and Sternberg, 2009). The N-terminus (residues 10-89) contains the bioinformatically-defined Sas10 domain found in the Sas10/C1D family of proteins (Pfam: PF04000) (Figure 1.6.A). This family includes the U3 ribonucleoprotein components Utp3 (also known as Sas10) and Lcp5 (Dragon et al., 2002; Wiederkehr et al., 1998), Rrp47 and its human homolog C1D (Mitchell et al., 2003) and the human initial factor 4e binding protein Neuroguidin (Jung et al., 2006). Functional studies of the Rrp47 protein reveal that residues 10-100, encompassing the Sas10/C1D domain, are critical for the protein function *in vivo* (Costello et al., 2011).

Rrp47 and Rrp6 interact physically through their N-terminal Sas10/C1D and PMC2NT domains respectively (Figure 1.6.B). This interaction is critical to the stability of Rrp47 *in vivo* as the loss of Rrp6 causes a strong decrease in expression levels of Rrp47 protein through proteasome degradation (Costello et al., 2011; Feigenbutz et al., 2013b; Stead et al., 2007). Recombinant Rrp47 can

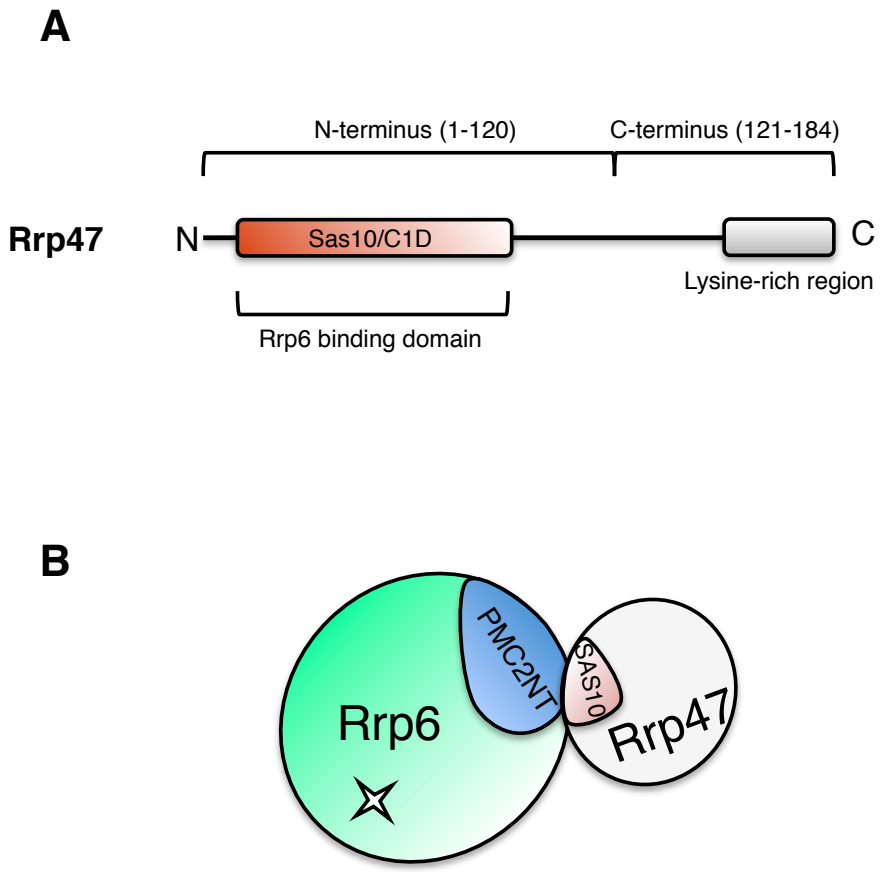

Figure 1.6. Domain architecture of Rrp47. (A) Schematic representation of Rrp47 domain architecture as defined by Pfam. Rrp47 contains an N-terminal Sas10/C1D domain (residues 10-89) and a conserved lysine rich region at the C-terminus (162-184). The N-terminus (1-120) is predicted to be α-helical where as the C-terminus (121-184) is predicted to be unstructured using bioinformatics tools. **(B)** Model schematic of Rrp47/Rrp6 interaction. The N-terminal Sas10/C1D domain of Rrp47 physical interacts with the N-terminal PMC2NT domain of Rrp6.

form homodimers *in vitro* and can form heterodimers with the N-terminus of Rrp6 ($Rrp6_{NT}$) in a 1:1 stoichiometry. Although Rrp47 and Rrp6 ultimately form a heterodimer in the nucleus *in vivo*, both proteins are independently imported into to the nucleus with Rrp6 transported via the importin complex (Feigenbutz et al., 2013b). These results suggest that Rrp47 is initially expressed as a homodimer in the cytoplasm and is dissociated following import to the nucleus to form the functional Rrp6/Rrp47 homodimer.

Rrp47 has been shown to bind nucleic acids *in vitro* with a preference for structured substrates (Stead et al., 2007). However, the protein does not possess any characterised RNA or DNA binding domains and therefore may possess a novel nucleic acid binding mechanism. It was initially thought that the highly basic lysine-rich C-terminus of Rrp47 provided an ideal region for RNA binding. Biochemical analysis revealed that RNA binding *in vitro* is dependent on both the C-terminal basic residues along with residues in the N-terminus (Costello et al., 2011).

The exact molecular function of Rrp47 is still to be elucidated entirely. Yeast strains lacking Rrp47 show defects in RNA processing and degradation pathways. These phenotypes closely resemble those seen in *rrp6* mutants such as the accumulation of pre-rRNA intermediates (including 5.8S+30, $27SA_2$, 23S and 35S rRNA species), a block in 3'-end Box C/D snoRNA maturation, the stabilisation of cryptic unstable transcripts (CUTs) and the accumulation of RNA surveillance targets including the 5'-external transcribed spacer region of 35S rDNA (5'ETS) (Costello et al., 2011; Garland et al., 2013; Milligan et al., 2008; Mitchell et al., 2003; Peng et al., 2003).

Taking together the RNA binding properties of Rrp47, the physical interaction between Rrp47 and Rrp6 and the similarities in RNA phenotypes upon the loss of either protein, it was suggested that Rrp47 might promote substrate binding to Rrp6 thus acting in RNA recruitment for Rrp6 dependent processing or degradation (Costello et al., 2011; Mitchell et al., 2003; Stead et al., 2007).

1.3.2 Mpp6 (M-phase phosophoprotein 6)

Yeast Mpp6 is a small, basic, exosome-associated RNA binding co-factor that shares many features with Rrp47. The human homolog, MPP6, was initially identified as a nuclear-specific protein in interphase cells that is subsequently targeted for MPF2-kinase-dependent phosphorylation during M-phase of the cell cycle (Matsumoto-Taniura et al., 1996). Both yeast Mpp6 and human MPP6 have been shown to co-purify with exosome complexes (Chen et al., 2001; Krogan et al., 2006; Milligan et al., 2008). MPP6 was found to be associated with exosome complexes that contained the Rrp6 homolog PM-Scl100 but lacked the Rrp44 homolog Dis3 (Chen et al., 2001).

Yeast Mpp6 was originally identified in a genetic screen for synthetic lethal interactions with the loss of Rrp47 or Air1, a zinc-knuckle protein component of the TRAMP complex (Milligan et al., 2008). Additionally, *mpp6Δ* alleles were shown to be synthetic lethal with a loss of Rrp6. This suggests that Mpp6 does not function redundantly with Rrp47 to promote substrate recognition for Rrp6-dependent processing or degradation. The Tollervey lab proposed the model that Mpp6 acts to target RNAs to the core-exosome for Rrp44-dependent exonuclease activity (Milligan et al., 2008). Mammalian MPP6 shows physical interactions with PM-Scl100 (Rrp6 in yeast) and hMtr4, a 3'-5' ATP-dependent helicase and part of the TRAMP complex (Schilders et al., 2007). Taken with the knowledge of the synthetic lethality between *mpp6Δ* and *air1Δ* alleles and the association of MPP6 with exosome complexes lacking Dis3 (Rrp44), an alternative model is that Mpp6 promotes functional coupling between Rrp6 and the TRAMP complex (Butler and Mitchell, 2011). A more recent study of the targeted degradation of aberrant mRNPs by Rrp6-dependent quality control pathways shows that Mpp6 is co-transcriptionally recruited along with Rrp47 and components of the TRAMP complex (Trf4/5 and Air2) to aberrant mRNPs (Stuparevic et al., 2013). Subsequent degradation of aberrant mRNPs is suggested to be generally dependent on Rrp6 catalytic activity and not Rrp44. Although no physical interaction between Mpp6 and Rrp6/Rrp47 has been

shown, it could be possible that Mpp6 recruits Rrp6 indirectly, possibly through the TRAMP complex.

Whilst Rrp47 shows a preference for binding of structured RNAs, Mpp6 was shown to bind unstructured pyrimidine-rich RNA sequences such as poly(U) RNA (Milligan et al., 2008; Schilders et al., 2007, 2005; Stead et al., 2007). Mpp6 contains no annotated RNA binding motifs and therefore represents a novel RNA binding protein. The physical association of Mpp6 to the exosome is independent of its ability to bind RNA as shown in tandem affinity purification experiments treated with RNaseA (Milligan et al., 2008). The C-terminus of Mpp6 is enriched with basic residues similar to the lysine-rich region of Rrp47. This could possible contribute to RNA binding through electrostatic attraction. However, in the case of Rrp47; both the basic C-terminus and the N-terminus were shown to contribute to RNA binding (Costello et al., 2011). There is no detailed structural data available for Mpp6. Primary sequence analysis reveals no presence of any annotated domain structures and secondary structure prediction software reveals inconclusive results yet suggests that the protein is highly disordered (Section 5.1, Kelley & Sternberg 2009). Sequence homology reveals two conserved motifs shared between Mpp6 homologs in model organisms (Milligan et al., 2008). These motifs will be discussed in further detail in Chapter 5.

The role of Mpp6 in RNA degradation has been poorly studied since its discovery. Whilst the physical and functional interactions between Rrp47 and Rrp6 have been thoroughly investigated (Costello et al., 2011; Feigenbutz et al., 2013a, 2013b; Stead et al., 2007), it is unknown how Mpp6 directly interacts with exosome complexes and how it stimulates targeted degradation of RNA surveillance substrates.

1.3.3. The TRAMP complex (Trf4/Air2/Mtr4 Polyadenylation complex)

TRAMP complexes are composed of a non-canonical poly(A) polymerase Trf4 or Trf5, a zinc-knuckle RNA-binding protein Air1 or Air2 and the putative RNA

helicase Mtr4. (Houseley and Tollervey, 2006; LaCava et al., 2005; Vanácová et al., 2005; Wyers et al., 2005). In a pathway completely distinct from the productive 3'-tail polyadenylation of mRNAs, the TRAMP complex functions to oligoadenylate ncRNA substrates for Rrp6 and core-exosome dependent processing and degradation. The TRAMP complex has been implicated in the 3'-end maturation of non-coding RNAs (snRNA and snoRNAs) and coding-RNAs (mRNAs). Additionally, TRAMP has been shown to be required for the turnover of functional mRNAs, aberrant ncRNAs and the rapid degradation of pervasive RNA PolII-generated cryptic unstable transcripts (Ciais et al., 2008; Grzechnik and Kufel, 2008; Vanácová et al., 2005; Wyers et al., 2005). Although a large number of TRAMP targets have been reported, it is still relatively unknown how the TRAMP complex is able to distinguish RNA substrates to target for constructive or destructive pathways involving the exosome.

1.3.4. Composition of TRAMP complexes

The TRAMP complex was originally identified through yeast two-hybrid analysis using Mtr4 as bait after previous studies identified the protein to be required for 3' end formation of 5.8S in yeast (de la Cruz et al., 1998; LaCava et al., 2005). Tandem affinity purification of interacting proteins revealed distinct complexes distinguished by the presence of Trf4 or Trf5 termed TRAMP4 and TRAMP5 respectively (Houseley and Tollervey, 2006; LaCava et al., 2005). The assembly of the TRAMP4 complex is dependent on bridging interactions with Air2. Mtr4 interacts with the N-terminus of Air2 and Trf4 is bound via a zinc-knuckle domain at the C-terminus of Air2 (Holub et al., 2012) (Figure 1.7). Although many crystal structures have been reported for the individual components of the TRAMP complex, a complete structure has yet to be solved (Hamill et al., 2010; Holub et al., 2012; Weir et al., 2010). Trf4 and Trf5 share 58% identity and double *trf4Δ trf5Δ* mutants are synthetic lethal (Castaño et al., 1996) Analogously, Air1 and Air2 are 45% identical and double *air1Δ air2Δ* mutants have a very strong growth defect (Inoue et al., 2000). Despite the obvious similarities between Trf4 and Trf5, TRAMP4 and TRAMP5 complexes have been reported to show different substrate

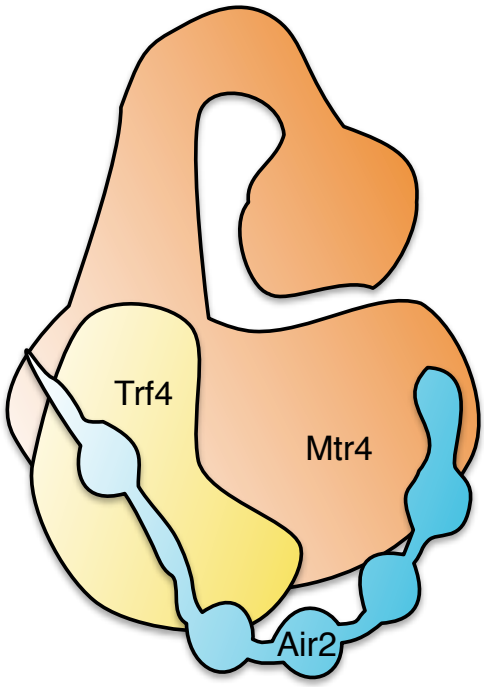

Figure 1.7. Structural composition of the TRAMP complex. Cartoon model of the arrangement of Air2/1, Trf4/5 and Mtr4 to form the TRAMP complex in yeast. Mtr4 interacts with the N-terminus of Air2 whereas Trf4 interacts with zinc-knuckles (ZnK) 4 and 5 at the C-terminus of Air2. The structure of Mtr4 is based on x-ray crystallography data (PDB = 2XGJ) whereas Trf4 and Air2 arrangements are based from a partial structure (PDB = 3NYB).

specificities (Houseley and Tollervey, 2006; Houseley et al., 2007; Roth et al., 2009). Likewise, the Air proteins have been shown to control the recognition of different classes of target substrates (Schmidt et al., 2012; Stuparevic et al., 2013).

1.3.4.1 Trf4/Trf5 (DNA topoisomerase I-related function 4/5)

Trf4, along with Trf5, was originally identified as a DNA polymerase in a genetic screen for mutations that are synthetic lethal with DNA topoisomerase 1

(Castaño et al., 1996). Further analysis reported that Trf4 and the *S. pombe* homolog Cid13 exhibit poly(A) polymerase activity *in vitro* and that Trf4 associates with poly(A) binding protein Pab1 (Ho et al., 2002; Saitoh et al., 2002; Vanácová et al., 2005). A link between Trf4 and the exosome was reported in studies showing that the activities of Rrp44, Rrp6 and Trf4 were required for the degradation of an aberrant pre-$tRNA_i^{Met}$ substrate (Kadaba et al., 2004).
Tandem affinity purification and mass spectrometry analysis revealed that Trf4 and Trf5 were the catalytic components part of a heterogenic polyadenylation protein complex comprised with Air1/2 and Mtr4 proteins. However, *in vitro* polyadenylation activity of Trf4 was only active with the addition of either Air1 or Air2 proteins suggesting a minimal active Trf4/5-Air1/2 complex (Vanácová et al., 2005). An independent report from the Tollervey lab identified the TRAMP complex initially through yeast-two hybrid analysis using Mtr4 as bait and more comprehensive analysis through tandem-affinity purification (LaCava et al., 2005). In contrast to related *S. pombe* and *C. elegans* cytoplasmic poly(A) polymerases (Cid13 and gld-2 respectively), Trf4 and Trf5 proteins were shown to be exclusively located in the nucleus (Huh et al., 2003; Kwak et al., 2004; Walowsky et al., 1999; Wang et al., 2000).

Trf4 and Trf5 proteins share 57% of identical sequence and 72% of similar sequences. The homology between the two proteins are suggested to have arisen due to the ancient whole genome-duplication event in *Saccharomyces cerevisiae* (Castaño et al., 1996; Kellis et al., 2004). Both Trf4 and Trf5 share characteristic

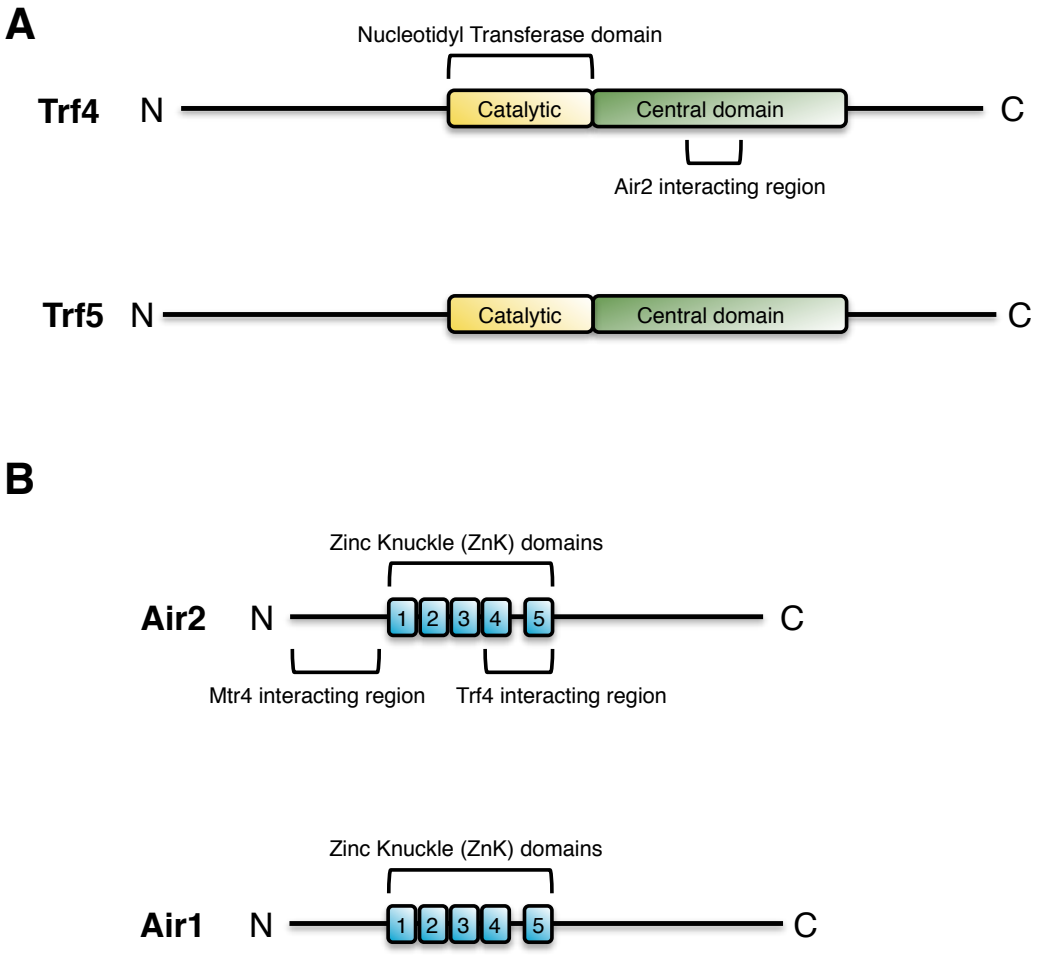

Figure 1.8. Domain architecture of Trf4/5 and Air2/1 proteins. (A) Trf4 and Trf5 share 57% identity. The N-terminal regions contain a Nucleotidyl Transferase domain (Residues 192-297 in Trf4 and 190-300 in Trf5) that provides poly(A) polymerase activity. The C-terminus contains a conserved Central domain which shares homology with Polβ family RNA Polymerases (297-481 in Trf4 and 300-484 in Trf5). The Air2 interacting region in Trf4 has been mapped to a conserved surface of the central domain. **(B)** Air2 and Air1 share 48% identity. Both proteins contain five Zinc Knuckle RNA binding domains (ZnK1 61-78, ZnK2 79-98, ZnK3 99-116, KnK4 121-143, ZnK5 162-179 in Air2). The N-terminal region of Air2 interacts with Mtr4 (residues 1-60). ZnK 4,5 and linker region are required for the interaction with Trf4 (121-179).

domain structure with canonical poly(A) polymerases such as Pap1, Cid13 and Gld-2. The N-terminal regions contain the catalytic domain bearing three highly conserved aspartate residues and a characteristic strand-loop motif. Additionally Trf proteins contain a Central domain that contains a short nucleotide recognition motif (Figure 1.8.A). In contrast to Pap1, Trf4 and Trf5 lack any characterised RNA-binding domains (Vanácová et al., 2005). The physical association with Air1/2 RNA binding proteins most likely contributes to RNA recognition. This model is corroborated by the observation that poly(A) polymerase activity of Trf4 *in vitro* requires the presence of Air1 or Air2 proteins (Vanácová et al., 2005; Wyers et al., 2005). A crystal structure of a Trf4/Air2 sub-complex lacking Mtr4 shows that the fourth and fifth zinc-knuckle domains of Air2 interact physically with a conserved surface in the central domain of Trf4 (Hamill et al., 2010). Although no structure exists for Trf4 complexes with Mtr4, it is presumed that the two proteins interact independently of the Air1/2 proteins as Trf4/5 co-precipitates Mtr4 in the absence of Air1 or Air2 (LaCava et al., 2005).

Polyadenylated RNA species, such as rRNAs, snRNAs, snoRNAs and CUTs, have been shown to increase in EXO9 and exosome-related mutants (Allmang et al., 1999a; Kuai et al., 2004; Mitchell et al., 2003; van Hoof et al., 2000a; Wyers et al., 2005). These species were subsequently shown to be polyadenylated by Trf4 and Trf5 but not by the canonical poly(A) polymerase Pap1 (Houseley and Tollervey, 2006; Wyers et al., 2005). It is proposed that Trf4 and Trf5 function to polyadenylate RNA substrates as part of the TRAMP complex to enhance processing or degradation pathways involving the nuclear exosome and Rrp6 (Egecioglu et al., 2006; LaCava et al., 2005; Vanácová et al., 2005; Wyers et al., 2005).

To distinguish from stable mRNA polyadenylation by Pap1, *in vitro* studies reported that Trf4/5 proteins add 10-50nt poly(A) tails to substrates in comparison to longer 60-80nt tails added by Pap1 (Egecioglu et al., 2006; Houseley and Tollervey, 2006; Kadaba et al., 2004; LaCava et al., 2005). However, more recent studies have shown that Mtr4 modulates poly(A) length to much shorter lengths of 4nt and complements a global analysis study on RNA surveillance targets in yeast

which reports poly(A) lengths of 3-5nt (Jia et al., 2011; Wlotzka et al., 2011). The general model for exosome activation due to polyadenylation by Trf4/5 is that the addition of unstructured poly(A) tails to RNA targets will make the transcripts more favourable to be recognised by the exosome. However, Trf4/5-dependent polyadenylation is not required for all substrates activated by TRAMP. This could be due to the helicase activity of Mtr4, which may unwind structured RNA to provide a more favourable substrate for exosome-dependent pathways. Nevertheless, a recent study has revealed that the polyadenylation activity of Trf4 can enable the helicase activity of Mtr4 to unwind substrates that otherwise could not be separated (Jia and Wang, 2012).
These findings fit a model of co-ordinated activity between Trf4/5 and Mtr4; Mtr4 modulates polyadenylation of substrates by Trf4 to ~4nt, Trf4-generated poly(A) tails aid in Mtr4-dependent unwinding and Trf4/Air1 directly stimulates the activity of Mtr4 (Jia and Wang, 2012; Jia et al., 2011).

TRAMP substrates fall into two categories of degradation targets and processing targets. The former group include hypermodified tRNAs, pre-rRNA processing intermediates, CUTs and aberrant RNAs (Allmang et al., 2000; Kadaba et al., 2006, 2004; Vanácová et al., 2005; Wyers et al., 2005). TRAMP dependent maturation targets include pre-rRNAs, snRNAs and snoRNAs (Allmang et al., 1999a; Houseley and Tollervey, 2006; Kuai et al., 2004). Trf4 and Trf5 dependent polyadenylation has been attributed to both processing and degradation pathways yet the mechanism to distinguish substrates is still relatively unknown. Microarray analysis of *trf4Δ* and *trf5Δ* showed little overlap in altered transcripts suggesting TRAMP4 and TRAMP5 complexes have distinct roles (San Paolo et al., 2009). It is more likely that the RNA binding proteins Air1 and Air2 confer substrate specificity. TRAMP4 complexes preferentially bind Air2 whilst TRAMP5 has only been shown to bind Air1 (Houseley and Tollervey, 2006; LaCava et al., 2005; Vanácová et al., 2005; Wyers et al., 2005). Air1 and Air2 proteins have recently been reported to show certain specificities and will be discussed below (Schmidt et al., 2012)

1.3.4.2 Air/Air2 (arginine methyl-transferase-interacting RING finger protein 1/2)

The Air1 and Air2 proteins are putative RNA binding proteins bearing five zinc-knuckle (ZnK) motifs (also known as RING finger motifs). As with *TRF4* and *TRF5* genes, the *AIR1* and *AIR2* alleles are thought to be an artefact of the whole genome duplication event in *S. cerevisiae* and share 45% identity (Inoue et al., 2000; Kellis et al., 2004). As part of the TRAMP polyadenylation complex, the Air1/2 proteins are suspected to be involved in substrate recognition to allow the complex to precisely polyadenylate and unwind targets for processing or degradation pathways. The mechanism by how TRAMP complexes distinguish substrates is still to be fully determined.

Both Air1 and Air2 contain five adjacent $C_{xx}C_{xxxx}H_{xxxx}C$ (CCHC) zinc knuckle (ZnK) domains that have been suggested to be involved in either RNA or protein binding (Figure 1.8.B). The domains are highly similar, sharing 67% identity and 80% similarity (Fasken et al., 2011; Inoue et al., 2000; LaCava et al., 2005; Vanácová et al., 2005). A crystal structure of Trf4 complexed with a fragment of Air2 revealed the zinc knuckles 4 and 5 (ZnK4 and ZnK5) interact with the central domain of Trf4 (Hamill et al., 2010). *In vivo* functional analysis of the ZnK domains in Air1 and Air2 revealed that ZnK4 and ZnK5 mutants exhibit TS growth phenotypes and are impaired in interactions with Trf4 (Fasken et al., 2011). This study also identified a highly conserved IWR*X*Y linker region between ZnK4 and ZnK5 that is critical for Trf4 interaction. *In vivo* northern blot analysis of Air1 ZnK4+5 and IWR*X*Y mutants revealed a strong accumulation of CUTs and pre-snoRNAs (Fasken et al., 2011). An independent analysis distinguished individual roles for the ZnK domains in Air2. ZnK4 was shown to have a key role in RNA binding and CUT recognition along with providing interactions with Trf4 whereas ZnK5 was shown to only be involved in Trf4 interaction (Holub et al., 2012).

The RNA binding properties of Air1 and Air2 were originally assumed due to the enhanced polyadenylation activity of recombinant Trf4 with the addition of Air2 (Hamill et al., 2010). *In vitro* binding assays reported that Air2 binds unstructured

RNA with a strong affinity whereas no binding to structured RNA substrates could be detected (Holub et al., 2012).

Due to a large degree of similarity, it was assumed that Air1 and Air2 were functionally redundant in TRAMP complexes. However further investigation revealed differential TRAMP complexes; TRAMP4 preferentially contains Air2 but has been shown to co-precipitate with Air1 whereas TRAMP5 only appears to contain Air1 (Houseley and Tollervey, 2006; LaCava et al., 2005; Vanácová et al., 2005; Wyers et al., 2005). The presence of different TRAMP complexes is most likely related to the multiple functions of the TRAMP complex in recognising different classes of substrates. Phenotypic analysis and RNA deep sequencing identified differential substrate specificities due to the presence of either Air protein (Schmidt et al., 2012). Air2 was shown to preferentially target polyadenylation of snoRNAs for subsequent degradation by Rrp6 and the exosome. It was also shown that Air2 plays a role in regulation of mRNAs involved in iron transport and carbon metabolism. Air1 was reported to be required for the stable copy number of the endogenous 2μ plasmid in concert with Rrp6 (Schmidt et al., 2012). Although non-redundant specific functions for each Air protein have been reported, the mechanisms behind this are yet to be understood.

1.3.4.3. Mtr4 (mRNA transport protein 4)

The putative 3'-5' RNA helicase, Mtr4 (also known as Dob1), was initially identified in a screen identifying mRNA transport mutants and later shown to be a co-factor to the nuclear exosome required for 5.8S rRNA maturation (Kadowaki et al. 1994; de la Cruz et al. 1998; van Hoof et al. 2000). Mtr4 was identified as part of the TRAMP complex through yeast-two hybrid interactions and mass spectrometry analysis of co-IPs (LaCava et al., 2005; Vanácová et al., 2005; Wyers et al., 2005). In addition to its association with TRAMP complexes, Mtr4 can function independently of TRAMP, a feature that is supported by an excess of cellular Mtr4 in comparison to other TRAMP components (Ghaemmaghami et al., 2003; LaCava et al., 2005; van Hoof et al., 2000a). Mtr4 is a member of the DE_XD/H-box

ATPase family of helicase proteins along with Ski2 that shares sequence identity (Anderson and Parker, 1998). Additionally, Mtr4 has been shown to be essential for growth in yeast (Liang et al., 1996). It has been reported that Mtr4 functions as an exosome co-factor in the processing of structured RNAs such as 5.8S rRNA (de la Cruz et al., 1998; Kadaba et al., 2004; LaCava et al., 2005; van Hoof et al., 2000a) and also functions with the TRAMP complex in processing and degradation of a wide range of substrates in concert with the exosome and Rrp6. The helicase activity of Mtr4 is thought to be required to unwind structured substrates to aid in recognition by the exosome and is stimulated by the polyadenylation activity of Trf4/5-Air1/2 complexes (Houseley and Tollervey, 2006; LaCava et al., 2005; Lebreton and Séraphin, 2008; Vanácová et al., 2005; Wyers et al., 2005).

Mtr4 shares 38% sequence identity with Ski2, another member of the DE_XH helicase family. However, the 110kDa Mtr4 is considerably larger than other helicases from this family (de la Cruz et al., 1998). Mtr4 comprises two canonical RecA domains (RecA1 and RecA2) that form the helicase core, a winged-helix (WH) domain and a C-terminal Helical bundle (Figure 1.9.A) (Jackson et al., 2010; Weir et al., 2010). The protein also features a large arched KOW domain inserted between the WH domain that shows structural similarities to a motif found in a variety of ribosomal proteins and a bacterial transcription factor NusG (Kyrpides et al., 1996). The KOW domain forms an arm and fist-like structure that is not found in related DE_XH helicases (Figure 1.9.B) (Jackson et al., 2010; Weir et al., 2010). Removal of the KOW arch domain results in slow-growth phenotypes, 5.8S processing defects similar to *rrp6Δ* mutants, reduces RNA binding and is unable to efficiently activate the exosome *in vitro* to process hypermodified $tRNA_i^{Met}$ (Holub et al., 2012; Jackson et al., 2010; Weir et al., 2010). Although individual crystal structures of Mtr4 have been solved, these have been independent of association with TRAMP components. However, mutational analysis revealed that the N-terminus of Air2 is required for the interaction with Mtr4 and was not required for the Trf4-Air2 interaction (Holub et al., 2012).

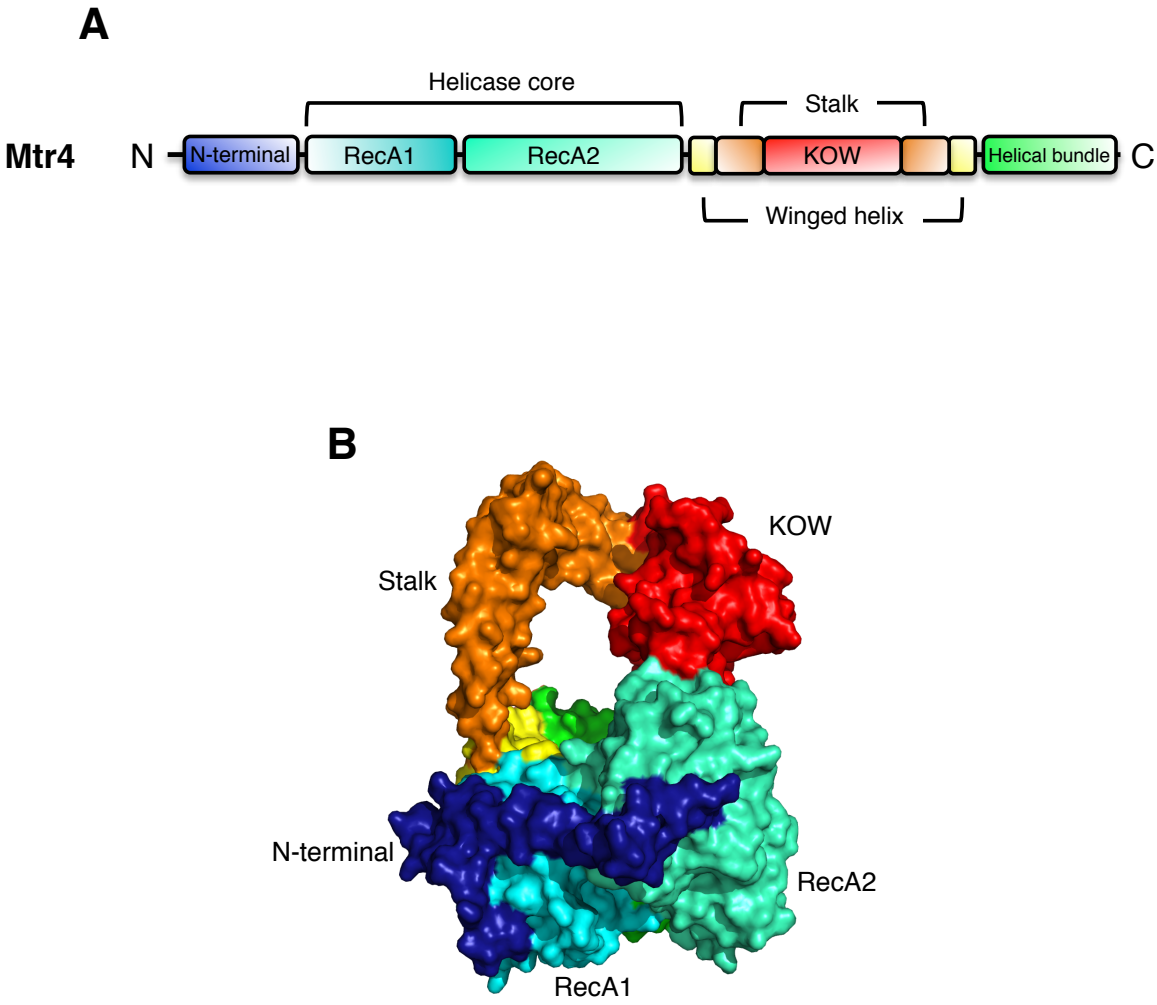

Figure 1.9. Domain architecture and structure of Mtr4. (A) Mtr4 contains a N-terminal domain (residues 80-143), two RecA domains (RecA1 150-320, RecA2 326-575), a Winged helix (WH) structure (575-615 and 876-900) separated by a stalk/KOW insertion domain (615-876) and a C-terminal Helical bundle domain (912-1073). The RecA2, WH2 and helical bundle domains are required for interaction with the Trf4/Air2 heterodimer (Holub et al. 2012). **(B)** X-ray crystal structure of Mtr4 from Weir *et al* (2010). Image was generated using PyMol and coloured by domain to match **A** (PDB = 2XGJ). The Stalk/KOW domains form a characteristic protruding structural unit from the central helicase core.

The function of the helicase activity of Mtr4 is presumed to unwind structured RNA and/or displace any associated protein complexes in order to present the exosome with a more favourable substrate (Houseley and Tollervey, 2009; Lebreton and Séraphin, 2008). Additionally, it has been proposed the hydrolysis of ATP by Mtr4 may be used to feed RNA substrates through the exosome core channel in a comparable mechanism to proteasome-associated ATPases (Makino et al., 2013b; Smith et al., 2007; van Hoof and Parker, 1999). Mutations in the helicase domain have been shown to result in the accumulation of pre-5.8S rRNA, 5'ETS and hypermodified $tRNA_i^{Met}$ substrates; all of which are processed or degraded by
the exosome and Rrp6. These mutations did not affect TRAMP stability of polyadenylation activity therefore suggesting that Mtr4 acts independently of Trf4-dependent polyadenylation (Allmang et al., 1999a; de la Cruz et al., 1998; Holub et al., 2012; Jackson et al., 2010). *In vitro* analysis has shown that Mtr4 can unwind RNA substrates with a high degree of secondary structure (Vanácová et al., 2005). As mentioned above, Mtr4 has been shown to modulate the nucleotide length of Trf4-generated poly(A) tails to 3-5 nt (Jia et al., 2011). These results suggest a mechanism by which Mtr4 regulates the polyadenylation of RNA targets by Trf4. Short poly(A) tails enhance the unwinding by Mtr4 to provide an accessible substrate for exosome activity. The unwinding activity may also serve to disassemble any RNP complexes associated with the transcript.

1.3.5 TRAMP-dependent targeting to the nuclear exosome

The TRAMP complex acts as a layer of control for RNA processing and degradation by the nuclear exosome. The ability to recognise and target specific substrates for differential pathways is a critical role needed to govern the exonuclease activity of Rrp44 and Rrp6. The TRAMP complex is proposed to function to recognise, polyadenylate and unwind RNA transcripts to provide a favourable substrate for the exosome and Rrp6. However, the mechanism by which TRAMP is able to distinguish substrates for productive or destructive processing is still poorly understood. The ability to modulate recognition may be

attributed to properties of components within the complex or due to the association with various co-factors. One proposed candidate is the exosome-associated RNA binding protein Mpp6 (Butler and Mitchell, 2011). In humans MPP6 physically associates with Rrp6 and Mtr4 homologs (PM-Scl100 and hMtr4 respectively) (Schilders et al., 2007). Additionally, *mpp6Δ* mutations are synthetic lethal with *air1Δ*, *rrp47Δ* and *rrp6Δ* suggesting a possible redundant coupling between Rrp6 and TRAMP complexes (Butler and Mitchell, 2011; Milligan et al., 2008).

1.3.6 The NNS (Nrd1/Nab3/Sen1) complex

The NNS complex, comprised of RNA binding proteins Nrd1, Nab3 and the putative nucleic acid helicase Sen1, plays an essential role in RNA quality control pathways through transcriptional termination and recruitment of RNA surveillance factors (Steinmetz et al., 2001). The NNS complex is involved in the transcriptional termination of RNA PolII transcripts coupled to TRAMP activity for the maturation of snRNAs, snoRNAs and some mRNAs (Carroll KL, Pradhan DA, Granek JA, Clarke ND, 2004; Ciais et al., 2008; Grzechnik and Kufel, 2008; Steinmetz et al., 2001). Additionally, NNS and TRAMP activity terminate and degrade cryptic unstable transcripts derived from pervasive intergenic transcription (Arigo et al., 2006; Thiebaut et al., 2006)

Nrd1 (Nuclear pre-mRNA Down-regulation protein 1) is an essential protein of 63kDa that features an N-terminal domain that allows interaction with the C-terminus of the large subunit of RNA PolII (CID, CTD interacting domain), an RNA recognition motif and a Nab3-interacting region (Figure 1.10.A) (Conrad et al., 2000; Vasiljeva et al., 2008a). The CTD of RNA PolII contains tandem heptameric repeats (TSPTSPS) that associate with various co/post-transcriptional factors. Differential binding to the CTD is modulated by phosphorylation at serine residues 2, 5 and 7 (TSPTSPS). *In vitro* analysis has shown that Nrd1 preferentially binds Ser5 phosphorylated CTD domain of RNA PolII whereas *in vivo* analysis shows

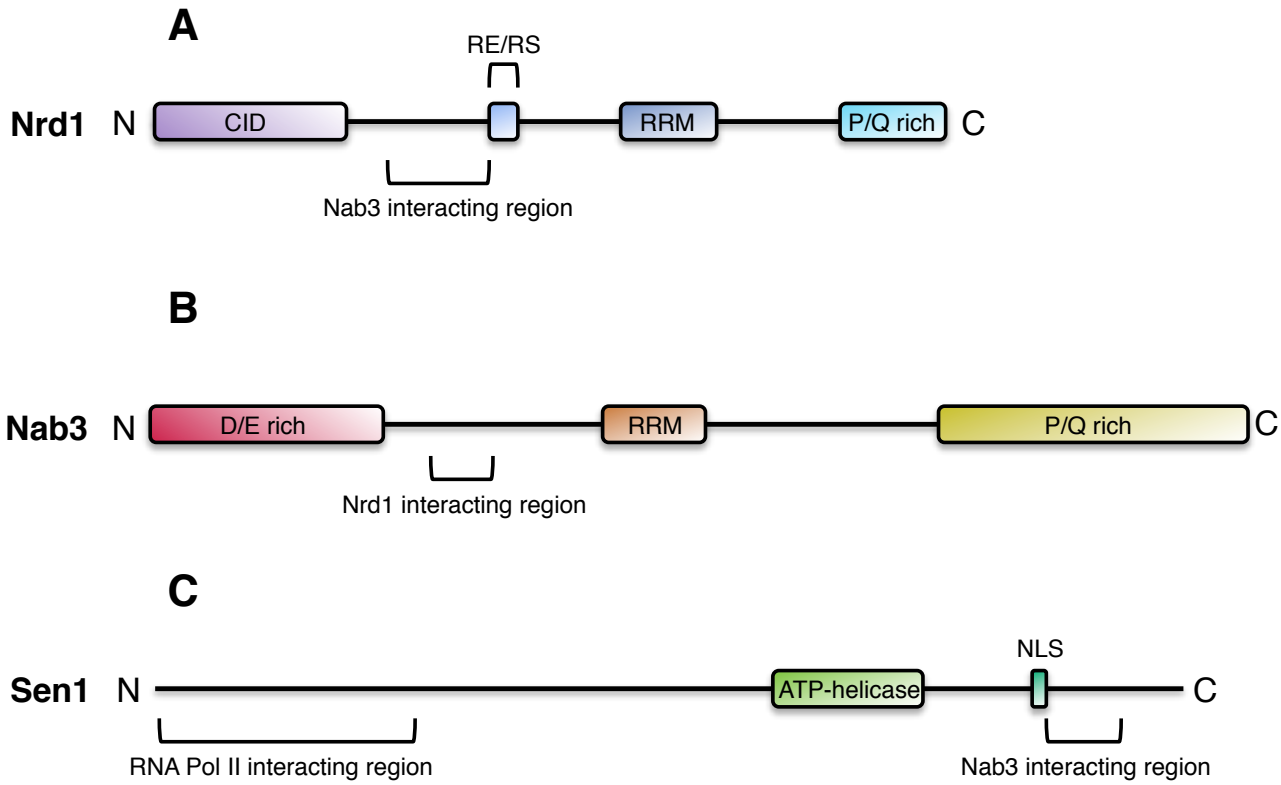

Figure 1.10. Domain architecture of Nrd1, Nab3 and Sen1. (A) Nrd1 contains an N-terminal RNA PolII CTD binding (CID) domain (residues 1-140), a RE/RS (argenine-glutamate/argenine-serine) rich region (245-265), a RNA binding motif (RRM) (340-410) and a P/Q (proline/glutamine)-rich region (500-575). The Nab3 interacting region is mapped to between residues 169 and 244. **(B)** Nab3 contains an N-terminal D/E (Aspartate/Glutamate)-rich region (residues 1-194), a RNA binding motif (RRM) (329-404) and a P/Q (Proline/Glutamine)-rich region (575-802). The Nrd1 interaction region is mapped to between residues 204 and 248. **(C)** Sen1 contains a Type I ATP-dependent DNA/RNA Helicase domain (residues 1327-1656)

Nrd1 to co-localise with the Ser7 phosphorylated form (Buratowski, 2009; Kim et al., 2010; Vasiljeva et al., 2008a).

The N-terminus of Nrd1, downstream of the CID, interacts physically with a second RNA binding protein, Nab3 (Nuclear polyadenylated RNA-binding protein 3), a 90kDa RNA binding protein shown to be essential in yeast (Conrad et al., 2000). Nab3 contains a C-terminal domain rich in acidic residues (D/E-rich), a central RNA recognition motif and an essential Proline/Glutamine-rich C-terminus with no characterised function (Figure 1.10.B) (Carroll et al., 2007; Conrad et al., 2000). The RNA-recognition motifs (RRMs) of Nrd1 and Nab3 have been reported to recognise GUAA/G and UCUU motifs as binding sites respectively (Carroll KL, Pradhan DA, Granek JA, Clarke ND, 2004; Hobor et al., 2011; Lunde et al., 2011).

The essential and highly conserved Type I 5'-3' ATP-dependent DNA/RNA helicase Sen1 (Splicing endonuclease protein 1) interacts with the Nrd1/Nab3 heterodimer through physical association with Nab3 but shows no direct interaction with Nrd1 (Nedea et al., 2008; Ursic et al., 2004; Winey and Culbertson, 1988). Although Sen1 is essential in yeast, *sen1* mutants bearing N-terminal deletions are viable with slow growth phenotypes. The N-terminus of Sen1 is involved in interactions with the CTD of RNA PolII whilst the C-terminal region contains the essential helicase domain (Figure 1.10.C) (Nedea et al., 2008; Ursic et al., 2004).

In yeast, the NNS complex is involved in productive pathways to generate mature snRNA and snoRNA transcripts and in destructive surveillance pathways to degrade pervasive intergenic-transcribed CUTs (Arigo et al., 2006; Grzechnik and Kufel, 2008; Kim et al., 2006; Steinmetz et al., 2001; Thiebaut et al., 2006). The RRM domains of Nrd1 and Nab3 have been reported to recognise specific RNA motifs in the 3'UTR regions of PolII transcripts (GUAA/G and UCUU respectively). These sequences are commonly found downstream of snRNA and snoRNA genes (Carroll KL, Pradhan DA, Granek JA, Clarke ND, 2004; Steinmetz and Brow, 1996, 1998). Binding of Nrd1/Nab3 has been suggested to stimulate the recruitment of the TRAMP complex and the exosome. Transcriptional termination

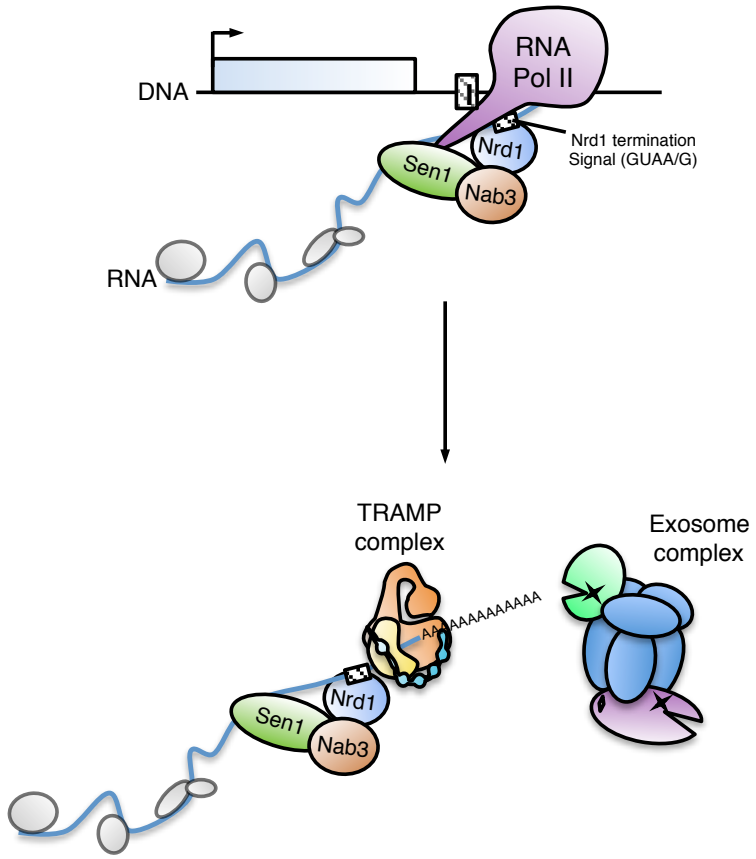

Figure 1.11. Nrd1-dependent termination of Pol II transcripts. Model of transcriptional termination of RNA Pol II transcripts (snRNAs, snoRNAs, CUTs) by the NNS complex. Nrd1 and Sen1 interact with Ser5 phosphorylated CTD of RNA Pol II. The RRM domains of Nrd1 and Nab3 bind specific RNA motifs that trigger transcriptional termination. The NNS complex recruits the TRAMP and exosome complexes for subsequence 3'-end processing by multiple rounds of polyadenylation and exonucleolytic trimming. This generates mature RNPs in the case of snRNAs and snoRNAs or complete degradation in the case of CUTs.

by the NNS is followed by polyadenylation and subsequent 3' end processing by the nuclear exosome (Figure 1.11) (LaCava et al., 2005; Perumal and Reddy, 2002; Vanácová et al., 2005; Vasiljeva and Buratowski, 2006; Wyers et al., 2005). Mutations in Nrd1, TRAMP and exosome components lead to an observable accumulation of 3' extended snRNAs and snoRNAs. In *rrp6Δ* mutants, two populations of 3' extended heterogeneous snR13, U14 and snR50 snoRNAs are observed to accumulate (Allmang et al., 1999a; Mitchell et al., 2003; van Hoof et al., 2000a; Vasiljeva and Buratowski, 2006). Subsequent analysis revealed that termination of snoRNAs is carried out by two complexes and in two distinct regions; a proximal NNS-dependent termination region (site I) and a distal "failsafe" mRNA 3' processing region (siteII) (Grzechnik and Kufel, 2008; Steinmetz and Brow, 2003). Both termination events are coupled to polyadenylation which leads to subsequent processing by the nuclear exosome and Rrp6 in the case of NNS-dependent termination, or degradation by the exosome and surveillance factors in the case of "failsafe" termination (Grzechnik and Kufel, 2008).

The discovery of pervasive transcription of intergenic regions has encouraged intense investigation into the nature of unstable-ncRNAs including cryptic unstable transcripts (CUTs). Originally identified in *rrp6Δ* strains, CUTs are rapidly degraded by the exosome in wildtype cells (Gudipati et al., 2012a; Schneider et al., 2012; Wyers et al., 2005). Like snoRNAs, CUTs are transcribed by RNA Pol II, have a defined 5' end and heterogeneous Trf4-dependent polyadenylated 3' ends. In the absence of Trf4, populations of non-polyadenylated CUTs are accumulated (Wyers et al., 2005). Transcriptional termination of CUTs is also dependent on the NNS complex in yeast (Arigo et al., 2006; Thiebaut et al., 2006). Many CUTs have been reported to contain Nrd1/Nab3 recognition motifs that recruit the NNS complex to trigger transcriptional termination. The NNS also stimulates the recruitment of the TRAMP complex and the exosome for subsequent Trf4-dependent polyadenylation and rapid degradation by Rrp44 and Rrp6 (Arigo et al., 2006; Thiebaut et al., 2006; Wyers et al., 2005). The well-characterised CUT, *NEL025c*, was shown to exist in two forms in exosome mutants. Shorter, heterogeneous transcripts were shown to be polyadenylated by Trf4 ($NEL025_S$) and a longer species were dependent on Pap1 polyadenylation ($NEL025c_L$)

(Thiebaut et al., 2006; Wyers et al., 2005). As with snoRNAs, these two species are due to termination events at either a proximal NNS-dependent region (site I) or a distal mRNA cleavage/polyadenylation site II. Depletion of Nrd1 in *rrp6Δ* mutants leads to a decrease in site I *NEL025c*$_S$ and subsequent increase in longer read-through transcripts terminating at site II (Thiebaut et al., 2006).

The NNS complex has been well characterised as part of RNA surveillance pathways in yeast as a level of quality control. With physical and functional connections to the TRAMP complex and the nuclear exosome, the action of the NNS can generate stable snRNA and snoRNA transcripts. Additionally, the NNS is well characterised in its role of termination of pervasive transcription and stimulation of rapid degradation by the exosome and Rrp6.

1.3.7. Rex1 (RNA exonuclease 1)

The 3'-5' exonuclease activity of the nuclear exosome is attributed to the exonuclease domain of Rrp44 and/or the exosome-associated Rrp6 (Allmang et al., 1999b; Mitchell et al., 1997). Rex1 (also known as Rnh70 and Rna82) is a member of the DEDDh superfamily of exoribonucleases along with Rrp6 (Ozanick et al., 2009; Zuo and Deutscher, 2001). Although Rex1 is localised to the nucleus, no physical association with the exosome complexes has been reported (Frank et al., 1999). Yeast *rex1Δ* strains accumulate 5S rRNA extended by ~3nt and show defects in processing of tRNAs (Ozanick et al., 2009; van Hoof et al., 2000b). Rex1 was initially characterised along with related 3' exonucleases Rex2 and Rex3 (van Hoof et al., 2000b). It was reported that Rex1 and Rex2 function redundantly in the 3' processing of 5.8S rRNA. Single mutants were shown to have no effect on 5.8S pre-cursors yet a *rex1Δ rex2Δ* double mutant showed an accumulation of 6S pre-rRNA species as initially reported in exosome mutants (Mitchell et al., 1996; van Hoof et al., 2000b). Yeast strains bearing *rex1Δ* alleles are synthetic lethal with *rrp6Δ* and *rrp47Δ* alleles (Costello et al., 2011; Peng et al., 2003; van Hoof et al., 2000b). Both *rrp6Δ* and *rex1Δ* strains show defects in 3'-end

processing of stable RNAs and the synthetic lethality genetic interaction may suggest redundancy in RNA substrate maturation.

1.4 Functional redundancy and synthetic lethal interactions

Functional redundancy is common within many biological systems and acts as a failsafe layer of 'genetic buffering' to protect the cell against the failure of one component or pathway(Kafri et al., 2009). The loss of function of two proteins independently may have little or no effect on the cell whereas the simultaneous loss of function may have a more dramatic and possible lethal impact. It has been widely documented that mutations in many exosome or exosome-related components result in similar phenotypes (Allmang et al., 1999a; LaCava et al., 2005; Milligan et al., 2008; Mitchell et al., 2003; van Hoof et al., 2000a; Vasiljeva and Buratowski, 2006). Corroborating this, recent transcriptome-wide analyses revealed a large degree of substrate overlap for the catalytic activities of both Rrp44 and Rrp6 as part of the nuclear exosome (Gudipati et al., 2012b; Schneider et al., 2012). Genetic redundancy is likely mirrored in synthetic lethal interactions. The functional overlap between Rrp44 and Rrp6 is supported by the synthetic lethality observed in *rrp6Δ rrp44*$^{exo-}$ mutants (Lebreton et al., 2008).

The exosome associated co-factor Rrp47 has been shown to interact directly with Rrp6 and function to promote Rrp6-dependent processes (Costello et al., 2011; Feigenbutz et al., 2013b; Mitchell et al., 2003; Stead et al., 2007). A second cofactor, Mpp6 is still relatively uncharacterised in terms of physical and functional interactions. It has been proposed that Rrp6-dependent processes are functionally redundant with Mpp6-related activities. This is supported by synthetic lethality observed in *rrp6Δ mpp6Δ* and *rrp47Δ mpp6Δ* mutants. It was therefore proposed that Mpp6 functions to stimulate the catalytic activity of Rrp44 (Milligan et al., 2008). An alternative model is that Mpp6 promotes the functional couple between Rrp6 and the TRAMP complex. This is supported by the synthetic lethality in *mpp6Δ air1Δ* mutants and physical interactions reported between human MPP6, PM-Scl100 and hMtr4 (Mpp6, Rrp6 and Mtr4 in yeast) (Milligan et

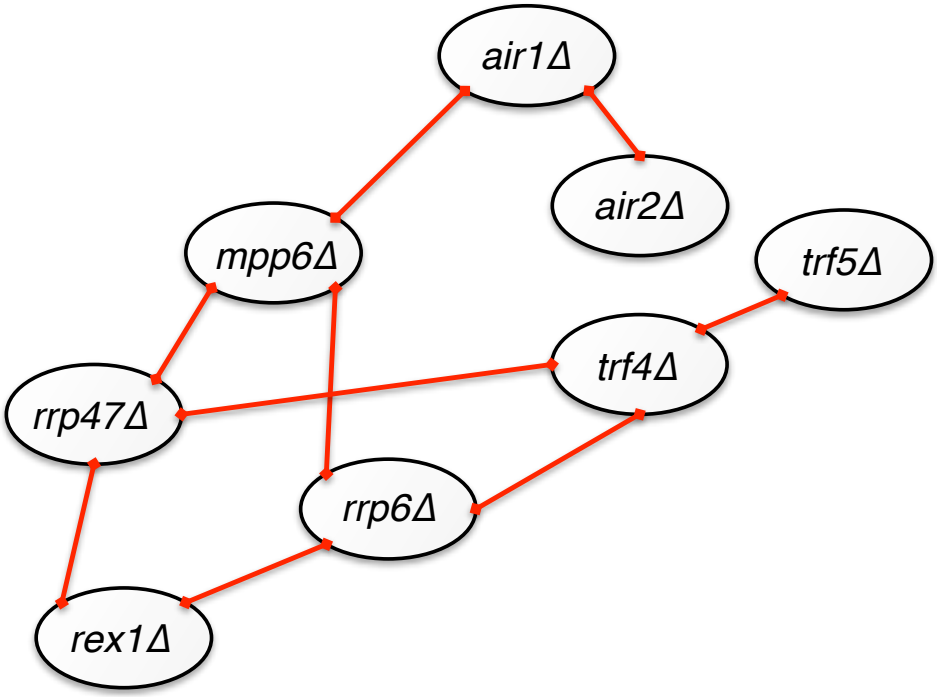

Figure 1.12. Synthetic lethal interactions between non-essential exosome co-factors. Generated from reported genetic interactions between null alleles. Data was obtained from BioGRID (http://thebiogrid.org/) or from observations during this study. Red connectors between two null alleles signifies that the double null mutant is synthetic lethal.

al., 2008; Schilders et al., 2007). A summary of synthetic lethal genetic interactions between exosome-related components is depicted in Figure 1.12.

1.5. Aims of this study

As described above, the eukaryotic exosome functions in a wide array of essential biological processes including RNA processing and RNA surveillance. It is still unclear how the complex is able to distinguish between transcripts from all characterised classes of RNA and discriminate between downstream productive or destructive processes. It is widely known that the exosome recruits a number of co-factors and additional complexes to distinguish the outcome of RNA substrates. Whilst the identification of these auxiliary factors has been widely documented, it is still generally unknown how exosome associate co-factors control the function of the exosome. This study aims to investigate the role of these additional proteins in RNA surveillance and processing pathways involving the nuclear exosome and the relationship between their individual functions.

The main aim of this work address the function of three proteins, Rrp6, Rrp47 and Mpp6. The relationship between Rrp6 and Rrp47 is investigated in Chapter 3 and 4. These proteins interact physically and functionally in RNA degradation processes and the stability of either protein is sensitive to this connection. These analyses look at the effects of separating the Rrp6/Rrp47 complex *in vivo* using a novel method and addressing the individual functions of either protein.

Mpp6 has been reported to associate with the nuclear exosome complex and is involved in RNA surveillance activities. However, little is known about the protein itself. Chapter 5 attempts to identify and characterise the functional regions of the Mpp6 protein through mutational analysis.

Finally, work throughout this study aims to address the redundant functions of these co-factors and provide insight into synthetic lethal interactions found in combined mutants.

Chapter 2: Materials and Methods

2.1 Materials

2.1.1. Reagents and enzymes

All general reagents used throughout this study were of molecular biology grade and purchased from Melford (Melford Laboratories Ltd., Ipswich, UK), Sigma (Sigma-Aldrich Co., St Louis, MO, USA), Fisher (Thermo Fisher Scientific., Waltham, MA, USA), VWR (VWR International LLC., Radnor, PA, USA) and Geneflow (Geneflow Ltd., Lichfield, Staffordshire, UK) as stated in the text. Water for stock solutions, buffers, media and other general uses was filtered through a Milli-Q 4 Bowl reagent grade water system (Millipore., Billerica, MA, USA). Enzymes were purchased from NEB (New England Biolabs., MA, USA), Fermentas (Fermentas International Inc., Canada), Promega (Promega Inc., Madison, WI, USA) and Roche (Roche Diagnostics Ltd., Surrey, UK) unless otherwise stated in the text.

2.1.2. Bacterial strains

E. coli strains XL1-Blue, DH5α (Stratagene., La Jolla, California, USA) and KC8 (Clontech., Mountain View, California, USA) were used for molecular cloning, plasmid recovery and amplification. For expression of recombinant proteins the *E. coli* strain BL21 (DE3) pLysS (Stratagene) was used. Genotypes of aforementioned strains are stated in Table 2.1

2.1.3. Bacterial growth

Bacterial strains were grown at 37°C unless otherwise stated. Liquid cultures were incubated in appropriate selective media (see Table 2.2) with sufficient aeration. All glassware and media were sterilised by autoclaving at 126°C, 121 psi for 20 minutes. Non-autoclavable components, such as IPTG, were sterilised by filtration

through 0.2 μm Minisart filters (Sartorius Stedim Biotech., Goettingen, Germany). Bacterial stocks were stored in 15% glycerol at -80°C.

2.1.4. Yeast strains

Unless otherwise stated, *S. cerevisiae* was the sole yeast used in this study. A list of background strains used in this study is described in Table 2.5

2.1.5. Yeast growth

Yeast strains were grown in appropriate media (see Table 2.2) at 30°C unless otherwise stated. Liquid cultures were incubated in sterilised glassware with sufficient aeration. Strains were stored on solid media plates or slants at 4°C for short-term storage or in 25% glycerol at -80°C for long-term storage.

Table 2.1. *E. coli* strains used during this study.

Strain	Genotype	Source
XL1-Blue	*RecA1 endA1 gyrA96 thi-1 hsdR17 supE44 relA1 lac* [F' *proAB lacI*^{q}*ZΔM15* Tn*10 (Tet*^{r}*)*]	Stratagene
DH5α	*fhuA2 Δ(argF-lacZ)U169 phoA glnV44 Φ80 Δ(lacZ) M15 gyrA96 recA1 relA1 endA1 thi-1 hsdR17*	Stratagene
KC8	*hsdR leu*B600 *trp*C9830 *pyr::*Tn5 *his*B463 *lac*DeltaX74 *str*A *gal*U *gal*K	Clontech
BL21 (DE3) pLysS	*F– dcm ompT hsdS(rb*$^-$*mb*$^-$*) gal λ(DE3) [pLysS Camr]*	Stratagene

Table 2.2. Media recipes used during this study.

Percentages given indicate weight per volume (w/v). For solid media, 2% Bacto-agar (BD., Becton Dickinson and Company, Sparks, MD, USA) was added prior to

autoclaving. Antibiotics/drugs were supplemented as necessary according to Table 2.4.

LB (Lysogeny Broth)	1% Tryptone (Melford), 0.5% Yeast Extract (Melford), 1% NaCl (Fisher).
M9 Minimal Media	1 X M9 Salts (3.4 mM Na_2HPO_4, 2.2 mM KH_2PO_4, 0.85 mM NaCl, 0.95 mM NH_4Cl). Amino acids and bases were supplemented as required from 100 X stocks, described in Table 2.3, prior to autoclaving. To cooled media 2 mM $MgSO_4$, 0.4% v/v Glucose and 100 μm $CaCl_2$ were added.
YPD	2% Peptone, 1% Yeast Extract, 2% Glucose
YPGal	2% Peptone, 1% Yeast Extract, 2% Galactose
Yeast Minimal Media	0.17% Yeast Nitrogen Base without amino acids (Melford), 0.5% Ammonium Sulphate, 2% Glucose. Amino acids and bases were supplemented as required from 100 X stocks prior to autoclaving (Table 2.3).
5'FOA Minimal Media	0.17% Yeast Nitrogen Base without amino acids, 0.5% Ammonium Sulphate, 2% Glucose. All amino acids and bases were supplemented from 100 X stocks. 5'-Fluoroortic Acid (Melford) was filter-sterilised to a final concentration of 1 mg/ml into cooled media after autoclaving.

Table 2.3. Weights of L-Amino Acids and Bases used to generate 100 X stocks.

100 X stock solutions were made up individually from solid reagents (Sigma) and stored at -20°C. Adenine and Tyrosine (*) required the addition of 20 mM and 30 mM NaOH respectively to neutralise pH.

Amino Acid/Base	Abbreviation	Mass per litre (g)
Adenosine hemisulphate*	Ade	2
Argenine monohydrochloride	Arg	2

Histidine monohydrochloride	His	2
Leucine	Leu	6
Lysine monohydrochloride	Lys	3
Methionine	Met	2
Phenyalanine	Phe	5
Threonine	Thr	20
Tryptophan	Trp	2
Tyrosine*	Tyr	3
Uracil	Ura	2

Table 2.4. Antibiotic/drug concentrations used in this study.

Antibiotic	Abbreviation	Source	Stock	Preparation	Final Concentration
Ampicillin Sodium Salt	Amp	Melford	1000 X	4 g in 50 ml ethanol	80 μg/ml
Chloramphenicol	Chl	Sigma	1000 X	250 mg in 10 ml ethanol	25 μg/ml
Kanamycin A Monosulphate (from *S. kanamyceticus)*	Kan	Sigma	1000 X	2.5 g in 50 ml sterile water	50 μg/ml
G418 Disulphate Salt (Geneticin)	Kan	Sigma	50 X	100 mg in 10 ml sterile water	200 μg/ml
Hygromycin B (from *S. hygroscopicus)*	Hyg	Sigma	50 X	100 mg in 10 ml sterile water	200 μg/ml
5'-Fluoroorotic Acid	5'FOA	Melford	50 X	100 mg in 1 ml DMSO	2 mg/ml

Table 2.5. *S. cerevisiae* strain backgrounds used in this study.

Strain	Genotype	Source
BMA38	*Mata/Matα ade2-1/ade2-1 his3-Δ200/his3-Δ200 leu2-3,112/leu2-3,112 trp1-1/trp1-1 ura3-1/ura3-1 can1-100/can1-100*	Laboratory stock (Baudin et al., 1993)
BY4741	*Mata his3Δ1 leu2Δ0 met15Δ0 ura3Δ0*	Euroscarf (University of Frankfurt, Germany) (Brachmann et al., 1998)
W303	*Mata/Matα ade2-1/ade2-1 his3-11,15/his3-11,15 leu2-3,112/leu2-3,112 trp1-1/trp1-1 ura3-1/ura3-1 can1-100 can1-100*	Laboratory stock (Rothstein, 1983)
158	*Mata ade2-1 his3-Δ200 leu2-3,112 trp1-1 ura3-1 can1-100 rrp6Δ::TRP1*	Laboratory stock
RS453	*Mata/Matα ade2-1/ade2-1 his3-11/his3-11 leu2-3/leu2-3 trp1-1/trp1-1 ura3-52/ura3-52 can1-100/can1-100*	Laboratory stock (Thomas and Rothstein, 1989)
575	*Mat1 ade2-1 his3-Δ200 leu2-3,112 trp1-1 ura3-1 can1-100*	Laboratory stock
SC0000	*Mata ade2 arg4 leu2-3,112 trp1-189 ura3-52*	Euroscarf (University of Frankfurt, Germany) (Gavin et al., 2006)

2.1.6. Media

Media background recipes are given in Table 2.2.

2.1.6.1. Bacterial Media

Sterilised antibiotics were used to select for bacterial strains expressing plasmids harboring the respective antibiotic resistant gene. Stocks were prepared at 1000 X concentrations by mixing the appropriate amount of antibiotic (shown in Table 2.4) in 50% v/v ethanol or dissolved in sterile MP H_2O before storage at -20°C. Antibiotics were added to sterile media following autoclaving after sufficient cooling.

2.1.6.2. Yeast Media

Amino acid dropout yeast minimal media (YMM) was used to select for strains harboring plasmid constructs containing selectable markers. A full list of amino acid supplements is described in Table 2.3
Minimal Raffinose- or Galactose-based media was prepared as described for YMM substituting Glucose with 2% Raffinose (Sigma) or Galactose (Sigma) respectively.
Antibiotics were supplemented to rich media (YPD) to select for deletion strains harboring Kanamycin (*kanMX4*) or Hygromycin B (*hphMX4*) resistance alleles. Antibiotics were filter sterilised from 50 X concentrated stocks, detailed in Table 2.4, into cooled media after autoclaving.

2.1.7. Buffers and solutions

All buffers and solutions were made from distilled water filtered through a Milli-Q 4 Bowl reagent grade water system (MP H_2O) and sterilised by autoclaving at 126°C, 121 psi for 20 minutes or filter sterilised though 0.2 μm Minisart filters (Sartorius Stedim). Recipes for buffer preparation are described in Table 2.6. All buffers and solutions were stored at room temperature unless otherwise stated.

Buffers as part of commercial kits were used according to the manufacturer's instructions unless otherwise stated.

Table 2.6. Buffers and solutions used in this study.

Buffer/Solution	Preparation
1 X TE Buffer	10 mM Tris-HCl (pH 8.0), 1 mM EDTA (pH 8.0)
1 X TBE (Tris/Borate/EDTA) running buffer	90 mM Tris, 90 mM Boric acid, 2 mM EDTA (pH 8.0)
1 X TGS (Tris/Glycine/SDS) running buffer	2.5 mM Tris, 19.2 mM Glycine, 0.1% w/v SDS
1 X TBS (Tris-buffered saline)	10 mM Tris-HCl (pH 7.4), 150 mM NaCl
1 X SSPE Buffer	150 mM NaCl, 9 mM NaH_2PO_4 , 1 mM EDTA, pH adjusted to 7.4 using NaOH
10 X MOPS Buffer	200 mM MOPS (pH 7.0), 50 mM NaAc, 10 mM EDTA. Filter sterilised.
6 X DNA Loading Dye	30% v/v Glycerol, 0.25% w/v Bromophenol Blue, 0.25% w/v Xylene cyanole
2 X Protein Loading Dye	160 mM Tris-HCl (pH 6.8), 10% v/v β-mercaptoethanol, 2% v/v SDS, 10% Glycerol, 0.05% w/v Bromophenol Blue
2 X RNA Loading Dye	95% v/v Formamide, 20 mM EDTA, 0.05% Bromophenol Blue, 0.05% w/v Xylene cyanole
1 X Glyoxal Loading Dye	50% v/v DMSO, 1 M Glyoxal, 1 X MOPS buffer, 10% v/v Glycerol, 20 μg/ml Ethidium Bromide, 0.025% w/v Bromophenol Blue, 0.025% Xylene cyanole
Western Blot Transfer Buffer	20% v/v Methanol, 0.5 X TGS, 0.05% v/v SDS

TMN150 Lysis Buffer	10 mM Tris-HCl (pH 7.6), 5 mM $MgCl_2$, 150 mM NaCl
HEPES Extraction Buffer	50 mM HEPES (pH 7.4), 50 mM KCl, 5 mM $MgCl_2$, 10% v/v Glycerol. Filter sterilised and stored at 4°C. PMSF was added to 2 mM prior to use.
GTC Mix	6.1 M Guanidine thiocyanate (GTC), 15 mM EDTA (pH 8.0), 75 mM Tris-HCl (pH 8.0), 3% v/v Sarkosyl, 1.5% v/v β-mercaptoethanol
NaAc Mix	10 mM Tris-HCl (pH 8.0), 100 mM Sodium Acetate (pH 5.0), 1 mM EDTA (pH 8.0)
ECL Solution 1	2.5 mM Luminol (Sigma), 400 μM p-coumaric acid (Sigma), 100 mM Tris-HCl (pH 8.7). Stored at 4°C
ECL Solution 2	5.4 mM H_2O_2, 100 mM Tris HCl (pH 8.7). Stored at 4°C
Alkaline Lysis Solution I	25 mM Tris-HCl (pH 8.0), 50 mM Glucose, 10 mM EDTA (pH 8.0)
Alkaline Lysis Solution II	0.2 M NaOH, 1% v/v SDS
Alkaline Lysis Solution III	3 M Potassium Acetate, 11.5% v/v Acetic Acid. Solution was pre-chilled on ice prior to use.
DEPC H_1O	0.1% Diethylpyrocarbonate (DEPC) in MP H_1O. Incubated overnight at 22°C before autoclaving.
Northern Blot Stripping Buffer	0.1% v/v SSPE, 0.1% v/v SDS
50 X Denhardt's Solution	0.04% w/v Ficoll, 0.04% w/v Polyvinylpyrrolidone, 0.04% w/v BSA. Stored at -20°C for short term storage and -80°C for long term storage.
Oligo-Hybridisation Buffer	6 X SSPE, 5 X Denhardt's Solution,

	0.2% v/v SDS. Made using DEPC treated MP H_2O
Formamide Oligo-Hybridisation Buffer	50% v/v Formamide, 5 X SSPE, 5 X Denhardt's Solution, 0.1% v/v SDS, 200 μg/ml Herring sperm DNA
LiT Buffer	10 mM Tris-HCl (pH 7.6), 1 mM EDTA (pH 8.0), 100 mM Lithium acetate (pH 7.5)
Western Blot Blocking Buffer	10% w/v dried, skimmed mlik powder (Marvel, Premier International Foods Ltd. Lincs, UK) in 1 X TBS.
STET	8% w/v Sucrose, 50 mM Tris-HCl (pH 8.0), 50 mM EDTA (pH 8.0), 5% v/v Triton X-100
Neutralisation Buffer	1.5 M NaCl, 0.5 M Tris, pH adjusted to 7.4 using HCl
Breaking Buffer	10 mM Tris-Hcl (pH 8.0), 1 mM EDTA (pH 8.0), 100 mM NaCl. 1% v/v SDS, 2% Triton X-100
Alkaline Lysis Extraction Buffer	0.2 M NaOH, 0.2% v/v β-mercaptoethanol. Stored at 4°C
TfbI Solution	10 mM KAc, 100 mM $RbCl_2$, 10 mM $CaCl_2$, 50 mM $MnCl_2$, 15% v/v Glycerol, pH adjusted to 5.8 using 0.2 M Acetic Acid.
TfbII Solution	10 mM MOPS, 75 mM $CaCl_2$, 10 mM $RbCl_2$, 15% v/v Glycerol, pH adjusted to 6.5 using 0.5 M KOH

2.1.8. Plasmids

All plasmids used or constructed during this study (unless otherwise stated) are described in Table 2.8. Vector backbones are detailed in Table 2.7.

Table 2.7. Backbone plasmids used in this study

Plasmid	Description	Source/Reference
pRSET-b	*E. coli* expression vector, ampicillin resistance, T7 promoter. For generating recombinant, N-terminal, His(6)-tagged fusion proteins.	Invitrogen (Schoepfer, 1993)
pGEX-2T	*E. coli* expression vector, ampicillin resistance, tac promoter. For generating recombinant, N-terminal GST fusion proteins.	Amersham (Smith and Johnson, 1988)
pRS313	Yeast/*E. coli* shuttle single-copy vector, ampicillin resistance, *HIS3* selection marker.	(Sikorski and Hieter, 1989)
pRS314	Yeast/*E. coli* shuttle single-copy vector, ampicillin resistance, *TRP1* selection marker.	(Sikorski and Hieter, 1989)
pRS415	Yeast/*E. coli* shuttle single-copy vector, ampicillin resistance, *LEU2* selection marker.	(Sikorski and Hieter, 1989)
pRS425	Yeast/*E. coli* shuttle multi-copy vector, ampicillin resistance, *LEU2* selection marker.	(Sikorski and Hieter, 1989)
pRS316	Yeast/*E. coli* shuttle single-copy vector, ampicillin resistance, *URA3* selection marker.	(Sikorski and Hieter, 1989)
pRS426	Yeast/*E. coli* shuttle multi-copy vector, ampicillin resistance, *URA3* selection marker.	(Sikorski and Hieter, 1989)
p44	Yeast/*E. coli* shuttle single-copy vector, ampicillin resistance, *URA3* selection. For generating N-terminal	(Mitchell et al., 1996)

	zz-tagged fusion proteins driven by the *RRP4* promoter.	
pEG(KT)	Yeast *2μ* high copy number vector, ampicillin resistance, *URA3* & *leu2-d* selection. For generating *Gal1/10* driven GST fusion proteins.	(Mitchell et al., 1993)
pTL26	Yeast/ *E. coli* shuttle single-copy vector, ampicillin resistance, *HIS3* selection. For generating *Gal1/10* driven proteins.	Euroscarf (Lafontaine and Tollervey, 1996)
pET24b[GB1]	*E. coli* expression vector, kanamycin resistance, T7 promoter. For generating N-terminal GB1 & His(6) fusion proteins.	A gift from G.Hautbergue (University of Sheffield) (Hautbergue et al., 2008)
pBS1479	Yeast / *E. coli* shuttle vector, ampicillin resistance, *TRP1* selection. For generating C-terminal TAP-tagged fusion proteins.	(Rigaut et al., 1999)

Plasmid numbers refer to the lab nomenclature reference system. Plasmids are prefixed with a lower case 'p' and numbered chronologically. Yeast selection markers are indicated in brackets.

Plasmid Number	Composition	Description	Source/Construction
p44	pRS416[zz]	For construction of N-terminal tagged zz-fusion proteins in yeast. Driven by *RRP4* promoter. (*URA3*)	P.J. Mitchell (University of Sheffield) (Mitchell et al., 1996)
p198	pEG(kt)	2μ yeast vector for high level expression of GST-fusion peptides under the control of the *GAL 1/10* promoter. (*URA3, leu2-d*)	(Mitchell et al., 1993)
p262	pRS314[RRP47]	Untagged Rrp47 yeast expression construct. Driven by the *RRP47* promoter. (*TRP1*)	R.M. Jones (University of Sheffield)
p263	pRS416[zz-RRP6]	zz-Rrp6 yeast expression construct. Driven by the *RRP4* promoter. (*URA3*)	P.J. Mitchell (University of Sheffield)
p280	pEG(kt)[rrp6Δ212-721]	2μ yeast vector for high level expression of GST-$Rrp6_{NT}$. Driven by *GAL1/10* promoter. (*URA3, leu2-d*)	J.A. Stead (Stead et al., 2007)
p425	pRS313[RRP47]	Untagged Rrp47 yeast expression construct under *RRP47* promoter. (*HIS3)*	P.J.Mitchell (University of Sheffield)
p426	pRS313[rrp47ΔC]	Untagged rrp47ΔC yeast expression construct under *RRP47* promoter. (*HIS3*)	P.J. Mitchell (University of Sheffield)

p428	pRS313[zz-RRP6]	zz-Rrp6 yeast expression construct. Driven by *RRP4* promoter. (*HIS3*)	P.J.Mitchell (Univeristy of Sheffield)
p430	pRS313[zz-rrp6-1]	zz-rrp6-1 yeast expression construct. Driven by *RRP4* promoter. (*HIS3*)	P.J. Mitchell (University of Sheffield)
p432	pRS313[zz-rrp6, L197X]	zz-$Rrp6_{NT}$ yeast expression construct. Driven by *RRP4* promoter. (*HIS3*)	P.J.Mitchell (University of Sheffield)
p514	pRS313[GAL::zz-RRP6]	zz-Rrp6 yeast expression construct. Under control of the *GAL1/10* promoter. (*HIS3*)	M. Turner (University of Sheffield)
p530	pRS425[NEL025c]	2μl NEL025c yeast expression construct. (*LEU2*)	M. Feigenbutz (University of Sheffield) (Garland et al., 2013)
p532	pRS426[NEL025c]	2μl NEL025c yeast expression construct. (*URA3*)	M. Feigenbutz (University of Sheffield) (Garland et al., 2013)
p593	pRS416[zz-MPP6]	zz-Mpp6 yeast expression construct. Driven by *RRP4* promoter. (*URA3*)	This study: o597 + o598 PCR on wildtype genomic DNA cloned into p44 using *Eco*R1 and *Hind*III
p599	pRS415[zz-MPP6]	zz-Mpp6 yeast expression construct. Driven by *RRP4* promoter. (*LEU2*)	This study: *Bam*HI/*Sal*I fragment from p593 subcloned into pRS415

p600	pEG(kt)[ura3-]	2μ yeast vector for high level expression of GST-fusion peptides under the control of the *GAL 1/10* promoter. *(leu2-d*)	This study: *URA3* allele of p198 disrupted by *Apa*I/*Stu*I digestion , treatment with Klenow fragment followed by blunt end ligation.
p601	pEG(kt)[Rrp6Δ212-721, ura3-]	2μ yeast vector for high level expression of GST-$Rrp6_{NT}$. Driven by *GAL1/10* promoter. (*leu2-d*)	This study: *URA3* allele of p280 disrupted by *Apa*I/*Stu*I digestion, treatment with Klenow fragment followed by blunt end ligation.
p602	pRS425[zz-RRP6]	2μ zz-RRP6 yeast expression construct. Driven by *RRP4* promoter. (*LEU2*)	This study: *Xho*I/*Sac*I fragment of p263 subcloned into pRS425.
p603	pRS425[zz-MPP6]	2μ zz-MPP6 yeast expression construct. Driven by *RRP4* promoter. (*LEU2*)	This study: *Bam*HI/*Sal*I fragment of p593 subcloned into pRS425.
p664	pRS415[zz-mpp6_L11A_S12A_V15A]	zz-mpp6 yeast expression construct with L11A_S12A_V15A substitutions. (*LEU2*)	This study: SDM on p599 using o758 + o759
p665	pRS415[zz-mpp6_M18A_K19A]	zz-mpp6 yeast expression construct with M18A_K19A substitutions. (*LEU2)*	This study: SDM on p599 using o760 + o761
p666	pRS415[zz-mpp6_F20A_M21A]	zz-mpp6 yeast expression construct with F20A_M21A substitutions. (*LEU2*)	This study: SDM on p599 using o762 + o763
p667	pRS415[zz-mpp6_G111A_R112A_F115A]	zz-mpp6 yeast expression construct with G111A_R112A_F115A substitutions. (*LEU2*)	This study: SDM on p599 using o764 + o765

p668	pRS415[zz-mpp6_D130X]	zz-mpp6 yeast expression construct with a D130X mutation. (*LEU2*)	This study: SDM on p599 using o844 + o845
p669	pRS415[zz-mpp6_K169X]	zz-mpp6 yeast expression construct with a K169X mutation. (*LEU2*)	This study: SDM on p599 using o766 + o767
p670	pRS313[RRP47-TAP,TRP1]	Rrp47-TAP yeast expression construct. Driven by *RRP47* promoter. (*HIS3, TRP1*)	This study: o878 + o879 PCR on pBS1479 was ligated with *Sal*I linearised p425 by *in vivo* recombination in yeast.
p671	pRS313[rrp47ΔC-TAP, TRP1]	Rrp47ΔC-TAP yeast expression construct. Driven by *RRP47* promoter. (*HIS3, TRP1*)	This study: o777 + o879 PCR on pBS1479 was ligated with *Sal*I linearised p425 by *in vivo* recombination in yeast.
p685	pRS415[zz-mpp6_M18I]	zz-mpp6 yeast expression construct with a M18I substitution. (*LEU2*)	This study: SDM on p599 using o846 + o847
p686	pRS415[zz-mpp6_N33D]	zz-mpp6 yeast expression construct with a N33D substitution. (*LEU2*)	This study: SDM on p599 using o850 + o851
p697	pRS415[zz-mpp6_S42P]	zz-mpp6 yeast expression construct with a S42P substitution. (*LEU2*)	This study: SDM on p599 using o854 + o855
p698	pRS415[zz-mpp6_D43N]	zz-mpp6 yeast expression construct with a D43N substitution. (*LEU2*)	This study: SDM on p599 using o858 + o859

p689	pRS415[zz-mpp6_L63P]	zz-mpp6 yeast expression construct with a L63P substitution. (*LEU2*)	This study: SDM on p599 using o852 + o853
p690	pRS415[zz-mpp6_Y66H]	zz-mpp6 yeast expression construct with a Y66H substitution. (*LEU2*)	This study: SDM on p599 using o856 + o857
p691	pRS415[zz-mpp6_E146K]	zz-mpp6 yeast expression construct with a E146K substitution. (*LEU2*)	This study: SDM on p599 using o848 + o849

2.1.9. Oligonucleotides

All oligonucleotides were purchased from Operon (Eurofins MWG Operon., Ebersberg, Germany) and were already purified and dephosphorylated. Oligos were typically diluted to a working stock concentration of 5 μM in DEPC treated H_2O. Tables 2.9, 2.10, 2.11 and 2.12 describe oligonucleotides used in this study categorized by usage. All sequences are written 5'-3'.

Table 2.9. Oligonucleotides used for Northern Probes in this study

Oligo Number refers to the lab nomenclature reference system.

Oligo Number	Sequence	Description/Use
o236	GCGTTGTTCATCGATGC	To detect 5.8S rRNA, complementary to B1S boundary in 5.8S rRNA
o237	TGAGAAGGAAATGACGCT	To detect 5.8S + 30nt rRNA, complementary to the 5.8S/ITS2 boundary
o238	TCACTCAGACATCCTAGG	To detect U14 snoRNA, complementary to 108-126 nt from the 5' end
o240	CACCGTTACTGATTTGGC	To detect snR13 snoRNA, complementary to 68-86 nt from the 5' end
o242	AAGGACCCAGAACTACCTTG	To detect SCR1 RNA, complementary to 295-315 nt from the 5' end
o243	GAGAGGTTACCTATTATTA	To detect snR38 snoRNA, complementary to 51-70 nt form the 5' end
o274	CGCTGCTCACCAATGG	To detect 5'ETS, complementary to 5'ETS 278 nt downstream of A_0
o319	GCTCTTTGCTCTTGCC	To detect 20S pre-rRNA, complementary between D and A_2
o405	CATGGCTTAATCTTTGAGAC	To detect 18S rRNA, complementary to 34-54 nt downstream of A_1
o406	CTCCGCTTATTGATATGC	To detect 25S rRNA, complementary to 41-59 nt downstream of C_1
o443	TTCGGTTTCTCACTCTGGGGTAC	To detect U3 snoRNA, complementary to 102-125 nt from the 5' end
o494	CTGCTGCAAATTGCTACCTC	To detect snR50 snoRNA, complementary to 13-23 nt from the 5' end
o517	ATCTCTGTATTGTTTCAAATTGACCAA	To detect U6 snRNA, complementary to 27-54 nt downstream from the 5' end
o717	TGTTACCTCTGGGCCC	To detect $27SA_2$ pre-rRNA, complementary to ITS1 between A_2 and A_3
o809	GGCTTCTACAGAACAAGTTGTATCGAAATGATTGTTGGCGAC	To detect NEL025c CUTs
o815	GATGTAAGAGAACAAGTGAACAGTGAACAGTGAACAGTGGGGACA	To detect IGS1-R CUTs
o820	ACTTGTCAGACTGCCATT	Complementary to the 3' end of U3 snoRNA
o821	GGTCAGATAAAAGTAAAAAAAGGTACG	Complementary to the 3' end of snR13 snoRNA
o822	AGATTGCAGCACCTGAGTTTC	Complementary to the 3' end of 5S rRNA
o925	CTACTCGGTCAGGCTC	To detect 5S rRNA, complementary to 64-80 nt from the 5' end

Table 2.10. Oligonucleotides used for site-directed mutagenesis in this study.
+/- denotes forward or reverse primers respectively.

Oligo Number	Sequence	Description/Use
o758	GTGCTAACAATGGTGTCACTGGCAAAGCCGCTAGTAGAGCCATGAATATGAAGTTTATGAAATTT	(+) To generate L11A, S12A, V15A substitutions in Mpp6
o759	AAATTTCATAAACTTCATATTCATGGCTCTACTAGCGGCTTTGCCAGTGACACCATTGTTAGCAC	(-) To generate L11A, S12A, V15A substitutions in Mpp6
o760	TGGCAAACTCTCTAGTAGAGTCATGAATGCGGCGTTTATGAAATTTGGTAAGACGGATGAC	(+) To generate M18A, K19A substitutions in Mpp6
o761	GTCATCCGTCTTACCAAATTTCATAAACGCCGCATTCATGACTCTACTAGAGAGTTTGCCA	(-) To generate M18A, K19A substitutions in Mpp6
o762	ACTCTCTAGTAGAGTCATGAATATGAAGGCTGCGAAATTTGGTAAGACGGATGACGAAGAG	(+) To generate F20A, M21A substitutions in Mpp6
o763	CTCTTCGTCATCCGTCTTACCAAATTTCGCAGCCTTCATATTCATGACTCTACTAGAGAGT	(-) To generate F20A, M21A substitutions in Mpp6
o764	CGAAAACCTGAGGGTGTGATAAGTGCGGCAAAAACCGCTGGCGATAATTCTGATGATAGT	(+) To generate G111A, R112A, F115A substitutions in Mpp6
o765	ACTATCATCAGAATTATCGCCAGCGGTTTTTGCCGCACTTATCACACCCTCAGGTTTCG	(-) To generate G111A, R112A, F115A substitutions in Mpp6
o766	GACCTAGATAAATTATTTAAGGATAGCATCTAGAAGAAAAAGACCAACCATAATGGTAAAAAT	(+) To generate a K169X truncation in Mpp6
o767	ATTTTTACCATTATGGTTGGTCTTTTTCTTCTAGATGCTATCCTTAAATAATTTATCTAGGTC	(-) To generate a K169X truncation in Mpp6
o844	GGTGGTTCCAGGAAGAGAAAGTTCTAGGAAGGCGAACAAAATGAAGAC	(+) To generate a D130X truncation in Mpp6
o845	GTGTTCATTTTGTTCGCCTTCCTAGAACTTTCTCTTCCTGGAACCAC	(-) To generate a D130X truncation in Mpp6
o846	CAAACTCTCTAGTAGAGTCATGAACATCAAGTTTCTGAAATTTGGTAAGAC	(+) To generate a M18I substitution in Mpp6

o847	GTCTTACCAAATTTCATAAACTTGATGTTCATGACTCTACTAGAGAGTTG	(-) To generate a M18I substitution in Mpp6
o848	GAAGACGAGAAAAGGGATGCTAAGGATAAAAAGTTTACAGGGAGCC	(+) To generate an E146K substitution in Mpp6
o849	GGCTCCCTGTAAACTTTTTATCCTTAGCATCCCTTTTCTCGTCTTC	(-) To generate an E146K substitution in Mpp6
o850	CGGATGACGAAGAGAGTTCAGATTCCAATACGCCGTCTAATATC	(+) To generate a N33D substitution in Mpp6
o851	GATATTAGACGGCGTATTGGAATCTGAACTCTCTTCGTCATCCG	(-) To generate a N33D substitution in Mpp6
o852	GTCTGGATGACTCAGCGTGGGATCCAAATAGCTACAAAGATGA	(+) To generate a L63P substitution in Mpp6
o853	TCATCTTTGTAGCTATTTGGATCCCACGCTGAGTCATCCAGAC	(-) To generate a L63P substitution in Mpp6
o854	CAATACGCCGTCTAATATCAATCCGGATGTGGAACCTATAGAGC	(+) To generate a S42P substitution in Mpp6
o855	GCTCTATAGGTTCCACATCCGGATTGATATTAGACGGCGTATTG	(-) To generate a S42P substitution in Mpp6
o856	CTGGATGACTCAGCGTGGGACCTCAATAGTCATAAAGATGATTT	(+) To generate a Y66H substitution in Mpp6
o857	AAATCATCTTTATGACTATTGAGGTCCCACGCTGAGTCATCCAG	(-) To generate a Y66H substitution in Mpp6
o858	CGCCGTCTAATATCAACTCTAACGTGGAACCTATAGAGCAGAAAG	(+) To generate a D43N substitution in Mpp6
o859	CTTTCTGCTCTATAGGTTCCACGTTAGAGTTGATATTAGACGGCG	(-) To generate a D43N substitution in Mpp6

Table 2.11. Oligonucleotides used for Southern probes in this study.

Oligo Number	Sequence	Description/Use
o778	GGCAAAGCCGCTAGTAG	To screen for L11A, S12A, V15A substitutions in Mpp6
o779	ATGAATGCGGCGTTTAT	To screen for M18A, K19A substitutions in Mpp6
o780	AGAAGGCTGCGAAATT	To screen for F20A, M21A substitutions in Mpp6
o781	ATAAGTGCGGCAAAAAC	To screen for G131A, R132A, F135A substitutions in Mpp6
o860	AGAAGTTCTAGGAAGGCG	To screen for D130X truncations in Mpp6
o861	GTCATGAACATCAAGTTTATG	To screen for M18I substitutions in Mpp6
o862	AGGATAAAAAGTTTACAGGG	To screen for E146K substitutions in Mpp6
o863	AGAGTTCAGATTCCAATACG	To screen for N33D substitutions in Mpp6
o864	GTGGGATCCAAATAGCTAC	To screen for L63P substitutions in Mpp6
o865	ATCAATCCGGATGTGG	To screen for S42P substitutions in Mpp6
o866	CCTCAATAGTCATAAAGATGATT	To screen for Y66H substitutions in Mpp6
o867	CAACTCTAACGTGGAACC	To screen for D43N substitutions in Mpp6

Table 2.12. Oligonucleotides used for PCR and molecular cloning during this study
+/- denotes forward or reverse primers respectively.

Oligo Number	Sequence	Description
o68	ATTAACCCTCACTAAAGGG	(+) PCR primer to amplify from the T3 promoter
o191	AAACTCGAGGAACTGACTACTGA	(+) Outlying PCR primer to amplify *RRP47* alleles
o192	AAAGAGCTCAAACTTTCGCTGG	(-) Outlying PCR primer to amplify *RRP47* alleles
o468	CTGGGATCCATGATACACGATGCAGG	(+) Outlying PCR primer to amplify *REX1* alleles
o512	ATGGCAACCCTACGAGTAA	(-) Outlying PCR primer to amplify *REX1* alleles
o594	CGCGAATTCTCTCGAATCTACACG	(+) PCR primer with *Eco*R1 site to amplify *MPP6* alleles
o595	CCTGCTCCCATTACAG	(+) Outlying PCR primer to amplify *MPP6* alleles
o597	ACGGAATTCAATGAGTGCTAACAATGG	(+) PCR primer with *Eco*RI site to amplify from the initiation site of *MPP6* alleles
o598	CGCAAGCTTGGCGTGCATGAGACG	(-) PCR primer with *Hin*DIII site to amplify *MPP6* alleles

o599	ACAAACAGATTCAAAGGG	(-) Outlying PCR primer to amplify *MPP6* alleles
o774	CGAAAGTAGACAACAAATTC	(+) PCR primer to amplify zz-tagged alleles.
o877	CAGGCAGAGCAAGAAAAAGCTAAGAATATCATTTCCAATGTTTTGGACTCCATGGAAAAGAGAAG	(+)PCR primer to amplify TAP-tag and *TRP1* marker from pBS1479. Contains regions of homology to target product to the *RRP47* locus to generate a *rrp47DC-TAP* allele
o878	AAAAGTAAAAGATTGGATAAAGTTGGAAAAAAGAAAGGAGGGAAGAAGTCCATGGAAAAGAGAAG	(+)PCR primer to amplify TAP-tag and *TRP1* marker from pBS1479. Contains regions of homology to target product to the *RRP47* locus to generate a *rrp47-TAP* allele
o879	TATAAGCATTTTTGCATTTGTGCTCTCACATCACCTTTAATCTACGACTCACTATAGGG	(-) PCR primer to amplify TAP-tag and downstream *TRP1* marker from pBS1479. Contains regions of homology to target downstream of the RRP47 locus.

2.1.10 Antibodies

Antibodies used in this study are described in Table 2.13. Bracketed names describe the abbreviations frequently used in this text and figures. Antibodies were stored at -80°C for long-term storage and either -20°C or 4°C as stated for short-term storage.

Table 2.13. Antibodies used in this study.

Name	Concentration used	Incubation period	Storage	Source
Mouse anti-penta-his (α-His)	1:10,000	2 hours	-20°C	QIAGEN
Rabbit anti-Glutathione-S-Transferase (α-GST)	1:14,000	2 hours	-20°C	SIGMA
Peroxidase/anti-Peroxidase (α-PAP)	1:10,000	2 hours	-20°C	SIGMA
Mouse anti-Phosphoglycerate Kinase 1 (α-PGK1)	1:10,000	2 hours	4°C	Invitrogen
Rabbit anti-Rrp4 (α-Rrp4)	1:10,000	2 hours	-20°C	P.J.Mitchell (University of Sheffield)
Rabbit anti-Rrp6 (α-Rrp6)	1:5,000	2 hours	-20°C	A kind gift from David Tollervey (Wellcome Trust Centre for Cell Biology, Edinburgh)
Rabbit anti-Rrp47 (α-Rrp47)	1:5,000	2 hours	-20°C	P.J.Mitchell (University of Sheffield)
Rabbit anti-Sba1 (α-Sba1)	1:20,000	1 hour	-20°C	A kind gift from Stephan Wilson (University of Sheffield)
Goat anti-Rabbit Peroxidase (GARPO)	1:10,000	1 hour	-20°C	SIGMA
Rabbit anti-Mouse Peroxidase (RAMPO)	1:20,000	1 hour	-20°C	SIGMA
Goat anti-Mouse Peroxidase (GAM)	1:10,000	1 hour	4°C	Bio-Rad

2.2. Methods

2.2.1. Generating competent *E. coli* cells: The Rubidium Chloride method

Saturated pre-cultures of appropriate *E. coli* strains (listed in Table 2.1) were diluted 100-fold into 100 ml LB media and grown at 37°C to an OD_{550} of 0.48. Cells were harvested by centrifugation at 3,200 x *g* at 4°C for 5 minutes and pellets were re-suspended in 40 ml TfbI solution. Following 10 minutes incubation on ice, cells were harvested as before and re-suspended in 5 ml TfbII solution before a further 15 minutes incubation on ice. Aliquots of 100 µl were snap-frozen in liquid nitrogen and stored at -80°C before use.

2.2.1.1. Determination of *E. coli* competency

Competent cells generated as above were routinely tested for their degree of competency by their transformation efficiency. An aliquot of cells was transformed as described in section 2.2.2 with 0.1 ng pUC18 DNA (Agilent), plated onto selective media and incubated for 16 hours. Transformation efficiency was calculated by the number of colony forming units per µg of pUC18 DNA (CFU/µg pUC18 DNA).

E. coli cells with a transformation efficiency of 10^5-10^7 CFU/µg pUC18 DNA were used for plasmid transformations. Cells with efficiencies of 10^7-10^9 CFU/µg pUC18 DNA were used for procedures that required a higher degree of competency such as molecular cloning or SDM transformations.

2.2.2. Transformation of competent *E. coli* cells

Competent *E. coli* cells were regularly transformed with varying nanogram quantities of DNA depending on the application. Cells were thawed on ice for 10 minutes before addition of transforming DNA and incubating for a further 15 minutes on ice. The cells were subjected to a heat-shock at 42°C for 1.5 minutes

followed by 2 minutes on ice before recovery at 37°C with the addition of 1ml LB media for 40 minutes. Following recovery, cells were centrifuged at 16,000 x *g* for 1 minute, re-suspended in LB media and plated onto selective media.

2.2.3. Isolation of plasmid DNA from *E. coli*

Plasmids were routinely extracted from transformed *E. coli* cells. Strains harboring plasmids were isolated from single colonies growing on solid LB media supplemented with appropriate antibiotics. Single colonies were used to inoculate 5ml LB media plus antibiotics and were grown to saturation overnight at 37°C with sufficient agitation. Cells were harvested at 16,300 x *g* for 1 minute and any supernatant was removed. Pellets were either used immediately or stored at -20°C for up to 1 week.

2.2.3.1 Alkaline lysis method

Based on method originally described by Birnboim & Doly (Birnboim and Doly, 1979). Cell pellets from 1.5 ml saturated pre-culture were re-suspended in 100 µl Alkaline lysis Solution I and 200 µl of Alkaline lysis solution II was added. After incubating on ice for 5 minutes, 150 µl of Alkaline lysis solution III was added before centrifugation at 16,300 x *g* for 10 minutes. The resulting supernatant was added to an equal volume of phenol/chloroform, briefly vortexed and centrifuged for 5 minutes. The aqueous phase was transferred to a fresh tube and mixed with 2 volumes of 100% ethanol and precipitated for 20 minutes at room temperature. Nucleic acids were pelleted by centrifugation for 20 minutes and washed with 200 µl 70% (v/v) ethanol. Pellets were air dried before re-suspending in 19 µl MP H_2O followed by the addition of 1 µg RNaseA. Plasmid mini-preps were routinely checked by agarose gel electrophoresis (see section 2.2.10) using 1 µl of sample.

2.2.3.2. Spin Miniprep Kit method

Plasmid preparations using E.Z.N.A.® Plasmid Miniprep Kit (Omega, Omega Bio-Tek Inc., Georgia, USA) were routinely used for lab stocks and sequencing. Cell

pellets were prepared as described above, re-suspended in chilled buffer provided by the manufacturer and plasmid DNA was isolated as per the manufacture's instructions.

2.2.4. Polymerase Chain Reaction (PCR)

PCR reactions were performed using *Taq* DNA polymerase (GoTaq®, Promega) unless otherwise stated. Thermocycling reactions were carried out using a Cleaver TC32/80 (Cleaver Scientific LTD., Warwickshire, UK) or a Techne TC312 (Techne., Cambridge, UK) thermocycler. PCR volumes ranged from 20-100 µl depending on the application. Two-step PCR was routinely used as a general protocol to optimize annealing.
Typical reaction mix:

30.5 µl	MP H_2O
10 µl	5 x GoTaq® Reaction Buffer (includes $MgCl_2$)
5 µl	2 mM dNTP mix
1 µl	Oligonucleotide primer A (5 µM stock)
1 µl	Oligonucleotide primer B (5 µM stock)
1 µl	Template DNA (~10 ng)
1.25 U	*Taq* DNA Polymerase

Typical thermocycler settings for two-step PCR:

95°C	2 mins	
95°C	30 secs	30 cycles
45°C	1 min	
50°C	1 min	
72°C	3 mins	
72°C	5 mins	
4°C	Hold	

PCR reaction products were regularly verified by agarose gel electrophoresis (see Section 2.2.10) and subjected to PCR cleanup (Section 2.2.9) or gel purification (Section 2.2.11) depending on the downstream application.

2.2.5. Colony PCR

Alleles were directly screened from yeast colonies without the need to isolate and purify DNA. Freshly growing cells were collected from solid media and added directly to a 50 μl PCR mix solution as described in Section 2.2.4 in place of the template DNA. A two-step PCR thermocycling program was used as described above with the addition of a 10-minute initial denaturation step. Cellular debris and other PCR contaminants were removed using a commercial PCR cleanup kit as described in section 2.2.8.

2.2.6. Error-prone PCR (EPPCR)

A variation on the PCR reaction was used to introduce random mutations into alleles to generate a mutant library. Cumulative rounds of PCR were performed on template DNA using GoTaq DNA Polymerase (Promega) that lacks proofreading activity.

The initial PCR product was generated using ~10 ng plasmid DNA harboring the gene of interest as a template. Outlying primers were designed to amplify the gene and flanking sequences. Reaction mixes of 100 μl (prepared in the same relative amounts as described in section 2.2.4) were split into 10 μl aliquots and PCR reactions were run in parallel before pooling the resulting products.

PCR products were purified by ethanol precipitation as described in Section 2.2.8. DNA was confirmed by agarose gel electrophoresis and approximately quantified in relation to GeneRuler 1 kb DNA ladder bands (Thermo Scientific). A 10 ng aliquot from the primary round (1°) of EPPCR was used for a subsequent secondary round (2°) of PCR as described above. This process was repeated for

5 rounds of EPPCR to generate 5 libraries (1°-5°) with cumulative degrees of nucleotide mis-incorporation for use in downstream applications.

2.2.7. Site-Directed Mutagenesis (SDM)

Site-Directed Mutagenesis was used to introduce nucleotide substitutions in plasmid expression constructs in order to generate specific mutations in the subsequent gene products. Briefly, two complementary oligonucleotides containing the desired mutation were used to amplify the appropriate plasmid DNA through a thermocycling reaction using *Pfu* Turbo high fidelity DNA polymerase. The Quickchange™ Site-Directed Mutagenesis I Kit (Stratagene) was used with slight variations to the manufacturers instructions.

Reaction mix:

15.5 µl	H_2O
2.5 µl	10 X Reaction Buffer
1 µl	Plasmid DNA (50-100 ng)
2.5 µl	Oligonucleotide Primer A
2.5 µl	Oligonucleotide Primer B
0.5 µl	dNTP Mix
2.5 U	*Pfu* DNA polymerase

Thermocycler conditions:

95°C	2 mins	
95°C	30s	30 cycles
55°C	1 min	
68°C	12 mins	
68°C	10 mins	
4°C	Hold	

After amplification, 20 U *DpnI* was added to digest methylated and hemimethylated parental plasmid at 37°C for 1 hour. A 10 μl aliquot was used to transform competent *E. coli* cells as described in section 2.2.2.

2.2.8. Ethanol precipitation of DNA

PCR products were precipitated to remove enzyme contaminants and excess dNTPs. To a standard 50 μl PCR reaction, NaAc pH 5.0 was added to a final concentration of 300mM after thermocycling. Nucleic acids were precipitated with the addition of 2 x volumes 100% ethanol and incubated at -20°C for 1 hour followed by centrifugation at 16,300 x *g* for 20 minutes. Pelleted DNA was washed with 70% (v/v) ethanol and centrifuged for a further 5 minutes. The supernatant was removed and DNA was air dried at room temperature before re-suspending in 50 μl TE buffer. DNA was confirmed by agarose gel electrophoresis.

2.2.9. PCR cleanup

Colony PCR DNA products were routinely purified for sequencing or downstream applications using an E.Z.N.A® Cycle-Pure Kit (Omega) with variations on the manufacturer's protocol. After thermocycling, cellular debris was pelleted by centrifugation at 16,300 x *g* for 2 minutes and the supernatant was transferred to a fresh tube. Buffer CP was added to 4 x volumes and the protocol was followed as described by the manufacturer's instructions.

2.2.10. Agarose gel electrophoresis of DNA

DNA was routinely separated by electrophoresis on 1% (w/v) agarose gels. High-resolution agarose (Geneflow) was dissolved in 0.5X TBE by microwaving. Agarose solutions were cooled to ~65°C and Ethidium bromide was added to a final concentration of 0.1 μg/μl. Gels were cast in a Bio-Rad gel caster and run at 76 V in a Mini-Sub Cell GT Agarose Gel Electrophoresis system (Bio-Rad, Bio-Rad

Laboratories., Munchen, Germany) using 0.5 X TBE as a running buffer. Prior to loading, samples were mixed with 6 X DNA Loading Buffer. DNA was visualized using a Syngene G:Box Gel Documentation UV transilluminator (Syngene, Synoptics., Cambridge, UK) and captured using GeneSnap software. Quantification was carried out using GeneTools software as described by the manufacturer's instructions.

2.2.11. Purification of DNA from agarose gels

After separation of DNA by agarose gel electrophoresis, DNA fragments were excised from the gel using a scalpel. A hand-held UV lamp was used to visualize the DNA whilst minimizing UV exposure where possible. DNA fragments were purified from agarose using an E.Z.N.A® Gel Extraction Kit (Omega) according to the manufacture's instructions. DNA was eluted from the column in 20-50 μl of TE buffer heated to 70°C. Eluted DNA was confirmed by agarose gel electrophoresis.

2.2.12. Restriction digest of DNA

DNA was digested using commercial enzymes provided by NEB and Promega according to the manufacturer's instructions. Digests were carried out in total volumes ranging 20-50 μl, using 100-500 ng of DNA for analytical digests and several micrograms of DNA for molecular cloning purposes. Typically, digests were carried out at 37°C for either 2-4 hours or 16 hours for analytical and preparative digestions respectively. Analysis of restriction digests was carried out using agarose gel electrophoresis as described in Section 2.2.10 and DNA fragments were routinely purified from agarose as described in Section 2.2.11.

2.2.13 Alkaline Phosphatase digestion of DNA

Calf-Intestinal Phosphatase (CIP) (Roche) was used to catalyse the removal of 5' phosphate groups from digested DNA to prevent self-ligation during molecular cloning.

Restriction digestion of DNA was carried out as described in Section 2.2.12 before adding 1 U CIP (1 U/μl) and incubating at 37°C for 1 hour. The sample was diluted 4 X using MP H_2O and NaAc pH 5.0 was added to a final concentration of 300 mM. An equal volume of phenol/chloroform was added before briefly vortexing and centrifuged at 16,300 x *g* for 5 minutes. The aqueous phase was transferred to a fresh tube and DNA precipitated with 2 volumes 100% (v/v) ethanol at -20°C for 1 hour. DNA was recovered by centrifugation at 16,3000 x *g* for 20 minutes before washing with 70% (v/v) ethanol and centrifugation for a further 5 minutes. The supernatant was removed before air-drying at room temperature. DNA was dissolved in a final volume of 50 μl.

2.2.14. Klenow fragment treatment of DNA

The Klenow fragment of DNA polymerase I from *E. coli* was used to fill in receded 3' ends of restriction digested DNA for blunt end ligation.
After restriction digestion of DNA (Section 2.2.12), 10 U of Klenow fragment (Fermentas) and dNTPs (to 200 μM) were added before incubating at 37°C for 10 minutes. The enzyme was heat-inactivated at 65°C for 5 minutes and DNA was purified by gel electrophoresis as described in Section 2.2.11.

2.2.15 *in vitro* DNA ligation

Ligation of DNA molecules with complementary overhanging sequences or blunt ends was routinely carried out as part of molecular cloning using T4 DNA ligase (Promega).
Typical ligation mix:

~200 ng purified, digested vector DNA
3 X molar equivalent purified, digested insert DNA
2 μl T4 Ligase Buffer
0.5 U T4 DNA Ligase
Volume to 20 μl with MP H_2O

Ligation reactions were left at room temperature overnight before addition of a further 0.5 U ligase and incubating for 4-6 hours. 10 μl of the ligation mixture was used to transform competent *E. coli* as described in Section 2.2.2.

2.2.16. 5'-end radiolabelling of Oligonucleotides

Short oligonucleotide probes were used to detect the presence of DNA or RNA molecules on Southern or Northern blots respectively. Nucleic acid probes were designed to be complementary to the desired target. Oligonucleotides were radiolabelled at the 5'-hydroxal group with γ[^{32}P]-ATP (PerkinElmer, PerkinElmer., MA, USA) using T4 Polynucleotide Kinase (PNK) (Promega)

Typical labeling reaction mix:

10 μl	DEPC H_2O
1.5 μl	10 X PNK Reaction Buffer
1 μl	DNA Oligonucleotide (5pmols/μl)
5 U	PNK
2 μl	γ[^{32}P]-ATP (~6 pmol total)

Reaction mixes were incubated at 37°C for 30-45 minutes before heat-inactivation at 65°C for 5 minutes. Labeled probes were diluted in oligo-hybridisation buffer and filter sterilised by passing through a 0.2 μm filter before use in Northern/Southern blot hybridisation.

2.2.17. Southern Blotting

As originally described by Southern (Southern et al, 1975). DNA separated by agarose gel electrophoresis was transferred using the 'turbo-blot' procedure. After electrophoresis, gels were soaked in 0.4 M NaOH for 15 minutes with gentle agitation. Excess NaOH was rinsed thoroughly with MP H_2O before soaking in neutralisation buffer for 15 minutes. The gel was washed thoroughly as previously

mentioned before a final soak in 10 X SSPE for 15 minutes. Nucleic acids were transferred to Hybond-N+ membrane (GE Healthcare, GE Healthcare Life Sciences., Buckinghamshire, UK) overnight by capillary action in 10X SSPE using reservoir pressure. After transfer, DNA was cross-linked to membranes using 1200 joules/cm^2 UV light at a distance of ~10 cm.

Southern blots were probed using γ[^{32}P]-ATP labeled oligonucleotides prepared as described in Section 2.2.16. Blots were hybridised overnight at 37°C with gentle agitation. Excess probe was decanted from the blot before being washed 3 x with 2 X SSPE at room temperature followed by a 30-minute incubation at 37°C. Blots were wrapped in saran wrap and placed under phosphor storage screens (Kodak). Exposures were scanned using a Personal Molecular Imager FX machine (Bio-Rad) and non-saturated images were obtained using the ImageJ64 program (NIH).

2.2.18. Genomic DNA extraction from yeast

Yeast genomic DNA (gDNA) was isolated in order to confirm alleles by PCR analysis or for amplification of genes for downstream applications. The method is based on the protocol originally described in (Cryer et al., 1975).

Yeast strains were grown to saturation in 50 ml of appropriate medium before harvesting at 3,200 x *g* for 5 minutes. Cell pellets were washed in 5 ml MP H_2O before spinning for a further 5 minutes. The supernatant was removed and the cell pellet was re-suspended in 1 ml breaking buffer and 1 ml phenol/chloroform. An equal volume of glass beads were added and cells were lysed by vortexing for 5 minutes. A further 4 ml of phenol/chloroform was added along with 4 ml TE buffer, the mixture was briefly vortexed and centrifuged for 5 minutes at 3,200 x *g*. The aqueous layer was removed to a fresh falcon tube and DNA was precipitated with 2 x volumes of 100% ethanol at -20°C for one hour. Samples were centrifuged for 20 minutes at 3,200 x *g* and re-suspended in 2 ml TE buffer. RNA was digested with the addition of 30 μg RNaseA and incubating at 37°C for 30 minutes. A further 5 ml 100% ethanol was added with 25 μl NH_4Ac and the mixture was

centrifuged for 20 minutes at 3,200 x *g*. The pellet was washed with 70% (v/v) ethanol before re-suspending in 500 μl TE buffer. DNA was re-precipitated 3 times with 1 volume isopropanol, pelleting by centrifugation at 16,300 x *g* and re-suspended in 0.5 ml TE buffer. Genomic DNA was air dried and dissolved in a final volume of 100 μl TE buffer.

2.2.19 Yeast Transformation

Yeast transformations were performed with variations on methods previously described (Schiestl and Gietz, 1989). Different methods were used depending on the desired efficiency of transformation.

2.2.19.1. Yeast Colony Transformation

For low yield, plasmid transformations (~10^2 cfu per μg Transforming DNA), yeast colonies were isolated from plates for transformation.

Several yeast colonies were picked from freshly growing selective media and re-suspended in 1 ml MP H_2O before pelleting at 16,300 x *g* for 1 minute. The cells were washed in 1 ml TE buffer and 1 ml LiT buffer consecutively before re-suspending in LiT buffer (50 μl per transformant). For each transformation, 50 μl of cells were mixed with 1 μg transforming DNA, 50 μg denatured- single-stranded herring sperm carrier DNA (Roche) and 100 μl sterile 40% (w/v) PEG4000 in LiT buffer. The mixture was incubated for 30 minutes at room temperature before adding 15 μl DMSO and heat-shocked at 42°C for 15 minutes. Cells were harvested and washed in 1 ml TE buffer before re-suspending in 100 μl TE buffer and plating onto selective media.

2.2.19.2. Yeast pre-culture Transformation

Alternatively to colony transformation, yeast cells were harvested from overnight liquid cultures grown in selective media.

1 ml of liquid cultures were pelleted by centrifugation at 16,300 x *g* for 1 minute before following the protocol described in section 2.2.19.1.

2.2.19.3. High-efficiency Yeast Transformation

For transformation of SDM plasmids, DNA libraries or genomic integrations, a high-efficiency transformation method was used.

A saturated overnight culture of the recipient strain was used to inoculate 50 ml YPD media to an OD_{600} of 0.1 and grown at 30°C with constant shaking to an OD_{600} of 0.5. Cells were harvested by centrifugation at 3,200 x *g* for 5 minutes, washed in 5 ml TE buffer and 5 ml LiT buffer concurrently and re-suspended in 500 µl LiT buffer. An aliquot of 100 µl cell suspension was used per transformation and was added to 50 µl LiT buffer containing 1 µg transforming DNA, 50 µg carrier DNA and 300 µl freshly prepared PEG4000 (40% w/v in LiT buffer). The mixture was incubated at room temperature for 30 minutes before the addition of 50 µl DMSO and heat-shocked at 42°C for 15 minutes. Cells were pelleted and washed in 1 ml TE buffer before re-suspending in 100 µl TE buffer and plating to the appropriate selective media.

2.2.20. Plasmid recovery from Yeast

Plasmid DNA was isolated from yeast strains using an E.Z.N.A® Yeast Plasmid kit (Omega) and amplified by transforming into KC8 *E. coli*. This allowed selection of plasmids using yeast auxotrophic markers and was ideal for recovery from yeast strains containing multiple plasmids bearing different auxotrophic markers.

Yeast strains were grown to saturation in YPD or selective minimal media before harvesting 3 ml of culture by centrifugation at 3,200 x *g* for 5 minutes. Cell pellets were used immediately or stored at -20°C. Cells were re-suspended in SE buffer/β-mercaptoethanol/lyticase solution as provided by the manufacturer and DNA was extracted according to the manufacturer's instructions. DNA was eluted from the column matrix in 30 µl elution buffer (10 mM Tris pH 8.5). 10 µl of DNA eluate was used to transform competent KC8 *E. coli* and selected on appropriate

drop out minimal M9 media. Isolated colonies were grown to saturation in LB media supplemented with the appropriate antibiotic before isolating plasmid DNA as described in section 2.2.3.

2.2.21. Yeast Replica Plating

Yeast colonies were routinely tested for the ability to grow on different selective media by replica plating.

Strains were grown on a master plate for 2-3 days at 30°C before pressing colonies onto a sterile velveteen disk. The disk was imprinted onto secondary selective media to transfer colonies and strains were incubated for a further 2-3 days at 30°C.

2.2.22. Spot Growth Tests

Yeast strains were compared for their relative growth in various different conditions by spotting onto selective media plates.

Strains were inoculated into 5ml of appropriate selective medium and grown to saturation over 1-2 days. Values for OD_{600} were measured and normalised for 1/1 samples. Ten-fold serial dilutions were made in sterile MP H_2O and 4 µl aliquots were spotted onto appropriate media. Strains were grown at various temperatures depending on the desired results.

2.2.23. Preparation of Protein Lysates from Yeast

2.2.23.1. Physical lysis method

Cells were grown in selective media at 30°C to an OD_{600} of 0.5-1.5 and harvested by centrifugation at 3,200 x *g* for 5 minutes and washed in 5 ml TE buffer. Pellets were either used immediately or stored at -80°C.

Cells were re-suspended in TMN150 buffer (2 ml/litre culture) and an equal volume of glass beads was added along with 2 mM PMSF. The cells were vortexed 10 times for 30 seconds with 1 minute rests on ice between beatings. Lysates were transferred to a 1.5 ml eppendorf tube and clarified at 15,000 x *g* for 20 minutes at 4°C.

Protein concentration was determined by measurement of OD_{280} and OD_{260} using a 6305 Genova Spectrophotometer (Jenway, Bibby Scientific., Stone, UK). Protein lysates were analysis by SDS-PAGE (described in Section 2.2.26).

2.2.23.2. Alkaline Lysis method

Protocol as described in (Motley et al., 2012) originally based on methods described in (von der Haar, 2007)

Yeast strains were grown in selective media before 10 ml cells at an OD_{600} of 1.0 were harvested by centrifugation at 3,200 x *g* for 5 minutes. The cells were washed in TE buffer and pellets were either stored at -80°C or used immediately.

Cell pellets were re-suspended in 500 µl cold Yeast Protein Alkaline Lysis Buffer and incubated on ice for 10 minutes. Trichloroacetic acid (TCA) was added to a final concentration of 5% (v/v) and incubated on ice for 10 minutes before centrifugation at 13,000 x *g* for 5 minutes in a cooled centrifuge. The pellet was re-suspended in 10 µl Tris HCl pH 9.4 before adding 90 µl 2 x SDS Protein Loading Dye and boiling the samples for 5 minutes at 95°C.
Protein lysates were stored at -20°C. Prior to use, the sample was cleared by centrifugation at 16,300 x *g* for 1 minute. Typically 10 µl (equivalent to 1 OD cells) was used for SDS-PAGE analysis as described in Section 2.2.26).

2.2.24 Purification of Tagged Proteins from Yeast

Endogenous TAP-tagged fusion proteins or plasmid-borne zz-tagged fusion constructs were used to isolate proteins from yeast and for pulldown analysis.

Yeast lysates were prepared as described in Section 2.2.23.1. However, the cells were lysed in HEPES Extraction Buffer in place of TMN150. A Bio-Rad Poly-Prep Chromatography Column (Bio-Rad) was washed with HEPES Extraction Buffer before adding 50 µl IgG Sepharose beads (GE Healthcare) and equilibrating with further HEPES Extraction Buffer. Clarified yeast protein lysates were incubated with the washed beads and passed through the column 10-15 times. The beads were washed thoroughly in HEPES Extraction Buffer followed by HEPES Wash Buffer.

Retained proteins were eluted either by boiling in 2 x SDS Loading Dye or incubating with 0.5 M Acetic Acid. Eluates from acid washing were concentrated by the addition of 10% (v/v) 2-butanol, vortexing and centrifugation at 16,300 x *g* for 5 minutes. The upper phase was removed and the process was repeated until ~50-100 µl of the lower phase remained. The samples were lyophilized in a Savant Speedvac SC 110A Concentrator (Thermo) before dissolving the pellet in 100 µl 2 x SDS Loading Dye and incubating at 95°C for 5 minutes.

Purified proteins were analysed by SDS-PAGE and Western Blotting (described in sections 2.2.26 and 2.2.28 respectively).

2.2.25 Glycerol gradient ultracentrifugation

Native yeast lysates were prepared by physical lysis and subjected to glycerol gradient ultracentrifugation through 12 ml 10-30% glycerol gradients prepared in HEPES extraction buffer.

Yeast cells were grown in 400 ml of appropriate media at 30°C to an OD_{600} of 1.0-1.5 before harvesting by centrifugation at 3,200 x *g* for 5 minutes. Cell pellets were washed in 5 ml TE buffer and centrifuged for a further 5 minutes before immediate use or storage at -80°C.

Cells were lysed by physical lysis (described in section 2.2.23.1) in cold HEPES Extraction Buffer. An equal volume of glass beads was added along with PMSF to a final concentration of 2 mM. Cells were vortexed for 10 x 30 second intervals interpolated with 1 minute incubations on ice. Lysates were clarified by centrifugation at 16,300 x *g* for 20 minutes.

Gradients were prepared by under-laying using a Beckman Model 385 former (Beckman-Coulter, Beckman Coulter UK LTD, High Wycombe, UK). The outer chamber was filled with 6 ml HEPES extraction buffer containing 30% v/v glycerol and mixed in the outlet chamber containing 6 ml HEPES extraction buffer containing 10% v/v glycerol before under-laying into 12 ml Beckman ultracentrifugation SW41 tubes.

Gradient tubes were weighed and calibrated using HEPES extraction buffer before loading 400 µl clarified yeast cell lysate on the top of the gradient. Ultracentrifugation was carried out in a Beckman-Optima LE-80X Ultracentrifuge using a SW41 rotor at 36,000 rpm for 24 hours at 4°C. Gradients were fractionated manually from the top of the gradient using a pipette into 18 x 680 µl fractions. Fractions were analysed by colloidal gel staining of SDS PAGE gels to compare resolution of whole cell lysates through gradients.

Proteins were precipitated from fractions by the addition of TCA to 20% v/v and incubating on ice for 30 minutes before centrifugation at 16,300 x *g* for 20 minutes. Precipitated proteins were washed in 1ml acetone before centrifugation at 16,300 x *g* for 5 minutes. Pellets were dried before re-suspending in 100 µl 2 x SDS Loading Dye and denaturing at 90°C for 5 minutes. Samples were analysed by SDS-PAGE followed by western blotting.

2.2.26. SDS-PAGE Analysis of Proteins

Proteins were routinely separated according to their electrophoretic mobility by Sodium Dodecyl Sulphate Polyacrylamide Gel Electrophoresis (SDS-PAGE) as originally described in (Shapiro et al., 1967). Acrylamide concentrations varied

from 8-15% (v/v) depending on the size of the protein(s) of interest. Typically, samples were run on a 12% Polyacrylamide gel using an Owl P81 Single Sided Vertical Electrophoresis System (Thermo-Fisher Scientific) or a Mini-Protean Cell electrophoresis system (BioRad). Larger SDS-PAGE gels were run in a Protean II electrophoresis system (BioRad).

12% SDS-PAGE Gel mixes;

Resolving fraction (10 ml);

3.0 ml	40% (w/v) 37.5:1 Acrylamide:Bis-Acrylamide (National Diagnostics Inc, Charlotte NC, USA)
2.8 ml	1.5 M Tris HCl pH 8.7
4 ml	MP H_2O
100 µl	10% (w/v) SDS
100 µl	10% (w/v) Ammonium Persulphate (APS)
10 µl	Tetramethylethylenediamine (TEMED) (Sigma)

Stacking fraction (3 ml);

350 µl	40% (w/v) Acrylamide 38:1 Bis-Acrylamide
350 µl	1 M Tris HCl pH 6.8
2.235 ml	MP H_2O
30 µl	10% (w/v) SDS
30 µl	10% (w/v) APS
5 µl	TEMED

Prior to loading, protein samples were denatured by boiling in 2 X SDS Loading Dye at 90°C for 5 minutes. Proteins were separated in 1 X TGS at 65 V through the stacking fraction and was raised to 115 V once the dye front reached the resolving fraction. Gels were typically run until the bromophenol blue dye reached the end of the resolving fraction.

SDS-PAGE gels were typicaly used for colloidal staining (Section 2.2.27) or subjected to Western Blot analysis (Section 2.2.28).

2.2.27. Coomassie staining of SDS-PAGE gels

To visualize proteins fractionated by SDS-PAGE, gels were incubated in 10 ml Instant Blue (Expedeon) after electrophoresis for 1 hour with gentle agitation followed by washing in MP H_2O to remove excess stain. Gels were visualized using a Syngene G:Box Gel Doc System using the GeneSnap software.

2.2.28. Western Blotting

SDS-PAGE gels were routinely subjected to Western Blot analysis in order to detect specific proteins of interest.

Following electrophoresis as described in section 2.2.26, proteins were transferred to Hybond-C nitrocellulose membrane (GE Healthcare) by electroblotting in Western Blot Transfer Buffer at 15 V overnight using a HSI, TE Series Transphor Electrophoresis Unit (HSI, Hoefer Scientific Instruments, San Francisco, USA).

Membranes were washed in TBS before staining with 10 ml Ponceau S solution (Thermo Scientific) to confirm protein transfer. Ponceau solution was removed by washing 3 times in TBS before incubating the membrane in Western Blot Blocking solution for 1 hour at room temperature with gentle agitation. Membranes were washed 3 times in TBS for 5-minute intervals before incubating with the relevant primary antibody (see Table 2.13 for concentration and incubation times of antibodies). Following a further 3 washes in TBS, membranes were incubated with the appropriate secondary antibody coupled to horseradish peroxidase (HRP). Excess antibody was removed with 3 further washes in TBS. A mixture of equal volumes of ECL solutions 1 and 2 was applied to the membrane and incubated at room temperature for 1 minute with gentle agitation. Immunofluorescence was

visualized primarily using a CCD camera as part of a Syngene G:Box Gel Doc System and captured using the GeneSnap software following the manufacturer's instructions. For larger Western Blots, membranes were wrapped in saran wrap after ECL incubation before being exposed to film (Kodak, Kodak Ltd., Herts, UK) and developed using a Compact X4 Developer (XOgraph, XOgraph Imaging Systems Inc., Gloucs, UK).

2.2.29. RNA Extraction from Yeast

Total RNA was extracted from Yeast using a variation on the guanidine thiocyanate/hot phenol method of extraction (T. Maniatis, E. F. Fritsch, 1982) with adaptations from a later study (Tollervey and Mattaj, 1987).

Cells of the appropriate strain were grown in 50 ml of selective media to an OD_{600} of 0.5 before harvesting at 3,200 x *g* for 5 minutes followed by washing in TE buffer and pelleting for a further 5 minutes. Cells were either used immediately or stored at -80°C until needed.
To the cell pellet, 1 ml of sterile DEPC treated glass beads were added along with 0.5 ml GTC mix and 0.5 ml phenol pH 4.0 before vortexing for 5 minutes. A further 1.5 ml GTC mix and 1.5 ml phenol pH 4.0 was added and briefly vortexed before incubating at 65°C for 10 minutes. The mixture was cooled on ice for 10 minutes before the addition of 2 ml chloroform and 1 ml NaAc mix. The aqueous phase was separated by centrifugation at 3,200 x *g* for 5 minutes before re-extracting with the addition of 2.5 ml phenol/chloroform pH 4.5 before centrifugation for a further 5 minutes. Nucleic acids were precipitated from the aqueous phase by the addition of 2 volumes of 100% (v/v) ethanol and incubating at -80°C overnight.

Precipitated RNA was pelleted by centrifugation at 3,200 x *g* for 20 minutes before washing with 70% (v/v) ethanol and air dried for 10 minutes at room temperature. Pellets were re-suspended in a final volume of 100 µl DEPC H_2O. RNA concentration (in µg/µl) was calculated by measuring the OD_{260} of diluted samples and assuming that 1 OD_{240} ~ 40µg. Typically a 160-fold dilution was used

and the OD_{260} value was multiplied by 6.4 to obtain the concentration. Samples were prepared by mixing with an equal volume of 2X RNA Loading Buffer and denatured at 65°C for 5 minutes before use or stored at -80°C.

2.2.30. Acrylamide gel electrophoresis of RNA

RNA samples were fractionated on 8% polyacrylamide (19:1), TBE buffered-gels containing 50% (w/v) urea. Gels were run in 0.5 X TBE using an EV200 Large Format PAGE Unit Gel Unit (Engineering and Design Plastics Ltd., Cambridge, UK).

Typically 5 μg total RNA was prepared in a total volume of 4 μl to which an equal volume of 2 X RNA loading buffer was added. Samples were denatured at 65°C for 5 minutes before loading. Gels were run overnight at 65 V until the Xylene Cyanole dye front reached the end of the gel. Fractionated RNA was stained by incubating the gel in Ethidium bromide diluted to 0.1 μg/ml in 0.5 X TBE for 15 minutes with gentle agitation before visualizing on a UV transilluminator.

2.2.31. Agarose gel electrophoresis of RNA

RNA was fractionated on 1.2% (w/v) agarose, MOPS buffered-gels in order to probe for pre-rRNA and mRNA species by northern blotting.

Aliquots of 10 μg total RNA were lyophilized in a Savant SpeedVac SC100A Plus Concentrator (Thermo Scientific) before dissolving in 15 μl Glyoxal loading dye (see Table 2.6) and denaturing for 1 hour at 55°C. Gels were prepared with 1.2% (w/v) agarose in 1 X MOPS buffer using DEPC treated MP H_2O and run in 1 X MOPS buffer in a OWL A1 Large Gel System (Thermo Scientific). Fractionated RNA was visualized on a UV transilluminator before transfer and northern blot analysis.

2.2.32. Northern Blotting

Northern blotting was performed based on original techniques described by Alwine *et al* (Alwine et al., 1977) and Littlehales (Littlehales, 1989).

Total RNA fractionated by polyacrylamide gel electrophoresis was transferred to Hybond-N+ membranes (GE Healthcare) by electroblotting at 10 V overnight in 0.5 X TBE. RNA separated by agarose gel electrophoresis was transferred to Hybond-N+ membranes by capillary action using the 'turbo-blot' procedure described in Section 2.2.17. Transferred RNA was cross-linked to membranes using 1200 joules/cm^2 UV light at a distance of ~10 cm. Membranes with RNA transferred from agarose gels were washed in 20 mM Tris HCl pH 8.0 at 65°C for 15 minutes to remove any excess glyoxal.

Membranes were incubated in 50 ml Oligo-hybridisation buffer for 1 hour at 37°C prior to hybridisation overnight with radiolabeled probes prepared as described in 2.2.16. Excess probe was decanted before washing three times for 1 minute in 6 X SSPE at room temperature before incubating at 37°C for 30 minutes. Membranes were wrapped in Saran wrap before placing under phosphor storage screens (Kodak) and analysed using a Personal Molecular Imager FX machine (BioRad). Non-saturated images were obtained using ImageJ64 software (NIH).

Radiolabelled probes were stripped from blots by incubating with 250 ml boiled Northern blot stripping buffer for 1 hour with strong agitation.

2.2.33. Bioinformatics

Yeast genome sequences were obtained from the *Saccharomyces* Genome Database (SGD) (http://www.yeastgenome.org). Bioinformatics tools and software were used extensively throughout this study and are referenced in the text.

Chapter 3: Resolving the Rrp6/Rrp47 complex *in vivo* using the DECOID approach

3.1 Introduction

The degradation of RNA is a fundamental biological process required for both productive and destructive pathways to maintain a stable transcriptome (Section 1.1). The RNA exosome complex harbors both endonuclease and 3'-5' exonuclease activities and functions in many fundamental degradation processes (Section 1.1.2). Rrp44 and Rrp6 associate with the exosome core (EXO9) to provide catalytic activity in the nucleus (Section 1.2). Whilst Rrp6 is not essential in yeast, *rrp6Δ* alleles are synthetic lethal in combination with *rrp44*$^{exo-}$ mutants and both proteins have overlapping functions in RNA processing and surveillance (Gudipati et al., 2012b; Schneider et al., 2012). With a wide array of RNA substrates for a multitude of degradation processes, the exosome requires the function of accessory factors to modulate its activity (Section 1.3).

The nuclear RNA binding protein Rrp47 (also known as Lrp1) functions in concert with Rrp6 in processing and degradation pathways. In the absence of Rrp47, most Rrp6-dependent processes are impeded (Mitchell et al., 2003). The N-terminal Sas10/C1D domain of Rrp47 ($Rrp47_{NT}$) physically interacts with the N-terminal PMC2NT domain of Rrp6 ($Rrp6_{NT}$). This interaction is essential for the normal expression levels of Rrp47 *in vivo*. In *rrp6Δ* or *rrp6ΔNT* mutants, Rrp47 levels are reduced to ~15% compared to wildtype cells (Feigenbutz et al., 2013b; Stead et al., 2007). Conversely in the absence of Rrp47, Rrp6 expression levels are reduced in cells grown in minimal media, but not to the extent as the loss of Rrp47 in *rrp6Δ* mutants (Feigenbutz et al., 2013a). Yeast *rrp47Δ* and *rrp6Δ* mutants are synthetic lethal in with the loss of Mpp6, another nuclear RNA binding protein, or the RNaseD related exonuclease Rex1 (Milligan et al., 2008; Peng et al., 2003). Like Rrp6, Rex1 functions in 3'-end processing of stable RNAs yet does not physically associate with the exosome (Ozanick et al., 2009; van Hoof et al., 2000b).

The C-terminus of Rrp47 is highly basic and is required for RNA binding *in vitro*. However, *rrp47ΔC* alleles encoding the N-terminal Sas10/C1D domain are still functional *in vivo* and are able to complement the synthetic lethality of *rrp47Δ rex1Δ* mutants (Costello et al., 2011). The C-terminus of Rrp47 was also reported to be required for the physical interaction with box C/D snoRNP proteins Nop56 and Nop58 and *rrp47ΔC* mutant show defects in the final stages of box C/D snoRNA maturation (Costello et al., 2011). Taken together, it has been proposed Rrp47 functions to aid in substrate recruitment to Rrp6 through its RNA binding properties. Additionally, as further discussed in Chapter 4, Rrp47 functions to maintain stable expression of Rrp6 (Feigenbutz et al., 2013a).

In this chapter, the effects of physically separating Rrp47 proteins from Rrp6-containing complexes were investigated. Rrp47 is unstable in the absence of the physical interaction with the N-terminal PMC2NT domain of Rrp6 ($Rrp6_{NT}$). To overcome this limitation, an overexpression system was used to induce expression of $Rrp6_{NT}$ and titrate Rrp47 out of functional complexes with Rrp6. This successfully divorces the Rrp6/Rrp47 homodimer whilst maintaining stable expression of Rrp47. This novel approach is referred to as DECOID (decreased expression of complexes by overexpression of interacting domains).
These results show that Rrp47 is functional when physically separated from the catalytic and exosome binding domains of Rrp6. The ability to function independent from Rrp6 is impaired upon deletion of the C-terminal region of Rrp47. Conditional *mpp6 rrp47* and *rex1 rrp47* mutants were generated using the DECOID approach. Overexpression of $Rrp6_{NT}$ in *mpp6Δ rrp47ΔC* and *rex1Δ rrp47ΔC* strains resulted in a conditional block in growth. RNA analyses revealed a widespread loss of RNA surveillance in the *mpp6 rrp47* mutant and a specific defect in snoRNA maturation in the *rex1 rrp47* mutant. This data supports the model that Rrp47 functions in substrate recognition prior to processing or degradation by Rrp6 and that these functions are redundant with pathways involving Rex1 or Mpp6.

3.1.1. A functional assay to screen for *mpp6* and *rrp47* alleles

A plasmid shuffle assay was developed to screen for loss of function mutations in Mpp6 or Rrp47 proteins. The plasmid shuffle and sectoring assays are well characterised as methods for testing genetic complementation of alleles using yeast centromeric plasmids (Elledge and Davis, 1988). These screens can be used to test for complementation of essential alleles or for synthetic lethal genetic interactions.

Yeast strains lacking Mpp6 are viable and have no strong growth or temperature sensitive phenotype. However, *mpp6Δ* alleles are synthetic lethal in combination with *rrp47Δ, rrp6Δ* or *air1Δ* alleles (Milligan et al., 2008). The viability of a *mpp6Δ rrp47Δ* double mutant can be complemented by the maintenance of a centromeric plasmid bearing either *MPP6* or *RRP47* alleles. The use of yeast shuttle vectors containing auxotrophic markers allows for selection or counterselection of plasmids in order to test for complementation of synthetic lethality.

A strain lacking the gene of interest is transformed with a *URA3* plasmid bearing a functional copy of the allele. The second gene is disrupted in the resulting strain and the double mutant is therefore reliant on the functional allele on the *URA3* maintenance plasmid for cell viability. This strain can be used to introduce plasmids bearing mutated alleles and test for complementation of the synthetic lethality by counterselection of the original maintenance plasmid on media containing 5-Floroorotic Acid (5'FOA). The use of 5'FOA is a common technique to cure yeast strains of plasmids containing *URA3* markers. 5'FOA is converted to the toxic 5-flurouracil in strains expressing the *URA3* allele coding for oritine-5-monophosphate decarboxylase (ODCase) involved in uracil biosynthesis.

For this study, an *mpp6Δ rrp47Δ* plasmid shuffle assay was constructed in order to test plasmids bearing mutated *mpp6* or *rrp47* alleles (summarised in Figure 3.1). The aim was to create a double knockout strain complemented with a wildtype copy of *MPP6* on a plasmid containing a *URA3* marker. The resulting

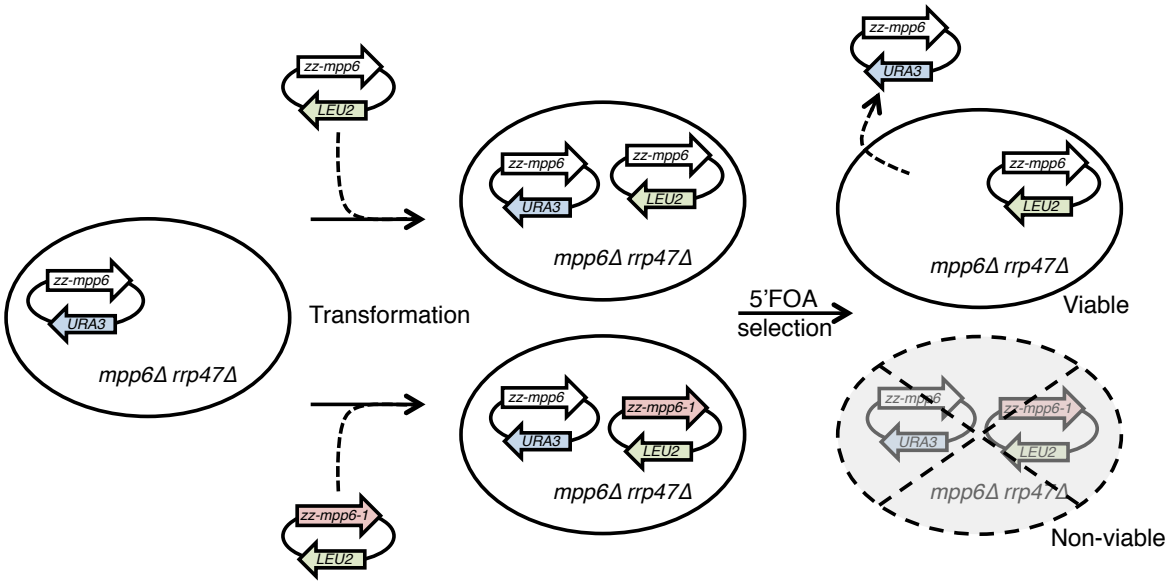

Figure 3.1. A functional assay to test for complementation of *mpp6Δ rrp47Δ* synthetic lethality. Schematic for a *mpp6Δ rrp47Δ* plasmid shuffle assay in yeast. A *mpp6Δ rrp47Δ* strain bearing a wildtype copy of *MPP6* on a URA3 plasmid can be used to test functionality of *mpp6* alleles on a *LEU2* plasmid by selection of transformants on minimal media containing 5'FOA. If the second plasmid contains a functional *mpp6* allele, cells are able to lose the *URA3* plasmid and are viable on 5'FOA media (*upper* route). However, if the second plasmid is unable to complement the *mpp6Δ rrp47Δ* synthetic lethality, the *URA3* plasmid is retained resulting in the production of toxic 5-flurouracil and cells lose viability (*lower* route).

strain can be transformed with a second plasmid bearing mutant copies of *mpp6* or *rrp47* and *LEU2* or *HIS3* selectable markers respectively. If the second plasmid coded for a functional copy of either gene, this would allow for the loss of the

URA3 expressing plasmid and strains would be viable on media containing 5'FOA. However, if the second plasmid coded for a non-functional allele, the strain would have to maintain the *URA3* plasmid to complement the synthetic lethality but as a result would be toxic to the cells. Such strains would be unable to grow on 5'FOA. The *mpp6Δ rrp47Δ* plasmid shuffle strain was used extensively for these studies.

3.2. Results

3.2.1. Generation of a tagged Mpp6 yeast expression construct

A *URA3* centromeric yeast plasmid expressing Mpp6 was created to serve as a maintenance plasmid in the plasmid shuffle strain. The presence of the *URA3* marker served as a tool to counterselect the plasmid on media containing 5'FOA. A fusion protein bearing two copies of the z domain of protein A from *Staphylococcus aureus* (Nilsson et al., 1987) was constructed in order to detect the expression of the protein by western blotting using available antibodies.

The wildtype *MPP6* ORF was amplified from genomic DNA isolated from a wildtype strain (P364) by PCR using o597 and o598. The primers introduced EcoR1 restriction site at the initiation codon of the *MPP6* ORF and a HindIII site ~430nt downstream of the stop codon. The PCR product of 998bp was cloned by ligation into EcoR1/HindIII cut p44 (pRS416[zz]), a yeast expression construct containing a zz-tag under the control of the *RRP4* promoter and bearing a *URA3* marker (Mitchell et al., 1996). Ligated plasmids were transformed into *E. coli* and recovered before screening by restriction digests using EcoR1/HindIII (Figure 3.2. A)

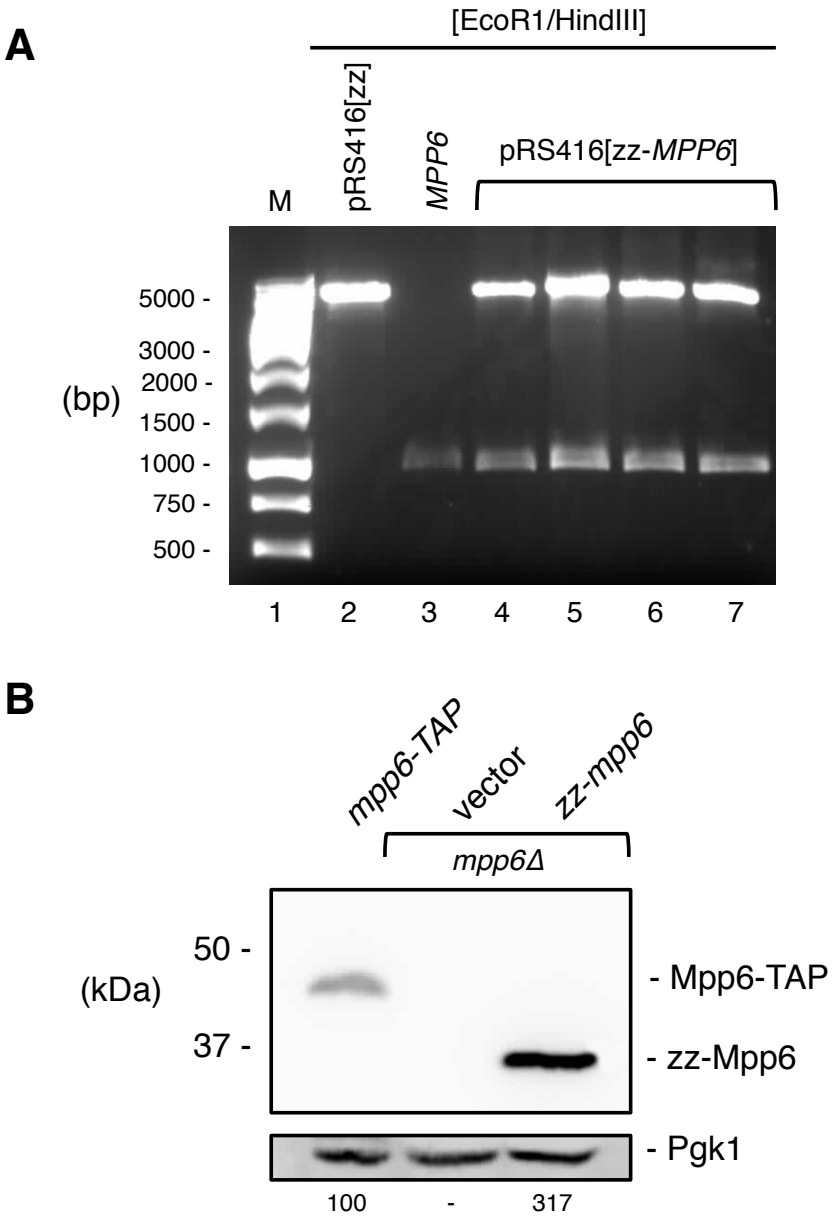

Figure 3.2. Generation of a tagged Mpp6 yeast expression construct. (A) Restriction digest screen of pRS416[zz-*MPP6*] constructs. The yeast *MPP6* ORF was amplified from gDNA from a wildtype strain by PCR using o597 + o598 and cloned into p44 (pRS416[zz]) using EcoR1 and HindIII restriction sites. Candidate plasmids (lanes 4-5) were screened by EcoR1/HindIII restriction digestion and confirmed by sequencing. **(B)** Western blot analysis of zz-Mpp6 protein expression. An *mpp6Δ* yeast strain was transformed with a plasmid encoding a zz-Mpp6 fusion protein under control of the *RRP4* promoter. An empty vector was transformed in parallel. Cells were lysed under denaturing conditions and analysed by SDS PAGE and western blotting. Lysates prepared from a endogenous *mpp6-TAP* tagged strain were analysed in parallel to compare expression levels. Mpp6 fusion proteins were detected with the PAP antibody (*upper* panel). An antiserum against Pgk1 was used as a loading control (*lower* panel). Expression levels of Mpp6 fusion proteins are given below the figures and are the average of three independent biological replicas. Values are expressed relative to the endogenous Mpp6-TAP protein.

To test for the expression of a zz-fusion peptide, the resulting plasmid (p593) was transformed into an *mpp6Δ* yeast strain (P548, Euroscarf, University of Frankfurt, Germany) and selected for growth on minimal media lacking uracil (SD-ura). The *mpp6Δ* strain was also transformed with an empty *URA3* containing vector as a negative control. Protein lysates were prepared by alkaline lysis and the tagged zz-Mpp6 fusion protein was visualised by western blot analysis using the PAP antibody (Figure 3.2. B). The migration of the zz-Mpp6 fusion protein corresponds to the estimated molecular weight of ~35kDa. No detectable fusions peptides were observed in lysates prepared from strains bearing the empty vector (lane 2). The steady state expression level of the zz-Mpp6 fusion protein was compared to levels of an endogenous C-terminal TAP tagged fusion peptide under the control of the *MPP6* promoter. The plasmid-borne zz-Mpp6 fusion protein is expressed ~3-fold greater than the Mpp6-TAP protein. Due to the nature of the plasmid construct, zz-Mpp6 is under the control of the *RRP4* promoter rather than the endogenous *MPP6* promoter. A global analysis of protein expression in yeast previously reported that Rrp4 and Mpp6 peptides are expressed at roughly 4840 and 1350 molecules per cell respectively (Ghaemmaghami et al., 2003). This translates to a 3.5:1 ratio of Rrp4:Mpp6 and roughly corresponds to the relative quantified values of zz-Mpp6:Mpp6-TAP in Figure 3.2. B.

To show that overexpression of Mpp6 has no detrimental effect on cell growth, the relative growth rates of strains expressing increased levels of Mpp6 protein were compared. Growth rates of isogenic wildtype, *mpp6Δ* and *mpp6Δ* strains expressing zz-Mpp6 from either a centromeric or 2μ plasmids were compared by spot growth assays on minimal- or rich-based media (Figure 3.3). The growth rates of all strains were comparable. Overexpression of Mpp6 showed no evident effect on growth in both minimal- and rich-based media.

3.2.2. Construction of an *mpp6Δ rrp47Δ* plasmid shuffle strain

In section 3.2.1, an *mpp6Δ* strain was transformed with a yeast expression shuttle plasmid encoding a zz-Mpp6 fusion protein. To generate an *mpp6Δ rrp47Δ*

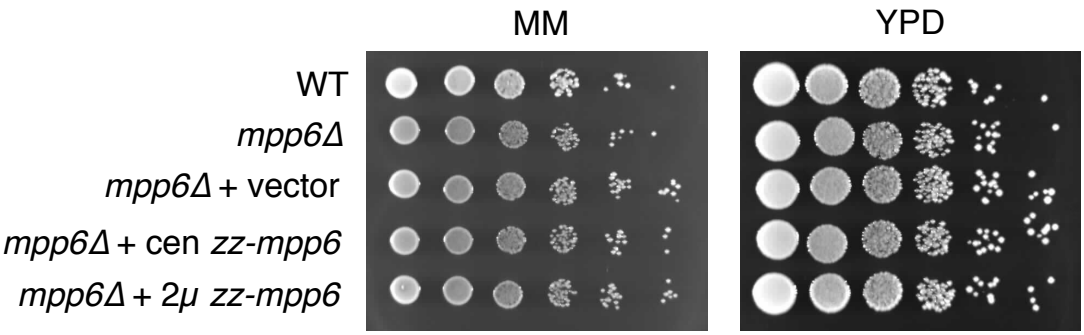

Figure 3.3. Overexpression of Mpp6 does not affect cell growth. Spot growth assays of isogenic wildtype (WT), *mpp6Δ* and *mpp6Δ* strains bearing an empty vector (pRS415), a centromeric plasmid encoding *zz-mpp6* (p599) and a 2μ plasmid encoding *zz-mpp6* (p603). Strains were grown in minimal medium and normalised by optical density (600nm). 10-fold serial dilutions were spotted onto solid minimal (MM) and rich (YPD) medium. Plates were incubated for 2 days at 30˚C before photographing.

plasmid shuffle strain in yeast the endogenous *RRP47* locus was disrupted by transposing an *rrp47Δ* deletion cassette into the aforementioned strain. The *MPP6* locus in the *mpp6Δ* parental strain was disrupted by a *KanMX4* deletion cassette (Wach et al., 1994), therefore the *RRP47* disruption would require a different marker for selection.

Genomic DNA was extracted from a strain harboring an *rrp47Δ* allele disrupted by the hygromycin B resistance gene, *hphMX4* (P913, Garland et al. 2013). PCR was used to amplify the *rrp47Δ::hphMX4* deletion cassette using primers complementary to sequences 500bp upstream and downstream of the *RRP47* ORF (o191 + o192). The *rrp47Δ* deletion cassette was used to transform the *mpp6Δ* strain complemented by plasmid borne zz-Mpp6 expression and selected on media containing hygromycin. The successful disruption of the *RRP47* locus was confirmed by PCR using outlying *RRP47* primers (o191 + o192) (Figure 3.4. A-B). The disruption of *RRP47* and viability of resulting transformants also confirms that the *zz-mpp6* allele is functional in yeast and complements the *mpp6Δ rrp47Δ* synthetic lethality.

The resulting *mpp6Δ rrp47Δ* plasmid shuffle strain (P1232) was assayed for the ability to lose the *URA3* maintenance plasmid encoding zz-Mpp6 through 5'FOA counterselection. The *zz-mpp6* allele was first subcloned into a centromeric plasmid bearing a *LEU2* allele (pRS415) before transforming into the *mpp6Δ rrp47Δ* plasmid shuffle strain. A parallel transformation was carried out using an empty *LEU2* vector. Transformants were selected on minimal medium lacking uracil and leucine before assaying for growth on minimal medium containing 5'FOA (Figure 3.4. C). Strains bearing *LEU2* plasmids encoding zz-Mpp6 were able to grow on media containing 5'FOA whereas strains transformed with an empty *LEU2* vector were not viable. The resulting strains viable on 5'FOA were tested for growth on minimal media lacking uracil to confirm the loss of the *URA3* plasmid. Strains passaged over 5'FOA were no longer viable on media lacking uracil confirming that the *URA3* plasmid had been lost.

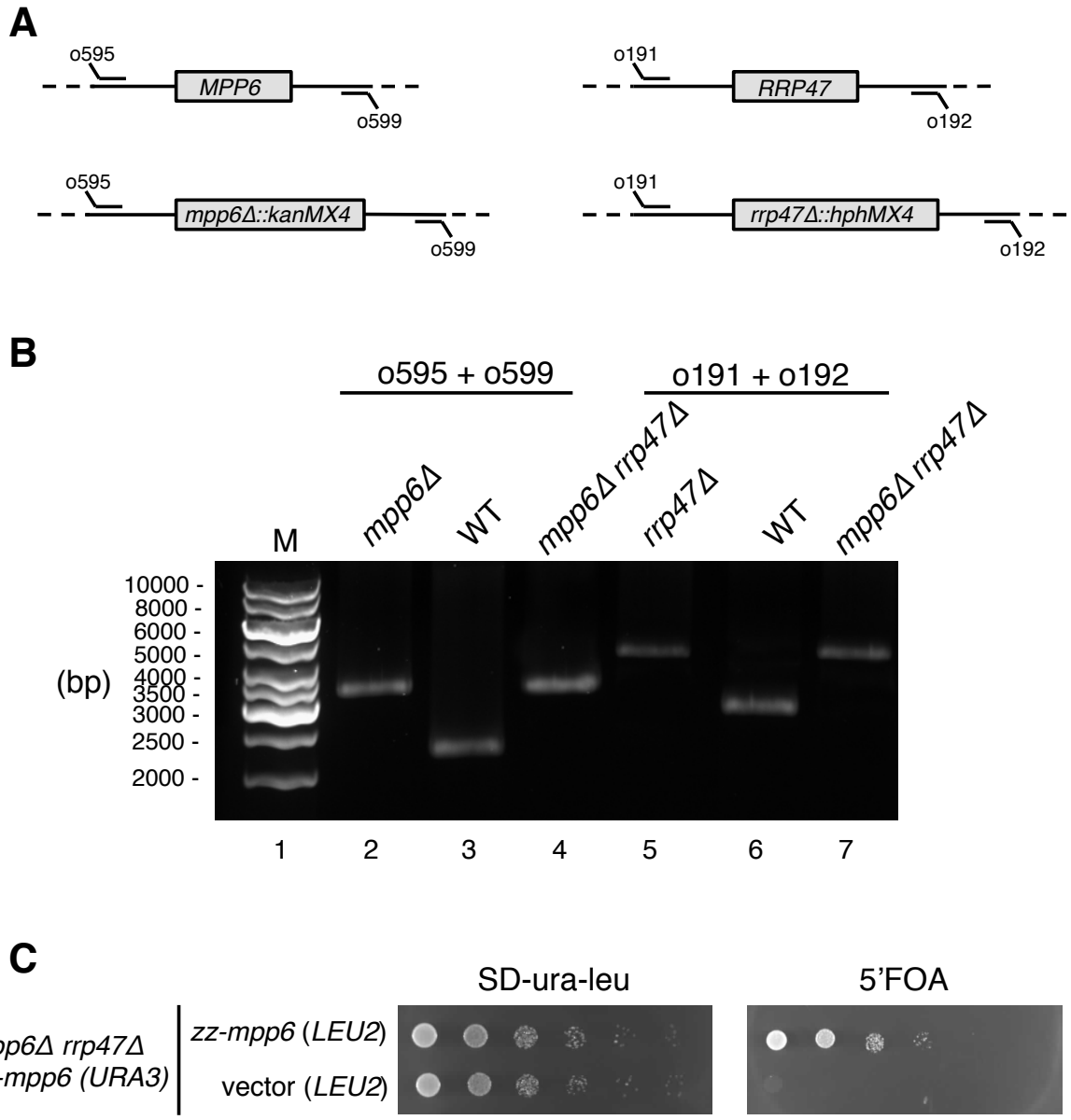

Figure 3.4. Validation of a *mpp6Δ rrp47Δ* plasmid shuffle assay. (A) Schematic of outlying *MPP6* and *RRP47* primers (B) PCR analysis of *mpp6Δ rrp47Δ* plasmid shuffle strain. A *mpp6Δ::kanMX4* strain was transformed with a *zz-MPP6* construct before disruption of the *RRP47* locus using a *rrp47Δ::hphMX4* allele. Double *mpp6Δ rrp47Δ* mutants were screened by PCR using outlying *MPP6* and *RRP47* primer pairs (o595 + o599 and o191 + o192 respectively). PCR was carried out on isogenic wildtype, *mpp6Δ* and *rrp47Δ* genomic DNA in parallel for comparison. (C) Spot growth assay to validate the plasmid shuffle assay. A *mpp6Δ rrp47Δ* plasmid shuffle strain was transformed with a *LEU2* centromeric plasmid encoding wildtype *zz-mpp6* and an empty *LEU2* vector. Transformants were grown to saturation in selective medium and normalised by optical density (600nm). Ten-fold serial dilutions were spotted onto solid glucose (SD-ura-leu) and 5'FOA media. Plates were incubated for 3 days at 30˚C before photographing.

These results describe the successful generation of an *mpp6Δ rrp47Δ* plasmid shuffle strain to be used as a method to assay for functionality of *mpp6* or *rrp47* alleles *in vivo*. The mitotic maintenance of the *URA3* maintenance plasmid encoding a functional copy of *MPP6* was disrupted by transformation with a secondary *LEU2* plasmid encoding zz-Mpp6 and growth on media containing 5'FOA. This provides a conditional assay to test for complementation of *mpp6Δ rrp47Δ* synthetic lethality using plasmids bearing *mpp6* or *rrp47* alleles.

3.2.3. *RRP47* and *rrp47ΔC* alleles complement the *mpp6Δ rrp47Δ* synthetic lethality

The plasmid shuffle assay, described in section 3.2.2 allows for testing plasmids bearing *mpp6* or *rrp47* alleles for functionality by complementation of a double *mpp6Δ rrp47Δ* mutant using 5'FOA to counterselect against a maintenance plasmid bearing *MPP6* and *URA3* alleles.

A C-terminal truncation of Rrp47, encoding the N-terminal 120 residues, has previously been shown to complement the synthetic lethality of *rrp47Δ rex1Δ* in a similar plasmid shuffle assay. The N-terminus of Rrp47 contains the bioinformatically defined Sas10/C1D domain that interacts physically with the N-terminal PMC2NT domain of Rrp6. The N-terminus of Rrp47 alone is functional in the absence of Rex1, however recombinant protein analyses report that the protein is unable to bind RNA *in vitro* (Costello et al., 2011).

To assay if the N-terminus of Rrp47 is sufficient to complement the *mpp6Δ rrp47Δ* synthetic lethality, centromeric *HIS3* plasmids encoding for *RRP47* and *rrp47ΔC* were transformed into the *mpp6Δ rrp47Δ* plasmid shuffle strain. Resulting transformants were assayed for complementation by growth on media containing 5'FOA to counterselect the *URA3* maintenance plasmid encoding zz-Mpp6 (Figure 3.5). Strains bearing plasmids containing *RRP47* and *rrp47ΔC* alleles were able to complement the *mpp6Δ rrp47Δ* synthetic lethality and were viable on 5'FOA

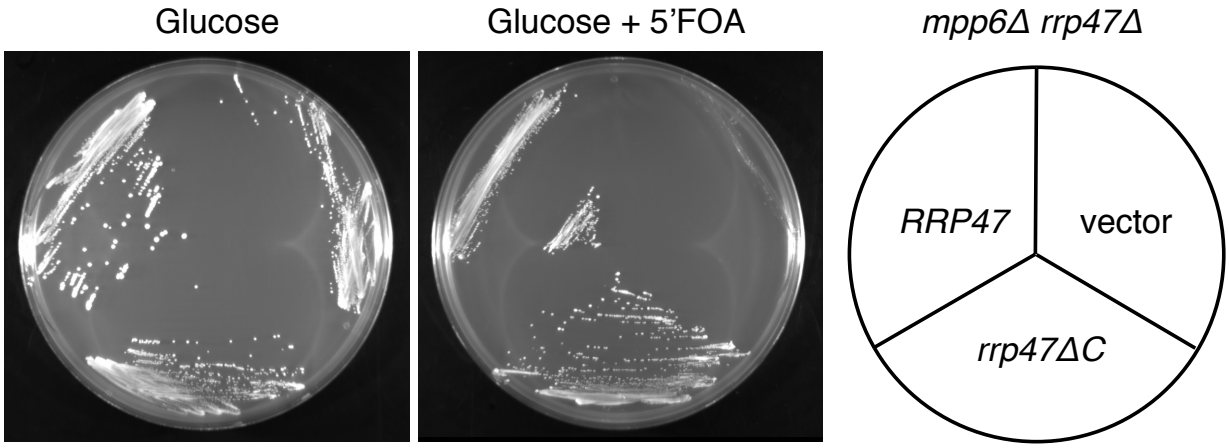

Figure 3.5. The *rrp47ΔC* allele complements the *mpp6Δ rrp47Δ* synthetic lethality.
A plasmid shuffle assay. Centromeric plasmids encoding the full length *RRP47* gene (p425), the *rrp47ΔC* allele (p426) and an empty vector (pTL26) were transformed into a *mpp6Δ rrp47Δ* strain complemented a *zz-MPP6* allele on a *URA3* vector. Transformants were assayed for the loss of the *URA3* plasmid by streaking out onto glucose-based minimal media containing 5'FOA.

media. Strains transformed with an empty *HIS3* vector (pTL26) were unable to grow on media containing 5'FOA.

The complementation assay revealed that the N-terminus of Rrp47 is sufficient to complement the synthetic lethality of an *mpp6Δ rrp47Δ* strain. The N-terminal Sas10/C1D domain of Rrp47 has been reported to interact physically with Rrp6 to form a heterodimer and this interaction is required for the stability of the Rrp47 protein *in vivo* (Feigenbutz et al., 2013b). The function of Rrp6 is partially dependent on its interaction with Rrp47 but the mechanisms behind this are unclear (Stead et al., 2007).

3.2.4. Using the DECOID strategy to resolve the Rrp6/Rrp47 complex *in vivo*.

The expression of Rrp47 is dramatically reduced in *rrp6Δ* mutants or strains lacking the N-terminal PMC2NT domain of Rrp6 (Stead et al., 2007). Because this interaction has a profound effect on the stability of Rrp47, it was presumed that RNA processing and degradation function of Rrp6 and Rrp47 was dependent on this physical association. It has been suggested that Rrp47 acts to promote the exonuclease activity of Rrp6 *in vivo* through substrate recognition from RNA binding activity (Costello et al., 2011; Mitchell et al., 2003; Stead et al., 2007). However, it was unclear whether the physical association of Rrp47 to Rrp6 was critical for its function in RNA processing and degradation pathways. As Rrp47 is degraded by the proteasome in the absence of Rrp6, analyses of *rrp6Δ* mutants are not ideal to address this question.

Previous work (established by M. Turner, M. Feigenbutz and P. Mitchell) developed a novel strategy to separate the physical interaction between the Rrp6/Rrp47 heterodimer complex. This employs an overexpression system to induce expression of the N-terminal PMC2NT domain of Rrp6 ($Rrp6_{NT}$) in order to titrate Rrp47 out of complexes with Rrp6 (Garland et al., 2013). We refer to this approach as DECOID (decreased expression of complexes by overexpression of

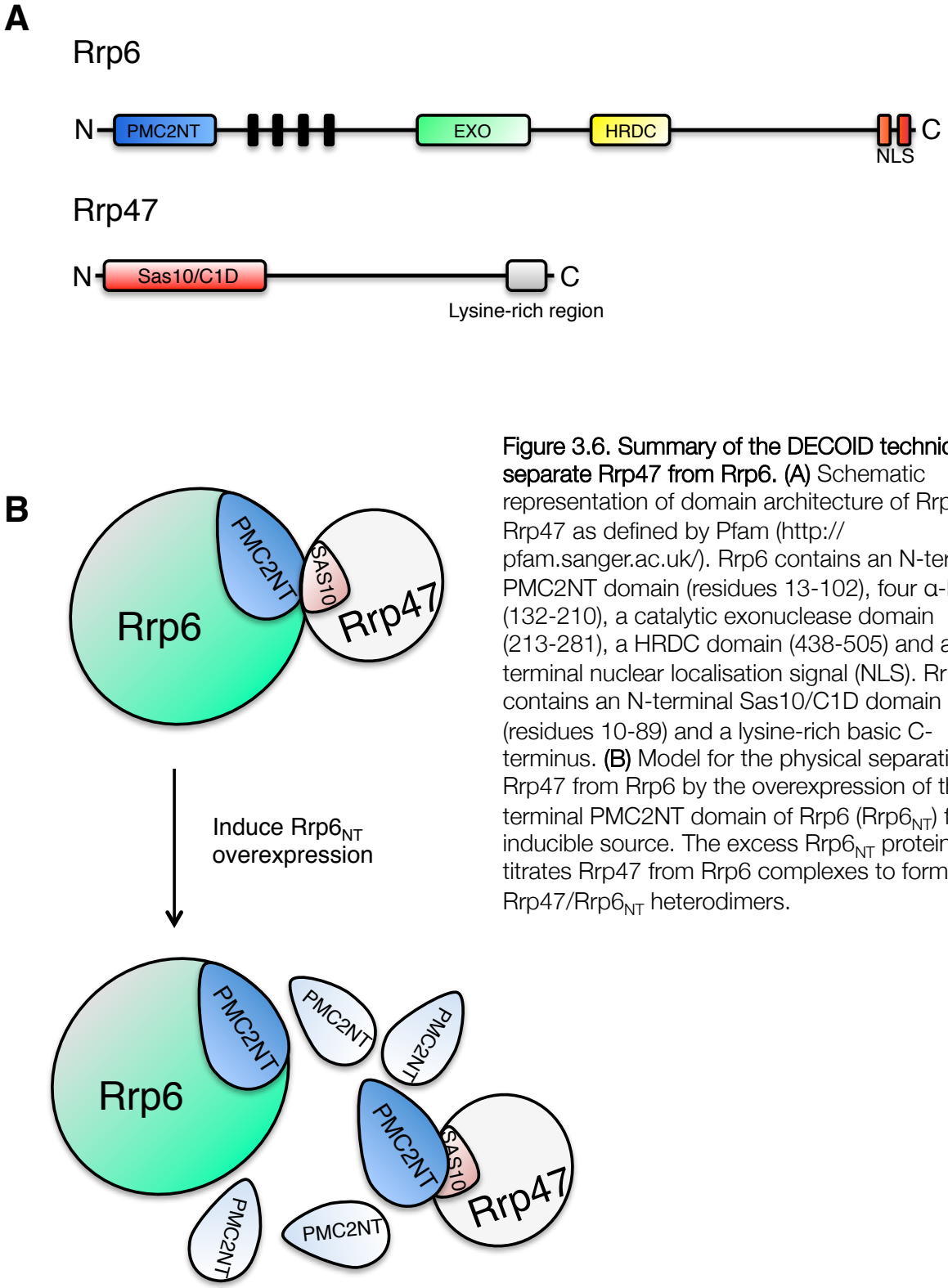

Figure 3.6. Summary of the DECOID technique to separate Rrp47 from Rrp6. (A) Schematic representation of domain architecture of Rrp6 and Rrp47 as defined by Pfam (http://pfam.sanger.ac.uk/). Rrp6 contains an N-terminal PMC2NT domain (residues 13-102), four α-helices (132-210), a catalytic exonuclease domain (213-281), a HRDC domain (438-505) and a C-terminal nuclear localisation signal (NLS). Rrp47 contains an N-terminal Sas10/C1D domain (residues 10-89) and a lysine-rich basic C-terminus. **(B)** Model for the physical separation of Rrp47 from Rrp6 by the overexpression of the N-terminal PMC2NT domain of Rrp6 ($Rrp6_{NT}$) from an inducible source. The excess $Rrp6_{NT}$ protein titrates Rrp47 from Rrp6 complexes to form $Rrp47/Rrp6_{NT}$ heterodimers.

interacting domains). A summary of the technique using the separation of Rrp47 and Rrp6 as an example is depicted in Figure 3.6. This approach would theoretically mimic the Rrp47/Rrp6 interaction through binding to the exogenously expressed $Rrp6_{NT}$ and prevent the degradation of Rrp47 in the absence of its normal binding partner. Overexpression of a *GAL*-inducible GST-$Rrp6_{NT}$ fusion protein was shown to effectively segregate Rrp47 from full-length Rrp6-containing complexes through glycerol gradient ultracentrifugation and pull-down assays (Garland et al., 2013)

Certain limitations of the DECOID technique must be considered. The possibility that residual amounts of Rrp47 protein remain bound to Rrp6 cannot be formally discounted. During the initial development of the method, it was shown that ~4% of Rrp47 remained bound to Rrp6 after induction of GST-$Rrp6_{NT}$ when compared to amounts bound after induction of a GST control. This was considered to be an efficient titration of Rrp47 from Rrp6. Additionally, by overexpressing a decoy protein, the possibility of off-target effects must be considered. It may be conceivable that overexpressed GST-$Rrp6_{NT}$ may interact or disrupt non-intended targets. However, overexpressing GST-$Rrp6_{NT}$ in an *rrp47Δ* strain showed no effect on growth in comparison to equivalent GST controls. With no Rrp47 in the cell, the decoy protein will have no target. Additionally, overexpression of GST-$Rrp6_{NT}$ in an *rrp47Δ* mutant showed no additive RNA processing or degradation phenotypes in comparison to a GST control (Garland et al., 2013). Furthermore, the N-terminal PMC2NT domain of Rrp6 has no reported function than to interact with Rrp47 in previous analyses.

Loss of Rrp47 function is synthetic lethal with *mpp6Δ* or *rex1Δ* alleles (Milligan et al., 2008; Peng et al., 2003). Surprisingly, segregation of Rrp47 from Rrp6 was tolerated in *mpp6Δ* and *rex1Δ* strains suggesting that Rrp47 is still functional when independent of full length Rrp6. Overexpression of the GST-$Rrp6_{NT}$ protein in *mpp6Δ* and *rex1Δ* strains induced slow growth phenotypes in comparison to cells overexpressing the GST domain.

3.2.5. Overexpression of $Rrp6_{NT}$ does not complement the *mpp6Δ rrp47Δ* synthetic lethality.

Induction of GST-$Rrp6_{NT}$ expression in *mpp6Δ* and *rex1Δ* mutants caused slow growth phenotypes in comparison to induction of the GST domain. Conversely, GST-$Rrp6_{NT}$ overexpression caused no change in growth rate in *rrp47Δ* strains (Garland et al., 2013). This suggests that Rrp47 is functional yet impaired upon GST-$Rrp6_{NT}$ induction.

Plasmid shuffle assays were carried out to test that overexpression of the $Rrp6_{NT}$ domain does not negate the requirement for Rrp47. The *mpp6Δ rrp47Δ* plasmid shuffle strain was transformed with 2μ plasmids encoding *GAL*-induced GST and GST-$Rrp6_{NT}$ proteins. Transformants were assayed for growth on minimal media containing 5'FOA to counterselect the *URA3* maintenance plasmid encoding wildtype *MPP6*. Strains expressing GST and GST-$Rrp6_{NT}$ were unable to grow on 5'FOA media whereas strains transformed with plasmids encoding wildtype *MPP6* allowed growth (Figure 3.7.) This shows that the overexpression of $Rrp6_{NT}$ does not suppress the *mpp6Δ rrp47Δ* synthetic lethality and that growth defects observed in *mpp6Δ* single mutants are not due to dominant-negative effects of $Rrp6_{NT}$ induction.

3.2.6. Yeast *mpp6Δ rrp47ΔC* and *rex1Δ rrp47ΔC* alleles are sensitive to $Rrp6_{NT}$ overexpression

In Section 3.2.3, a C-terminal truncation of Rrp47, encompassing the bioinformatically defined Sas10/C1D domain, was shown to complement the *mpp6Δ rrp47Δ* synthetic lethality through a plasmid shuffle assay. Additionally, the *rrp47ΔC* allele was previously shown to complement the *rex1Δ rrp47Δ* synthetic lethality through a similar plasmid shuffle assay (Costello et al., 2011). The DECOID strategy was employed to assay if the Rrp47ΔC protein was functional when divorced from Rrp6 by overexpression of the $Rrp6_{NT}$ protein in *mpp6Δ* and *rex1Δ* strains.

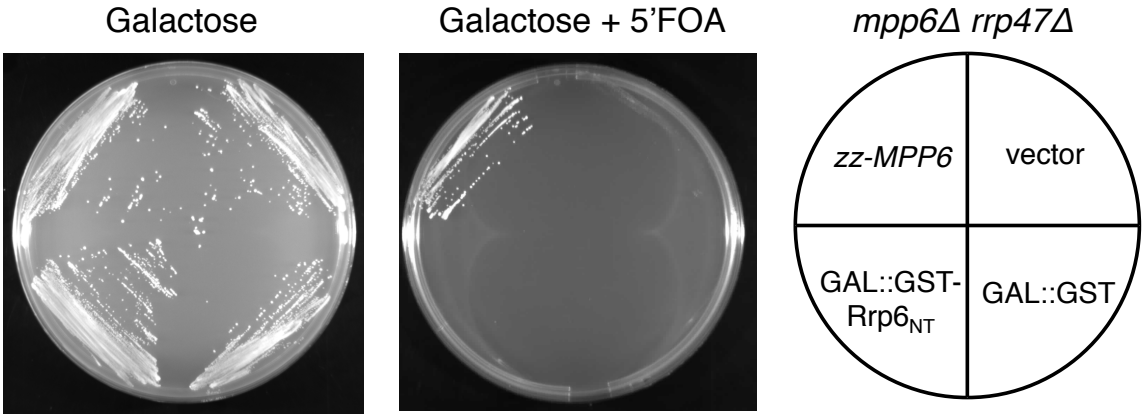

Figure 3.7. Overexpression of $Rrp6_{NT}$ does not complement the *mpp6Δ rrp47Δ* synthetic lethality. A plasmid shuffle assay. A *mpp6Δ rrp47Δ* strain maintained by a *URA3* plasmid encoding *zz-MPP6* was transformed with 2-micron plasmids encoding GAL::GST (p198) and GAL::GST-$Rrp6_{NT}$ (p280). Centromeric vector (pRS415) and *zz-MPP6* (p599) control plasmids were transformed in parallel. Transformants were assayed for the ability to lose the *URA3* maintenance plasmid by streaking onto galactose media containing 5'FOA.

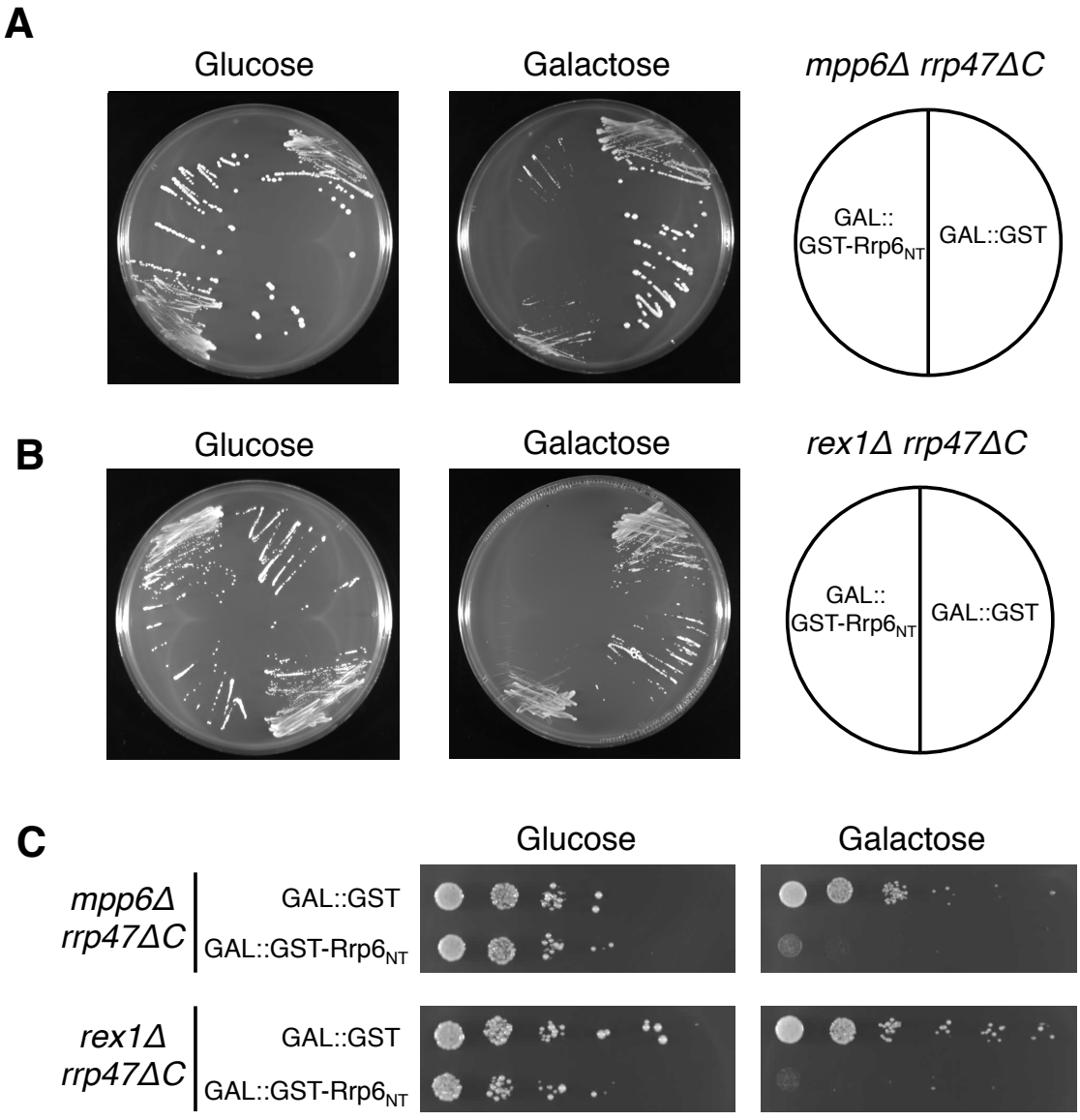

Figure 3.8. Yeast *mpp6Δ rrp47ΔC* and *rex1Δ rrp47ΔC* strains are sensitive to $Rrp6_{NT}$ overexpression. Plate growth assays of yeast strains on permissive glucose-based medium and non-permissive galactose-based medium. (A) Growth of *mpp6Δ rrp47ΔC* strains bearing plasmids encoding either *GAL*-regulated GST or GST-$Rrp6_{NT}$. (B) Growth of *rex1Δ rrp47ΔC* strains bearing plasmids encoding either *GAL*-regulated GST or GST-$Rrp6_{NT}$. (C) Spot growth assays of *mpp6Δ rrp47ΔC* and *rex1Δ rrp47ΔC* strains bearing plasmids encoding *GAL*-regulated GST or GST-$Rrp6_{NT}$. Strains were grown to saturation in permissive raffinose-based medium and normalised by optical density (600nm). Ten-fold serial dilutions were spotted onto solid glucose- or galactose based minimal medium. Plates were photographed after 3 days incubation at 30˚C.

Yeast *mpp6Δ rrp47Δ* and *rex1Δ rrp47Δ* strains harboring plasmids encoding Rrp47ΔC were transformed with 2μ plasmids encoding GST or GST-Rrp6$_{NT}$ under the control of the *GAL1/10* promoter (Stead et al., 2007). Transformants were assayed for growth on glucose- and galactose-based media (Figure 3.8. A-C). Strikingly, induction of the GST-Rrp6$_{NT}$ domain caused a significant reduction in growth in both *mpp6Δ rrp47ΔC* and *rex1Δ rrp47ΔC* mutants whereas induction of the GST domain allowed for viability on galactose-based media. This suggests that the C-terminus of Rrp47 is required for Rrp6-independent functions that are redundant with pathways involving Mpp6 and Rex1.

The C-terminus of Rrp47 was previously shown to not be required for protein function yet is necessary for RNA binding *in vitro*. Additionally, the C-terminus is required for interactions with snoRNP proteins Nop56 and Nop58 and C-terminal deletion mutants show defects in the maturation of Box C/D snoRNAs (Costello et al., 2011).

3.2.7. Rrp47 and Rrp47ΔC proteins are stabilised by Rrp6$_{NT}$

The stability of Rrp47 is sensitive to the physical interaction with the N-terminus of Rrp6. In the absence of Rrp6, steady state expression levels of Rrp47 are reduced to ~15 % compared to wildtype cells (Costello et al., 2011; Feigenbutz et al., 2013b). Separating full length Rrp47 from Rrp6 in wildtype, *mpp6Δ* and *rex1Δ* strains allowed for viability. However, divorcing Rrp47ΔC from Rrp6 results in a conditional lethal growth phenotype in *mpp6Δ* and *rex1Δ* strains. This suggests that the C-terminus of Rrp47 is required for Rrp6-independent functions that are redundant with Mpp6- and Rex1-dependent pathways. One possibility is that the physical separation of Rrp47ΔC and Rrp6 though Rrp6$_{NT}$ overexpression results in the destabilisation of Rrp47ΔC protein expression.

To check for expression levels of Rrp47 and Rrp47ΔC proteins, C-terminal TAP-tagged fusion constructs were generated through homologous recombination cloning in yeast. PCR was carried out on pBS1479 to amplify the TAP-tag, consisting of two IgG binding domains (zz) from *S. aureus* protein A and a calmodulin binding peptide separated by a TEV cleavage site, along with a *TRP1*

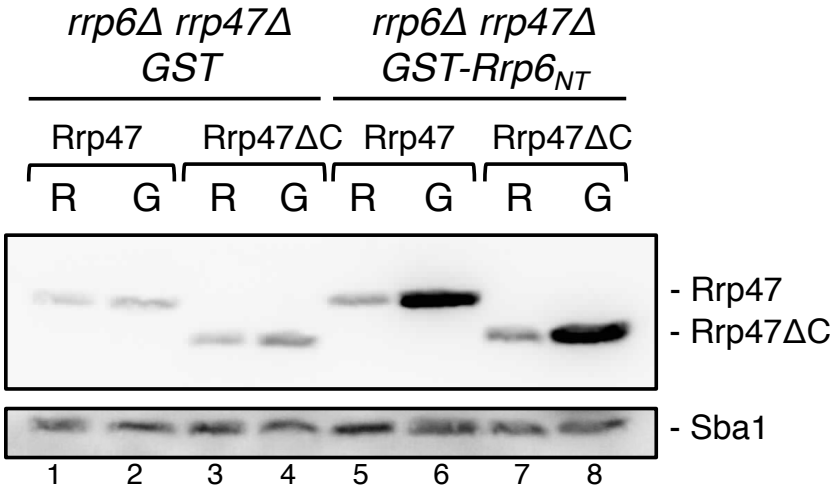

Figure 3.9. Rrp47 and Rrp47ΔC protein expression is stabilised by $Rrp6_{NT}$ in *rrp6Δ* mutants. Western blot analysis of Rrp47 and Rrp47ΔC protein expression in *rrp6Δ* strains. Yeast *rrp6Δ rrp47Δ* strains harboring *GAL*-inducible GST or GST-$Rrp6_{NT}$ constructs were transformed with plasmids encoding C-terminal TAP tagged Rrp47 and Rrp47ΔC fusion proteins. Strains were grown in raffinose- (R) or galactose- (G) based minimal medium. Log phase cells were harvested and lysed under denaturing conditions before analysis by SDS PAGE and western blotting. Rrp47 and Rrp47ΔC fusion proteins were detected with the PAP antibody (*upper* panel). An antiserum against Sba1 was used as a loading control (*lower* panel).

marker (Puig et al., 2001). Primers were designed to amplify the TAP tag and introduce regions of homology to target the tag the *RRP47* locus to generate *RRP47-TAP* and *rrp47ΔC-TAP* alleles (o878 + o879 and o877 + o879 respectively). A plasmid bearing the wildtype *RRP47* allele (p425) was linearised downstream of the ORF by digestion using SalI and co-transformed with the PCR products into *rrp6Δrrp47Δ* strains either harboring the *GAL*::*GST-rrp6*$_{NT}$ construct (p280) or *GAL::GST* (p198). Transformants were isolated on selective medium and screened for positive clones by western blot analysis. Rrp47-TAP and Rrp47ΔC-TAP proteins were detected using the PAP antibody. Plasmids harboring *RRP47-TAP* and *rrp47ΔC-TAP* alleles were recovered from yeast and sequenced to confirm the junction between the ORF and the TAP-tag.

Lysates were prepared from *rrp6Δ* strains expressing either full length Rrp47 or truncated Rrp47ΔC proteins before and after induction of GST-Rrp6$_{NT}$ protein or GST control in raffinose- and galactose-based media respectively. Raffinose is used as a non-inducing/non-repressing neutral carbon source. This allows for rapid induction of proteins under control of the *GAL* promoter upon shift to synthetic galactose-based medium. Steady state expression levels of TAP-tagged Rrp47 proteins were analysed by western blotting using the PAP antibody (Figure 3.9). As reported in previous analyses (Feigenbutz et al., 2013b), the expression level of Rrp47 was increased in the *rrp6Δ* mutant upon expression of the GST-Rrp6$_{NT}$ (Figure 3.9, compare lanes 5 and 6). Furthermore, the expression of the Rrp47ΔC protein was increased comparably upon expression of GST-Rrp6$_{NT}$ protein (lanes 7-8). Induction of the GST control showed no significant effect on the expression levels of Rrp47 or Rrp47ΔC proteins (lanes 1-4). These results show that both the full length Rrp47 and the truncated Rrp47ΔC protein are stable in complex with the Rrp6$_{NT}$ protein in the absence of full length Rrp6.

A possible explanation for the loss of growth observed in *mpp6Δ rrp47ΔC* and *rex1Δ rrp47ΔC* mutants upon Rrp6$_{NT}$ expression is that the stability of Rrp47ΔC proteins is compromised in the absence of Mpp6 or Rex1. To address this, the expression levels of full-length and C-terminally truncated Rrp47 proteins were analysed in *mpp6Δ* and *rex1Δ* mutants. Plasmids encoding C-terminal TAP-tagged Rrp47 and Rrp47ΔC (described above) were transformed into *mpp6Δ*

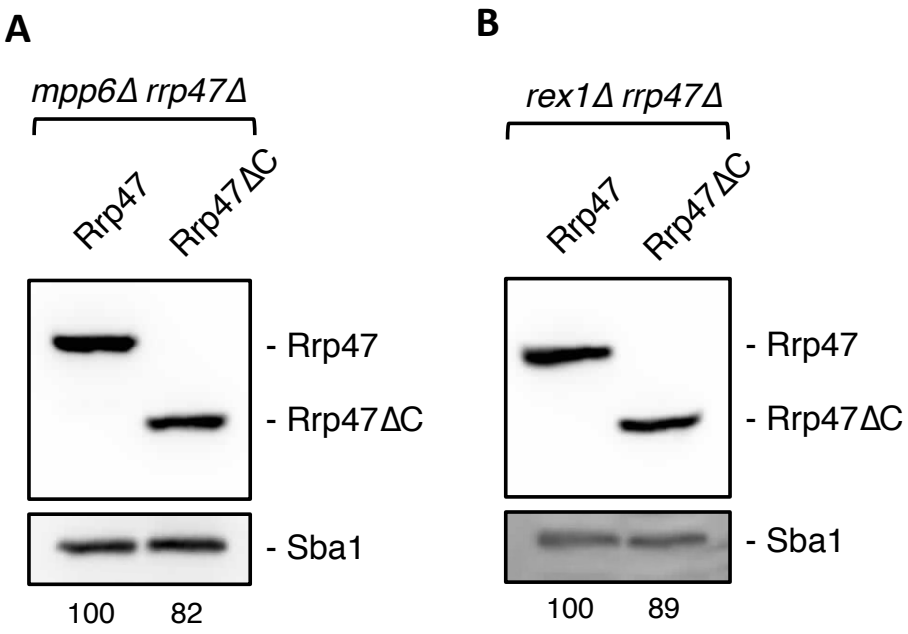

Figure 3.10. Rrp47 and Rrp47ΔC proteins are stable in *mpp6Δ* and *rex1Δ* mutants. Western blot analysis of Rrp47 and Rrp47ΔC protein expression in *mpp6Δ* (A) and *rex1Δ* (B) strains. Plasmids encoding C-terminal TAP-tagged fusion proteins of wildtype Rrp47 (p670) or the C-terminal truncation Rrp47ΔC (p671) were transformed into yeast *mpp6Δ rrp47Δ* and *rex1Δ rrp47Δ* plasmid shuffle strains bearing URA3 maintenance plasmids encoding wildtype *MPP6* and *RRP47* alleles respectively. Cells were passaged over media containing 5'FOA to purge the strains of the *URA3* maintenance plasmid. Cells were lysed under denaturing conditions and analysed by SDS PAGE and Western blotting. Rrp47 and Rrp47ΔC fusion proteins were detected with the PAP antibody (*upper* panel). An antiserum against Sba1 was used as a loading control (*lower* panel). Expression levels of Rrp47 proteins are given below the figures and are the average of three independent biological replicas. Values are expressed relative to the corresponding wildtype Rrp47 proteins in each strain.

rrp47Δ and *rex1Δ rrp47Δ* plasmid shuffle strains. As shown in Section 3.2.3 and Costello et al. 2011, both *RRP47* and *rrp47ΔC* alleles are able to complement the *mpp6Δ rrp47Δ* and *rex1Δ rrp47Δ* synthetic lethality. Transformants were viable on media containing 5'FOA and recovered strains were validated for the loss of the *URA3* maintenance plasmid encoding wildtype *MPP6* or *RRP47* alleles. Lysates were prepared from the resulting *mpp6Δ* and *rex1Δ* strains harboring plasmids encoding Rrp47-TAP and Rrp47ΔC-TAP tagged proteins and analysed by western blotting using the PAP antibody (Figure 3.10). Quantitative analysis from three independent biological replicas shows that the expression of Rrp47 proteins is not markedly altered in strains lacking Mpp6 or Rex1. Levels of Rrp47ΔC are slightly reduced to 82% and 89% in *mpp6Δ* and *rex1Δ* mutants, respectively, in comparison to the expression of full length Rrp47.

In conclusion, Rrp47 and Rrp47ΔC proteins are stable in complex with the N-terminal region of Rrp6 ($Rrp6_{NT}$). Additionally; Rrp47ΔC proteins are stable in the absence of Mpp6 or Rex1.

3.2.8 Rrp47 and rrp47ΔC proteins retain function when separated from Rrp6-containing complexes.

The separation of Rrp47 and Rrp6 using the DECOID method in *mpp6Δ* or *rex1Δ* mutants causes slow growth phenotypes, yet strains are viable (Garland et al., 2013). In *mpp6Δ rrp47ΔC* and *rex1Δ rrp47ΔC* mutants, overexpression of the $Rrp6_{NT}$ domain causes a strong conditional block in growth. This suggests that the C-terminus of Rrp47 is required to function with Mpp6 or Rex1 when separated from Rrp6-containing complexes.

To address if Rrp47ΔC is functional when segregated from Rrp6, northern blot hybridisation analyses were carried out in *rrp47ΔC* mutants upon GST-$Rrp6_{NT}$ induction. Yeast *rrp47Δ* strains harboring plasmids encoding either full length or C-terminally truncated Rrp47 proteins were transformed with plasmids encoding *GAL*-driven GST-$Rrp6_{NT}$ proteins. Total RNA was analysed in parallel with wildtype and *rrp47Δ* strains before and after induction of GST-$Rrp6_{NT}$. Northern blot

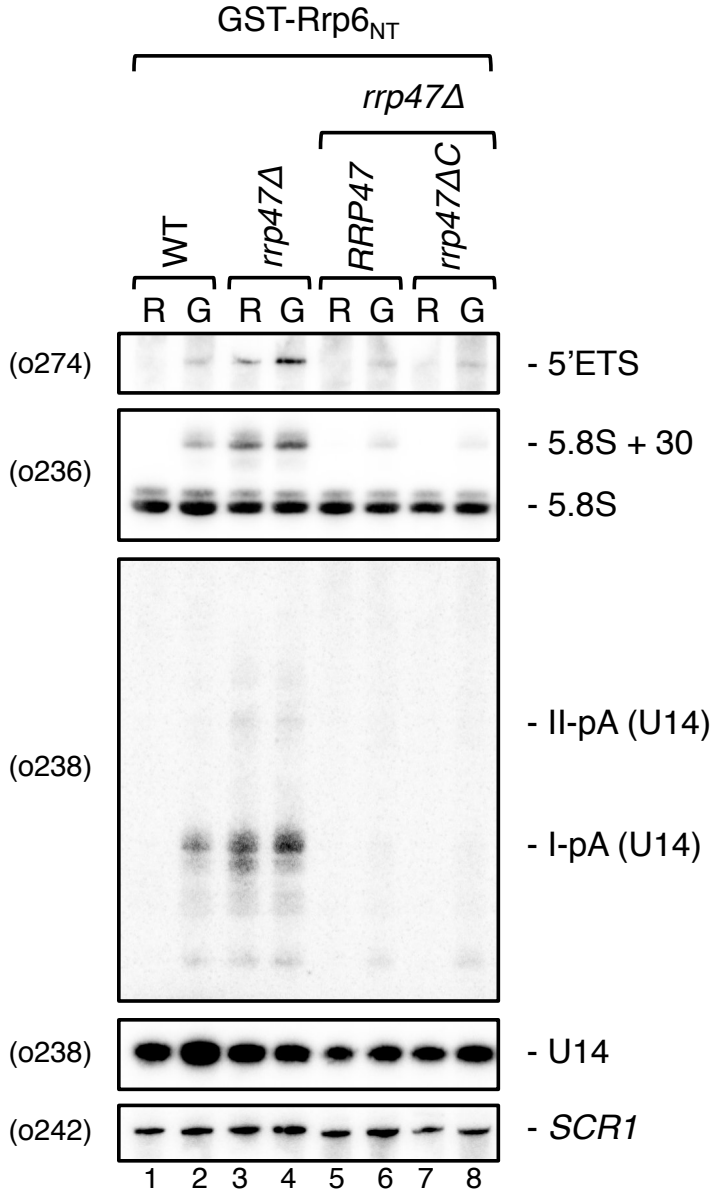

Figure 3.11. Rrp47 and Rrp47ΔC proteins are functional when segregated from Rrp6. Northern analyses of $Rrp6_{NT}$ induction in wildtype, *rrp47Δ* and *rrp47Δ* strains transformed with plasmids encoding *RRP47* or *rrp47ΔC* alleles. Cells were harvested in during growth in raffinose (lanes labeled R) or galactose (lanes labeled G)-based medium. RNA was fractionated through an 8% denaturing acrylamide gel and analysed by Northern blot hybridisation using probes complementary to the RNAs indicated. To compare relative levels of mature and 3' extended forms of U14 snoRNA, two images are shown of the same hybridisation. Dispersed bands labeled I-pA and II-pA correspond with pre-snoRNAs that are polyadenylated at termination sites I or II respectively. *SCR1* was used as a loading control.

hybridisation analyses of 5.8S rRNA revealed that both full length Rrp47 and truncated Rrp47ΔC proteins retained function when segregated from Rrp6. A mild accumulation of 3' extended 5.8S + 30 pre-rRNA species was observed in *rrp47ΔC* ffmutants upon $Rrp6_{NT}$ induction. However, the levels of this processing intermediate were markedly less than those observed in the *rrp47Δ* mutants (Figure 3.11 compare lanes 8 with 3-4). Additionally, the *rrp47ΔC* mutant showed a lower accumulation of 5' external transcribed spacer (5'ETS) and 3' extended snoRNAs when overexpressing GST-$Rrp6_{NT}$ in comparison to levels detected in the *rrp47Δ* mutant. In general, the *rrp47ΔC* and *RRP47* complemented strains showed comparably mild *rrp47Δ*-phenotypes upon $Rrp6_{NT}$ expression. This suggests that both full length and C-terminally truncated Rrp47 proteins are functional when segregated from Rrp6 in otherwise wildtype cells.

3.2.9. Expression of $Rrp6_{NT}$ is not sufficient to complement the *rrp6Δ mpp6Δ* or *rrp6Δ rex1Δ* synthetic lethality

Expression levels of Rrp47 are dramatically reduced in the absence of Rrp6. It has previously been reported that the stability of Rrp47 is dependent upon its physical interaction with the N-terminus of Rrp6 (Feigenbutz et al., 2013b). Both *rrp6Δ* and *rrp47Δ* alleles are synthetic lethal in combination with *mpp6Δ* or *rex1Δ* mutants. One possibility for the basis of the synthetic lethality in *rrp6Δ mpp6Δ* and *rrp6Δ rex1Δ* mutants is that the protein levels of Rrp47 are reduced in the absence of Rrp6. Exogenous expression of the N-terminal domain of Rrp6 is sufficient to maintain stable expression of Rrp47 *in vivo* in the absence of Rrp6 (Section 3.2.7. and Feigenbutz et al. 2013). If the synthetic lethality of *rrp6Δ mpp6Δ* and *rrp6Δ rex1Δ* strains is due to the indirect loss of Rrp47 protein levels, expression of $Rrp6_{NT}$ should complement the double mutants.

To address this, plasmid shuffle strains were generated to assay if overexpression of $Rrp6_{NT}$ could complement the synthetic lethality observed in *rrp6Δ mpp6Δ* and *rrp6Δ rex1Δ* strains. As shown in Figure 3.9, expression of the GST-$Rrp6_{NT}$ protein increases the levels of Rrp47 in *rrp6Δ* mutants. The N-terminal domain of Rrp6

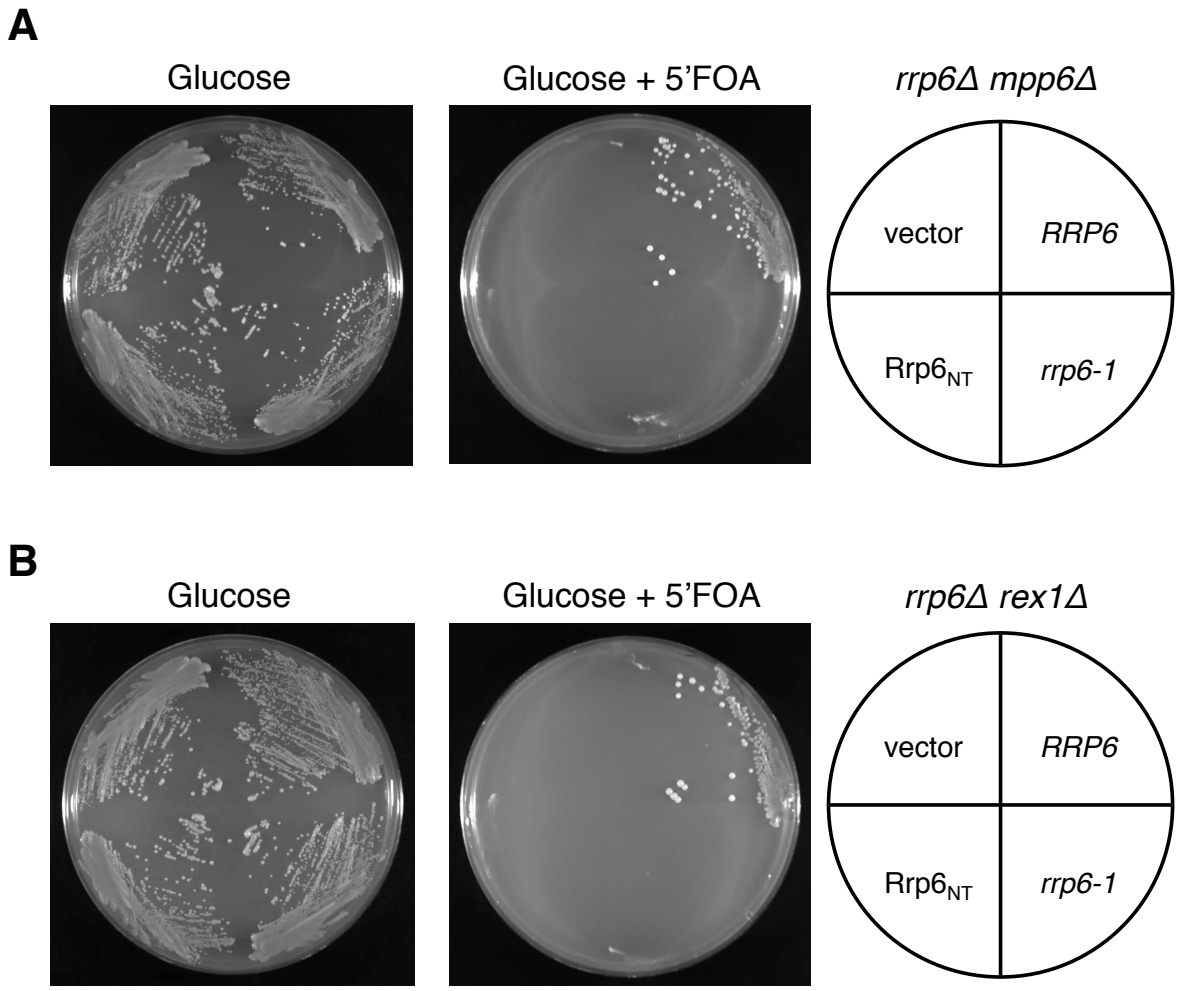

Figure 3.12. Expression of $Rrp6_{NT}$ is not sufficient to complement the *rrp6Δ mpp6Δ* or *rrp6Δ rex1Δ* synthetic lethality. Plasmid shuffle assay to test complementation *rrp6Δ mpp6Δ* or rrp6*Δ rex1Δ* synthetic lethality by the *rrp6-1* allele or expression of the $Rrp6_{NT}$ domain. **(A)** Plasmids encoding Rrp6 (p428), rrp6-1 (p430) and $Rrp6_{NT}$ (p432) were transformed into a *rrp6Δ mpp6Δ* strain harboring a wildtype *RRP6* allele on a *URA3* vector. A parallel transformation was carried out with an empty vector (pTL26). Strains were assayed for the ability to lose the *URA3* maintenance plasmid by streaking onto minimal media containing 5'FOA. **(B)** Plasmids encoding Rrp6 (p428), rrp6-1 (p430) and $Rrp6_{NT}$ (p432) were transformed into a *rrp6Δ rex1Δ* strain harboring a wildtype *RRP6* allele on a *URA3* vector. A parallel transformation was carried out with an empty vector (pTL26). Strains were assayed for the ability to lose the *URA3* maintenance plasmid by streaking onto minimal media containing 5'FOA.

does not contain exonuclease or exosome-binding regions of Rrp6 and therefore is assumed to have no other function than to bind and stabilise Rrp47.

Yeast *rrp6Δ mpp6Δ* and *rrp6Δ rex1Δ* strains were generated through targeting the *kanMX4* disruption cassette to *MPP6* and *REX1* loci in an *rrp6Δ::TRP1* strain bearing a *URA3* plasmid encoding zz-Rrp6. Genomic DNA was isolated from *mpp6Δ::kanMX4* and *rex1Δ::kanMX4* strains and PCR was used to amplify the disruption cassettes using outlying *MPP6* and *REX1* specific primers (o595 + o599 and o468 + o512 respectively). The amplicons were used to transform the *rrp6Δ* strain complemented by exogenous expression of zz-Rrp6. Disruption of *MPP6* and *REX1* loci was confirmed by PCR using outlying primers.

Yeast *rrp6Δ mpp6Δ* and *rrp6Δ rex1Δ* plasmid shuffle strains were transformed with plasmids encoding zz-tagged Rrp6 constructs and assayed for growth on media containing 5'FOA to screen for complementation of synthetic lethality. Plasmids bearing wildtype *RRP6* alleles allowed for complementation of the *rrp6Δ mpp6Δ* and *rrp6Δ rex1Δ* double mutants and were viable on media containing 5'FOA (Figure 3.12. A-B) No complementation was observed upon transformation with a plasmid encoding the N-terminal domain of Rrp6 ($Rrp6_{NT}$) in both mutants. Additionally, a plasmid encoding a catalytically inactive D238N Rrp6 mutant (*rrp6-1*) was not sufficient to allow growth on 5'FOA in both mutants.

These results show that the synthetic lethality observed in *rrp6Δ mpp6Δ* and *rrp6Δ rex1Δ* strains is not dependent on expression levels of Rrp47. Furthermore, the catalytic activity of Rrp6 is required in the absence of Mpp6 or Rex1.

3.2.10. Analysis of $Rrp6_{NT}$ overexpression in *mpp6Δrrp47ΔC* and *rex1Δrrp47ΔC* mutants

A block of growth was observed in conditional *mpp6Δ rrp47ΔC* and *rex1Δ rrp47ΔC* mutants by inducing overexpression of the N-terminus of Rrp6. To address the loss-of-growth phenotypes, changes in the levels of specific RNA

were analysed from the aforementioned strains upon transfer from permissive to non-permissive conditions by northern blot hybridisation.

Exosome mutants, including *rrp6Δ, rrp47Δ* and *mpp6Δ* strains, have previously been shown to stabilise a subset of non coding RNAs known as cryptic unstable transcripts (CUTs) (Milligan et al., 2008; Wyers et al., 2005). CUTs are barely detectable by northern hybridisation analysis in wildtype strains due to rapid degradation aided by the Exosome. To aid detection of a model CUT, *NEL025c*, a 2μ high-copy number plasmid encoding the *NEL025c* gene was transformed into the analysed strains. Plasmid-borne expression of the *NEL025c* gene has previously been shown to recapitulate the expression and degradation pattern of endogenous *NEL025c* transcript (Thiebaut et al., 2006). In Section 3.2.11, RNA analysis of wildtype cells overexpressing *NEL025c* shows that the transcript levels are still barely detectable.

To investigate the basis for the conditional lethal growth phenotype, *mpp6Δ rrp47ΔC* and *rex1Δ rrp47ΔC* strains bearing plasmids encoding *GAL*-regulated GST or GST-Rrp6$_{NT}$ proteins were grown in synthetic raffinose-based media before shifting to galactose-based media. All analysed strains also bore a 2μ high-copy number plasmid encoding *NEL025c* (p532). Cells were harvested during logarithmic growth in raffinose media and after every cell doubling in galactose media. The growth rate of both mutants expressing GST-Rrp6$_{NT}$ slowed considerably when shifted from permissive raffinose to non-permissive galactose based media in comparison to cells expressing GST (Figure 3.13. A-B). The *mpp6Δ rrp47ΔC* mutant showed a slowed growth rate before the fourth doubling after induction of the Rrp6$_{NT}$ domain in galactose-based media (Figure 3.13. A). Equivalent strains expressing the GST domain alone grew at a constant rate with a doubling time of ~ 4 hours. The *rex1Δ rrp47ΔC* mutant showed a more rapid reduction in growth upon expression of the Rrp6$_{NT}$ domain with a strong growth defect observable before two doublings in galactose-based media (Figure 3.13. B). Strains lacking Rex1 grew considerably slower in galactose-based media as observed in previous analysis (Garland et al., 2013).

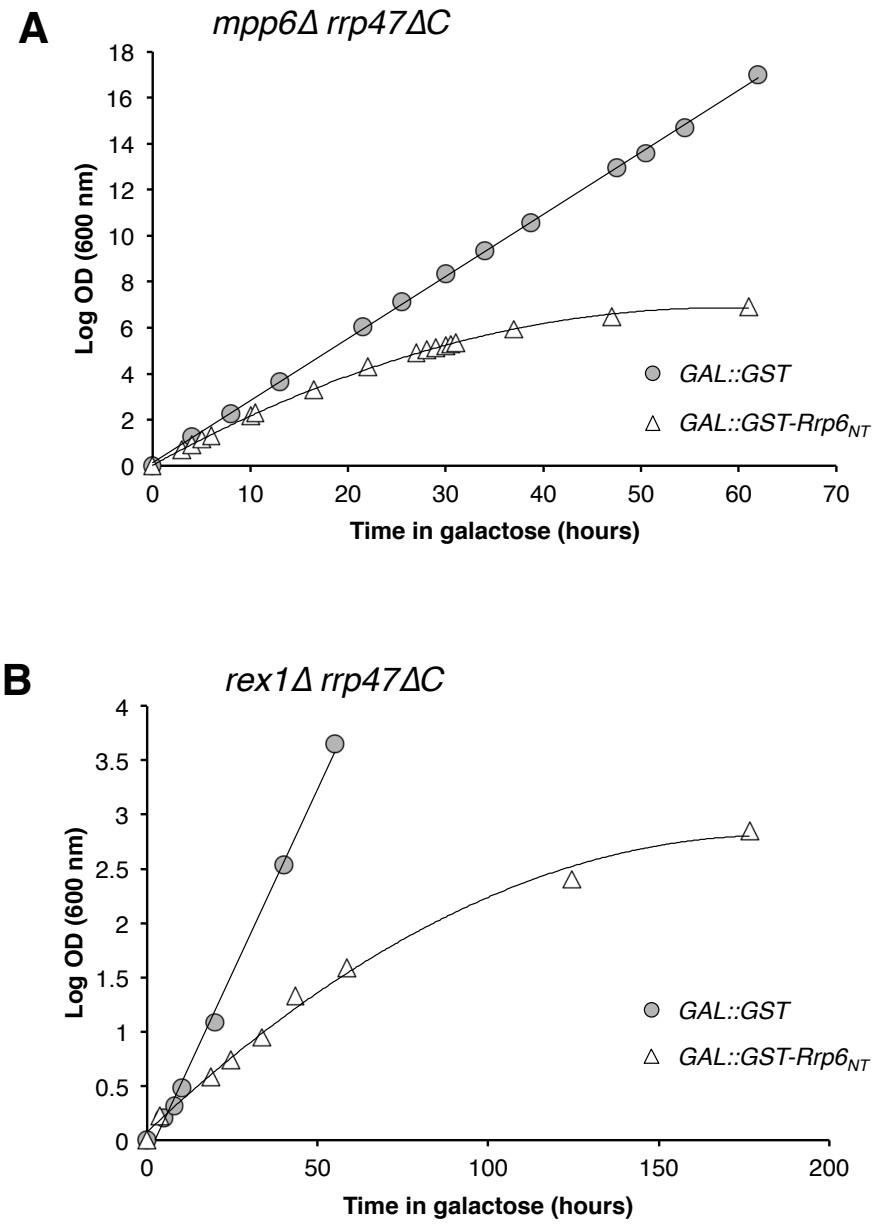

Figure 3.13. Growth rate of *mpp6Δ rrp47ΔC* and *rex1Δ rrp47ΔC* mutants upon $Rrp6_{NT}$ induction. Growth rate assays of **(A)** *mpp6Δ rrp47ΔC* and **(B)** *rex1Δ rrp47ΔC* strains after induction of GST or GST-$Rrp6_{NT}$. Cultures were grown in raffinose-based medium at 30°C to mid-log phase before shifting to galactose-based medium. Strains were kept in early exponential growth by dilution with pre-warmed media. The cumulative increase in OD_{600} is expressed as log_2 values.

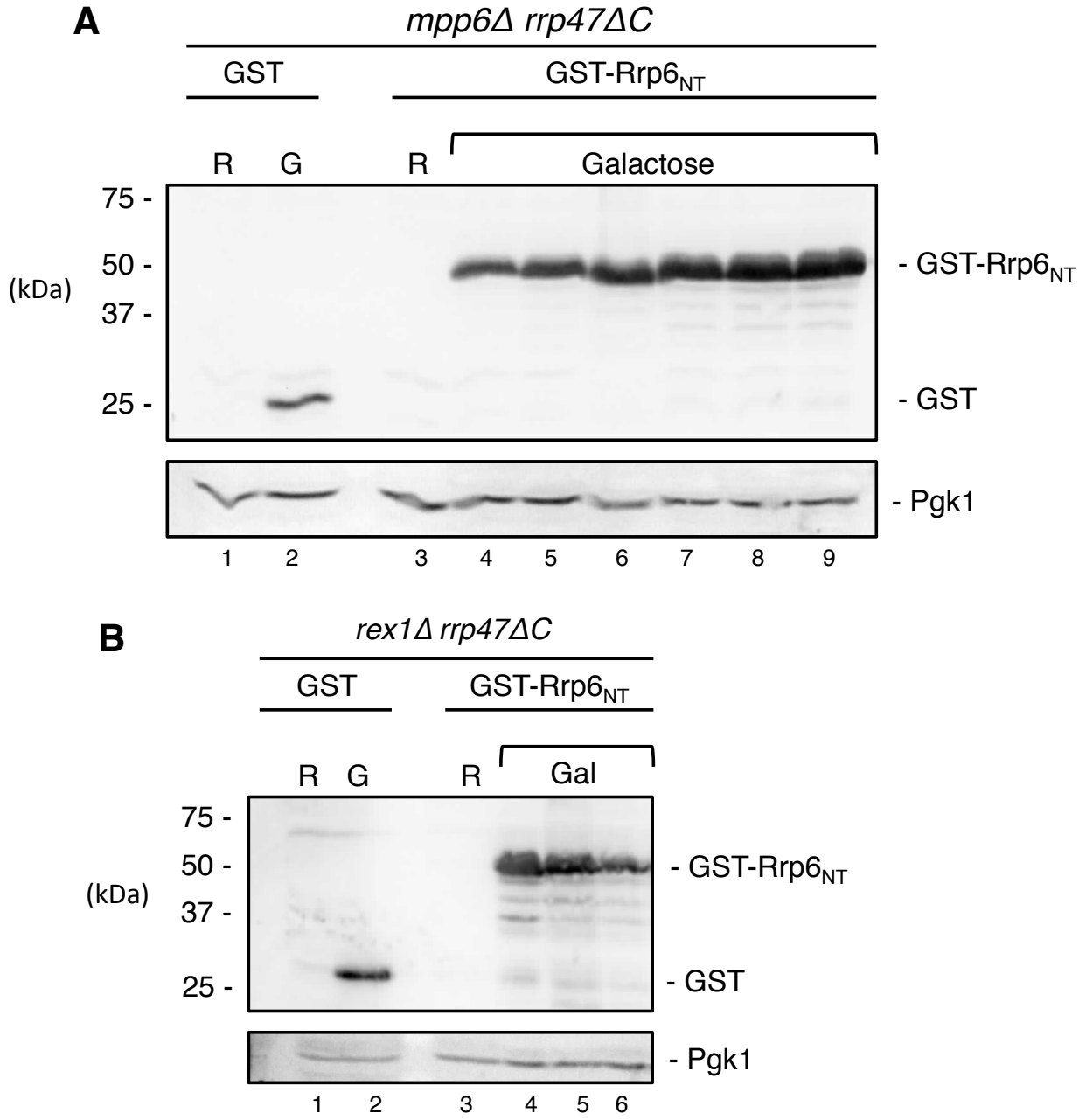

Figure 3.14. Induction of the GST-Rrp6$_{NT}$ protein in *mpp6Δ rrp47ΔC* and *rex1Δ rrp47ΔC* mutants. Western blot analysis of **(A)** *mpp6Δ rrp47ΔC* and **(B)** *rex1Δ rrp47ΔC* mutants upon induction of GST or GST-Rrp6$_{NT}$. Cells were harvested during growth in raffinose based medium (R) and at each doubling of cell density after transfer to galactose based medium (G). Lysates were fractionated by SDS PAGE and analysed by western blot using an antibody against the GST domain (*upper* panel). An antiserum against Pgk1 was used as a loading control (*lower* panel).

Cells harvested from raffinose and galactose time points were assayed by western blot analysis to detect the induction of GST or GST-Rrp6$_{NT}$ proteins. Lysates from cells harvested pre- and post-induction of *GAL*-regulated proteins were fractionated by SDS PAGE and analysed by western blotting using the GST antibody (Figure 3.14. A-B). No detectable expression of GST or GST-Rrp6$_{NT}$ was observed in cells grown in raffinose-based synthetic media (Figure 3.14. A and B, lanes 1 and 3). Expression of GST-Rrp6$_{NT}$ is tolerated in *mpp6Δ rrp47ΔC* strains and is relatively stable throughout the time course (Figure 3.14.A, lanes 4-9). The expression of GST-Rrp6$_{NT}$ decreases slightly after three cell doublings in the *rex1Δ rrp47ΔC* mutant upon shifting to galactose-based media (Figure 3.14.B, lanes 4-6). The stability of the fusion protein may decrease over time due to the long induction and doubling time of the *rex1Δ rrp47ΔC* mutant. Nevertheless, the Rrp6$_{NT}$ protein is still highly overexpressed.

Total RNA was isolated from cells harvested at every cell doubling timepoint and extensive northern blot hybridisation analyses were carried out to investigate the effects on the levels of known exosome target transcripts.
In the absence of either Mpp6 or Rrp47, cells have previously been reported to accumulate cryptic unstable transcripts (CUTs) including *NEL025c*, a well characterised CUT transcript (Milligan et al., 2008). Hybridisation analysis of RNA extracted from the *mpp6Δ rrp47ΔC* mutant revealed a striking accumulation of the *NEL025c* transcript from early time points upon Rrp6$_{NT}$ induction (Figure 3.15, lanes 5-10). This transcript was barely detectable in equivalent control samples expressing the GST domain (lane 2). *NEL025c* transcripts are heterogeneous due to 3' polyadenylation and therefore appear as a smear upon northern blot hybridisation. The degree of heterogeneity of the *NEL025c* CUT observably decreases in the later time points of the time course, corresponding to slowed growth. A similar accumulation of the *IGS1-R* CUT (also known as NTS1) was observed in later time points in the *mpp6Δ rrp47ΔC* mutant (Lanes 8-10). This non-coding RNA arises from pervasive transcription of intergenic regions between ribosomal DNA (rDNA) tandem repeats and has previously been characterised to have 3' heterogeneity due to polyadenylation analogous to the *NEL025c* transcript (Houseley et al., 2007; Vasiljeva et al., 2008b)

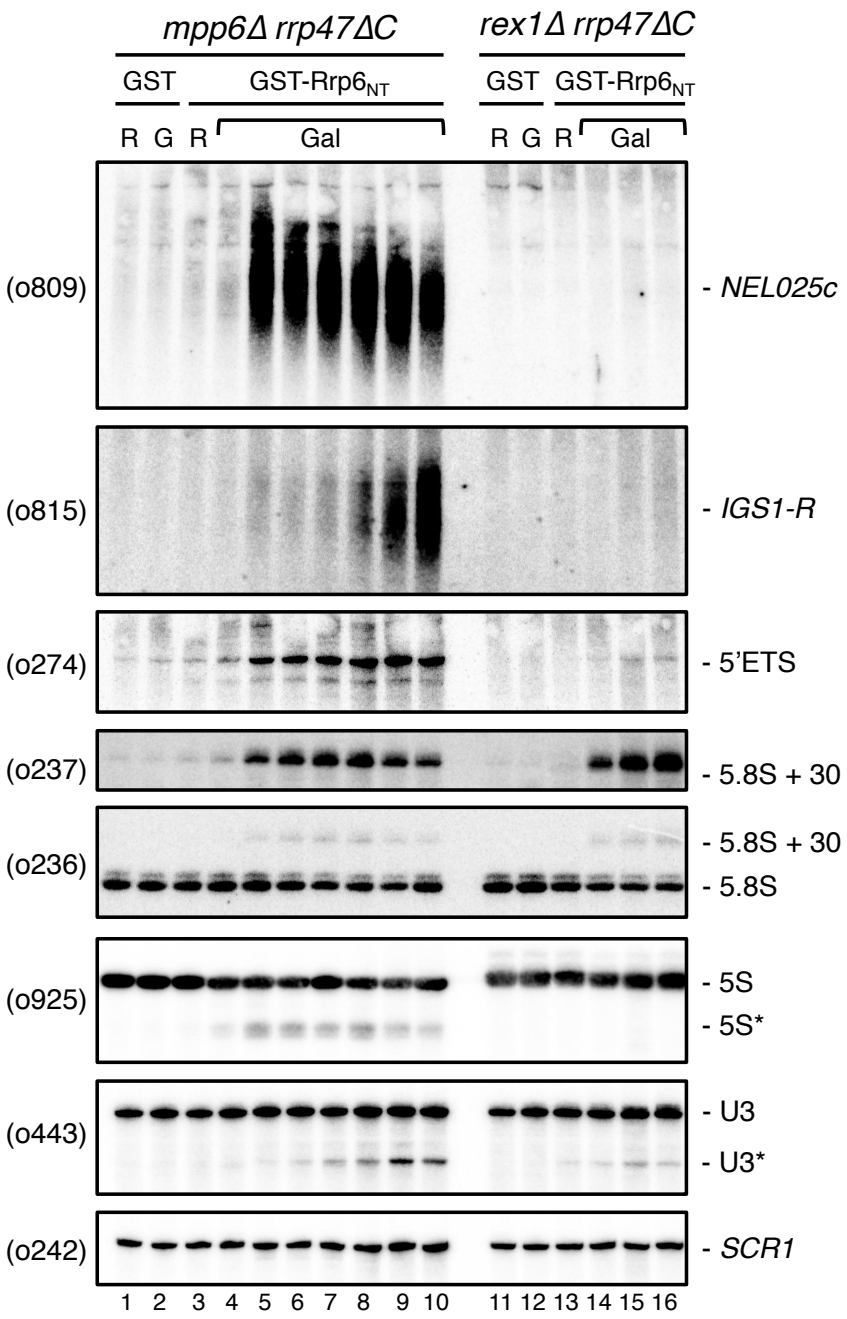

Figure 3.15. Northern blot analysis of conditional *mpp6 rrp47* and *rex1 rrp47* mutants. Total RNA was isolated from *mpp6Δ rrp47ΔC* and *rex1Δ rrp47ΔC* mutants expressing GST-Rrp6$_{NT}$ from the *GAL* promoter. Cells were harvested during growth in raffinose based medium (R) and at each doubling of cell density after transfer to galactose based medium (G). RNA was also isolated from strains expressing *GAL*-regulated GST in raffinose and galactose- based medium (lanes 1, 2, 11 and 12). RNA was fractionated through 8% polyacrylamide gels containing 50% urea and analysed by northern blot hybridisation using oligonucleotide probes as indicated. Asterisks (*) denote truncated transcripts.

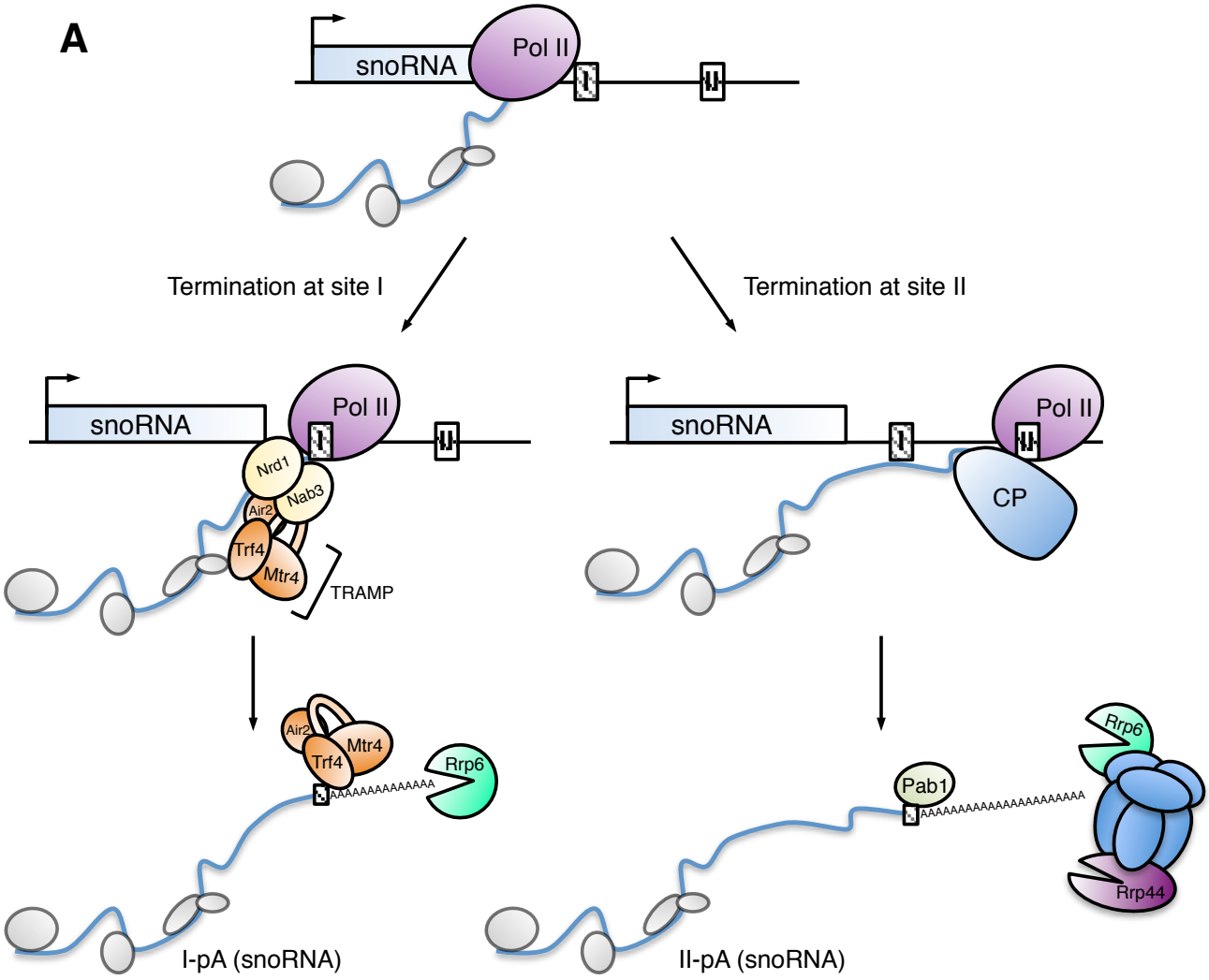

Figure 3.16.A. Model of transcriptional termination, polyadenylation and termination of snoRNAs. The major pathway of snoRNA termination is at the Nrd1/Nab3-dependent site I. Released pre-snoRNAs undergo multiple rounds of polyadenylation by Trf4/5 and exonucleolytic digestion by Rrp6 to generate mature snoRNAs. Failsafe termination occurs at a distal site II by cleavage polyadenylation pathways. Site II-termination pre-snoRNAs are exclusively polyadenylated by Pab1 and undergo further processing or complete degradation by the exosome/Rrp6. Adapted from Grzechnik P et al (2008).

B

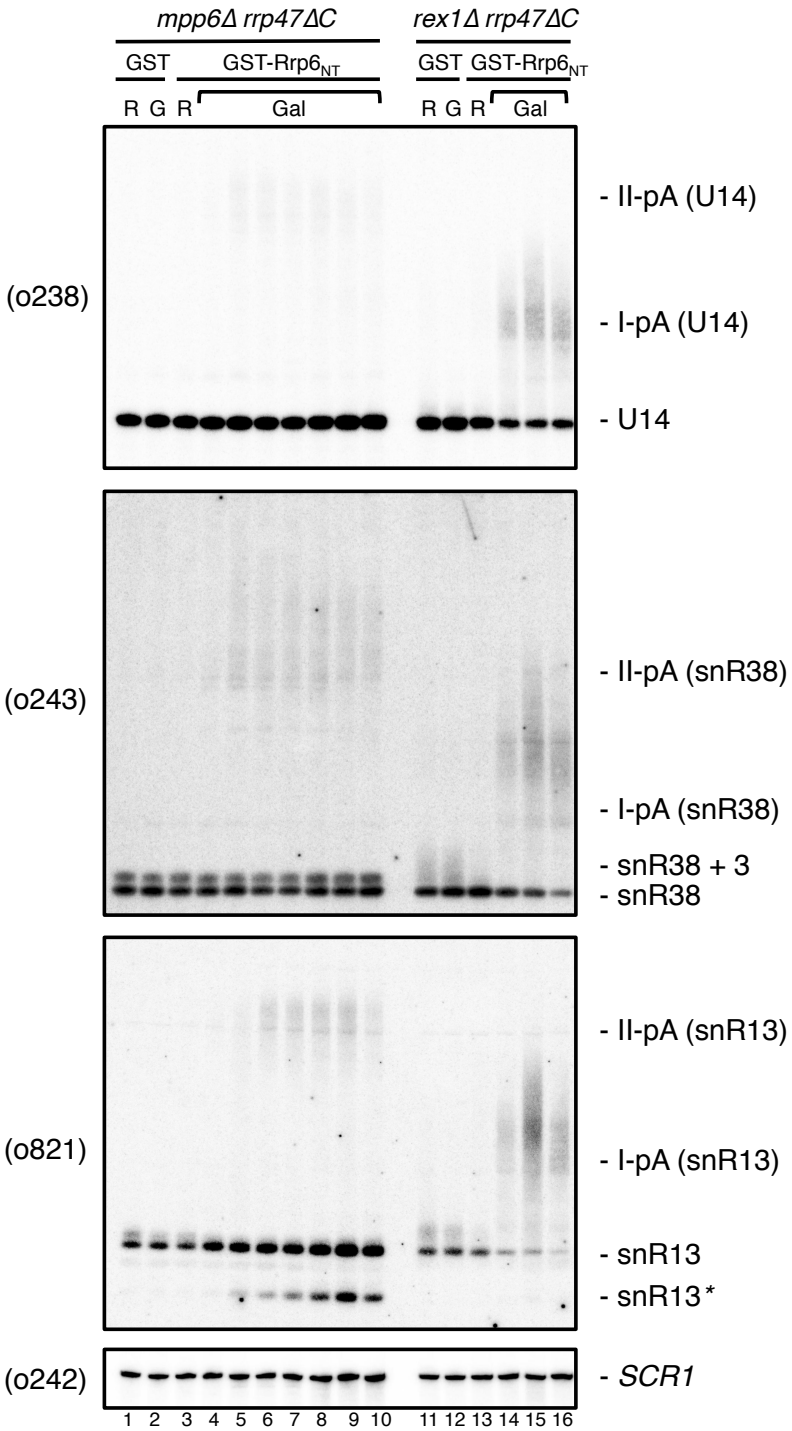

Figure 3.16.B Northern blot analysis of box C/D snoRNAs in conditional *mpp6 rrp47* and *rex1 rrp47* mutants. RNA isolated as described in Figure 3.15 was resolved through denaturing polyacrylamide gels and analysed by northern blot hybridisation using indicated probes. Dispersed bands labeled I-pA and II-pA correspond with pre-snoRNAs that are polyadenylated at termination sites I or II respectively. Asterisks (*) denote truncated transcripts. *SCR1* was used as a loading control.

The *mpp6 rrp47* conditional mutant showed a strong accumulation of the 5'external transcribed spacer (5'ETS) region generated from A_0 cleavage of the 35S pre-rRNA. The 5'ETS RNA is a byproduct of rRNA processing and undergoes rapid turnover in wildtype cells. Exosome mutants show defects in the turnover of 5'ETS with stronger accumulations reported in cells depleted of core-exosome or TRAMP components (Allmang et al., 1999a; de la Cruz et al., 1998). Similarly, defects in the degradation of truncated fragments of 5S rRNA, U3 and snR13 snoRNAs (5S*, U3* and snR13* respectively) are observed in the *mpp6Δ rrp47ΔC* mutant upon $Rrp6_{NT}$ induction (Figure 3.15 and 3.16). The accumulation of these species will be discussed further below.

The *rex1Δ rrp47ΔC* mutant exhibited less striking RNA phenotypes in comparison to the *mpp6Δ rrp47ΔC* mutant upon induction of the GST-$Rrp6_{NT}$ protein, yet growth was more rapidly impeded. There was no observable accumulation of the *NEL025c* or *IGSR-1* CUTs throughout the time-course. A mild accumulation of 5'ETS and truncated U3 (U3*) was observed in later time-points (Lanes 14-16), but the effect was not as pronounced as the *mpp6Δ rrp47ΔC* mutant. Previous analyses have shown Rex1 to be required for 3' end maturation of 5S rRNA and *rex1Δ* mutants exhibit an ~3nt extended 5S species (Piper et al., 1983; van Hoof et al., 2000b). This 5S processing phenotype was observed in the *rex1Δ rrp47ΔC* mutant but induction of $Rrp6_{NT}$ had no further effect on the 5S rRNA. Both *mpp6 rrp47* and *rex1 rrp47* conditional mutants exhibited an accumulation of the 5.8S + 30 rRNA processing intermediate and corresponding decrease of mature 5.8S upon $Rrp6_{NT}$ induction consistent with a loss of Rrp47 function (Mitchell et al., 2003)

Hybridisation with probes against box C/D snoRNAs revealed distinct phenotypes in the *mpp6Δ rrp47ΔC* and *rex1Δ rrp47ΔC* mutants upon $Rrp6_{NT}$ induction (Figure 3.16.B). The *mpp6* mutant showed an accumulation of heter ogeneous extended forms of U14, snR38 and snR13 with no effect on mature snoRNAs (Lanes 4-10). However, the *rex1* mutant showed an accumulation of shorter extended forms of U14, snR38 and snR13 with a corresponding loss of mature snoRNA (11-16). Transcriptional termination of snoRNAs is dependent on a

bipartite signal at the 3' region of the alleles consisting of a proximal Nrd1/Nab3 binding region (site I) and a more distal 'failsafe' cleavage/polyadenylation signal (site II) (Steinmetz and Brow, 2003) (Figure 3.16.A). Both termination events are followed by polyadenylation to target the transcript for either 3' processing or degradation by the exosome respectively (Steinmetz et al., 2001). Nrd1-dependent termination at site I, and subsequent Trf4-dependent polyadenylation results in productive 3'-end processing of snoRNAs. Termination events at site II are consistent with a loss of Nrd1-dependent termination and result in aberrant snoRNAs. Site II transcripts are suggested to be targeted by surveillance pathways for rapid degradation by the exosome to prevent transcriptional interference with adjacent downstream promoters (Steinmetz et al., 2001). Heterogeneous transcripts, polyadenylated at sites I and II (pA-I and pA-II, respectively), are accumulated in core-exosome, *rrp6,* TRAMP and NNS mutants (Allmang et al., 1999a; Mitchell et al., 2003; van Hoof et al., 2000a; Vasiljeva and Buratowski, 2006).

The *mpp6Δ rrp47ΔC* mutant accumulated site II terminated snoRNAs upon $Rrp6_{NT}$ expression. The accumulation of II-pA snoRNAs is consistent with a loss of degradation pathways and corroborates the accumulation of aberrant transcripts noted above. The levels of mature U14 and snR38 remain relatively unchanged in the *mpp6* mutant yet the levels of snR13 appear to increase in later time points. This suggests that normal productive snoRNA processing pathways are present and do not require the function of Mpp6.

A prominent depletion of mature snoRNAs coupled with an accumulation of extended heterogeneous snoRNAs was observed in the *rex1Δ rrp47ΔC* mutant upon induction of the $Rrp6_{NT}$ protein (Figure 3.16.B, lanes 11-16). The extended forms of U14, snR38 and snR13 correspond to transcripts terminated at the Nrd1-dependent site I (marked as I-pA) and have been previously characterised as 3' extended precursor transcripts that undergo 3'-end exonuclease processing to generate mature snoRNAs. This processing was previously attributed to Rrp6, yet these data suggests that the 3'-5' exonuclease activity of Rex1 may also contribute to redundant 3' processing pathways of snoRNAs. The final step in 3'

end processing of box C/D snoRNAs requires the catalytic activity of Rrp6 with the co-operation of Rrp47. Functional analysis of *rrp47* mutants revealed that the C-terminus of the protein is required for this process. Cells expressing Rrp47ΔC show the accumulation of short 3' extensions of 1-6 nucleotides (Costello et al., 2011; Mitchell et al., 2003). In the case of snR38, these can be resolved as mature snR38 and snR38 + 3 species on 8% polyacrylamide gels as observed in the *mpp6Δ rrp47ΔC* mutant (Figure 3.16.B., lanes 1-10). However, expression of Rrp47ΔC in a *rex1Δ* mutant shows an accumulation of short heterogeneous snoRNAs (Figure 3.16.B, lanes 11-12). These species are lost upon $Rrp6_{NT}$ induction in concordance with a block in a prior processing step.

A number of truncated transcripts were identified from northern blot hybridisation analysis of the *mpp6 rrp47* and *rex1 rrp47* conditional mutants including U3*, 5S* and snR13*. Similar transcripts have previously been identified and characterised in exosome mutants with U3* and snR13* transcripts being truncated from the 5' end and 5S* truncated from the 3' end (Kadaba et al., 2006; Kufel et al., 2000; Rasmussen and Culbertson, 1998). To confirm these species, northern blot hybridisation was carried out using probes complementary to the 3' ends of the transcripts (Figure 3.17). The U3* and snR13* transcripts were still detectable upon hybridisation with the 3' end probes in the *mpp6 rrp47* and *rex1 rrp47* conditional mutants, therefore these species are truncated at the 5' end in agreement with previous studies. Additionally, the 5S* truncated species was not detectable upon hybridisation with a 3' end probe showing that these transcripts are truncated at the 3' end, also in concordance with previous observations in *rrp6* and *trf4* mutants(Kadaba et al., 2006). These transcripts are suggested to be aberrant RNA species that are targeted for rapid degradation by the exosome.

These observations suggest a widespread loss of RNA surveillance and degradation pathways in the *mpp6Δ rrp47ΔC* mutant upon $Rrp6_{NT}$ overexpression. This results in the accumulation of RNAs normally targeted for rapid degradation including CUTs, aberrant ncRNAs, read-through snoRNA transcripts and rRNA processing byproducts. The block in growth could be attributed to the inhibition of RNA surveillance and CUTs degradation. However, it

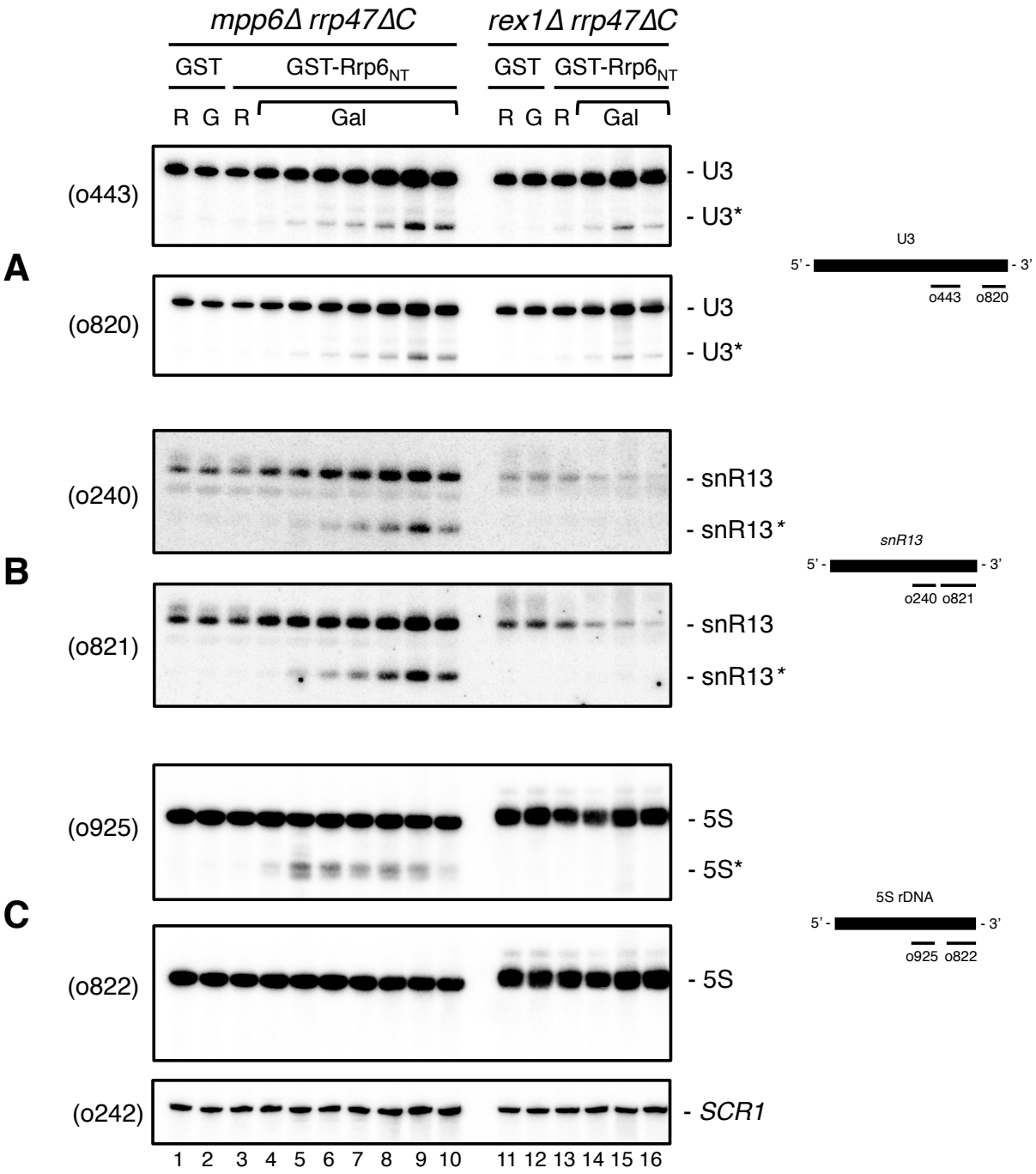

Figure 3.17. Northern blot analysis of truncated RNA species in conditional *mpp6 rrp47* and *rex1 rrp47* mutants. RNA, prepared as described in Figure 3.15 was resolved through 8% polyacrylamide gels containing 50% urea and analysed by northern blot hybridisation using oligonucleotide probes as indicated. Probes were complementary to either the center or 3' end region of **(A)** U3, **(B)** snR13 or **(C)** 5S transcripts as indicated on the schematics. Asterisks (*) denote truncated transcripts. *SCR1* was used as a loading control

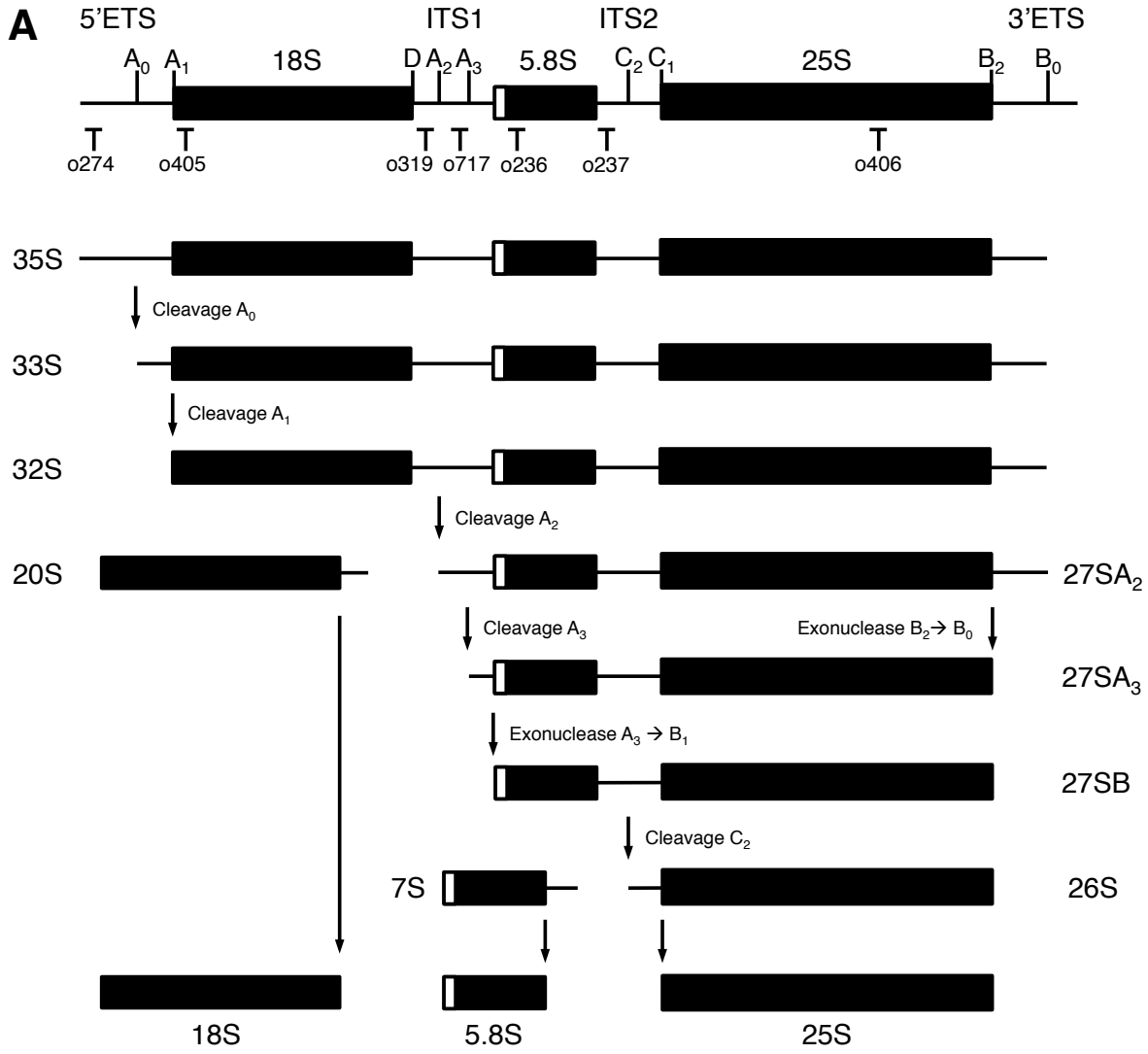

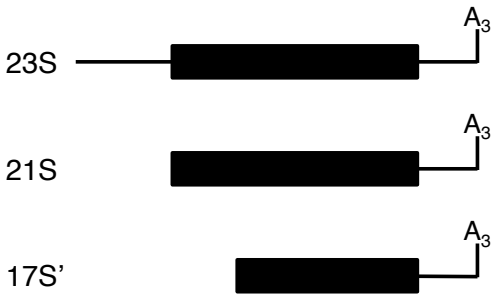

Figure 3.18.A. The yeast pre-rRNA processing pathway. Summary of 35S processing including intermediate and aberrant pre-rRNA species. The 18S, 5.8S and 25S rRNA are separated by internal transcribed spacers (ITS1, ITS2) and flanked by external transcribed spacers (5'ETS, 3'ETS). Sites complementary to probes used in this study are indicated. Endonucleolytic cleavage and exonucleolytic steps are indicated at processing sites. The aberrant 23S and 25S pre-rRNA species are generated by premature cleavage at site A_3. The aberrant 17S' species arises from 5' degradation of pre-rRNA fragments generated as a result of a block in ITS1 processing. Adapted from Mitchell *et al* (2003). Sites within the 35S pre-rRNA complementary to oligonucleotide probes are indicated.

B

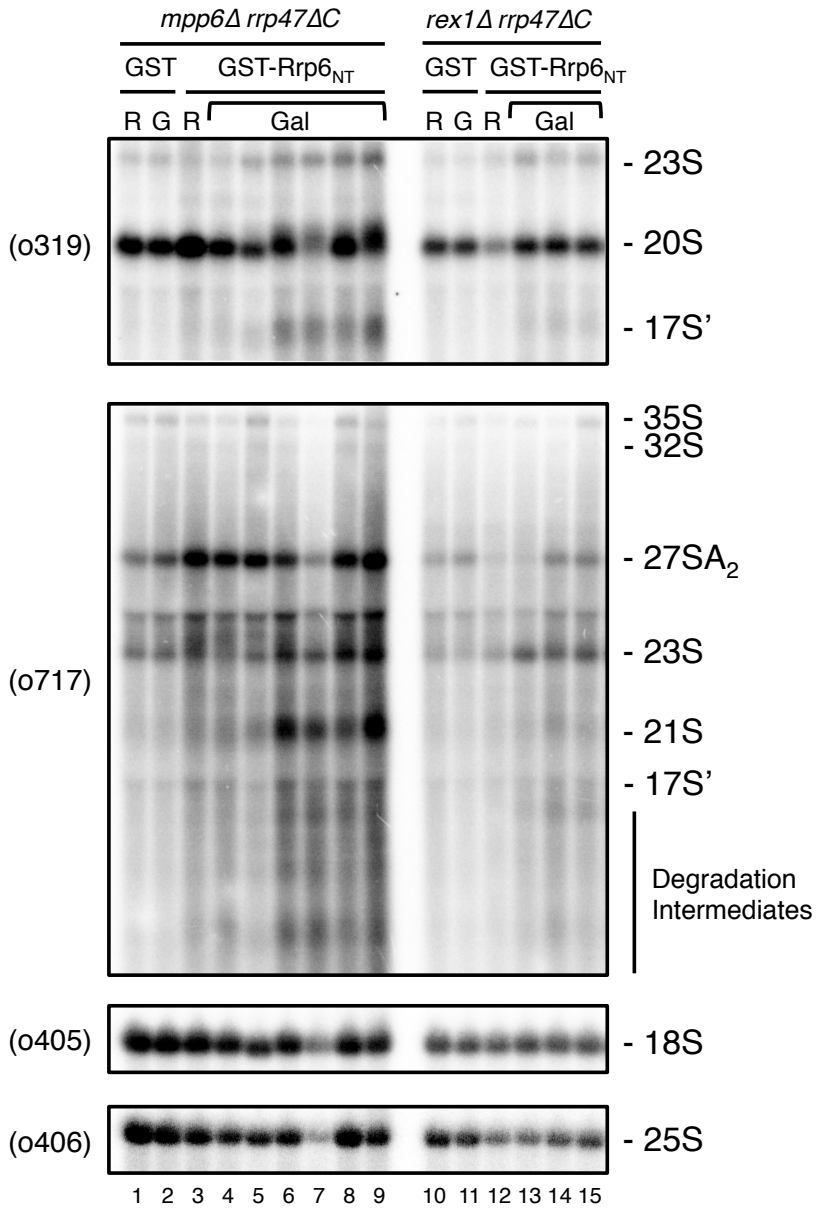

Figure 3.18.B. Analysis of pre-ribosomal rRNA species in conditional *mpp6 rrp47* and *rex1 rrp47* mutants. Total RNA was isolated from *mpp6 rrp47* and *rex1* rrp47 mutants as described in Figure 3.15. Samples containing 10µg RNA were glyoxal denatured before fractionating by electrophoresis on a 1.2% agarose gel and analysed by northern blot hybridisation using labeled oligonucleotides as indicated. 18S and 25S served as loading controls.

is not as clear as to why *rex1Δ rrp47ΔC* strains stop growing upon $Rrp6_{NT}$ induction. The *rex1 rrp47* conditional mutant showed a block in 3'-end processing of box C/D snoRNAs resulting in the accumulation of 3'-extended pre-snoRNAs and a corresponding loss of mature transcripts. The function of snoRNAs is important in the biogenesis of ribosomes by guiding modifications of pre-rRNA. A depletion of mature snoRNA may have a critical impact on the levels of mature rRNA. The conditional *rex1 rrp47* mutant showed a depletion of U14, snR38 and snR50 box C/D snoRNAs which target sites in 18S and 25S rRNA (Li et al., 1990; Lowe and Eddy, 1999). To investigate the effects on larger pre-rRNA species in *mpp6Δ rrp47ΔC* and *rex1Δ rrp47ΔC* upon $Rrp6_{NT}$ induction, agarose gel northern analyses were carried out using RNA from the samples described above. Northern blots were analysed with probes complimentary to known pre-rRNA species (Figure 3.18.A). The *mpp6 rrp47* mutant showed an accumulation of pre-rRNA species upon induction of $Rrp6_{NT}$ including 23S, 21S and 17S' transcripts along with a number of smaller uncharacterised degradation intermediates (Figure 3.18.B, lanes 1-9). These species were previously characterised in strains lacking Rrp6 (Allmang et al., 2000). Some of these effects were previously reported in RNA analysis of a conditional *mpp6 rrp47* mutant albeit not as detailed (Milligan et al., 2008). The levels of mature 18S and 25S remain relatively unchanged in the *mpp6Δ rrp47ΔC* samples (Figure 3.18 with the exception of lane 7 due to an error in loading. The accumulation of aberrant pre-rRNA species in the *mpp6Δ rrp47ΔC* mutant upon $Rrp6_{NT}$ induction is consistent with previous observations described above.

The *rex1Δ rrp47ΔC* mutant showed mild accumulation of pre-rRNA degradation intermediates upon expression of the $Rrp6_{NT}$ protein (lanes 10-15) but not to the extent of the *mpp6 rrp47* mutant. Depletion of essential snoRNAs such as U3 or U14 results in a loss of 18S rRNA. However, no effect on mature 18S or 25S rRNA was observed in the *rex1 rrp47* mutant.

3.2.11 Comparing conditional *mpp6 rrp47* and *rex1 rrp47* mutant phenotypes with RNA processing and degradation mutants

Northern blot hybridisation of the *mpp6Δ rrp47ΔC* mutant upon $Rrp6_{NT}$ overexpression exhibited a block in the degradation of RNA surveillance substrates including CUTs, aberrant 5S, snoRNAs and pre-rRNA species. These phenotypes have been extensively described previously in *rrp6, nrd1* and TRAMP complex mutants (Allmang et al., 1999a; Briggs et al., 1998; LaCava et al., 2005; Thiebaut et al., 2006; van Hoof et al., 2000a). Similarly, species observed in the *rex1Δ rrp47ΔC* mutant upon $Rrp6_{NT}$ induction have previously been identified in strains lacking Rrp6 (Allmang et al., 1999a). The levels of these RNA transcripts were compared in *mpp6 rrp47* and *rex1 rrp47* conditional double mutants with the corresponding single mutants. Additionally, these strains were compared with previously characterised RNA processing and degradation mutants including *rrp6,* TRAMP and NNS-complex mutants.

In Section 3.2.10 the *mpp6Δ rrp47ΔC* mutant showed a striking accumulation of the *NEL025c* CUT transcript upon induction of the $Rrp6_{NT}$ protein. Isogenic wild type, *rrp47Δ, mpp6Δ* and *rex1Δ* strains were transformed with a multicopy plasmid encoding the *NEL025c* along with a second 2μ plasmid encoding for the GST-$Rrp6_{NT}$ protein under the control of the *GAL1/10* promoter. Strains were grown in synthetic raffinose- and galactose-based minimal media. Cells grown in galactose media were pre-grown in raffinose and allowed to double 5 times in galactose before harvesting. This allowed a comparison the effects seen after equivalent cell doubling in the time-course experiment described in Section 3.2.10. The *mpp6Δ rrp47ΔC* and *rex1Δ rrp47ΔC* strains were harvested equivalent to the end time points in the experiment in Section 3.2.10. Isogenic *rrp6Δ* and *trf4Δ* strains harboring a multicopy plasmid encoding the *NEL025c* gene were grown in minimal media and harvested at mid-log phase. Conditional *GAL::NRD1* and *GAL::NAB3* strains were used to analyse the loss of NNS complex components. Both Nrd1 and Nab3 are essential in yeast; therefore a conditional system is required. The aforementioned strains were transformed with the multicopy plasmid encoding *NEL025c* and pre-grown in permissive galactose-based minimal media before shifting to non-permissive glucose-based media. Cells were harvested after 4 doublings in glucose-based medium. Total RNA was

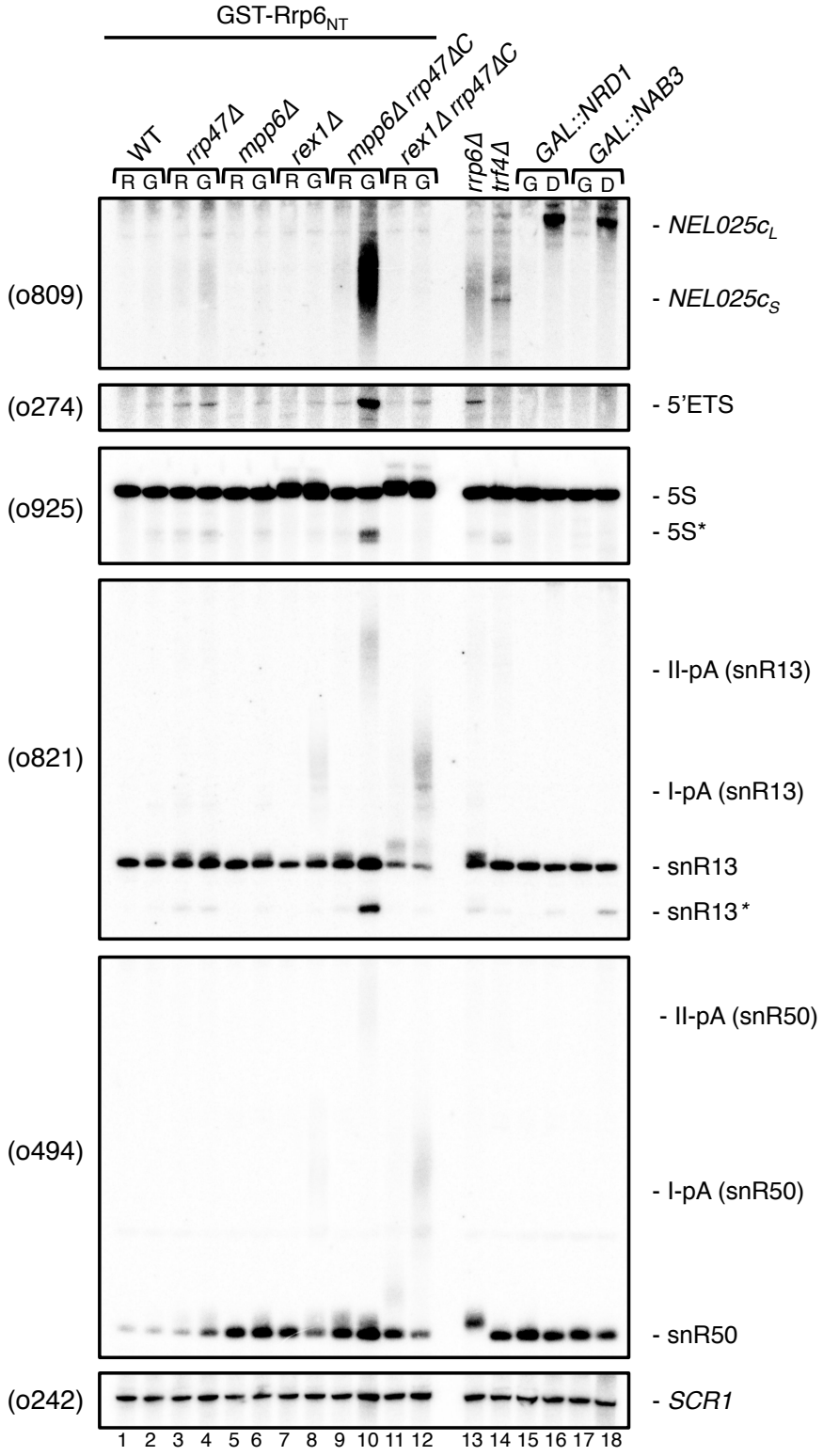

Figure 3.19. Conditional *mpp6Δ rrp47Δ* mutants show markedly strong RNA degradation phenotypes in comparison with RNA surveillance mutants. Northern blot analysis of isogenic WT, *rrp47Δ*, *mpp6Δ*, *rex1Δ*, *mpp6Δ rrp47ΔC* and *rex1Δ rrp47ΔC* strains bearing a 2-micron plasmid encoding the GST-Rrp6$_{NT}$ fusion protein under the control of the *GAL* promoter. Cells were grown in raffinose(R)- and galactose(G)-based media and harvested after 6 doublings of cell density. Isogenic *rrp6Δ* and *trf4Δ* mutants were grown in glucose-based minimal medium. *GAL::NRD1* and *GAL::NAB3* strains were grown in permissive galactose(G)-and non-permissive glucose(D)-based minimal medium and harvested after 4 doublings of cell density. Total RNA was extracted from all samples and fractionated on 8% denaturing polyacrylamide gels and analysed by northern blot hybridisation using radiolabelled oligonucleotides as indicated. Asterisks (*) denote truncated transcripts. Dispersed bands labeled I-pA and II-pA correspond with pre-snoRNAs that are polyadenylated at termination sites I or II respectively. *SCR1* was used a loading control

fractionated by denaturing polyacrylamide gel electrophoresis and analysed by northern blot hybridisation using probes against RNA species that exhibited strong phenotypes in the analysis of *mpp6Δ rrp47ΔC* and *rex1Δ rrp47ΔC* mutants (Section 3.2.10).

The initial identification and characterisation of cryptic unstable transcripts was previously carried out in yeast strains defective in nuclear exosome functions. As *rrp6Δ* strains are viable, these have proven to be a useful tool to analyse stabilised CUT transcripts such as *NEL025c* (Thiebaut et al., 2006; Wyers et al., 2005). Conditional *mpp6 rrp47* mutants previously exhibited a strong accumulation of cryptic unstable transcripts. The levels of the *NEL025c* CUT in the *mpp6Δ rrp47ΔC* mutant upon $Rrp6_{NT}$ induction showed a markedly higher accumulation in comparison to strains lacking Rrp6 or Trf4 (Figure 3.19 compare lane 10 with 13-14). Quantitative analysis of heterogeneous transcripts is not entirely accurate but the level of *NEL025c* transcripts was roughly estimated at 5-fold higher in the *mpp6 rrp47* conditional mutant in comparison to the *rrp6Δ* mutant (Figure 3.20. A). The TRAMP complex targets RNA surveillance substrates, including CUTs, to the nuclear exosome by Trf4/5-dependent polyadenylation (LaCava et al., 2005; Vanácová et al., 2005; Wyers et al., 2005). Strains lacking Trf4 accumulate *NEL025c* transcripts that are non-adenylated and appear as more distinct bands in comparison to the heterogeneous smear observed in *rrp6Δ* strains (Figure 3.19 compare lanes 13 and 14). Some level of heterogeneity is observed in *trf4Δ* strains, most likely due to redundant polyadenylation activity by the major yeast nuclear poly(A) polymerase, Pap1. Transcriptional termination of CUTs is dependent on the activity of Nrd1 and Nab3 as part of the NNS complex (Arigo et al., 2006). Depletion of Nrd1 or Nab3 results in the accumulation of read-through transcripts that terminate at downstream terminator regions. In the initial characterisation of the *NEL025c* CUT, two forms of the transcript were reported; shorter, heterogeneous transcripts that undergo Nrd1-dependent termination (termed $NEL025c_S$) and a longer homogenous species ($NEL025c_L$) that terminates at a downstream terminator region. The *mpp6 rrp47* conditional mutant shows a strong accumulation of the $NEL025c_S$ transcript consistent with a block in the rapid turnover of Nrd1-dependent termination products. In conditional *nrd1* or

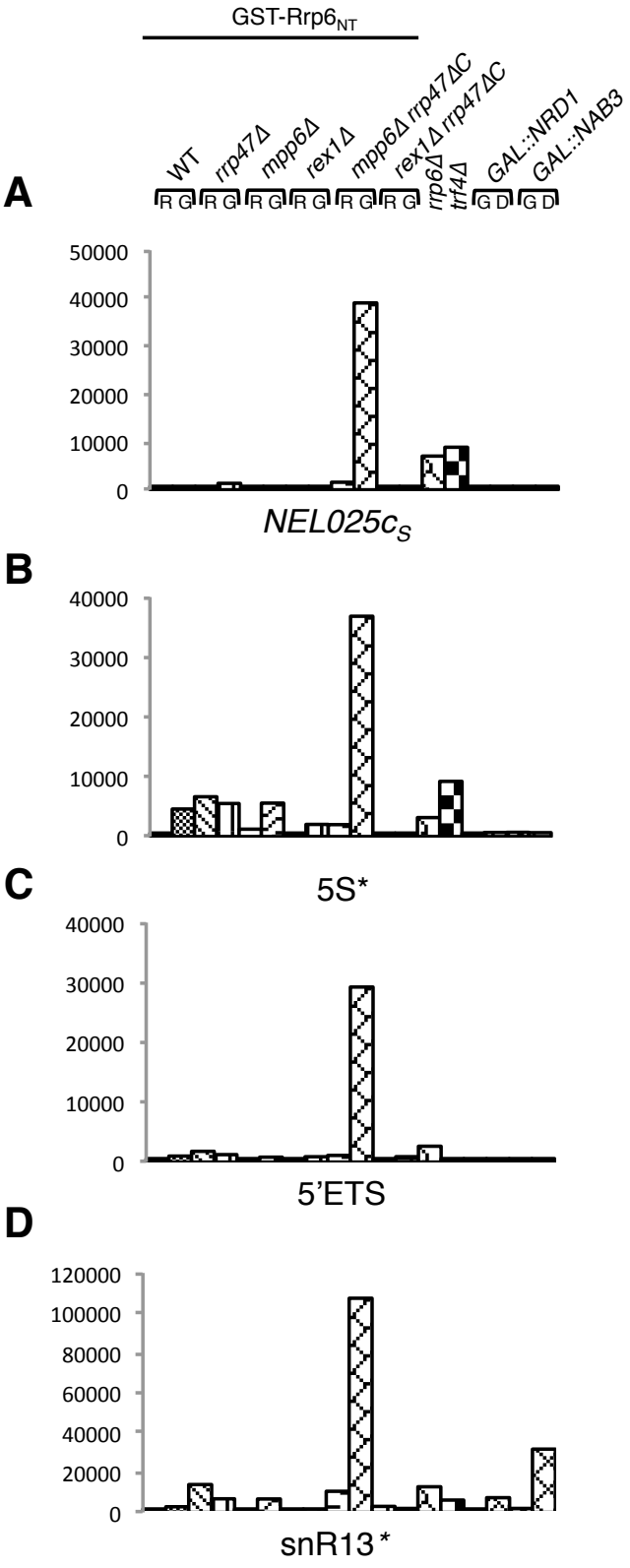

Figure 3.20. Quantification of accumulated transcripts from RNA surveillance mutants. Quantification of northern blot signals from strains analysed in Figure 3.19. Values of *NEL025c*$_S$, 5S*, 5'ETS and snR13* are given for each strain. Asterisks (*) denote truncated RNA species. Averages from two data sets are normalised to *SCR1* levels and expressed relative to the signals from the wildtype (WT) strain.

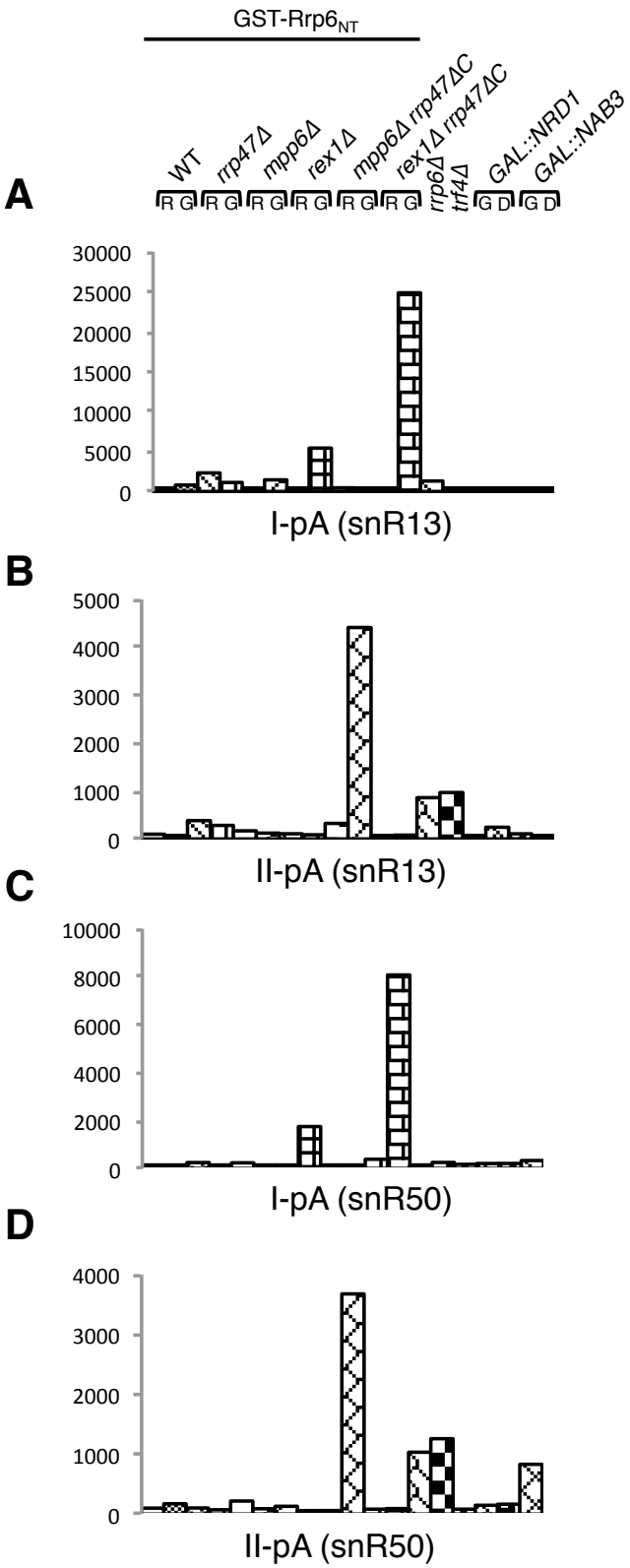

Figure 3.21. Quantification of box C/D snoRNA phenotypes in RNA surveillance mutants. Quantification of northern blot signals from analysis of box C/D snoRNAs from strains analysed in Figure 3.19. Values of I-pA and II-pA snoRNAs are shown for each strain. Averages from two data sets are normalised to *SCR1* levels and expressed relative to the signals from the wildtype (WT) strain.

nab3 mutants, the longer *NEL025c*$_L$ transcript is accumulated upon shifting to non-permissive conditions (Figure 3.19, lanes 15-18).

The conditional *mpp6 rrp47* mutant also showed a greater accumulation of RNA surveillance substrates such as the 5'ETS, 5S* and snR13* species in comparison to the *rrp6Δ, trfΔ* and conditional *nrd1/nab3* mutants. In comparison to the *rrp6Δ* mutant, the *mpp6Δ rrp47ΔC* strain expressing Rrp6$_{NT}$ showed a ~10 fold greater accumulation of the 5S* and 5'ETS species (Figure 3.19 compare lanes 10 and 13, Figure 3.20. B-C). Additionally, the *mpp6Δ rrp47*ΔC mutant shows a 4-fold accumulation of site II terminated snoRNAs on average in comparison to *rrp6Δ* strains (Figure 3.21. B,D). These results strongly corroborate the model that Rrp47/Rrp6 and Mpp6 function in redundant RNA surveillance pathways. The separation of Rrp47ΔC from Rrp6-containing complexes in the absence of Mpp6 results in disruption of both pathways resulting in a critical loss of RNA surveillance and accumulation of target transcripts.

The *rex1Δ rrp47ΔC* showed a stronger depletion of mature snoRNAs compared to the single *rex1Δ* mutant upon Rrp6$_{NT}$ overexpression (Figure 3.19, compare lanes 8 and 12). This, in turn, is matched by a stronger accumulation of I-pA extended snoRNAs suggesting a cumulative block in the 3' end processing of pre-snoRNAs from the loss of Rex1 and functional Rrp47. This suggests that 3'-end processing of box C/D snoRNAs is primarily dependent on redundant pathways involving Rrp6/Rrp47 and Rex1. However, 3'-end processing may still be functional through the activity of other exonucleases such as Rrp44 or Rex2/3 proteins albeit less efficient.

3.3 Discussion

Rrp47 has previously been shown to function as an exosome-associated cofactor in RNA processing and surveillance pathways. The function and stability of Rrp47 is dependent on the physical interaction with the Rrp6 exonuclease (Costello et al., 2011; Feigenbutz et al., 2013b; Mitchell et al., 2003; Stead et al., 2007). The

specific molecular function of Rrp47 still remains largely elusive although it has generally been proposed that Rrp47 acts to stimulate the activity of Rrp6 through RNA binding (Butler and Mitchell, 2011).

In this chapter we set out to analyse the function of Rrp47 when physically separated from Rrp6. In the absence of Rrp6, Rrp47 is rapidly degraded by the proteasome and steady state expression levels of Rrp47 are reduced to below 10% in comparison to wildtype cells (Feigenbutz et al., 2013b). Therefore, to overcome the issue of protein stability, a novel approach was developed to segregate the Rrp6/Rrp47 homodimer *in vivo* whilst maintaining the stability of Rrp47. The DECOID (**d**ecreased **e**xpression of **c**omplexes by **o**verexpression of **i**nteracting **d**omains) strategy was utilized to divorce Rrp47 from Rrp6 by overexpression the N-terminal interacting domain of Rrp6 ($Rrp6_{NT}$). The use of *GAL*-inducible vector constructs allows a conditional system in which the expression of the interacting domain can be switched on. Glycerol gradient ultracentrifugation and pulldown analyses reported that the segregation of the Rrp6/Rrp47 complex was ~96% effective (Garland et al., 2013). We cannot fully eliminate the possibility that a small fraction of residual Rrp47 remains bound to Rrp6. However, using DECOID on a truncated *rrp47* mutant in resulted conditional lethal phenotypes in combination with *mpp6Δ* or *rex1Δ* alleles. This suggests that the *rrp47* mutant is functional under permissive conditions and loses function upon segregation from Rrp6 by the induction of the $Rrp6_{NT}$ protein.

RNA analysis of wildtype and *rrp47ΔC* strains upon induction of the $Rrp6_{NT}$ protein revealed that the cells still have functional RNA processing and surveillance mechanisms upon separation of the Rrp47/Rrp6 complex. The loss of Rrp47 or Rrp6 function is synthetic lethal in combination with *mpp6Δ* or *rex1Δ* alleles. Overexpression of $Rrp6_{NT}$ in *mpp6Δ* and *rex1Δ* strains was tolerated yet induced slow growth phenotypes and mild RNA processing and degradation phenotypes. However, inducing $Rrp6_{NT}$ expression in *mpp6Δ* and *rex1Δ* mutants combined with a C-terminal truncation *rrp47* mutant (*rrp47ΔC*) resulted in a block in growth. This suggests that full length Rrp47 is functional when segregated from Rrp6-containing complexes yet requires the C-terminal domain for sufficient function.

The C-terminus of Rrp47 contains a highly basic, lysine-rich region that is required for RNA binding *in vitro*. However, this property is not required for the function of Rrp47 *in vivo* as shown by the complementation of *mpp6Δ rrp47Δ* and *rex1Δ rrp47Δ* synthetic lethality (Costello et al., 2011). The C-terminus is suggested to provide substrate recognition for the Rrp47/Rrp6 complex through RNA binding. Additionally, the C-terminal domain is required for the physical interaction between snoRNP proteins Nop56 and Nop58 (Costello et al., 2011). Furthermore, an interaction between Rrp47 and the Nrd1/Nab3 (NNS) termination complex has been observed but is lost in *rrp47ΔC* mutants (P. Mitchell, M. Feigenbutz, personal communication). This suggests that the C-terminus is required to function in the recognition of RNP substrates through both RNA and protein contacts (Figure 3.22)

In the absence of a functional Rrp47/Rrp6 complex, cells require the activities of either Mpp6 or Rex1. Mpp6 is a nuclear exosome-associated RNA binding protein with many similarities to Rrp47, however the exact molecular function is yet to be determined. Previous analyses of conditional *mpp6 rrp47* double mutants reported defects in the degradation of pre-rRNAs, cryptic unstable transcripts and aberrant mRNAs (Milligan et al., 2008). This suggests that Mpp6 functions in redundant RNA surveillance pathways, possibly through stimulation of the core-exosome and Rrp44. The data in this chapter supports the conclusion that Rrp6/Rrp47 and Mpp6 function in redundant RNA surveillance pathways and extensive northern blot hybridisation analysis expands on RNA targets of these pathways. These conditional *mpp6 rrp47* mutants show accumulations of CUTs, pre-rRNA processing byproducts, truncated forms of stable RNAs and site II-terminated snoRNA transcripts. Analyses of *rex1 rrp47* double mutants revealed distinct phenotypes from the *mpp6 rrp47* mutants. The Rex1 exonuclease functions in 3' end maturation of 5S rRNA and tRNAs (Copela et al., 2008; Ozanick et al., 2009; van Hoof et al., 2000b). Conditional *rex1 rrp47* double mutants showed a strong accumulation of site I terminated pre-snoRNAs matched with a depletion of mature snoRNAs. These observations support a model that mature snoRNA transcripts are terminated at site I by Nrd1/Nab3

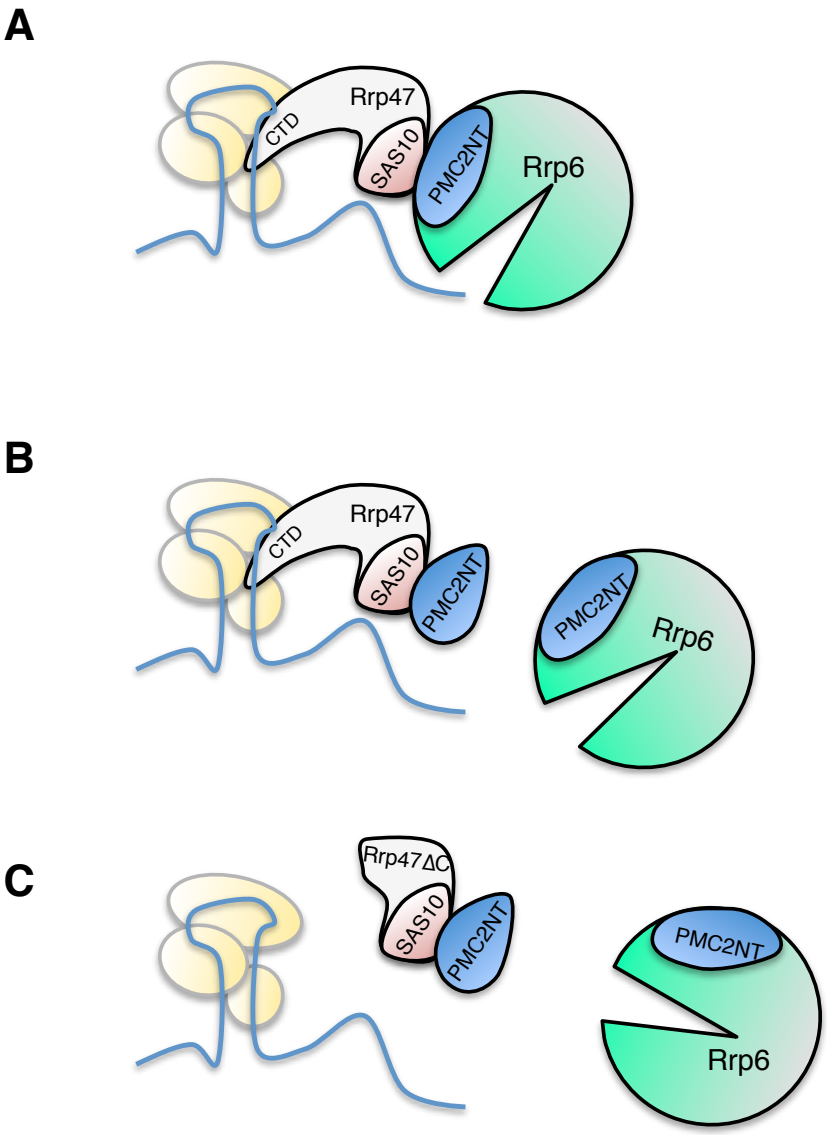

Figure 3.22. Model for substrate recognition by Rrp47. **(A)** Rrp47 is bound to Rrp6 in wildtype cells via an interaction between the Sas10/C1D and PMC2NT domains respectively. The C-terminus of Rrp47 (CTD) forms interactions with RNA and proteins and contribute to substrate recognition prior to Rrp6-dependent catalysis. **(B)** Rrp47 is functional when physically separated from Rrp6 using the DECOID method. The CTD of Rrp47 can still engage in RNA and protein interactions to recruit substrates. **(C)** The functional capability of Rrp47 is dependent on the CTD when physically segregated from Rrp6. Upon separation, Rrp47 is can no longer interact with substrates. When Rrp47/Rrp6 pathways are blocked, the strain is dependent on redundant pathways involving Rex1 and Mpp6.

followed by polyadenylation (Grzechnik and Kufel, 2008) and that subsequent 3' end processing requires redundant pathways involving a functional Rrp6/Rrp47 complex or Rex1.

A block in growth was observed in *mpp6Δ rrp47ΔC* and *rex1Δ rrp47ΔC* double mutants upon expression of the $Rrp6_{NT}$ protein. The significant accumulation of CUTs and aberrant RNAs may contribute to the growth defect in *mpp6 rrp47* mutants. Whilst the role of CUTs, if any, is generally unknown, previous studies have identified possible roles in transcriptional regulation (Camblong et al., 2007; Castelnuovo et al., 2013; Martens et al., 2004). With this in mind, a loss of cryptic transcription regulation may impact normal transcription of genes that are regulated by CUTs. Additionally, a loss in RNA surveillance pathways would result in the stabilisation of aberrant transcripts that incorporate into RNP complexes and cause adverse cellular effects. The possible basis of a block in growth in the *rex1Δ rrp47ΔC* mutant upon $Rrp6_{NT}$ induction is less clear. Whilst cells showed a block in snoRNA processing and subsequent depletion of mature snoRNA transcripts, no adverse effects on the levels of mature ribosomal RNA were observed. Both *mpp6 rrp47* and *rex1 rrp47* conditional mutants showed a significant accumulation of polyadenylated snoRNAs and CUTs. The stabilisation of polyadenylated transcripts may result in the titration of poly(A)-binding proteins such as Pab1, Nab2 or the Nrd1/Nab3 termination complex and impact on normal gene expression profiles. The effects observed in northern blot hybridisation analysis are limited by the use of complementary probes for specific RNA transcripts. With the advent of high throughput next generation RNA sequencing methods, a transcriptome-wide analysis on RNA isolated from conditional *mpp6 rrp47* and *rex1 rrp47* mutants may reveal a more comprehensive understanding on the changes in transcription profiles upon loss of RNA surveillance or processing pathways.

Transcriptome wide analysis of exosome targets and the identification of cryptic unstable transcripts has historically been performed on *rrp6Δ* strains. The loss of Rrp6 is tolerated by cells yet serves as a tool to stabilise pervasive transcripts and RNA surveillance targets. As described in Section 3.2.11, the levels of *NEL025c* CUTs are accumulated to a larger degree in the *mpp6 rrp47* mutant in

comparison to levels in *rrp6Δ* or *trf4Δ* mutants. This effect is most likely due to a cumulative loss of redundant Rrp6/Rrp47 and Mpp6-dependent processes required for efficient RNA surveillance pathways. The *mpp6Δ rrp47ΔC GAL::GST-rrp6*$_{NT}$ mutant may provide an ideal conditional host strain to analyse CUT transcripts and could be used purify CUT RNPs from yeast.

Mpp6 was previously identified as a nuclear exosome-associated cofactor and shown to be involved in RNA surveillance and quality control pathways (Milligan et al., 2008). This chapter expands on the molecular basis of the synthetic lethality of *mpp6Δ rrp47Δ* double mutants using a conditional system. However, the exact role of Mpp6 is still poorly understood. The work in Chapter 5 investigates Mpp6 in further detail through mutational analysis.

The use of DECOID allowed the successful segregation of Rrp47 from Rrp6-containing complexes whilst maintaining the normal expression of Rrp47. The DECOID approach provides a simple method to determine if components of protein complexes are able to function when separated. Using the technique only requires knowledge of the interacting domain one of the protein components within a complex. The use of an inducible promoter allows conditional expression of the interacting domain. The stability of the induced protein would generally be aided by the use of a neutral N-terminal tag such as GST which would also allow for detection by western blot analysis using widely available antibodies. We have already begun work on physically separating other exosome-associated components using the DECOID method. The use of the technique can be applied to any protein complex with prior knowledge of interacting domain architecture.

Chapter 4: Analysis of functional and redundant relationships between Rrp6, Rrp47 and Mpp6.

4.1. Introduction

As described in Chapter 1, the function of Rrp6 is largely dependent on the physical and functional interaction with the small nuclear RNA binding protein Rrp47. It was recently shown that in the absence of Rrp6, the expression level of Rrp47 protein is dramatically reduced to ~15% in comparison to wild-type *RRP6* strains with no significant change to mRNA levels (Feigenbutz et al., 2013b). Previous reports have observed that Rrp6 protein expression levels are not sensitive to the loss of Rrp47 (Mitchell and Tollervey, 2003; Stead et al., 2007). However, these studies were carried out on strains grown in rich medium. Further studies have shown that Rrp6 protein levels are reduced in *rrp47Δ* strains grown in synthetic minimal media. The decrease in protein expression is due to both protein and *RRP6* transcript stability. *RRP6* mRNA levels are decreased to ~ 44% in *rrp47Δ* strains compared to *RRP47* cells. Concurrently, the expression levels of Rrp6 protein are reduced to ~ 30% in *rrp47Δ* mutants (Feigenbutz et al., 2013a). Taken together, these results suggest that the stability of Rrp6 and Rrp47 are mutually dependent on their physical interaction with Rrp47 being more sensitive to the loss of Rrp6. This proposes that a function of Rrp47 is to maintain the normal expression levels of Rrp6 *in vivo*. It was subsequently shown that artificially increasing the expression of Rrp6 in *rrp47Δ* mutants was able to suppress RNA processing and turnover phenotypes observed from the lack of Rrp47 (Feigenbutz et al., 2013a).

In this chapter it is observed that overexpression of Rrp6 is sufficient to complement the synthetic lethality of *mpp6Δ rrp47Δ* double mutants through genetic shuffling assays. Chapter 3 reported a loss of RNA surveillance and degradation pathways in conditional *mpp6 rrp47* mutants. Consistent with these observations, northern blot analysis of complemented *mpp6Δ rrp47Δ* mutants

showed a strong accumulation of RNA surveillance targets. Increased expression of Rrp6 suppressed the severity of RNA phenotypes in the *mpp6Δ rrp47Δ*. These results provide an insight into the molecular nature of the synthetic lethality of *mpp6Δ* and *rrp47Δ/rrp6Δ* alleles and corroborates the proposal that Rrp6/Rrp47 function in RNA turnover pathways redundant with Mpp6. A parallel study carried out by colleagues in the lab reported similar findings: *RRP6* overexpression complements the *rex1Δ rrp47Δ* synthetic lethality and that increased levels of Rrp6 suppresses RNA processing phenotypes observed in conditional *rex1 rrp47* mutants (reported in Feigenbutz, Garland et al. 2013). The analysis of complemented *rex1Δ rrp47Δ* mutants corroborates the model that Rrp6/Rrp47 and Rex1 have a redundant function in RNA processing pathways. These results complement the results observed in Chapter 3.

Results in this chapter contribute to the work published in Feigenbutz et al (2013)b (Appendix IV).

4.2. Results

4.2.1. Increased *RRP6* expression complements the *mpp6Δ rrp47Δ* synthetic lethality

It has been previously reported that the stability of Rrp47 is strongly dependent on the physical interaction with the N-terminal PMC2NT domain of Rrp6 ($Rrp6_{NT}$) *in vivo* (Feigenbutz et al., 2013b; Stead et al., 2007). Subsequent analyses have revealed that the levels of Rrp6 protein are also sensitive to the loss of Rrp47 in strains grown in minimal media. By artificially increasing levels of Rrp6 through exogenous plasmid-borne expression, RNA defects in *rrp47Δ* mutants are suppressed (Feigenbutz et al., 2013a). This suggests that a key function of Rrp47 is to maintain the stable expression of Rrp6. However, increased expression of Rrp6 did not fully suppress *rrp47Δ* RNA processing defects to the extent of complementation with wildtype *RRP47* therefore suggesting that Rrp47 has functions in addition to maintaining Rrp6 levels (Feigenbutz et al., 2013a).

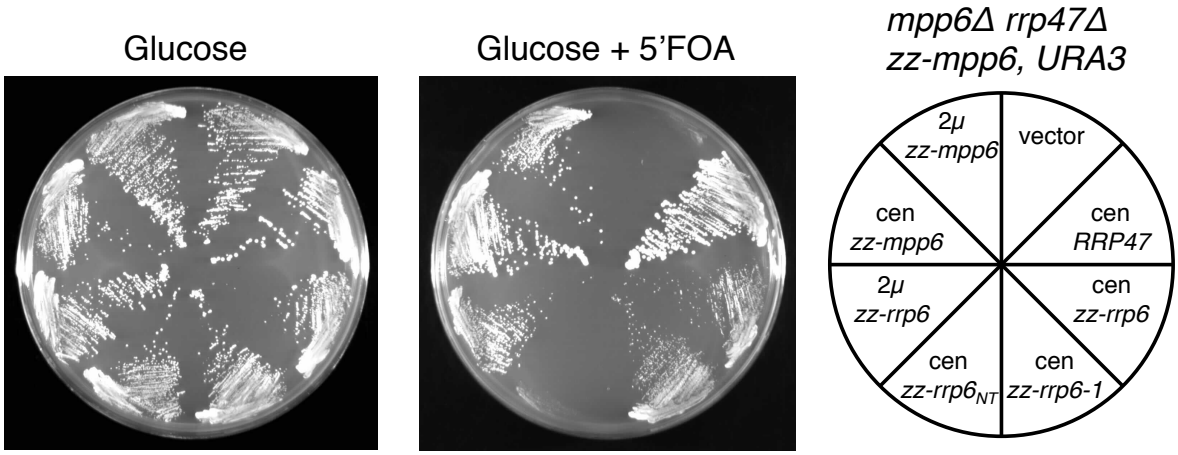

Figure 4.1. Exogenous expression of Rrp6 complements the *mpp6Δ rrp47Δ* synthetic lethality. A plasmid shuffle assay. Centromeric plasmids encoding *RRP47* (p425), *zz-rrp6* (p428), *zz-rrp6-1* (p430), *zz-rrp6*$_{NT}$ (p432), *zz-mpp6* (p599) and 2μ plasmids encoding *zz-rrp6* (p602) and *zz-mpp6* (p603) were transformed into a *mpp6Δ rrp47Δ* yeast strain bearing a *URA3*-containing gene encoding for a wildtype copy of *MPP6*. Transformants were isolated on selective minimal media and assayed for viability on minimal media containing 5'FOA. Plates were incubated at 30°C for 3 days before photographing. The nature of each transformant is indicated on the right panel.

Loss of function *rrp47* alleles are synthetic lethal with *mpp6Δ* mutants. To determine if increased expression levels of Rrp6 can complement the dependency of *RRP47* expression in an *mpp6Δ* mutant, an *mpp6Δ rrp47Δ* plasmid shuffle strain (previously described in Section 3.1.2) was transformed with single-copy centromeric (cen) and high-copy 2-micron (2μ) plasmids encoding *rrp6* alleles under the control of the *RRP4* promoter. Transformants were assayed for growth on minimal medium containing 5'FOA to counterselect against the *URA3* plasmid bearing a wildtype copy of *MPP6*.

Plasmid-borne expression of a tagged zz-Rrp6 fusion protein allowed for viability of the *mpp6Δ rrp47Δ* strain (Figure 4.1). Similarly, expression of the *zz-rrp6* allele on a 2μ multicopy plasmid also complemented the *mpp6Δ rrp47Δ* double mutant. Interestingly, a catalytically inactive *rrp6-1* ($rrp6_{D238N}$) was able to complement the *mpp6Δ rrp47Δ* double mutant and grew comparable to strains complemented by exogenous expression of function zz-Rrp6. The catalytically inactive *rrp6-1* allele ($rrp6_{D238N}$) was unable to complement the synthetic lethality of *rex1Δ rrp47Δ* double mutants in a similar plasmid shuffle assay (Feigenbutz et al., 2013a). This suggests that Rrp6 has other roles important in strains lacking Mpp6 that do not require its exonuclease activity. A single copy plasmid encoding the N-terminal PMC2NT domain of Rrp6 ($Rrp6_{NT}$) was unable to complement the *mpp6Δ rrp47Δ* synthetic lethality. Single copy plasmids encoding *RRP47* and *zz-MPP6* allowed for complemented viability of the plasmid shuffle strain whereas strains transformed with an empty vector (pTL26) were inviable on 5'FOA media.

These results show that exogenous overexpression of Rrp6 can suppress the synthetic lethality of *mpp6Δ rrp47Δ* mutants and that complementation is not dependent on the catalytic activity of Rrp6.

4.2.2. Slow growth rates are observed in Rrp6-complemented *mpp6 rrp47* mutants

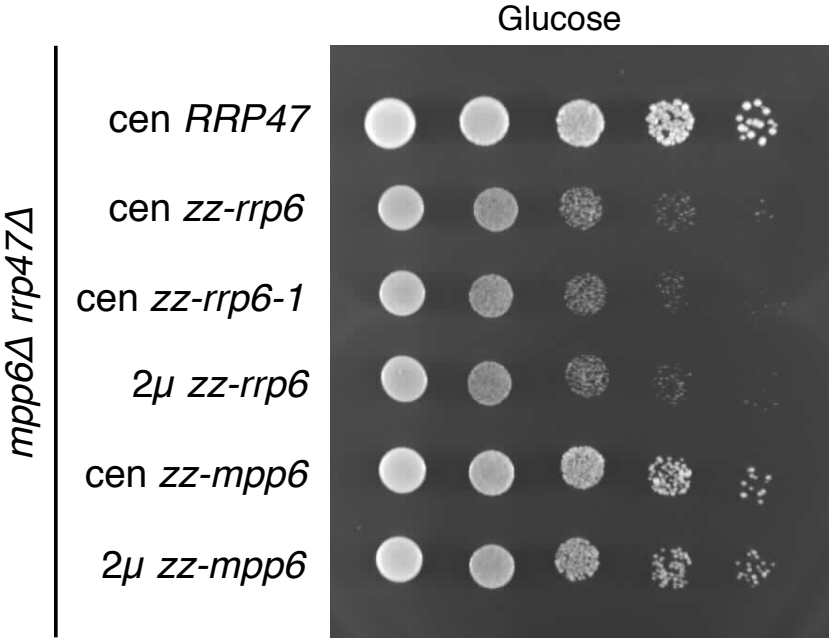

Figure 4.2. Slow growth phenotypes are observed in *mpp6Δ rrp47Δ* mutants bearing exogenous *rrp6* alleles. Spot growth assay of *mpp6Δ rrp47Δ* mutants transformed with centromeric plasmids encoding *RRP47* (p425), *zz-rrp6* (p428), *zz-rrp6-1* (p430), *zz-rrp6*$_{NT}$ (p432), *zz-mpp6* (p599) and 2μ plasmids encoding *zz-rrp6* (p602) and *zz-mpp6* (p603). Strains were grown in liquid selective minimal medium and normalised by optical density ($A600_{nm}$) before spotting 10-fold serial dilutions onto selective solid medium. Plates were incubated for 3 days at 30˚C before photographing.

Increased expression of Rrp6 was shown to be able to complement the synthetic lethality of *mpp6Δ rrp47Δ* double mutants in a plasmid shuffle. Single colony isolates were recovered from 5'FOA media and assayed for growth on solid minimal medium by spot growth tests.

A markedly decreased growth rate was observed in *mpp6Δ rrp47Δ* strains complemented with cen *zz-rrp6, zz-rrp6-1* and 2μ *zz-rrp6* plasmids in comparison to strains complemented by wildtype *RRP47* or *MPP6* alleles (Figure 4.2). Expression of the multicopy *zz-rrp6* plasmid did not show any significant improvement in growth compared to the single-copy *zz-rrp6* plasmid.

These results show that artificially increasing the expression levels of Rrp6 in an *mpp6Δ rrp47Δ* mutant is able to complement the synthetic lethality. Strains are viable but show markedly slow growth phenotypes in comparison to strains complemented with wildtype *RRP47* or *MPP6* alleles. Interestingly, no significant growth defect was observed in *rex1Δ rrp47Δ* mutants complemented with either *RRP6* or *RRP47* alleles (Feigenbutz et al., 2013a). This suggests that *mpp6Δ* mutants are more sensitive to the loss of Rrp47 and corroborates the proposition that Mpp6 and Rrp6/Rrp47 function in redundant pathways.

4.2.3. Rrp6 can be overexpressed in *mpp6Δ rrp47Δ* mutants

Artificially increasing the copy number of *RRP6* in an *rrp47Δ mpp6Δ* strain allows for cell viability and complemented the genetic synthetic lethality of the double mutant. This was assumed to be due to increased Rrp6 protein expression. It has been shown that expression levels of Rrp47 are dramatically decreased in strains lacking Rrp6 (Costello et al., 2011; Feigenbutz et al., 2013b). Likewise, it has been shown that Rrp6 transcript and protein expression levels are decreased in strains lacking Rrp47 when grown in minimal media. However, Rrp47 is more sensitive to the loss of Rrp6. By increasing Rrp6 levels through exogenous overexpression on plasmids, this could negate the requirement of Rrp47 for Rrp6 stability.

Expression of Rrp6 was assayed in *mpp6Δ rrp47Δ* strains complemented with *RRP47, MPP6* and *rrp6* alleles. Lysates were also prepared from isogenic wildtype, *rrp47Δ* and *mpp6Δ* strains and assayed in parallel by SDS PAGE and western blot analysis using an Rrp6-specific antibody (Figure 4.3). Levels of endogenous Rrp6 are decreased in the *rrp47Δ* strain and *mpp6Δ rrp47Δ* double mutant complemented with zz-Mpp6 in comparison to wildtype levels (Figure 4.3 compare lanes 1,2 and 4). The loss of Mpp6 has no effect on the expression level of Rrp6 (compare lanes 1 and 3).

Exogenous expression of zz-Rrp6 and zz-rrp6-1 fusion proteins from centromeric plasmids under the control of the *RRP4* promoter were analysed in *mpp6Δ rrp47Δ* strains. Endogenous levels of Rrp6 remained comparable to *rrp47* mutants whereas the tagged proteins showed a marked overexpression effect (Figure 4.3 lanes 6 & 7). Greater levels of overexpression were observed in strains bearing a high copy number 2μ plasmid encoding zz-Rrp6 (Lane 8). Lower molecular weight bands observed in strains expressing zz-Rrp6 fusion proteins are due to C-terminal degradation products and are typical of plasmid-borne Rrp6 expression. These degradation products are more distinct in lane 8 due to a greater expression level of the zz-Rrp6 protein. Due to the high level of degradation observed in samples expressing zz-Rrp6, these westerns could not be accurately quantified.

Overexpression of zz-Mpp6 from a 2μ plasmid had no stabilizing effect on the levels of endogenous Rrp6 in the *mpp6Δ rrp47Δ* plasmid. This suggests that Mpp6 does not function to maintain normal expression levels of Rrp6.

These results show that Rrp6 can be overexpressed in strains lacking Rrp47, with greater expression in strains bearing 2μ plasmids encoding for zz-Rrp6 fusion proteins. Exogenous overexpression of Rrp6 can therefore negate the requirement for Rrp47 in strains lacking Mpp6.

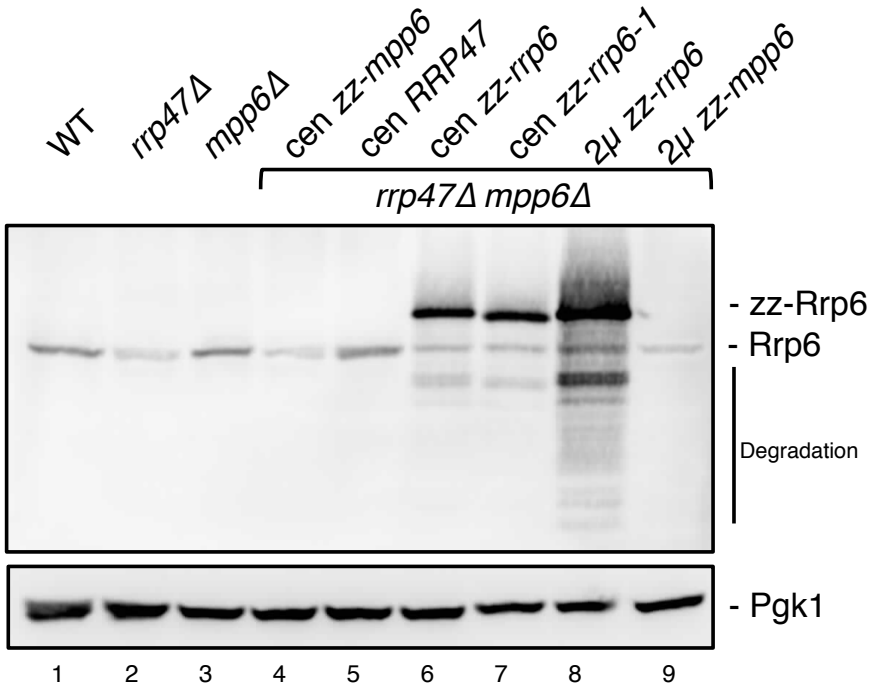

Figure 4.3. Rrp6 can be overexpressed in *rrp47Δ mpp6Δ* strains. Lysates prepared from *mpp6Δ rrp47Δ* strains bearing centromeric plasmids encoding *zz-mpp6, RRP47, zz-rrp6, zz-rrp6-1* or 2μ plasmids encoding *zz-rrp6* or *zz-mpp6* were fractionated by SDS PAGE and analysed by western blotting. Lysates from isogenic wildtype, *rrp47Δ* and *mpp6Δ* strains were assayed in parallel. Rrp6 proteins were detected upon incubation with an Rrp6-specific antibody (*upper* panel). A second incubation using a Pgk1-specific antibody was used for a loading control (*lower* panel).

4.2.4 The stability of Rrp6 is not dependent on Mpp6 or Rex1

Rrp6 protein levels are reduced in yeast strains lacking Rrp47. Loss of function *rrp47* alleles are synthetic lethal in with *mpp6Δ* or *rex1Δ* alleles (Milligan et al., 2008; Peng et al., 2003). It could be proposed that the basis of synthetic lethality is due the cumulative destabilisation of Rrp6 due to additive loss of Mpp6 or Rex1 in combination with *rrp47Δ* alleles. However, *rrp6Δ* strains are viable, therefore an additive loss of Rrp6 expression would not be the sole reason for synthetic lethality, but could be a contributing factor. An alternative proposition is that the expression levels of Rrp6 are increased in *mpp6Δ* or *rex1Δ* mutants to compensate for the lack of Mpp6- or Rex1-dependent pathways.

MPP6 and *REX1* loci were individually targeted for disruption by homologous recombination of a *kanMX4* deletion cassette in an *rrp6Δ* strain bearing a centromeric plasmid encoding for a zz-Rrp6 fusion protein under the control of the *RRP4* promoter. Transformants were selected on rich media containing G418 and candidates were screened by PCR for disruption of *MPP6* and *REX1* loci (Garland et al., 2013). The expression levels of zz-Rrp6 were assayed in the resulting *mpp6Δ* and *rex1Δ* strains grown in minimal medium by SDS PAGE and western blot analysis (Figure 4.4). Compared to *MPP6* strains, there was no significant change in the relative zz-Rrp6 expression levels in the *mpp6Δ* mutant (Figure 4.4A). The *rex1Δ* mutant showed a slight but not substantial increase in zz-Rrp6 expression (Figure 4.4B).

Therefore, Rrp6 stability is not significantly affected by the loss of Mpp6 or Rex1 expression. Any loss of endogenous Rrp6 protein in *mpp6 rrp47* mutants can be predominantly attributed to the loss of Rrp47.

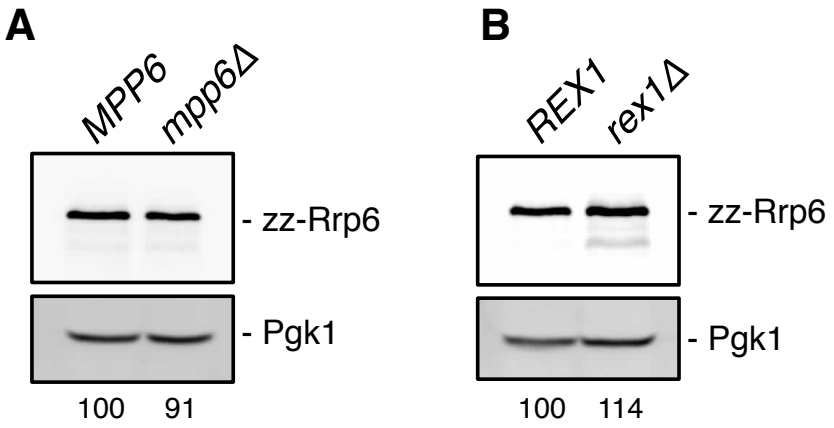

Figure 4.4. Rrp6 expression levels are unchanged in *mpp6Δ* or *rex1Δ* strains. Lysates were prepared from yeast strains expressing zz-Rrp6 fusion proteins either carrying a wildtype or a deletion allele of the *MPP6* (A) or *REX1* (B) genes. Proteins were fractionated by SDS PAGE and analysed by western blotting using the PAP antibody (*upper* panel). Blots were incubated with a Pgk1-specific antibody as a loading control (*lower* panel). Expression levels of zz-Rrp6 in each strain are given below the figure and are the average of of three independent biological replicas. Values are expressed relative to the corresponding wildtype *MPP6* or *REX1* strains respectively.

4.2.5 RNA analysis of *mpp6Δ rrp47Δ* mutants

Chapter 3 investigated RNA processing and degradation phenotypes in a conditional *mpp6 rrp47* double mutant. This strain exhibited defects in surveillance and degradation of CUTs, pre-rRNA and other aberrant RNAs. Northern blot hybridisation was carried out on complemented *mpp6Δ rrp47Δ* strains to investigate if these phenotypes could be suppressed with increasing exogenous levels of Rrp6.

Total cellular RNA was isolated from *mpp6Δ rrp47Δ* strains complemented with *RRP47, MPP6* or *rrp6* alleles. Strains were grown in minimal media and harvested during mid-log phase. Isogenic wildtype, *rrp47Δ* and *mpp6Δ* strains were analysed in parallel. Northern blot analyses were performed on total cellular RNA fractionated by denaturing polyacrylamide electrophoresis.

A strong accumulation of cryptic unstable transcripts (CUTs) was exhibited in *mpp6Δ rrp47Δ* mutants complemented by single copy plasmids encoding *zz-rrp6* and *zz-rrp6-1* alleles (Figure 4.5 lanes 6 and 7). The accumulation of *NEL025c* and *IGS1-R* CUTs was markedly increased in comparison to *rrp47Δ* and *mpp6Δ* single mutants (Figure 4.5 compare lanes 2-3, 6-7, Figure 4.6A-B). This is in concordance with previous observations in conditional *mpp6 rrp47* mutants (Chapter 3 and Milligan et al. 2008). Additionally, *mpp6Δ rrp47Δ* mutants expressing the zz-Rrp6 and zz-rrp6-1 fusion proteins revealed defects in the degradation of RNA surveillance targets including truncated fragments of 5S rRNA, U3 and snR13 snoRNAs (Figures 4.6 and 4.8 lanes 6-7, denoted 5S*, U3* and snR13* respectively). These transcripts have previously been characterised as aberrant species in RNA surveillance mutants (Kadaba et al., 2006; Kufel et al., 2000; Rasmussen and Culbertson, 1998). A similar accumulation of a truncated fragment of the U6 snRNA was also observed (data not shown).

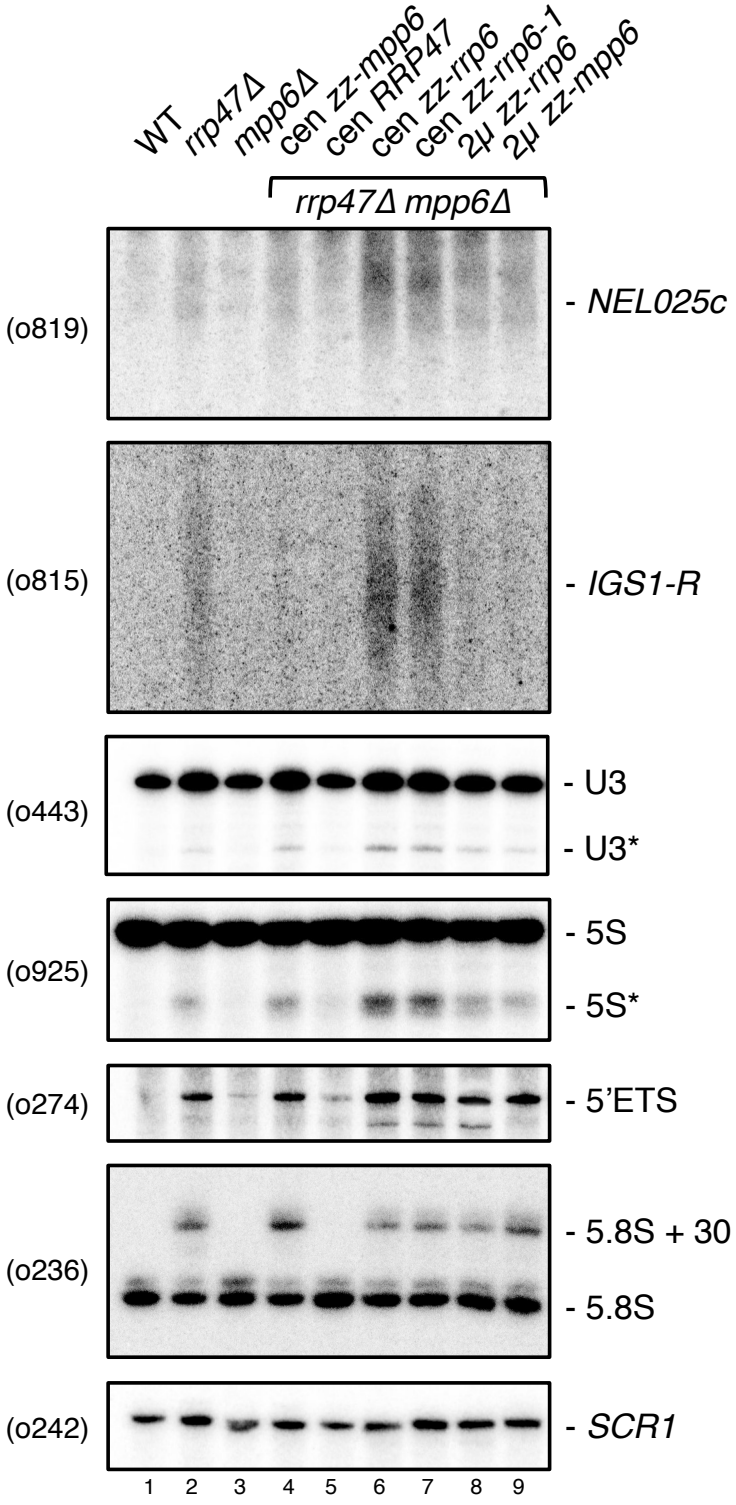

Figure 4.5. Northern blot analysis of *mpp6Δ rrp47Δ* mutants. Total cellular RNA was isolated from isogenic wild-type (WT), *rrp47Δ* and *mpp6Δ* strains (lanes 1-3), and *mpp6Δ rrp47Δ* double mutants complemented with either centromeric (cen) plasmids encoding *zz-mpp6, RRP47, zz-rrp6, zz-rrp6-1* or 2-micron (2μ) plasmids encoding *zz-rrp6* and *zz-mpp6* (lanes 4-9). RNA was fractionated on 8% denaturing polyacrylamide gels and analysed by northern blot hybridisation using radiolabeled oligonucleotides as indicated. Detected RNA species are indicated to the right of each panel. Truncated RNA transcripts are indicated with an asterisk (*). *SCR1* served as a loading control.

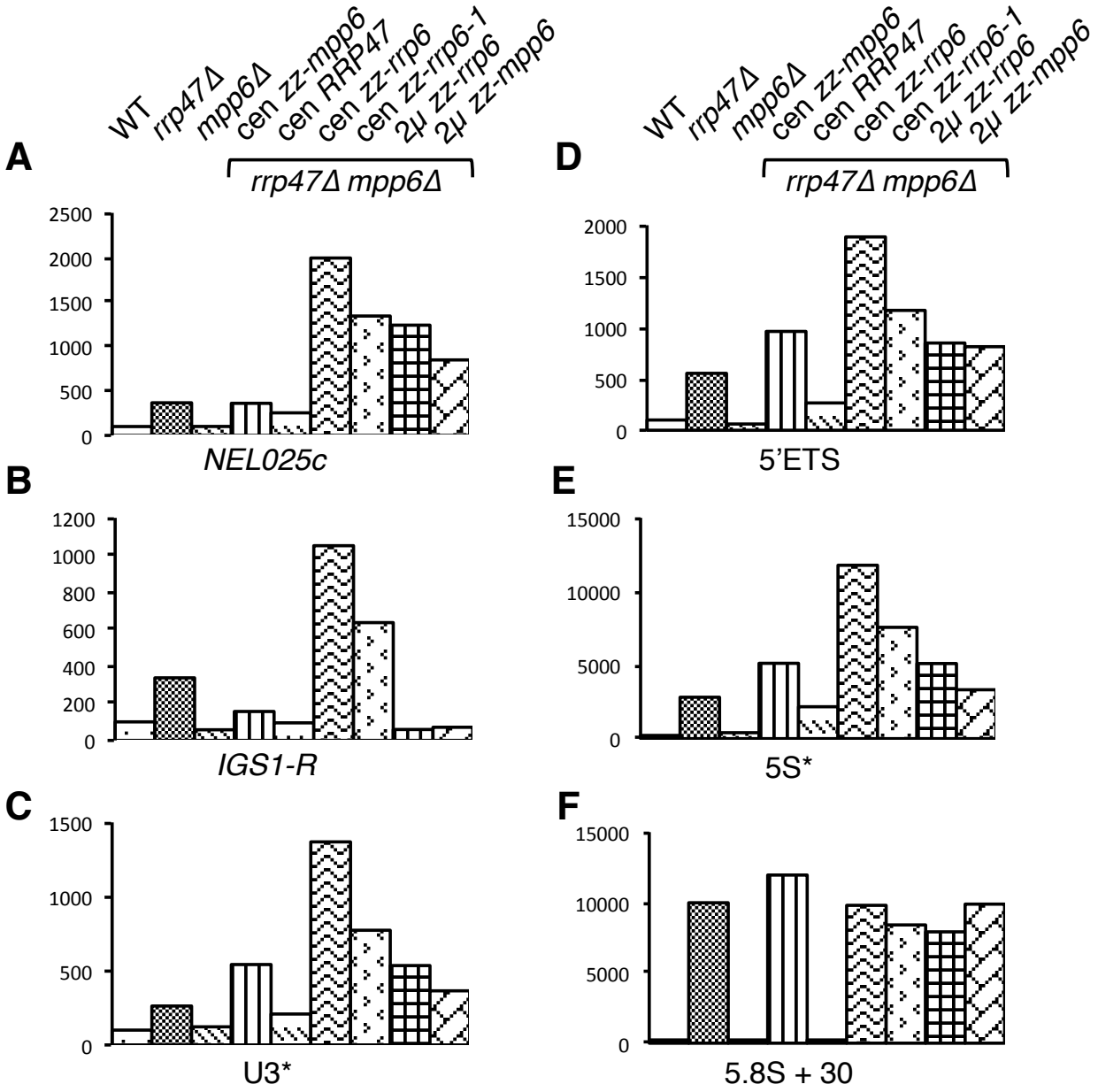

Figure 4.6. Quantification of RNA degradation phenotypes in *mpp6Δ rrp47Δ* mutants.
Quantification of northern blot signals from analysis of *mpp6Δ rrp47Δ* mutants shown in Figure 4.5. Values from *NEL025, IGS1-R,* U3*, 5S*, 5'ETS and 5.8S + 30 species are shown for each strain. Averages from two data sets are normalised to *SCR1* levels and expressed relative to the signals from the wildtype (WT) strain.

As observed in conditional *mpp6 rrp47* mutants (Chapter 3), the *mpp6Δ rrp47Δ* strains expressing zz-rrp6 and zz-rrp6-1 proteins revealed an accumulation of 3' extended U14 and snR13 snoRNAs (Figure 4.7, lanes 6-7). The *rrp47Δ* strain displays two populations of extended U14 snoRNAs that are proposed to correspond to transcriptional termination at a proximal Nrd1-dependent site (site I) and a more distal cleavage/polyadenylation site (site II). Both termination events result in polyadenylation and appear as smears on northern blot hybridizations (Grzechnik and Kufel, 2008). The *mpp6Δ rrp47Δ* strains complemented by *zz-rrp6* and *zz-rrp6-1* alleles show a stronger accumulation of site II polyadenylated transcripts (dubbed II-pA (U14) and II-pA (snR13)) in comparison to the *rrp47Δ* single mutant (Figure 4.7 compare lanes 2 with 6-7). These transcripts read through into distal alleles and are targeted for rapid degradation in wild type cells through RNA surveillance pathways (Allmang et al., 1999a; Steinmetz and Brow, 2003). These results agree with previous analyses in Chapter 3 and show that degradation of RNA surveillance targets is impeded in the absence of Mpp6 and Rrp47.

The final step in 3' end processing of box C/D snoRNAs requires the catalytic activity of Rrp6 with the co-operation of Rrp47 (Costello et al., 2011; Mitchell et al., 2003). Short 3' extensions of 1-6 nucleotides are present in the absence of Rrp6 and Rrp47. In the case of snR38, these can be resolved as mature snR38 and snR38 + 3 species on 8% polyacrylamide gels as seen in the *rrp47Δ* mutant (Figure 4.7, lane 2). The *mpp6Δ rrp47Δ* strain expressing zz-Rrp6 shows complementation of the snR38 + 3 phenotype when compared with the *rrp47Δ* single mutant (Figure 4.7, compare lanes 2 and 6). Interestingly, the strain expressing zz-rrp6-1 shows a stronger accumulation of the snR38+3 species and subsequent depletion of mature snR38. This shows the *rrp6-1* mutant is unable to efficiently process short 3'-extended snoRNAs in comparison to strains complemented by functional Rrp6 (Figure 4.7, compare lanes 6 and 7).

A suppression of all observed phenotypes was detected in the *mpp6Δ rrp47Δ* strain expressing zz-Rrp6 from a multicopy plasmid. Accumulation of CUTs,

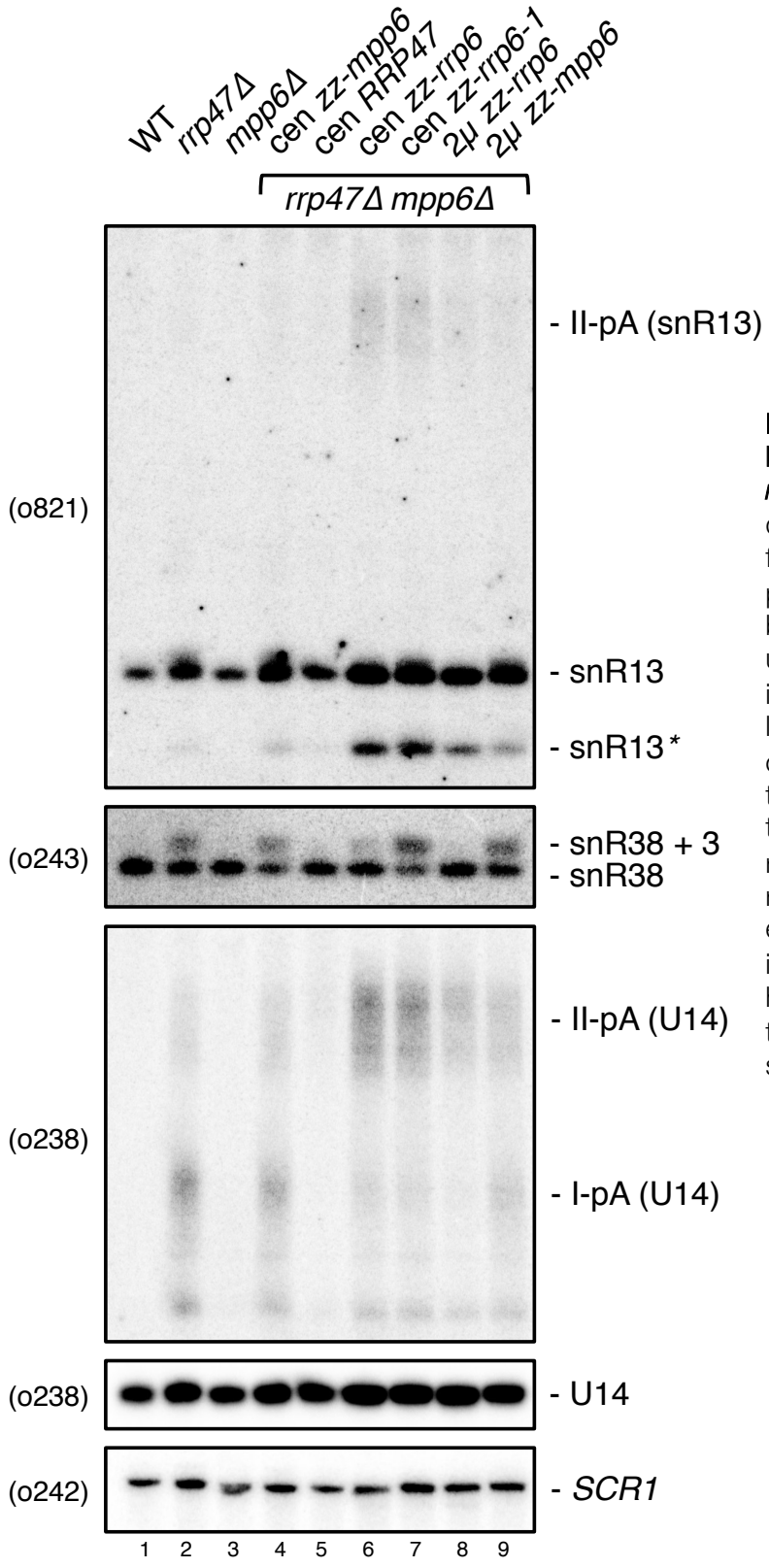

Figure 4.7. Northern analysis of box C/D snoRNAs in *mpp6Δ rrp47Δ* mutants. RNA isolated as described in Figure 4.5 was fractionated on 8% denaturing polyacrylamide gels and analysed by northern blot hybridisation using radiolabeled probes as indicated. Dispersed bands labeled I-pA and II-pA correspond with pre-snoRNAs that are polyadenylated at termination sites I or II respectively. To compare the relative levels of mature and extended U14 transcripts, two images are shown from the same hybridisation. Asterisks (*) denote truncated transcripts. *SCR1* served as a loading control.

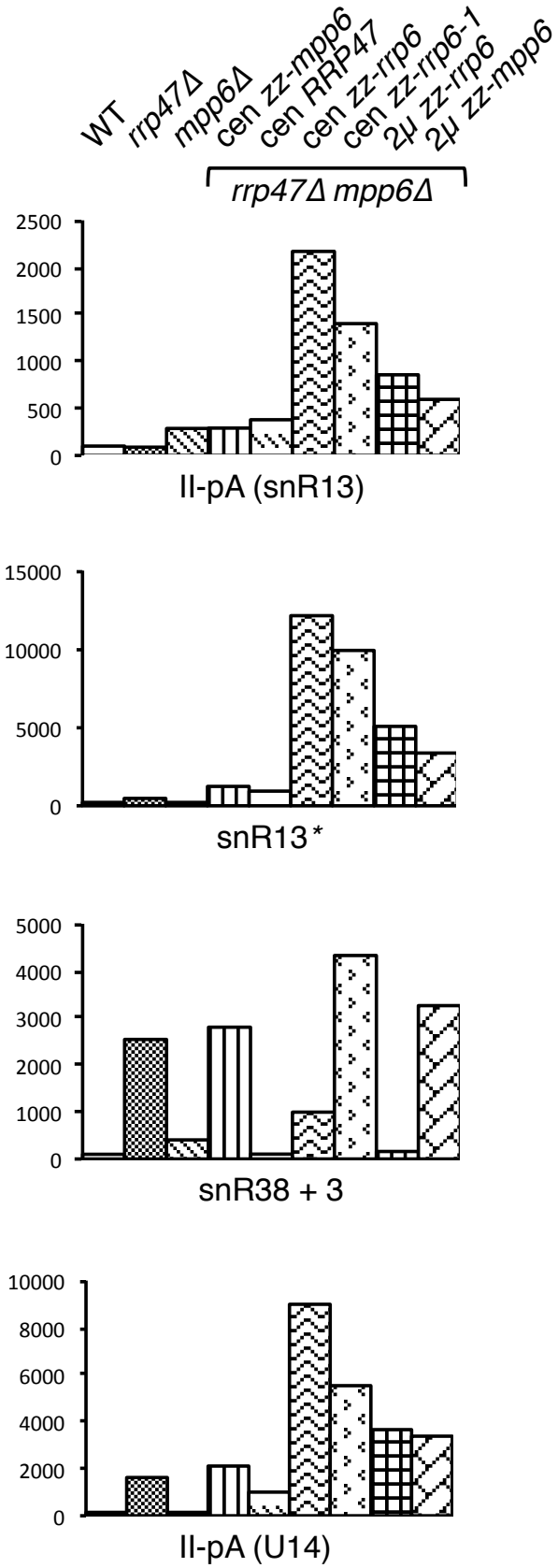

Figure 4.8. Quantification of box C/D snoRNA phenotypes in *mpp6Δ rrp47Δ* mutants. Quantification of northern blot signals from analysis of box C/D snoRNAs in *mpp6Δ rrp47Δ* mutants from Figure 4.7. Values of II-pA (snR13), snR13*, snR38 + 3 and II-pA(U14) are shown for each strain . Averages from two data sets are normalised to *SCR1* levels and expressed relative to the signals from the wildtype (WT) strain.

5'ETS, II-pA snoRNAs, truncated 5S*, U3* and snR13* transcripts are less severe in comparison to strains complemented with single copy plasmids encoding zz-Rrp6 and zz-rrp6-1 (Figures 4.5 and 4.7, compare lanes 6-8). Quantitative analysis shows reduction of at least 50% of the aforementioned RNA species when comparing the 2μ zz-Rrp6 mutants with the cen zz-Rrp6 strain (Figures 4.6 and 4.8). Strikingly, overexpression of Rrp6 showed almost complete suppression of the *IGS1-R* CUT transcript. However, CUTs have a very low expression level and any changes may seem more modest in comparison to more abundant transcripts.

No substantial suppression of phenotypes was seen in *mpp6Δ rrp47Δ* double mutants expressing zz-Mpp6 from a multicopy vector (Figures 4.5 and 4.7, lane 9). On average, accumulated RNA transcripts were comparable to strains expressing single copy zz-Mpp6 (Figures 4.6 and 4.8, compare lanes 4 and 9). Steady state protein analysis previously showed that overexpression of zz-Mpp6 does not stabilise normal expression levels of Rrp6 in an *rrp47Δ* strain (Figure 4.3, lane 9). This suggests that Mpp6 does not function to maintain normal levels of Rrp6 and that increased levels of Mpp6 protein does not complement RNA phenotypes observed in *rrp47Δ* mutants.

Strains assayed in the aforementioned RNA analyses were initially isolated by the plasmid shuffle method using 5'FOA to counter-select against a *URA3* plasmid. Exposure to 5'FOA can be highly mutagenic to cells with some studies reporting large levels of chromosomal instability (Wellington and Rustchenko, 2005). To validate that the above results are not due to genetic instability from 5'FOA exposure, 4 sets of independent *mpp6Δ rrp47Δ* strains bearing *RRP47, MPP6* and *rrp6* plasmids were isolated by the 5'FOA plasmid shuffle assay. Transformants were recovered from 5'FOA-containing media as soon as colonies were observable to minimize exposure. Total cellular RNA was isolated from independent isolates and analysed by acrylamide gel Northern analysis (Figure 4.9). The phenotypes observed in Figures 4.7 and 4.9 were shown to be reproducible in independent isolates. The *mpp6Δ rrp47Δ* double mutants complemented by zz-Rrp6 and zz-rrp6-1 expressed from centromeric plasmids

showed consistent accumulations of 3' extended snR13 transcripts and the 5S* truncated transcript in concordance with previous analyses (Figure 4.9 lanes 3-4, 9-10, 15-16 and 21-22). Complementation of the double mutant with a 2μ plasmid encoding zz-Rrp6 showed a suppression of said phenotypes (lanes 5, 11, 17 and 23). This validates that the effects seen in *mpp6Δ rrp47Δ* mutants are reproducible and are not due to mutations through 5'FOA exposure.

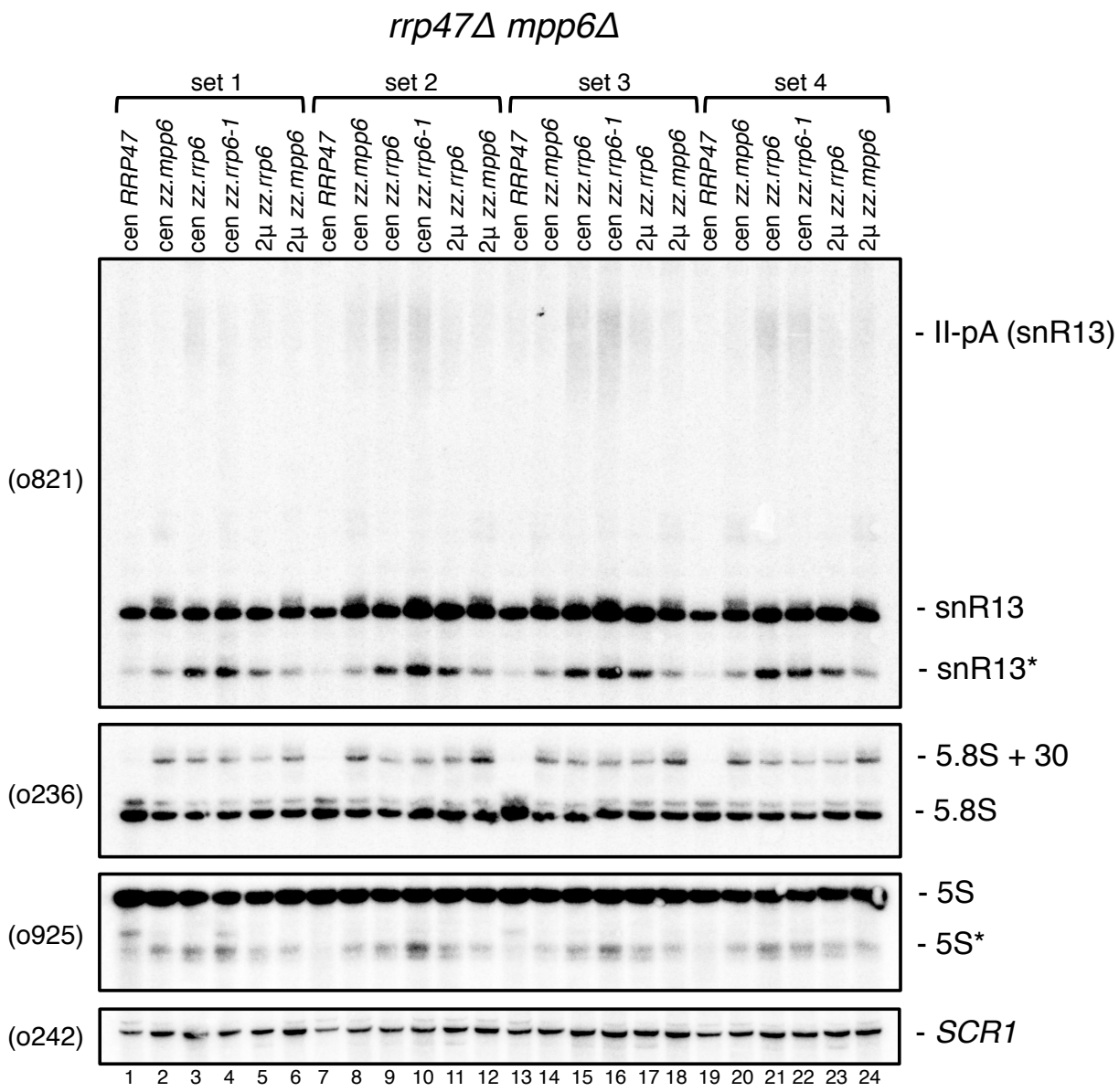

Figure 4.9. RNA analyses from independent *mpp6Δ rrp47Δ* isolates. Northern blot hybridisation analysis of total cellular RNA independently isolated *mpp6Δ rrp47Δ* mutants complemented with either centromeric (cen) plasmids encoding *zz-mpp6, RRP47, zz-rrp6, zz-rrp6-1* or 2-micron (2µ) plasmids encoding *zz-rrp6* and *zz-mpp6.* RNA from four sets os isolates (labelled sets 1-4) was analysed by hybridisation using the probes as indicated. Truncated RNA transcripts are indicated with an asterisk (*). *SCR1* served as a loading control.

4.3 Discussion

The functional relationship between Rrp6 and Rrp47 has been widely characterized in a number of previous analyses (Costello et al., 2011; Feigenbutz et al., 2013b; Mitchell et al., 2003; Stead et al., 2007). The normal function of Rrp6 in RNA processing and surveillance pathways relies on the presence of Rrp47. In turn, the stability of Rrp47 is dependent on the physical interaction with Rrp6 through their respective N-terminal domains. More recently it has been shown that the stability of Rrp6 is also dependent on this interaction, albeit less sensitive (Feigenbutz et al., 2013a). Whilst the relationship with Rrp6 has been well studied, the exact molecular function of Rrp47 has remained largely unknown. From recent analyses, it has been proposed that one role of Rrp47 is to maintain stable expression of Rrp6. Here, it is shown that by artificially increasing the expression levels of Rrp6, the requirement of Rrp47 for normal Rrp6 stability is negated. This allowed the isolation and analysis of *mpp6 rrp47* double mutants and supports previous observations in conditional *mpp6 rrp47* double mutants as described in Chapter 3.

Initially, it was found that plasmid-borne overexpression of Rrp6 was sufficient to complement the synthetic lethality of *mpp6Δ rrp47Δ* double mutants. This suggests that the requirement of Rrp47 for normal Rrp6 function could be circumvented. Loss of function *mpp6* alleles are synthetic lethal in combination with *rrp47Δ* or *rrp6Δ* mutants. As it has been widely characterised that Rrp47 and Rrp6 work in concert, it has been proposed that Mpp6 functions in pathways redundant with the Rrp6/Rrp47 homodimer. Therefore, in the absence of Mpp6, a functional Rrp6 pathway is required to maintain cell viability. If one function of Rrp47 is to maintain the normal expression levels of Rrp6, the synthetic lethality observed in *mpp6Δ rrp47Δ* mutants could be a result of the decreased amounts of Rrp6 protein. By increasing Rrp6 levels in these mutants, it was possible to maintain cell viability.

Interestingly, exogenous expression of a catalytically inactive *rrp6-1* mutant was able to complement the synthetic lethality of *mpp6Δ rrp47Δ* mutants. In parallel

analyses, the *rrp6-1* mutant was unable to complement the synthetic lethality of *rex1Δ rrp47Δ* mutants. This suggests that Rrp6 may have important non-catalytic roles in RNA surveillance pathways redundant with Mpp6-dependent pathways. One possibility, irrespective of catalytic function, is that the association of Rrp6 with the exosome stimulates the activity of Rrp44. Recent analyses have suggested that Rrp6 allosterically promotes the activity of Rrp44 through physical interactions with the nuclear exosome (Makino et al., 2013a; Wasmuth and Lima, 2012). Additionally, analysis of RNA substrates targeted by Rrp6- and Rrp44-dependent pathways shows a large degree of overlap (Gudipati et al., 2012b; Schneider et al., 2012). Therefore, it may be possible that the overexpression of catalytically inactive Rrp6 proteins would function to stimulate the function of Rrp44 in RNA surveillance pathways that are redundant with Rrp6-dependent pathways. Furthermore, Rrp6 could contribute to the recruitment of other proteins or complexes through physical interaction. Nevertheless, catalytic activity of Rrp6 is required for some processes in the absence of Mpp6 as *mpp6Δ rrp6-1* mutants were previously shown to be inviable in Chapter 3 (Section 3.2.9).

Increased expression of Rrp6 proteins allowed the isolation of *mpp6Δ rrp47Δ* double mutants. Strains complemented with centromeric (cen) or 2μ plasmids bearing *rrp6* alleles showed slow growth phenotypes in comparison to equivalent strains complemented by *RRP47* or *MPP6* alleles. Growth was not markedly improved in strains expressing Rrp6 from a high copy number vector in comparison to a single copy plasmid, although western blot analysis shows that Rrp6 expression was clearly increased. Additionally, the absence of Mpp6 or Rex1 did not have a negative effect on normal Rrp6 protein expression. This suggests that the growth rate limiting effect in complemented *mpp6Δ rrp47Δ* strains was not due to the amount of Rrp6 protein but due to the synergystic absence of Mpp6 and Rrp47.

Northern blot analyses of complemented *mpp6Δ rrp47Δ* mutants corroborated previous observations described in Chapter 3 and provides an insight into the molecular basis of the synthetic lethal association between *mpp6Δ* and *rrp47Δ* alleles. Conditional *mpp6 rrp47* mutants were extensively analysed in Chapter 3

and shown to accumulate a wide array of RNA transcripts that are normally degraded by the exosome complex in wildtype conditions. This was observed in *mpp6Δ rrp47Δ* mutants complemented by increased expression of Rrp6. Cells showed an accumulation of cryptic unstable transcripts (CUTs), truncated forms of stable RNAs, pre-rRNA processing byproducts and extended snoRNAs consistent with impaired RNA surveillance pathways. These phenotypes were partially suppressed upon increased expression of Rrp6 from a high copy number plasmid. This suggests that increased Rrp6 expression is able to maintain RNA surveillance pathways to an extent in the absence of Mpp6 and Rrp47. However, overexpression of Rrp6 was not able to fully suppress the observed phenotypes. This indicates that despite being required for normal Rrp6 expression, Rrp47 has other functions required for efficient RNA surveillance pathways. Interestingly, *mpp6Δ rrp47Δ* strains complemented by *rrp6-1* alleles showed comparable RNA surveillance phenotypes to equivalent strains complemented by a wildtype *RRP6* gene. This indicates, as previously mentioned, that Rrp6 has non-catalytic roles in targeting aberrant RNAs and CUTs for rapid degradation.

The functional redundancy between Rrp47/Rrp6- and Mpp6-dependent processes is supported by synthetic lethality observed in *mpp6Δ rrp47Δ* and *mpp6Δ rrp6Δ* mutants. In the absence of either pathway, cells are viable. However, as shown in Chapter 3, destabilisation of functional Rrp6/Rrp47 complexes in *mpp6Δ* mutants results in a block in growth. This may be explained by the strong accumulation of aberrant ncRNA species and stabilisation of cryptic unstable transcripts consistent with a loss of RNA surveillance and quality control mechanisms. This also highlights the biological importance of RNA surveillance as a loss in these pathways results in a loss of cell viability.

Functional redundancy is common in many biological systems and provides failsafe pathways in case one pathway is impaired. The results in this Chapter and Chapter 3 suggest a model where Rrp6/Rrp47 function in redundant RNA processing pathways with Rex1 (Figure 4.10.A) and in redundant discard pathways with Mpp6 (Figure 4.10.B).

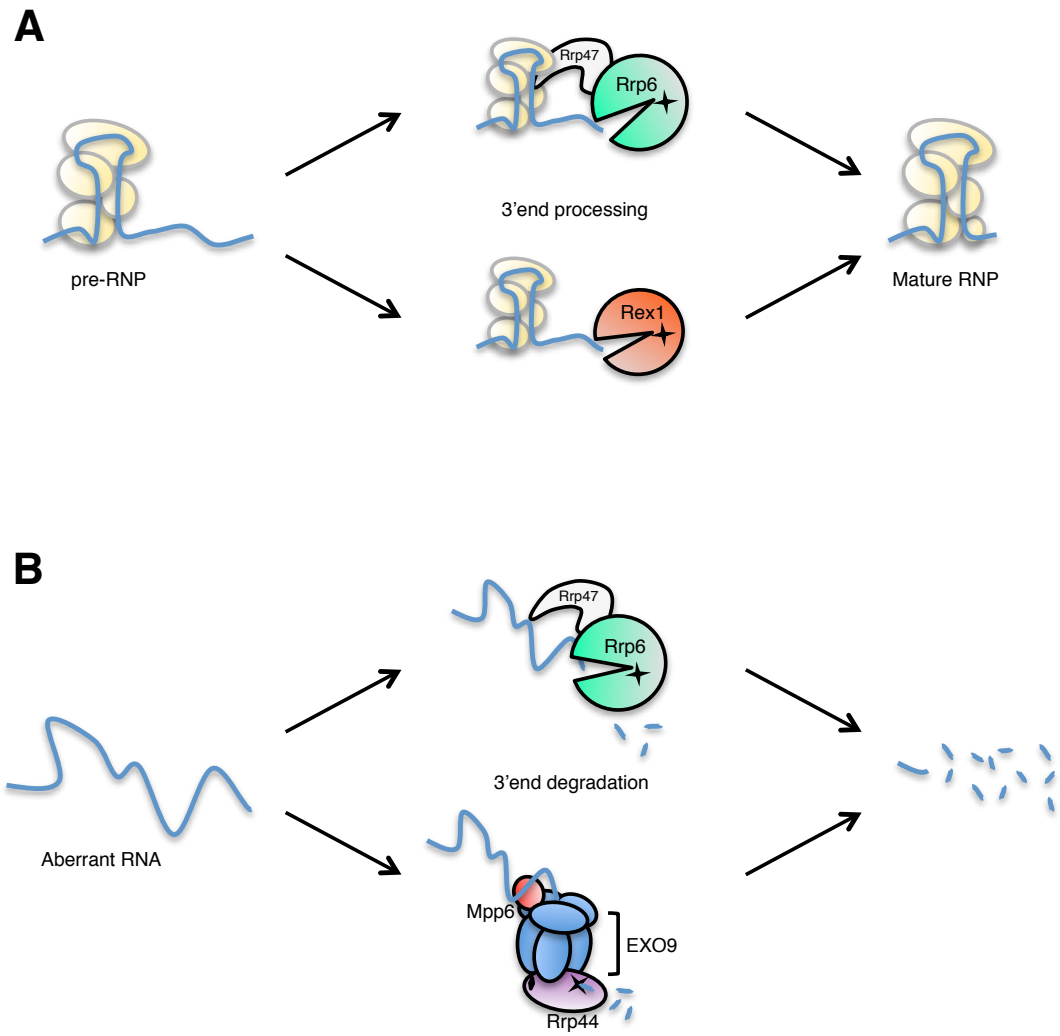

Figure 4.10. Rrp6/Rrp47, Rex1 and Mpp6 function in redundant RNA processing and degradation pathways. Model for 3'-end processing or degradation of transcripts via alternative, redundant pathways. **(A)** Rrp6 and Rex1 are required for the 3'-end exonucleolytic trimming of pre-RNAs to form mature RNPs. Both pathways can function in the absence of the other. However, a cumulative loss of both pathways results in loss of viability. **(B)** RNA transcripts targeted for discard pathways require either Rrp6/Rrp47- or Mpp6-dependent pathways. It is assumed that Mpp6-dependent pathways target substrates for degradation by Rrp44. Disruption of either pathway is tolerated *in vivo* yet *rrp6Δ mpp6Δ* or *rrp47Δ mpp6Δ* double mutants are synthetic lethal. Proteins with exonuclease domains are marked with a cross.

Whist it has been shown that Mpp6 is required for redundant RNA surveillance pathways; the molecular basis of its function is not understood. Mpp6 has been shown to associate with the exosome core and given that Rrp6 and Rrp44 share a common set of substrates, it has been proposed that Mpp6 acts to stimulate the function of Rrp44 in pathways redundant with Rrp6 (Milligan et al., 2008). An alternative proposition is that Mpp6 functions with the TRAMP polyadenylation complex and Rrp6 to target RNA substrates to the exosome core. This is supported by observed physical interactions between human Mpp6, Rrp6 and Mtr4 homologues (MPP6, PM-Scl100 and hMtr4 respectively) (Butler and Mitchell, 2011; Schilders et al., 2007). A more comprehensive characterisation of the Mpp6 protein is described in Chapter 5.

Chapter 5: Mutagenesis and functional characterisation of Mpp6

5.1 Introduction

In Chapters 3 and 4, the physical and functional interactions between the nuclear exosome associated exonuclease Rrp6 and cofactor partner Rrp47 were investigated. The Rrp6/Rrp47 heterodimer functions in RNA processing and surveillance pathways in concert with the nuclear exosome and a number of associated proteins and complexes. Functional disruption of the Rrp6/Rrp47 complex was shown to be synthetic lethal in combination with *mpp6Δ* and *rex1Δ* alleles. This is in agreement with previous studies that showed *rrp6Δ* or *rrp47Δ* mutants are synthetic lethal in combination with *mpp6Δ* or *rex1Δ* alleles (Milligan et al., 2008; Peng et al., 2003). RNA analyses of conditional *mpp6 rrp47* showed a block in RNA surveillance and turnover pathways, while *rex1 rrp47* mutants showed a specific defect in snoRNA maturation pathways (Chapter 1., Garland et al. 2013). These results support the conclusion that Mpp6 and Rex1 function in RNA surveillance and processing pathways redundant with the function of Rrp6/Rrp47.

The small, nuclear protein Mpp6 was originally identified in yeast in a genome-wide screen for synthetic lethal interactions with *rrp47Δ* mutants and subsequently shown to associate with the nuclear exosome. Additionally, *mpp6Δ* mutants were shown to be synthetic lethal in combination with *rrp6Δ* mutants or the loss of Air1, an RNA binding protein and part the TRAMP polyadenylation complex (Milligan et al., 2008). Mpp6 shows RNA binding activity in yeast and human homologues with a preference for pyrimidine-rich sequences (Milligan et al., 2008; Schilders et al., 2005). However, Mpp6 is devoid of any characterised RNA binding motifs. Cells lacking Mpp6 show mild defects in RNA surveillance and degradation pathways including the accumulation of cryptic unstable transcripts (CUTs), pre-rRNA processing byproducts and aberrant forms of stable ncRNAs. These effects are exacerbated in combination with conditional *rrp47* mutants (Feigenbutz et al., 2013a; Garland et al., 2013; Milligan et al., 2008). Whilst is has been proposed

that Mpp6 functions in RNA surveillance pathways redundant with the function of the Rrp6/Rrp47 complex, the molecular basis of this is still not understood. One model is that Mpp6 functions to stimulate the activity of the core-exosome associated exonuclease Rrp44 (also known as Dis3) (Milligan et al., 2008). However, any possible stimulation may be indirect, as human MPP6 has been shown to associate with the exosome core in the absence of DIS3 (Chen et al., 2001). An alternative proposal is that Mpp6 acts to promote the functional coupling between Rrp6 and the TRAMP complex. This is supported by the reported physical interaction between human homologues of Mpp6, Rrp6 and Mtr4 (MPP6, PM-Scl-100 and hMtr4, respectively) (Schilders et al., 2007).

The amino acid sequence of Mpp6 contains no characterised domains that may hint to the function of the protein. Alignment of known Mpp6 homologues in model organisms identifies two regions of high conservation (Figure 5.1) (Milligan et al., 2008). In the yeast Mpp6 protein, these sequences map to an N-terminal motif I (residues L11 to F23) and a distal motif II (residues G111-S119). Using these sequences for consecutive PSI-blast searches only identifies other Mpp6 homologues. The secondary structure of Mpp6 was predicted using the Phyre^2 web server (Kelley and Sternberg, 2009). These analyses predicted that 61% of the protein sequence is disordered (Figure 5.2). Additionally, predicted secondary structure features are modeled with a low confidence score (26%). The N-terminal conserved motif I (residues L11-F23) is predicted to form an alpha-helix structure with mid-high confidence scores. However, the reliability of such data is not ideal with such a low confidence score. The C-terminal region of Mpp6 contains a high proportion of lysine and arginine residues. A lysine-rich domain is also found in the C-terminus of Rrp47. This region was shown to be required for RNA binding *in vitro* but not for the function of the protein *in vivo* (Costello et al., 2011). The C-terminal lysine-rich region is found in other yeast Mpp6 homologues (Appendix II) but not as conserved between homologues in higher eukaryotes (Appendix I).

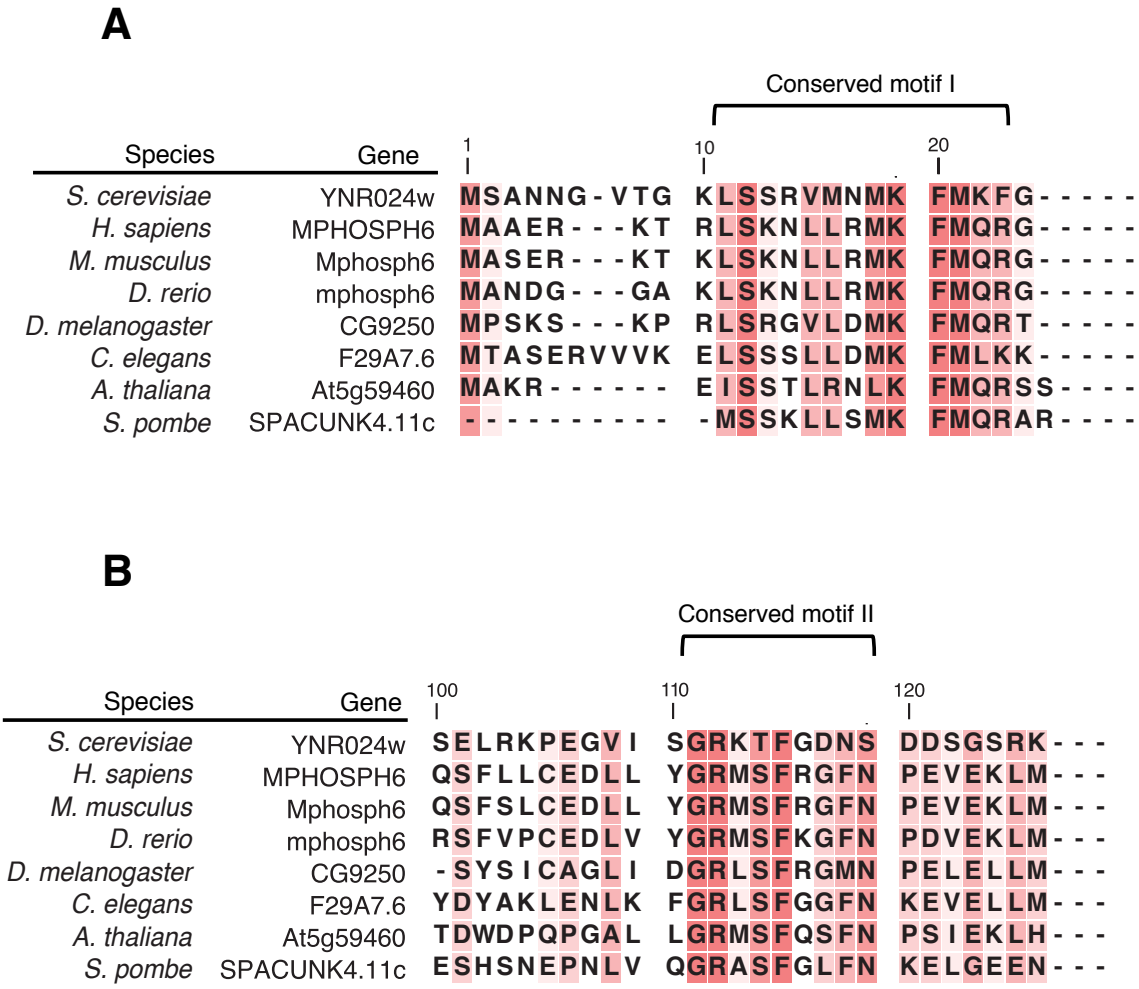

Figure 5.1. Mpp6 contains two highly conserved motifs. Amino acid sequence alignment of Mpp6 homologues from model eukaryotes. Sequences from *Saccharomyces cerevisiae*, *Homo sapiens*, *Mus musculus*, *Danio rerio*, *Drosophila melanogaster*, *Caenorhabditis elegans*, *Arabidopsis thaliana* and *Schizosaccharomyces pombe* were aligned using Clustal Omega (Sievers et al. 2011) and edited using CLC Main Workbench 6 (CLC Bio, Aahus, Denmark). Residues with high conservation are highlighted in red. Yeast Mpp6 contains an N-terminal motif I between residues L11 and F23 (A) and a distal motif II between residues G111 and S119 (B). Amino acid numbers are according to residues in the yeast Mpp6 sequence. A full alignment is found in Appendix I

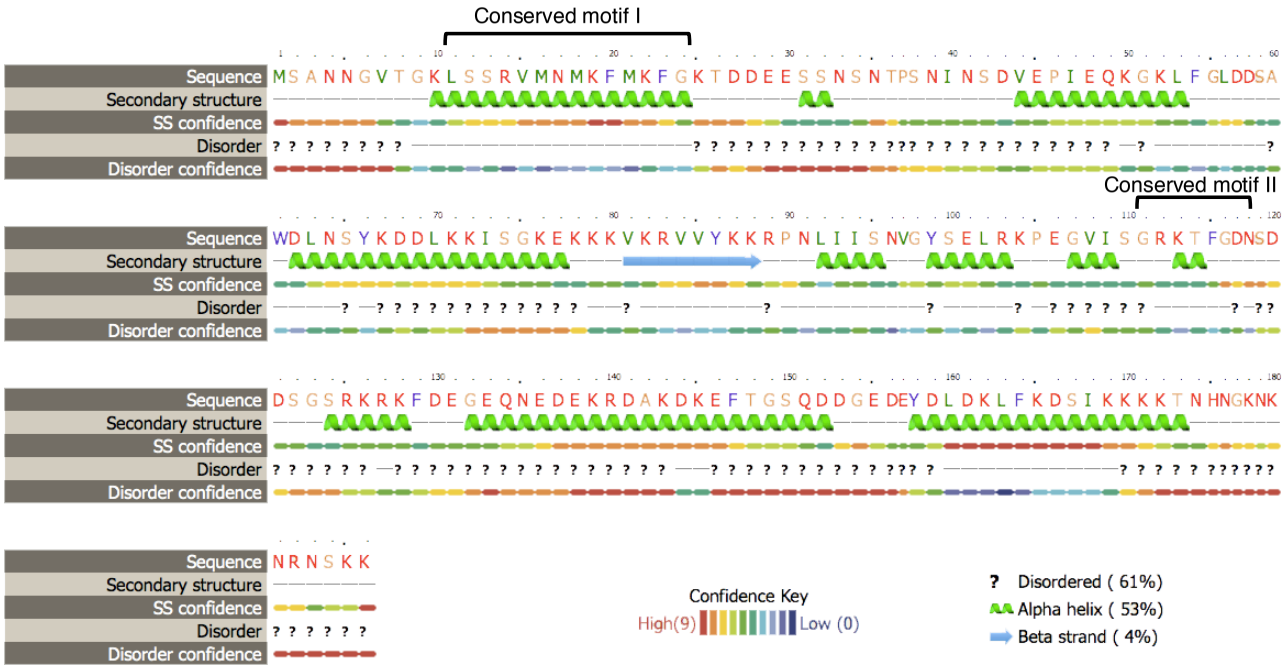

Figure 5.2. Secondary structure prediction of Mpp6. RAW output of the secondary structure prediction obtained for yeast Mpp6 using Phyre[2] web server. Three independent secondary structure predictions using PSIPRED, JNet and Sspro score each residue for structure and give a confidence value of 0 (low, blue) to 9 (high, red) which are averaged to form a consensus. Phyre also uses the DISOPRED server to prodive a prediction score for disordered (?) or ordered (-) residues. Two conserved motifs found in Mpp6 are also indicated.

In the absence of domain information or structural data for Mpp6, this Chapter describes a mutagenesis study to characterise functional regions of the protein. A random mutagenesis approach was employed to generate a library of *mpp6* mutants that were screened for function using an *mpp6Δ rrp47Δ* plasmid shuffle assay. Loss-of function mutations were identified in the N-terminal conserved region in addition to sites in areas of low conservation. The DECOID approach, described in Chapter 3, was used to analyse RNA phenotypes of conditional *mpp6 rrp47* mutants and revealed regions in Mpp6 required for function in RNA surveillance and degradation pathways. Finally, possible links between Mpp6 and larger complexes was investigated in *rrp6* and TRAMP complex mutants using glycerol gradient ultracentrifugation. Sedimentation analysis of Mpp6 mutants identifies critical residues required for complex association.

5.1.1 Random mutagenesis methods for *in vitro* evolution

Random mutagenesis is a powerful tool used to alter the chemical and physical properties of proteins. When combined with precise screening procedures to identify loss-of function mutations, this provides a viable method to map functional regions of a protein.

With no identifiable domain features or structural data, a random mutagenesis approach seemed ideal to investigate the functional regions of Mpp6. A library of random *mpp6* mutants could be screen could be screened for functionality by the ability to complement the *mpp6Δ rrp47Δ* synthetic lethality using a plasmid shuffle assay generated in Chapter 3.

Various methods for generating random mutations *in vitro* have been well documented including the use of chemical mutagens, passing DNA through mutator strains or using error-prone PCR (EPPCR) (Labrou, 2010). Each method is effective depending on the application. Chemical mutagens such as nitrous acid (HNO_2) or ethyl methanesulfonate (EMS) alter the chemical structure of nucleotides by deamination or alkylation respectively and promote base-pair substitutions

(Kaudewitz, 1959; Lai et al., 2004). Chemical mutagenesis can be used on DNA *in vitro* or on whole cells to introduce random mutations. Random mutations can be introduced into DNA by passaging plasmids through mutator strains lacking DNA repair mechanisms (Cox, 1976). The mutagenic *E. coli* strain XL1-Red (Stratagene) contains *mutS*, *mutD* and *mutT* mutations that disrupt primary DNA repair pathways. The rate of mutation of DNA is measured to be ~5000-fold higher than wildtype cells (Greener et al., 1996). This method has the advantage that a wide array of mutations can be incorporated including insertions, deletions and frameshifts. However, the drawback is that the bacterial strain becomes chromosomally unstable due to errors in replication of endogenous genes (Labrou, 2010). Finally, error-prone PCR methods promote random copying errors by imposing low-fidelity conditions to PCR reactions. PCR can be used to amplify the DNA of interest under mutagenic conditions to lower the fidelity of the DNA polymerase. *Taq* DNA polymerase is generally used due to its lack of 3'-5' proofreading activity and exhibits a mutation rate of 2.2×10^{-5} errors per nt per cycle (Lundberg et al., 1991). Altering standard PCR conditions can increase the degree of mutagenesis. Increasing $MgCl_2$ concentrations, the addition of $MnCl_2$, using an unbalanced ratio of dNTPs and increasing the polymerase concentration are all methods of increasing the rate of mutation in PCR (Pritchard et al., 2005). An advantage to using PCR-based mutagenesis over other methods is that mutations can be specifically directed to the ORF of interest before cloning into plasmids for analysis. Whilst the cloning step may be rate limiting, this prevents mutations forming in regions of plasmids outside of the site of interest.

For the purposes of this study, error-prone based PCR methods were employed to introduce random mutations into the *MPP6* open reading frame. Libraries of *mpp6* mutants were generating through consecutive rounds of standard PCR using *Taq* polymerase. For each round of PCR, a reaction volume of 100 μl was divided into 10 x 10 μl volumes before thermocycling and pooled at the end. This was to prevent the predominance of mutations arising early in PCR cycles and would allow a more heterogeneous population of unique mutations. DNA generated after the primary PCR round (1°) was used as a template for the secondary PCR round (2°) and so on for five rounds of PCR. This allowed the

generation of five libraries of *mpp6* DNA fragments with increasing degrees of mutation that were subsequently cloned into plasmids using homologous recombination methods in yeast.

5.2 Results

5.2.1. Construction of a mutational library in *MPP6* using error-prone PCR (EPPCR)

PCR based random mutagenesis was employed to generate a library of mutants in the *MPP6* open reading frame in order to determine functionally important regions of *MPP6*. Section 5.1.2. describes various methods of *in vitro* mutagenesis including pros, cons and mutational biases. However, this study utilized PCR-based mutagenesis using *Taq* DNA polymerase isolated from *Thermus aquaticus*. *Taq* polymerase is commonly used as a method to introduce random mutations due to its naturally high error rate from a lack of proofreading activity (Keohavong and Thilly, 1989). Mutational bias can be manipulated by modifications to the PCR protocol including using unequal ratios of dNTPs, increasing $MgCl_2$ concentration or the addition of $MnCl_2$ (Leung et al., 1989). This study employed consecutive rounds of standard PCR on the *MPP6* ORF to create a library of PCR products with increasing degrees of mutagenicity. Products were cloned into plasmids through yeast recombinational cloning (Ma et al., 1987). An overview schematic describing the generation of the random mutant library is depicted in Figure 5.3.

PCR was performed on a yeast centromeric plasmid encoding an epitope-tagged *zz-MPP6* allele (p599) using a forward primer complementary to the T3 RNA polymerase promoter (o68) and a reverse primer complementary to downstream regions of the *MPP6* ORF (o598). Standard PCR reaction mixes were prepared in 100µl volumes before splitting into 10 x 10µl volumes prior to thermocycling and pooled after the procedure. This method was employed to prevent a bias of certain mutations that may arise during early cycles of PCR and increase the

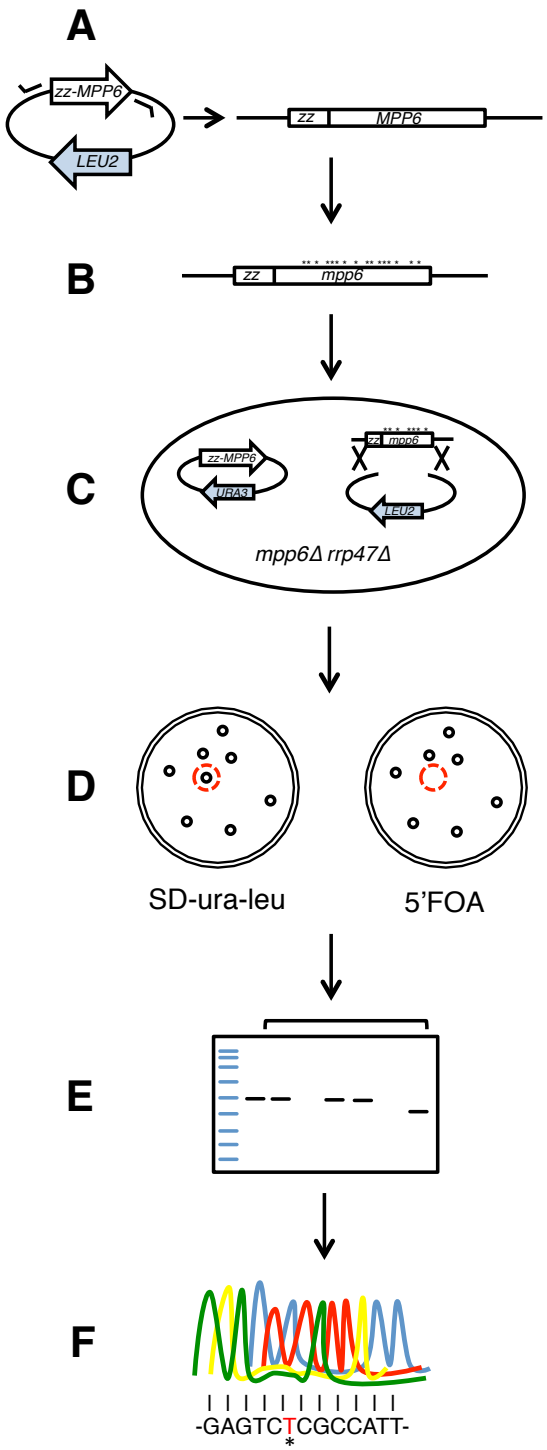

Figure 5.3. Generation of a library of random mutations in the *MPP6* ORF and subsequent screening steps. A library of random mutations in the *MPP6* ORF was created using error prone PCR and resulting transformants were selected for loss of function in a plasmid shuffle assay. (A) The *zz-MPP6* ORF was amplified from plasmid p599 by PCR to generate a wildtype template fragment. (B) *in vitro* evolution using error-prone PCR. Consecutive rounds of PCR were carried out on the template fragment using low fidelity *Taq* DNA polymerase to generate a library of mutant *mpp6* ORF fragments. (C) Libraries of mutant *mpp6* ORFs were co-transformed along with a gapped *LEU2* plasmid into a *rrp47Δ mpp6Δ* plasmid shuffle strain bearing a *URA3* plasmid encoding wildtype zz-Mpp6. Mutant *mpp6* ORF fragments contained regions of homology with the gapped plasmid to allow for homologous recombination in yeast. (D) Transformants were selected for functionality by replica plating colonies from solid SD-ura-leu media to 5'FOA media. Colonies that were unable to grow on 5'FOA after 3 days at 30°C were recovered from the permissive plate for further analysis. (E) Strains that were non-viable on 5'FOA media were screened for expression of mutant zz-fusion proteins. The wildtype *zz-MPP6*, *URA3* plasmid was purged from strains by transforming with a *RRP47, HIS3* plasmid (p425) and passaging over 5'FOA. Denatured lysates were fractioned by SDS PAGE and analysed by western blotting using the PAP antibody. (F) Screened *mpp6* mutants were analysed by sequencing to determine mutation sites. Mutant *mpp6* ORFs were amplified direct from yeast using colony PCR before analysis by Sanger sequencing.

heterogeneity of mutations. Following PCR, DNA products were analysed by agarose gel electrophoresis to validate the thermocycling reaction and determine DNA concentration (Figure 5.4. B). The PCR generated a 1650 nt fragment consisting of the coding regions for *zz*-tag, the *MPP6* ORF plus flanking sequences. DNA was purified using a PCR cleanup kit before using 20ng as a template for the second PCR reaction. Five consecutive PCR reactions (termed 1°- 5°) were carried out and products were confirmed by agarose gel electrophoresis (Figure 5.4. A-B).

Yeast recombinational cloning can be used to insert DNA fragments into plasmids by exploiting the efficient homologous recombination machinery in *S. cerevisiae* (Oldenburg et al., 1997). By co-transforming a DNA fragment with a linearised plasmid bearing regions of sufficient homology, a ligated plasmid will be generated through homologous recombination *in vivo*.

A yeast centromeric *LEU2* plasmid encoding for zz-Mpp6 under the control of the *RRP4* promoter (p599) was digested with NcoI and PshAI to remove the *MPP6* open reading frame sequence. This allows for 590 nt of homologous sequence with the EPPCR generated *MPP6* fragment (Figure 5.5. A). Gapped plasmids were recovered by agarose gel electrophoresis and gel purified to remove the digested. Purified gapped plasmid was co-transformed into the *mpp6Δ rrp47Δ* plasmid shuffle strain (described in Section 3.2.2) along with PCR fragments from EPPCR libraries 1° through 5°. A parallel transformation was carried out with the gapped plasmid alone. Roughly ~7500 colonies were scored on plates with strains transformed with both gapped vector and insert DNA. The gapped-plasmid control transformation yielded ~ 1000 background colonies on average, most likely due to ligated plasmids generated through non-homologous end joining pathways in yeast (Daley et al., 2005). Primary transformants were washed off plates and stored in glycerol at -80°C. This allowed for re-plating of cells at suitable densities to distinguish single colonies.

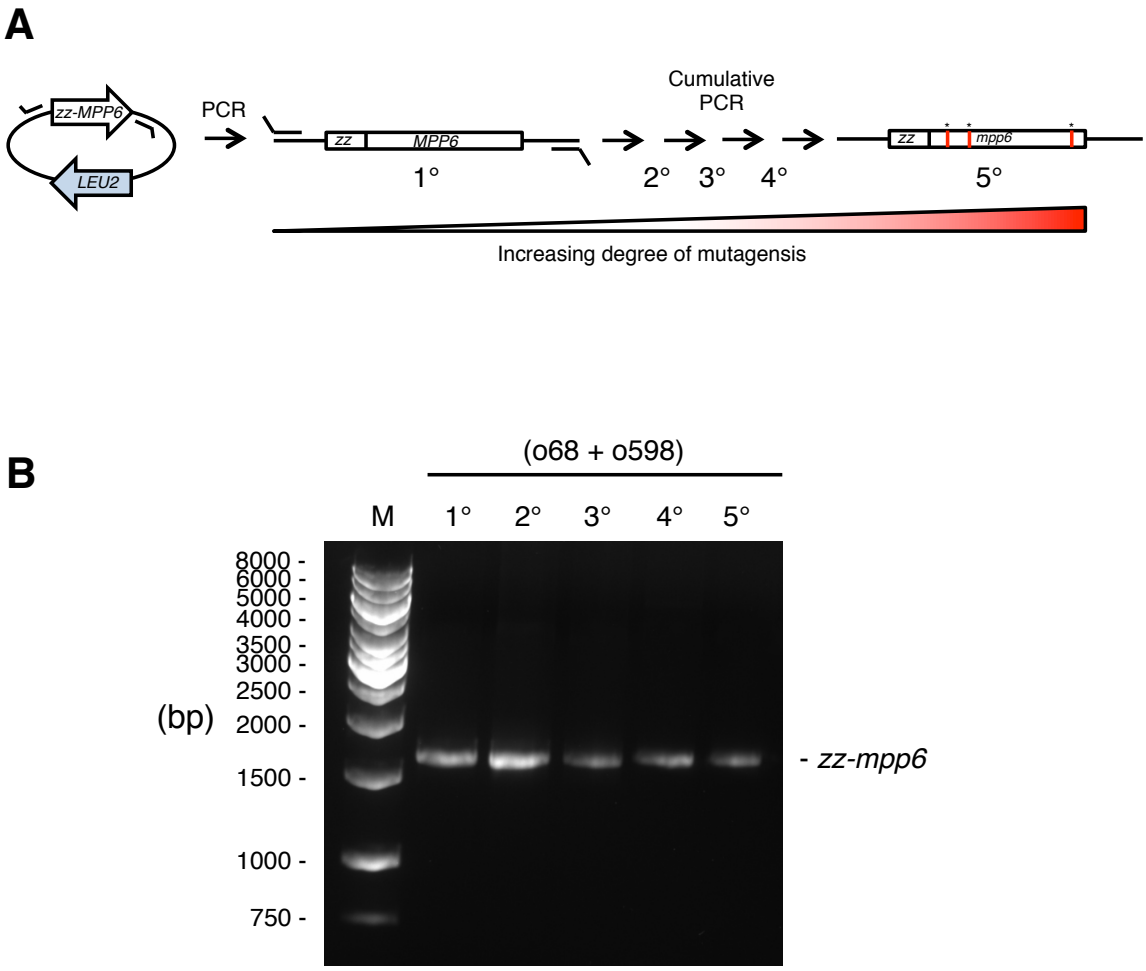

Figure 5.4. Generation of random mutant library using error-prone PCR. (A) Schematic of error prone PCR method. The *zz-MPP6* allele and flanking regions was amplified from a plasmid construct (p599) by PCR using oligonucleotides o68 and o598 using *Taq* DNA polymerase. PCR products were purified before use in 5 sequential rounds of PCR to generate independent libraries of increasing mutagensis. **(B)** Validation of error-prone PCR products from each PCR step. A 1/50 volume of each PCR reaction was fractionated by agarose gel electrophoresis to confirm successful PCR products. Each round number of error-prone PCR is suffixed by the degrees symbol for the primary (1°) to quinary (5°) EPPCR cycling reaction.

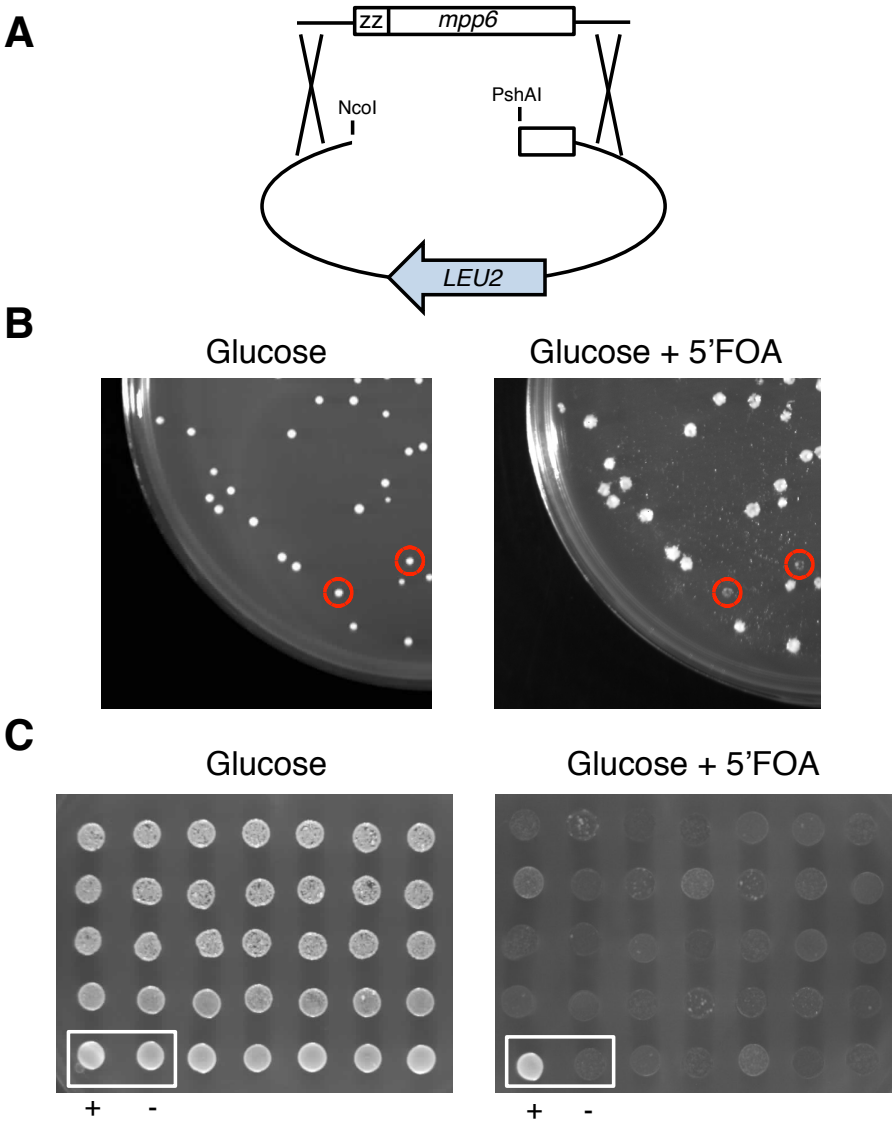

Figure 5.5. Cloning of mutant libraries by *in vivo* homologous recombination and screening by 5'FOA selection. (A) Schematic of recombination event to generate library of plasmids bearing mutant *mpp6* alleles. A *LEU2* plasmid encoding wildtype zz-Mpp6 (p599) was linearised by NcoI/PshAI digestion and co-transformed with insert DNA, generated by error-prone PCR, into a *mpp6Δ rrp47Δ* plasmid shuffle strain bearing a *URA3* plasmid encoding wildtype zz-Mpp6 (p593). Transformants were selected on synthetic glucose medium lacking uracil and leucine (SD-ura-leu). **(B)** Mpp6 mutants were assayed for function for complementation of the *mpp6Δ rrp47Δ* synthetic lethality. Strains harboring *mpp6* mutants were grown on SD-ura-leu media at 30°C for 3 days before replica plating to minimal media containing 5'FOA and growing for a further 3 days. Non-viable strains on 5'FOA were recovered from the glucose plate for further screening. **(C)** Recovered mutants were confirmed for loss of viability on 5'FOA media. Candidate strains were grown to saturation in liquid SD-ura-leu medium before diluting 100 fold and spotting onto solid glucose- and glucose + 5'FOA media. The plasmid shuffle strain was transformed with a wildtype *MPP6*, *LEU2* plasmid and an empty *LEU2* vector as positive (+) and negative (-) controls. Plates were incubated at 30°C for 3 days before photographing.

5.2.2. Scoring *mpp6* mutants for loss of function in a *mpp6Δ rrp47Δ* plasmid shuffle assay

The *mpp6Δ rrp47Δ* plasmid shuffle assay (described in Section 3.2.2 and Figure 3.1) was constructed in order to test *MPP6* and *RRP47* alleles for functionality. In brief, a double *mpp6Δ rrp47Δ* strain bearing a wildtype *MPP6* allele on a *URA3* plasmid is transformed with a second plasmid bearing mutated *MPP6* alleles and a *LEU2* marker. Transformants are tested for viability on media containing 5-Fluoroorotic Acid (5'FOA), which counter-selects against strains expressing the *URA3* gene. If the second plasmid bears a functional *MPP6* allele, the strain is able to lose the *URA3* plasmid through mitotic destabilisation and is viable on 5'FOA media. If the second plasmid bears a non-functional *MPP6* allele, the *URA3* plasmid is not lost through segregation and the strain generates toxic 5-flourouracil on 5'FOA media and loses viability.

Section 5.2.1. describes the creation of a library of mutant *mpp6* plasmids generated in the *mpp6Δ rrp47Δ* plasmid shuffle strain. In order to screen mutants for loss of function alleles, mutant libraries were assayed for growth on media containing 5'FOA. Cells from libraries produced from tertiary and quinary EPPCR DNA fragments (termed 3° and 5°), were plated onto selective media at suitable density to distinguish single colonies (~200-400 colonies per plate). Colonies formed after 3 days incubation at 30°C were replica plated onto minimal media containing 5'FOA and incubated at 30°C for a further 3 days. Strains unable to grow on 5'FOA were recovered from the original plate and stored for further analysis. Figure 5.5. B shows an example of mutant screening by 5'FOA selection. Roughly 8000 colonies per library were screened to cover the initial estimate of transformants on the primary plate. From the 3° and 5° libraries, 55 and 68 strains were scored as non-viable on 5'FOA media respectively. Loss of function mutants were validated by growing to saturation in liquid media before spotting onto solid glucose- and glucose + 5'FOA media (Figure 5.5. C). The proportion of mutants isolated from the 5° library was not significantly greater than that of the 3° library. In total, 123 non-functional mutants were scored from screening of ~14,000 colonies, roughly a 1% hit-rate.

5.2.3 Screening loss of function *mpp6* mutants for protein expression

From initial screening, 123 strains bearing loss-of function *mpp6* alleles were isolated by 5'FOA counterselection using the *mpp6Δ rrp47Δ* plasmid shuffle assay. Loss of function phenotypes can be attributed to a loss of protein expression through mutation. For the purposes of this investigation, such mutants are not useful for study. Additionally, a high background of transformants was observed in cells transformed with a gapped plasmid alone suggesting a significant proportion of re-ligated plasmids are formed through non-homologous end joining. Such plasmids would give false-positive results when screening for loss of function alleles by 5'FOA counterselection. Mutant plasmids generated by homologous recombination were constructed to encode epitope tagged zz-Mpp6 fusion peptides in order to assay for protein expression using the PAP antibody. However, these plasmids were constructed in an *mpp6Δ rrp47Δ* plasmid shuffle strain complemented by a *URA3* plasmid encoding zz-Mpp6. In order to assay for the expression of the mutant proteins, strains were cured of the *URA3* maintenance plasmid by genetic shuffling. A yeast centromeric plasmid encoding *RRP47* and *HIS3* alleles was transformed into yeast *mpp6Δ rrp47Δ* strains bearing plasmids encoding wildtype and mutant zz-Mpp6 fusion proteins on *URA3* and *LEU2* vectors respectively. An *RRP47* allele would complement the synthetic lethality of *mpp6Δ rrp47Δ* and allow for loss of the *URA3* plasmid encoding wildtype *MPP6.* Successful transformants were grown on media containing 5'FOA to purge the *URA3* containing plasmid. Resulting *mpp6Δ rrp47Δ* strains contained *LEU2* plasmids bearing mutant *mpp6* alleles and a *HIS3* plasmid encoding Rrp47.

Lysates from strains expressing epitope tagged Mpp6 mutants were screened by SDS PAGE and western blotting using the PAP antibody. Parallel lysates from *mpp6Δ rrp47Δ* strains bearing either zz-Mpp6 encoding plasmids or an empty vector were used to compare relative expression of wildtype and mutant zz-Mpp6 proteins. In addition, lysates from a strain encoding an endogenous C-terminal TAP tagged *MPP6* allele was used to compare mutant protein expression to wildtype Mpp6 under the control of its endogenous promoter. As described in

Section 3.2.1, zz-Mpp6 fusion proteins under the control of the *RRP4* promoter are expressed 3 fold greater than Mpp6-TAP fusion proteins under the control of the endogenous *MPP6* promoter. Of the 123 strains isolated from the 5'FOA screen (Section 5.2.2), 66 (54%) expressed zz-Mpp6 fusion proteins detectable by western blot analyses using the PAP antibody.

An example of screening by western blot analysis is shown in Figure 5.6. The western screen identified zz-Mpp6 proteins of variable size and expression level. Fusion proteins were categorized into sub-groups depending on size. In total, 44% of strains screened expressed a full-length zz-Mpp6 protein (Figure 5.6. Lanes 7, 10, 12 and 14). The majority of proteins detected (48.5%) were truncated to varying sizes between 20 - 25 kDa as determined by comparison with molecular weight standards (Lanes 5-6, 9, 13, 15-17). Additionally, a small number of strains (7.5%) expressed zz-fusion proteins that migrated slower than wildtype zz-Mpp6 (Lane 8). Upon further analysis, described below, these extended proteins arise due to a mutation in the natural *MPP6* stop codon resulting in translational read-through to the next available stop codon.

This screen removed Mpp6 mutants that did not express detectable protein. A loss of expression could be attributed to mutations causing destabilisation of correct protein folding and are therefore targeted for rapid degradation. Another possibility is that a low percentage of gapped plasmids were re-circularised upon transformation in yeast by non-homologous end joining and did not contain EPPCR-generated insert DNA.

A more comprehensive analysis of Mpp6 mutant protein expression is detailed in Section 5.2.8.

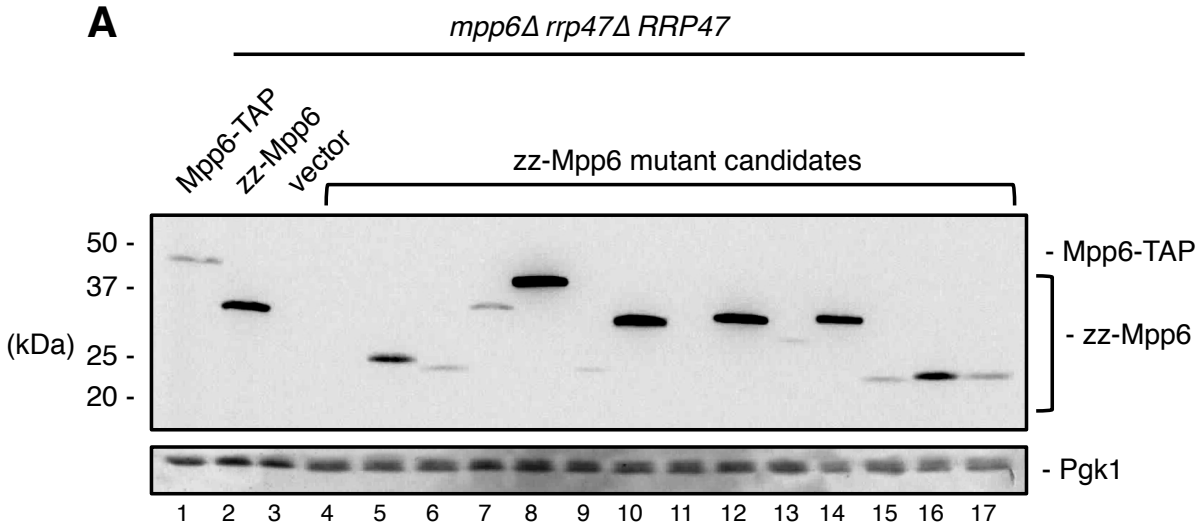

B

Protein type	Number of mutants isolated	Percentage of non-functional mutants (%)	Percentage of protein-expressing mutants (%)
Full length	29	23.6	44.0
Truncation	32	26.0	48.5
Extension	5	4.1	7.5
No protein	57	46.3	–
	123		

Figure 5.6. Screening *mpp6* mutants by protein expression. (A) Western blot analysis of strains harbouring loss of function *mpp6* alleles to screen for expression of a zz-Mpp6 protein. Lysates from strains expressing wildtype Mpp6-TAP and zz-Mpp6, under control of *MPP6* and *RRP4* promoters respectively, were analysed in parallel. Denatured protein samples were fractionated on a 10% polyaderylamide gel and analysed by western blotting using the PAP antibody to detect tagged Mpp6 proteins (*upper* panel). An antiserum against Pgk1 was using as a loading control (*lower* panel). (B) Relative percentages of proteins identified by western blot analysis. Candidate strains were grouped by expression of either full length, truncated and extended zz-Mpp6 proteins. Additionally, strains were identified that did not express detectable proteins.

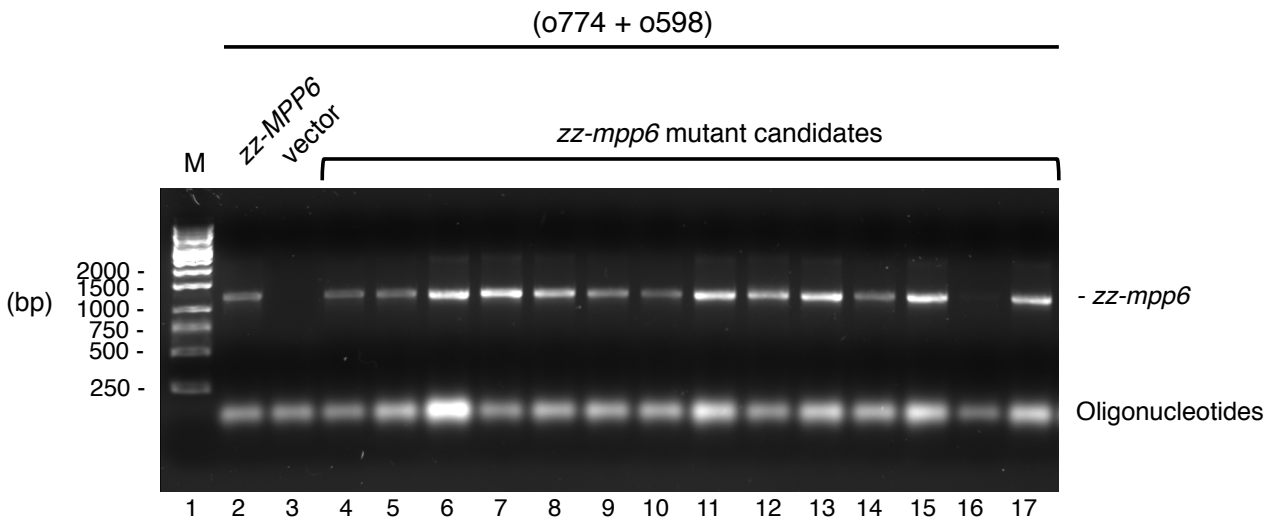

Figure 5.7. Amplification of *mpp6* alleles from yeast colonies. Colony PCR to amplify *mpp6* alleles from loss of function mutants. Fresh growing yeast colonies were added to PCR reactions directly and lysed during an extended initial heating step. A forward primer complementary to the zz-tag and a reverse primer complementary to downstream *MPP6* sequences were used to amplify *zz-mpp6* alleles (1194 nt). PCR products were confirmed by agarose gel electrophoresis before sequencing. Unincorporated oligonucleotides are indicated

5.2.4. Sequence analysis of *mpp6* mutants

In order to analyse the extent of mutation in the library of loss of function *mpp6* mutants, DNA sequences of mutagenised ORFs were analysed by Sanger sequencing. Initial attempts to recover plasmids bearing mutant *mpp6* alleles from yeast were unsuccessful. Therefore a colony PCR-based method was employed to amplify the *mpp6* ORF directly from yeast colonies. Primers complementary to sequences in the *zz*-tag (o774) and downstream of the *MPP6* open reading frame (o598) were used to generate a DNA fragment of 1194 nt. The forward primer complementary to the zz-tag was used to prevent amplification of the endogenous *mpp6Δ::kanMX4* allele. PCR products were confirmed by agarose gel electrophoresis (Figure 5.7) and purified using spin columns before submission for sequencing analysis.

Raw DNA sequences were translated into amino acid sequences *in silico* using the ExPASy Translate tool (Artimo et al., 2012) and aligned using Clustal Omega (Sievers et al., 2011). Mutants were sub-categorized and arranged into point mutations and frameshift mutations (Figure 5.8). In some cases, duplicate mutations arose from independent clones. Duplicated point mutants were included in the alignment. However, a frameshift mutation at residue I73 was found in 12 individual mutants and duplicated sequences were omitted from the alignment.

Analysis of point mutant sequences identified two single point mutants: V15D and K145R. The V15D mutation lies in a highly conserved motif found in Mpp6 homologues (Milligan et al., 2008) as shown in Figure 5.1 However, the K145R mutation resides in a previously un-characterised region of Mpp6. The C-terminal domain of Mpp6 has a large fraction of basic residues including K145. A highly basic C-terminus is also found in the nuclear exosome-associated RNA binding protein, Rrp47. A *rrp47* mutant lacking the C-terminal domain (*rrp47ΔC*) is unable to bind RNA *in vitro* yet is still functional *in vivo* (Costello et al., 2011).

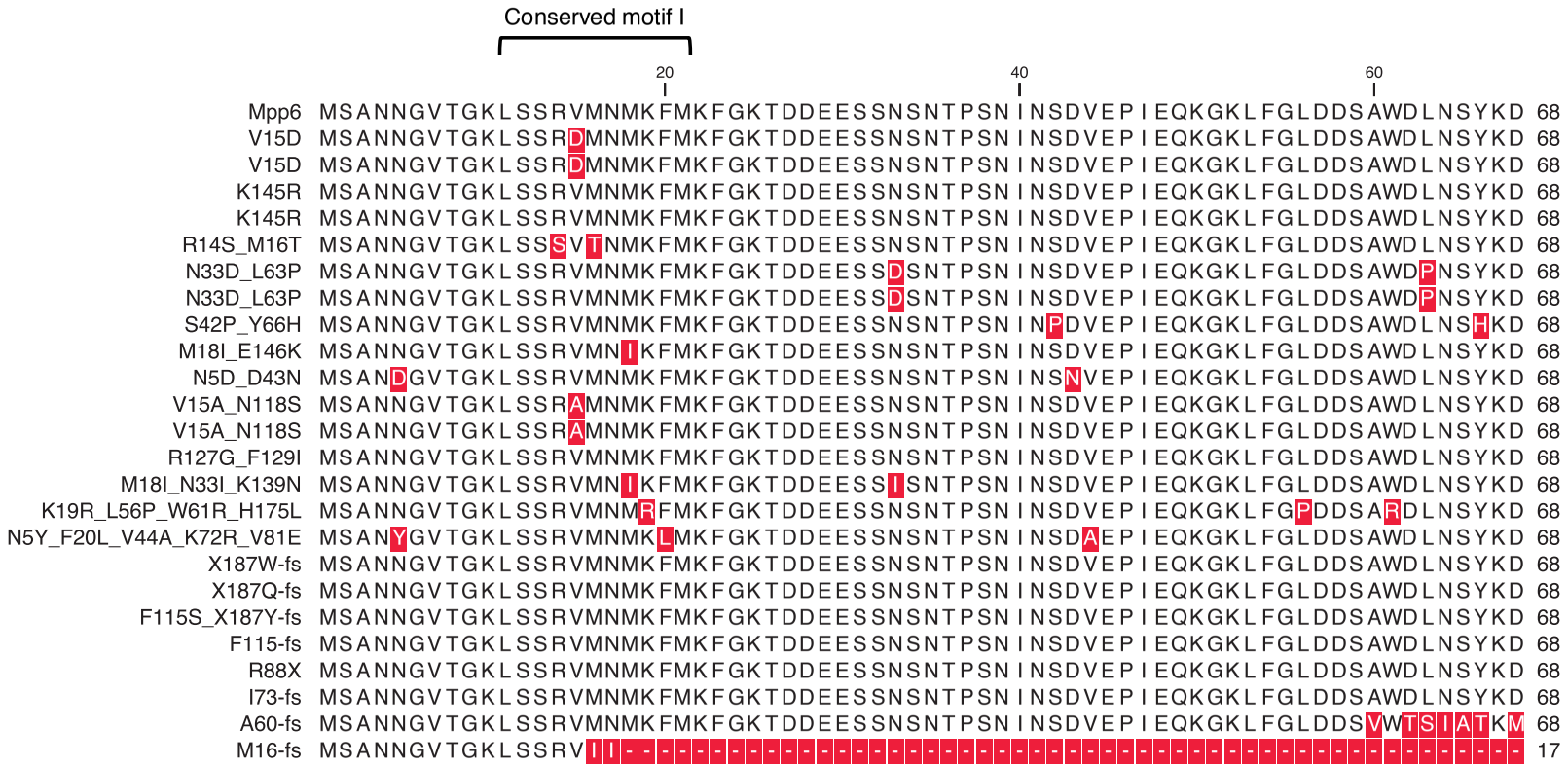

Figure 5.8. Sequence analysis of non-functional *mpp6* mutants. Amino acid alignment of translated nucleotide sequences from isolated *mpp6* mutants. Mutant *mpp6* alleles were sequenced by Source BioScience (Nottingham., UK) using Sanger sequencing. Raw nucleotide sequences from trace files were obtained using FinchTV (Geospiza) and translated *in silico* using the ExPASy Translate tool (Artimo et al. 2012) and aligned using Clustal Omega (Sievers et al. 2011). Multiple sequence alignments were edited using CLC Main Workbench 6 (CLC Bio, Aahus, Denmark). Conserved regions found in Mpp6 homologues are indicated above. Highlighted residues indicate sites of amino acid substitution in comparison to wildtype Mpp6 protein sequence. Sequence absent from truncated proteins is indicateg by highlighting.


Conserved motif II
80
100
120
Mpp6 DLKKISGKEKKKVKRVVYKKRPNLIISNVGYSELRKPEGVISGRKTFGDNSDDSGSRKRKFDEGEQNE 136
V15D DLKKISGKEKKKVKRVVYKKRPNLIISNVGYSELRKPEGVISGRKTFGDNSDDSGSRKRKFDEGEQNE 136
V15D DLKKISGKEKKKVKRVVYKKRPNLIISNVGYSELRKPEGVISGRKTFGDNSDDSGSRKRKFDEGEQNE 136
K145R DLKKISGKEKKKVKRVVYKKRPNLIISNVGYSELRKPEGVISGRKTFGDNSDDSGSRKRKFDEGEQNE 136
K145R DLKKISGKEKKKVKRVVYKKRPNLIISNVGYSELRKPEGVISGRKTFGDNSDDSGSRKRKFDEGEQNE 136
R14S_M16T DLKKISGKEKKKVKRVVYKKRPNLIISNVGYSELRKPEGVISGRKTFGDNSDDSGSRKRKFDEGEQNE 136
N33D_L63P DLKKISGKEKKKVKRVVYKKRPNLIISNVGYSELRKPEGVISGRKTFGDNSDDSGSRKRKFDEGEQNE 136
N33D_L63P DLKKISGKEKKKVKRVVYKKRPNLIISNVGYSELRKPEGVISGRKTFGDNSDDSGSRKRKFDEGEQNE 136
S42P_Y66H DLKKISGKEKKKVKRVVYKKRPNLIISNVGYSELRKPEGVISGRKTFGDNSDDSGSRKRKFDEGEQNE 136
M18I_E146K DLKKISGKEKKKVKRVVYKKRPNLIISNVGYSELRKPEGVISGRKTFGDNSDDSGSRKRKFDEGEQNE 136
N5D_D43N DLKKISGKEKKKVKRVVYKKRPNLIISNVGYSELRKPEGVISGRKTFGDNSDDSGSRKRKFDEGEQNE 136
V15A_N118S DLKKISGKEKKKVKRVVYKKRPNLIISNVGYSELRKPEGVISGRKTFGDSSDDSGSRKRKFDEGEQNE 136
V15A_N118S DLKKISGKEKKKVKRVVYKKRPNLIISNVGYSELRKPEGVISGRKTFGDSSDDSGSRKRKFDEGEQNE 136
R127G_F129I DLKKISGKEKKKVKRVVYKKRPNLIISNVGYSELRKPEGVISGRKTFGDNSDDSGSRKGKIDEGEQNE 136
M18I_N33I_K139N DLKKISGKEKKKVKRVVYKKRPNLIISNVGYSELRKPEGVISGRKTFGDNSDDSGSRKRKFDEGEQNE 136
K19R_L56P_W61R_H175L DLKKISGKEKKKVKRVVYKKRPNLIISNVGYSELRKPEGVISGRKTFGDNSDDSGSRKRKFDEGEQNE 136
N5Y_F20L_V44A_K72R_V81E DLKRISGKEKKKEKRVVYKKRPNLIISNVGYSELRKPEGVISGRKTFGDNSDDSGSRKRKFDEGEQNE 136
X187W-fs DLKKISGKEKKKVKRVVYKKRPNLIISNVGYSELRKPEGVISGRKTFGDNSDDSGSRKRKFDEGEQNE 136
X187Q-fs DLKKISGKEKKKVKRVVYKKRPNLIISNVGYSELRKPEGVISGRKTFGDNSDDSGSRKRKFDEGEQNE 136
F115S_X187Y-fs DLKKISGKEKKKVKRVVYKKRPNLIISNVGYSELRKPEGVISGRKTSGDNSDDSGSRKRKFDEGEQNE 136
F115-fs DLKKISGKEKKKVKRVVYKKRPNLIISNVGYSELRKPEGVISGRKTLAIIILMIVVPGRESLMKANKMK 136
R88X DLKKISGKEKKKVKRVVYKK-- 88
I73-fs DLKKFQVRRRKR-- 80
A60-fs I-- 69
M16-fs --- 17

T

140
160
180
200
Mpp6 DEKRDAKDKEFTGSQDDGEDEYDLDKLFKDSIKKKKTNHNGKNKNRNSKK------------ 186
V15D DEKRDAKDKEFTGSQDDGEDEYDLDKLFKDSIKKKKTNHNGKNKNRNSKK------------ 186
V15D DEKRDAKDKEFTGSQDDGEDEYDLDKLFKDSIKKKKTNHNGKNKNRNSKK------------ 186
K145R DEKRDAKDREFTGSQDDGEDEYDLDKLFKDSIKKKKTNHNGKNKNRNSKK------------ 186
K145R DEKRDAKDREFTGSQDDGEDEYDLDKLFKDSIKKKKTNHNGKNKNRNSKK------------ 186
R14S_M16T DEKRDAKDKEFTGSQDDGEDEYDLDKLFKDSIKKKKTNHNGKNKNRNSKK------------ 186
N33D_L63P DEKRDAKDKEFTGSQDDGEDEYDLDKLFKDSIKKKKTNHNGKNKNRNSKK------------ 186
N33D_L63P DEKRDAKDKEFTGSQDDGEDEYDLDKLFKDSIKKKKTNHNGKNKNRNSKK------------ 186
S42P_Y66H DEKRDAKDKEFTGSQDDGEDEYDLDKLFKDSIKKKKTNHNGKNKNRNSKK------------ 186
M18I_E146K DEKRDAKDKKFTGSQDDGEDEYDLDKLFKDSIKKKKTNHNGKNKNRNSKK------------ 186
N5D_D43N DEKRDAKDKEFTGSQDDGEDEYDLDKLFKDSIKKKKTNHNGKNKNRNSKK------------ 186
V15A_N118S DEKRDAKDKEFTGSQDDGEDEYDLDKLFKDSIKKKKTNHNGKNKNRNSKK------------ 186
V15A_N118S DEKRDAKDKEFTGSQDDGEDEYDLDKLFKDSIKKKKTNHNGKNKNRNSKK------------ 186
R127G_F129I DEKRDAKDKEFTGSQDDGEDEYDLDKLFKDSIKKKKTNHNGKNKNRNSKK------------ 186
M18I_N33I_K139N DENRDAKDKEFTGSQDDGEDEYDLDKLFKDSIKKKKTNHNGKNKNRNSKK------------ 186
K19R_L56P_W61R_H175L DEKRDAKDKEFTGSQDDGEDEYDLDKLFKDSIKKKKTNLNGKNKNRNSKK------------ 186
N5Y_F20L_V44A_K72R_V81E DEKRDAKDKEFTGSQDDGEDEYDLDKLFKDSIKKKKTNHNGKNKNRNSKK------------ 186
X187W-fs DEKRDAKDKEFTGSQDDGEDEYDLDKLFKDSIKKKKTNHNGKNKNRNSKKWRRQCTGRSTYSYIIMRT 204
X187Q-fs DEKRDAKDKEFTGSQDDGEDEYDLDKLFKDSIKKKKTNHNGKNKNRNSKKQRRQCTSRSTYSYIIMRT 204
F115S_X187Y-fs DEKRDAKDKEFTGSQDDGEDEYDLDKLFKDSIKKKKTNHNGKNKNRNSKKYRRQCTSRSTYSYIIMRT 204
F115-fs TRKGMLRITRNLQGAKTMERMNMT---------- 159
R88X ---------- 88
I73-fs ---------- 80
A60-fs ---------- 69
M16-fs ---------- 17

he sequencing data also identified multiple point mutants including 7 unique double mutants. Not surprisingly, a large proportion of amino acid substitutions were identified in the highly conserved domain in the N-terminus of Mpp6 spanning roughly the first 30 amino acids. However, more interestingly, a number of mutations in non-conserved regions of the protein were identified. A S42P substitution was present as part of a S42P_Y66H double mutant. S42 was previously identified as a phosphorylated residue in two independent mass spectrometry analysis of phosphorylation sites in yeast (Gnad et al., 2009; Smolka et al., 2007) although it has not been directly shown. Bioinformatics analysis reveals that S42 is part of a casein kinase II motif (SXXE/D). Phosphorylation status may be of functional importance to Mpp6, which itself was initially identified as a phosphoprotein in humans (Matsumoto-Taniura et al., 1996). However, further investigation into Mpp6 phosphorylation was not explored in this study.

Analysis of *mpp6* mutant sequences also identified 8 unique mutations that encode truncated or extended proteins either through frameshift deletions or point mutations. Frameshift mutations including F115-fs, I73-fs and A60-fs are the result of single nucleotide deletions. The I73-fs mutation was found in 12 independently isolated mutants and results from a single adenine deletion in a stretch of 8 consecutive adenine bases in the nucleotide sequence. This mutation causes a frameshift and the encoded protein terminates after a further 8 amino acids. A nonsense R88X mutation causes a CGA>TGA mutation resulting in a premature stop codon and encoding for just under 50% of the wildtype protein. Interestingly, nucleotide analysis of three mutants that encode extended proteins reveals three independent mutations of the natural *MPP6* stop codon. Substitutions are found in all three nucleotides of the stop codon triplet (TAG>TGG, CAG and TAC), each encoding for different amino acids (X187W, X187Q and X187Y respectively). Stop codon mutants encode an additional 18 amino acids before termination. Interestingly, 2 out of 3 X187 mutants contain no other amino acid substitutions suggesting that the extension of 18 amino acids causes the loss of protein function.

In summary, sequence analysis of random *mpp6* mutants identified 2 single point mutations (V15D, K145R) and 7 double point mutations that cause a loss of protein function *in vivo*. Additionally, 8 mutations were identified that encode for truncated or extended Mpp6 proteins. Whilst a number of amino acid substitutions arose in a highly conserved region in the N-terminal domain, mutations were found in other regions of the protein.

5.2.5. Separating loss of function amino acid substitutions in *mpp6* mutants.

Sequence analysis of loss of function *mpp6* alleles encoding full-length proteins identified 7 mutants with two single amino acid substitutions (Figure 5.8) Loss of function could be attributed to the effect of one single mutation or the combination of both. To investigate the nature of each substitution, site directed mutations were generated in a plasmid encoding zz-Mpp6 to separate identified double mutants. For these investigations, double mutants were chosen depending on their vicinity to each other in primary sequence. Without a 3D structure of Mpp6, it is impossible to know the relative spatial proximity of these residues. Double substitutions identified in close proximity, such as R14S_M16T and R127_F129I, were omitted from further analysis by separation. Single M18I, N33D, S42P, D43N, L63P, Y66H and E146K mutations (Figure 5.9) were generated through site-directed mutagenesis using oligonucleotide pairs o846/o847, o850/o851, o854/o855, o858/o859, o852/o853, o856/o857 and o848/o849 respectively. SDM was carried out as described in Section 2.2.7 using a *LEU2* centromeric plasmid encoding a wildtype copy of zz-Mpp6 (p599). Candidate plasmids were screened by southern blot hybridisation before confirming mutations though sequencing analysis.

Single point mutated *mpp6* alleles were screened for functionality using the *mpp6Δ rrp47Δ* plasmid shuffle assay described in Section 3.1.2. Plasmids encoding zz-Mpp6 proteins harboring single amino acid substitutions were transformed into an *mpp6Δ rrp47Δ* strain complemented by a *URA3* plasmid

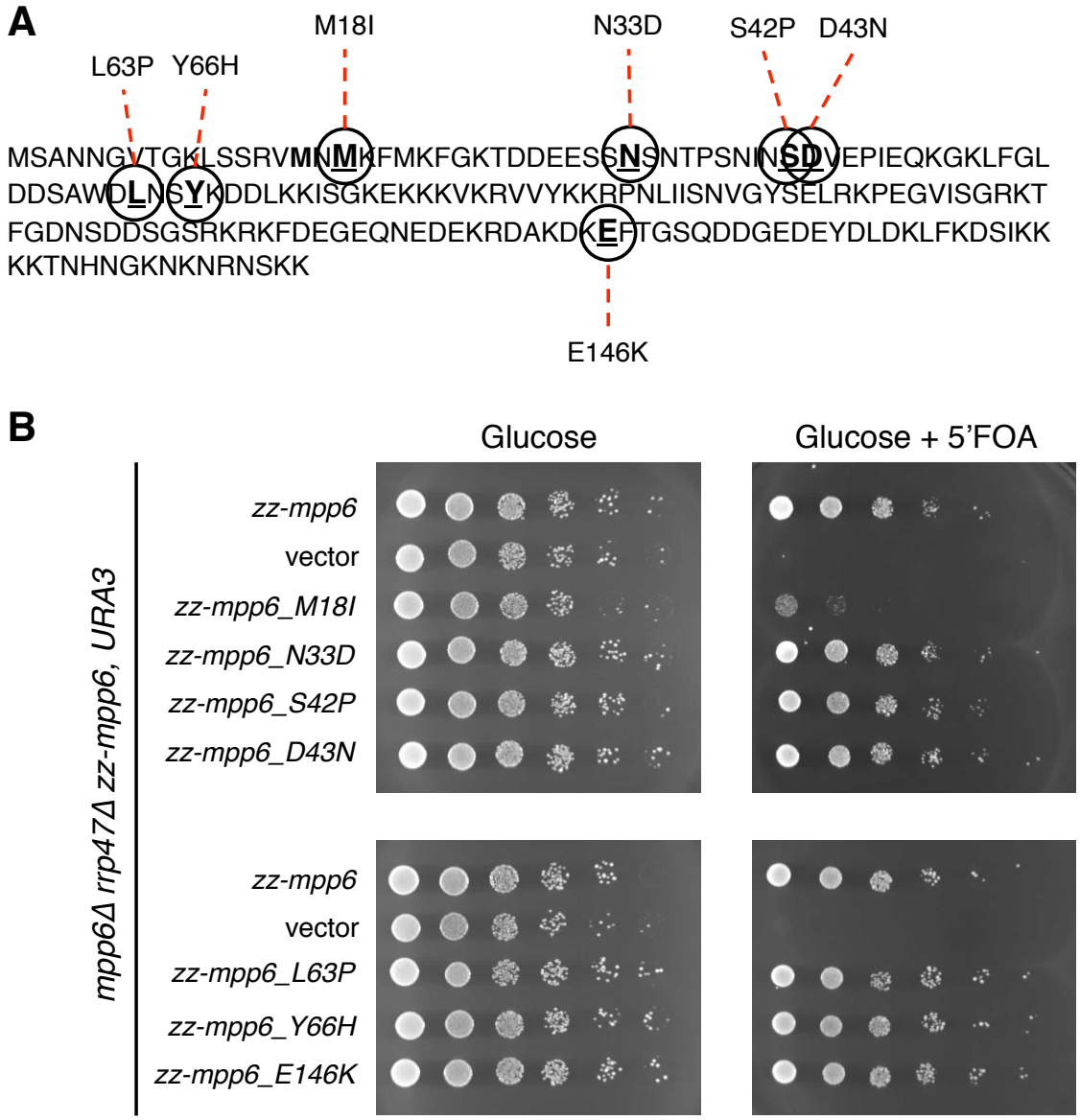

Figure 5.9. Separation of non-functional *mpp6* double mutants. **(A)** Schematic of mutation targets for amino acid subsitution. Double point mutations were identified in a random mutageneis approach and separated using SDM. A list of SDM primers for each mutation is detailed in Table 2.10. **(B)** Plasmid shuffle assay to test for functionality of mutants. Plasmids generated through SDM were transformed into a *mpp6Δ rrp47Δ* plasmid shuffle strain and assayed for growth on medium containing 5'FOA. Strains were grown to saturation in selective medium and normalised by optical densitiy before spotting 10-fold serial dilutions onto solid glucose- and 5'FOA media. Plates were incubated 3 days at 30°C before photographing.

bearing a wildtype *MPP6* allele. A *LEU2* plasmid encoding wildtype zz-Mpp6 and an empty *LEU2* vector were transformed in parallel. Transformants were screened for complementation of the *mpp6Δ rrp47Δ* synthetic lethality by assaying growth on media containing 5'FOA to counterselect against the *URA3* maintenance plasmid bearing a wildtype *MPP6* allele (Figure 5.9) All single point mutants complemented the *mpp6Δ rrp47Δ* synthetic lethality and were viable on media containing 5'FOA. Each complemented mutant grew comparable to the wildtype *MPP6* complemented strain with the exception of the M18I mutant that showed a strong growth defect. The M18I mutation was originally identified as a non-functional M18I_E146K double mutant. It is worth noting that an adjacent single K145R mutation was identified as non-functional, however the E146K single mutant showed no apparent growth defect in the plasmid shuffle strain. M18 is a highly conserved residue shared in Mpp6 homologues from model organisms (Milligan et al., 2008).

Separating *mpp6* double point mutations reveals that the loss of function phenotypes observed in the double point mutants are most likely due to a cumulative effects from each single point mutation. Whilst the majority of single point mutations show no apparent growth phenotype, the combined double mutations show a synergistic loss of function. The notable exception identified here is a single M18I amino acid substitution, which shows a strong growth defect combined with an *rrp47Δ* allele.

5.2.6. Conserved regions of Mpp6 are functionally important.

Sequence analysis of *mpp6* mutants generated by random mutagenesis showed that a high number of point mutations were found in a highly conserved N-terminal region of Mpp6. This region was initially identified in a previous analysis of Mpp6 along with a second region closer to the C-terminus (Milligan et al., 2008). Appendices I and II shows the conservation of these regions from homologues found in model organisms and orthologs found in other *Saccharomyces* species. To investigate the importance of these regions in Mpp6, site directed mutagenesis

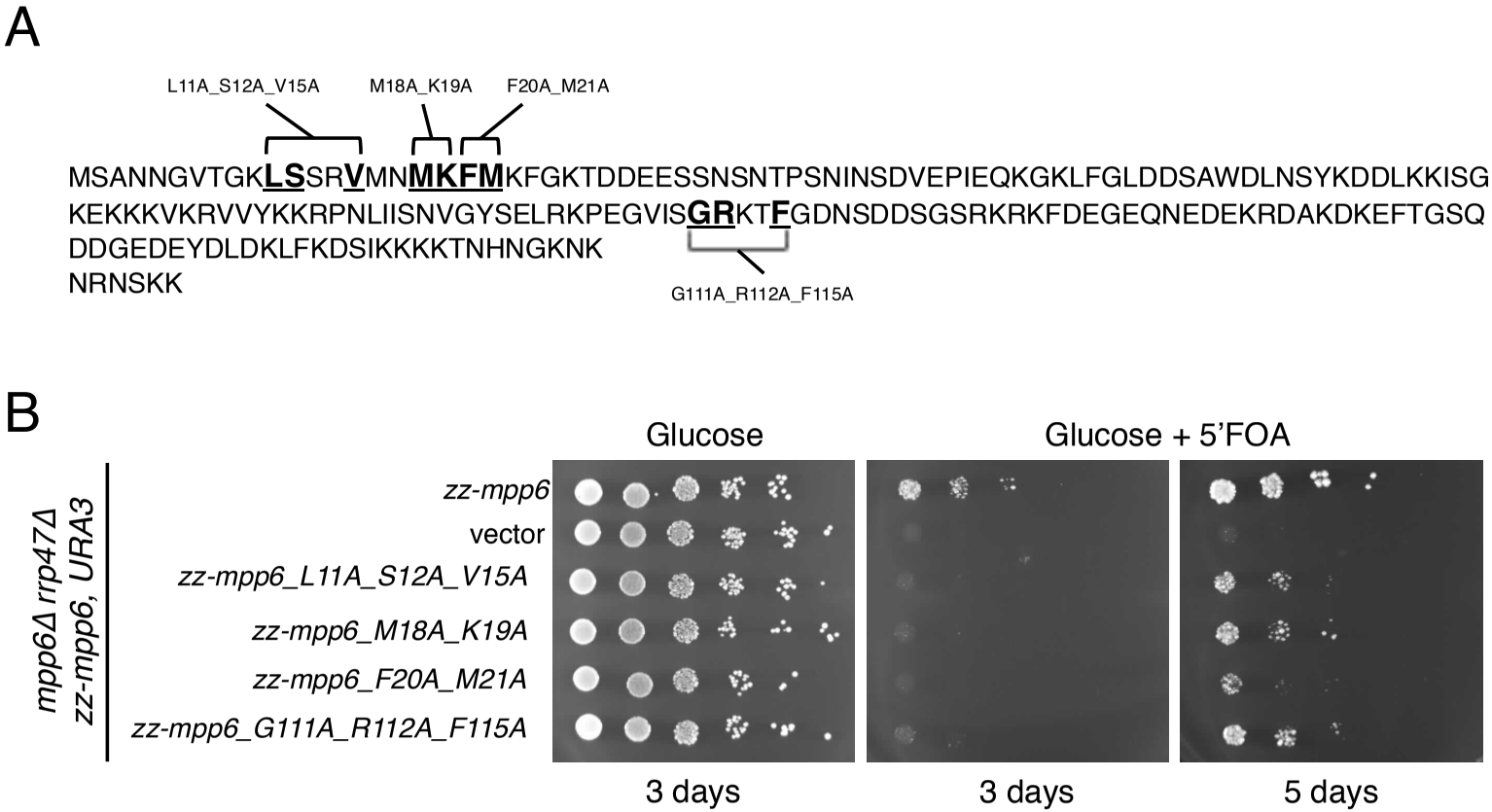

Figure 5.10. Conserved motifs are important for Mpp6 function *in vivo*. Plasmid shuffle assay to test function of *mpp6* mutants bearing alanine substitutions in conserved residues. **(A)** Sites of engineered mutation Mpp6. L11A_S12A_V15A, M18A_K19A, F20A_M21A and G11A_R112A_F115A mutations were introduced into a zz-Mpp6 expression construct (p599) by SDM using oligonucleotides indicated in the text. **(B)** Conserved motif mutants generated by SDM were transformed into a *mpp6Δ rrp47Δ* plasmid shuffle strain bearing a *URA3* plasmid encoding wildtype zz-Mpp6. Strains were grown to saturation in selective medium and normalised by optical densitiy before spotting 10-fold serial dilutions onto solid glucose- and 5'FOA media. Plates were incubated 3 days at 30°C before photographing. The 5'FOA plate was incubated for a further 2 days before photographing.

was used to introduce alanine substitutions in conserved residues. Mutations were grouped together for initial characterisation of these regions (Figure 5.10 A)

Mutations were introduced into the coding sequence of a zz-Mpp6 expression construct on a *LEU2* plasmid (p599) using site directed mutagenesis. L11A_S12A_V15A, M18A_K19A, F20A_M21A and G111A_R112A_F115A

mutations (Figure 5.10. A) were introduced using oligonucleotide pair's o758/o759, o760/o761, o762/o763 and o764/o765 respectively. Mutant plasmids were screened by southern blot analysis and validated by sequencing.

Plasmids harboring *mpp6* mutants were transformed into the *mpp6Δ rrp47Δ* plasmid shuffle strain bearing a *URA3* maintenance plasmid encoding wildtype zz-Mpp6. Transformants were assayed for growth on medium containing 5'FOA to counterselect against the *URA3* maintenance plasmid. Parallel strains transformed with a *LEU2* plasmid encoding wildtype zz-Mpp6 and an empty vector were assayed in parallel as positive and negative controls respectively. Analysis of growth on 5'FOA revealed that all mutants were able to complement the *mpp6Δ rrp47Δ* synthetic lethality. However, resulting strains displayed reduced growth phenotypes with the strongest effect noted in the F20A_M21A mutant. This suggests that these regions are functionally important in Mpp6 and corroborates observations in loss of function mutations identified above.

5.2.7. Short, C-terminal deletions of Mpp6 are functional *in vivo*.

Through random mutagenesis, four unique *mpp6* mutants were isolated that encoded truncated proteins. Sequence analysis revealed that proteins containing the first 115 amino acids, or less, were not able to function *in vivo*. The C-terminus of Mpp6 contains a high abundance of basic residues including a 17 residue lysine-rich stretch. This basic region is reminiscent of the C-terminus of Rrp47 that also contains a lysine-rich peptide sequence. Short deletions in the C-terminus of Rrp47 abolished RNA binding *in vitro*. However, these mutants were shown to be

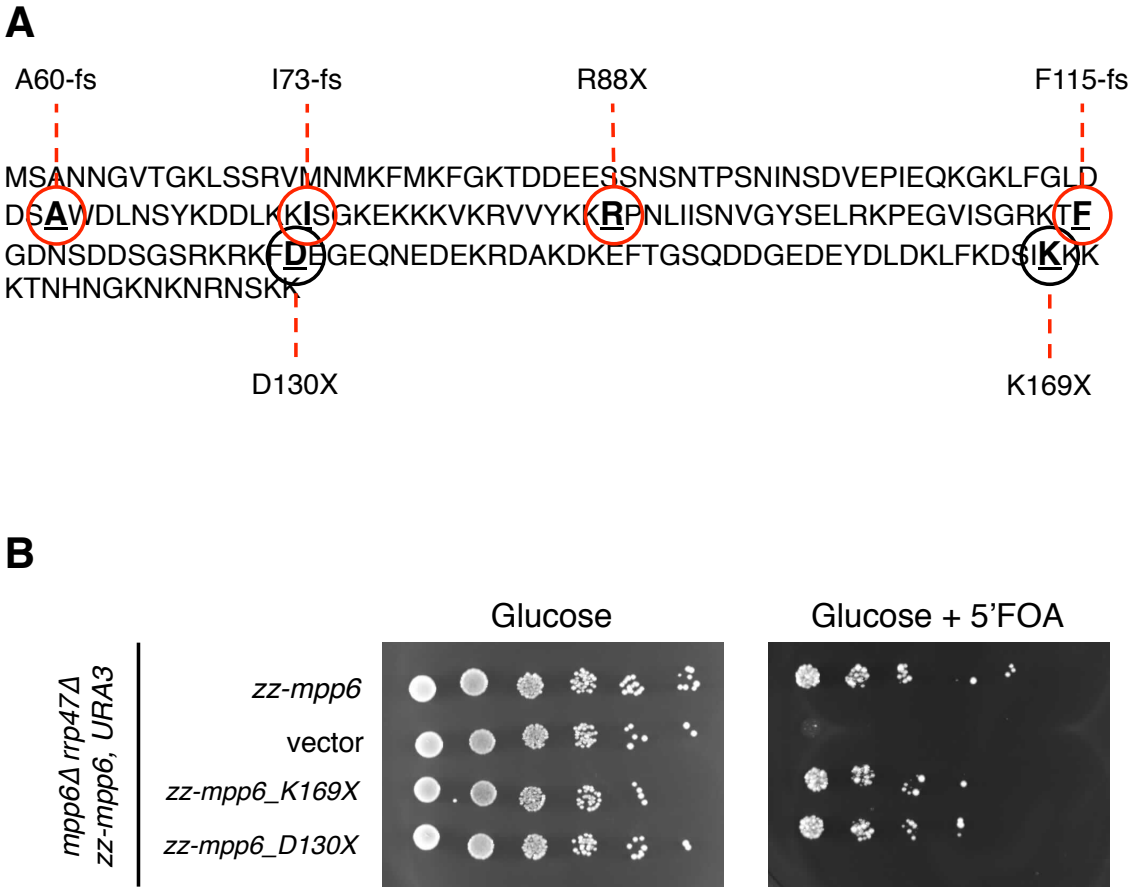

Figure 5.11. The C-terminal lysine-rich region is not required for Mpp6 function *in vivo*. (A) Schematic of truncated *mpp6* mutants generated during this study. Highlighted residues mark the site of mutation. Red circles correspond to mutations that cause a loss of protein function. D130X and K169X mutations were introduced by SDM using oligonucleotide pairs o766/o767 and o844/o845 respectively. (B) A plasmid shuffle assay to test K169X and D130X mutations for function. Yeast expression constructs encoding zz-Mpp6 and K169X, D130X derivatives were transformed into a *mpp6Δ rrp47Δ* plasmid shuffle strain. An empty *LEU2* vector was transformed in parallel. Strains were grown to saturation in liquid selective media before normalising by optical density and spotting 10-fold serial dilutions onto solid glucose- and 5'FOA-based media. Plates were incubated 3 days at 30°C before photographing.

functional *in vivo* through plasmid shuffle assays suggesting that RNA binding is not required for protein function (Costello et al., 2011).

To investigate the requirement of the C-terminus of Mpp6 for protein function *in vivo*, two directed mutations were generated in a zz-Mpp6 expression construct and assayed for functionality using the *mpp6Δ rrp47Δ* plasmid shuffle assay. A K169X mutant was generated to remove the furthermost lysine-rich peptide region of the C-terminus. Furthermore, a D130X mutation was generated as an intermediate truncation between F115 and K169 sites. A schematic of mutation sites are shown in Figure 5.11 A.

K169X and D130X mutations were introduced to the zz-Mpp6 expression construct (p599) by site-direction mutagenesis using oligonucleotide pairs o766/o767 and o844/o845 respectively. Candidate plasmids were screened by southern blot hybridisation and validated by sequencing before transforming into the *mpp6Δ rrp47Δ* plasmid shuffle strain. Transformants were screened for functionality by assaying for growth on media containing 5'FOA to counterselect against the *URA3* plasmid bearing a wildtype *MPP6* allele (Figure 5.11. B). Both K169X and D130X mutations complemented the *mpp6Δ rrp47Δ* synthetic lethality and were viable on media containing 5'FOA. Additionally, both strains grew comparably to an *mpp6Δ rrp47Δ* strain transformed with a wildtype zz-Mpp6 expression construct. These results show that the last 56 residues of Mpp6, including a lysine-rich domain, are not required for protein function *in vivo*.

5.2.8. Steady state expression levels of *mpp6* mutants

The library of *mpp6* mutants was first screened for loss of function alleles in an *mpp6Δ rrp47Δ* plasmid shuffle assay followed by a second round of screening to confirm expression of a tagged zz-Mpp6 protein. The expression levels of Mpp6 mutant proteins were assayed further to investigate the effects of specific mutations on protein stability. Loss of function phenotypes could be attributed to protein mis-folding as a result of amino acid substitutions, truncations or extensions. The library of *mpp6* mutants was generated from a zz-Mpp6

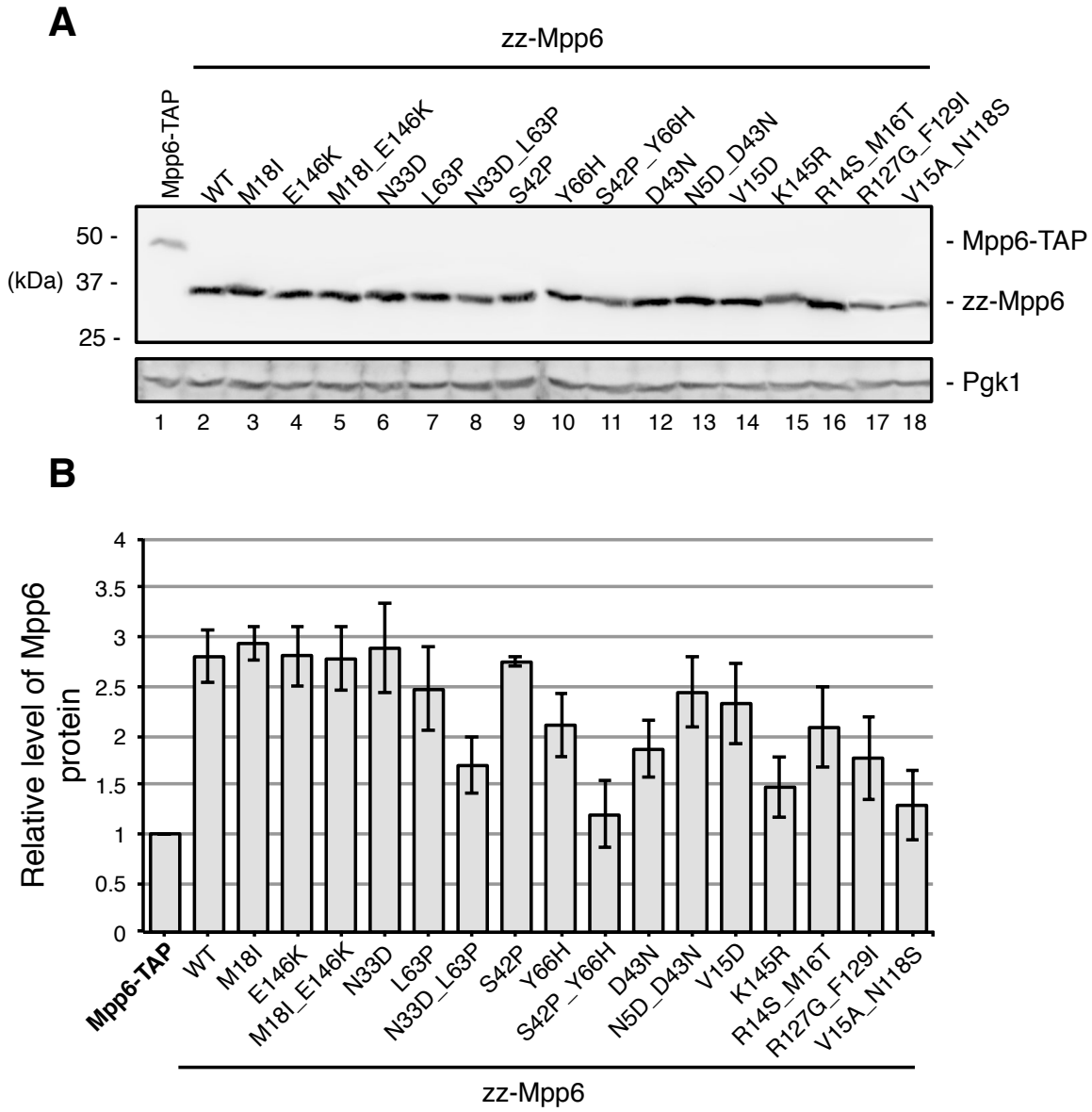

Figure 5.12. Relative stability of Mpp6 proteins bearing single and double amino acid substitutions. (A) SDS PAGE and western blot analysis of full length zz-Mpp6 mutant proteins. Lysates were prepared from strains harbouring plasmids encoding mutant zz-Mpp6 proteins and wildtype zz-Mpp6 as a control. Additionally, lysates were prepared from a strain encoding a C-terminally TAP-tagged Mpp6 fusion promoter from the endogenous *MPP6* locus. Fusion peptides were detected using the PAP antibody (*upper* panel). An antiserum against Pgk1 was used as a loading control (*lower* panel). **(B)** Quantification of relative steady state levels of Mpp6 proteins. Data is representative of three independent experiments. Relative expression levels of Mpp6 proteins are normalised for Pgk1 expression values and standardised to levels in the Mpp6-TAP strain. Error bars represent the standard error of the mean for each set of values.

expression construct under the control of the *RRP4* promoter. In a global analysis of yeast protein expression, it was reported that Rrp4 proteins are expressed roughly 3.5-fold greater than Mpp6 proteins (4830 molecular per cell compared to 1350 respectively) (Ghaemmaghami et al., 2003). As shown in Section 3.2.1, zz-Mpp6 fusion proteins are expressed roughly 3-fold greater than endogenous Mpp6 under the wildtype promoter. Therefore, *mpp6* mutants are already overexpressed compared to endogenous *MPP6*.

Lysates were prepared from strains harboring plasmids encoding loss of function zz-Mpp6 mutants and a wildtype *RRP47* plasmid to complement the *mpp6Δ rrp47Δ* strain background. Proteins were fractionated by SDS PAGE and analysed by western blotting using the PAP antibody to detect zz-tagged fusion proteins. Lysates were also prepared from an endogenous C-terminal TAP tagged *MPP6* strain in parallel to compare relative steady state expression levels.

Western blot analysis of *mpp6* mutants encoding full-length proteins with amino acid substitutions revealed that the steady state expression profiles were generally similar to the wildtype zz-Mpp6 protein with a couple of exceptions (Figure 5.12. A). Quantitative analysis of independent samples showed that protein expression is reduced in some double mutants, including N33D_L63P and S42P_Y66H (Figure 5.12). However, these expression levels still remain greater in comparison to endogenous levels of Mpp6. (Figure 5.12. A,B compare lanes 1 with 2-18). These results suggest that loss of function phenotypes observed in *mpp6* point mutants are not due to decreased stability of Mpp6 proteins. This implies that substitutions in residues critical for protein function are the basis of observed phenotypes.

Steady state protein expression levels were analysed in *mpp6* mutants expressing zz-Mpp6 proteins bearing alanine substitutions in conserved residues. These mutants were constructed through site directed mutagenesis and shown to complement the synthetic lethality of *mpp6Δ rrp47Δ* double mutants (Section 5.2.6). Lysates were fractionated by SDS PAGE and analysed by western blotting along with samples from strains expressing wildtype Mpp6-TAP and zz-Mpp6

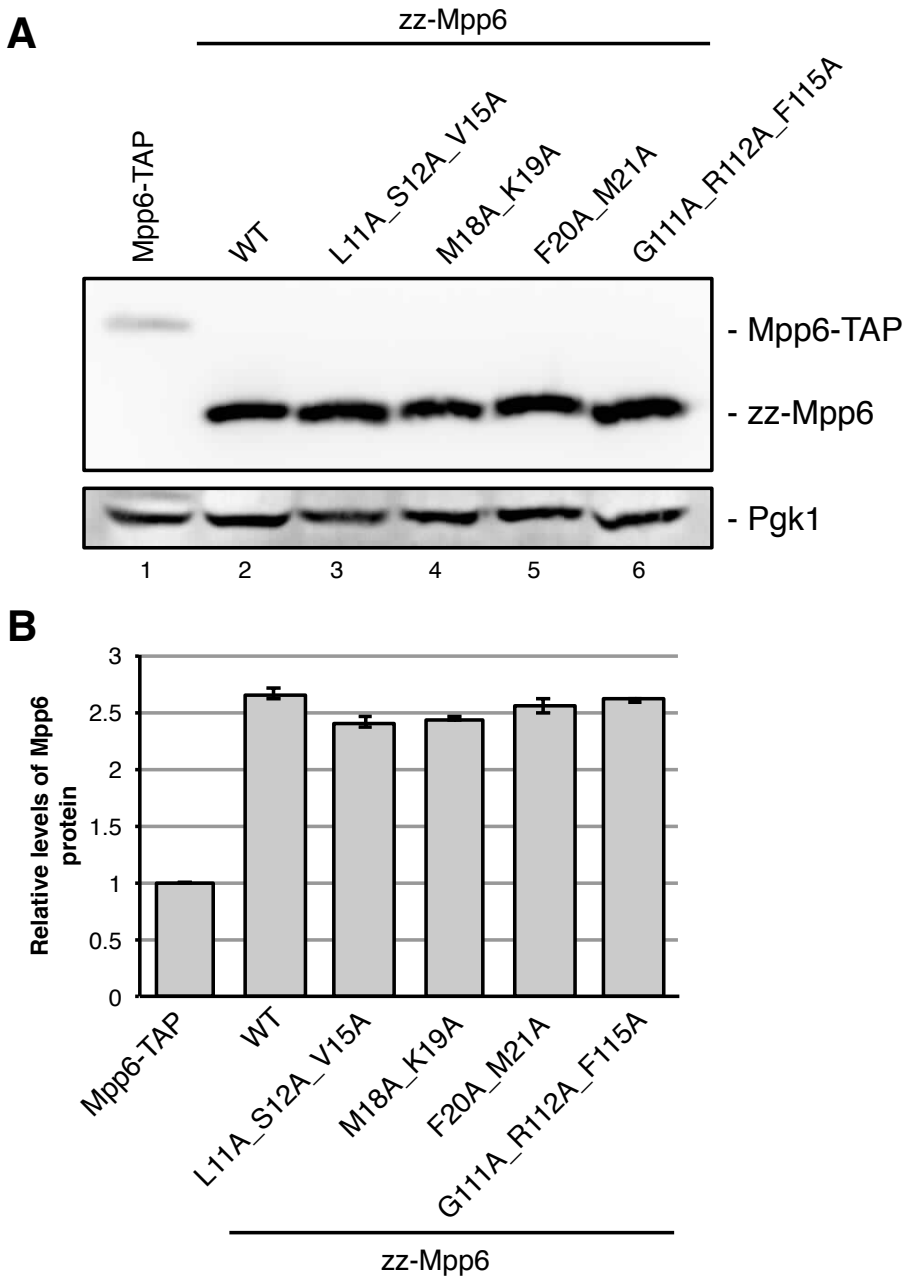

Figure 5.13. Mutations in conserved regions of Mpp6 do not affect protein stabiltiy. (A) Western blot analysis of strains harboring *mpp6* mutants encoding zz-Mpp6 proteins bearing alanine substitutions in conserved motifs. Denatured lysates from strains expressing wildtype Mpp6-TAP, zz-Mpp6 and mutant L11A_S12A_V15A, M18A_K19A, F20A_M21A and G111A_R112A_F115A proteins were analysed by SDS PAGE and western blotting using the PAP antibody to detect Mpp6 fusion proteins (*upper* panel). An antiserum against Pgk1 served as a loading control (*lower* panel). **(B)** Quantitative analysis of relative levels of Mpp6 proteins in each strain. Data is representative of three independent experiments. Relative expression levels of Mpp6 proteins are normalised for Pgk1 expression values and standardised to levels in the Mpp6-TAP strain. Error bars represent the standard error of the mean for each set of values.

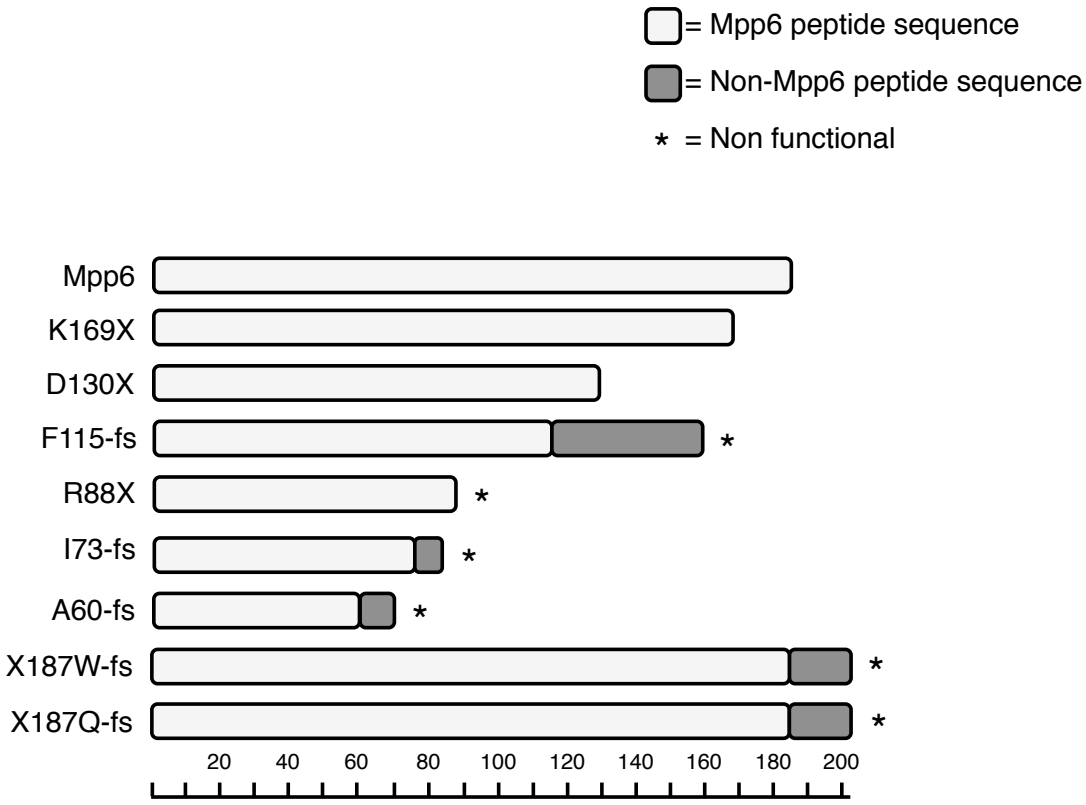

Figure 5.14. Truncation and extension mutations generated in Mpp6. Relative comparison schematic of truncated or extended Mpp6 proteins generated in this study through random or directed mutagenesis. The nature of the mutation is indicated according to the amount of Mpp6 sequence expressed. Mpp6-peptide sequences are depicted in light grey and non-Mpp6 peptide sequence as a result of frameshift is depicted in dark grey. Asterisks (*) denote non-function Mpp6 proteins. The scale indicates the relative length of each protein in amino acid residues.

proteins as previously described (Figure 5.13. A). Western blot analysis displayed that all conserved motif mutants expressed Mpp6 proteins comparable to the wildtype zz-Mpp6 protein that, in turn, is expressed roughly 2.5-3 fold higher than endogenously expressed Mpp6-TAP (Figure 5.13. B). This suggests that these conserved regions of Mpp6 are not required for normal protein stability. The slow growth phenotypes observed in Section 5.2.6 are therefore presumed to be due to the nature of the substitutions rather than a loss of normal protein expression. The random mutagenesis approach also generated frameshift mutations resulting from nucleotide deletions. Such mutations produce truncated or extended proteins, often with nonsense peptide sequences following the frameshift site. A scaled schematic of truncation and extension mutants generated during this study are depicted in Figure 5.14 including SDM generated K169X and D130X mutations.

Western blot analysis of truncated proteins showed a general trend of decreased stability correlating with the length of Mpp6 proteins. Mutant strains expressing functional proteins (WT, K169 and D130X) showed relatively comparable expression levels at steady state (Figure 5.15. A, lanes 2-4). The F115-fs mutant shows a 2.5-fold decrease in expression level compared to wildtype zz-Mpp6 proteins (compare lanes 2 and 5). However, the expression level is equivalent to levels of endogenous Mpp6 under the control of the wildtype promoter (Lanes 1 and 5). It is worth reiterating that the F115-fs protein is longer than the D130X protein due to a 44 amino acid extension as a result of the frameshift. It can be inferred that this long nonsense peptide extension interferes with folding of the protein resulting in a loss of stability. The R88X mutant is produced from single nucleotide change resulting in a premature stop codon and therefore contains no peptide extension. As a result, this protein appears to be more stable than the F115-fs protein yet the expression level is lower in comparison to the wildtype zz-Mpp6 (Compare lanes 2, 5-6). Finally, I73-fs and A60-fs mutations express proteins with short peptide extensions of ~10 amino acids. The resulting proteins are expressed considerably lower than wildtype zz-Mpp6 and have steady state levels of 81% and 28% in comparison to endogenous Mpp6 under the control of the wildtype promoter (compare lanes 1, 7-8).

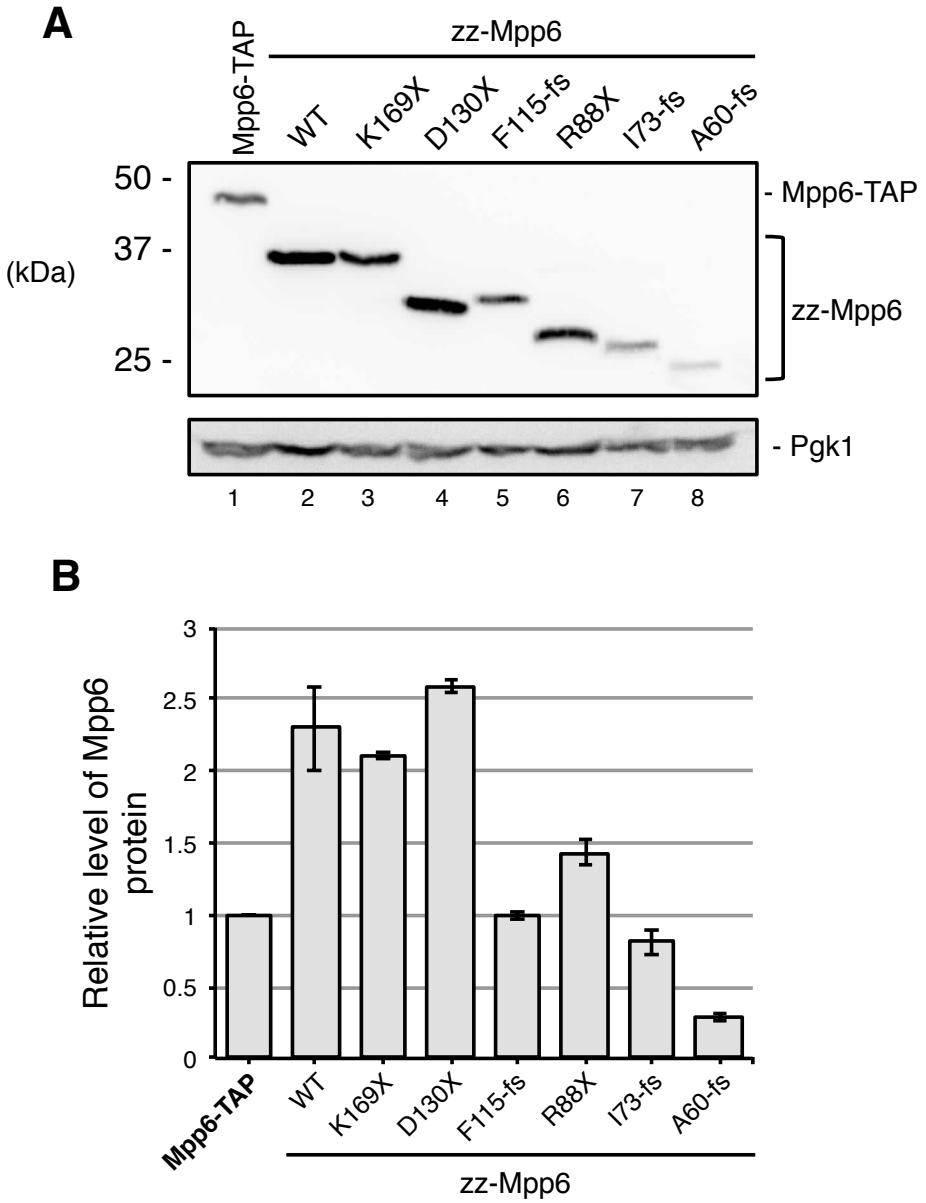

Figure 5.15. C-terminal truncations of Mpp6 result in reduced protein expression. (A) Western blot analysis of truncated Mpp6 proteins. Lysates from strains harbouring plasmids encoding Mpp6 truncations depicted in Figure 5.14 were fractionated on 10% polyacrylamide gels and analysed by western blotting. Lysates from a Mpp6-TAP and wildtype zz-Mpp6 strain were analysed in parallel. TAP- and zz- fusion proteins were detected using the PAP antibody. An antiserum against Pgk1 served as a loading control. (B) Quantification of relative levels of Mpp6 protein expression from western blot analysis. Data is representative of three independent experiments. Values are standardised to levels in the Mpp6-TAP strain and expressed as relative quantities. Error bars represent the standard error of the mean for each set of values.

T

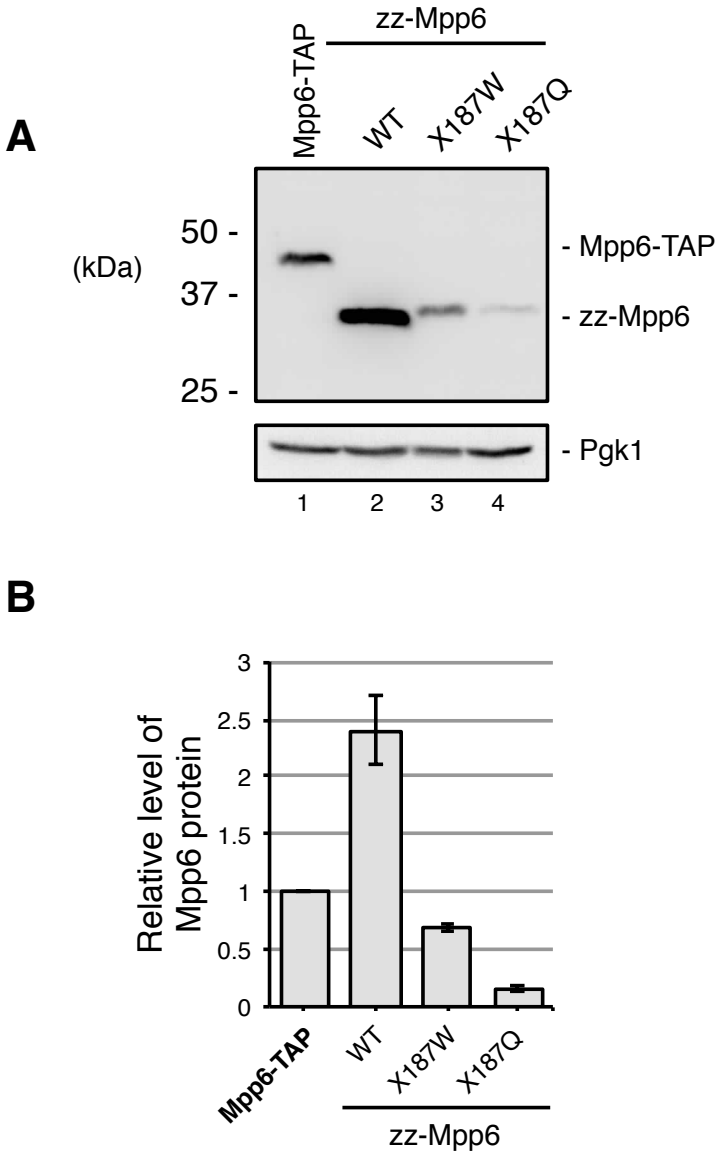

Figure 5.16. C-terminal peptide extensions in Mpp6 result in reduced protein expression. (A) Western blot analysis of extended Mpp6 proteins. Lysates from strains harboring plasmids encoding Mpp6 extensions depicted in Figure 5.14 were fractionated on 10% polyacrylamide gels and analysed by western blotting. Lysates from a Mpp6-TAP and wildtype zz-Mpp6 strain were analysed in parallel. TAP- and zz- fusion proteins were detected using the PAP antibody. An antiserum against Pgk1 served as a loading control. **(B)** Quantification of relative levels of Mpp6 protein expression from western blot analysis. Data is representative of three independent experiments. Relative expression levels of Mpp6 proteins are normalised for Pgk1 expression values and standardised to levels in the Mpp6-TAP strain. Error bars represent the standard error of the mean for each set of values.

hree non-functional *mpp6* mutants were identified from the random mutagenesis screen that encodes extended proteins. These arise from mutations in the natural stop codon and encode an additional peptide sequence of 18 amino acids. Each mutant differs in the nature of the stop-codon mutation (X187W, X187Q, X187Y) yet encodes the same 18 residue extension. The X187Y mutant was omitted from further investigation due to an additional F115S mutation in the sequence. Western blot analysis of strains expressing extended Mpp6 proteins reveals a considerable loss of protein expression in comparison to wildtype zz-Mpp6 levels (Figure 5.16. A, compare lanes 2 and 3-4). Expression levels of X187W and X187Q proteins are reduced to 29% and 6% respectively in comparison to wildtype zz-Mpp6. These expression levels are also below steady state levels of endogenous Mpp6 (compare lanes 1 and 3-4). It is interesting to note that the X187Q mutation causes a stronger destabilisation of protein expression in comparison to the X187W mutant. These values were consistent in independently prepared samples. These data suggest that short C-terminal extensions destabilise Mpp6 proteins resulting in reduced expression levels. It is unsure if loss-of function phenotypes are observed due to the reduced protein expression or that the peptide extension interferes with protein function. Curiously, strains bearing C-terminally tagged Mpp6 alleles produce functional proteins. In Section 5.2.11 the endogenous *RRP6* allele is disrupted in an *MPP6-TAP* strain and the resulting transformant is viable. As *rrp6Δ mpp6Δ* double mutants are synthetic lethal, taken together this shows that the C-terminally TAP-tagged Mpp6 protein is functional *in vivo*. Therefore, loss of function in the X187W and X187Q mutants can be attributed to either a reduced protein expression or the specific nature of the 18-residue extension.

Taken together, analysis of steady state protein expression in *mpp6* mutants shows that single amino acid substitutions do not significantly affect stable protein expression. As zz-Mpp6 mutant proteins are overexpressed in comparison to endogenous Mpp6 levels, it can be assumed that loss of function phenotypes are not due to reduced protein levels but due to a loss of essential protein function. Additionally, truncated and extended non-functional proteins show decreased expression levels in comparison to wildtype zz-Mpp6. Loss of function in C-

terminal truncation mutants is likely due to the absence of regions critical to protein function. Additionally, a loss of normal peptide sequence may result in protein mis-folding and prevent possible interactions with either RNA or proteins. Curiously, short C-terminal peptide extensions results in destabilisation of Mpp6 proteins. This indicates that the distal C-terminal region is required for the stability of the protein either by *cis*-interactions to maintain tertiary conformation or *trans*-interactions with other proteins to form quaternary structure.

5.2.9. Using the DECOID approach to analyse *mpp6* mutants.

Loss-of function *mpp6* mutants were generated through a random mutagenesis approach to identify regions of Mpp6 that are critical to function. Sequencing data revealed the nature of mutations and protein analyses showed that most mutants encoded in zz-Mpp6 fusion constructs are expressed equal or greater than levels of endogenous Mpp6 proteins. In Chapters 3 and 4, it was identified that Mpp6 and the Rrp6/Rrp47 complex function in redundant RNA surveillance pathways. Loss of function *mpp6* alleles are synthetic lethal with *rrp6Δ* or *rrp47Δ* alleles. A conditional system was used to investigate the effects of *mpp6* mutations on RNA surveillance pathways. Initially, a *GAL*-regulated Mpp6 expression construct was generated to make a conditional *GAL::mpp6 rrp47Δ* double mutant. However, control of Mpp6 expression could not be tightly regulated and strains were viable in non-permissive glucose- based media (data not shown). Chapter 3 described a novel method of separating protein complexes *in vivo* by the overexpression of one of the interacting domains of either protein. This novel method is called DECOID (decreased expression of complexes by overexpression of interacting domains). Rrp6 and Rrp47 interact physically via their respective N-terminal PMC2NT and Sas10/C1D domains. Overexpression of the N-terminal PMC2NT domain of Rrp6 ($Rrp6_{NT}$) allowed the successful segregation of the Rrp6/Rrp47 complex *in vivo* by titrating Rrp47 from Rrp6 (Garland et al., 2013). Segregation of Rrp47 from Rrp6 was tolerated in *mpp6Δ* strains suggesting that Rrp47 retained function when divorced from the exonuclease and exosome-binding domains of Rrp6. Separation of a Rrp47ΔC protein, expressing the N-terminal Sas10/C1D domain, from Rrp6 was not tolerated in *mpp6Δ* strains resulting in a block to cell

growth. RNA analyses of conditional *mpp6 rrp47* mutants show a global loss of RNA surveillance pathways resulting in the accumulation of RNA degradation targets including CUTs, pre-rRNA processing byproducts and aberrant forms of stable ncRNAs. The DECOID approach was used as a conditional system to induce loss of Rrp6/Rrp47 function in strains harboring *mpp6* mutants to analyse their phenotypic effects on RNA surveillance.

Plasmids were recovered from strains bearing *mpp6* mutations originally identified in the 5'FOA screen described in Section 5.2.1. However, these strains harbored *LEU2* plasmids encoding *mpp6* mutant alleles and an *URA3* maintenance plasmid bearing a wildtype *MPP6* allele. The maintenance plasmid was required for complementation of the *mpp6Δ rrp47Δ* synthetic lethal genetic background. Normal plasmid extraction from yeast involves DNA isolation followed by recovery of plasmid DNA using *E. coli* (Robzyk and Kassir, 1992). However, initial attempts proved to be unsuccessful and DNA preps were unable to transform competent *E. coli* cells. This procedure was vastly improved upon the use of a commercial kit to isolate plasmid DNA from yeast cells (Section 2.2.20) and plasmids were successfully recovered in *E. coli*. However, recovered DNA was a mixture of *LEU2* plasmids encoding *mpp6* mutants and *URA3* plasmids encoding a wildtype *MPP6* allele and required time-consuming downstream screening to isolate the *LEU2* plasmids. To overcome this issue, heterogeneous plasmid DNA isolated from yeast strains was used to transform competent KC8 *E. coli* cells (Clontech). The KC8 strain bears *leuB, trpC, pryR* and *hisB* auxotrophic mutations that can be complemented by *LEU2, TRP1, URA3* and *HIS3* yeast alleles (Struhl et al., 1979). Transformed KC8 *E. coli* cells were selected for growth on M9 minimal media plates lacking leucine to only select for cells harboring *LEU2* plasmids. This only allowed the isolation of *LEU2* plasmids bearing mutated *mpp6* alleles and prevented contamination by the *URA3* maintenance plasmid.

Centromeric yeast plasmids bearing *mpp6* alleles were transformed into an *mpp6Δ rrp47Δ* strain complemented by a *HIS3* plasmid bearing an *rrp47ΔC* allele. As shown in Section 3.2.3 and 3.2.7, the *rrp47ΔC* allele is sufficient for complementation of the *mpp6Δ rrp47Δ* synthetic lethality and Rrp47ΔC proteins

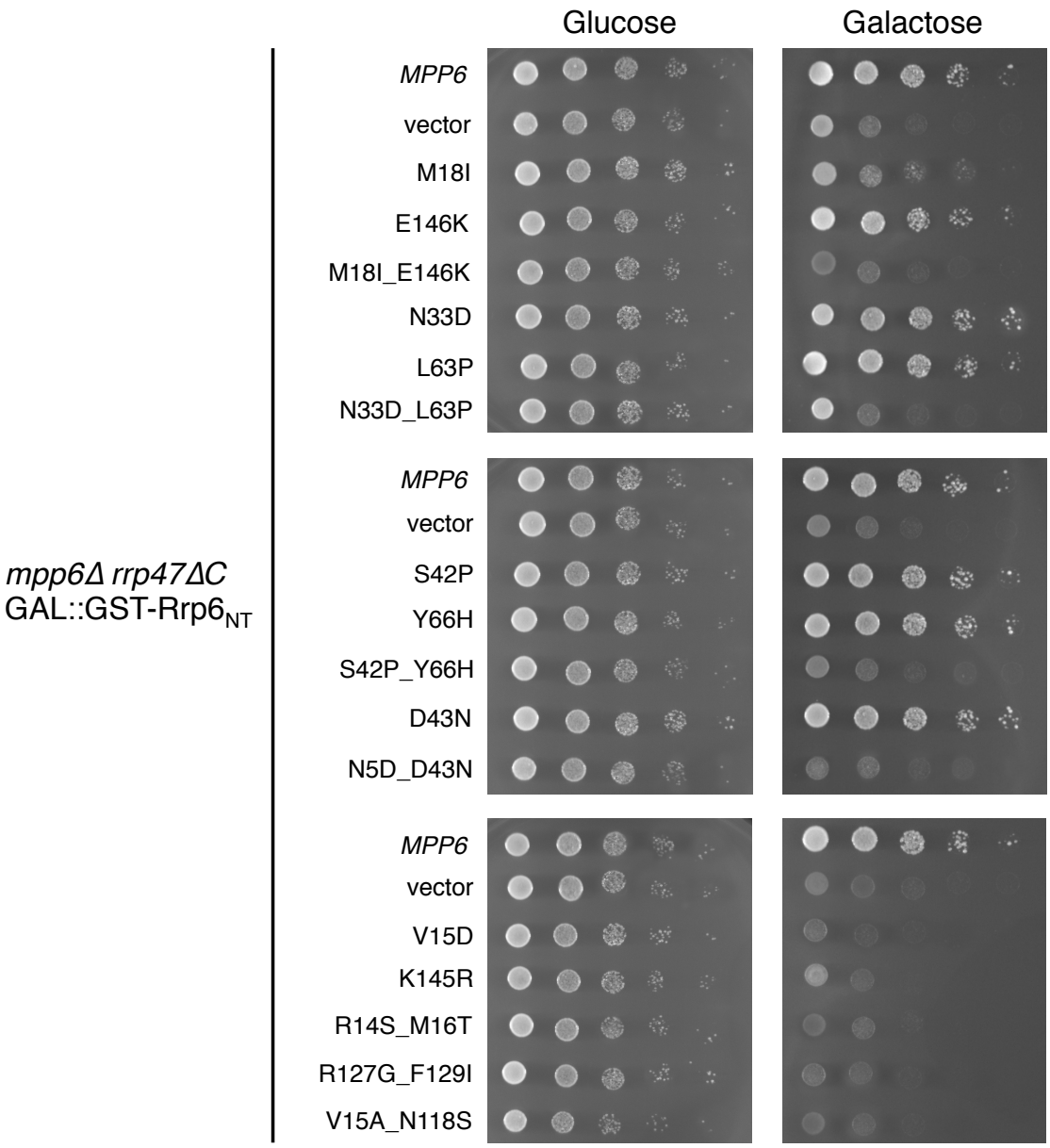

Figure 5.17. Growth analyses of conditional *rrp47 mpp6* mutants using DECOID. Spot growth assays of yeast *mpp6Δ rrp47ΔC GAL::GST-Rrp6$_{NT}$* strains transformed with plasmids bearing *mpp6* alleles. The nature of mutations is indicated for each strain. Parallel transformations with a wildtype zz-Mpp6 expression construct or an empty vector were carried out as positive and negative controls respectively. Cells from raffinose-based cultures were normalised by optical density (600 nm) before spotting 10- fold serial dilutions onto solid glucose- or galactose-based media. Plates were incubated for 3 days at 30°C before photographing.

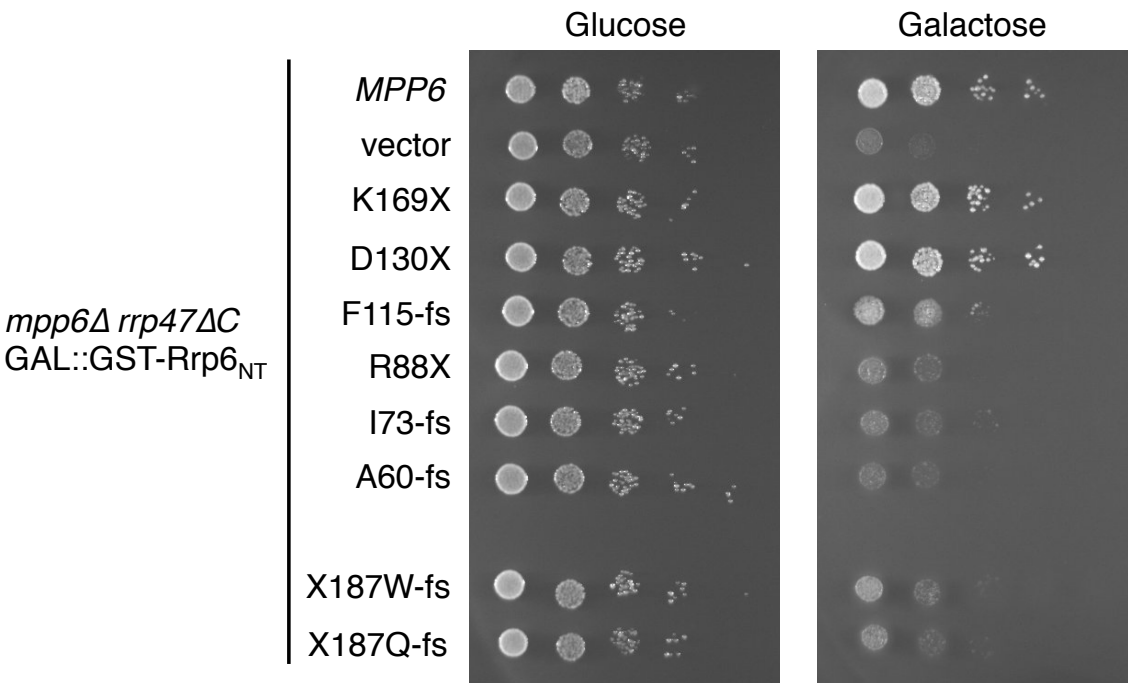

Figure 5.18. Growth analyses of *mpp6* frameshift mutants using DECOID. Spot growth assays of yeast *mpp6Δ rrp47ΔC GAL::GST-Rrp6$_{NT}$* strains transformed with plasmids bearing *mpp6* alleles encoding truncated and extended proteins. The nature of mutations is indicated for each strain. Parallel transformations with a wildtype zz-Mpp6 expression construct or an empty vector were carried out as positive and negative controls respectively. Cells from raffinose-based cultures were normalised by optical density (600 nm) before spotting 10- fold serial dilutions onto solid glucose- or galactose-based media. Plates were incubated for 3 days at 30°C before photographing.

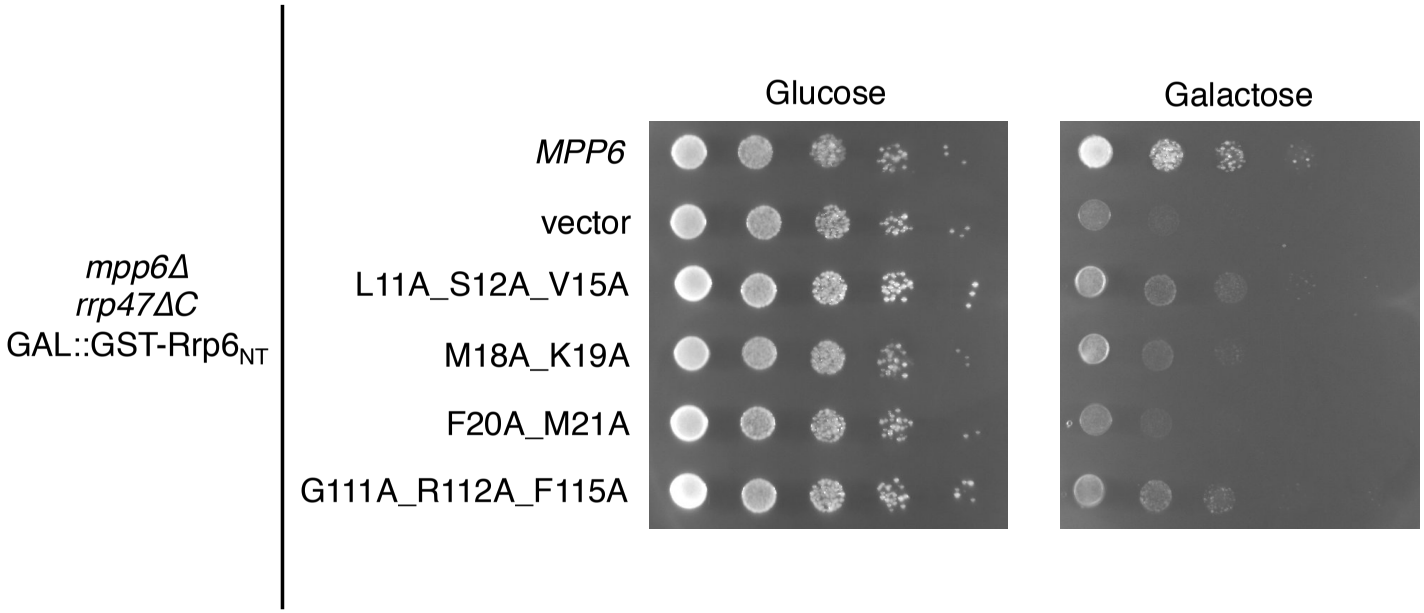

Figure 5.19. Growth analyses of conditional *rrp47 mpp6* mutants using DECOID. Spot growth assays of yeast *mpp6Δ rrp47ΔC GAL::GST-Rrp6$_{NT}$* strains transformed with plasmids bearing *mpp6* alleles. The nature of mutations is indicated for each strain. Parallel transformations with a wildtype zz-Mpp6 expression construct or an empty vector were carried out as positive and negative controls respectively. Cells from raffinose-based cultures were normalised by optical density (600 nm) before spotting 10- fold serial dilutions onto solid glucose- or galactose-based media. Plates were incubated for 3 days at 30°C before photographing.

are stable in the absence of Mpp6. Resulting transformants were transformed with a 2μ plasmid that encodes a *GAL*-inducible GST-Rrp6$_{NT}$ fusion protein (Stead et al., 2007). Conditional overexpression of Rrp6$_{NT}$ allows the segregation of Rrp47ΔC from Rrp6. Combined with loss of function *mpp6* mutations; this induces synthetic lethality and results in a strong growth defect. Strains were assayed for growth on glucose and galactose plates to validate the assay (Figure 5.17). Mutations causing loss of function showed slow growth phenotypes upon induction of the GST-Rrp6$_{NT}$ protein equivalent to strains transformed with an empty vector. Yeast cells bearing functional copies of Mpp6 such as E146K, N33D and L63P, permitted growth on galactose media comparable to strains bearing wildtype *MPP6* alleles.

Strains bearing *mpp6* truncation and extensions mutations showed similar effects on growth upon induction of the Rrp6$_{NT}$ protein (Figure 5.18). K169X and D130X mutations were previously shown to be functional in a plasmid shuffle assay (Section 5.2.7) and permitted growth on galactose medium comparable to the wildtype *MPP6* complemented strain. All non-functional truncation and extension mutants showed slow growth phenotypes upon Rrp6$_{NT}$ induction. The F115-fs mutant showed slightly improved growth compared to other non-functional mutants, yet was much slower compared to K169X and D130X mutants (Figure 5.18).

DECOID growth analysis of strains bearing mutations in conserved regions of Mpp6 showed an equivalent growth pattern observed in the functionality assay (Section 5.2.6. Figure 5.10) All conserved motif mutants showed slow growth phenotypes upon induction of Rrp6$_{NT}$ with the F20_M21 mutant displaying the strongest effect (Figure 5.19)

These results corroborate previous growth analyses and are consistent with loss of growth phenotypes observed in *mpp6Δ rrp47ΔC* mutants upon GST-Rrp6$_{NT}$ expression. The DECOID technique to separate Rrp47ΔC proteins from Rrp6 complexes successfully works as a conditional system to induce loss of functional Rrp6/Rrp47 complexes *in vivo*.

5.2.10. RNA analyses of *mpp6* mutants

The DECOID approach allows a conditional system to induce destabilisation of functional Rrp6/Rrp47 complexes *in vivo*. In wildtype cells, separation of Rrp47 and Rrp47ΔC proteins from Rrp6 is tolerated and mild RNA processing and surveillance phenotypes are observed. Segregation of Rrp47ΔC proteins in strains lacking Mpp6 results in a block in growth and cells exhibit a widespread loss of RNA surveillance. This suggests that Rrp6/Rrp47 and Mpp6 function in redundant RNA surveillance pathways and loss of both mechanisms results in loss-of growth phenotypes. Using this technique in strains harboring *mpp6* mutants allows characterisation of specific mutations in order to map functional regions of the protein.

Yeast *mpp6Δ rrp47ΔC GAL::GST-rrp6*$_{NT}$ strains harboring plasmids encoding *mpp6* mutants (as described in Section 5.2.9) were harvested in selective raffinose- based minimal media and after five doublings of cell density following transfer to galactose- based minimal media. In parallel, cells from *GAL::GST-rrp6*$_{NT}$ and *mpp6Δ rrp47ΔC GAL::GST-rrp6*$_{NT}$ strains transformed with a wildtype zz-Mpp6 construct or an empty vector were harvested as described above. Samples of 5μg total RNA were fractionated through denaturing acrylamide gels and analysed by northern blot hybridisation. Blots were probed for RNAs shown to accumulate in conditional *mpp6 rrp47* mutants including *NEL025c* cryptic unstable transcripts (CUTs), the 5' external transcribed spacer (5'ETS), truncated fragments of 5S rRNA U3 snoRNA and site II extended snoRNAs (II-pA). Hybridisation of *NEL025c* CUTs appears as a homogenous smear on blots transferred from an 8% polyacrylamide gel and cross-hybridises with high molecular weight RNAs. To aid the detection of CUTs, separate acrylamide gels were loaded with 10 μg RNA and fractionated for 1.5 x longer than normal before analysis by northern blot hybridisation. Under non-permissive conditions, upon Rrp6$_{NT}$ induction, *mpp6Δ rrp47ΔC GAL::GST-rrp6*$_{NT}$ strains transformed with an empty vector show strong RNA surveillance phenotypes as described in detail in Chapter 3 (Figure 5.20. A-C lane 4). However, equivalent strains bearing a plasmid encoding wildtype zz-Mpp6 show virtually no phenotype upon Rrp6$_{NT}$ induction

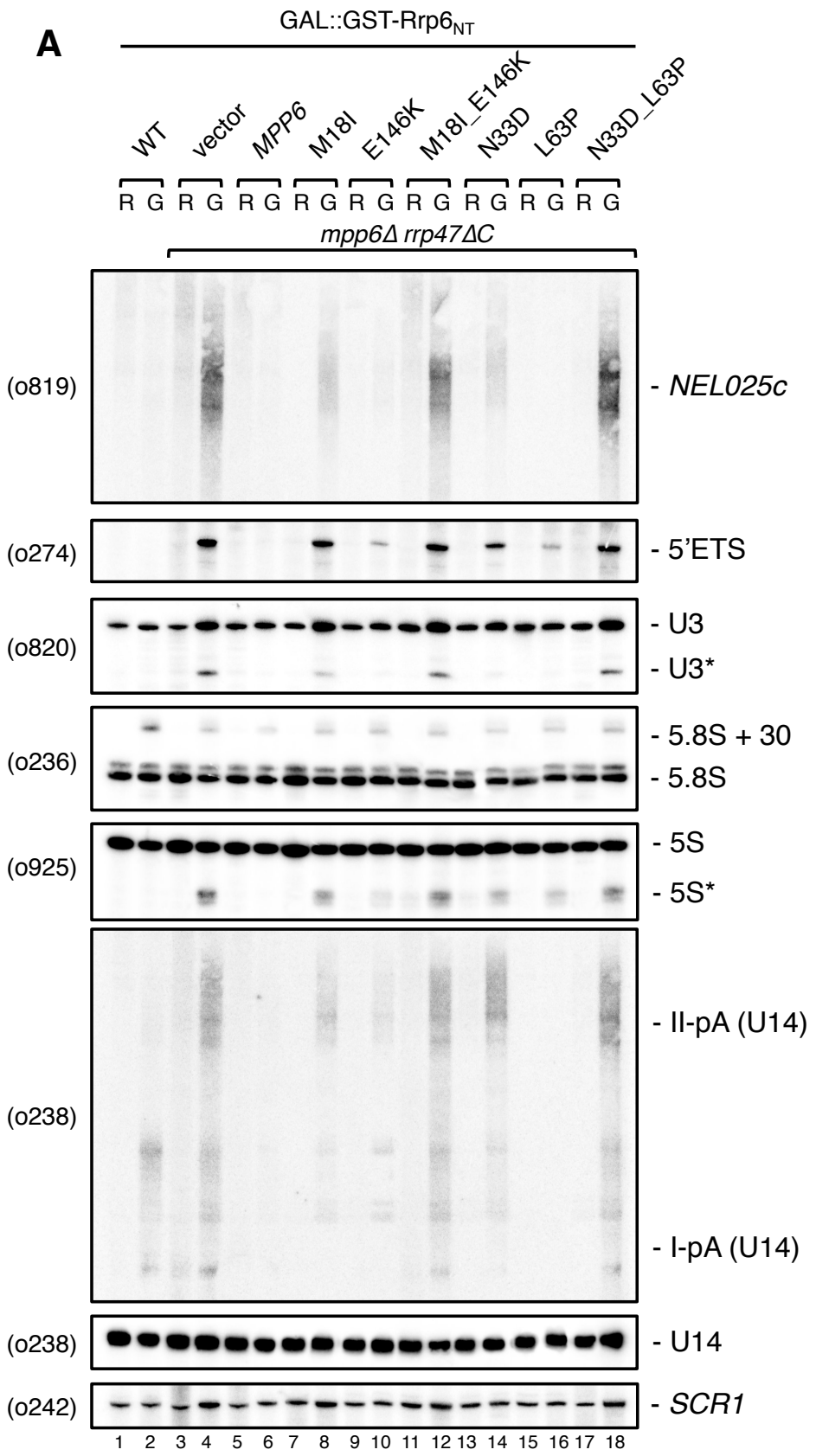

Figure 5.20. RNA analysis of conditional *mpp6 rrp47* mutants using DECOID. Northern blot hybridisation analysis of *mpp6Δ rrp47ΔC GAL::GST-rrp6$_{NT}$* strains transformed with plasmids encoding *mpp6* mutants. Equivalent strains transformed with a plamid encoding wildtype zz-Mpp6 or an empty vector were assayed in parallel. The nature of *mpp6* mutations are indicated. Cells were grown in raffinose(R)- and galactose(G)-based media and harvested after 6 doublings of cell density. Total RNA was fractionated on denaturing polyacrylamide gels and analysed by northern blot hybridisation using radiolabelled oligonucleotide probes as indicated (*left* of panels). Asterisks (*) denote truncated transcripts. Dispersed bands labeled I-pA and II-pA correspond with pre-snoRNAs that are polyadenylated at termination sites I or II respectively. *SCR1* was used a loading control (B) and (C) continued overleaf

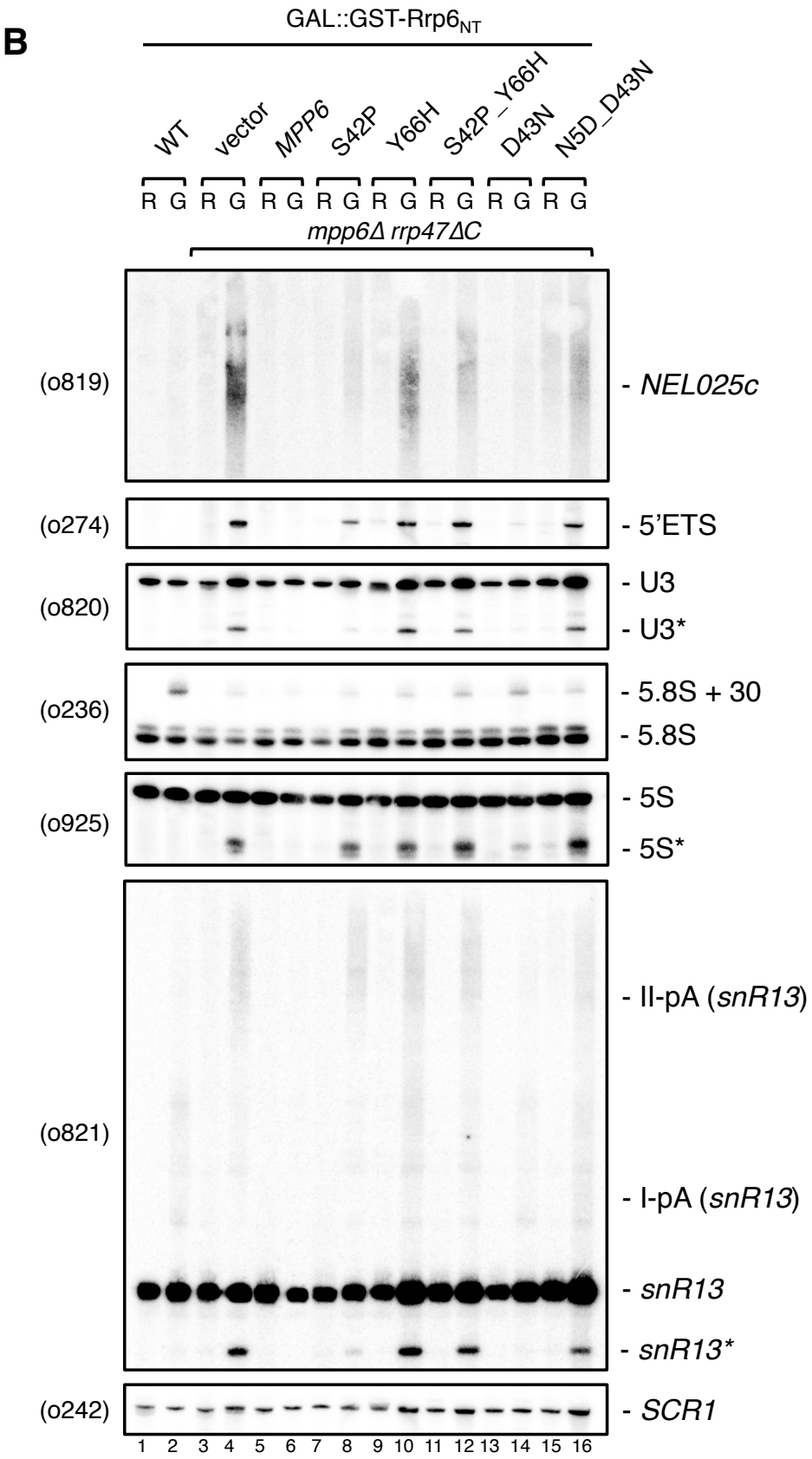
B
GAL::GST-Rrp6NT
WT
vector
MPP6
S42P
Y66H
S42P_Y66H
D43N
N5D_D43N
R G R G R G R G R G R G R G R G
mpp6Δ rrp47ΔC
(o819)
- NEL025c
(o274)
- 5'ETS
(o820)
- U3
- U3*
(o236)
- 5.8S + 30
- 5.8S
(o925)
- 5S
- 5S*
(o821)
- II-pA (snR13)
- I-pA (snR13)
- snR13
- snR13*
(o242)
- SCR1
1 2 3 4 5 6 7 8 9 10 11 12 13 14 15 16

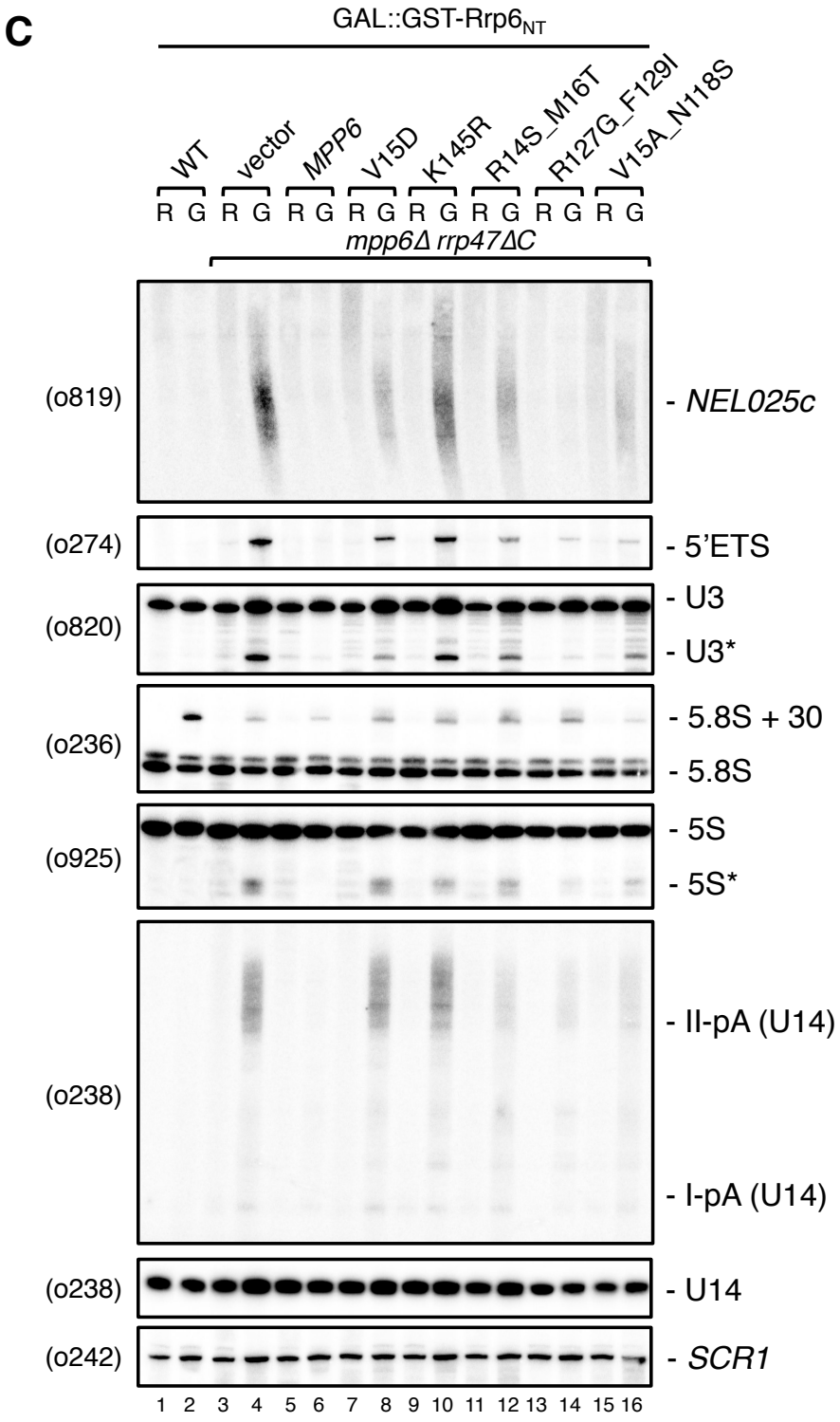
C
GAL::GST-Rrp6NT
WT
vector
MPP6
V15D
K145R
R14S_M16T
R127G_F129I
V15A_N118S
R G R G R G R G R G R G R G R G
mpp6Δ rrp47ΔC
(o819)
- NEL025c
(o274)
- 5'ETS
(o820)
- U3
- U3*
(o236)
- 5.8S + 30
- 5.8S
(o925)
- 5S
- 5S*
(o238)
- II-pA (U14)
- I-pA (U14)
(o238)
- U14
(o242)
- SCR1
1 2 3 4 5 6 7 8 9 10 11 12 13 14 15 16

(Figures 5.20. A-C lane 6). These control samples act as standards for either complete loss of function or no loss of function respectively. This allows a comparable measure to determine if *mpp6* mutations cause phenotypes equivalent to a total loss of Mpp6 function or show milder effects.

RNA analysis of *mpp6* mutants bearing single or double amino acid substitutions were grouped together to examine if the phenotypes of double mutants are the result of one single mutation or have a cumulative effect (Figures 5.20 A-B) M18_E146K and N33D_L63P double mutants showed a strong accumulation of *NEL025c*, 5'ETS, U3*, 5S* and II-pA (U14) upon induction of $Rrp6_{NT}$ comparable to the null *mpp6* mutant (Figure 5.20. A. compare lanes 4 with 12 and 18). Analyzing the separated point mutations shows mild phenotypes in M18I and N33D mutants and weaker phenotypes in E146K and L63P mutants. This suggests that M18I and N33D mutations are the main contributors to loss of function in their respective double mutants but their effects are exacerbated in combination with E146K and L63P substitutions respectively. Interestingly some mutants displayed specific phenotypes: The N33D mutant showed a strong accumulation of site II terminated snoRNAs comparable to the null mutant (Figure 5.20 A compare lanes 4 and 14). However, this mutant showed a relatively weak CUTs phenotype and almost undetectable levels of the aberrant truncated U3* snoRNA. All mutants in Figure 5.20 showed a detectable amount of 5'ETS and 5S* transcripts upon $Rrp6_{NT}$ induction. However, as these species are derived from pre-rRNA and 5S rRNA species respectively, their relative abundance will be much greater in comparison to other analysed transcripts.
Hybridisation analysis of the S42P_Y66H double mutant and separated single mutants shows that the Y66H mutation has the greater effect in the pair. Curiously, the Y66H single mutation shows a stronger accumulation of *NEL025c* CUTs, aberrant U3* and snR13* transcripts in comparison to the double mutant (Figure 5.20 B compare lanes 10 and 12). Y66 is mildly conserved in fungal Mpp6 homologs (Appendix II) and not conserved in homologues in model organisms (Appendix I) however; these results suggest the residue is important for Mpp6 function *in vivo*. The D43N mutant shows relatively weak RNA surveillance phenotypes upon $Rrp6_{NT}$ expression in comparison to a N5D_D43N double

mutant (Figure 5.20 B compare lanes 14 and 16). The N5D mutation was not separated by SDM because it was assumed be causing loss-of function phenotypes due to the proximity to the N-terminal conserved motif in Mpp6. In hindsight, it would be interesting to investigate this mutant in isolation.
V15D and K145R were identified as single amino acid substitutions that cause a loss of function. RNA analyses show comparable phenotypes upon $Rrp6_{NT}$ induction in comparison to the *mpp6Δ* mutant (Figure 5.20 C compare lanes 8 and 10 with 4). Specifically, the K145 mutant shows comparable accumulations of *NEL025c* CUTs, 5'ETS, U3* and II-pA (U14) whereas the V15D mutant shows slightly milder phenotypes with the possible exception of 5S*. As mentioned previously, due to the higher levels of 5S rRNA, the 5S* phenotype may appear to be more distinct in comparison to transcripts that are weakly expressed.
R14S_M16T and V15A_N118S double mutants show comparable CUT and aberrant ncRNA accumulations. These mutants share substitutions in a highly conserved N-terminal domain motif in Mpp6 that appears to be a critical region for protein function.

Taken together, analysis of *mpp6* mutants encoding full-length proteins identifies critical regions for protein function. Firstly, mutations in a highly conserved N-terminal motif cause loss of function or slow growth phenotypes in combination with *rrp47* mutants. RNA analyses show that this region is important for the function of Mpp6 in RNA surveillance pathways. Loss of function proteins show an accumulation of RNA substrates normally targeted for degradation in wildtype cells. Mutational analysis has also identified residues between N33 and Y66 that also seem important for Mpp6 function *in vivo*. This region is not conserved in Mpp6 homologues found in model organisms. However, N33, S42, D43 and L63 residues are relatively well conserved when comparing fungal homologues suggesting that this region may be functionally important in other yeast species.

RNA analysis using DECOID was carried out in strains harboring *mpp6* mutants bearing alanine substitutions in conserved residues. These analyses corroborate results described above. Mutations in the highly conserved N-terminal motif were previously shown to cause slow growth phenotypes in combination with *rrp47Δ*

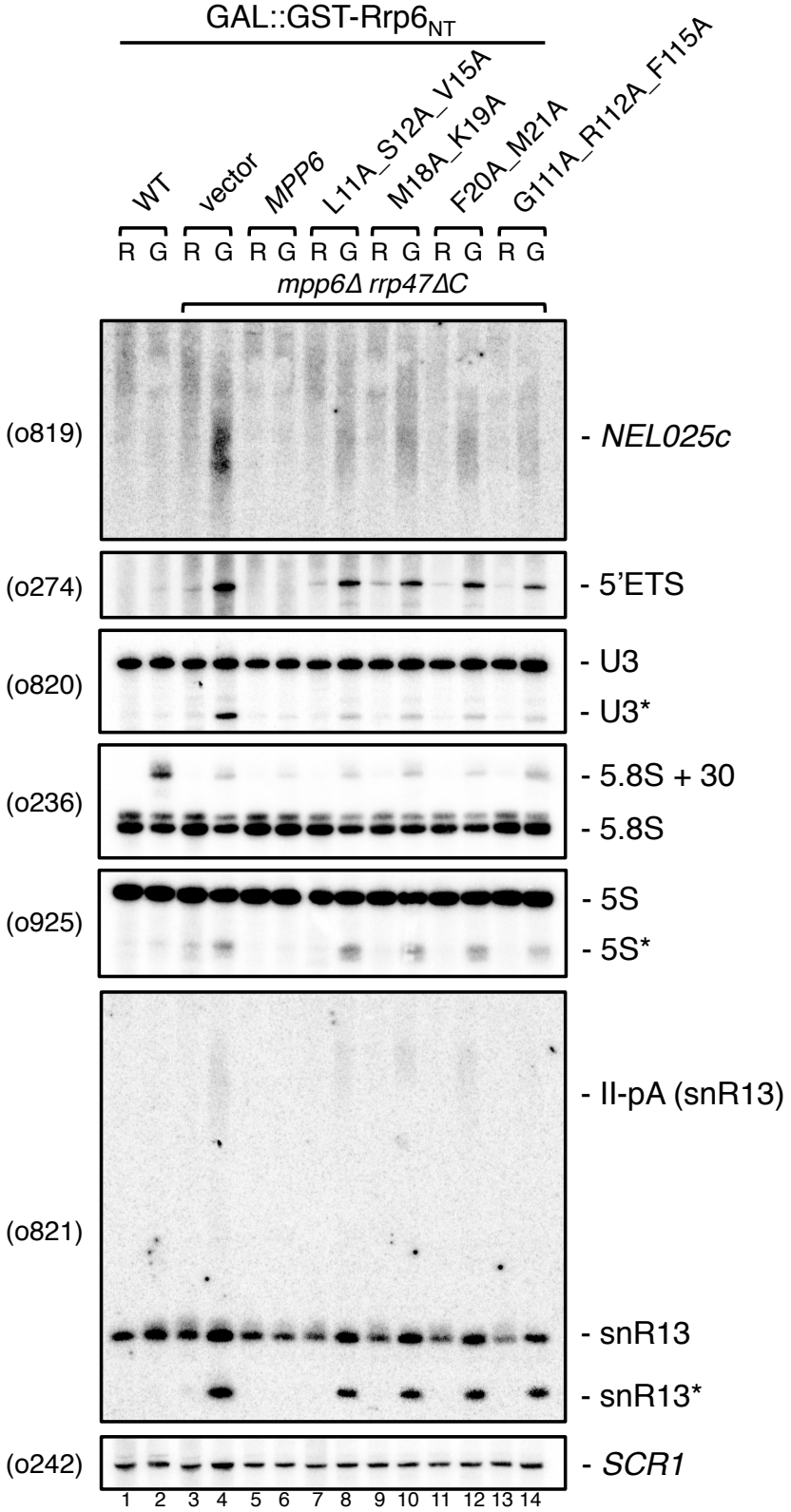

Figure 5.21. RNA analysis of conserved motif *mpp6* mutants. Northern blot hybridisation analysis of *mpp6Δ rrp47ΔC GAL::GST-rrp6$_{NT}$* strains transformed with plasmids encoding *mpp6* mutants. Equivalent strains transformed with a plamid encoding wildtype zz-Mpp6 or an empty vector were assayed in parallel. The nature of *mpp6* mutations are indicated. Cells were grown in raffinose(R)- and galactose(G)-based media and harvested after 6 doublings of cell density. Total RNA was fractionated on denaturing polyacrylamide gels and analysed by northern blot hybridisation using radiolabelled oligonucleotide probes as indicated (*left* of panels). Asterisks (*) denote truncated transcripts. Dispersed bands labeled I-pA and II-pA correspond with pre-snoRNAs that are polyadenylated at termination sites I or II respectively. *SCR1* was used a loading control.

alleles. Northern blot hybridisation analysis revealed that these strains accumulate RNA surveillance targets including CUTs, 5'ETS and aberrant ncRNAs (Figure 5.21 lanes 8-12). Additionally, a triple mutant bearing substitutions in a second conserved motif revealed similar phenotypes suggesting that both regions are important for normal Mpp6 function (Figure 5.21 lane 14). Mutations in the N-terminal motif but not the second, more distal motif were identified in loss-of function mutants isolated by random mutagenesis.

Finally, *mpp6* mutants encoding truncated or extended Mpp6 proteins were analysed using DECOID as a tool to induce Rrp6/Rrp47 destabilisation as described above. In Section 5.2.7, Mpp6 proteins bearing K169X and D130X mutations were shown to be functional *in vivo* using a plasmid shuffle assay and were also included in this RNA analysis. All mutants bearing C-terminal truncations or extensions showed an accumulation of the 5' external transcribed spacer region (5'ETS) (Figure 5.22). This fragment is a byproduct of 35S pre-rRNA maturation and is usually degraded by the exosome in wildtype cells. The accumulation of 5'ETS in all truncated and extended mutants suggests that the C-terminus of Mpp6 is important in normal 5'ETS turnover. Mutants encoding Mpp6 proteins truncated at D130 and shorter showed a strong accumulation of *NEL025c* cryptic unstable transcripts comparable to conditional *mpp6Δ rrp47* strains (Figure 5.22 compare lanes 4 with 10-18). Additionally, X187W-fs and X187Q-fs mutations, encoding extended Mpp6 proteins showed an accumulation of CUTs with X187Q-fs mutant displaying a stronger phenotype (Figure 5.22 Lanes 19-22). Accumulations of aberrant ncRNA species were observed in truncation and extension mutants including U3* and 5S* truncated transcripts. Consistent with previous observations, an accumulation of box C/D snoRNAs terminated at the failsafe site-II (Grzechnik and Kufel, 2008) was detected in non-functional *mpp6* mutants. A mild accumulation of II-pA (U14) was observed in K169X and D130X mutants but not to the extent of loss-of function mutants (Compare lanes 7-10 with 11-18).

Consistent with conditional *mpp6Δ rrp47* mutant strains explored in Chapter 3, loss-of function *mpp6* mutants display a block in RNA surveillance pathways when

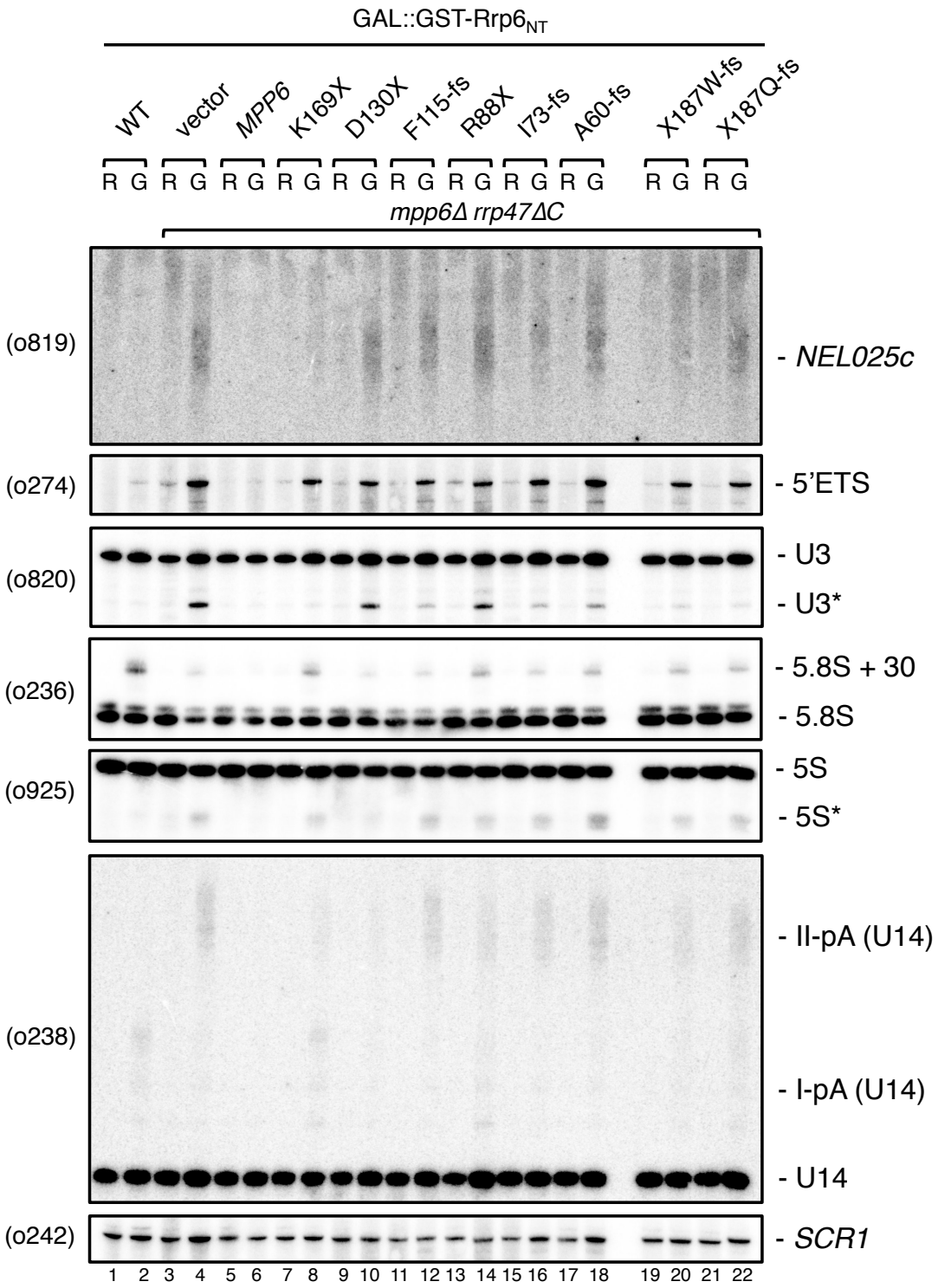

Figure 5.22. RNA analysis of *mpp6* truncation and extension mutants using DECOID. Northern blot hybridisation analysis of *mpp6Δ rrp47ΔC GAL::GST-rrp6*$_{NT}$ strains transformed with plasmids encoding *mpp6* mutants. Equivalent strains transformed with a plamid encoding wildtype zz-Mpp6 or an empty vector were assayed in parallel. The nature of *mpp6* mutations are indicated. Cells were grown in raffinose(R)- and galactose(G)-based media and harvested after 6 doublings of cell density. Total RNA was fractionated on denaturing polyacrylamide gels and analysed by northern blot hybridisation using radiolabelled oligonucleotide probes as indicated (*left* of panels). Asterisks (*) denote truncated transcripts. Dispersed bands labeled I-pA and II-pA correspond with pre-snoRNAs that are polyadenylated at termination sites I or II respectively. *SCR1* was used a loading control.

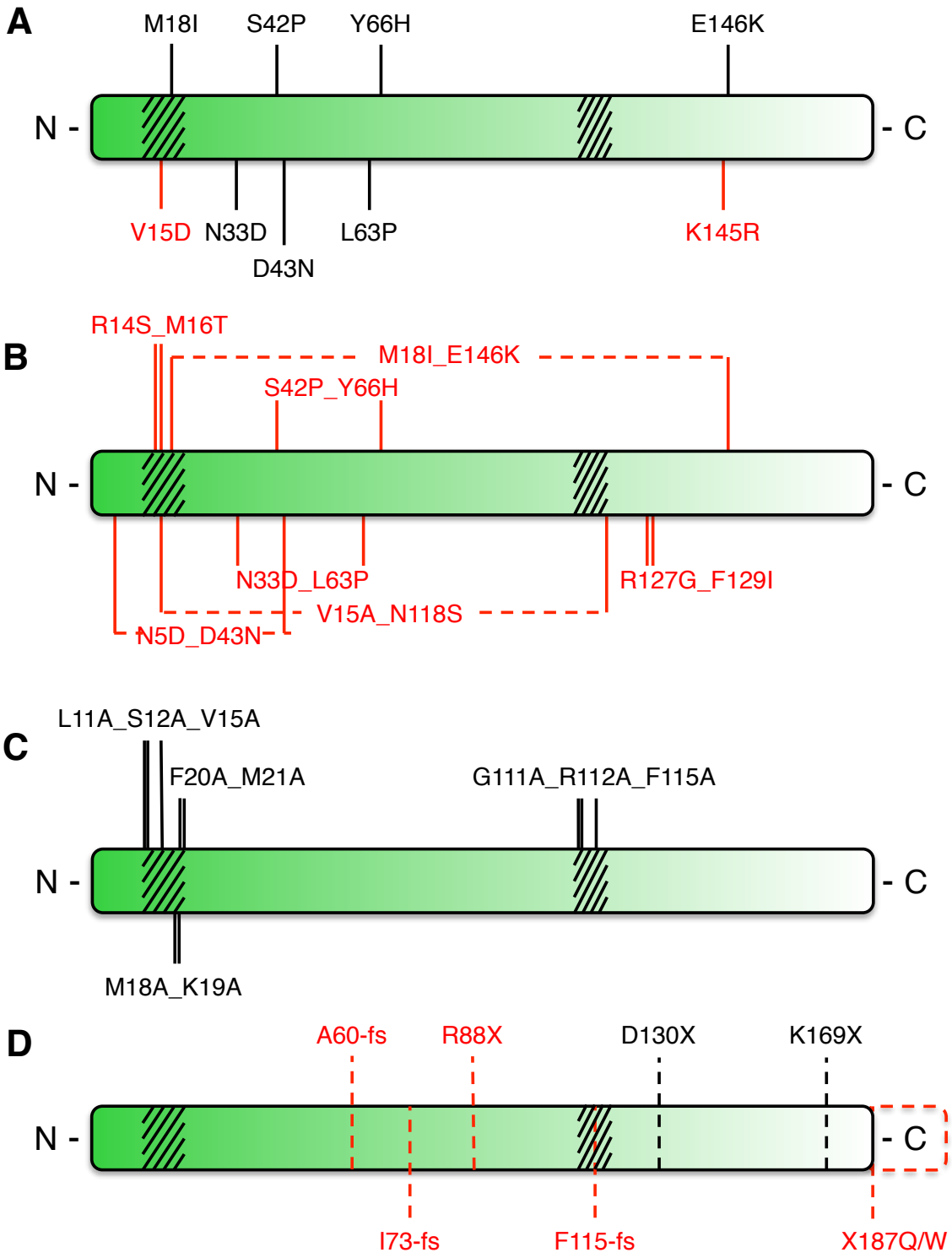

Figure 5.23. Summary of *mpp6* mutants generated in this study. Schematic of mutation sites generated through random or directed methods. Loss of function mutations are marked in red. Mutations are separated into groups of (A) single amino acid substitutions, (B) double amino acid substitutions, (C) alanine substitutions in conserved motifs and (D) C-terminal truncation and extensions.

combined with conditional *rrp47* mutants. Cells accumulate transcripts that usually undergo rapid turnover in wildtype cells such as CUTs and aberrant ncRNAs. This study has characterised a number of loss-of function *mpp6* mutants and identified functionally important regions of the Mpp6 protein (Summarised in Figures 5.23). However, it is still not known how Mpp6 functions with the nuclear exosome in RNA surveillance pathways and what proteins/complexes it may contact.

5.2.11. Mpp6 expression is decreased in the absence of Rrp6 or Trf4

Mutational studies and RNA analysis have shown that Mpp6 is required for RNA surveillance and degradation pathways involving the nuclear exosome. Additionally, functional pathways involving Mpp6 are redundant with pathways requiring functional Rrp6 and Rrp47. In the absence of both pathways, cells accumulate a wide range of aberrant RNA species and stabilise cryptic unstable transcripts (CUTs). Many of the RNA species shown to accumulate in conditional *rrp47 mpp6* mutants have been previously characterised in exosome mutants. Specifically, nuclear exosome surveillance pathways have been shown to require the function of the Trf4/Air2/Mtr4 polyadenylation (TRAMP) complex (Houseley et al., 2006; Wolin et al., 2012). The TRAMP complex targets RNAs for degradation by the nuclear exosome by the addition of short poly(A) tails (~ 4-5 nt) which are suggested to enhance the activity of the exosome by providing a more favorable single stranded RNA substrate. The complex is typically composed of a non-canonical poly(A) polymerase Trf4 or Trf5, a zinc-knuckle RNA binding protein Air1 or Air2 and the ATP-dependent 3'-5' helicase Mtr4. The helicase action of Mtr4 is predicted to function in unwinding of structured RNA substrates, such as 5'ETS, to aid in recognition by the exosome. Many RNA surveillance targets detected in northern hybridisation analysis of *mpp6* mutants are known substrates for the TRAMP complex. Transcriptional termination of CUTs is dependent on the activity of the Nrd1/Nab3/Sen1 (NNS) complex that recruits the TRAMP complex for subsequent polyadenylation prior to rapid degradation by the nuclear exosome (Wolin et al., 2012). Yeast *trf4Δ* cells accumulate non-polyadenylated CUTs (Wyers et al., 2005). Additionally, truncated forms of stable ncRNAs such as a 5'-

truncated form of 5S rRNA (5S*) have been shown to accumulate in *trf4* mutants (Kadaba et al., 2006).

Mpp6 has previously been proposed to function by stimulating the activity of Rrp44, possibly by substrate recognition/recruitment through RNA binding activity (Milligan et al., 2008). This was inferred as *mpp6Δ* mutations are synthetic lethal with *rrp47Δ* or *rrp6Δ* alleles, suggesting that Mpp6 and Rrp47 do not both function to target substrates to Rrp6. An alternative model is that Mpp6 promotes functional coupling between Rrp6 and the TRAMP complex (Butler and Mitchell, 2011). This is supported by a physical interaction observed between human homologs of Mpp6, Rrp6 and Mtr4 (MPP6, PM-Scl100 and hMtr4 respectively) (Schilders et al., 2007). Additionally, *mpp6Δ* mutations are synthetic lethal with *air1Δ* alleles (Milligan et al., 2008).

To investigate possible functional and/or physical interactions between Mpp6 and TRAMP components, a C-terminal TAP-tagged *MPP6* allele was transposed into isogenic strains lacking TRAMP components or Rrp6. Previous analysis of the Rrp6/Rrp47 heterodimer revealed that the stability of either protein was dependent on their physical interaction, with Rrp47 more sensitive to the loss of Rrp6 (Feigenbutz et al., 2013a, 2013b). Deletions in TRAMP components and Rrp6 were used as a method to possibly identify proteins that interact physically with Mpp6 and are required for protein stability *in vivo*.

A C-terminally TAP tagged *MPP6* allele was amplified from yeast genomic DNA by PCR using outlying primers (o595 + o598). PCR products were validated by agarose gel electrophoresis and purified using commercial PCR clean up kits. The *MPP6-TAP* cassette fragment contains sufficient regions of homology to target to *MPP6* loci and also included a *HIS3* selectable marker (Ghaemmaghami et al., 2003). Isogenic *rrp6Δ, trf4Δ, trf5Δ* and *air1Δ* strains were transformed with purified *MPP6-TAP, HIS3* DNA and selected on minimal medium lacking histidine. Transformants were screened for successful integration by PCR using outlying *MPP6* primers (o595 + o598). Lysates were prepared from isogenic wildtype,

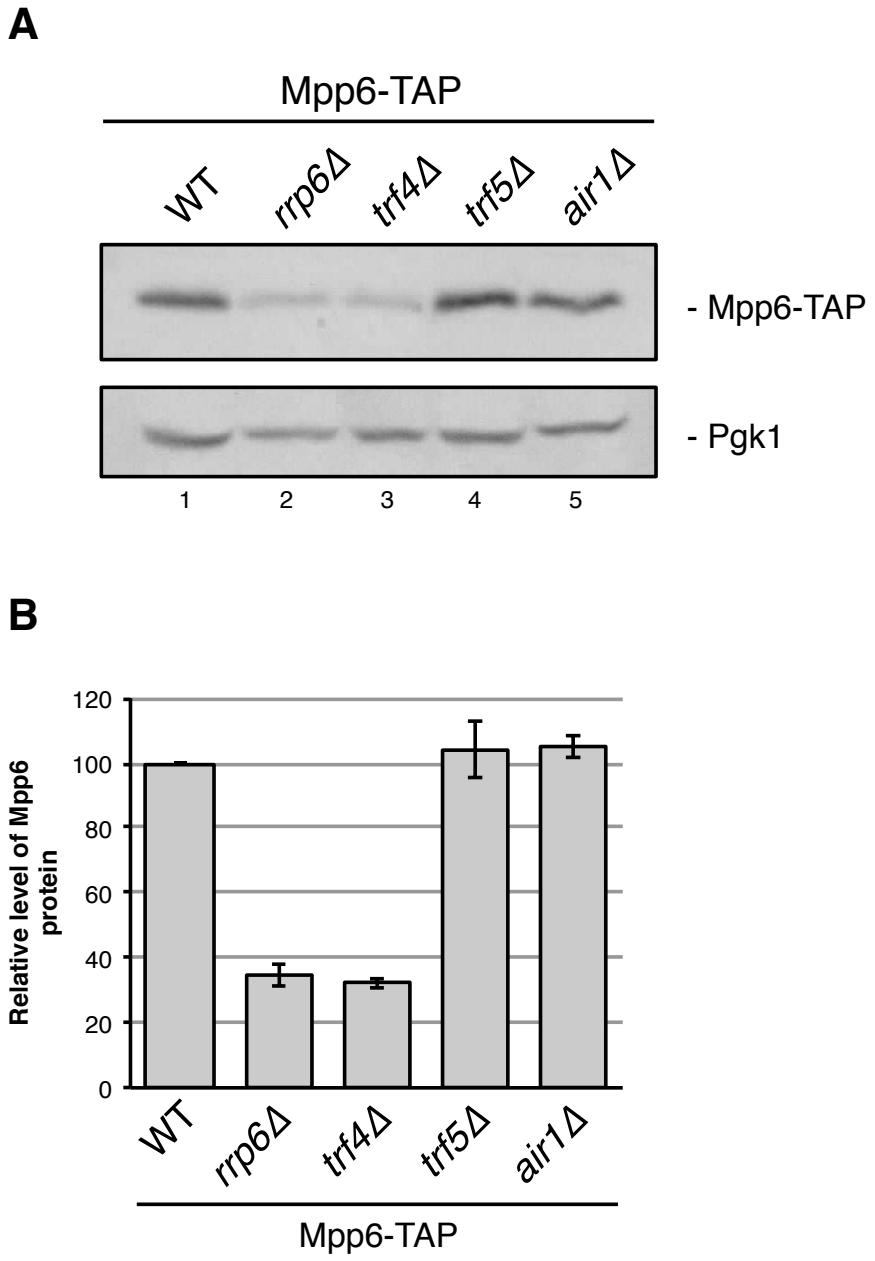

Figure 5.24. Stable expression of Mpp6 is dependent on Rrp6 or Trf4. Western blot analysis of Mpp6-TAP expression in *rrp6* and TRAMP mutants. The *MPP6-TAP* allele was transposed into isogenic wildtype (WT), *rrp6Δ, trf4Δ, trf5Δ* and *air1Δ* strains. **(A)** Lysates were fractionated by SDS PAGE and the expression of Mpp6 proteins were analysed by western blot using the PAP antibody (*upper* panel). An antiserum against Pgk1 was used as a loading control (*lower* panel). **(B)** Quantitative analysis of of relative Mpp6-TAP protein expression. Data is representative of three independent experiments. Values were normalised against Pgk1 levels and standardised to the amount of protein in wild-type cells. Error bars represent the standard error of the mean for each set of values.

rrp6Δ, *trf4Δ*, *trf5Δ* and *air1Δ* strains bearing *MPP6-TAP* alleles and analysed by SDS PAGE and western blot analysis using the PAP antibody (Figure 5.24. A).

Steady state expression levels of Mpp6 were decreased to 34 % and 32 % in *rrp6Δ* and *trf4Δ* strains in comparison to wildtype cells (compare lanes 1-3). These values were consistent upon independent analysis of biological replicas. Interestingly, levels of Mpp6 were unchanged in cells lacking Trf5 or Air1 in comparison to wildtype levels (compare lanes 1 with 4-5). This suggests that both Rrp6 and Trf4 are required for stable expression of Mpp6.

The non-canonical poly(A) polymerases Trf4 and Trf5 form distinct TRAMP complexes (TRAMP4 and TRAMP5 respectively) which have been reported to target distinct groups of RNAs for degradation with some functional overlap (Egecioglu et al., 2006; San Paolo et al., 2009). TRAMP4 complexes contain either Air1 or Air2 proteins whereas TRAMP5 complexes exclusively contain Air1 (Houseley and Tollervey, 2006; LaCava et al., 2005). These results suggest a possible functional and/or physical link between Mpp6, Rrp6 and the TRAMP complex, specifically TRAMP4.

Mpp6 has previously been reported to physically associate with the nuclear exosome through pull-down analyses and shown to cosediment with core-exosome components in glycerol gradient ultracentrifugation experiments (Milligan et al., 2008). However, the physical contacts between Mpp6 and the core-exosome complex are unknown. Interactions could either be direct or via another associated protein. To investigate interactions with exosome-containing complexes, the sedimentation of Mpp6 proteins were analysed in *rrp6Δ* and TRAMP mutants described above.

Native cell lysates prepared from isogenic wildtype, *rrp6Δ*, *trf4Δ*, *trf5Δ* and *air1Δ* strains expressing Mpp6-TAP proteins were fractionated by ultracentrifugation through glycerol gradients and the sedimentation behavior of Mpp6 was visualised by western blot analysis (Figure 5.25. A). Colloidal staining of fractions separated by SDS PAGE was used to validate the distribution of total cellular protein profiles and were comparable in each gradient (Figure 5.25. B). Additionally, lysates from

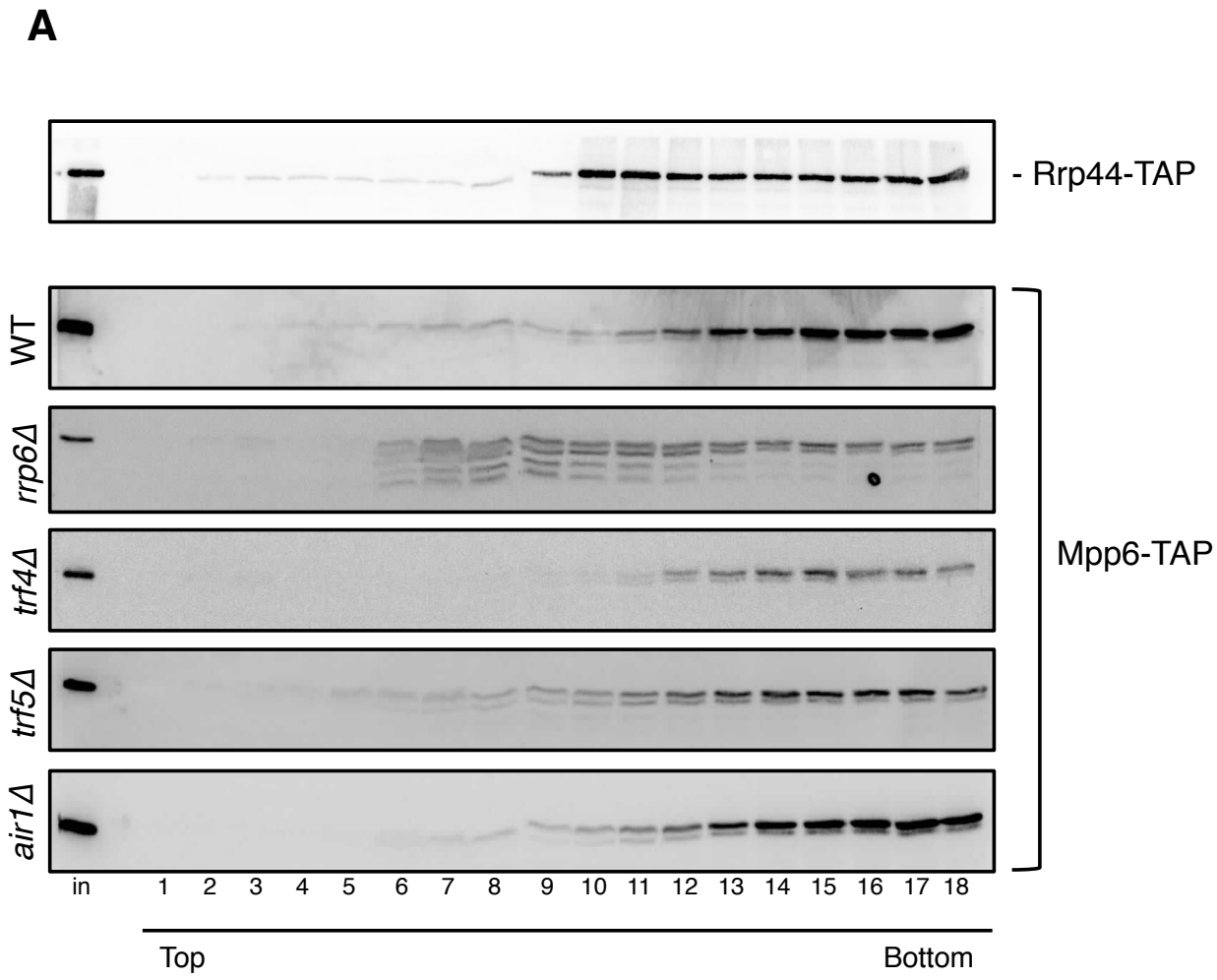

Figure 5.25. The association of Mpp6 with larger complexes is destabilised in the absence of Rrp6. Glycerol gradient ultracentrifugation analysis of Mpp6-TAP proteins expressed in *rrp6* and TRAMP mutants. Lysates from isogenic wildtype, *rrp6Δ*, *trf4Δ*, *trf5Δ* and *air1Δ* strains expressing Mpp6-TAP proteins were sedimented through 10 – 30% glycerol gradients. Lysate from a Rrp44-TAP strain was sedimented in parallel. (A) Gradient fractions 1-18 were resolved by SDS PAGE and analysed by (A) western blotting using the PAP antibody and (B) coomassie staining (*overleaf).*

B

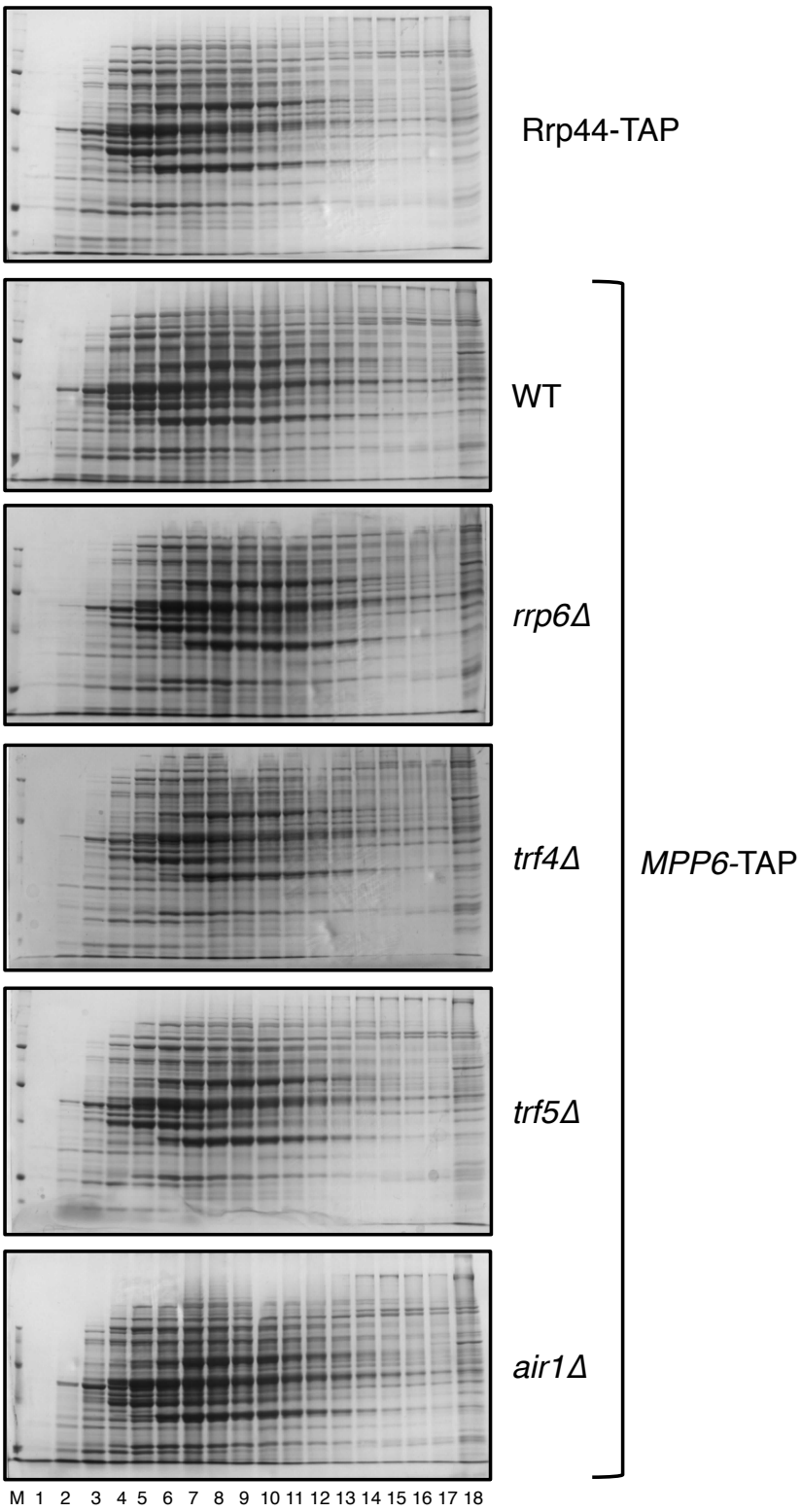
Rrp44-TAP
WT
rrp6Δ
trf4Δ
trf5Δ
air1Δ
MPP6-TAP
M 1 2 3 4 5 6 7 8 9 10 11 12 13 14 15 16 17 18

cells expressing C-terminally TAP tagged Rrp44 were fractionated in parallel as a marker for the sedimentation profile of nuclear exosome complexes. The sedimentation behavior of Mpp6 in wildtype cells clearly displays that the protein is found in large complexes. The distribution of sedimentation showed a peak in fractions 15-17 and exhibited clear overlaps with the sedimentation profile of Rrp44. This corroborates previous analyses in which Mpp6 showed cosedimentation with the core-exosome subunit Rrp43 (Milligan et al., 2008). Analysis of the sedimentation of Mpp6 in *rrp6Δ* strains reveals that the distribution of Mpp6-TAP is shifted further to the top of the gradient. Additionally, the protein shows a high degree of degradation in fractions 6-12. This pattern was reproducible upon repeat glycerol gradient analyses. The shift in sedimentation distribution suggests that Rrp6 is partly required for the association of Mpp6 with larger complexes. As the protein is still present in fractions 14-18, this implies that Mpp6 may form other contacts with the exosome independent of Rrp6. The increased degradation pattern of Mpp6 suggests that the protein is less stable in the absence of Rrp6. This agrees with the observable decrease in steady state protein expression of Mpp6 in *rrp6Δ* cells.
Analysis of the sedimentation behavior of Mpp6 in cells lacking Trf4 shows that the protein sedimentation retains a similar distribution pattern to the wildtype in fractions 12-18 (Figure 5.25). However, no protein is observed in upper fractions (4-10). This may be due to relative signal intensities as Mpp6 expression is decreased to ~30% in *trf4Δ* cells. However, another possibility is that the fraction of Mpp6 proteins represented in fractions 4-10 corresponds to sub-exosome complexes composed of TRAMP complexes associated with Mpp6, specifically TRAMP4 complexes. In *trf5Δ* and *air1Δ* samples, Mpp6 shows a normal distribution profile comparable to wildtype cells.

These results suggest the possibility that Mpp6 is found in two distinct subcomplexes and that the connection between these complexes is partially dependent on Rrp6. In the absence of Rrp6, Mpp6 expression is decreased to ~30% of normal steady state levels. Glycerol gradient analysis shows that the distribution of Mpp6 sedimentation shifts from larger complexes to moderately sized complexes where the protein appears to be less stable. In the absence of

Trf4, Mpp6 expression is also decreased to ~30% compared to wildtype cells. Glycerol gradient sedimentation shows that Mpp6 is still found in larger complexes but is not detected in fractions corresponding to smaller complexes. This suggests that Mpp6 may contribute to connections between the TRAMP complex and the nuclear exosome. Additionally, Rrp6 may be partially required for the association of Mpp6 with the exosome complex that also maintains normal protein stability of Mpp6. Interestingly; this interaction appears to be specific for TRAMP4 complexes as no effect is observed in cells lacking Trf5 or Air1.

5.2.12. Glycerol gradient ultracentrifugation analysis of Mpp6 mutants.

Section 5.2.11 identified possible connections that mediate the interaction of Mpp6 with larger complexes using glycerol gradient ultracentrifugation analyses to analyse the sedimentation pattern of tagged-Mpp6 proteins. Additionally, a library of *mpp6* mutants has been generated through either random or directed mutagenesis methods. Using glycerol gradient ultracentrifugation methods, the sedimentation behavior of Mpp6 proteins was analysed in *mpp6* mutants in order to characterise regions of the protein that may be required for interactions with larger complexes.

A number of *mpp6* mutants identified in the random mutagenesis screen were shown to contain amino acid substitutions in a highly conserved motif at the N-terminus of the protein. Using site directed mutagenesis methods, four mutants were previously constructed with alanine substitutions in conserved regions of Mpp6 including the N-terminal motif (L11A_S12A_V15A, M18A_K19A and F20A_M21A) and a second, more distal motif (G111A_R112A_F115A). Mutations were generated in a N-terminal zz-tagged Mpp6 expression construct under the control of the *RRP4* promoter. Glycerol gradient ultracentrifugation analysis of the wildtype zz-Mpp6 construct showed a slightly different distribution profile to that observed in cells expressing a C-terminal TAP-tagged Mpp6 protein under the control of the endogenous *MPP6* promoter (Figure 5.26) In addition to

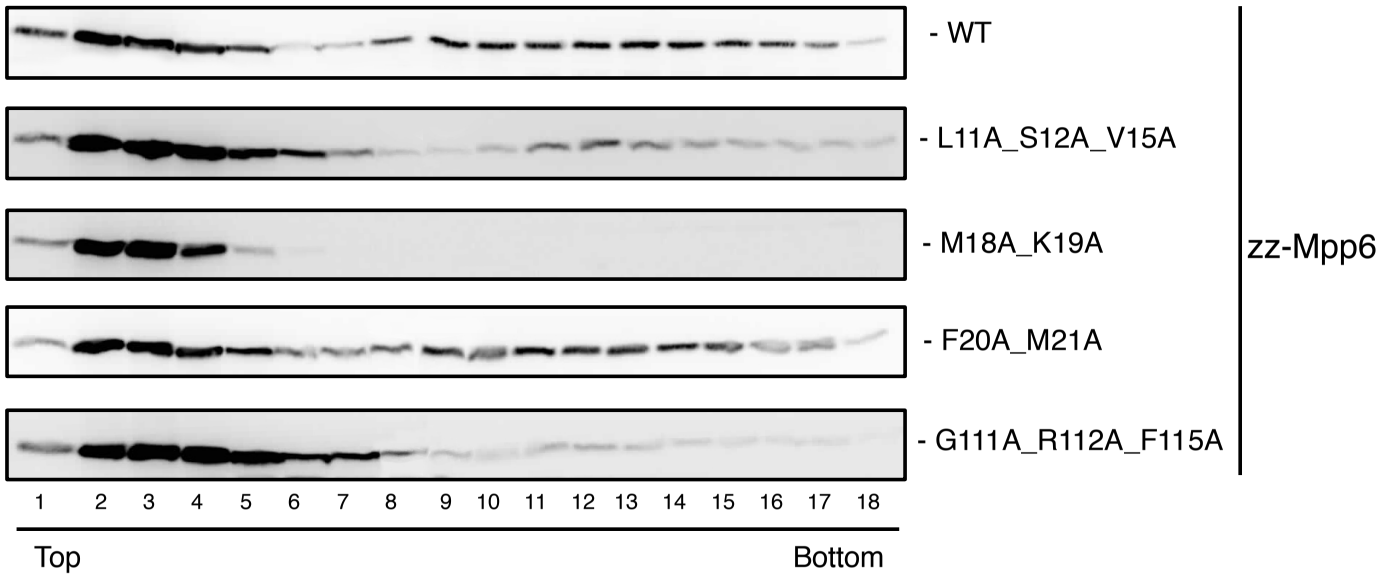

Figure 5.26. M18A_K19A substitutions in Mpp6 inhibit associations with larger complexes. Glycerol gradient ultracentrifugation analysis of zz-Mpp6 proteins bearing mutations in conserved residues. Lysates from cells expressing widltype zz-Mpp6 or L11A_S12A_V15A, M18A_K19A, F20A_M21A and G111A_R112A_F115A mutant proteins were sedimented through 10 – 30% glycerol gradients. Fractions 1-18 were separated by SDS PAGE and analysed by western blotting using the PAP antibody.

sedimentation in larger complexes in fractions 8-18, a large pool of zz-Mpp6 protein is found in fractions 1-6. As proteins found in these fractions are generally

not incorporated in complexes, it is inferred that this distribution represents a population of Mpp6 proteins that are not part of larger complexes. Due to the nature of the zz-Mpp6 construct, these proteins are overexpressed in comparison to endogenous Mpp6-TAP proteins under the control of the *MPP6* promoter. It is presumed that overexpressing Mpp6 generates an excess of the protein that is not incorporated into larger complexes.

Lysates prepared from yeast *mpp6Δ rrp47Δ* strains harboring *LEU2* plasmids encoding *mpp6* mutants and a *HIS3* plasmid encoding *RRP47* were fractionated by ultracentrifugation and the relative distribution of Mpp6 proteins was compared using western blot analysis. The *mpp6* mutant encoding zz-Mpp6 with M18A_K19A substitutions showed a striking loss of sedimentation with larger complexes (Figure 5.26) The majority of M18A_K19A proteins were observed in fractions from the top of the glycerol gradient corresponding to proteins not incorporated into complexes. Upon longer exposures of M18A_K19A western blots, trace amounts of proteins are observed in larger fractions yet the majority of signal was found in fractions 1-5. Interestingly, alanine substitutions in adjoining F20_M21 residues did not have an effect on the distribution of Mpp6 sedimentation and was comparable to the profile of the wildtype zz-Mpp6 protein. This suggests that M18 and/or K19 residues are specifically required for the interaction of Mpp6 with larger complexes.
The profiles of L11A_S12A_V15A and G111A_R112A_F115A mutants show weaker signals for larger complexes in fractions 10-18 and a corresponding stronger signal in fractions 5-8. This effect is difficult to analyse due to the excess of free zz-Mpp6 protein in fractions 1-5. An interpretation could be that M18 and/or K19 are required for the interaction with larger complexes and these interactions are stabilised by residues in L11-V15 and G111-F115 motifs.

In the screen for loss-of function *mpp6* mutants, substitutions at the M18 residue were observed in a M18I_E146K mutant. Generation of a single M18I mutant was shown to complement the *mpp6Δ rrp47Δ* synthetic lethality yet cells showed a

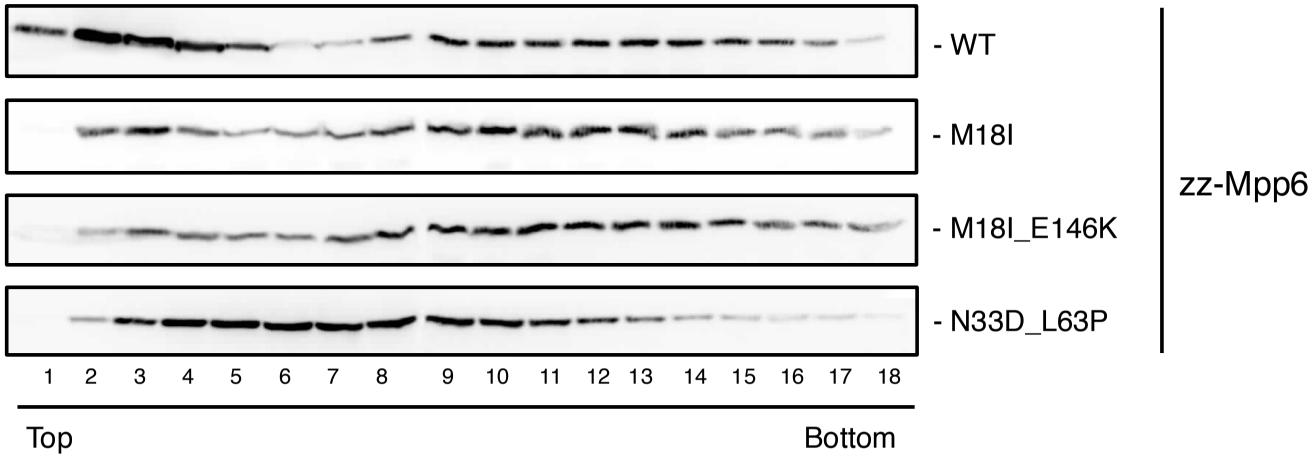

Figure 5.27. Glycerol gradient analysis of *mpp6* point mutations. Lysates from cells expressing widltype zz-Mpp6 or M18I, M18I_E146K and N33D_L63P mutant varients were sedimented through 10 – 30% glycerol gradients. Fractions 1-18 were separated by SDS PAGE and analysed by western blotting using the PAP antibody to detect zz-tagged Mpp6 proteins.

strong growth defect (Section 5.2.5) The sedimentation profiles of single M18I and double M18I_E146K mutants were analysed using glycerol gradient ultracentrifugation to determine if M18I mutations cause a loss of cosedimentation with larger complexes (Figure 5.27) Interestingly both single and double mutants showed Mpp6 protein distributions comparable to the wildtype zz-Mpp6 protein profile. This suggests that the K19A substitution in M18A_K19A double mutants causes the loss of interaction with complexes. Alternatively, the nature of the mutation may be responsible for this effect. Methionine and isoleucine residues are hydrophobic whereas alanine is generally considered to be a neutral amino acid. The differences in amino acid properties may contribute differential effects upon substitutions in the same residue.

The vast majority of *mpp6* mutants isolated showed no significant change in sedimentation profiles in comparison to the wildtype zz-Mpp6 protein (data not shown). However, the distribution of a N33D_L63P double mutant showed a shift of sedimentation from larger complexes to moderately sized complexes (Figure 5.27) This mutant was isolated as non-functional in the random mutagenesis screen and sequence analysis showed that amino acid substitutions were found in regions of Mpp6 with low conservation. This observation suggests that N33D, L63P substitutions or the combined double mutant causes destabilisation of the interaction of Mpp6 with larger complexes.

Finally, the sedimentation profile of truncated and extended Mpp6 proteins were analysed by glycerol gradient ultracentrifugation. Previous analysis in Section 5.2.7 showed that K169X and D130X truncations were functional *in vivo* whereas proteins encoding the first 115 residues of Mpp6 or shorter were identified as non-functional. Glycerol gradient and western blot analyses showed that K169X and D130X proteins maintained a similar sedimentation profile as the wildtype protein (Figure 5.28) Proteins truncated at residue 88 or shorter (R88X, I73-fs and A60-fs mutations) showed a loss of incorporation into larger complexes and were predominantly found in fractions 1-5 consistent with un-complexed protein distributions. The F115-fs mutant showed protein sedimentation corresponding to complex proteins (Fractions 10-18) yet did not have a pool of excess protein in lower fraction numbers. The relative expression level of the F115-fs protein is

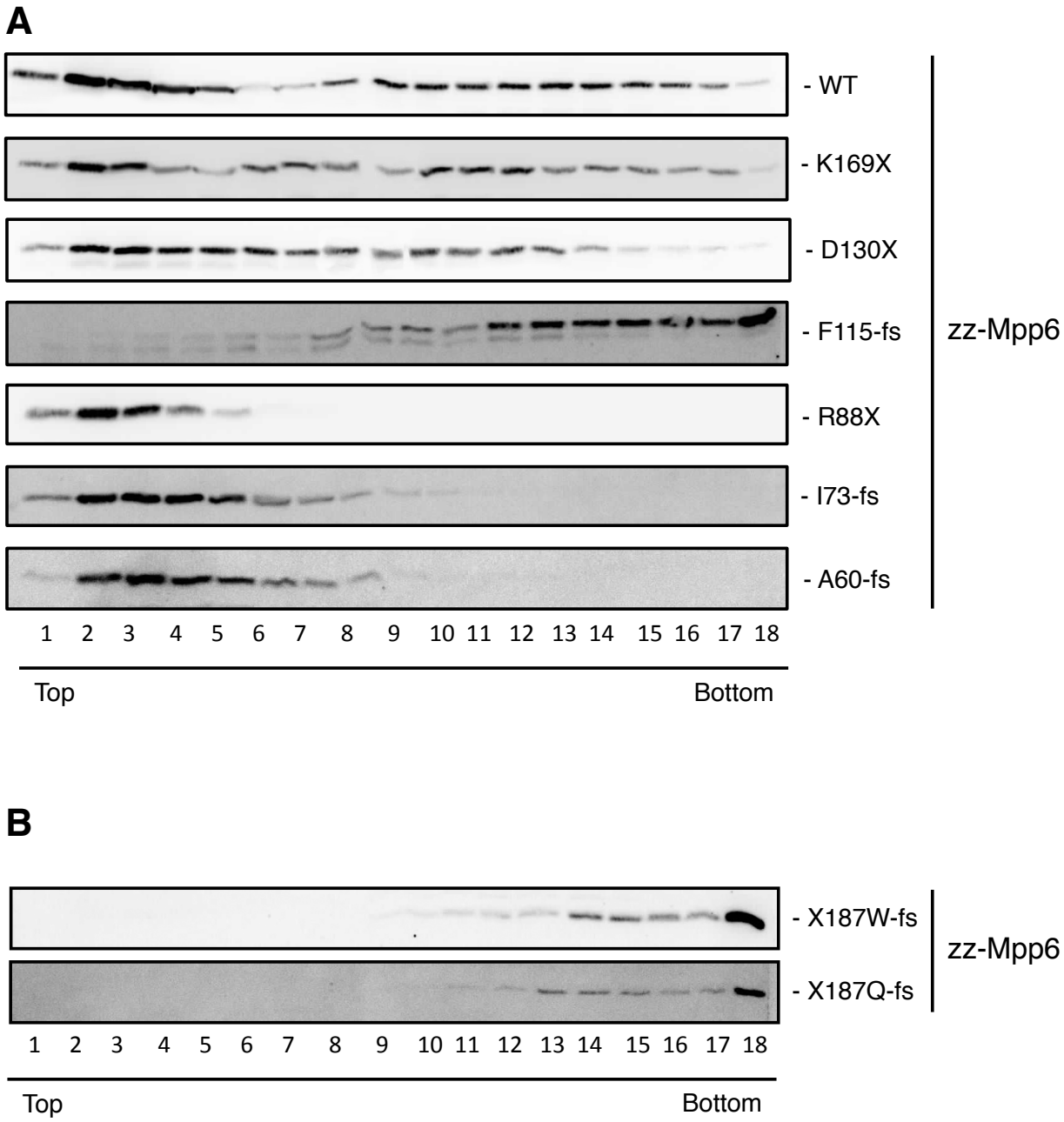

Figure 5.28. C-terminal truncations inhibit the association of Mpp6 with larger complexes.
Glycerol gradient ultracentrifugation analysis of (A) truncated and (B) extended Mpp6 proteins. Strains expressing either wildtype zz-Mpp6 or C-terminal truncation and extension mutants were lysed and fractionated through 10 – 30% glycerol gradients. Fractions 1-18 were separated by SDS PAGE and analysed by western blotting using the PAP antibody to detect zz-tagged proteins.

comparable to the levels of endogenously expressed Mpp6-TAP under control of the wildtype promoter (Figure 5.15) and protein distribution through glycerol gradients matches this accordingly as in Figure 5.25. These results show that the first 115 residues of Mpp6 are sufficient for incorporation into larger complexes whereas proteins truncated at R88 and shorter remain unincorporated. Loss of sedimentation with larger complexes could be attributed to a loss of accessible domain features due to misfolding. This is increasingly likely in truncated proteins that may be stably expressed but lack structural features found in the conformation of full-length proteins. Assuming that Mpp6 is functional in larger complexes, loss of function could be due to the loss of incorporation into complexes. Analysis of a G111A_R112A_F115A mutant showed a reduced distribution of Mpp6 proteins in larger complexes. This agrees with a loss of complex incorporation in the R88X mutant that lacks G111-F115 residues. Analysis of mutants expressing Mpp6 proteins with short C-terminal extensions (X187W-fs and X187Q-fs) revealed distributions in higher fractions (13-18) consistent with proteins associated with larger complexes (Figure 5.28 B). This suggests that the short peptide extensions do not interfere with normal association in larger complexes. Due to the low expression of these mutants, the full distribution through gradient fractions was difficult to detect.

These results identify sites within Mpp6 that may contribute to interactions with larger protein complexes. The M18A_K19A mutation in a highly conserved region of Mpp6 showed a striking loss of sedimentation with larger complexes. Analysis of different M18 mutations showed that this effect may be dependent on the nature of amino acid substitution or is solely due to the K19A mutation. Isolation of K19 mutants would characterise this region more critically. Additionally, mutations in a second region of conservation (G111-F115) showed a reduced sedimentation of Mpp6 proteins with larger complexes suggesting that this region is also important for protein-protein contacts. Finally, mutations in a region of poor conservation (N33D_L63P) displayed a shift in Mpp6 sedimentation from larger complexes to moderately sized complexes.

5.3 Discussion

The exosome complex requires a wide range of auxiliary factors to modulate the recognition and fate of transcripts from all known classes of RNA. In the nucleus the exosome associates with the small, basic, RNA-binding protein Mpp6. Whilst Mpp6 is not essential in yeast, *mpp6Δ* mutants are synthetic lethal with the loss of Rrp6 or Rrp47. Functional redundancy is an inherent feature common to many biological systems where multiple pathways exist to perform overlapping functions. This 'genetic buffering' would provide cells with failsafe mechanisms in the failure of one pathway. It was proposed that Mpp6 functions in pathways redundant with Rrp6/Rrp47-dependent processes. Consistent with previous analyses (Milligan et al., 2008), destabilisation of the Rrp6/Rrp47 complex in *mpp6* mutants resulted in a widespread loss of RNA surveillance and degradation pathways (Chapter 3 and Garland et al. 2013). Conditional *mpp6 rrp47* mutants accumulate a wide range of RNA surveillance targets including cryptic unstable transcripts (CUTs), pre-rRNA processing byproducts and aberrant forms of stable RNAs.

Although it has been shown that Mpp6 functions in surveillance pathways, little is known about the protein itself and what interactions it forms within the network of the nuclear exosome complex and associated proteins. Mpp6 lacks any characterised domains that are associated with nucleic acid- or protein-binding activity. A previous report described two highly conserved motifs found in Mpp6 homologues in higher eukaryotes (Milligan et al., 2008) but was not investigated. Here, a random mutagenesis approach was used to isolate loss-of function *mpp6* mutants in order to map the functional regions of the protein.

A library of *mpp6* mutants was generated through *in vitro* error-prone PCR based mutagenesis. Loss of function mutants were initially screened using an *mpp6Δ rrp47Δ* plasmid shuffle assay before analyzing protein expression. The mutagenesis screen identified 66 strains bearing non-functional *mpp6* alleles. Sequence analysis revealed two *mpp6* mutants bearing single amino acid substitutions (V15D and K145R) along with a larger fraction of mutants with

multiple point substitutions. Furthermore, a number of *mpp6* mutants bearing frameshift mutations were shown to encode truncated and extended proteins.

A high proportion of amino acid substitutions in *mpp6* mutants were found in an N-terminal region that is highly conversed in Mpp6 homologues. Alanine-scanning mutagenesis of conserved motifs showed that these regions are functionally important. Glycerol gradient analyses suggest that these regions may be required for protein-protein interactions. Specifically, the sedimentation of a M18A_K19A mutant showed a striking loss of association with larger complexes in comparison to the wildtype protein. Interestingly, an M18I single mutant did not show this effect suggesting that either the K19A mutation is critical for complex formation or the effect is specific to the amino acid substitution. Isolation of separated M18A and K19A single mutations would be interesting to expand these observations.

Sequence analysis of *mpp6* mutants revealed a number of mutants encoding proteins with double substitutions in residues with weak conservation in homologues. To determine the effects of each individual substitution, single point mutants were isolated by SDM and were tested for functionality using the *mpp6Δ rrp47Δ* plasmid shuffle assay. Separated point mutations were revealed to be functional *in vivo* suggesting that the action of double mutants had synergistically lethal effects on protein function. This was substantiated by RNA analyses of single and double mutants.

A loss of RNA surveillance is observed in conditional *mpp6 rrp47* mutants (Garland et al., 2013; Milligan et al., 2008). The DECOID approach, described in Chapter 3, was used as a conditional system to destabilise the Rrp6/Rrp47 complex by the overexpression of the interacting domain of Rrp6 ($Rrp6_{NT}$). This method was used in *mpp6* mutants to analyse levels of RNA surveillance targets. Consistent with a loss of Mpp6, using DECOID in cells encoding loss of function *mpp6* mutations resulted in a strong accumulation of CUTs, aberrant ncRNAs and pre-rRNA processing byproducts. All *mpp6* mutants displayed phenotypes comparable or weaker than those observed in the null mutant. No specific phenotypes were attributed to isolated mutants. This suggests that Mpp6

functions as a general factor in RNA surveillance pathways rather than in the recognition of specific substrates.

The random mutagenesis approach generated a number of *mpp6* mutants encoding proteins truncated or extended at the C-terminus. Additional mutations generated by SDM showed that truncations to D130 were functional *in vivo*. An *mpp6* mutant expressing the first 115 residues of Mpp6 was identified as non-functional. However, the protein also encoded a further 44 amino acids due to a frameshift mutation. Therefore, the loss of function may be due to the additional foreign peptide sequence. Nevertheless, a R88X mutant was also shown to be non-functional which suggests a cut-off point exists between R88 and D130 in which the protein no longer functions. This region, which includes a stretch of highly conserved residues (G111 - S119), may be required for interactions with larger complexes. Cosedimentation analysis showed that the F115-fs mutant was found in larger complexes whereas a R88X mutant lost this association. Directed alanine substitution mutations in conserved residues in this region (G111-F115) resulted in reduced cosedimentation with larger complexes. These proteins were still identified in higher complexes suggesting that this conserved region may only stabilise more critical interactions from other parts of the protein. Systematic directed mutational analysis may help to define this region.
Curiously, short C-terminal peptide extensions resulting from mutations in the natural *MPP6* stop codon resulted in a loss of function. Western blot analysis showed that these proteins are relatively unstable which suggests that the C-terminus is crucial for normal protein stability. Interestingly, the destabilisation appears to be specific to the nature of the sequence. A strain encoding a C-terminally tagged Mpp6 protein has been used extensively in other experiments. Successful isolation of *rrp6Δ MPP6-TAP* strains demonstrates that the Mpp6-TAP protein is functional *in vivo* as *mpp6Δ rrp6Δ* double mutants are synthetic lethal.

The library of *mpp6* mutants was generated from a zz-tagged Mpp6 expression construct under the control of the *RRP4* promoter. As shown in Section 3.2.1, zz-Mpp6 is expressed ~3-fold higher than endogenous Mpp6-TAP under the control of the natural *MPP6* promoter. This system has both advantages and limitations

for the purposes of these studies. With no Mpp6-specific antibody available, using a tagged expression construct allows detection of the fusion protein in western blot analyses using commercial antibodies. Additionally, using an overexpression system allowed the detection of *mpp6* mutants that exhibited reduced levels of zz-Mpp6 protein at steady state. However, this system does not represent endogenous Mpp6 expression conditions due to the use of a different promoter and addition of a stabilising tag. Additionally, the zz-tag may interfere with possible protein-protein interactions at the N-terminus of Mpp6. The zz-Mpp6 expression construct was able to complement an *mpp6Δ rrp47Δ* double mutant and is therefore functional. However, this does not account for non-essential functions of Mpp6 including protein-protein interactions. Furthermore, overexpression of mutant Mpp6 proteins may suppress more distinct phenotypes due to increased expression. For a more precise analysis of the effects of *mpp6* mutations *in vivo*, it would be interesting to integrate isolated mutants into the chromosomal *MPP6* locus. This would allow endogenous expression from the natural promoter and may give stronger phenotypes when combined with conditional *rrp47* mutations.

In analyzing RNA phenotypes in conditional *mpp6 rrp47* mutants, it was noted that a large number of accumulated transcripts were also targets of Rrp6 and the TRAMP complex. It has previously been proposed that Mpp6 may be involved in the functional coupling between Rrp6 and the TRAMP complex (Butler and Mitchell, 2011). This is supported by observed physical interactions between the human MPP6 protein and PM-Scl100 and hMtr4 (Rrp6 and Mtr4 in yeast) (Schilders et al., 2007). By analyzing relative steady state levels of Mpp6 proteins in *rrp6Δ* and TRAMP mutants it was shown that Mpp6 expression is reduced to ~30% in the absence of Rrp6 or Trf4. Protein stability is often dependent on physical interactions with other proteins. For example, the mutual stability of Rrp6 and Rrp47 is dependent on the physical interaction between their respective N-terminal domains (Feigenbutz et al., 2013a, 2013b; Stead et al., 2007). Glycerol gradient analysis of Mpp6 proteins in *rrp6Δ* mutants showed a shift in distribution from larger complexes to moderately sized complexes with increased amounts of protein degradation. In the absence of Trf4, Mpp6 does not co-sediment with moderately sized complexes. These results

Mutation (*= highly conserved residue)	Functional	Protein expression (relative to WT) (%)	RNA surveillance phenotype (s=strong, m=weak, n=none)	Association in larger complexes (✓=yes, ✗ = no, ? = partial, n/a= not tested)
V15D*	✗	82	S	✓
M18I*	✓	103	W	✓
N33D	✓	103	W	✓
S42P	✓	97	W	n/a
D43N	✓	66	N	n/a
L63P	✓	88	W	n/a
Y66H	✓	75	S	n/a
K145R	✗	53	S	✓
E146K	✓	101	W	
N5D_D43N	✗	86	S	n/a
R14S*_M16T*	✗	78	S	✓
V15A*_N118S	✗	46	W	n/a
M18I*_E146K	✗	98	S	✓
N33D_L63P	✗	60	S	?
S42P_Y66H	✗	43	S	n/a
R127G_F129I	✗	63	W	✓
L11A*_S12A*_V15A*	✓	90	W/S	?
M18A*_K19A*	✓	92	W/S	✗
F20A*_M21A*	✓	95	W/S	✓
G111A*_R112A*_F115A*	✓	98	W/S	?
K169X	✓	91	N	✓
D130X	✓	109	W	✓
F115-fs	✗	43	W/S	✓
R88X	✗	62	S	✗
I73-fs	✗	35	S	✗
A60-fs	✗	12	S	✗
X187W	✗	28	S	✓
X187Q	✗	6	S	✓

Figure 5.29. Summary of *mpp6* mutants and corresponding phenotypes. Mutations are separated into groups of single amino acid substitutions, double amino acid substitutions, alanine substitutions in conserved motifs and C-terminal truncation and extensions according to the schematic in Figure 5.28. Relative protein expression is the average of three independent values. RNA surveillance phenotypes are compared to phenotypes observed in equivalent *mpp6Δ* strains.

suggest that Mpp6 may associate physically with both the TRAMP complex and the exosome and that these interactions are partially mediated through Trf4 and Rrp6 respectively. Mpp6 is still found in larger complexes in the absence of Rrp6 but the association appears to be less stable. This suggests that other factors may be involved in this recruitment or that Rrp6 has a more indirect role. It has not been possible to observe a direct interaction between Rrp6 and Mpp6 using recombinant proteins (data not shown). This suggests that other factors are employed.

With a library of functional and non-functional mutants (summarised in Figures 5.23 and 5.29) it may be possible to identify the regions of Mpp6 that contribute to RNA binding. Both yeast and human Mpp6 proteins have been shown to bind pyrimidine-rich RNA sequences yet have no characterised nucleic-acid binding domains (Milligan et al., 2008; Schilders et al., 2005). Furthermore, it would be interesting to see if RNA binding is required for the function of Mpp6 *in vivo* or if Mpp6 simply serves as a bridging protein for various complexes. Analogously, the RNA binding properties of Rrp47 are not required for protein function *in vivo* (Costello et al., 2011).

Finally, after initial observations it would be interesting to further analyse the interactions between Mpp6, Rrp6 and the TRAMP complex. Mpp6 shows a specific sensitivity to the loss of Trf4 over Trf5 that form analogous TRAMP4 and TRAMP5 complexes respectively and have been shown to have a specific set of RNA targets (San Paolo et al., 2009; Schmidt and Butler, 2013). Mpp6 may function in quality control pathways to recruit TRAMP4/Rrp6 complexes to the exosome and stimulate the degradation of RNA surveillance targets including cryptic unstable transcripts and aberrant ncRNAs.

Chapter 6: Conclusions and future studies

This study has focused on the function of the exosome associated co-factors Rrp6, Rrp47 and Mpp6, which are involved in RNA processing and degradation activities in the nucleus. Whilst these proteins are non-essential, they appear to share redundant essential processes. This is highlighted by the synthetic lethality observed in double *rrp47Δ mpp6Δ* and *rrp6Δ mpp6Δ* mutants. The exosome requires a high level of modulation to recognise all known classes of RNA and target transcripts for processing or degradation in both the nucleus and cytoplasm. It is believed that co-factors play important roles in forming specific pathways for RNAs and associated proteins to interact with the exosome. The details of how these proteins provide specificity is yet to be elucidated and remains a rich source of investigation.

The relationship between Rrp6 and Rrp47 was investigated in Chapters 3 and 4. Whilst the catalytic activity and function of Rrp6 has been widely characterised, the exact molecular function of Rrp47 has remained elusive. Using the DECOID technique to separate Rrp47 from Rrp6, it appears that Rrp47 can function independently from Rrp6. However, this Rrp6-independent function requires the C-terminus of Rrp47. The results in Chapter 3 support the model that Rrp47 functions as a substrate adaptor, recognising substrates prior to Rrp6-dependent catalysis. This role is dependent on the C-terminus of the Rrp47 that has been reported to mediate interactions with RNA and snoRNP proteins Nop56/58 (Costello et al., 2011). In addition, an interaction between Rrp47 and the NNS complex has been observed that is lost upon deletion of the C-terminal domain (M. Feigenbutz, P. Mitchell, personal communication). The C-terminus of Rrp47 requires further investigation to understand how the protein specifically recruits substrates prior to Rrp6-dependent catalysis. Previous attempts at identifying *in vivo* RNA targets using the CRAC (cross-linking and analysis of cDNAs) technique (Granneman et al., 2009) have been unsuccessful using full length Rrp47 (P. Mitchell, personal communication). As RNA binding is not essential to the function of Rrp47, it may be of more interest to further investigate protein interactions such as Nrd1.

Furthermore, the results in Chapter 4 and (Feigenbutz et al., 2013a) suggest that Rrp47 functions to maintain normal expression levels of Rrp6. Artificially increasing the copy number of Rrp6 was able to suppress the synthetic lethality of *rrp47 mpp6* and *rrp47 rex1* double mutants and partially suppress RNA processing and degradation phenotypes. Whilst Rrp47 has a key impact on the expression levels of Rrp6, it must also perform additional functions as part of the Rrp6/Rrp47 complex. Overexpressing Rrp6 in *rrp47Δ* mutants does not fully suppress RNA phenotypes consistent with impaired processing and degradation pathways (Feigenbutz et al., 2013a). This complements the model that Rrp47 aids in substrate recognition and may bridge contacts with other proteins.

The DECOID technique provides a simple method to determine whether proteins are functional when physically separated from interactions in complexes. This method can be widely applied as a tool to dissect complexes with minimum knowledge of the interacting domain within only one of the protein partners. With an every increasing wealth of structural biology data, this technique can be used to complement *in vivo* investigations of protein complexes. However, the limitations must also be considered. This method relies inducing the expression of a 'decoy' interaction domain to outcompete the natural interaction between two partner proteins. Using a *GAL*-regulated promoter to overexpress the interaction domain will increase the equilibrium in favour of disrupting the intended targets. However, the possibility of residual proteins left unaffected cannot be eliminated and must be considered. It was shown that ~4% of Rrp47 remained bound to Rrp6 upon $Rrp6_{NT}$ induction in pulldown experiments. This shows that the titration is efficient but not absolute. The stability of the decoy protein must be considered as this process relies on its overexpression.
Additionally, when investigating the consequences of separating protein complexes using the DECOID technique, the possibility of off-target effects must be considered. It can be possible that overexpression of a decoy protein may interact with or disrupt non-intended targets. In this work, the N-terminal PMC2NT domain of Rrp6 ($Rrp6_{NT}$) has no known role other than to interact with Rrp47. Overexpressing GST-$Rrp6_{NT}$ in an *rrp47Δ* strain showed no effect on growth compared to the overexpression of a GST control and RNA analyses showed no

discernable effect to processing and degradation phenotypes. Controls as such must be introduced to confirm off-target effects of overexpressing decoy proteins.

The DECOID approach can be utilized to disrupt characterised interactions between proteins known to associate with the exosome complex. It would be interesting to investigate the effects of disrupting EXO9 associated proteins and analyse the effects of divorced complexes. Notably Rrp44, Rrp6 and Ski7 all interact with the core-exosome complex and have characterised binding domains. In the case of Rrp44, it would be of interest to investigate whether the protein can function independent of the exosome. It has been proposed that Rrp44 requires threading of substrates through the exosome for some processes but can also degrade substrates more direct. Disruption of Rrp44 from EXO9 using DECOID and subsequent RNA analyses may reveal subsets of transcript targets that specifically require exosome-threading.

A previous study has shown that Rrp6 can function independently from the EXO9 but used a C-terminal deletion that lacks a characterised exosome-interacting region (Callahan and Butler, 2008). However, this may have a negative impact on the activity of Rrp44 as it has been shown that Rrp6 interaction with EXO9 allosterically promotes the catalytic activity of Rrp44 (Wasmuth and Lima, 2012). By overexpressing the C-terminus of Rrp6 ($Rrp6_{CT}$), this should disrupt Rrp6 from the core-exosome whilst maintaining any allosteric effects of $Rrp6_{CT}$ binding to EXO9.

Further studies using the DECOID method will develop the technique whilst addressing key experimental questions involving the exosome and associated proteins.

RNA analyses of conditional *rrp47 mpp6* and *rrp47 rex1* mutants have revealed distinct phenotypes that hint the basis of synthetic lethality of the double mutants. In Chapters 3-5 and previous studies, Mpp6 and the Rrp6/Rrp47 complex function in redundant RNA degradation pathways to remove transcripts targeted for discard. Extensive RNA analysis was carried out using northern blot hybridisation. However this technique is restricted to analyzing RNAs with complementary probes available in the lab. With the advent of next generation

sequencing technologies, RNA-seq transcriptome analyses can be used to investigate a more global dataset. It would be of interest to analyse the RNA from the conditional mutants used in Chapter 3. Comparing the data from *mpp6 rrp47ΔC* and *rex1Δ rrp47ΔC* after GST or GST-Rrp6$_{NT}$ induction would reveal RNA substrates that are inefficiently degraded or processed due to the loss of functional redundant pathways. More interestingly, a global RNA analysis may reveal the basis of synthetic lethality in *rrp47 rex1* mutants, as this was not obvious from the northern analyses in this study.

Chapter 5 employed a mutagenesis strategy to define the functional regions of the exosome-associated co-factor Mpp6. It is accepted that Mpp6 functions in RNA degradation pathways that are redundant with Rrp6/Rrp47, the molecular basis of this function is still unknown. With a library of non-functional mutants, this will aid further analyses of Mpp6.

Previous studies reported that Mpp6 can bind RNA with a preference for unstructured RNAs such as poly(U) (Milligan et al., 2008). The RNA binding activity of Mpp6 was not thoroughly investigated during this study but would be of interest to see if it was required for protein function. Mpp6 shares many features with Rrp47 as both proteins are small, basic and have a lysine-rich C-terminus. Interestingly, the RNA binding activity of Rrp47 is not essential to protein function (Costello et al., 2011). The ability of Mpp6 mutants to bind RNA could be assayed in a recombinant protein system using poly(U)-agarose affinity resins. Initial studies have shown that recombinant GB1-tagged Mpp6 is able to bind poly(U)-agarose whereas a GB1 control could not (data not shown). An alternative method would be to use an *in vitro* transcription/translation system to generate radiolabelled protein from PCR-generated DNA and assay for the ability to bind poly(U) RNA-agarose resin.

Mpp6 has been identified as associated to the nuclear exosome by mass spectrometry of purified exosome complexes and through biochemical cosedimentation analyses (Milligan et al., 2008). However, the specific physical interactions have yet to be shown. Analyses of *rrp47 mpp6* mutants show that the majority of RNAs that accumulate are known targets of the TRAMP complex. This

suggests possible physical interactions between Mpp6, TRAMP and the exosome. This is also indicated by the reduced stability of Mpp6 in *rrp6Δ* and *trf4Δ* strains (Section 5.2.11). The loss of function of *mpp6* mutants generated in this study may be due to impaired interactions between either TRAMP and/or the exosome. This was initially investigated using glycerol gradient ultracentrifugation (Section 5.2.12) which identified some Mpp6 mutants that no longer co-sedimented with larger complexes. These mutations could be combined with tagged exosome or TRAMP components and assayed for detection in a pulldown assay.

The library of Mpp6 mutations was created in a zz-Mpp6 expression construct under the control of the *RRP4* promoter. By using an overexpression system it was possible to detect mutant proteins that may otherwise not be detectable by western blot analysis. The downside of this method is that the mutants are not under the control of the *MPP6* promoter and subsequent functional analyses may not be indicative of endogenous conditions. For a more comprehensive analysis of the effects of *mpp6* mutants *in vivo*, it would be of worth to integrate the alleles generated during this study at the *MPP6* chromosomal loci. It would also be advantageous to integrate these alleles into a C-terminally tagged Mpp6 strain (Mpp6-TAP) in order to analyse relative protein expression and for use in pulldown experiments.

Bibliography

Alderuccio, F., 1991. Molecular characterization of an autoantigen of PM-Scl in the polymyositis/scleroderma overlap syndrome: a unique and complete human cDNA encoding an apparent 75-kD acidic protein of the nucleolar complex. J Exp Med 173, 941–952.

Allmang, C., Kufel, J., Chanfreau, G., Mitchell, P., Petfalski, E., Tollervey, D., 1999a. Functions of the exosome in rRNA, snoRNA and snRNA synthesis. EMBO J 18, 5399–5410.

Allmang, C., Mitchell, P., Petfalski, E., Tollervey, D., 2000. Degradation of ribosomal RNA precursors by the exosome. Nucleic Acids Res 28, 1684–1691.

Allmang, C., Petfalski, E., Podtelejnikov, A., Mann, M., Tollervey, D., Mitchell, P., 1999b. The yeast exosome and human PM-Scl are related complexes of 3' --> 5' exonucleases. Genes Dev 13, 2148–2158.

Alwine, J., Kemp, D., Stark, G., 1977. Method for detection of specific RNAs in agarose gels by transfer to diazobenzyloxymethyl-paper and hybridization with DNA probes. Proc Natl Acad Sci USA 74, 5350–5354.

Anderson, J.S., Parker, R.P., 1998. The 3' to 5' degradation of yeast mRNAs is a general mechanism for mRNA turnover that requires the SKI2 DEVH box protein and 3' to 5' exonucleases of the exosome complex. EMBO J 17, 1497–1506.

Araki, Y., Takahashi, S., Kobayashi, T., Kajiho, H., Hoshino, S., Katada, T., 2001. Ski7p G protein interacts with the exosome and the Ski complex for 3'-to-5' mRNA decay in yeast. EMBO J 20, 4684–4693.

Arigo, J.T., Eyler, D.E., Carroll, K.L., Corden, J.L., 2006. Termination of cryptic unstable transcripts is directed by yeast RNA-binding proteins Nrd1 and Nab3. Mol Cell 23, 841–851.

Artimo, P., Jonnalagedda, M., Arnold, K., Baratin, D., Csardi, G., de Castro, E., Duvaud, S., Flegel, V., Fortier, A., Gasteiger, E., Grosdidier, A., Hernandez, C., Ioannidis, V., Kuznetsov, D., Liechti, R., Moretti, S., Mostaguir, K., Redaschi, N., Rossier, G., Xenarios, I., Stockinger, H., 2012. ExPASy: SIB bioinformatics resource portal. Nucleic Acids Res 40, 597–603.

Astuti, D., Morris, M.R., Cooper, W.N., Staals, R.H.J., Wake, N.C., Fews, G.A., Gill, H., Gentle, D., Shuib, S., Ricketts, C.J., Cole, T., van Essen, A.J., van Lingen, R.A., Neri, G., Opitz, J.M., Rump, P., Stolte-Dijkstra, I., Müller, F., Pruijn, G.J.M., Latif, F., Maher, E.R., 2012. Germline mutations in DIS3L2 cause the Perlman syndrome of overgrowth and Wilms tumor susceptibility. Nat. Genet. 44, 277–84.

Baudin, A., Ozier-Kalogeropoulos, O., Denouel, A., Lacroute, F., Cullin, C., 1993. A simple and efficient method for direct gene deletion in Saccharomyces cerevisiae. Nucleic Acids Res 21, 3329–3330.

Beelman, C.A., Stevens, A., Caponigro, G., LaGrandeur, T.E., Hatfield, L., Fortner, D.M., Parker, R., 1996. An essential component of the decapping enzyme required for normal rates of mRNA turnover. Nature 382, 642–646.

Bertone, P., Stolc, V., Royce, T.E., Rozowsky, J.S., Urban, A.E., Zhu, X., Rinn, J.L., Tongprasit, W., Samanta, M., Weissman, S., Gerstein, M., Snyder, M., 2004. Global identification of human transcribed sequences with genome tiling arrays. Science 306, 2242–6.

Birnboim, H.C., Doly, J., 1979. A rapid alkaline extraction procedure for screening recombinant plasmid DNA. Nucleic Acids Res 7, 1513–1523.

Bonneau, F., Basquin, J., Ebert, J., Lorentzen, E., Conti, E., 2009. The yeast exosome functions as a macromolecular cage to channel RNA substrates for degradation. Cell 139, 547–559.

Brachmann, C.B., Davies, A., Cost, G.J., Caputo, E., Li, J., Hieter, P., Boeke, J.D., 1998. Designer deletion strains derived from Saccharomyces cerevisiae S288C: a useful set of strains and plasmids for PCR-mediated gene disruption and other applications. Yeast 14, 115–132.

Briggs, M.W., Burkard, K.T., Butler, J.S., 1998. Rrp6p, the Yeast Homologue of the Human PM-Scl 100-kDa Autoantigen, Is Essential for Efficient 5.8S rRNA 3' End Formation. J Biol Chem 273, 13255–13263.

Buratowski, S., 2009. Progression through the RNA polymerase II CTD cycle. Mol Cell 36, 541–546.

Burkard, K.T., Butler, J.S., 2000. A nuclear 3'-5' exonuclease involved in mRNA degradation interacts with Poly(A) polymerase and the hnRNA protein Npl3p. Mol Cell Biol 20, 604–616.

Butler, J.S., Mitchell, P., 2011. Rrp6, Rrp47 and cofactors of the nuclear exosome. Adv Exp Med Biol 702, 91–104.

Callahan, K.P., Butler, J.S., 2008. Evidence for core exosome independent function of the nuclear exoribonuclease Rrp6p. Nucleic Acids Res 36, 6645–6655.

Camblong, J., Iglesias, N., Fickentscher, C., Dieppois, G., Stutz, F., 2007. Antisense RNA stabilization induces transcriptional gene silencing via histone deacetylation in S. cerevisiae. Cell 131, 706–717.

Carpousis, A.J., 2002. The Escherichia coli RNA degradosome: structure, function and relationship in other ribonucleolytic multienzyme complexes. Biochem Soc Trans 30, 150–155.

Carroll, K., Ghirlando, R., Ames, J., Corden, J., 2007. Interaction of yeast RNA-binding proteins Nrd1 and Nab3 with RNA polymerase II terminator elements. RNA 13, 361–373.

Carroll KL, Pradhan DA, Granek JA, Clarke ND, C.J., 2004. Identification of cis elements directing termination of yeast nonpolyadenylated snoRNA transcripts. Mol Cell Biol 24, 6241–6252.

Castaño, I.B., Heath-Pagliuso, S., Sadoff, B.U., Fitzhugh, D.J., Christman, M.F., 1996. A novel family of TRF (DNA topoisomerase I-related function) genes required for proper nuclear segregation. Nucleic Acids Res 24, 2404–2410.

Castelnuovo, M., Rahman, S., Guffanti, E., Infantino, V., Stutz, F., Zenklusen, D., 2013. Bimodal expression of PHO84 is modulated by early termination of antisense transcription. Nat Struct Mol Biol 20, 851–858.

Chapman, M.A., Lawrence, M.S., Keats, J.J., Cibulskis, K., Sougnez, C., Schinzel, A.C., Harview, C.L., Brunet, J.-P., Ahmann, G.J., Adli, M., Anderson, K.C., Ardlie, K.G., Auclair, D., Baker, A., Bergsagel, P.L., Bernstein, B.E., Drier, Y., Fonseca, R., Gabriel, S.B., Hofmeister, C.C., Jagannath, S., Jakubowiak, A.J., Krishnan, A., Levy, J., Liefeld, T., Lonial, S., Mahan, S., Mfuko, B., Monti, S., Perkins, L.M., Onofrio, R., Pugh, T.J., Rajkumar, S.V., Ramos, A.H., Siegel, D.S., Sivachenko, A., Stewart, A.K., Trudel, S., Vij, R., Voet, D., Winckler, W., Zimmerman, T., Carpten, J., Trent, J., Hahn, W.C., Garraway, L.A., Meyerson, M., Lander, E.S., Getz, G., Golub, T.R., 2011. Initial genome sequencing and analysis of multiple myeloma. Nature 471, 467–472.

Chen, C.Y., Gherzi, R., Ong, S.E., Chan, E.L., Raijmakers, R., Pruijn, G.J., Stoecklin, G., Moroni, C., Mann, M., Karin, M., 2001. AU binding proteins recruit the exosome to degrade ARE-containing mRNAs. Cell 107, 451–464.

Chlebowski, A., Lubas, M., Jensen, T.H., Dziembowski, A., 2013. RNA decay machines: The exosome. Biochim Biophys Acta 1829, 552–560.

Ciais, D., Bohnsack, M.T., Tollervey, D., 2008. The mRNA encoding the yeast ARE-binding protein Cth2 is generated by a novel 3' processing pathway. Nucleic Acids Res 36, 3075–3084.

Conrad, N.K., Wilson, S.M., Steinmetz, E.J., Patturajan, M., Brow, D.A., Swanson, M.S., Corden, J.L., 2000. A yeast heterogeneous nuclear ribonucleoprotein complex associated with RNA polymerase II. Genetics 154, 557–571.

Copela, L., Fernandez, C., Sherrer, R., Wolin, S., 2008. Competition between the Rex1 exonuclease and the La protein affects both Trf4p-mediated RNA quality control and pre-tRNA maturation. RNA 14, 1214–1227.

Costello, J.L., Stead, J., Feigenbutz, M., Jones, R.M., Mitchell, P., 2011. The C-terminal region of the exosome-associated protein Rrp47 is specifically required for box C/D small nucleolar RNA 3'-maturation. J Biol Chem 286, 4535–4543.

Cox, E.C., 1976. Bacterial mutator genes and the control of spontaneous mutation. Annu Rev Genet 10, 135–156.

Cryer, D.R., Eccleshall, R., Marmur, J., 1975. Isolation of yeast DNA. Methods Cell Biol 12, 39–44.

Daley, J.M., Palmbos, P.L., Wu, D., Wilson, T.E., 2005. Nonhomologous end joining in yeast. Annu Rev Genet 39, 431–451.

David, L., Huber, W., Granovskaia, M., Toedling, J., Palm, C.J., Bofkin, L., Jones, T., Davis, R.W., Steinmetz, L.M., 2006. A high-resolution map of transcription in the yeast genome. Proc Natl Acad Sci U 103, 5320–5325.

Davis, C.A., Ares, M., 2006. Accumulation of unstable promoter-associated transcripts upon loss of the nuclear exosome subunit Rrp6p in Saccharomyces cerevisiae. Proc Natl Acad Sci USA 103, 3262–3267.

De la Cruz, J., Kressler, D., Tollervey, D., Linder, P., 1998. Dob1p (Mtr4p) is a putative ATP-dependent RNA helicase required for the 3' end formation of 5.8S rRNA in Saccharomyces cerevisiae. EMBO J 17, 1128–1140.

Doma, M.K., Parker, R., 2006. Endonucleolytic cleavage of eukaryotic mRNAs with stalls in translation elongation. Nature 440, 561–564.

Dragon, F., Gallagher, J.E.G., Compagnone-Post, P., Mitchell, B.M., Porwancher, K. a, Wehner, K. a, Wormsley, S., Settlage, R.E., Shabanowitz, J., Osheim, Y., Beyer, A.L., Hunt, D.F., Baserga, S.J., 2002. A large nucleolar U3 ribonucleoprotein required for 18S ribosomal RNA biogenesis. Nature 417, 967–970.

Dunckley, T., Parker, R., 1999. The DCP2 protein is required for mRNA decapping in Saccharomyces cerevisiae and contains a functional MutT motif. EMBO J 18, 5411–5422.

Dutrow, N., Nix, D.A., Holt, D., Milash, B., Dalley, B., Westbroek, E., Parnell, T.J., Cairns, B.R., 2008. Dynamic transcriptome of Schizosaccharomyces pombe shown by RNA-DNA hybrid mapping. Nat Genet 40, 977–986.

Dziembowski, A., Lorentzen, E., Conti, E., Séraphin, B., 2007. A single subunit, Dis3, is essentially responsible for yeast exosome core activity. Nat Struct Mol Biol 14, 15–22.

Egecioglu, D., Henras, A., Chanfreau, G., 2006. Contributions of Trf4p-and Trf5p-dependent polyadenylation to the processing and degradative functions of the yeast nuclear exosome. RNA 12, 26–32.

Elledge, S., Davis, R., 1988. A family of versatile centromeric vectors designed for use in the sectoring-shuffle mutagenesis assay in Saccharomyces cerevisiae. Gene 70, 303–312.

Erdemir, T., Bilican, B., Cagatay, T., Goding, C.R., Yavuzer, U., 2002. Saccharomyces cerevisiae C1D is implicated in both non-homologous DNA end joining and homologous recombination. Mol Microbiol 46, 947–957.

Fang, F., Phillips, S., Butler, J.S., 2005. Rat1p and Rai1p function with the nuclear exosome in the processing and degradation of rRNA precursors. RNA 11, 1571–1578.

Fasken, M.B., Leung, S.W., Banerjee, A., Kodani, M.O., Chavez, R., Bowman, E. a, Purohit, M.K., Rubinson, M.E., Rubinson, E.H., Corbett, A.H., 2011. Air1 zinc knuckles 4 and 5 and a conserved IWRxY motif are critical for the function and integrity of the TRAMP RNA quality control complex. J Biol Chem 286, 37429–47445.

Feigenbutz, M., Garland, W., Turner, M., Mitchell, P., 2013a. The Exosome Cofactor Rrp47 Is Critical for the Stability and Normal Expression of Its Associated Exoribonuclease Rrp6 in Saccharomyces cerevisiae. PLoS One 8, e80752.

Feigenbutz, M., Jones, R., Besong, T.M.D., Harding, S.E., Mitchell, P., 2013b. Assembly of the yeast exoribonuclease Rrp6 with its associated cofactor Rrp47 occurs in the nucleus and is critical for the controlled expression of Rrp47. J Biol Chem 288, 15959–15970.

Frank, P., Braunshofer-reiter, C., Karwan, A., Grimm, R., Wintersberger, U., 1999. Purification of Saccharomyces cerevisiae RNase H(70) and identification of the corresponding gene. FEBS lett 450, 251–256.

Frazão, C., McVey, C.E., Amblar, M., Barbas, A., Vonrhein, C., Arraiano, C.M., Carrondo, M.A., 2006. Unravelling the dynamics of RNA degradation by ribonuclease II and its RNA-bound complex. Nature 443, 110–114.

Frischmeyer, P.A., van Hoof, A., O'Donnell, K., Guerrerio, A.L., Parker, R., Dietz, H.C., 2002. An mRNA surveillance mechanism that eliminates transcripts lacking termination codons. Science (80-.). 295, 2258–2261.

Garland, W., Feigenbutz, M., Turner, M., Mitchell, P., 2013. Rrp47 functions in RNA surveillance and stable RNA processing when divorced from the exoribonuclease and exosome-binding domains of Rrp6. RNA 19, 1659–1668.

Gavin, A.-C., Aloy, P., Grandi, P., Krause, R., Boesche, M., Marzioch, M., Rau, C., Jensen, L.J., Bastuck, S., Dümpelfeld, B., Edelmann, A., Heurtier, M.-A., Hoffman, V., Hoefert, C., Klein, K., Hudak, M., Michon, A.-M., Schelder, M., Schirle, M., Remor, M., Rudi, T., Hooper, S., Bauer, A., Bouwmeester, T., Casari, G., Drewes, G., Neubauer, G., Rick, J.M., Kuster, B., Bork, P., Russell, R.B., Superti-Furga, G., 2006. Proteome survey reveals modularity of the yeast cell machinery. Nature 440, 631–636.

Ge, Q., Frank, M.B., O'Brien, C., Targoff, I.N., 1992. Cloning of a complementary DNA coding for the 100-kD antigenic protein of the PM-Scl autoantigen. J Clin Invest 90, 559–570.

Gelpi, C., Algueró, A., Angeles Martinez, M., Vidal, S., Juarez, C., Rodriguez-Sanchez, J.L., 1990. Identification of protein components reactive with anti-PM/Scl autoantibodies. Clin Exp Immunol 81, 59–64.

Ghaemmaghami, S., Huh, W.-K., Bower, K., Howson, R.W., Belle, A., Dephoure, N., O'Shea, E.K., Weissman, J.S., 2003. Global analysis of protein expression in yeast. Nature 425, 737–741.

Gnad, F., de Godoy, L.M.F., Cox, J., Neuhauser, N., Ren, S., Olsen, J. V, Mann, M., 2009. High-accuracy identification and bioinformatic analysis of in vivo protein phosphorylation sites in yeast. Proteomics 9, 4642–4652.

Granneman, S., Kudla, G., Petfalski, E., Tollervey, D., 2009. Identification of protein binding sites on U3 snoRNA and pre-rRNA by UV cross-linking and high-throughput analysis of cDNAs. Proc Natl Acad Sci USA 106, 9613–9618.

Greener, A., Callahan, M., Jerpseth, B., 1996. An efficient random mutagenesis technique using an E. coli mutator strain. Methods Mol. Biol. 57, 375–385.

Groll, M., Ditzel, L., Löwe, J., Stock, D., Bochtler, M., Bartunik, H.D., Huber, R., 1997. Structure of 20S proteasome from yeast at 2.4 A resolution. Nature 386, 463–471.

Grzechnik, P., Kufel, J., 2008. Polyadenylation linked to transcription termination directs the processing of snoRNA precursors in yeast. Mol Cell 32, 247–258.

Gudipati, R.K., Neil, H., Feuerbach, F., Malabat, C., Jacquier, A., 2012a. The yeast RPL9B gene is regulated by modulation between two modes of transcription termination. EMBO J 31, 2427–2437.

Gudipati, R.K., Xu, Z., Lebreton, A., Séraphin, B., Steinmetz, L.M., Jacquier, A., Libri, D., 2012b. Extensive Degradation of RNA Precursors by the Exosome in Wild-Type Cells. Mol Cell 48, 409–421.

Halbach, F., Reichelt, P., Rode, M., Conti, E., 2013. The Yeast Ski Complex: Crystal Structure and RNA Channeling to the Exosome Complex. Cell 154, 814–826.

Hamill, S., Wolin, S.L., Reinisch, K.M., 2010. Structure and function of the polymerase core of TRAMP, a RNA surveillance complex. Proc Natl Acad Sci USA 107, 15045–15050.

Harlow, L.S., Kadziola, A., Jensen, K.F., Larsen, S., 2004. Crystal structure of the phosphorolytic exoribonuclease RNase PH from Bacillus subtilis and implications for its quaternary structure and tRNA binding. Protein Sci 13, 668–677.

Hautbergue, G.M., Hung, M.-L., Golovanov, A.P., Lian, L.-Y., Wilson, S. a, 2008. Mutually exclusive interactions drive handover of mRNA from export adaptors to TAP. Proc Natl Acad Sci USA 105, 5154–5159.

Ho, Y., Gruhler, A., Heilbut, A., Bader, G.D., Moore, L., Adams, S.-L., Millar, A., Taylor, P., Bennett, K., Boutilier, K., Yang, L., Wolting, C., Donaldson, I., Schandorff, S., Shewnarane, J., Vo, M., Taggart, J., Goudreault, M., Muskat, B., Alfarano, C., Dewar, D., Lin, Z., Michalickova, K., Willems, A.R., Sassi, H., Nielsen, P.A., Rasmussen, K.J., Andersen, J.R., Johansen, L.E., Hansen, L.H., Jespersen, H., Podtelejnikov, A., Nielsen, E., Crawford, J., Poulsen, V., Sørensen, B.D., Matthiesen, J., Hendrickson, R.C., Gleeson, F., Pawson, T., Moran, M.F., Durocher, D., Mann, M., Hogue, C.W. V, Figeys, D., Tyers, M., 2002. Systematic identification of protein complexes in Saccharomyces cerevisiae by mass spectrometry. Nature 415, 180–183.

Hobor, F., Pergoli, R., Kubicek, K., Hrossova, D., Bacikova, V., Zimmermann, M., Pasulka, J., Hofr, C., Vanacova, S., Stefl, R., 2011. Recognition of transcription termination signal by the nuclear polyadenylated RNA-binding (NAB) 3 protein. J Biol Chem 286, 3645–3657.

Holub, P., Lalakova, J., Cerna, H., Pasulka, J., Sarazova, M., Hrazdilova, K., Arce, M.S., Hobor, F., Stefl, R., Vanacova, S., 2012. Air2p is critical for the assembly and RNA-binding of the TRAMP complex and the KOW domain of Mtr4p is crucial for exosome activation. Nucleic Acids Res 40, 1–15.

Houseley, J., Kotovic, K., El Hage, A., Tollervey, D., 2007. Trf4 targets ncRNAs from telomeric and rDNA spacer regions and functions in rDNA copy number control. EMBO J 26, 4996–5006.

Houseley, J., LaCava, J., Tollervey, D., 2006. RNA-quality control by the exosome. Nat Rev Mol Cell Biol 7, 529–539.

Houseley, J., Tollervey, D., 2006. Yeast Trf5p is a nuclear poly(A) polymerase. EMBO Rep 7, 205–211.

Houseley, J., Tollervey, D., 2009. The many pathways of RNA degradation. Cell 136, 763–776.

Hsu, C.L., Stevens, A., 1993. Yeast cells lacking 5'-->3' exoribonuclease 1 contain mRNA species that are poly(A) deficient and partially lack the 5' cap structure. Mol Cell Biol 13, 4826–4835.

Huh, W.-K., Falvo, J. V, Gerke, L.C., Carroll, A.S., Howson, R.W., Weissman, J.S., O'Shea, E.K., 2003. Global analysis of protein localization in budding yeast. Nature 425, 686–691.

Inoue, K., Mizuno, T., Wada, K., Hagiwara, M., 2000. Novel RING finger proteins, Air1p and Air2p, interact with Hmt1p and inhibit the arginine methylation of Npl3p. J Biol Chem 275, 32793–32799.

Ishii, R., Nureki, O., Yokoyama, S., 2003. Crystal structure of the tRNA processing enzyme RNase PH from Aquifex aeolicus. J Biol Chem 278, 32397–32404.

Jackowiak, P., Nowacka, M., Strozycki, P.M., Figlerowicz, M., 2011. RNA degradome--its biogenesis and functions. Nucleic Acids Res 39, 7361–7370.

Jackson, R.N., Klauer, A., Hintze, B.J., Robinson, H., van Hoof, A., Johnson, S.J., 2010. The crystal structure of Mtr4 reveals a novel arch domain required for rRNA processing. EMBO J 29, 2205–2216.

Januszyk, K., Liu, Q., Lima, C.D., 2011. Activities of human RRP6 and structure of the human RRP6 catalytic domain. RNA 17, 1566–1577.

Jia, H., Wang, X., 2012. RNA unwinding by the Trf4/Air2/Mtr4 polyadenylation (TRAMP) complex. Proc Natl Acad Sci USA 109, 7292–7297.

Jia, H., Wang, X., Liu, F., Guenther, U.-P., Srinivasan, S., Anderson, J.T., Jankowsky, E., 2011. The RNA helicase Mtr4p modulates polyadenylation in the TRAMP complex. Cell 145, 890–901.

Johnson, A.W., Kolodner, R.D., 1995. Synthetic lethality of sep1 (xrn1) ski2 and sep1 (xrn1) ski3 mutants of Saccharomyces cerevisiae is independent of killer virus and suggests a general role for these genes in translation control. Mol Cell Biol 15, 2719–2727.

Jung, M.-Y., Lorenz, L., Richter, J.D., 2006. Translational control by neuroguidin, a eukaryotic initiation factor 4E and CPEB binding protein. Mol Cell Biol 26, 4277–4287.

Kadaba, S., Krueger, A., Trice, T., 2004. Nuclear surveillance and degradation of hypomodified initiator tRNAMet in S. cerevisiae. Genes Dev 18, 1227–1240.

Kadaba, S., Wang, X., Anderson, J.T., 2006. Nuclear RNA surveillance in Saccharomyces cerevisiae: Trf4p-dependent polyadenylation of nascent hypomethylated tRNA and an aberrant form of 5S rRNA. RNA 12, 508–521.

Kadowaki, T., Chen, S., Hitomi, M., Jacobs, E., Kumagai, C., Liang, S., Schneiter, R., Singleton, D., Wisniewska, J., Tartakoff, A.M., 1994. Isolation and characterization of Saccharomyces cerevisiae mRNA transport-defective (mtr) mutants. J Cell Biol 126, 649–659.

Kafri, R., Springer, M., Pilpel, Y., 2009. Genetic redundancy: new tricks for old genes. Cell 136, 389–392.

Karolina Drążkowska, Rafał Tomecki, Krystian Stoduś, Katarzyna Kowalska, Mariusz Czarnocki-Cieciura, A.D., 2013. The RNA exosome complex central channel controls both exonuclease and endonuclease Dis3 activities in vivo and in vitro. Nucleic acids … 41, 3845–3858.

Kaudewitz, F., 1959. Production of bacterial mutants with nitrous acid. Nature 183, 1829–1830.

Kelley, L.A., Sternberg, M.J.E., 2009. Protein structure prediction on the Web: a case study using the Phyre server. Nat Protoc 4, 363–371.

Kellis, M., Birren, B.W., Lander, E.S., 2004. Proof and evolutionary analysis of ancient genome duplication in the yeast Saccharomyces cerevisiae. Nature 428, 617–624.

Keohavong, P., Thilly, W.G., 1989. Fidelity of DNA polymerases in DNA amplification. Proc Natl Acad Sci USA 86, 9253–9257.

Kim, H., Erickson, B., Luo, W., Seward, D., Graber, J.H., Pollock, D.D., Megee, P.C., Bentley, D.L., 2010. Gene-specific RNA polymerase II phosphorylation and the CTD code. Nat Struct Mol Biol 17, 1279–1286.

Kim, M., Vasiljeva, L., Rando, O.J., Zhelkovsky, A., Moore, C., Buratowski, S., 2006. Distinct pathways for snoRNA and mRNA termination. Mol Cell 24, 723–734.

Krogan, N.J., Cagney, G., Yu, H., Zhong, G., Guo, X., Ignatchenko, A., Li, J., Pu, S., Datta, N., Tikuisis, A.P., Punna, T., Peregrín-Alvarez, J.M., Shales, M., Zhang, X., Davey, M., Robinson, M.D., Paccanaro, A., Bray, J.E., Sheung, A., Beattie, B., Richards, D.P., Canadien, V., Lalev, A., Mena, F., Wong, P., Starostine, A., Canete, M.M., Vlasblom, J., Wu, S., Orsi, C., Collins, S.R., Chandran, S., Haw, R., Rilstone, J.J., Gandi, K., Thompson, N.J., Musso, G., St Onge, P., Ghanny, S., Lam, M.H.Y., Butland, G., Altaf-Ul, A.M., Kanaya, S., Shilatifard, A., O'Shea, E., Weissman, J.S., Ingles, C.J., Hughes, T.R., Parkinson, J., Gerstein, M., Wodak, S.J., Emili, A., Greenblatt, J.F., 2006. Global landscape of protein complexes in the yeast Saccharomyces cerevisiae. Nature 440, 637–643.

Kuai, L., Fang, F., Butler, J.S., Sherman, F., 2004. Polyadenylation of rRNA in Saccharomyces cerevisiae. Proc Natl Acad Sci USA 101, 8581–8586.

Kufel, J., Allmang, C., Chanfreau, G., Petfalski, E., Lafontaine, D.L., Tollervey, D., 2000. Precursors to the U3 small nucleolar RNA lack small nucleolar RNP proteins but are stabilized by La binding. Mol Cell Biol 20, 5415–5424.

Kumar, A., Agarwal, S., Heyman, J. a, Matson, S., Heidtman, M., Piccirillo, S., Umansky, L., Drawid, A., Jansen, R., Liu, Y., Cheung, K.-H., Miller, P., Gerstein, M., Roeder, G.S., Snyder, M., 2002. Subcellular localization of the yeast proteome. Genes Dev 16, 707–719.

Kwak, J.E., Wang, L., Ballantyne, S., Kimble, J., Wickens, M., 2004. Mammalian GLD-2 homologs are poly(A) polymerases. Proc Natl Acad Sci USA 101, 4407–4412.

Kyrpides, N.C., Woese, C.R., Ouzounis, C.A., 1996. KOW: a novel motif linking a bacterial transcription factor with ribosomal proteins. Trends Biochem Sci 21, 425–426.

Labrou, N.E., 2010. Random mutagenesis methods for in vitro directed enzyme evolution. Curr Protein Pept Sci 11, 91–100.

LaCava, J., Houseley, J., Saveanu, C., Petfalski, E., Thompson, E., Jacquier, A., Tollervey, D., 2005. RNA degradation by the exosome is promoted by a nuclear polyadenylation complex. Cell 121, 713–724.

Lafontaine, D., Tollervey, D., 1996. One-step PCR mediated strategy for the construction of conditionally expressed and epitope tagged yeast proteins. Nucleic Acids Res 24, 3469–3471.

Lai, Y.-P., Huang, J., Wang, L.-F., Li, J., Wu, Z.-R., 2004. A new approach to random mutagenesis in vitro. Biotechnol Bioeng 86, 622–627.

Lebreton, A., Séraphin, B., 2008. Exosome-mediated quality control: substrate recruitment and molecular activity. Biochim Biophys Acta 1779, 558–565.

Lebreton, A., Tomecki, R., Dziembowski, A., Séraphin, B., 2008. Endonucleolytic RNA cleavage by a eukaryotic exosome. Nature 456, 993–996.

Leung, D., Chen, E., Goeddel, D., 1989. A method for random mutagenesis of a defined DNA segment using a modified polymerase chain reaction. Technique 1, 11–15.

Li, H.D., Zagorski, J., Fournier, M.J., 1990. Depletion of U14 small nuclear RNA (snR128) disrupts production of 18S rRNA in Saccharomyces cerevisiae. Mol Cell Biol 10, 1145–1152.

Li, L., Wang, X., Stolc, V., Li, X., Zhang, D., Su, N., Tongprasit, W., Li, S., Cheng, Z., Wang, J., Deng, X.W., 2006. Genome-wide transcription analyses in rice using tiling microarrays. Nat Genet 38, 124–129.

Liang, S., Hitomi, M., Hu, Y.H., Liu, Y., Tartakoff, A.M., 1996. A DEAD-box-family protein is required for nucleocytoplasmic transport of yeast mRNA. Mol Cell Biol 16, 5139–5146.

Littlehales, W.J., 1989. Electroblotting technique for transferring specimens from a polyacrylamide electrophoresis or like gel onto a membrane.

Liu, Q., Greimann, J.C., Lima, C.D., 2006. Reconstitution, activities, and structure of the eukaryotic RNA exosome. Cell 127, 1223–1237.

Lorentzen, E., Basquin, J., Tomecki, R., Dziembowski, A., Conti, E., 2008. Structure of the active subunit of the yeast exosome core, Rrp44: diverse modes of substrate recruitment in the RNase II nuclease family. Mol Cell 29, 717–728.

Lorentzen, E., Conti, E., 2006. The exosome and the proteasome: nano-compartments for degradation. Cell 125, 651–654.

Lorentzen, E., Walter, P., Fribourg, S., Evguenieva-Hackenberg, E., Klug, G., Conti, E., 2005. The archaeal exosome core is a hexameric ring structure with three catalytic subunits. Nat Struct Mol Biol 12, 575–581.

Lowe, T.M., Eddy, S.R., 1999. A computational screen for methylation guide snoRNAs in yeast. Science (80-.). 283, 1168–1171.

Lundberg, K.S., Shoemaker, D.D., Adams, M.W., Short, J.M., Sorge, J.A., Mathur, E.J., 1991. High-fidelity amplification using a thermostable DNA polymerase isolated from Pyrococcus furiosus. Gene 108, 1–6.

Lunde, B.M., Hörner, M., Meinhart, A., 2011. Structural insights into cis element recognition of non-polyadenylated RNAs by the Nab3-RRM. Nucleic Acids Res 39, 337–346.

Lykke-Andersen, S., Brodersen, D.E., Jensen, T.H., 2009. Origins and activities of the eukaryotic exosome. J Cell Sci 122, 1487–94.

Ma, H., Kunes, S., Schatz, P.J., Botstein, D., 1987. Plasmid construction by homologous recombination in yeast. Gene 58, 201–216.

Makino, D.L., Baumgärtner, M., Conti, E., 2013a. Crystal structure of an RNA-bound 11-subunit eukaryotic exosome complex. Nature 485, 70–75.

Makino, D.L., Halbach, F., Conti, E., 2013b. The RNA exosome and proteasome: common principles of degradation control. Nat Rev Mol Cell Biol 14, 654–660.

Malet, H., Topf, M., Clare, D.K., Ebert, J., Bonneau, F., Basquin, J., Drazkowska, K., Tomecki, R., Dziembowski, A., Conti, E., Saibil, H.R., Lorentzen, E., 2010. RNA channelling by the eukaryotic exosome. EMBO Rep 11, 936–942.

Marquardt, S., Hazelbaker, D.Z., Buratowski, S., 2011. Distinct RNA degradation pathways and 3' extensions of yeast non-coding RNA species. Transcription 2, 145–154.

Martens, J.A., Laprade, L., Winston, F., 2004. Intergenic transcription is required to repress the Saccharomyces cerevisiae SER3 gene. Nature 429, 571–574.

Martens, J.A., Wu, P.-Y.J., Winston, F., 2005. Regulation of an intergenic transcript controls adjacent gene transcription in Saccharomyces cerevisiae. Genes Dev 19, 2695–2704.

Matsumoto-Taniura, N., Pirollet, F., Monroe, R., Gerace, L., Westendorf, J.M., 1996. Identification of novel M phase phosphoproteins by expression cloning. Mol Cell Biol 7, 1455–1469.

Midtgaard, S.F., Assenholt, J., Jonstrup, A.T., Van, L.B., Jensen, T.H., Brodersen, D.E., 2006. Structure of the nuclear exosome component Rrp6p reveals an interplay between the active site and the HRDC domain. Proc Natl Acad Sci USA 103, 11898–11903.

Milligan, L., Decourty, L., Saveanu, C., Rappsilber, J., Ceulemans, H., Jacquier, A., Tollervey, D., 2008. A yeast exosome cofactor, Mpp6, functions in RNA surveillance and in the degradation of noncoding RNA transcripts. Mol Cell Biol 28, 5446–5457.

Mitchell, D.A., Marshall, T.K., Deschenes, R.J., 1993. Vectors for the inducible overexpression of glutathione S-transferase fusion proteins in yeast. Yeast 9, 715–722.

Mitchell, P., Petfalski, E., Houalla, R., Mann, M., Tollervey, D., Podtelejnikov, A., 2003. Rrp47p is an exosome-associated protein required for the 3' processing of stable RNAs. Mol Cell Biol 23, 6982–6992.

Mitchell, P., Petfalski, E., Shevchenko, A., Mann, M., Tollervey, D., 1997. The exosome: a conserved eukaryotic RNA processing complex containing multiple 3'-->5' exoribonucleases. Cell 91, 457–466.

Mitchell, P., Petfalski, E., Tollervey, D., 1996. The 3' end of yeast 5.8S rRNA is generated by an exonuclease processing mechanism. Genes Dev 10, 502–513.

Mitchell, P., Tollervey, D., 2003. An NMD pathway in yeast involving accelerated deadenylation and exosome-mediated 3'-->5' degradation. Mol Cell 11, 1405–1413.

Morozov, V., Mushegian, A.R., Koonin, E. V., Bork, P., 1997. A putative nucleic acid-binding domain in Bloom's and Werner's syndrome helicases. Trends Biochem Sci 22, 417–418.

Motley, A.M., Nuttall, J.M., Hettema, E.H., 2012. Pex3-anchored Atg36 tags peroxisomes for degradation in Saccharomyces cerevisiae. EMBO J 31, 2852–2868.

Muhlrad, D., Parker, R., 1994. Premature translational termination triggers mRNA decapping. Nature 370, 578–581.

Nedea, E., Nalbant, D., Xia, D., Theoharis, N.T., Suter, B., Richardson, C.J., Tatchell, K., Kislinger, T., Greenblatt, J.F., Nagy, P.L., 2008. The Glc7 phosphatase subunit of the cleavage and polyadenylation factor is essential for transcription termination on snoRNA genes. Mol Cell 29, 577–587.

Nehls, P., Keck, T., Greferath, R., Spiess, E., Glaser, T., Rothbarth, K., Stammer, H., Werner, D., 1998. cDNA cloning, recombinant expression and characterization of polypetides with exceptional DNA affinity. Nucleic Acids Res 26, 1160–1166.

Neil, H., Malabat, C., d'Aubenton-Carafa, Y., Xu, Z., Steinmetz, L.M., Jacquier, A., 2009. Widespread bidirectional promoters are the major source of cryptic transcripts in yeast. Nature 457, 1038–1042.

Nilsson, B., Moks, T., Jansson, B., Abrahmsén, L., Elmblad, A., Holmgren, E., Henrichson, C., Jones, T.A., Uhlén, M., 1987. A synthetic IgG-binding domain based on staphylococcal protein A. Protein Eng 1, 107–113.

Nurmohamed, S., Vaidialingam, B., Callaghan, A.J., Luisi, B.F., 2009. Crystal structure of Escherichia coli polynucleotide phosphorylase core bound to RNase E, RNA and manganese: implications for catalytic mechanism and RNA degradosome assembly. J Mol Biol 389, 17–33.

Oldenburg, K.R., Vo, K.T., Michaelis, S., Paddon, C., 1997. Recombination-mediated PCR-directed plasmid construction in vivo in yeast. Nucleic Acids Res 25, 451–452.

Ozanick, S.G., Wang, X., Costanzo, M., Brost, R.L., Boone, C., Anderson, J.T., 2009. Rex1p deficiency leads to accumulation of precursor initiator tRNAMet and polyadenylation of substrate RNAs in Saccharomyces cerevisiae. Nucleic Acids Res 37, 298–308.

Parker, R., 2012. RNA degradation in Saccharomyces cerevisae. Genetics 191, 671–702.

Peng, W.T., Robinson, M.D., Mnaimneh, S., Krogan, N.J., Cagney, G., Morris, Q., Davierwala, A.P., Grigull, J., Yang, X., Zhang, W., Mitsakakis, N., Ryan, O.W., Datta, N., Jojic, V., Pal, C., Canadien, V., Richards, D., Beattie, B., Wu, L.F., Altschuler, S.J., Roweis, S., Frey, B.J., Emili, A., Greenblatt, J.F., Hughes, T.R., 2003. A panoramic view of yeast noncoding RNA processing. Cell 113, 919–933.

Perumal, K., Reddy, R., 2002. The 3' end formation in small RNAs. Gene Expr 10, 59–78.

Phillips, S., Butler, J., 2003. Contribution of domain structure to the RNA 3′ end processing and degradation functions of the nuclear exosome subunit Rrp6p. RNA 9, 1098–1107.

Piper, P.W., Bellatin, J.A., Lockheart, A., 1983. Altered maturation of sequences at the 3' terminus of 5S gene transcripts in a Saccharomyces cerevisiae mutant that lacks a RNA processing endonuclease. EMBO J 2, 353–359.

Pritchard, L., Corne, D., Kell, D., Rowland, J., Winson, M., 2005. A general model of error-prone PCR. J Theor Biol 234, 497–509.

Puig, O., Caspary, F., Rigaut, G., Rutz, B., Bouveret, E., Bragado-Nilsson, E., Wilm, M., Séraphin, B., 2001. The tandem affinity purification (TAP) method: a general procedure of protein complex purification. Methods 24, 218–229.

Rasmussen, T.P., Culbertson, M.R., 1998. The Putative Nucleic Acid Helicase Sen1p Is Required for Formation and Stability of Termini and for Maximal Rates of Synthesis and Levels of Accumulation of Small Nucleolar RNAs in Saccharomyces cerevisiae The Putative Nucleic Acid Helicase Sen1p Is Requi. Mol Cell Biol 18, 6885–6896.

Reimer, G., Scheer, U., Peters, J.M., Tan, E.M., 1986. Immunolocalization and partial characterization of a nucleolar autoantigen (PM-Scl) associated with polymyositis/scleroderma overlap syndromes. J Immunol 137, 3802–3808.

Rigaut, G., Shevchenko, A., Rutz, B., Wilm, M., Mann, M., Séraphin, B., 1999. A generic protein purification method for protein complex characterization and proteome exploration. Nat Biotechnol 17, 1030–1032.

Robzyk, K., Kassir, Y., 1992. A simple and highly efficient procedure for rescuing autonomous plasmids from yeast. Nucleic Acids Res 20, 3790.

Roth, K.M., Byam, J., Fang, F., Butler, J.S., 2009. Regulation of NAB2 mRNA 3 9 -end formation requires the core exosome and the Trf4p component of the TRAMP complex. RNA 15, 1045–1058.

Rothstein, R.J., 1983. One-step gene disruption in yeast. Methods Enzym. 101, 202–211.

Saccharomyces cerevisiae, 1998. . Trends Genet.

Saitoh, S., Chabes, A., McDonald, W.H., Thelander, L., Yates, J.R., Russell, P., 2002. Cid13 is a cytoplasmic poly(A) polymerase that regulates ribonucleotide reductase mRNA. Cell 109, 563–573.

San Paolo, S., Vanacova, S., Schenk, L., Scherrer, T., Blank, D., Keller, W., Gerber, A.P., 2009. Distinct roles of non-canonical poly(A) polymerases in RNA metabolism. PLoS Genet 5, e1000555.

Schaeffer, D., Reis, F.P., Johnson, S.J., Arraiano, C.M., van Hoof, A., 2012. The CR3 motif of Rrp44p is important for interaction with the core exosome and exosome function. Nucleic Acids Res 40, 9298–9307.

Schaeffer, D., Tsanova, B., Barbas, A., Reis, F.P., Dastidar, E.G., Sanchez-Rotunno, M., Arraiano, C.M., van Hoof, A., 2009. The exosome contains domains with specific endoribonuclease, exoribonuclease and cytoplasmic mRNA decay activities. Nat Struct Mol Biol 16, 56–62.

Schiestl, R.H., Gietz, R.D., 1989. High efficiency transformation of intact yeast cells using single stranded nucleic acids as a carrier. Curr Genet 16, 339–346.

Schilders, G., Raijmakers, R., Raats, J.M.H., Pruijn, G.J.M., 2005. MPP6 is an exosome-associated RNA-binding protein involved in 5.8S rRNA maturation. Nucleic Acids Res 33, 6795–6804.

Schilders, G., van Dijk, E., Pruijn, G.J.M., 2007. C1D and hMtr4p associate with the human exosome subunit PM/Scl-100 and are involved in pre-rRNA processing. Nucleic Acids Res 35, 2564–2572.

Schmidt, K., Butler, J.S., 2013. Nuclear RNA surveillance: role of TRAMP in controlling exosome specificity. Wiley Interdiscip Rev RNA 4, 217–231.

Schmidt, K., Xu, Z., Mathews, D.H., Butler, J.S., 2012. Air proteins control differential TRAMP substrate specificity for nuclear RNA surveillance. RNA 18, 1934–1945.

Schneider, C., Anderson, J.T., Tollervey, D., 2007. The exosome subunit Rrp44 plays a direct role in RNA substrate recognition. Mol Cell 27, 324–331.

Schneider, C., Kudla, G., Wlotzka, W., Tuck, A., Tollervey, D., 2012. Transcriptome-wide Analysis of Exosome Targets. Mol Cell 48, 422–433.

Schneider, C., Leung, E., Brown, J., Tollervey, D., 2009. The N-terminal PIN domain of the exosome subunit Rrp44 harbors endonuclease activity and tethers Rrp44 to the yeast core exosome. Nucleic Acids Res 37, 1127–1140.

Schoepfer, R., 1993. The pRSET family of T7 promoter expression vectors for Escherichia coli. Gene 124, 83–85.

Shapiro, A.L., Viñuela, E., Maizel, J. V, 1967. Molecular weight estimation of polypeptide chains by electrophoresis in SDS-polyacrylamide gels. Biochem Biophys Res Commun 28, 815–820.

Shi, Z., Yang, W.-Z., Lin-Chao, S., Chak, K.-F., Yuan, H.S., 2008. Crystal structure of Escherichia coli PNPase: central channel residues are involved in processive RNA degradation. RNA 14, 2361–2371.

Sievers, F., Wilm, A., Dineen, D., Gibson, T.J., Karplus, K., Li, W., Lopez, R., McWilliam, H., Remmert, M., Söding, J., Thompson, J.D., Higgins, D.G., 2011. Fast, scalable generation of high-quality protein multiple sequence alignments using Clustal Omega. Mol Syst Biol 7, 539.

Sikorski, R.S., Hieter, P., 1989. A System of Shuttle Vectors and Yeast Host Strains Designed for Efficient Manipulation of DNA in. Genetics 122, 19–27.

Smith, D.B., Johnson, K.S., 1988. Single-step purification of polypeptides expressed in Escherichia coli as fusions with glutathione S-transferase. Gene 67, 31–40.

Smith, D.M., Chang, S.-C., Park, S., Finley, D., Cheng, Y., Goldberg, A.L., 2007. Docking of the proteasomal ATPases' carboxyl termini in the 20S proteasome's alpha ring opens the gate for substrate entry. Mol Cell 27, 731–744.

Smolka, M.B., Albuquerque, C.P., Chen, S., Zhou, H., 2007. Proteome-wide identification of in vivo targets of DNA damage checkpoint kinases. Proc Natl Acad Sci USA 104, 10364–10369.

Staub, E., Fiziev, P., Rosenthal, A., Hinzmann, B., 2004. Insights into the evolution of the nucleolus by an analysis of its protein domain repertoire. Bioessays 26, 567–581.

Stead, J.A., Costello, J.L., Livingstone, M.J., Mitchell, P., 2007. The PMC2NT domain of the catalytic exosome subunit Rrp6p provides the interface for binding with its cofactor Rrp47p, a nucleic acid-binding protein. Nucleic Acids Res 35, 5556–5567.

Steinmetz, E.J., Brow, D., 1996. Repression of gene expression by an exogenous sequence element acting in concert with a heterogeneous nuclear ribonucleoprotein-like protein, Nrd1, and the putative helicase Sen1. Mol Cell Biol 16, 6993–7003.

Steinmetz, E.J., Brow, D.A., 1998. Control of pre-mRNA accumulation by the essential yeast protein Nrd1 requires high-affinity transcript binding and a domain implicated in RNA polymerase II association. Proc Natl Acad Sci USA 95, 6699–6704.

Steinmetz, E.J., Brow, D.A., 2003. Ssu72 protein mediates both poly(A)-coupled and poly(A)-independent termination of RNA polymerase II transcription. Mol Cell Biol 23, 6339–6349.

Steinmetz, E.J., Conrad, N.K., Brow, D.A., Corden, J.L., 2001. RNA-binding protein Nrd1 directs poly(A)-independent 3'-end formation of RNA polymerase II transcripts. Nature 413, 327–331.

Steinmetz, E.J., Ng, S.B.H., Cloute, J.P., Brow, D.A., 2006. cis- and trans-Acting determinants of transcription termination by yeast RNA polymerase II. Mol Cell Biol 26, 2688–2696.

Steitz, T.A., Steitz, J.A., 1993. A general two-metal-ion mechanism for catalytic RNA. Proc Natl Acad Sci USA 90, 6498–6502.

Stolc, V., Gauhar, Z., Mason, C., Halasz, G., van Batenburg, M.F., Rifkin, S.A., Hua, S., Herreman, T., Tongprasit, W., Barbano, P.E., Bussemaker, H.J., White, K.P., 2004. A gene expression map for the euchromatic genome of Drosophila melanogaster. Science (80-.). 306, 655–660.

Struhl, K., Stinchcomb, D.T., Scherer, S., Davis, R.W., 1979. High-frequency transformation of yeast: autonomous replication of hybrid DNA molecules. Proc Natl Acad Sci USA 76, 1035–1039.

Stuparevic, I., Mosrin-Huaman, C., Hervouet-Coste, N., Remenaric, M., Rahmouni, a R., 2013. Co-transcriptional recruitment of the RNA exosome cofactors Rrp47p, Mpp6p and two distinct TRAMP complexes assists the exonuclease Rrp6p in the targeting and degradation of an aberrant mRNP in yeast. J Biol Chem 288, 31816–31829.

Synowsky, S.A., Heck, A.J.R., 2008. The yeast Ski complex is a hetero-tetramer. Protein Sci 17, 119–125.

Synowsky, S.A., Wijk, M. Van, Raijmakers, R., Heck, A.J.R., 2009. Comparative Multiplexed Mass Spectrometric Analyses of Endogenously Expressed Yeast Nuclear and Cytoplasmic Exosomes. J Mol Biol 385, 1300–1313.

T. Maniatis, E. F. Fritsch, J.S., 1982. Molecular cloning: a laboratory manual, Molecular cloning: a laboratory manual.

Takahashi, S., Araki, Y., Sakuno, T., Katada, T., 2003. Interaction between Ski7p and Upf1p is required for nonsense-mediated 3'-to-5' mRNA decay in yeast. EMBO J 22, 3951–3959.

Thiebaut, M., Kisseleva-Romanova, E., Rougemaille, M., Boulay, J., Libri, D., 2006. Transcription termination and nuclear degradation of cryptic unstable transcripts: a role for the nrd1-nab3 pathway in genome surveillance. Mol Cell 23, 853–864.

Thomas, B.J., Rothstein, R., 1989. Elevated recombination rates in transcriptionally active DNA. Cell 56, 619–630.

Thompson, D.M., Parker, R., 2007. Cytoplasmic decay of intergenic transcripts in Saccharomyces cerevisiae. Mol Cell Biol 27, 92–101.

Thomson, E., Tollervey, D., 2010. The final step in 5.8S rRNA processing is cytoplasmic in Saccharomyces cerevisiae. Mol Cell Biol 30, 976–984.

Tollervey, D., Mattaj, I., 1987. Fungal small nuclear ribonucleoproteins share properties with plant and vertebrate U-snRNPs. EMBO J 6, 469–476.

Uhler, J.P., Hertel, C., Svejstrup, J.Q., 2007. A role for noncoding transcription in activation of the yeast PHO5 gene. Proc Natl Acad Sci USA 104, 8011–8016.

Ursic, D., Chinchilla, K., Finkel, J.S., Culbertson, M.R., 2004. Multiple protein/protein and protein/RNA interactions suggest roles for yeast DNA/RNA helicase Sen1p in transcription, transcription-coupled DNA repair and RNA processing. Nucleic Acids Res 32, 2441–2452.

Van Hoof, a, Lennertz, P., Parker, R., 2000a. Yeast exosome mutants accumulate 3'-extended polyadenylated forms of U4 small nuclear RNA and small nucleolar RNAs. Mol Cell Biol 20, 441–452.

Van Hoof, a, Lennertz, P., Parker, R., 2000b. Three conserved members of the RNase D family have unique and overlapping functions in the processing of 5S, 5.8S, U4, U5, RNase MRP and RNase P RNAs in yeast. EMBO J 19, 1357–1365.

Van Hoof, a, Staples, R.R., Baker, R.E., Parker, R., 2000c. Function of the ski4p (Csl4p) and Ski7p proteins in 3'-to-5' degradation of mRNA. Mol Cell Biol 20, 8230–8243.

Van Hoof, A., Frischmeyer, P.A., Dietz, H.C., Parker, R., 2002. Exosome-mediated recognition and degradation of mRNAs lacking a termination codon. Science (80-.). 295, 2262–2264.

Van Hoof, A., Parker, R., 1999. The exosome: a proteasome for RNA? Cell 99, 347–350.

Vanácová, S., Wolf, J., Martin, G., Blank, D., Dettwiler, S., Friedlein, A., Langen, H., Keith, G., Keller, W., 2005. A new yeast poly(A) polymerase complex involved in RNA quality control. PLoS Biol 3, e189.

Vasiljeva, L., Buratowski, S., 2006. Nrd1 interacts with the nuclear exosome for 3' processing of RNA polymerase II transcripts. Mol cell 21, 239–248.

Vasiljeva, L., Kim, M., Mutschler, H., Buratowski, S., Meinhart, A., 2008a. The Nrd1-Nab3-Sen1 termination complex interacts with the Ser5-phosphorylated RNA polymerase II C-terminal domain. Nat Struct Mol Biol 15, 795–804.

Vasiljeva, L., Kim, M., Terzi, N., Soares, L.M., Buratowski, S., 2008b. Transcription termination and RNA degradation contribute to silencing of RNA polymerase II transcription within heterochromatin. Mol Cell 29, 313–323.

Von der Haar, T., 2007. Optimized protein extraction for quantitative proteomics of yeasts. PLoS One 2, e1078.

Wach, A., Brachat, A., Pöhlmann, R., Philippsen, P., 1994. New heterologous modules for classical or PCR-based gene disruptions in Saccharomyces cerevisiae. Yeast 10, 1793–1808.

Walowsky, C., Fitzhugh, D.J., Castaño, I.B., Ju, J.Y., Levin, N.A., Christman, M.F., 1999. The topoisomerase-related function gene TRF4 affects cellular sensitivity to the antitumor agent camptothecin. J Biol Chem 274, 7302–7308.

Wang, H.-W., Wang, J., Ding, F., Callahan, K., Bratkowski, M. a, Butler, J.S., Nogales, E., Ke, A., 2007. Architecture of the yeast Rrp44 exosome complex suggests routes of RNA recruitment for 3' end processing. Proc Natl Acad Sci USA 104, 16844–16849.

Wang, S.W., Toda, T., MacCallum, R., Harris, A.L., Norbury, C., 2000. Cid1, a fission yeast protein required for S-M checkpoint control when DNA polymerase delta or epsilon is inactivated. Mol Cell Biol 20, 3234–3244.

Wasmuth, E. V., Lima, C.D., 2012. Exo- and Endoribonucleolytic Activities of Yeast Cytoplasmic and Nuclear RNA Exosomes Are Dependent on the Noncatalytic Core and Central Channel. Mol Cell 48, 133–144.

Weir, J.R., Bonneau, F., Hentschel, J., Conti, E., 2010. Structural analysis reveals the characteristic features of Mtr4, a DExH helicase involved in nuclear RNA processing and surveillance. Proc Natl Acad Sci USA 107, 12139–12144.

Wellington, M., Rustchenko, E., 2005. 5-Fluoro-orotic acid induces chromosome alterations in Candida albicans. Yeast 22, 57–70.

Wiederkehr, T., Prétôt, R.F., Minvielle-Sebastia, L., 1998. Synthetic lethal interactions with conditional poly(A) polymerase alleles identify LCP5, a gene involved in 18S rRNA maturation. RNA 4, 1357–13572.

Winey, M., Culbertson, M.R., 1988. Mutations affecting the tRNA-splicing endonuclease activity of Saccharomyces cerevisiae. Genetics 118, 609–617.

Wlotzka, W., Kudla, G., Granneman, S., Tollervey, D., 2011. The nuclear RNA polymerase II surveillance system targets polymerase III transcripts. EMBO J 30, 1790–1803.

Wolin, S.L., Sim, S., Chen, X., 2012. Nuclear noncoding RNA surveillance: is the end in sight? Trends Genet 28, 306–313.

Wyers, F., Rougemaille, M., Badis, G., Rousselle, J.-C., Dufour, M.-E., Boulay, J., Régnault, B., Devaux, F., Namane, A., Séraphin, B., Libri, D., Jacquier, A., 2005. Cryptic pol II transcripts are degraded by a nuclear quality control pathway involving a new poly(A) polymerase. Cell 121, 725–737.

Xu, Z., Wei, W., Gagneur, J., Perocchi, F., Clauder-Münster, S., Camblong, J., Guffanti, E., Stutz, F., Huber, W., Steinmetz, L.M., 2009. Bidirectional promoters generate pervasive transcription in yeast. Nature 457, 1033–1037.

Yavuzer, U., Smith, G.C., Bliss, T., Werner, D., Jackson, S.P., 1998. DNA end-independent activation of DNA-PK mediated via association with the DNA-binding protein C1D. Genes Dev 12, 2188–2199.

Zuo, Y., Deutscher, M.P., 2001. Exoribonuclease superfamilies: structural analysis and phylogenetic distribution. Nucleic Acids Res 29, 1017–1026.

Zuo, Y., Vincent, H. a, Zhang, J., Wang, Y., Deutscher, M.P., Malhotra, A., 2006. Structural basis for processivity and single-strand specificity of RNase II. Mol Cell 24, 149–156.

Zuo, Y., Wang, Y., Malhotra, A., 2005. Crystal structure of Escherichia coli RNase D, an exoribonuclease involved in structured RNA processing. Structure 13, 973–984.

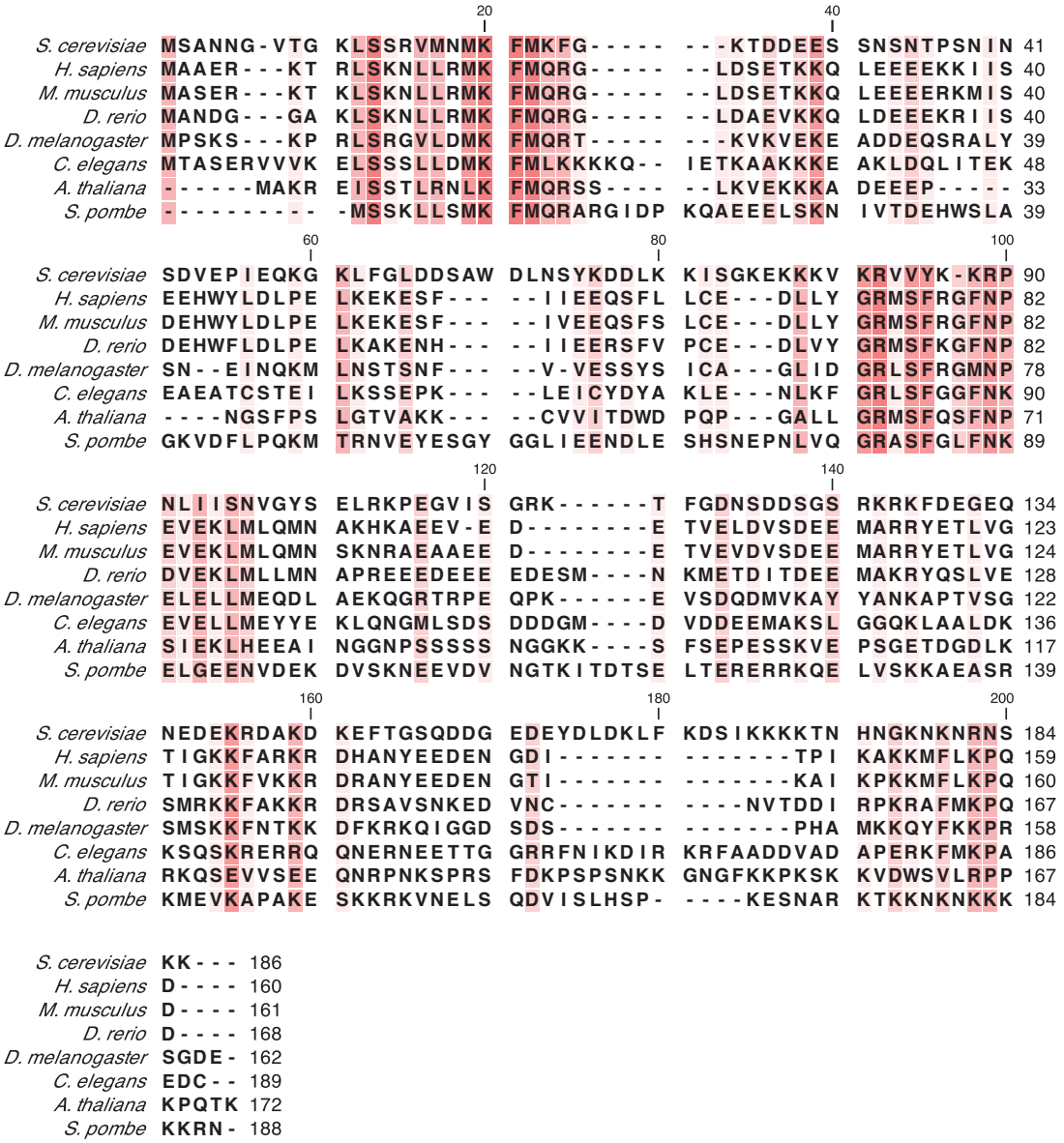

Appendix I. Amino acid sequence alignment of Mpp6 homologues from model organisms. Sequences of Mpp6 proteins from *Saccharomyces cerevisiae*, *Homo sapiens*, *Mus musculus*, *Danio rerio*, *Drosophila melanogaster*, *Caenorhabditis elegans*, *Arabidopsis thaliana* and *Schizosaccharomyces pombe* were aligned using Clustal Omega (Sievers et al. 2011) and edited using CLC Main Workbench 6 (CLC Bio, Aahus, Denmark). Conserved residues are highlighted in red.

Appendix II. Amino acid sequence alignment of Mpp6 orthologs in other *Saccharomyces* species. Sequences of predicted Mpp6 proteins from *Saccharomyces cerevisiae, Saccharomyces paradoxus, Saccharomyces mikatae, Saccharomyces bayanus and Saccharomyces castellii* were aligned using Clustal Omega (Sievers et al. 2011) and edited using CLC Main Workbench 6 (CLC Bio, Aahus, Denmark). Conserved residues are highlighted in red.

Appendix III. Garland, W., Feigenbutz, M., Turner, M., Mitchell, P., 2013. Rrp47 functions in RNA surveillance and stable RNA processing when divorced from the exoribonuclease and exosome-binding domains of Rrp6. RNA 19, 1659–1668.

Rrp47 functions in RNA surveillance and stable RNA processing when divorced from the exoribonuclease and exosome-binding domains of Rrp6

WILLIAM GARLAND, MONIKA FEIGENBUTZ, MARTIN TURNER, and PHIL MITCHELL[1]
Molecular Biology and Biotechnology Department, The University of Sheffield, Sheffield S10 2TN, United Kingdom

ABSTRACT

The eukaryotic exosome exoribonuclease Rrp6 forms a complex with Rrp47 that functions in nuclear RNA quality control mechanisms, the degradation of cryptic unstable transcripts (CUTs), and in the 3′ end maturation of stable RNAs. Stable expression of Rrp47 is dependent upon its interaction with the N-terminal domain of Rrp6 ($Rrp6_{NT}$). To address the function of Rrp47 independently of Rrp6, we developed a DECOID (decreased expression of complexes by overexpression of interacting domains) strategy to resolve the Rrp6/Rrp47 complex in vivo and employed *mpp6Δ* and *rex1Δ* mutants that are synthetic lethal with loss-of-function *rrp47* mutants. Strikingly, Rrp47 was able to function in *mpp6Δ* and *rex1Δ* mutants when separated from the catalytic and exosome-binding domains of Rrp6, whereas a truncated Rrp47 protein lacking its C-terminal region caused a block in cell growth. Northern analyses of the conditional mutants revealed a specific block in the 3′ maturation of box C/D snoRNAs in the *rex1 rrp47* mutant and widespread inhibition of Rrp6-mediated RNA surveillance processes in the *mpp6 rrp47* mutant. In contrast, growth analyses and RNA northern blot hybridization analyses showed no effect on the *rrp47Δ* mutant upon overexpression of the $Rrp6_{NT}$ domain. These findings demonstrate that Rrp47 and Rrp6 have resolvable functions in Rrp6-mediated RNA surveillance and processing pathways. In addition, this study reveals a redundant requirement for Rrp6 or Rex1 in snoRNA maturation and demonstrates the effective use of the DECOID strategy for the resolution and functional analysis of protein complexes.

Keywords: RNA surveillance; RNA processing; yeast; synthetic lethality; protein overexpression; exosome

INTRODUCTION

The degradation of RNA is a fundamentally important biological process. Firstly, cellular RNAs are typically generated by the accurate, limited degradation of larger precursor molecules. RNA fragments released through such processing reactions are also subjected to degradation. In addition, mRNA transcripts have defined functional lifetimes and are degraded in a temporally controlled manner. Furthermore, both mRNAs and noncoding RNAs are subjected to quality control systems that eliminate incorrectly processed transcripts or misassembled ribonucleoprotein particles (Houseley and Tollervey 2009; Wolin et al. 2012). A significant proportion of transcripts are degraded by such "RNA surveillance" processes, even in normally growing, healthy cells (Gudipati et al. 2012). Finally, low level antisense and inter-genic transcription generates a large number of noncoding RNAs, many of which are subjected to rapid degradation (Wyers et al. 2005).

A major source of 3′→5′ ribonucleolytic activity in eukaryotic cells is the exosome ribonuclease complex (Mitchell et al. 1997; Allmang et al. 1999b). The exosome functions in both the limited trimming of RNA precursors in RNA processing pathways and in the complete destruction of RNAs as part of RNA surveillance mechanisms, the removal of RNA fragments generated during RNA processing, and the elimination of transiently expressed, cryptic unstable transcripts (CUTs) (Chlebowski et al. 2013). The core of the eukaryotic exosome is itself catalytically inert, ribonuclease activity being provided by two additional associated proteins; Rrp44 (also known as Dis3) is bound to the base of the core, while Rrp6 is associated with the cap region (Bonneau et al. 2009; Makino et al. 2013). Rrp44 is a member of the RNase II family of exoribonucleases that also has an N-terminal PIN domain with associated endonucleolytic activity and is found tightly associated with the core exosome in both the nucleus and cytoplasmic

[1]**Corresponding author**
E-mail p.j.mitchell@shef.ac.uk
Article published online ahead of print. Article and publication date are at http://www.rnajournal.org/cgi/doi/10.1261/rna.039388.113. Freely available online through the *RNA* Open Access option.

© 2013 Garland et al. This article, published in *RNA*, is available under a Creative Commons License (Attribution-NonCommercial 3.0 Unported), as described at http://creativecommons.org/licenses/by-nc/3.0/.

regions. Rrp6 is an RNase D-related 3′→5′ exoribonuclease (Burkard and Butler 2000) that contains an N-terminal PMC2NT domain, a "DEDD" catalytic domain, an HRDC domain, and a C-terminal region that is required for interaction with the exosome complex. A C-terminal truncation of Rrp6 that prevents its stable association with the exosome does not inhibit Rrp6-dependent processes (Callahan and Butler 2008), suggesting that Rrp6 can function largely independently of its association with the exosome.

The activity of the nuclear exosome is dependent upon additional proteins or complexes, including the Trf/Air/Mtr4 polyadenylation complex TRAMP, the Nrd1/Nab3/Sen1 complex, and the nuclear RNA-binding proteins Rrp47 (also known as Lrp1) and Mpp6 (Chlebowski et al. 2013). The Nrd1/Nab3/Sen1 complex functions in the transcription termination of short RNA polymerase II transcripts (Steinmetz et al. 2001), copurifies together with RNA polymerase II and exosomes in large transcription/processing complexes, and promotes exosome-mediated degradation of transcripts containing Nrd1/Nab3 binding sites (Vasiljeva and Buratowski 2006). TRAMP promotes Nrd1/Nab3-dependent transcription termination of snoRNAs (Grzechnik and Kufel 2008) and adds poly(A) tails onto RNA substrates, which promotes their subsequent degradation (LaCava et al. 2005; Vanacova et al. 2005; Wyers et al. 2005). Rrp47 interacts directly with Rrp6 and functions specifically to promote Rrp6-mediated processes (Mitchell et al. 2003; Peng et al. 2003). In contrast, the exosome-associated protein Mpp6 has been proposed to function as an Rrp44-specific cofactor (Milligan et al. 2008).

Functional redundancy is a common feature of biological systems. Yeast *rrp6* and *rrp44* mutants have synergistic phenotypes, and both Rrp6 and Rrp44 function in the processing of stable RNAs, in RNA surveillance pathways, and in the degradation of CUTs (Gudipati et al. 2012; Schneider et al. 2012). Redundancy between Rrp6 and an Mpp6-stimulated activity, presumably that of Rrp44, is supported by the synthetic lethality observed for *rrp6Δ mpp6Δ* and *rrp47Δ mpp6Δ* double mutants (Milligan et al. 2008). Yeast *rrp6Δ* and *rrp47Δ* mutants are also synthetic lethal with loss-of-function mutations in *REX1/RNA82* (van Hoof et al. 2000a; Peng et al. 2003), a gene that encodes another RNase D-related 3′→5′ exoribonuclease (Ozanick et al. 2009) that is not physically associated with the exosome. Like *rrp6* mutants, *rex1* strains are defective in the 3′ end maturation of stable RNAs and accumulate polyadenylated RNAs (Piper et al. 1983; van Hoof et al. 2000a).

Rrp6 and Rrp47 interact directly through their N-terminal PMC2NT and Sas10/C1D domains, respectively, and normal Rrp47 expression levels are strongly dependent upon this interaction. In contrast, Rrp6 expression and nuclear localization are not significantly affected in the *rrp47Δ* mutant (Stead et al. 2007; Feigenbutz et al. 2013). Both Rrp47 and the homologous human protein C1D show nucleic acid binding activity in vitro, with a specificity for structured substrates (Schilders et al. 2007; Stead et al. 2007). Notably, purified recombinant Rrp6 exonuclease shows poor processivity through structured RNA (Burkard and Butler 2000; Liu et al. 2006). This led to the proposal that Rrp47 may promote the Rrp6-mediated degradation of structured RNA. However, Rrp6 lacking the PMC2NT domain shows comparable exonucleolytic activity to the full-length protein on the substrates tested in vitro (Assenholt et al. 2008; Wasmuth and Lima 2012). Furthermore, the N-terminal Sas10/C1D domain is able to complement the synthetic lethality of an *rrp47Δ rex1Δ* mutant but is itself insufficient for the RNA-binding activity of Rrp47 (Costello et al. 2011).

In these studies, we sought to address whether the physical association of Rrp47 with the Rrp6 exonuclease is critical for its function in RNA processing and degradation. Demonstration that Rrp6 and Rrp47 can function when the proteins are divorced would provide prima facie evidence that Rrp47 functions in substrate recognition or activation, before catalysis. Rrp47 stability is dependent upon its interaction with the $Rrp6_{NT}$ domain (Feigenbutz et al. 2013). We therefore used an overexpression system to induce expression of the $Rrp6_{NT}$ domain and titrate Rrp47 out of Rrp6 complexes. We refer to this approach as DECOID (decreased expression of complexes by overexpression of interacting domains).

Our results reveal that Rrp47 is functional as a full-length protein when separated from the catalytic and exosome-binding domains of Rrp6 but that its ability to function is lost upon deletion of the C-terminal region of the protein. This region of Rrp47 has previously been shown to be required for its interaction with the snoRNP proteins Nop56 and Nop58 and for binding to RNA (Costello et al. 2011). Genetic assays and Northern analyses show that the resolved Rrp6/Rrp47 complex functions in the processing or degradation of all Rrp6 substrates tested. Intriguingly, conditional *rrp47 rex1* mutants showed a specific defect in snoRNA production, while *rrp47 mpp6* mutants were blocked in RNA turnover pathways. These findings are consistent with a function for Rrp47 in the recognition of most, if not all, substrates prior to RNA processing or degradation by Rrp6.

RESULTS AND DISCUSSION

Overexpression of the $Rrp6_{NT}$ domain segregates Rrp47 from full-length Rrp6

To determine whether Rrp47 could be titrated out of complexes containing full-length Rrp6 by overexpression of the $Rrp6_{NT}$ domain, a yeast strain expressing an Rrp47-GFP fusion protein from its own promoter (Feigenbutz et al. 2013) was transformed with plasmids that encode either a *GAL*-inducible GST-$Rrp6_{NT}$ fusion protein or just the GST domain. Lysates from cells grown in galactose-based medium were fractionated by ultracentrifugation through glycerol gradients, and the sedimentation behavior of Rrp47 was

compared to the total cellular protein profiles and to protein markers that were resolved in parallel gradients.

In control cells expressing GST, Rrp47 sedimented as part of a moderately sized complex with a sedimentation coefficient between that of BSA (4.6 S) and catalase (11.3 S) (Fig. 1A). A similar distribution of Rrp47, with a peak in fraction 7, was observed in lysates from nontransformed cells grown in glucose-based minimal medium (data not shown). GST sedimented in a distinct region of the gradient from Rrp47-GFP, being observed in fractions 3 and 4. Upon overexpression of GST-Rrp6$_{NT}$, Rrp47 exhibited a slower sedimentation rate, and the two proteins showed a clear overlap, with a peak in fraction 5 (Fig. 1A). The observed shift in sedimentation profile for Rrp47 upon induction of GST-Rrp6$_{NT}$ was supported by completely reproducible protein patterns of these gradient fractions upon SDS-PAGE analyses.

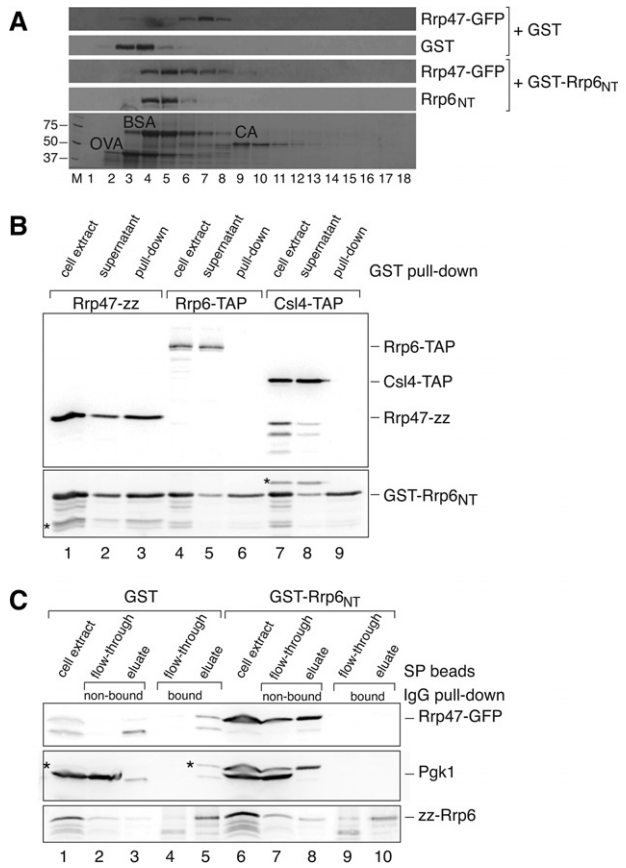

FIGURE 1. Rrp6$_{NT}$ induction leads to disruption of the Rrp6/Rrp47 complex. (*A*) Glycerol gradient analyses of extracts from strains expressing epitope-tagged Rrp47-GFP after induction of GST-Rrp6$_{NT}$ or GST. Gradient fractions 1–18 were resolved by SDS-PAGE and analyzed by Western blotting. Bovine serum albumin (BSA), ovalbumin (OVA), and catalase (CA) markers were resolved in a parallel gradient and fractions analyzed by SDS-PAGE; molecular weight markers (masses indicated in kDa) are resolved in lane M. (*B*) Pull-down analysis of Rrp47-zz, Rrp6-TAP, and Csl4-TAP fusion proteins with GST-Rrp6$_{NT}$. The *upper* panel shows a Western analysis of Rrp47-zz, Rrp6-TAP, and Csl4-TAP proteins in equivalent aliquots of the cell extract, supernatant, and pull-down fractions. The *lower* panel shows a subsequent Western analysis of the same blot using a GST antibody. Asterisks indicate bands due to residual signal from the initial Western. (*C*) Pull-down analysis of Rrp47-GFP binding to zz-Rrp6 upon induction of either GST or GST-Rrp6$_{NT}$. Cell extracts were initially resolved into "flow-through" and "eluate" fractions by SP sepharose chromatography. Both fractions were then incubated with IgG-sepharose beads, giving "bound" and "nonbound" fractions. Equivalent aliquots of each fraction were then analyzed by Western blotting for the presence of Rrp47-GFP (*upper* panel), Pgk1 (*center* panel), and zz-Rrp6 (*lower* panel). Asterisks in the center panel indicate bands due to residual signal from the Rrp47-GFP Western.

To determine whether the observed cosedimentation of GST-Rrp6$_{NT}$ and Rrp47 reflects an interaction between these two proteins, GST pull-down assays were performed on lysates from strains expressing an Rrp47-zz fusion protein from its own promoter (Mitchell et al. 2003) after induction of GST-Rrp6$_{NT}$ overexpression. Parallel assays were also performed on strains expressing C-terminal TAP-tagged fusion proteins of Rrp6 or the core exosome subunit Csl4, both expressed from their own promoter. The pull-down data shown in Figure 1B clearly demonstrate that Rrp47, but not full-length Rrp6 or Csl4, is associated with the induced GST-Rrp6$_{NT}$ protein (Fig. 1B). We have previously shown that no interaction is observed between Rrp47-zz and GST (see also Fig. 1A; Stead et al. 2007). Depletion of Rrp47-zz and GST-Rrp6$_{NT}$ from the cell lysates upon incubation with glutathione sepharose beads occurred at comparable efficiencies (cf. the band intensities for Rrp47-zz and GST-Rrp6$_{NT}$ in Fig. 1B, lanes 1–3), suggesting that the majority of Rrp47 is associated with the GST fusion protein.

We then determined whether Rrp47 could still be detected in complexes with Rrp6 upon overexpression of GST-Rrp6$_{NT}$. GST or the GST-Rrp6$_{NT}$ protein was induced in an *rrp47-GFP rrp6Δ* strain expressing a plasmid-encoded zz-Rrp6 fusion protein, and Rrp6 complexes were captured in IgG pull-down assays. We have previously shown that the zz-Rrp6 fusion protein, which is expressed from the *RRP4* promoter in this construct (Allmang et al. 1999b), is expressed at a level comparable to that of the Rrp6-TAP fusion protein (Stead et al. 2007). To reduce the degree of Rrp6 proteolysis observed during pull-down reactions, Rrp6 complexes were initially enriched from whole cell lysates by ion exchange chromatography using SP-sepharose beads (Allmang et al. 1999b). IgG pull-down assays were performed on both the flow-through and eluate fractions obtained by ion exchange chromatography, and Western analyses were performed on equivalent aliquots of the cell extracts, flow-through, and eluate fractions.

Western analyses revealed that Rrp47 efficiently copurified with Rrp6 from lysates of strains overexpressing the GST protein (Fig. 1C; cf. "nonbound" lanes 2 and 3 with "bound" lanes 4 and 5), demonstrating that Rrp47 and Rrp6 remained stably associated under the experimental conditions used in the pull-down assay. In contrast, the interaction between Rrp47 and endogenous Rrp6 was barely detectable upon overexpression of the GST-Rrp6$_{NT}$ fusion protein (Fig. 1C; cf. lanes 7 and 8 with 9 and 10). A significantly higher level of

expression of Rrp47-GFP was observed in the cells expressing GST-Rrp6$_{NT}$, presumably because the increased availability of this domain serves to stabilize Rrp47 (Feigenbutz et al. 2013). Comparison of the amount of Rrp47 present in the Rrp6 pull-down samples upon induction of GST or GST-Rrp6$_{NT}$ was therefore standardized to the expression level of Pgk1 in the cell extracts. Pgk1 is clearly visible as the major band in the cell extract and the SP sepharose flow-through fractions in the center panel of Figure 1C and is absent from the upper panel. Quantitative analyses revealed that the amount of Rrp47 associated with Rrp6 upon overexpression of GST-Rrp6$_{NT}$ was ~4% of that observed upon overexpression of GST. Comparable amounts of Rrp6 protein were observed in the pull-downs in both samples (Fig. 1C, lower panel; cf. lanes 4 and 5 with 9 and 10). Taken together, the data from glycerol gradient analyses and pull-down experiments demonstrate that Rrp47 is effectively titrated out of full-length Rrp6-containing complexes upon overexpression of the Rrp6$_{NT}$ "decoy" domain.

Rrp47 is functional when physically segregated from the catalytic and exosome-binding domains of Rrp6

To test genetically whether Rrp47 can function when physically separated from full-length Rrp6, *mpp6Δ* and *rex1Δ* mutants were transformed with plasmids expressing either GST or GST-Rrp6$_{NT}$ from the *GAL* promoter, and the resultant transformants were assayed for growth on glucose- and galactose-based media. Isogenic wild-type and *rrp47Δ* strains were also transformed with the same plasmids and assayed in parallel. Strikingly, transformants of both *mpp6Δ* and *rex1Δ* mutants expressing GST-Rrp6$_{NT}$ were viable on galactose-based medium. We then compared the growth rates of transformants expressing either GST or GST-Rrp6$_{NT}$ during incubation in galactose-based medium. There was only a very slight decrease in growth rate seen in the wild-type strain upon induction of the GST-Rrp6$_{NT}$ protein. In contrast, *mpp6Δ* and *rex1Δ* strains overexpressing GST-Rrp6$_{NT}$ clearly grew slower than transformants overexpressing the GST domain (Fig. 2A). No detectable difference was observed in the growth rate of transformants of the *rrp47Δ* mutant, demonstrating that induction of the GST-Rrp6$_{NT}$ domain does not elicit an Rrp47-independent dominant negative growth phenotype. Plasmid shuffle assays showed that overexpression of GST-Rrp6$_{NT}$ in itself did not suppress the synthetic lethality of the *mpp6Δ rrp47Δ* double mutant (data not shown). These analyses demonstrate that the function of Rrp47 is impaired, but nevertheless not blocked, when Rrp47 is segregated from full-length Rrp6.

To address the nature of the slow growth phenotypes in *mpp6Δ* and *rex1Δ* strains observed upon induction of GST-Rrp6$_{NT}$ expression, Northern analyses were performed on RNA isolated from transformants of a wild-type strain and from *rrp47Δ*, *mpp6Δ*, or *rex1Δ* mutants (Fig. 2B). RNA processing and degradation phenotypes were observed upon induction of GST-Rrp6$_{NT}$ in the wild-type strain that are similar in nature to those observed in *rrp47Δ* mutants (Mitchell et al. 2003; Costello et al. 2011) but considerably weaker, consistent with a mild inhibition of Rrp47 function in wild-type cells upon segregation of Rrp47 from full-length Rrp6 (Fig. 2B; cf. lanes 1–3). Specifically, induction of GST-Rrp6$_{NT}$ in the wild-type strain led to a detectable accumulation of the "5.8S + 30" rRNA processing intermediate and 3′ extended forms of the snoRNA snR38, a modest accumulation of the excised RNA polymerase I 5′ external transcribed spacer (5′ ETS) fragment, and the accumulation of extended

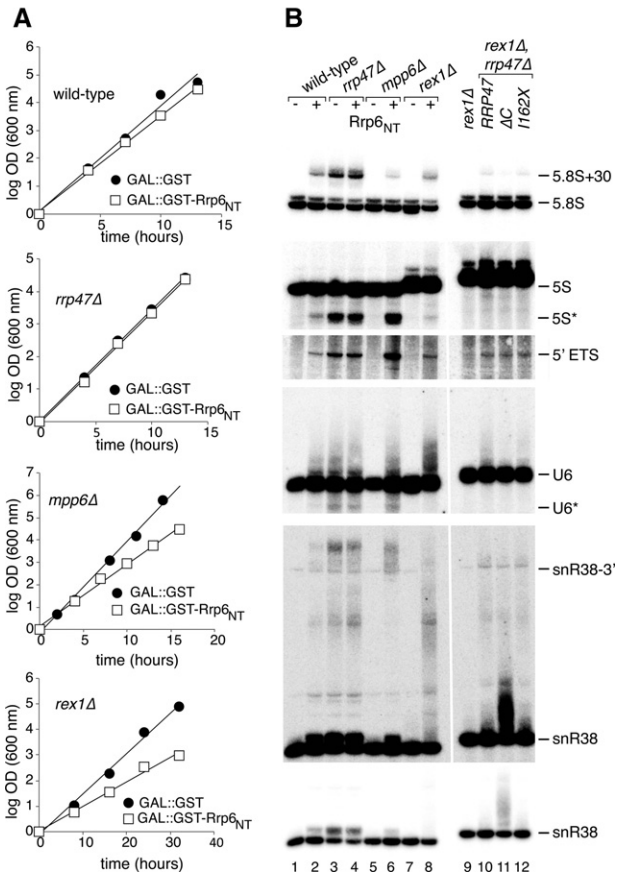

FIGURE 2. Growth rate and RNA analyses of *mpp6Δ* and *rex1Δ* mutants upon Rrp6$_{NT}$ induction. (*A*) Growth rate analyses of wild-type, *rrp47Δ*, *mpp6Δ*, and *rex1Δ* strains after induction of GST or GST-Rrp6$_{NT}$. Cultures were grown in galactose-based minimal medium at 30°C and maintained in early exponential growth by dilution with pre-warmed medium. The increase in OD_{600} is expressed as $\log_2$ values. All plotted lines of best fit have Rf values greater than 0.98. (*B*) Lanes *1–8*, acrylamide gel Northern analyses of RNA from wild-type, *rrp47Δ*, *mpp6Δ*, or *rex1Δ* strains expressing either GST (−) or GST-Rrp6$_{NT}$ (+). RNA was isolated from cultures grown in selective galatose-based medium. Lanes *9–12*, Northern analyses of RNA from a *rex1Δ* mutant and from a *rex1Δ rrp47Δ* mutant expressing either the full-length *RRP47* gene, the *rrp47ΔC* allele, or the *rrp47*$_{I162X}$ allele. RNA was isolated from cultures grown in glucose-based selective minimal medium. The blot was successively hybridized with probes complementary to the RNA species indicated. Identical hybridizations and exposure times are shown for lanes *1–8* and *9–12*.

forms and shorter degradation intermediates of U6 snRNA (the degradation product is denoted U6* in Fig. 2B). A discrete, truncated 5S rRNA fragment was observed (also labeled with an asterisk in Fig. 2B) that was not detected with a probe complementary to the 3′ terminus and, hence, is shortened from the 3′ end; a similarly sized, 3′ truncated 5S rRNA degradation fragment has previously been reported in *rrp44*, *rrp6Δ*, and *trf4* mutants and is proposed to reflect an RNA surveillance substrate (Kadaba et al. 2006; Callahan and Butler 2008).

In contrast to the wild-type strain, induction of GST-Rrp6$_{NT}$ expression in the *rrp47Δ* strain had no significant discernible effect. Thus, GST-Rrp6$_{NT}$ expression induced no detectable Rrp47-independent "off-target" effects in either growth rate or the RNA processing and degradation pathways analyzed.

Notably, induction of GST-Rrp6$_{NT}$ in the *mpp6Δ* mutant caused a greater accumulation of the truncated 5S rRNA and the 5′ ETS fragment than was observed in the *rrp47Δ* mutant, while the 3′ end maturation of 5.8S rRNA was only modestly affected (Fig. 2B; cf. lanes 4–6). This strain also accumulated the U6 snRNA degradation fragments seen in the *rrp47Δ* mutant. Furthermore, hybridization with a probe against the box C/D snoRNA snR38 revealed a specific accumulation of the longest extended forms seen in the *rrp47Δ* mutant. Overexpression of GST-Rrp6$_{NT}$ in the *rex1Δ* mutant largely caused the modest defects observed in the wild-type strain. However, there was a specific accumulation of extended snR38 and snR50 RNAs (Fig. 2B; data not shown).

The data shown in Figures 1 and 2 strongly supports the conclusion that Rrp47 is able to function effectively in Rrp6-dependent RNA processing and degradation pathways when the two proteins are physically uncoupled from one another. We cannot formally eliminate the possibility that the small fraction of Rrp47 that remains associated with full-length Rrp6 upon GST-Rrp6$_{NT}$ induction is sufficient for Rrp47 function. However, further analyses with an *rrp47* mutant detailed below provide additional support for our interpretation. These data also suggest that Rrp47 and Mpp6 function in redundant pathways that largely target RNA for degradation, while Rex1 and Rrp47 are required for redundant pathways that mediate productive processing of snoRNA.

The C-terminal region of Rrp47 is critical for its function when segregated from the catalytic and exosome-binding domains of Rrp6

As noted above, expression of the N-terminal Sas10/C1D domain of Rrp47 complements the synthetic lethality of *rex1Δ rrp47Δ* strains (Costello et al. 2011). We performed Northern analyses on RNA from a *rex1Δ rrp47ΔC* strain, which encodes essentially only the Sas10/C1D domain of Rrp47, and from a *rex1Δ rrp47$_{I162X}$* mutant, which encodes a mutant Rrp47 protein lacking a cluster of basic residues at the C terminus of the protein that is required for RNA binding activity in vitro (Costello et al. 2011). The *rex1Δ rrp47ΔC* double mutant, but not the *rex1Δ rrp47$_{I162X}$* double mutant or either *rex1Δ* or *rrp47Δ* single mutants, showed a strong accumulation of a heterogeneous population of snR38 molecules with short 3′ extensions (Fig. 2B, lane 11). Again, similar results were observed for snR50 (data not shown). Thus, either

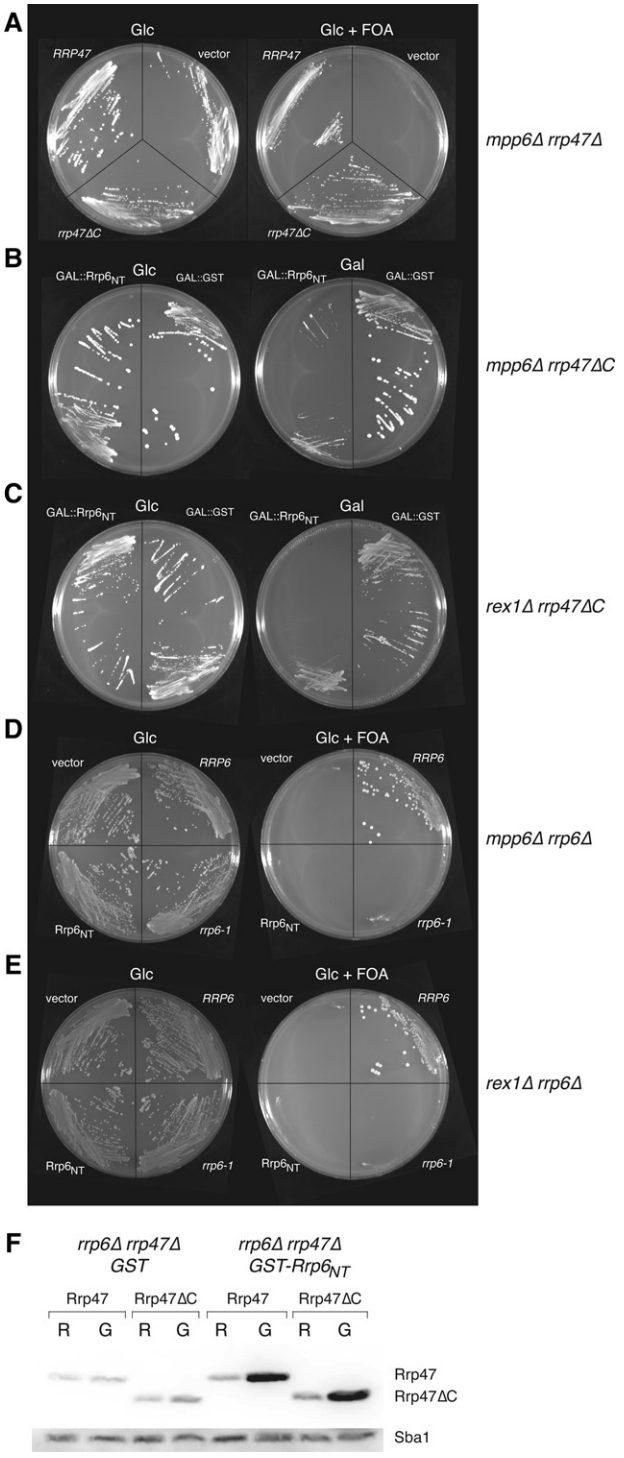

FIGURE 3. (Legend on next page)

segregation of Rrp47 from full-length Rrp6 or deletion of the C-terminal region of Rrp47 causes a specific defect in snoRNA 3′ end maturation in the *rex1Δ* mutant.

The observation that similar snoRNA processing defects are observed in *rex1Δ* mutants expressing the *rrp47ΔC* mutant or upon GST-Rrp6$_{NT}$ induction suggested that the C-terminal region of Rrp47 may be important for the function of the protein when it is segregated from full-length Rrp6. To test this hypothesis, a *rex1Δ rrp47ΔC* double mutant was transformed with plasmids encoding *GAL*-regulated GST or GST-Rrp6$_{NT}$, and the transformants were assayed for growth on glucose- and galactose-based medium. Strikingly, induction of GST-Rrp6$_{NT}$ in the *rex1Δ rrp47ΔC* mutant caused a strong block in growth, while a transformant harboring plasmids encoding *GAL*-regulated GST grew on both glucose- and galactose-based medium (Fig. 3C). A plasmid shuffle assay demonstrated that the *rrp47ΔC* allele also complements the synthetic lethality of the *mpp6Δ rrp47Δ* double mutant (Fig. 3A). Similarly, *mpp6Δ rrp47ΔC* mutants transformed with a plasmid encoding GAL-regulated GST-Rrp6$_{NT}$ showed growth inhibition on galactose-based medium, while the transformant expressing GST grew on both glucose- and galactose-based medium (Fig. 3B).

Since the Rrp47ΔC protein is functional when expressed in a complex with Rrp6 (Costello et al. 2011), these data argue against the interpretation that the residual Rrp47/Rrp6 complex upon GST-Rrp6$_{NT}$ induction is sufficient for growth. Based on previous work (Costello et al. 2011), we envisage that the C-terminal region of Rrp47 engages with RNP substrates of Rrp6 through contacts with protein and/or RNA and promotes their subsequent processing or degradation, even when Rrp47 is divorced from catalytically active Rrp6.

A caveat to this model is that the truncated Rrp47ΔC protein is stably expressed when associated with the GST-Rrp6$_{NT}$ protein. We generated TAP-tagged alleles of full-length Rrp47 and the C-terminal truncated mutant and compared their expression levels in *rrp6Δ* mutants before and after induction of GST-Rrp6$_{NT}$ protein or the GST control (Fig. 3F). As previously observed (Feigenbutz et al. 2013), expression of full-length Rrp47 was increased in the *rrp6Δ* mutant upon expression of the Rrp6$_{NT}$ fusion protein. In contrast, no difference in the Rrp47 expression level was observed upon induction of GST. Importantly, expression of the Rrp47ΔC mutant was increased upon expression of GST-Rrp6$_{NT}$ protein in a comparable manner to that observed for the full-length protein.

Since *rrp6Δ* mutants express very low levels of Rrp47 (Feigenbutz et al. 2013), it is formally possible that the synthetic lethality observed in *rrp6Δ mpp6Δ* and *rrp6Δ rex1Δ* mutants is due to the lack of Rrp47 protein rather than a requirement for Rrp6. We, therefore, tested whether expression of the Rrp6$_{NT}$ domain was sufficient to complement the synthetic lethality of *mpp6Δ rrp6Δ* and *rex1Δ rrp6Δ* mutants, using a plasmid shuffle assay. No complementation was observed upon transformation with a plasmid encoding only the N-terminal region of Rrp6 (Fig. 3, panels D and E). Moreover, the *rrp6-1* mutation also failed to allow growth of the plasmid shuffle strain on 5-FOA medium, whereas complementation was observed for the wild-type *RRP6* gene. Thus, separable activities provided by both Rrp47 and Rrp6 are required in the absence of Mpp6 or Rex1.

FIGURE 3. Full-length Rrp47, but not the Rrp47ΔC mutant, is functional when divorced from the catalytic and exosome-binding domains of Rrp6. (*A–E*) Plate growth assays of yeast strains on permissive glucose-based medium (Glc, *left*-hand side) and on galactose-based medium (Gal) or medium containing 5-FOA (Glc + FOA) (*right*-hand side). Relevant genotypes of the yeast strains are indicated on the *right*. (*A*) Plasmid shuffle assay for complementation of the *mpp6Δ rrp47Δ* strain by the *rrp47ΔC* allele. (*B*) Growth of the *mpp6Δ rrp47ΔC* strain bearing a plasmid encoding either *GAL*-regulated GST or GST-Rrp6$_{NT}$. (*C*) Growth of the *rex1Δ rrp47ΔC* strain bearing a plasmid encoding either *GAL*-regulated GST or GST-Rrp6$_{NT}$. (*D*) Plasmid shuffle assay for complementation of the *mpp6Δ rrp6Δ* mutant by the *rrp6-1* allele or expression of Rrp6$_{NT}$ domain. (*E*) Plasmid shuffle assay for complementation of the *rex1Δ rrp6Δ* mutant by the *rrp6-1* allele or expression of Rrp6$_{NT}$ domain. (*F*) Western analysis of Rrp47 and Rrp47ΔC protein expression. Yeast *rrp6Δ rrp47Δ* strains harboring plasmids expressing C-terminal TAP-tagged fusion proteins of wild-type Rrp47, or the C-terminal truncation mutant and the galactose-inducible GST, or GST-Rrp6$_{NT}$ proteins were lysed under denaturing conditions and analyzed by SDS-PAGE/Western blotting. Rrp47 and Rrp47ΔC fusion proteins were detected with the PAP antibody (*upper* panel). An antiserum against Sba1 was used as a loading control on the same blot (*lower* panel).

Processing and degradation defects in *rrp47 mpp6* and *rrp47 rex1* mutants

To determine the basis of the loss-of-growth phenotypes upon induction of GST-Rrp6$_{NT}$ in the *mpp6Δ rrp47ΔC* and *rex1Δ rrp47ΔC* mutants, changes in the levels of specific RNAs upon transfer from raffinose-based medium to galactose-based medium were assayed by Northern blot hybridization. The analyzed strains also harbored a high-copy-number plasmid encoding the well-characterized *NEL025c* gene (Wyers et al. 2005; Arigo et al. 2006b); a previous study has shown that plasmid-based expression of the *NEL025c* gene recapitulates the expression and degradation pattern of the chromosomal transcripts (Thiebaut et al. 2006). Control strains expressing GST were harvested during growth in raffinose- and galactose-based medium and analyzed in parallel.

The *mpp6Δ rrp47ΔC* mutant showed slowed growth before the fourth doubling after induction of the Rrp6$_{NT}$ domain. Northern hybridization analyses revealed a dramatic accumulation of the *NEL025c* CUT well before this time-point, with the length of the CUT becoming less heterogeneous and shorter after the onset of slow growth (Fig. 4, lanes 4–10). The IGS1-R CUT from the inter-genic region of the rDNA repeat (Houseley et al. 2007; Vasiljeva et al. 2008) also accumulated upon transfer to galactose-based medium, with a strong increase at later time-points. The *mpp6Δ rrp47ΔC* mutant also

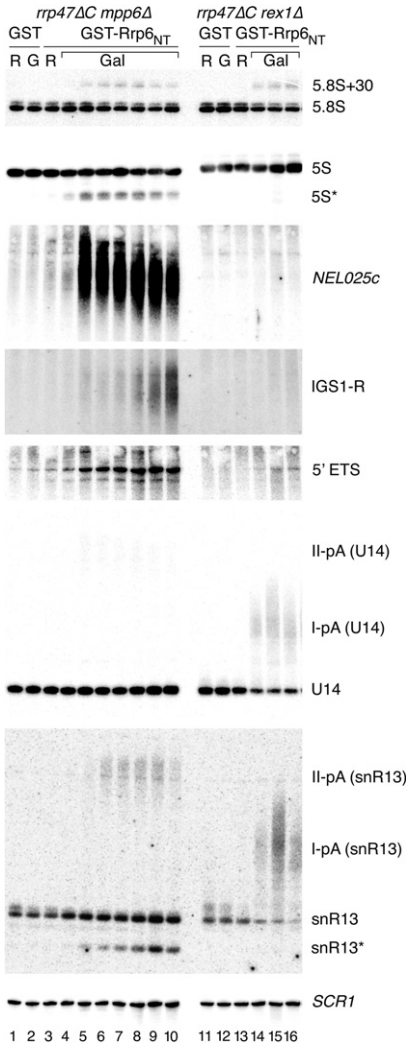

FIGURE 4. Northern analyses of conditional *rrp47 mpp6* and *rrp47 rex1* mutants. RNA was isolated from *mpp6Δ rrp47ΔC* and *rex1Δ rrp47ΔC* mutants expressing GST-Rrp6$_{NT}$ from the *GAL* promoter. Cells were harvested during growth in raffinose-based medium (lanes labeled R) and at each doubling of cell density after transfer to galactose-based medium (lanes labeled Gal). RNA was also isolated from cells expressing *GAL*-regulated GST during growth in raffinose- or galactose-based medium (lanes *1*,*2*,*11*, and *12*; labeled R or G, respectively). RNA was resolved through denaturing acrylamide gels and analyzed by Northern blot hybridization, using probes complementary to the RNAs indicated. Lanes *1–10*, RNA isolated from the *mpp6Δ rrp47ΔC* mutant. Lanes *11–16*, RNA from the *rex1Δ rrp47ΔC* mutant. Asterisks denote truncated fragments of the full-length, mature 5S rRNA, and snR13. Dispersed bands labeled I-pA and II-pA denote snoRNA precursors that are polyadenylated at termination sites I or II, respectively.

showed defects in the degradation of the 5′ ETS fragment and truncated fragments of 5S, snR13, U3, and U6 at early timepoints (Fig. 4; data not shown; truncated 5S and snR13 species are denoted with asterisks in Fig. 4).

Transcription termination of snoRNA genes occurs at a proximal Nrd1-dependent site I and a more distal, "fail-safe" mRNA 3′ processing site II (Steinmetz and Brow 2003; Steinmetz et al. 2006). In *rrp6Δ* mutants, heterogeneous 3′ extended forms of snR13, U14, and snR50 accumulate due to polyadenylation after termination at both sites I and II (Allmang et al. 1999a; van Hoof et al. 2000b; Grzechnik and Kufel 2008), denoted I-pA and II-pA. Hybridization with probes complementary to the snoRNAs U14, snR13, and snR50 revealed that the *mpp6Δ rrp47ΔC* mutant specifically accumulated snoRNAs before inhibition of growth that correspond in length to transcripts terminating at the distal site II (Fig. 4; data not shown; denoted II-pA in Fig. 4). The level of mature snoRNA was not affected. A weak accumulation of the 5.8S + 30 fragment equivalent to that seen upon induction in the presence of full-length Rrp47 was also observed (cf. Figs. 2B and 4). Agarose gel Northern analyses of the *mpp6 rrp47ΔC* mutant revealed the accumulation of a range of apparent pre-rRNA degradation intermediates of diverse sizes upon induction of the Rrp6$_{NT}$ domain that are not seen in *rrp47Δ* or *rrp6Δ* mutants (data not shown). In sum, these data are consistent with the loss of redundant RNA surveillance pathways upon inactivation of both Rrp47 and Mpp6 (Milligan et al. 2008).

The *rex1Δ rrp47ΔC* mutant was impeded in growth more rapidly upon induction of the Rrp6$_{NT}$ domain than the *mpp6Δ rrp47ΔC* mutant, with a clear effect within less than two doublings after transfer to galactose-based medium. There was no clear defect in the degradation of CUTs or truncated stable RNAs in this mutant, and the defects in the processing of the 5.8S + 30 species, U6 processing, or the degradation of the 5′ ETS fragment were equivalent to those seen upon induction of the Rrp6$_{NT}$ domain in the *rex1Δ* mutant expressing full-length Rrp47 (see Fig. 2B). In contrast, there was a striking, rapid depletion of U14, snR13, snR38, and snR50 snoRNAs and an associated accumulation of longer, heterogeneous species corresponding in length to transcripts that are terminated at site I and subsequently polyadenylated (Fig. 4, lanes 13–16; data not shown; denoted I-pA in Fig. 4). These data support the model that normal productive snoRNA synthesis is mediated by termination at site I followed by polyadenylation (Grzechnik and Kufel 2008) and requires either Rrp6 or Rex1 activity for snoRNA 3′ end maturation. In contrast, fail-safe termination at site II generates RNAs that can apparently be targeted to exosome-mediated RNA surveillance by either Rrp6 or an Mpp6-dependent activity. The 5S rRNA and dimeric tRNA^{Arg}-tRNA^{Asp} processing defects of *rex1Δ* mutants (Piper et al. 1983; van Hoof et al. 2000a) were not exacerbated (Fig. 4; data not shown).

Widespread inhibition of the degradation of CUTs and RNA surveillance substrates may well significantly contribute to the block in cell growth. In contrast, it is less obvious how the depletion of snoRNAs could cause rapid growth inhibition. A small number of snoRNAs are essential for viability in yeast and function in pre-rRNA processing (Watkins and Bohnsack 2011). However, agarose gel Northern blot analyses did not reveal a pre-rRNA processing defect upon Rrp6$_{NT}$ induction in the *rex1Δ rrp47ΔC* strain, and conditional ribosome synthesis mutants are slow-acting because the pre-

existing pool of ribosomes must be depleted through growth. We envisage that a significant accumulation of polyadenylated snoRNAs or CUTs could lead to the depletion of the free pool of nuclear poly(A)-binding proteins such as Pab1 and Nab2, or the Nrd1/Nab3 termination complex, and have widespread effects on gene expression profiles.

Our data are consistent with the model that Rrp47 functions in the recognition of Rrp6 substrates, prior to RNA degradation or processing. Rrp47, Rrp6, and the TRAMP component Trf4 have been proposed to promote Nrd1/Nab3-dependent transcription termination (Arigo et al. 2006a; Grzechnik and Kufel 2008; Castelnuovo et al. 2013), in addition to subsequent RNA hydrolysis. We envisage that the Rrp47/Rrp6$_{NT}$ complex, perhaps in combination with TRAMP, retains the ability to recognize Nrd1/Nab3-mediated termination events when separated from full-length Rrp6. Deletion of the C-terminal region of Rrp47, which is known to mediate interactions with RNA and RNA-bound proteins (Costello et al. 2011), would be predicted to weaken this activity and thereby impede subsequent recognition of RNP substrates by Rrp6. In strains expressing the truncated Rrp47 protein bound to full-length Rrp6, substrate recognition may be more effective due to contacts between the TRAMP complex and both Nrd1/Nab3 (Arigo et al. 2006a) and Rrp6 (Callahan and Butler 2010).

The DECOID approach provides a simple method to determine whether proteins that are normally expressed within a complex are able to function when resolved from one another. Most proteins function as part of larger complexes, and the majority of proteins are predicted to be significantly overexpressed when placed under the control of the *GAL* promoter. Use of a neutral N-terminal tag such as GST would generally allow stable expression of individual protein domains. Application of the technique requires only knowledge of the interacting domain within one of the partner proteins. It is of note that we were able to obtain far tighter conditional growth phenotypes using the DECOID strategy than we observed with *GAL::rrp47 rex1Δ* and *GAL::mpp6 rrp47Δ* mutants. Given the accelerating wealth of detailed structural biology data, DECOID could provide a widely applicable, additional approach for the functional dissection of protein complexes.

MATERIALS AND METHODS

Plasmids

The *URA3* marker gene in the *GAL::rrp6*$_{NT}$ construct (p280) (Stead et al. 2007) was inactivated by restriction digestion with ApaI and StuI, treatment with Klenow fragment, and religation. Selection of the resultant plasmid (p601) in yeast was dependent upon the *leu2-d* marker. The *NEL025c* gene was amplified from wild-type yeast genomic DNA using primers o636 (catggatccatatgctgtctttaagcc) and o637 (catgtcgacgaacgtaacgacttttcc) and cloned into the 2μ *URA3* vector pRS426 (Christianson et al. 1992) after digestion with BamHI and SalI, giving p532. The *MPP6* ORF and downstream ~500 nt were amplified from wild-type yeast genomic DNA using primers o597 (acggaattcaatgagtgctaacaatgg) and o598 (cgcaagcttggcgtgcatgagacg) and cloned in-frame into p44 (Mitchell et al. 1996) by digestion with EcoRI and HindIII. The resultant plasmid (p593) encodes an N-terminal Mpp6 protein fusion bearing two copies of the z domain of protein A from *Staphylococcus aureus* that is expressed under the control of the *RRP4* promoter and also bears the *URA3* marker. Analogous constructs expressing a functional N-terminal full-length Rrp6 fusion protein (zz-Rrp6, p263) or *rrp6* mutants expressing only the N-terminal 196 aa residues (Rrp6$_{NT}$, p287) or expressing the catalytically inactive D238N mutant (Burkard and Butler 2000) (p389) have been described (Allmang et al. 1999b; Feigenbutz et al. 2013). Constructs encoding the full-length Rrp47 protein (p262) or a C-terminally truncated mutant that encodes the first 120 aa (denoted Rrp47ΔC) (p293) have also been described previously (Costello et al. 2011). For plasmid shuffle assays, inserts from *RRP6* or *RRP47* constructs were transposed into pRS313 (Sikorski and Hieter 1989), which contains the *HIS3* marker. Plasmids expressing C-terminal TAP-tagged fusion proteins of full-length Rrp47 or the first 120 aa were generated by homologous recombination in yeast, as follows. The pRS313-based *RRP47* genomic clone p425 was linearized downstream from the *RRP47* ORF by digestion with SalI and transformed into an *rrp6Δ rrp47Δ* strain, together with amplicons generated from pBS1479 (Puig et al. 2001) that comprise the TAP tag and the downstream *TRP1* marker into an *rrp6Δ rrp47Δ* strain harboring the *GAL::rrp6*$_{NT}$ construct. PCR was performed using the reverse primer o879 (tataagcatttttgcatttgtgctctcacatcacctttaatc tacgactcactataggg) and the forward primer o878 (aaaagtaaaagattgg ataaagttggaaaaaagaaaggagggaagaagtccatggaaaagagaag) or o877 (cagg cagagcaagaaaaagctaagaatatcatttccaatgttttggactccatggaaaagagaag) for the full-length clone (p670) or truncated clone (p671), respectively. Transformants were isolated on selective medium and screened for expression of the zz fusion protein by Western analyses. Positive clones were recovered from yeast and confirmed by sequence analysis of the ORF/TAP tag junction.

Strains

Strains were grown at 30°C in selective medium comprising 2% glucose, raffinose, or galactose, 0.5% ammonium sulphate, and 0.17% yeast nitrogen base, supplemented with appropriate amino acids and bases. Isogenic wild-type, *rrp47Δ::kanMX4*, *rex1Δ::kanMX4*, and *mpp6Δ::kanMX4* strains were obtained from Euroscarf (University of Frankfurt, Germany). The *rrp47Δ::kanMX4* disruption allele was converted to an *rrp47Δ::hphMX4* allele by PCR-mediated homologous recombination of the *rrp47Δ::kanMX4* recipient strain, using the hygromycin B resistance gene in plasmid pAG32 (Goldstein and McCusker 1999). An *mpp6 rrp47* plasmid shuffle strain was generated by transforming the *mpp6Δ::kanMX4* strain with the *MPP6* expression construct p593 and disruption of the *RRP47* gene by transposing the *rrp47Δ::hphMX4* allele. The *mpp6Δ rrp6Δ* and *rex1Δ rrp6Δ* shuffle strains were made by targeting the *kanMX4* cassette to the *MPP6* or *REX1* locus in an *rrp6Δ::TRP1* strain bearing the plasmid p263, which encodes the zz-Rrp6 fusion protein and the *URA3* gene (Allmang et al. 1999b). The *rrp6Δ::kanMX4 rrp47Δ::hphMX4* strain was generated by PCR-mediated gene disruption of the *RRP6* locus in the *rrp47Δ::hphMX4* strain. Csl4-TAP and Rrp6-TAP strains were obtained from Open Biosystems. The

rrp47-zz, *rrp47-GFP*, and *rrp47-GFP::HIS3 rrp6Δ::kanMX4* strains have been described (Mitchell et al. 2003; Feigenbutz et al. 2013). The chromosomally encoded Csl4-TAP, Rrp6-TAP, Rrp47-zz, and Rrp47-GFP fusion protein and the plasmid-encoded Rrp47-TAP fusion proteins were expressed from their homologous promoters. Expression of the plasmid-encoded zz-Rrp6 fusion protein, which is driven from the *RRP4* promoter, is comparable to that of the Rrp6-TAP fusion protein (Stead et al. 2007).

RNA analyses

For $Rrp6_{NT}$ induction analyses, cultures were harvested during growth in permissive, raffinose-based medium and upon every doubling of OD_{600} after transfer to medium containing 2% galactose. RNA was isolated by glass bead extraction in the presence of phenol and guanidinium isothiocyanate (Tollervey and Mattaj 1987). Total cellular RNA was resolved through 8% polyacrylamide gels containing 50% urea or 1.2% agarose gels and transferred to Hybond-N^+ (GE Healthcare) for hybridization analyses. The sequences of the oligonucleotide probes used were as follows: 5.8S, gcgttgttcatc gatgc; 5S, ctactcggtcaggctc; 5′ ETS, cgctgctcaccaatgg; U6, atctctgtatt gtttcaaattgaccaa; snR38, gagaggttacctattattacccattcagacagggataactg; *NEL025c*, ggcttctacagaacaagttgtatcgaaatgattgttggcgac; IGS1-R, gatg taagagacaagtgaacagtgaacagtgaacagtggggaca; U14, tcactcagacatcctagg; snR13 3′, ggtcagataaaagtaaaaaaaggtagc; *SCR1*, aaggacccagaactaccttg. Hybridized blots were placed under phosphor storage screens, analyzed using a Personal Molecular Imager FX machine (BioRad), and nonsaturated images were obtained using the ImageJ64 package (NIH).

Protein analyses

Yeast cell extracts for gradient centrifugation analyses and pull-down assays were made by glass bead disruption in TMN150 buffer (10 mM Tris, pH 7.6, 150 mM NaCl, 5 mM $MgCl_2$, 1 mM PMSF) (Mitchell et al. 1996), while the protein expression analyses in Figure 3 were done on alkaline denatured cell lysates (Motley et al. 2012). Samples were analyzed by Western blotting, using the peroxidase-antiperoxidase conjugate (PAP, Sigma), mouse anti-GFP (Roche), mouse anti-Pgk1 (Invitrogen), rabbit anti-GST (Sigma), and rabbit anti-Sba1 (Mollapour and Piper 2012) primary antibodies, and HRP-conjugated goat anti-mouse (BioRad) or anti-rabbit (Sigma) secondary antibodies. Proteins were detected by ECL and visualized using a G:Box iChemi XL system running GeneSnap and GeneTools software packages (Syngene).

For sedimentation analyses, the *rrp47-GFP* strain was transformed with plasmids encoding either GST or GST-$Rrp6_{NT}$ under the control of the *GAL* promoter. Strains were grown in galactose-based medium, and cell lysates were resolved through 12 mL 10%–30% glycerol gradients in TMN150 buffer at 36,000 rpm for 24 h using an SW40 rotor (Beckman Coulter). 0.65 mL fractions were collected and analyzed by Western blotting. Protein markers (BSA, 4.6 S; chicken ovalbumin, 3.6 S; bovine catalase, 11.3 S) (Erickson 2009) were resolved in parallel gradients. Protein profiles of glycerol gradients were routinely assessed by SDS-PAGE analysis of the fractions and staining with InstantBlue colloidal Coomassie Blue stain (Expedion).

For $Rrp6_{NT}$ pull-down experiments, yeast strains expressing Rrp47-zz, Rrp6-TAP, or Csl4-TAP fusion proteins were transformed with a plasmid expressing *GAL*-driven GST-$Rrp6_{NT}$ and grown in galactose-based medium. Clarified lysates were passed over glutathione beads, and retained protein was eluted with lysis buffer containing 25 mM glutathione. For the Rrp6 pull-down experiments, the *rrp47-GFP::HIS3 rrp6Δ::kanMX4* strain was transformed with plasmids encoding zz-Rrp6 and either GAL-driven GST or GST-$Rrp6_{NT}$. Cell extracts were initially fractionated by binding with SP sepharose beads; retained protein was eluted with buffer containing 500 mM NaCl. After adding NaCl to the flow-though fraction to a final concentration of 500 mM, both flow-through and eluate fractions were incubated with IgG sepharose beads (GE Healthcare) to trap Rrp6 complexes. The beads were washed with buffer containing 500 mM NaCl, and retained protein was recovered by elution with 0.5 M acetic acid and lyophilized.

ACKNOWLEDGMENTS

This work was supported by a grant from the Wellcome Trust to P. M. (08836/Z/09/Z) and BBSRC-funded PhD studentships to W.G. and M.T. We thank Stefan Millson and Peter Piper (University of Sheffield) for the Sba1 antibody.

Received March 29, 2013; accepted August 7, 2013.

REFERENCES

Allmang C, Kufel J, Chanfreau G, Mitchell P, Petfalski E, Tollervey D. 1999a. Functions of the exosome in rRNA, snoRNA and snRNA synthesis. *EMBO J* **18:** 5399–5410.

Allmang C, Petfalski E, Podtelejnikov A, Mann M, Tollervey D, Mitchell P. 1999b. The yeast exosome and human PM–Scl are related complexes of 3′→5′ exonucleases. *Genes Dev* **13:** 2148–2158.

Arigo JT, Carroll KL, Ames JM, Corden JL. 2006a. Regulation of yeast *NRD1* expression by premature transcription termination. *Mol Cell* **21:** 641–651.

Arigo JT, Eyler DE, Carroll KL, Corden JL. 2006b. Termination of cryptic unstable transcripts is directed by yeast RNA-binding proteins Nrd1 and Nab3. *Mol Cell* **23:** 841–851.

Assenholt J, Mouaikel J, Andersen KR, Brodersen DE, Libri D, Jensen TH. 2008. Exonucleolysis is required for nuclear mRNA quality control in yeast THO mutants. *RNA* **14:** 2305–2313.

Bonneau F, Basquin J, Ebert J, Lorentzen E, Conti E. 2009. The yeast exosome functions as a macromolecular cage to channel RNA substrates for degradation. *Cell* **139:** 547–559.

Burkard KT, Butler JS. 2000. A nuclear 3′-5′ exonuclease involved in mRNA degradation interacts with Poly(A) polymerase and the hnRNA protein Npl3p. *Mol Cell Biol* **20:** 604–616.

Callahan KP, Butler JS. 2008. Evidence for core exosome independent function of the nuclear exoribonuclease Rrp6p. *Nucleic Acids Res* **36:** 6645–6655.

Callahan KP, Butler JS. 2010. TRAMP complex enhances RNA degradation by the nuclear exosome component Rrp6. *J Biol Chem* **285:** 3540–3547.

Castelnuovo M, Rahman S, Guffanti E, Infantino V, Stutz F, Zenklusen D. 2013. Bimodal expression of *PHO84* is modulated by early termination of antisense transcription. *Nat Struct Mol Biol* **20:** 851–858.

Chlebowski A, Lubas M, Jensen TH, Dziembowski A. 2013. RNA decay machines: The exosome. *Biochim Biophys Acta***1829:** 552–560.

Christianson TW, Sikorski RS, Dante M, Shero JH, Hieter P. 1992. Multifunctional yeast high-copy-number shuttle vectors. *Gene* **110:** 119–122.

Costello JL, Stead JA, Feigenbutz M, Jones RM, Mitchell P. 2011. The C-terminal region of the exosome-associated protein Rrp47 is

specifically required for box C/D small nucleolar RNA 3′-maturation. *J Biol Chem* **286:** 4535–4543.
Erickson HP. 2009. Size and shape of protein molecules at the nanometer level determined by sedimentation, gel filtration, and electron microscopy. *Biol Proced Online* **11:** 32–51.
Feigenbutz M, Jones R, Besong TMD, Harding SE, Mitchell P. 2013. Assembly of the yeast exoribonuclease Rrp6 with its associated cofactor Rrp47 occurs in the nucleus and is critical for the controlled expression of Rrp47. *J Biol Chem* **288:** 15959–15970.
Goldstein AL, McCusker JH. 1999. Three new dominant drug resistance cassettes for gene disruption in *Saccharomyces cerevisiae*. *Yeast* **15:** 1541–1553.
Grzechnik P, Kufel J. 2008. Polyadenylation linked to transcription termination directs the processing of snoRNA precursors in yeast. *Mol Cell* **32:** 247–258.
Gudipati RK, Xu Z, Lebreton A, Séraphin B, Steinmetz LM, Jacquier A, Libri D. 2012. Extensive degradation of RNA precursors by the exosome in wild-type cells. *Mol Cell* **48:** 409–421.
Houseley J, Tollervey D. 2009. The many pathways of RNA degradation. *Cell* **136:** 763–776.
Houseley J, Kotovic K, Hage El A, Tollervey D. 2007. Trf4 targets ncRNAs from telomeric and rDNA spacer regions and functions in rDNA copy number control. *EMBO J* **26:** 4996–5006.
Kadaba S, Wang X, Anderson JT. 2006. Nuclear RNA surveillance in *Saccharomyces cerevisiae*: Trf4p-dependent polyadenylation of nascent hypomethylated tRNA and an aberrant form of 5S rRNA. *RNA* **12:** 508–521.
LaCava J, Houseley J, Saveanu C, Petfalski E, Thompson E, Jacquier A, Tollervey D. 2005. RNA degradation by the exosome is promoted by a nuclear polyadenylation complex. *Cell* **121:** 713–724.
Liu Q, Greimann JC, Lima CD. 2006. Reconstitution, activities, and structure of the eukaryotic RNA exosome. *Cell* **127:** 1223–1237.
Makino DL, Baumgärtner M, Conti E. 2013. Crystal structure of an RNA-bound 11-subunit eukaryotic exosome complex. *Nature* **495:** 70–75.
Milligan L, Decourty L, Saveanu C, Rappsilber J, Ceulemans H, Jacquier A, Tollervey D. 2008. A yeast exosome cofactor, Mpp6, functions in RNA surveillance and in the degradation of noncoding RNA transcripts. *Mol Cell Biol* **28:** 5446–5457.
Mitchell P, Petfalski E, Tollervey D. 1996. The 3′ end of yeast 5.8S rRNA is generated by an exonuclease processing mechanism. *Genes Dev* **10:** 502–513.
Mitchell P, Petfalski E, Shevchenko A, Mann M, Tollervey D. 1997. The exosome: A conserved eukaryotic RNA processing complex containing multiple 3′→5′ exoribonucleases. *Cell* **91:** 457–466.
Mitchell P, Petfalski E, Houalla R, Podtelejnikov A, Mann M, Tollervey D. 2003. Rrp47p is an exosome-associated protein required for the 3′ processing of stable RNAs. *Mol Cell Biol* **23:** 6982–6992.
Mollapour M, Piper PW. 2012. Activity of the yeast zinc-finger transcription factor War1 is lost with alanine mutation of two putative phosphorylation sites in the activation domain. *Yeast* **29:** 39–44.
Motley AM, Nuttall JM, Hettema EH. 2012. Pex3-anchored Atg36 tags peroxisomes for degradation in *Saccharomyces cerevisiae*. *EMBO J* **31:** 2852–2868.
Ozanick SG, Wang X, Costanzo M, Brost RL, Boone C, Anderson JT. 2009. Rex1p deficiency leads to accumulation of precursor initiator $tRNA^{Met}$ and polyadenylation of substrate RNAs in *Saccharomyces cerevisiae*. *Nucleic Acids Res* **37:** 298–308.
Peng WT, Robinson MD, Mnaimneh S, Krogan NJ, Cagney G, Morris Q, Davierwala AP, Grigull J, Yang X, Zhang W, et al. 2003. A panoramic view of yeast noncoding RNA processing. *Cell* **113:** 919–933.
Piper PW, Bellatin JA, Lockheart A. 1983. Altered maturation of sequences at the 3′ terminus of 5S gene transcripts in a *Saccharomyces cerevisiae* mutant that lacks a RNA processing endonuclease. *EMBO J* **2:** 353–359.
Puig O, Caspary F, Rigaut G, Rutz B, Bouveret E, Bragado-Nilsson E, Wilm M, Séraphin B. 2001. The tandem affinity purification (TAP) method: A general procedure of protein complex purification. *Methods* **24:** 218–229.
Schilders G, van Dijk E, Pruijn GJM. 2007. C1D and hMtr4p associate with the human exosome subunit PM/Scl-100 and are involved in pre-rRNA processing. *Nucleic Acids Res* **35:** 2564–2572.
Schneider C, Kudla G, Wlotzka W, Tuck A, Tollervey D. 2012. Transcriptome-wide analysis of exosome targets. *Mol Cell* **48:** 422–433.
Sikorski RS, Hieter P. 1989. A system of shuttle vectors and yeast host strains designed for efficient manipulation of DNA in *Saccharomyces cerevisiae*. *Genetics* **122:** 19–27.
Stead JA, Costello JL, Livingstone MJ, Mitchell P. 2007. The PMC2NT domain of the catalytic exosome subunit Rrp6p provides the interface for binding with its cofactor Rrp47p, a nucleic acid-binding protein. *Nucleic Acids Res* **35:** 5556–5567.
Steinmetz EJ, Brow DA. 2003. Ssu72 protein mediates both poly(A)-coupled and poly(A)-independent termination of RNA polymerase II transcription. *Mol Cell Biol* **23:** 6339–6349.
Steinmetz EJ, Conrad NK, Brow DA, Corden JL. 2001. RNA-binding protein Nrd1 directs poly(A)-independent 3′-end formation of RNA polymerase II transcripts. *Nature* **413:** 327–331.
Steinmetz EJ, Ng SBH, Cloute JP, Brow DA. 2006. *cis*- and *trans*-Acting determinants of transcription termination by yeast RNA polymerase II. *Mol Cell Biol* **26:** 2688–2696.
Thiebaut M, Kisseleva-Romanova E, Rougemaille M, Boulay J, Libri D. 2006. Transcription termination and nuclear degradation of cryptic unstable transcripts: A role for the Nrd1-Nab3 pathway in genome surveillance. *Mol Cell* **23:** 853–864.
Tollervey D, Mattaj IW. 1987. Fungal small nuclear ribonucleoproteins share properties with plant and vertebrate U-snRNPs. *EMBO J* **6:** 469–476.
van Hoof A, Lennertz P, Parker R. 2000a. Three conserved members of the RNase D family have unique and overlapping functions in the processing of 5S, 5.8S, U4, U5, RNase MRP and RNase P RNAs in yeast. *EMBO J* **19:** 1357–1365.
van Hoof A, Lennertz P, Parker R. 2000b. Yeast exosome mutants accumulate 3′-extended polyadenylated forms of U4 small nuclear RNA and small nucleolar RNAs. *Mol Cell Biol* **20:** 441–452.
Vanacova S, Wolf J, Martin G, Blank D, Dettwiler S, Friedlein A, Langen H, Keith G, Keller W. 2005. A new yeast poly(A) polymerase complex involved in RNA quality control. *PLoS Biol* **3:** e189.
Vasiljeva L, Buratowski S. 2006. Nrd1 interacts with the nuclear exosome for 3′ processing of RNA polymerase II transcripts. *Mol Cell* **21:** 239–248.
Vasiljeva L, Kim M, Terzi N, Soares LM, Buratowski S. 2008. Transcription termination and RNA degradation contribute to silencing of RNA polymerase II transcription within heterochromatin. *Mol Cell* **29:** 313–323.
Wasmuth EV, Lima CD. 2012. Exo- and endoribonucleolytic activities of yeast cytoplasmic and nuclear RNA exosomes are dependent on the noncatalytic core and central channel. *Mol Cell* **48:** 133–144.
Watkins NJ, Bohnsack MT. 2011. The box C/D and H/ACA snoRNPs: Key players in the modification, processing and the dynamic folding of ribosomal RNA. *WIREs RNA* **3:** 397–414.
Wolin SL, Sim S, Chen X. 2012. Nuclear noncoding RNA surveillance: Is the end in sight? *Trends Genet* **28:** 306–313.
Wyers F, Rougemaille M, Badis G, Rousselle J-C, Dufour M-E, Boulay J, Régnault B, Devaux F, Namane A, Séraphin B, et al. 2005. Cryptic pol II transcripts are degraded by a nuclear quality control pathway involving a new poly(A) polymerase. *Cell* **121:** 725–737.

Appendix IV. Feigenbutz M., Garland, W., Turner, M., Mitchell, P., 2013a. The Exosome Cofactor Rrp47 Is Critical for the Stability and Normal Expression of Its Associated Exoribonuclease Rrp6 in Saccharomyces cerevisiae. PLoS ONE 8, e80752

OPEN ACCESS Freely available online

PLOS ONE

The Exosome Cofactor Rrp47 Is Critical for the Stability and Normal Expression of Its Associated Exoribonuclease Rrp6 in *Saccharomyces cerevisiae*

Monika Feigenbutz, William Garland, Martin Turner, Phil Mitchell*

Molecular Biology and Biotechnology Department, The University of Sheffield, Sheffield, United Kingdom

Abstract

Rrp6 is a conserved catalytic subunit of the eukaryotic nuclear exosome ribonuclease complex that functions in the productive 3' end maturation of stable RNAs, the degradation of transiently expressed noncoding transcripts and in discard pathways that eradicate the cell of incorrectly processed or assembled RNAs. The function of Rrp6 in these pathways is at least partially dependent upon its interaction with a small nuclear protein called Rrp47/Lrp1, but the underlying mechanism(s) by which Rrp47 functions in concert with Rrp6 are not established. Previous work on yeast grown in rich medium has suggested that Rrp6 expression is not markedly reduced in strains lacking Rrp47. Here we show that Rrp6 expression in *rrp47*Δ mutants is substantially reduced during growth in minimal medium through effects on both transcript levels and protein stability. Exogenous expression of Rrp6 enables normal levels to be attained in *rrp47*Δ mutants. Strikingly, exogenous expression of Rrp6 suppresses many, but not all, of the RNA processing and maturation defects observed in an *rrp47*Δ mutant and complements the synthetic lethality of *rrp47*Δ *mpp6*Δ and *rrp47*Δ *rex1*Δ double mutants. Increased Rrp6 expression in the resultant *rrp47*Δ *rex1*Δ double mutant suppresses the defect in the 3' maturation of box C/D snoRNAs. In contrast, increased Rrp6 expression in the *rrp47*Δ *mpp6*Δ double mutant diminishes the block in the turnover of CUTs and in the degradation of the substrates of RNA discard pathways. These results demonstrate that a principal function of Rrp47 is to facilitate appropriate expression levels of Rrp6 and support the conclusion that the Rrp6/Rrp47 complex and Rex1 provide redundant exonuclease activities for the 3' end maturation of box C/D snoRNAs.

Citation: Feigenbutz M, Garland W, Turner M, Mitchell P (2013) The Exosome Cofactor Rrp47 Is Critical for the Stability and Normal Expression of Its Associated Exoribonuclease Rrp6 in *Saccharomyces cerevisiae*. PLoS ONE 8(11): e80752. doi:10.1371/journal.pone.0080752

Editor: Sander Granneman, Univ. of Edinburgh, United Kingdom

Received August 2, 2013; **Accepted** October 15, 2013; **Published** November 5, 2013

Copyright: © 2013 Feigenbutz et al. This is an open-access article distributed under the terms of the Creative Commons Attribution License, which permits unrestricted use, distribution, and reproduction in any medium, provided the original author and source are credited.

Funding: This work was funded by research grant 08836/Z/09/Z from the Wellcome Trust (www.wellcome.ac.uk) and BBSRC-funded PhD studentships to WG and MT. The funders had no role in study design, data collection and analysis, decision to publish, or preparation of the manuscript.

Competing interests: The authors have declared that no competing interests exist.

* E-mail: p.j.mitchell@shef.ac.uk

Introduction

Ribonucleases are of fundamental importance for the expression of both coding and non-coding RNA in all cells. All characterised RNA transcripts are generated from longer precursor molecules through processing reactions involving the nuclease activities of exo- and/or endonucleases. Furthermore, the large amount of RNA fragments that are released as by-products of such processing reactions, such as pre-mRNA introns, must be degraded. The ultimate degradation of mRNA in the cytoplasm is also an essential biological process, individual mRNAs being degraded at transcript-specific rates that contribute to the expression levels of each gene [1]. Furthermore, both coding and non-coding RNAs are subjected to quality control systems that degrade incorrectly processed or assembled ribonucleoprotein (RNP) particles [2]. There is a substantial flux through such RNA surveillance pathways, even in normal healthy cells [3,4].

A major source of 3' →5' exoribonuclease activity in eukaryotic cells is the exosome RNase complex, which plays key roles in both the productive 3' end processing of precursor transcripts to their mature RNAs, and in the complete degradation of RNAs that are targeted to RNA discard pathways [5]. The exosome was initially identified as a nuclease complex that functions in the 3' end maturation of 5.8S rRNA, snoRNAs and snRNAs [6,7] and subsequently shown to function in cytoplasmic mRNA turnover, and in nuclear and cytoplasmic RNA surveillance pathways for both coding and non-coding RNAs. In addition, the analysis of RNA from yeast strains compromised in exosome activity allowed the discovery of a new class of low abundance RNAs known as cryptic unstable transcripts (CUTs) [8-10].

The exosome has two associated catalytic subunits, Rrp44 (also known as Dis3) and Rrp6. Yeast and mammalian Rrp44 is found exclusively associated with the exosome complex [11,12]. Rrp44 belongs to the RNase R/RNase II family of exoribonucleases [13] but is restricted to eukaryotes and contains an additional N-terminal PIN domain that has endonuclease activity [14-16]. Rrp44 has a highly processive hydrolytic exonuclease activity when expressed as a recombinant protein [6] but shows a largely reduced activity when associated with the exosome core complex [17]. Interaction with the exosome is through the N-terminal PIN domain of Rrp44 and the exosome core subunits Rrp41 and Rrp45 [16,18]. The core of the exosome structure functions to channel the RNA substrate to the active site of the Rrp44 exonuclease [19]. Rrp6 is related to the RNase D family of exonucleases [20] that have a "DEDD" catalytic domain named after four highly conserved acidic residues that coordinate the binding of two metal cations required for catalysis [21,22]. The *RRP6* gene was originally cloned by complementation of a catalytically inactive allele (*rrp6-1*) that contains an asparagine in place of the conserved D238 residue [23,24]. In addition to the catalytic domain, Rrp6 also has an N-terminal PMC2NT domain, a central HRDC domain and a C-terminal region that is required for its association with the exosome. Loss of interaction with the exosome has little effect on the ability of Rrp6 to function in RNA processing or RNA degradation pathways [25]. However, association of Rrp6 with the exosome allosterically stimulates the activity of Rrp44 [19,26].

RNA analyses have revealed that most Rrp6-mediated RNA processing and degradation pathways are impeded in strains lacking the nuclear RNA-binding protein Rrp47 (also known as Lrp1) [11]. Rrp47 directly interacts with the PMC2NT domain of Rrp6 through its N-terminal Sas10/C1D domain, while the C-terminal region of the protein is required for RNA binding activity and contributes to substrate recognition [27,28]. Another RNA-binding protein, Mpp6, interacts with exosome complexes and has been proposed to stimulate the activity of Rrp44 [29] or to promote the functional coupling between Rrp6 and the TRAMP/exosome complexes [30]. Strains lacking Rrp6 or Rrp47 are synthetic lethal with *mpp6*Δ mutants, probably reflecting a degree of functional redundancy between the Rrp6 and Rrp44 enzymes [3,31]. Similarly, *rrp6*Δ and *rrp47*Δ mutants are also synthetic lethal with mutants lacking Rex1, another RNase D-related 3'→5' exoribonuclease [32,33].

Cellular ribonucleases represent effective modulators of changes in gene expression profiles. However, little data is available concerning how these enzymes might be regulated in response to changes in physiological conditions or as a result of developmental programmes. Rrp6 expression in diploid yeast is decreased upon shift from fermentation to respiration, and further depleted upon entry into meiosis. This fluctuation of Rrp6 expression occurs without a significant alteration in *RRP6* mRNA levels, indicative of a post-transcriptional mode of regulation [34]. Furthermore, both the *RRP6* and *RRP47* genes are potentially regulated by transcription factors that modulate gene expression in response to nutrient availability or stress [35-37]. In prokaryotes, the 3'→5' exoribonucleases RNase II and RNase R are both regulated in response to nutrient availability at the level of protein stability. Notably, RNase II protein levels are decreased upon shift from rich medium to minimal medium in a manner dependent upon the protein Gmr [38]. In contrast, RNase R is a highly unstable protein during growth in rich medium and its expression is induced by protein stabilisation upon entry into the stationary phase or upon cold shock [39]. RNase R instability during rapid growth is mediated by acetylation and involves its interaction with the SmpB/tmRNA trans-translation complex [40,41]. The SmpB mRNA accumulates in the absence of RNase R, indicative of a mutually dependent regulation of expression [42].

We have recently reported that the absence of Rrp6 has a profound effect on the stability of its associated protein Rrp47, without a substantial change in transcript levels [43]. Previous studies on cultures in rich medium suggested Rrp6 expression levels are not markedly affected in strains lacking Rrp47 [11,27]. Here we report that Rrp6 levels are decreased substantially in the absence of Rrp47 during growth in minimal medium, reflecting both a decrease in protein stability and *RRP6* transcript abundance. Overexpression of Rrp6 suppressed RNA processing and degradation defects observed in the *rrp47*Δ mutant and complemented the synthetic lethality of *rrp47*Δ *mpp6*Δ and *rrp47*Δ *rex1*Δ double mutants. Furthermore, analyses of RNA from the *rrp47*Δ *mpp6*Δ and *rrp47*Δ *rex1*Δ double mutants are consistent with studies proposing that either the Rrp6/Rrp47 complex or an Mpp6-dependent activity is required for RNA surveillance pathways and the degradation of CUTs, while the Rrp6/Rrp47 complex and Rex1 provide redundant activities for the 3' maturation of box C/D snoRNAs [29,44].

Materials and Methods

Plasmids

The plasmid expressing an N-terminal Rrp6 fusion protein (zz-Rrp6) with two copies of the z domain of protein A from *Staphylococcus aureus* (p263) has been described previously [45]. This construct expresses the Rrp6 fusion protein from the *RRP4* promoter. An analogous *MPP6* construct has been recently reported [44]. Mutant variants of the *RRP6* construct that express the catalytically inactive *rrp6-1* (D238N) derivative (p389) [24] or just the N-terminal domain truncation (L197X) (p287) were generated by site directed mutagenesis with appropriate primers [43]. A genomic clone of the *RRP6* gene encompassing approximately 400 nucleotides up- and downstream of the ORF (p436) was constructed by amplification of the *RRP6* locus from wild-type genomic DNA by PCR using Vent DNA polymerase and primers o457 (cagtctagacttcgagatgagcttg) and o458 (gctgggcccacctcagtattacagc), and cloning into pRS416 (*URA3* marker) as an *Xba*I-*Eco*RI fragment [46] (the *Eco*RI site is genomically encoded). The *RRP6* promoter region contains the *CEN* element of chromosome 15. To prevent recombination of plasmids containing the genomic *RRP6* sequence during growth in yeast due to the presence of two *CEN* elements, the *CEN6* element within the vector backbone was deleted by site-directed mutagenesis. *Hpa*I sites were introduced either side of the *CEN6* element using the sense primers o839

(gttggcgatccccctagagtcgttaacatcttcggaaaacaaaaactat) and o841 (aattatttttatagcacgtgatgttaacgacccaggtggcacttttcgg) and the intervening sequence was deleted by restriction digestion and religation. A genomic clone of the *RRP47* gene [28] was generated by PCR amplification of wild-type genomic DNA using the primers o191 (aaactcgaggaactgactactga) and o192 (aaagagctcaaactttcgctgg), and the product was cloned into pRS416 as a *Xho*I-*Sac*I fragment. High copy number derivatives of these plasmids were generated by subcloning the inserts into the 2 micron plasmids pRS424 (*TRP1* marker), pRS425 (*LEU2* marker) and pRS426 (*URA3* marker) [47] using appropriate restriction enzymes. *RRP6* and *RRP47* alleles were also subcloned into pRS314 (*TRP1* marker) for plasmid shuffle assays in the *rex1*Δ *rrp47*Δ strain, and into pRS313 (*HIS3* marker) or pRS415 (*LEU2* marker) for plasmid shuffle assays in the *mpp6*Δ *rrp47*Δ strain.

Strains

Strains were grown at 30 ° C in YPD medium (2 % glucose, 2 % bactopeptone, 1 % yeast extract) or in selective minimal growth medium, comprising 2 % glucose, 0.5 % ammonium sulphate, 0.17 % yeast nitrogen base and the appropriate amino acids and bases. Plasmid shuffle assays were performed on complete minimal medium containing 50 µg/ml uracil and 1 mg/ml 5-flouro-orotic acid (5 FOA) (Melford Laboratories). Colonies recovered from 5 FOA plates were streaked out on appropriate selective solid medium and shown to be cured of the parental *RRP47* or *MPP6* plasmids by lack of growth on SD medium lacking uracil.

For spot growth assays, precultures were diluted to a standard OD at 600 nm and then 10-fold serially diluted with fresh medium. Aliquots were applied to the surface of minimal medium plates and incubated at 30 °C for 3 days. Cells were harvested from liquid medium cultures at OD at 600 nm of less than 1.0 for protein analyses, or less than 0.5 for RNA analyses.

Strains expressing the C-terminal Rrp47-zz fusion protein, with or without the *rrp6*Δ*::TRP1* allele, have been described previously [11]. Yeast *rrp47*Δ*::KANMX4*, *mpp6*Δ*::KANMX4* and *rex1*Δ*::KANMX4* deletion strains were obtained from Euroscarf (University of Frankfurt, Germany). The *rrp47*Δ*::KANMX4* allele was introduced into the *rrp6-TAP::HIS3* strain (Thermo Fisher Scientific) by PCR-mediated homologous recombination, as described [43]. The *mpp6*Δ*::KANMX4 rrp47::hphMX4* double mutant was made by converting the *KANMX4* marker in the *rrp47::KANMX4* strain to the *hphMX4* marker, using the plasmid pAG32 [48], and then targeting the *RRP47* locus of the *mpp6*Δ strain by PCR-mediated integration after transformation with a plasmid encoding a functional *MPP6* gene. The *rex1*Δ*::KANMX4 rrp47*Δ*::KANMX4* double mutant strain has been described previously [28] and was made by crossing *rex1*Δ and *rrp47*Δ single mutants, transforming the diploid strain with a plasmid encoding a wild-type copy of the *RRP47* gene, and isolating meiotic progeny bearing both null alleles. Strains expressing the plasmid-borne zz-Rrp6 fusion protein as the sole form of the protein and lacking either the *MPP6* or *REX1* gene have been recently reported [44].

Protein Analyses

Cell extracts were prepared under alkaline denaturing conditions to minimise protein degradation [49]. Translational shut-off experiments were performed by addition of cycloheximide to a final concentration of 100 µg/ml and aliquots of the culture were harvested at 10 minute intervals thereafter. Lysates were resolved by SDS-PAGE and the proteins transferred to Hybond C membranes (GE Healthcare) for western analyses. An Rrp6-specific polyclonal antiserum was kindly provided by David Tollervey [11]. Pgk1 was used as a loading control and was detected with a mouse monoclonal antibody (clone 22C5D8, Life Technologies). TAP-tagged and zz fusion proteins were detected using the PAP antibody (P1291, Sigma). For the analysis of non-tagged proteins, blots were incubated with either goat anti-rabbit (A4914, Sigma) or goat anti-mouse (1706516, BioRad) HRP-conjugated secondary antibodies. ECL images were captured and quantified using a G:Box iChemi XL system (Syngene). Expression levels of Rrp6 and Rrp47 proteins were determined relative to the amount of Pgk1 detected on the identical blot for a minimum of 4 independent biological replicates.

RNA analyses

Total cellular RNA was isolated from cell pellets by glass bead extraction in the presence of phenol and guanidinium isothiocyanate solution, followed by phenol/chloroform extraction and ethanol precipitation [50]. RNA was resolved through 8 % polyacrylamide gels containing 50 % urea and transferred to Hybond N^+ membranes (GE Healthcare). Northern blots were hybridised at 37 °C with 5' ^{32}P-labelled oligonucleotide probes in 6 x SSPE buffer, 5 x Denhardt's solution and 0.2 % SDS. The sequences of the oligonucleotide probes used were as follows: U14, tcactcagacatcctagg (o238); snR38, gagaggttacctattattacccattcagacagggataactg (o272); snR13, caccgttactgatttggc (o240); *SCR1*, aaggacccagaactaccttg (o242); U6, atctctgtattgtttcaaattgaccaa (o517); U3, ttcggtttctcactctggggtac (o443); 5.8S, gcgttgttcatcgatgc (o221); *NEL025c*, ggcttctacagaacaagttgtatcgaaatgattgttggcgac (o809); 5S, ctactcggtcaggctc (o925); *IGS1-R*, gatgtaagagacaagtgaacagtgaacagtgaacagtggggaca (o815). Hybridised blots were placed under phosphor storage screens and analysed using a personal molecular imager FX scanner (Biorad). Figures were generated from nonsaturated images using ImageJ64 (NIH, Bethesda).

For cDNA synthesis reactions, RNA samples were cleaned up using RNeasy miniprep kits (Qiagen) and their integrity confirmed by analysis on glyoxal agarose gels. Reverse transcription reactions were performed on DNase I treated RNA, using random hexamer primers with the Tetro cDNA synthesis kit (BioLine). Quantitative real time PCR (qPCR) primers were designed using Primer3Plus software [51] and their specificity confirmed by melt curve analyses and analytical PCR reactions. The qPCR primers used in this study were as follows: *RRP6*(+), tggcttcagcgagatttagg (o650); *RRP6*(-), gcggtcttatacgccagtca (o651); *SCR1*(+), gagagtccgttctgaagtgtcc (o654); *SCR1*(-), cctaaggacccagaactaccttg (o655). Triplicate qPCR reactions were performed on 4 biological replicates in a

Corbett Rotor-Gene cycler (Qiagen) using SensiMix SYBR kits (Bioline). Assays were analysed using RotorGene 6000 software and *RRP6* mRNA levels were normalized to the *SCR1* reference transcript using the comparative C_T method [52].

Results

Rrp6 expression levels are decreased in *rrp47*Δ strains

We recently showed that the expression of Rrp47 is strongly dependent upon its ability to interact with Rrp6 and form the Rrp6/Rrp47 complex [43]. Previous work had shown that the lack of Rrp47 does not have a significant impact on the expression level of Rrp6 [11,27] but these earlier studies were nonquantitative and limited to analyses of cultures in rich YPD medium. We therefore reanalysed the relative expression level of Rrp6 in wild-type strains and *rrp47*Δ mutants by quantitative western blotting during growth in rich medium (YPD) and in complete minimal medium (SD). Cell lysates were prepared under alkaline denaturing conditions to minimise protein degradation *in vitro* [49].

As previously reported [43], the expression level of the Rrp47-zz fusion protein was considerably less in the *rrp6*Δ mutant than in the wild-type strain (Figure 1A). In the reciprocal experiment, Rrp6-TAP expression levels in the *rrp47*Δ mutant were ~ 80 % of that observed in the wild-type strain during growth in YPD medium (Figure 1B) but were reduced more than two-fold during growth in minimal medium (Figure 1B). The reduction in Rrp6 expression levels in the *rrp47*Δ mutant was independent of the TAP tag fusion, since comparable reductions in Rrp6 levels were observed for the Rrp6-TAP fusion protein and for non-tagged, wild-type Rrp6 protein (Figure 1B and C). These data clearly demonstrate that Rrp6 levels are reduced in the absence of Rrp47, and that this effect is responsive to alterations in growth medium. The expression levels of Rrp6 and Rrp47 are mutually dependent, with Rrp47 being more sensitive than Rrp6 to the absence of its partner protein.

The reduction in Rrp47 observed in an *rrp6*Δ mutant is principally due to a decrease in protein stability when Rrp6 is not available for interaction [43]. To determine whether Rrp6 is less stable in the absence of Rrp47, cultures of isogenic wild-type and *rrp47*Δ strains were treated with the translation inhibitor cycloheximide and the depletion of non-tagged, wild-type Rrp6 was followed by western analyses of cell extracts. Rrp6 levels showed a clear decrease through the 80 minute time-course in the *rrp47*Δ mutant, compared to the wild-type strain (Figure 2A,B). Quantitative analyses show that after 60 minutes incubation the Rrp6 levels were reduced by ~ 25 % in the wild-type strain, whereas the reduction was nearly 10-fold in the *rrp47*Δ mutant (Figure 2C). The half-life of the Rrp6 protein was estimated to be ~ 25 minutes in the *rrp47*Δ mutant and greater than 80 minutes in the wild-type strain (Figure S1). The stability of Rrp6 in the *rrp47*Δ mutant relative to the wild-type strain was not further decreased when the cultures were grown in minimal medium (Figures 2 and S1). These results show that Rrp6 is more rapidly degraded in the absence of Rrp47, and suggest that an additional mechanism is responsible for the exacerbated decrease in Rrp6 steady state levels during growth in minimal medium. Quantitative real time PCR (qPCR) analyses revealed that the expression level of *RRP6* mRNA in the *rrp47*Δ mutant was reduced to ~ 60% of the level observed in wild-type cells during growth in minimal medium (62.5 %, SEM=3.6 %, n=4), while a slight increase in *RRP6* mRNA levels was observed in the *rrp47*Δ mutant during growth in rich medium (114 %, SEM=8.7 %, n=4) (Figure 3). Taken together with the western blotting data, these results are consistent with a decrease in Rrp6 levels in the *rrp47*Δ mutant due to a general decrease in Rrp6 protein stability that is augmented by a decrease in *RRP6* mRNA levels during growth in minimal medium.

To determine whether the expression level of Rrp6 can be increased in the *rrp47*Δ mutant by exogenous expression of *RRP6*, isogenic wild-type and *rrp47*Δ strains were transformed with low copy, centromeric (cen) or high copy, 2 micron (2μ) plasmids encoding the wild-type *RRP6* gene (see Materials and Methods) and cell extracts from cultures grown in selective minimal medium were analysed by western blotting using an Rrp6-specific antibody [11]. Rrp6 levels were clearly increased in both the wild-type strain and the *rrp47*Δ mutant upon transformation with a high copy number plasmid encoding the *RRP6* gene (Figure 4, compare lanes 1-4), with higher expression levels achieved in the *rrp47*Δ mutant than are seen in wild-type cells transformed with the vector alone.

We also analysed the relative expression levels of an N-terminal zz-Rrp6 fusion protein [45] expressed from the *RRP4* promoter within either a centromeric or 2μ plasmid. Expression of the zz-Rrp6 fusion protein from a 2μ plasmid was greater than from a centromeric plasmid in both wild-type and *rrp47*Δ strains. Thus, although normal Rrp6 expression levels are dependent upon Rrp47 it is nevertheless possible to overexpress Rrp6 in the *rrp47*Δ mutant. The lower molecular weight bands observed in Figure 4 upon overexpression of the zz-Rrp6 fusion protein are C-terminal degradation products. These polypeptide fragments are also visible upon expression of the zz-Rrp6 fusion protein from a centromeric plasmid (Figure 4, lane 5) or upon overexpression of non-tagged Rrp6 (Figure 4, lane 4), although at a much reduced level.

RRP6 overexpression suppresses RNA defects in *rrp47*Δ mutants

To address whether the RNA processing and degradation defects observed in the *rrp47*Δ mutant can be ascribed to an indirect effect of decreased expression of Rrp6, rather than the absence of Rrp47 protein, we performed acrylamide gel northern blot analyses on RNA isolated from *rrp47*Δ strains that harboured centromeric and 2μ plasmids expressing Rrp6. It has previously been shown that *rrp6*Δ and *rrp47*Δ mutants accumulate 3' extended, polyadenylated forms of snoRNAs [7,11,53]. These extended snoRNA transcripts are thought to arise due to transcription termination at either the downstream proximal site I or the more distal site II, followed by polyadenylation [54]. Exogenous expression of the *RRP6* gene from the 2μ vector substantially reduced the levels of U14, snR38 and snR13 box C/D snoRNAs that are 3' extended to site I and site II (Figure 5A-C,J) in the *rrp47*Δ mutant. Expression of the *RRP6* gene in the *rrp47*Δ mutant from a

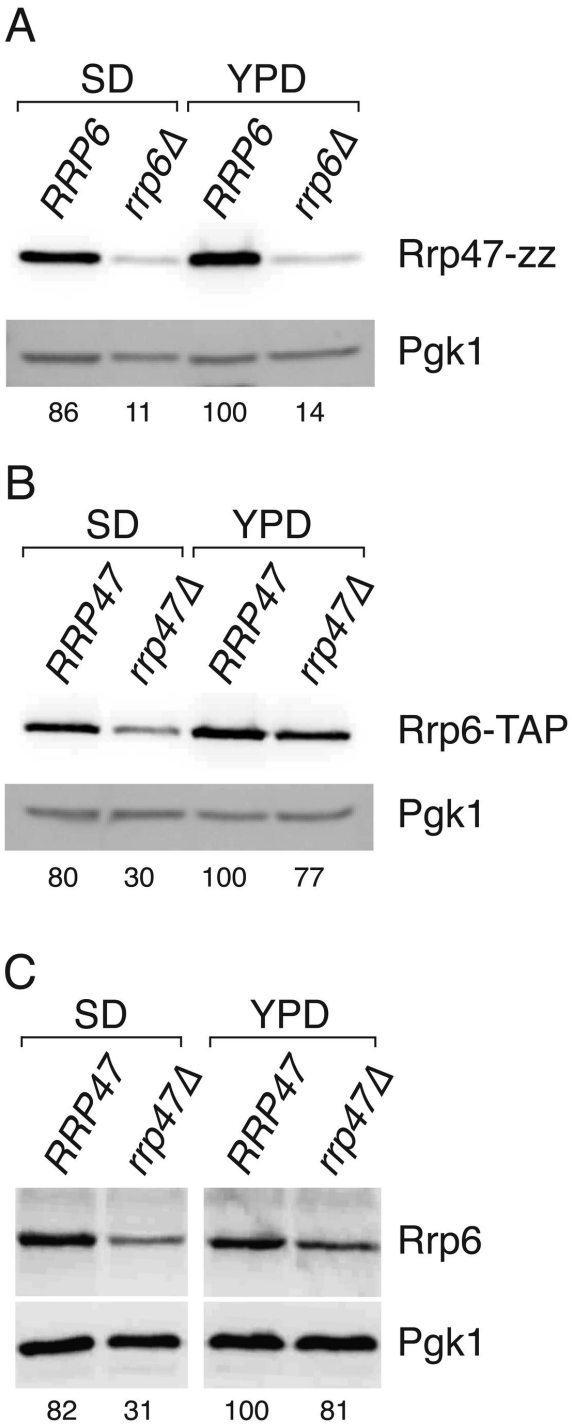

Figure 1. The Expression of Rrp6 and Rrp47 is mutually dependent. Isogenic wild-type and *rrp6*Δ or *rrp47*Δ strains were grown in selective minimal medium (SD) or in nonselective rich medium (YPD) and extracts were prepared under alkaline denaturing conditions. Extracts were resolved by SDS-PAGE and western blots were incubated with PAP antibody (Panels A and B) to detect fusion proteins, or with an Rrp6-specific antibody (Panel C). Blots were also incubated with an antibody specific to detect Pgk1, which serves as a loading control. (A) Western analysis of Rrp47-zz in isogenic wild-type *RRP6* and *rrp6*Δ strains. (B) Western analysis of Rrp6-TAP in isogenic wild-type *RRP47* and *rrp47*Δ strains. (C) Western analysis of non-tagged Rrp6 in isogenic wild-type *RRP47* and *rrp47*Δ strains. Relative expression levels of Rrp6 or Rrp47, indicated as percentages under each panel, are normalised for Pgk1 expression levels and standardised to the amount of protein in the wild-type strain grown in YPD. Values are the mean of at least 4 independent experiments.

doi: 10.1371/journal.pone.0080752.g001

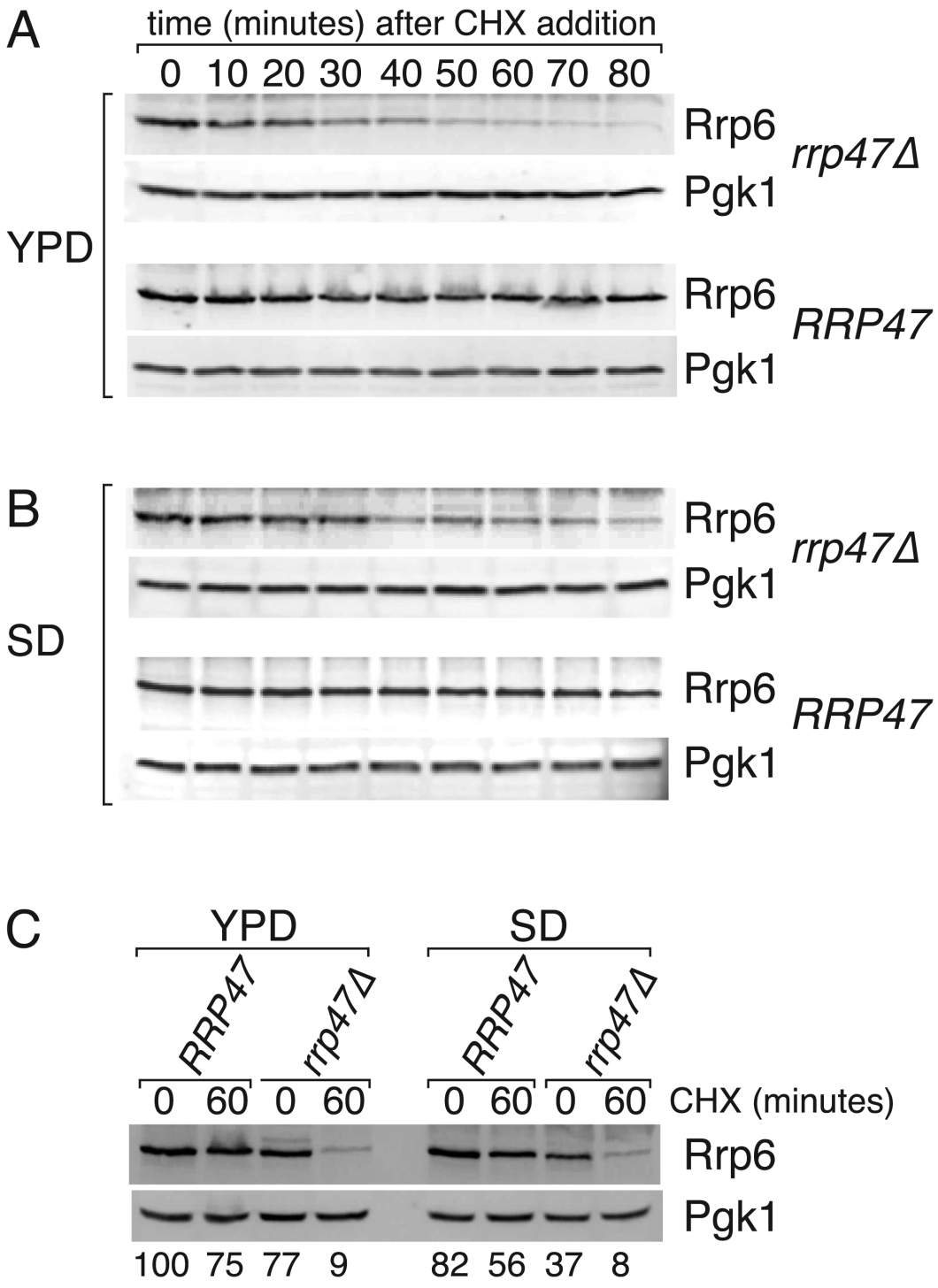

Figure 2. Rrp6 protein stability is decreased in the *rrp47*Δ mutant. Isogenic wild-type and *rrp47*Δ strains were harvested during growth in selective minimal medium (SD) or rich medium (YPD) and at time-points after addition of the translation inhibitor cycloheximide (CHX), as indicated. Extracts were prepared under denaturing conditions and identical western blots were incubated with antiserum specific to Rrp6 and the loading control Pgk1. (A) Translational shut-off experiment in YPD medium. (B) Translational shut-off experiment in SD medium. (C) Quantitative analysis of the amount of Rrp6 in extracts from wild-type and *rrp47*Δ strains before addition of cycloheximide ("0" lanes) and 60 minutes after treatment ("60" lanes). The relative amount of Rrp6, normalised to Pgk1 expression levels and standardised to the level observed in the wild-type strain during growth in YPD medium (average of 2 experiments), is given below each lane.

doi: 10.1371/journal.pone.0080752.g002

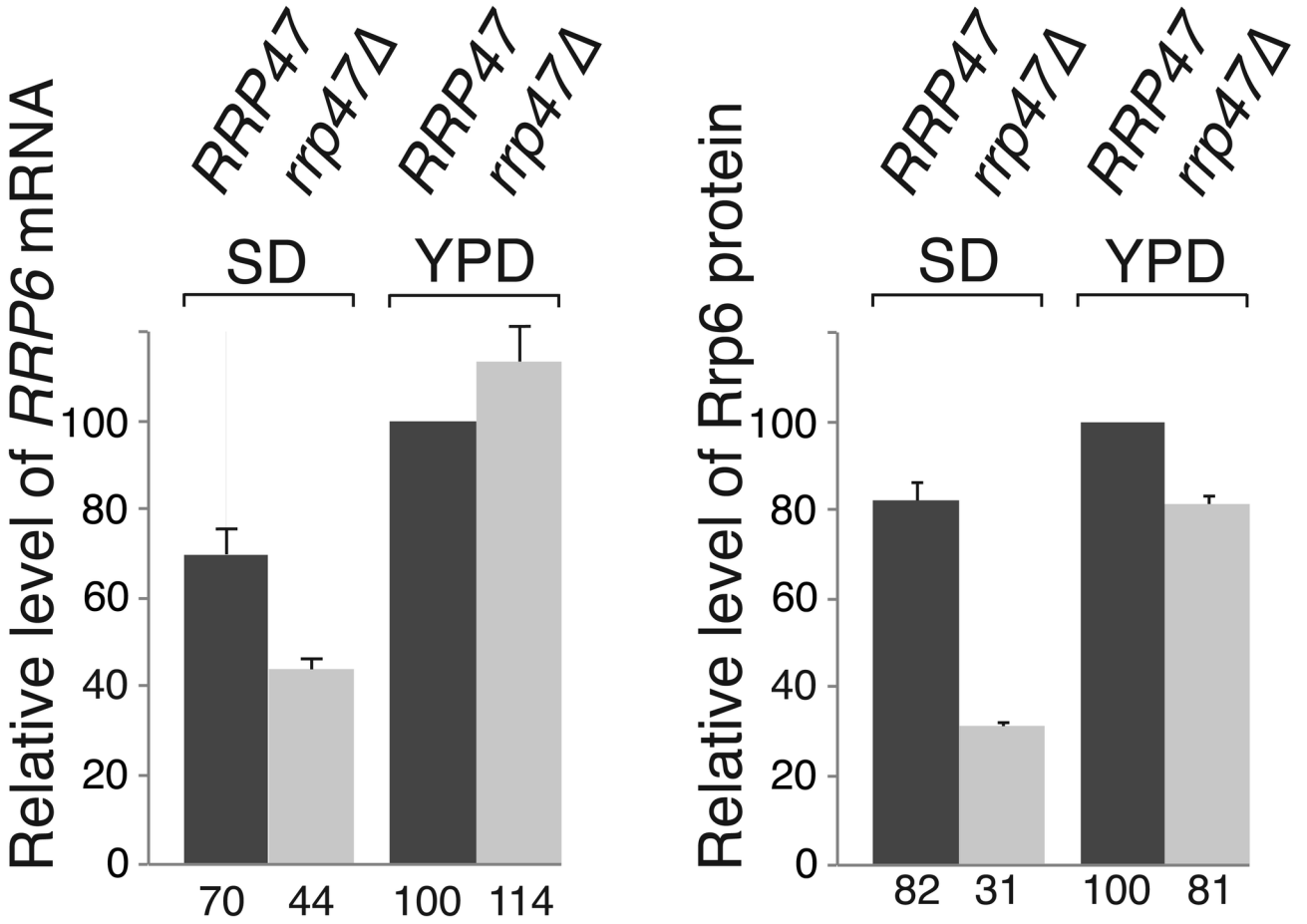

Figure 3. *RRP6* mRNA levels are decreased in the *rrp47*Δ mutant. Relative expression levels of *RRP6* mRNA in wild-type and *rrp47*Δ mutants during growth in either selective minimal medium (SD) or rich medium (YPD). Expression levels, indicated as percentages, are standardised to the amount in wild-type cells grown in YPD medium. *RRP6* mRNA levels were determined by qRT-PCR and normalised to the *SCR1* RNA. Expression levels of non-tagged Rrp6 protein, determined as in Figure 1, are shown for comparison. Error bars indicate the positive range of the standard error of the mean for each set of values.

doi: 10.1371/journal.pone.0080752.g003

centromeric vector also had a clear effect but the suppression was less marked than when *RRP6* was expressed from the multicopy plasmid (Figure 5A-C, compare lanes 2-5). This suppression in the absence of a clear increase in Rrp6 steady state levels (see Figure 4) may reflect a differential nuclear localization of Rrp6 or an increase in the effective concentration of Rrp6/TRAMP and/or Rrp6/exosome complexes. The accumulation of extended forms of U6 snRNA, truncated forms of U3 and snR13 snoRNAs (denoted as U3* and snR13* in Figure 5) and the *NEL025c* CUT observed in the *rrp47*Δ mutant was also suppressed (Figure 5C,E,F,H,J). Notably, some RNAs that accumulate in the *rrp47*Δ mutant, such as the "+30" 3' extended form of 5.8S rRNA were not clearly reduced upon Rrp6 overexpression (Figure 5G,J). This difference may reflect either the extensive degree of secondary structure found at the 3' end of the 3' extended 5.8S rRNA [55], its nucleolar localisation or the large degree of flux through the pre-rRNA processing pathway [56]. Increased expression of Rrp6 in the *rrp47*Δ mutant did not suppress the RNA processing defects to the extent seen upon transformation with a plasmid bearing the wild-type *RRP47* gene (Figure 5A-G, compare lanes 5 and 6), indicating that Rrp47 has functions in RNA processing and degradation in addition to ensuring adequate expression levels of Rrp6. Overexpression of Rrp6 *per se* is not detrimental to the cell, since no alteration in phenotype was detected upon Rrp6 overexpression in a wild-type strain (unpublished data). These data suggest that the requirement for Rrp47 in box C/D snoRNA maturation, the degradation of CUTs and in RNA surveillance pathways mediated by Rrp6 can be partially attributed to its indirect effect on Rrp6 expression.

RRP6 overexpression suppresses the genetic requirement for *RRP47* expression

Yeast *rrp47*Δ *rex1*Δ and *rrp47*Δ *mpp6*Δ double mutants are synthetic lethal [29,33]. To determine whether normal wild-type

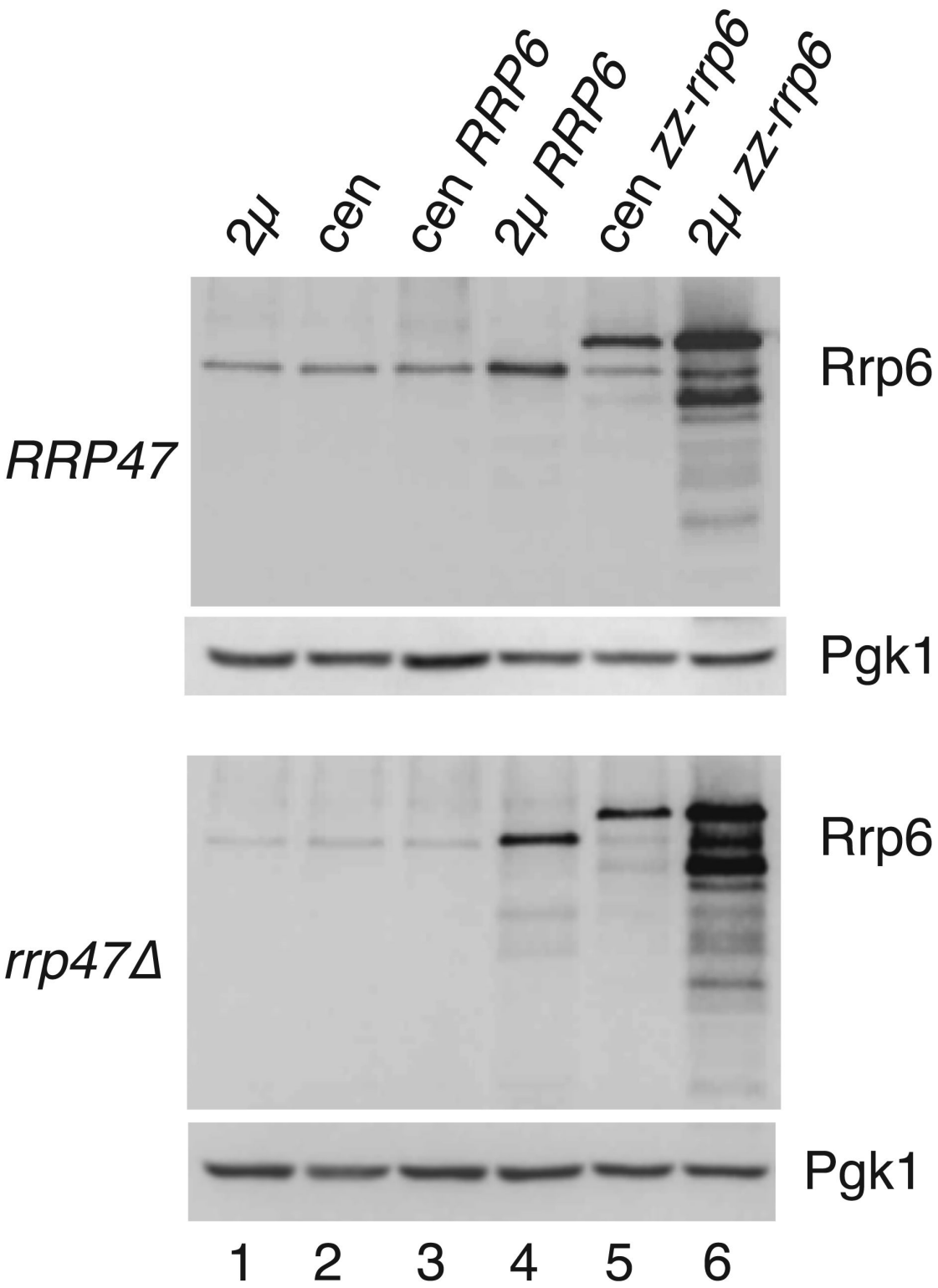

Figure 4. Rrp6 can be overexpressed in wild-type and *rrp47*Δ strains. Western analyses of Rrp6 in isogenic wild-type and *rrp47*Δ strains that are transformed with *RRP6* expression constructs. Strains were transformed with either the 2 micron (2μ) vector pRS426 (lane 1), the centromeric (cen) plasmid pRS416 (lane 2), an *RRP6* genomic clone in pRS416 (lane 3) or in pRS426 (lane 4), as well as constructs expressing an N-terminal zz fusion of Rrp6 from the *RRP4* promoter in pRS416 (lane 5) or pRS426 (lane 6). Identical blots were analysed for Rrp6 levels using an Rrp6-specific antiserum, followed by analysis of the loading control Pgk1.

doi: 10.1371/journal.pone.0080752.g004

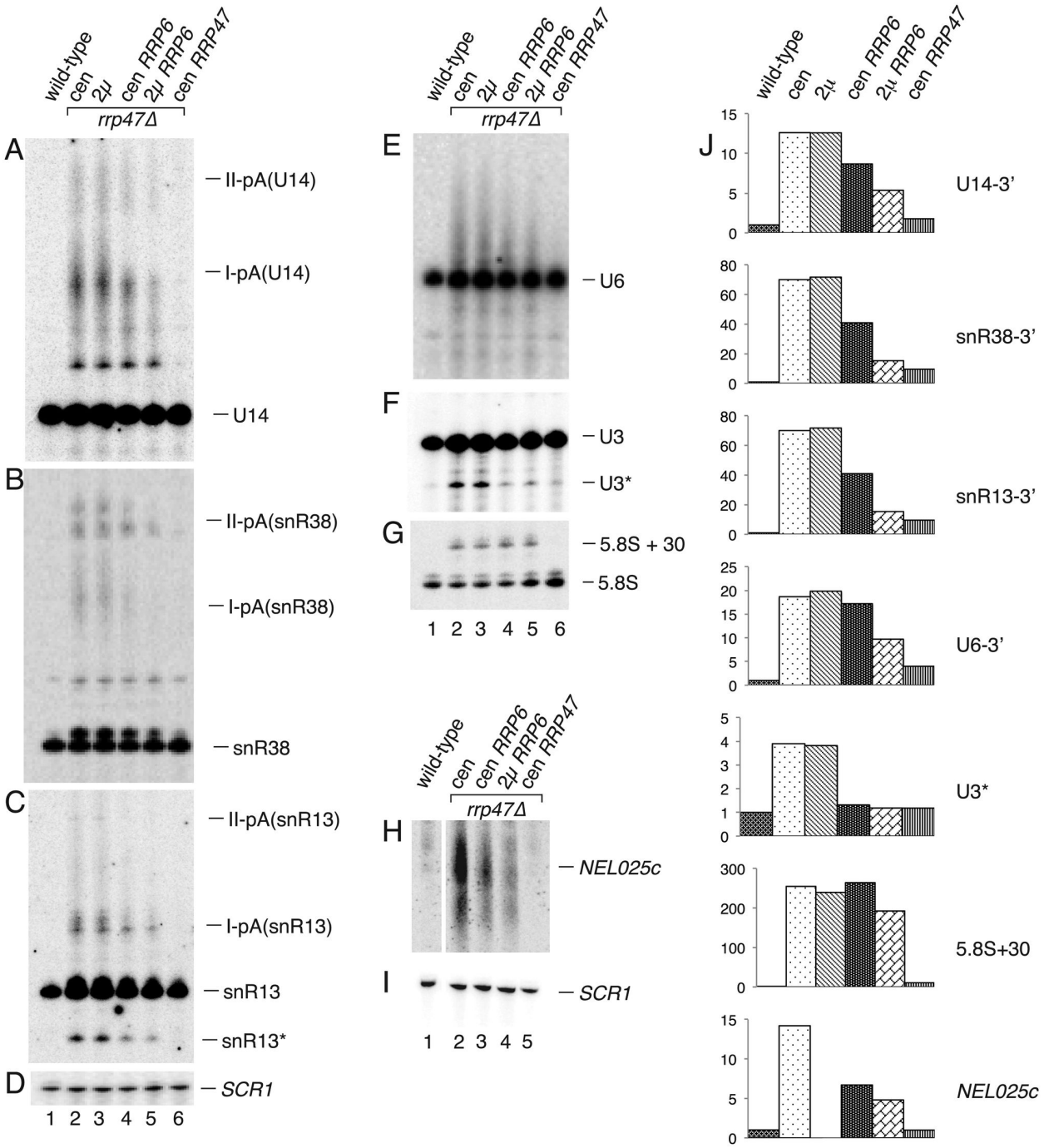

Figure 5. Rrp6 overexpression suppresses RNA phenotypes in *rrp47*Δ mutants. Northern analyses of total cellular RNA isolated from a wild-type strain, an isogenic *rrp47*Δ mutant and from *rrp47*Δ mutants expressing exogenous Rrp6 or Rrp47 from either centromeric (cen) plasmids or 2 micron-based (2μ) constructs. RNA was resolved through 8% denaturing acrylamide gels, transferred to nylon membranes and hybridised with probes complementary to specific RNAs, as follows: (A) U14; (B) snR38; (C) snR13; (D) SCR1; (E) U6; (F) U3; (G) 5.8S; (H) *NEL025c*; (I) *SCR1*. Blots shown in A-G and H-I are from distinct gels. Dispersed bands labelled I-pA and II-pA in panels A-C represent snoRNAs that are polyadenylated after termination at sites I and II, respectively. The bands labelled snR13* and U3* are 5' truncated forms of snR13 and U3. (J) Quantification of signals for the 3' extended forms of U14, snR38, snR13, U6 and 5.8S, the truncated U3 RNA and the *NEL025c* mRNA are shown for each strain. Average values of two data sets are normalised to *SCR1* loading controls and expressed relative to the level of the RNA observed in the wild-type strain.

doi: 10.1371/journal.pone.0080752.g005

expression levels of Rrp6 can alleviate the requirement for *RRP47* expression in *rex1*Δ or *mpp6*Δ mutants, centromeric and 2μ plasmids encoding *rrp6* alleles were transformed into *rrp47*Δ *rex1*Δ and *rrp47*Δ *mpp6*Δ plasmid shuffle strains and the resulting transformants were assayed for growth on medium containing 5 FOA. Isolates were obtained for the *rrp47*Δ *rex1*Δ transformants expressing either wild-type Rrp6 or the zz-Rrp6 fusion protein from both centromeric and 2μ vectors, but not from the vector control, growth being most readily observed upon transformation with the 2μ plasmid encoding the Rrp6 fusion protein (Figure 6A,B). In contrast, no growth was observed upon transformation with constructs encoding the catalytically inactive $rrp6_{D238N}$ mutant (Figure 6B) or just the N-terminal PMC2NT domain of Rrp6 ($rrp6_{NT}$) (Figure 6C). These data demonstrate that exogenous expression of Rrp6 suppresses the synthetic lethality of *rrp47*Δ *rex1*Δ mutants, and that the suppression is dependent upon the expression of catalytically active Rrp6. Exogenous expression of the zz-Rrp6 fusion protein also allowed growth of the *rrp47*Δ *mpp6*Δ mutant (Figure 6D). Notably, the *rrp47*Δ *mpp6*Δ double mutant was complemented by expression of the $rrp6_{D238N}$ mutant. This suggests that Rrp6 has an important noncatalytic function in cells lacking Mpp6.

Isolates were recovered from the 5 FOA plates and assayed for growth on solid minimal medium. The growth rates of all the complemented *rrp47*Δ *rex1*Δ double mutants were comparable, whether the plasmids encoded the *RRP6* gene or the *RRP47* gene (Figure 7). In contrast, *rrp47*Δ *mpp6*Δ transformants expressing an increased amount of Rrp6 showed a markedly slow growth phenotype relative to transformants that were complemented by copies of the *RRP47* or *MPP6* gene. This suggests that the *mpp6*Δ mutant shows a higher degree of dependence upon expression of the Rrp47 protein for optimal growth than the *rex1*Δ mutant.

Northern analyses of *rrp47*Δ *rex1*Δ and *rrp47*Δ *mpp6*Δ mutants

Northern blot analyses were performed on total cellular RNA isolated from the complemented *rrp47*Δ *rex1*Δ and *rrp47*Δ *mpp6*Δ double mutants during growth in minimal medium and compared to RNA from a wild-type strain and from the *rrp47*Δ, *rex1*Δ and *mpp6*Δ single mutants. The amount of the shorter 3' extended forms of U14, snR13 and snR38 was dramatically increased in the *rrp47*Δ *rex1*Δ mutant complemented by expression of the *RRP6* gene from the centromeric plasmid, compared to the *rrp47*Δ single mutant (labelled I-pA in Figure 8A-C, compare lanes 3 and 5). Complementation of the *rrp47*Δ *rex1*Δ mutant with cen or 2μ plasmids encoding the zz-Rrp6 fusion protein caused a weaker defect in snoRNA 3' maturation (Figure 8A, lanes 7 and 8). Northern analyses of RNA from multiple *rrp47*Δ *rex1*Δ isolates showed that this effect was reproducible (Figure S2). The milder phenotypes observed in the *rrp47*Δ *rex1*Δ strain expressing the zz-Rrp6 fusion protein presumably reflect the increased expression of this form of Rrp6 (Figure 4). We conclude that the accumulation of 3' extended snoRNAs in the *rrp47*Δ *rex1*Δ mutants can be alleviated by increased expression of Rrp6. As in the case of the *rrp47*Δ single mutant (Figure 5), the extended forms of U6 snRNA were depleted in the *rrp47*Δ *rex1*Δ double mutant upon overexpression of Rrp6 (Figure 8E) and there was no suppression of the 5.8S rRNA processing defect (Figure 8D).

Conditional *rrp47 mpp6* double mutants exhibit defects in the degradation of CUTs and in discard pathways that degrade defective nuclear pre-mRNAs and pre-rRNA fragments [29]. Consistent with this earlier study, northern analyses of RNA from the *rrp47*Δ *mpp6*Δ mutants expressing the zz-Rrp6 fusion protein from a centromeric plasmid revealed defects in the degradation of truncated fragments of 5S rRNA and snR13 (denoted as 5S* and snR13* in Figure 8G and H, respectively) that are presumably targeted to discard pathways [11,57], as well as the accumulation of the *NEL025c* and *IGS1-R* CUTs (Figure 8J,K). In all cases, these RNAs accumulated substantially more in the *rrp47*Δ *mpp6*Δ double mutant expressing zz-Rrp6 from a centromeric plasmid than in the *rrp47*Δ or *mpp6*Δ single mutants (Figure 8G-K, compare lanes 2,3 and 6). Northern analyses using probes complementary to box C/D snoRNAs revealed that the *rrp47*Δ *mpp6*Δ mutant expressing zz-Rrp6 from a centromeric plasmid also accumulated 3' extended U14 and snR13 RNAs (Figure 8H,L). In contrast to the *rrp47*Δ *rex1*Δ mutants, however, the longer forms of snR13 and U14 detected in the *rrp47*Δ *mpp6*Δ mutant were extended to site II (labelled II-pA in Figure 8).

The severity of the phenotypes observed in the *rrp47*Δ *mpp6*Δ double mutant expressing exogenously supplied zz-Rrp6 was suppressed upon expression of the protein from a multicopy plasmid (Figure 8G-N, compare lanes 6 and 8). The analysis of RNA from multiple independent isolates showed that this effect is reproducible (Figure S3). Taken together, the data shown in Figure 8 supports a role for Rrp6, directly or indirectly, in the processing or degradation of RNAs that accumulate in the *rrp47*Δ *rex1*Δ or *rrp47*Δ *mpp6*Δ mutants. Yeast snoRNA maturation is dependent upon the exonuclease activity of Rrp6 in the case of the *rrp47*Δ *rex1*Δ mutant, since no complementation was observed for the catalytically inactive $rrp6_{D238N}$ mutant (Figure 6B). In contrast, the *rrp47*Δ *mpp6*Δ mutant could be complemented by expression of the $rrp6_{D238N}$ mutant and the severity and nature of the RNA phenotypes seen upon complementation were generally indistinguishable to that seen upon expression of the wild-type protein (Figure 8G-N, compare lanes 6 and 7). These observations provide support for an important non-catalytic role of Rrp6 in RNA surveillance and degradation pathways that has been noted in previous studies [58]. The $rrp6_{D238N}$ mutant was not, however, able to process the short 3' extensions of snoRNAs (resolved from the mature RNA well in the case of snR38 in Figure 8I, compare lanes 6 and 7) that arise through the addition of short oligoadenylate tails [54].

Given that the exonuclease activity of Rrp6 is redundant with activities dependent upon either Mpp6 or Rex1 [44](Figure 6), we hypothesised that the expression of Rrp6 may be increased when Mpp6- or Rex1-dependent pathways are blocked. To address this, we determined the relative levels of Rrp6 in extracts of isogenic strains that carry either a wild-type or null allele of the *MPP6* or *REX1* gene. Western analyses of cultures grown in minimal medium showed that Rrp6 expression levels

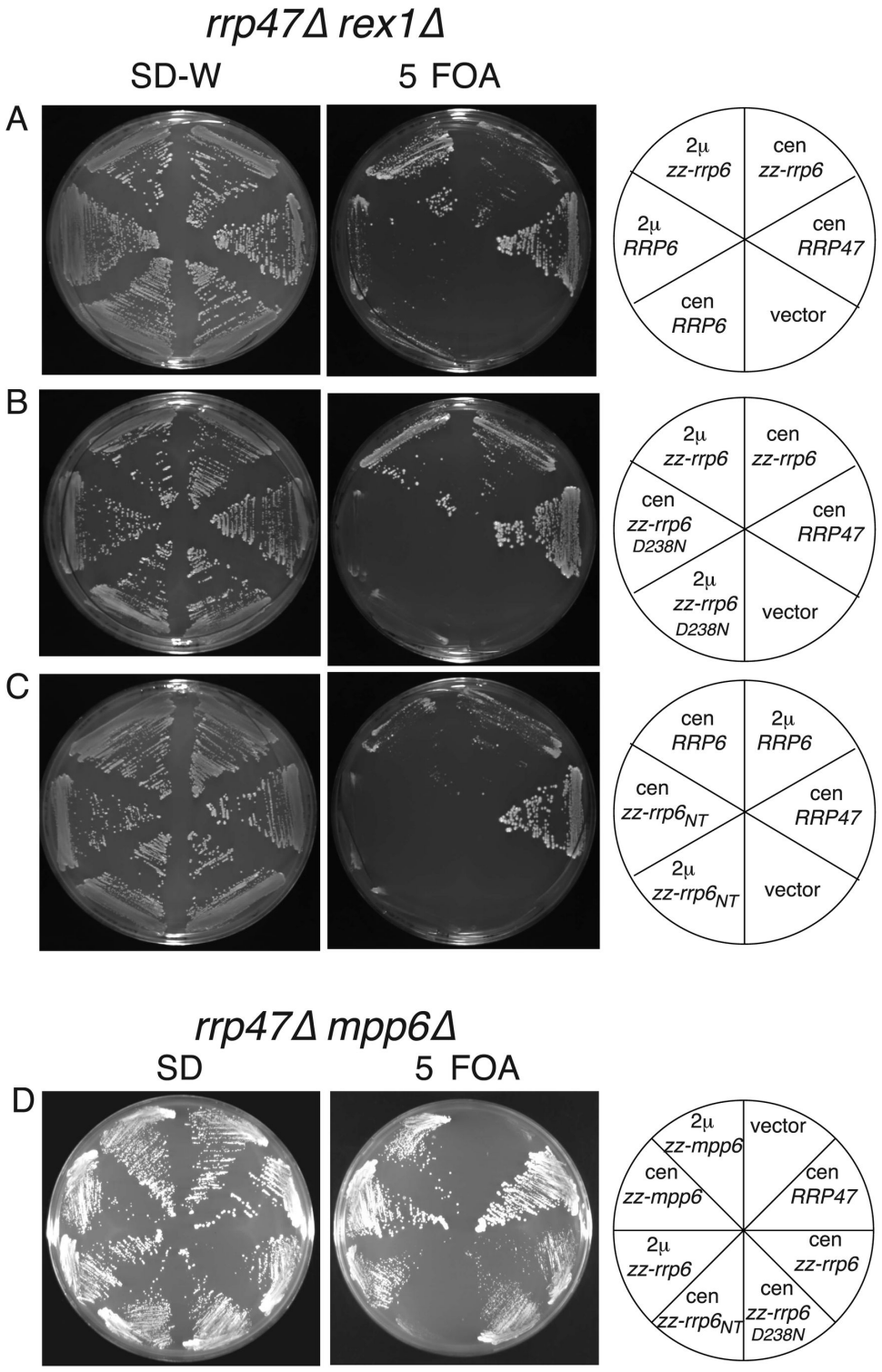

Figure 6. Exogenous expression of Rrp6 complements the synthetic lethality of *rrp47*Δ *rex1*Δ and *rrp47*Δ *mpp6*Δ mutants. Yeast *rrp47*Δ *rex1*Δ and *rrp47*Δ *mpp6*Δ double mutants bearing plasmids with a *URA3* marker and a wild-type copy of either the *RRP47* (panels A-C) or *MPP6* gene (panel D) were transformed with *RRP6* constructs. Transformants were isolated on selective minimal medium and tested for growth in parallel on permissive minimal medium (left panel) and on medium containing 5 FOA (right panel). Plates were incubated at 30 °C for 3 days. The nature of the expression construct is indicated for each segment on the right.

doi: 10.1371/journal.pone.0080752.g006

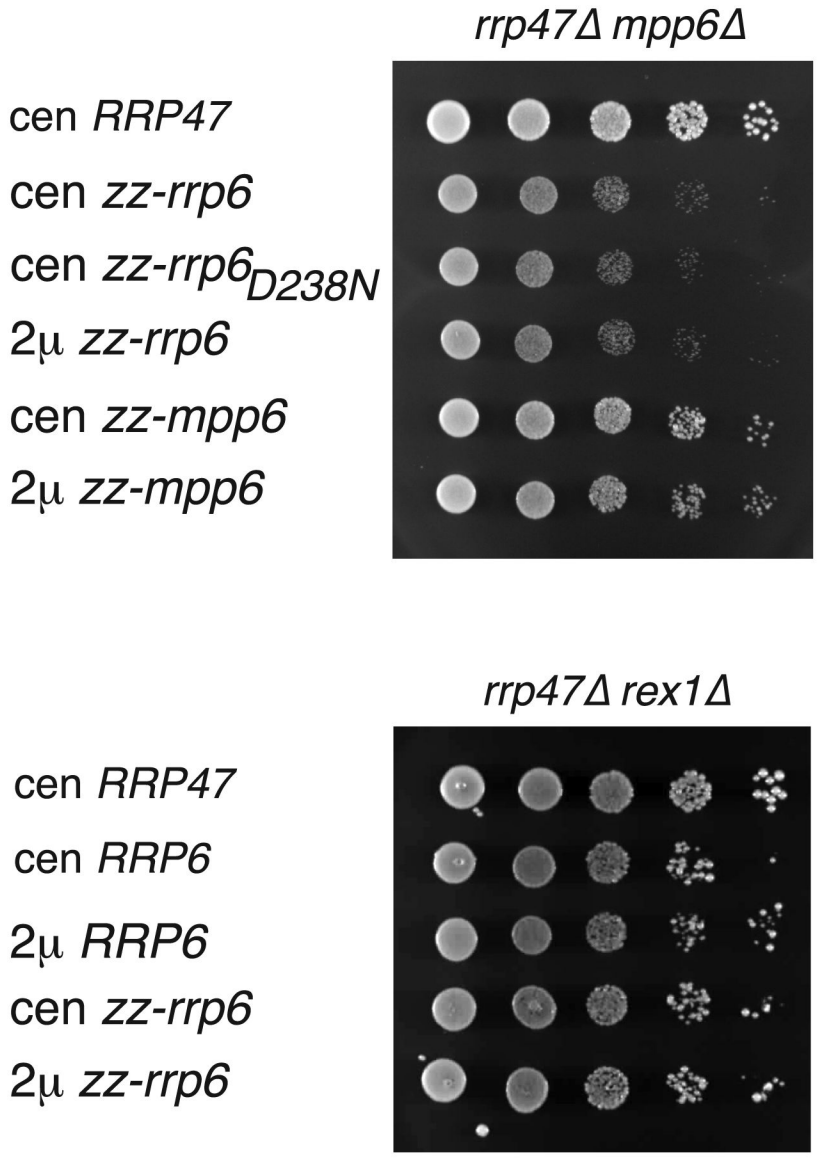

Figure 7. Growth assays of *rrp47*Δ *rex1*Δ and *rrp47*Δ *mpp6*Δ mutants. Spot growth assays of *rrp47*Δ *mpp6*Δ (upper panel) and *rrp47*Δ *rex1*Δ (lower panel) double mutant isolates. The complementing construct is indicated on the left. 10-fold serial dilutions of standardised precultures were spotted on to selective solid medium and the plates were incubated at 30 °C. Plates were photographed after incubation for 3 days.

doi: 10.1371/journal.pone.0080752.g007

are not markedly altered in the presence or absence of Mpp6 or Rex1 (Figure 9). Thus, Rrp6 expression levels are responsive to the availability of its interacting protein Rrp47 but not the status of redundant Mpp6- or Rex1-dependent processing or degradation pathways.

Discussion

The yeast protein Rrp47 was identified 10 years ago as an exosome-associated protein that is functionally linked to the Rrp6 exonuclease [11,33,59]. The exact molecular function(s) of this protein has, however, remained largely elusive. We have recently shown that the stability of Rrp47 is drastically reduced in the absence of Rrp6 [43]. Here we demonstrate that Rrp6 protein levels are reduced in the absence of Rrp47, and that this effect is reinforced when strains are grown in minimal medium rather than rich medium. Down-regulation of Rrp6 expression occurs both at the level of protein stability and at the *RRP6* transcript level. Strikingly, restoration of Rrp6 expression in an *rrp47*Δ mutant to wild-type levels is largely sufficient to compensate for the lack of Rrp47, suppressing RNA processing and turnover defects observed in the *rrp47*Δ

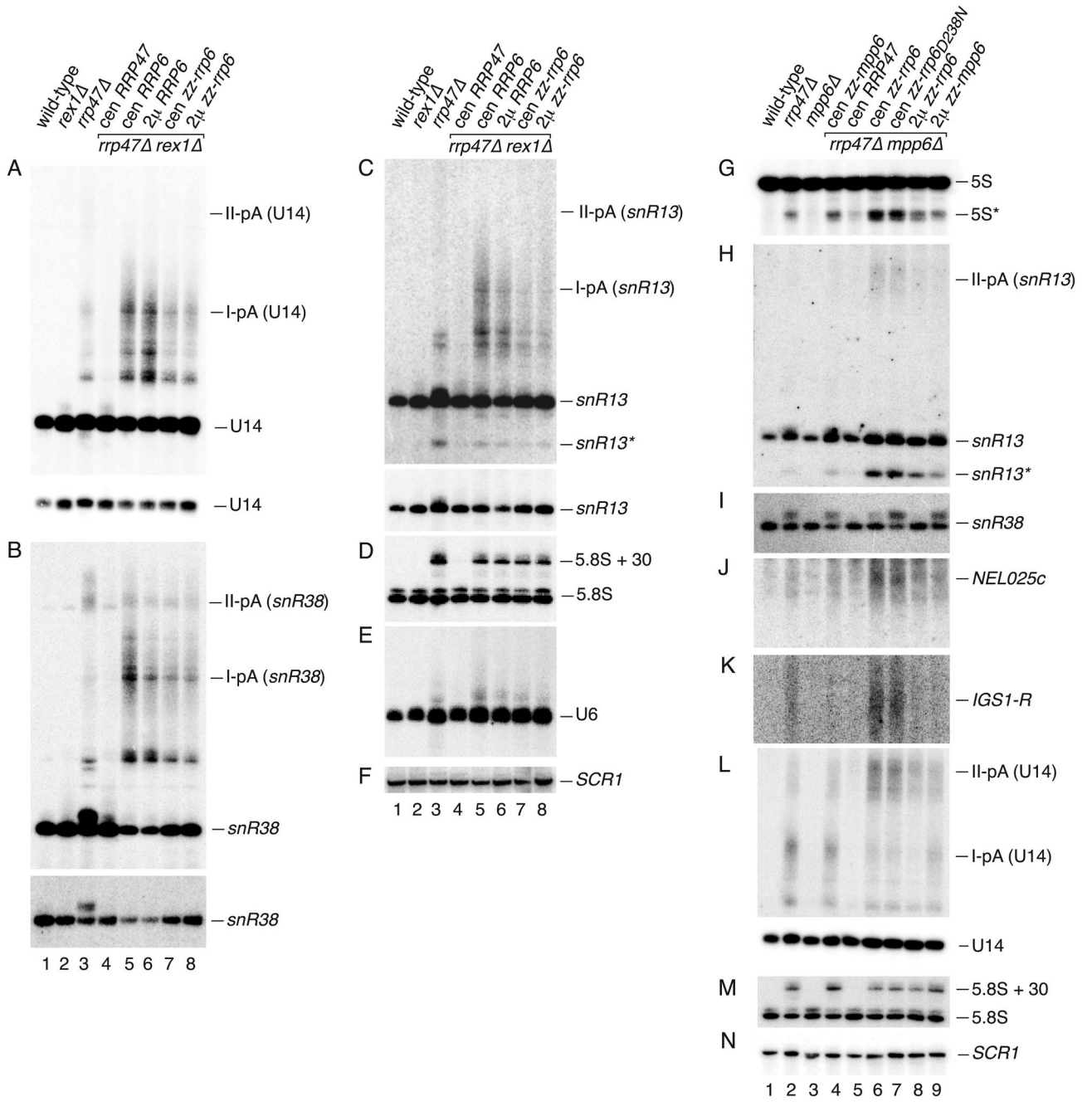

Figure 8. Northern analyses of *rrp47*Δ *rex1*Δ and *rrp47*Δ *mpp6*Δ mutants. Total cellular RNA was isolated from isogenic wild-type, *rex1*Δ, *rrp47*Δ and *mpp6*Δ strains, and from *rrp47*Δ *rex1*Δ *rrp47*Δ or *rrp47*Δ *mpp6*Δ double mutants that are complemented by centromeric (cen) or 2 micron (2μ) plasmids expressing *RRP47*, *MPP6* or *RRP6* alleles. *RRP6* constructs encoded either non-tagged or zz-tagged fusion proteins. RNA was resolved through 8% denaturing polyacrylamide gels and northern blot analyses performed, using probes complementary to the RNAs indicated on the right of each panel. (A-F) Analysis of *rrp47*Δ *rex1*Δ mutants. (G-N) Analysis of *rrp47*Δ *mpp6*Δ mutants. To compare the relative levels of both mature and 3' extended forms of snoRNAs in the different strains in panels A-C, two images are shown from the same hybridisation. Dispersed bands labelled I-pA and II-pA represent snoRNAs that are polyadenylated after termination at sites I or II, respectively. Bands labelled 5S* and snR13* represent truncated RNAs.

doi: 10.1371/journal.pone.0080752.g008

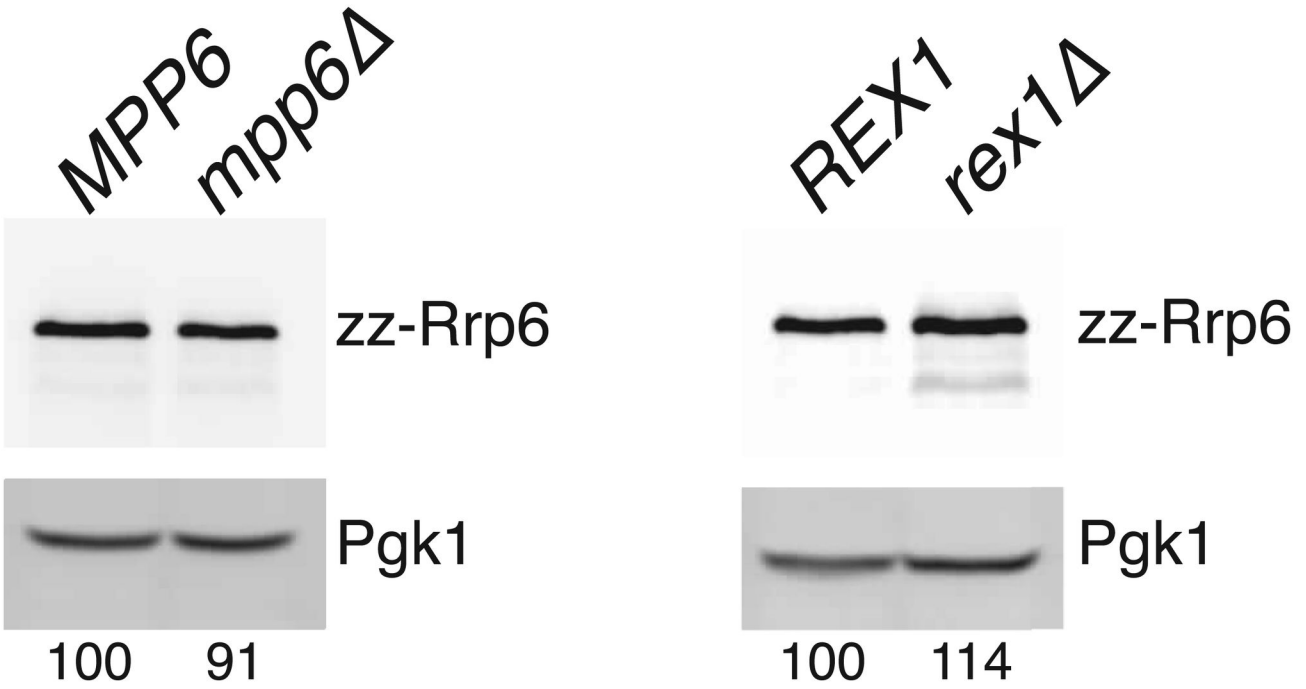

Figure 9. Rrp6 levels are not altered in *mpp6*Δ or *rex1*Δ mutants. Western analyses were performed on extracts from strains that either carry a wild-type or a deletion allele of the *MPP6* or *REX1* gene and that express the zz-Rrp6 fusion protein. Blots were successively incubated with the PAP antibody and antibody specific to the Pgk1 protein. Expression levels of zz-Rrp6 in the *mpp6*Δ and *rex1*Δ mutants, relative to the level observed in the corresponding wild-type strain, are given at the bottom of the figure and are the average of three independent biological replicates.

doi: 10.1371/journal.pone.0080752.g009

mutant and complementing the synthetic lethal growth phenotypes of *rrp47*Δ *rex1*Δ and *rrp47*Δ *mpp6*Δ double mutants. This demonstrates that an important function of Rrp47 is to facilitate a critical expression level of Rrp6. Similar findings have been independently reported recently [60]. In contrast to the study by Stuparevic et al., we did not observe a complete depletion of Rrp6 in the absence of Rrp47. Our findings are more consistent with observed differences in the growth phenotypes and genetic interactions of *rrp47*Δ and *rrp6*Δ mutants [11].

The Rrp6 and Rrp47 proteins interact directly with one another [27]. The mutual stabilisation of two interacting proteins has the consequence of limiting the expression of the constituent proteins to functional, assembled complexes and suppressing the potential titration of substrates or factors by the one or other subunit. In the case of Rrp47 and Rrp6, this would limit the expression of the proteins to their site of assembly and functional location in the cell nucleus [43]. Consistent with a key function of Rrp47 being its ability to facilitate normal Rrp6 expression levels, the Sas10/C1D domain of Rrp47 that is required for the interaction with Rrp6 is sufficient for the function of the protein *in vivo* [28]. Notwithstanding this impact of Rrp47 on Rrp6 expression levels, Rrp47 performs additional functions as part of the Rrp6/Rrp47 complex that contribute to RNA processing and degradation and which involve the C-terminal region of the protein [28,44]. This is underlined by the observation that expression of exogenous Rrp6 protein restored Rrp6 levels but did not suppress the defects in RNA processing and degradation in the *rrp47*Δ single mutant or either double mutant as efficiently as expression of the *RRP47* gene.

The ability of increased Rrp6 expression to suppress the requirement for Rrp47 facilitated the isolation of viable *rrp47*Δ *rex1*Δ and *rrp47*Δ *mpp6*Δ strains, and the analyses of the complemented strains provided some insight into the molecular basis of the synthetic lethal relationship between *rrp47*Δ mutations and *rex1*Δ or *mpp6*Δ alleles. Northern analyses of the *RRP6*-complemented *rrp47*Δ *rex1*Δ double mutants revealed an accumulation of 3' extended box C/D snoRNAs that was suppressed upon increased expression of Rrp6. Furthermore, the exonuclease activity of Rrp6 is required for complementation of the *rrp47*Δ *rex1*Δ mutant. We recently reported that segregation of Rrp47 from catalytically active form of Rrp6 in the *rex1*Δ mutant causes a block in the 3' end maturation of box C/D snoRNAs [44]. This strongly suggests that Rrp6 and Rex1 have a redundant function in snoRNA processing that cannot be carried out by other cellular exonucleases. There are no additional detectable snoRNA processing intermediates in the *rrp47*Δ mutant upon loss of Rex1, suggesting that the redundancy between Rrp6 and Rex1 does not stem from a cooperative pathway. This is further supported by the lack of data supporting a physical interaction

between these two proteins or with a mutual partner. Rather, the redundancy of processing activities in snoRNA maturation appears to reflect genetic buffering. Rex1 is a member of a family of related exonucleases in yeast that remain relatively poorly characterised [32,61]. It will be of interest to address whether the substrate specificity or availability of Rex1 is regulated by an associated protein in a manner similar to the effect of Rrp47 on Rrp6.

In contrast to the specific snoRNA processing defect observed in the *rrp47*Δ *rex1*Δ mutant, a set of RNAs accumulated in the *rrp47*Δ *mpp6*Δ mutant that are normally destined for rapid degradation. These phenotypes were also suppressed upon increased expression of Rrp6, indicative of a functional redundancy between the Rrp6/Rrp47 complex and an Mpp6-dependent activity in RNA discard pathways and the degradation of CUTs [29]. Interestingly, exogenous expression of either the *rrp6-1* allele or the wild-type *RRP6* gene had comparable effects on the growth of the *rrp47*Δ *mpp6*Δ double mutant and the viable transformants were compromised to a similar degree in their ability to degrade truncated stable RNAs, CUTs or extended snoRNA transcripts. These observations are consistent with a previous study proposing that Rrp6 has an important noncatalytic role in RNA surveillance [58]. One noncatalytic mechanism by which Rrp6 might promote RNA surveillance is through its interaction with the exosome complex, which promotes channelling of RNA substrates through the core to Rrp44 [19,26]. However, *rrp6-1 mpp6*Δ double mutants are nonviable [44], suggesting that at least one essential biological process is dependent upon the catalytic activity of either Rrp6 or an Mpp6-dependent activity. This most likely reflects the substrate overlap observed for Rrp6 and Rrp44 [3,31]. The molecular function of Mpp6 remains unclear. The human Mpp6 protein physically interacts with homologues of Mtr4 and the Rrp47/Rrp6 complex [62] and contacts the exosome independently of Rrp44 [63], while yeast *mpp6*Δ mutants show strong genetic interactions with mutants lacking the TRAMP component Air1 [29,64], as well as mutations of the Rrp6/Rrp47 complex. One possibility is that Mpp6 might act to functionally couple the TRAMP and Rrp6/exosome complexes [30].

Studies on the prokaryotic exoribonucleases RNase R and RNase II have revealed changes in the expression levels of these enzymes upon changes in nutrient availability or other forms of stress [38,39]. The wide-ranging impact on diverse aspects of RNA metabolism that are seen for mutants of the exosome complex, or the 5'→3' exoribonucleases Xrn1 and Rat1, suggests that modulation of the expression of eukaryotic exoribonucleases may orchestrate similar changes in the transcriptome associated with cellular responses to physiological signals. More detailed analyses of the expression levels of eukaryotic ribonucleases in response to altered growth conditions may be a fruitful area of future research.

Supporting Information

Figure S1. Rrp6 stability is decreased in *rrp47*Δ mutants. Western analyses were performed on cell extracts from wild-type strains and *rrp47*Δ mutants during growth in rich medium (YPD) or minimal medium (SD) following treatment with cycloheximide (CHX) for the times indicated. The amount of Rrp6 detected was normalised to the level of endogenous Pgk1 protein and expressed as a percentage of the protein present in the cell lysates as a function of time.
(TIF)

Figure S2. RNA analyses of independent *rrp47*Δ *rex1*Δ isolates. Acrylamide gel Northern analyses were performed on total cellular RNA from independent isolates of the *rrp47*Δ *rex1*Δ mutant that harbor either the centromeric *RRP6* plasmid (lanes 1-3), the 2μ *RRP6* plasmid (lanes 4-6), a centromeric plasmid encoding the zz-Rrp6 fusion protein (lanes 7-9) or a 2μ plasmid encoding zz-Rrp6 (lanes 10-12). The blot was successively hybridised with probes complementary to snR13, U14, 5.8S rRNA and SCR1.
(TIF)

Figure S3. RNA analyses of independent *rrp47*Δ *mpp6*Δ isolates. Acrylamide gel Northern analyses of total cellular RNA from independent isolates of the *rrp47*Δ *mpp6*Δ mutant harbouring centromeric plasmids encoding Rrp47 (cen *RRP47*), the zz-Mpp6 fusion (cen *zz-mpp6*), the zz-Rrp6 fusion (cen *zz-rrp6*) or the catalytically inactive *rrp6* mutant (cen *zz-rrp6*$_{D238N}$), or 2μ plasmids encoding the zz-Rrp6 fusion (2μ *zz-rrp6*) or the zz-Mpp6 fusion (2μ *zz-mpp6*). RNA from four sets of isolates (labelled sets 1-4: lanes 1-6, 7-12, 13-18 and 19-24, respectively) was analysed by hybridisation using probes complementary to the RNAs indicated on the right.
(TIF)

Acknowledgements

We thank David Tollervey (University of Edinburgh) for provision of the Rrp6-specific antiserum.

Author Contributions

Conceived and designed the experiments: MF WG PM. Performed the experiments: MF WG MT. Analyzed the data: MF PM. Contributed reagents/materials/analysis tools: MF WG MT. Wrote the manuscript: PM.

References

1. Parker R (2012) RNA degradation in *Saccharomyces cerevisae*. Genetics 191: 671–702. doi:10.1534/genetics.111.137265. PubMed: 22785621.
2. Houseley J, Tollervey D (2009) The Many Pathways of RNA Degradation. Cell 136: 763–776. doi:10.1016/j.cell.2009.01.019. PubMed: 19239894.
3. Gudipati RK, Xu Z, Lebreton A, Séraphin B, Steinmetz LM et al. (2012) Extensive degradation of RNA precursors by the exosome in wild-type cells. Mol Cell 48: 409–421. doi:10.1016/j.molcel.2012.08.018. PubMed: 23000176.
4. Porrua O, Libri D (2013) RNA quality control in the nucleus: the angel's share of RNA. Biochim Biophys Acta 1829: 604–611. doi:10.1016/j.bbagrm.2013.02.012. PubMed: 23474120.
5. Chlebowski A, Lubas M, Jensen TH, Dziembowski A (2013) RNA decay machines: the exosome. Biochim Biophys Acta 1829: 552–560. doi:10.1016/j.bbagrm.2013.01.006. PubMed: 23352926.
6. Mitchell P, Petfalski E, Shevchenko A, Mann M, Tollervey D (1997) The exosome: a conserved eukaryotic RNA processing complex containing multiple 3'5 exoribonucleases. Cell 91: 457–466. doi:10.1016/S0092-8674(00)80432-8. PubMed: 9390555.
7. Allmang C, Kufel J, Chanfreau G, Mitchell P, Petfalski E et al. (1999) Functions of the exosome in rRNA, snoRNA and snRNA synthesis. EMBO J 18: 5399–5410. doi:10.1093/emboj/18.19.5399. PubMed: 10508172.
8. Wyers F, Rougemaille M, Badis G, Rousselle J-C, Dufour M-E et al. (2005) Cryptic pol II transcripts are degraded by a nuclear quality control pathway involving a new poly(A) polymerase. Cell 121: 725–737. doi:10.1016/j.cell.2005.04.030. PubMed: 15935759.
9. Neil H, Malabat C, d'Aubenton-Carafa Y, Xu Z, Steinmetz LM et al. (2009) Widespread bidirectional promoters are the major source of cryptic transcripts in yeast. Nature 457: 1038–1042. doi:10.1038/nature07747. PubMed: 19169244.
10. Xu Z, Wei W, Gagneur J, Perocchi F, Clauder-Münster S et al. (2009) Bidirectional promoters generate pervasive transcription in yeast. Nature 457: 1033–1037. doi:10.1038/nature07728. PubMed: 19169243.
11. Mitchell P, Petfalski E, Houalla R, Podtelejnikov A, Mann M et al. (2003) Rrp47p is an exosome-associated protein required for the 3' processing of stable RNAs. Mol Cell Biol 23: 6982–6992. doi:10.1128/MCB.23.19.6982-6992.2003. PubMed: 12972615.
12. Tomecki R, Kristiansen MS, Lykke-Andersen SOR, Chlebowski A, Larsen KM et al. (2010) The human core exosome interacts with differentially localized processive RNases: hDIS3 and hDIS3L. EMBO J 29: 2342–2357. doi:10.1038/emboj.2010.121. PubMed: 20531386.
13. Mian IS (1997) Comparative sequence analysis of ribonucleases HII, III, II PH and D. Nucleic Acids Res 25: 3187–3195. doi:10.1093/nar/25.16.3187. PubMed: 9241229.
14. Lebreton A, Tomecki R, Dziembowski A, Séraphin B (2008) Endonucleolytic RNA cleavage by a eukaryotic exosome. Nature 456: 993–996. doi:10.1038/nature07480. PubMed: 19060886.
15. Schaeffer D, Tsanova B, Barbas A, Reis FP, Dastidar EG et al. (2009) The exosome contains domains with specific endoribonuclease, exoribonuclease and cytoplasmic mRNA decay activities. Nat Struct Mol Biol 16: 56–62. doi:10.1038/nsmb.1528. PubMed: 19060898.
16. Schneider C, Leung E, Brown J, Tollervey D (2008) The N-terminal PIN domain of the exosome subunit Rrp44 harbors endonuclease activity and tethers Rrp44 to the yeast core exosome. Nucleic Acids Res 37: 1127–1140. doi:10.1093/nar/gkn1020. PubMed: 19129231.
17. Liu Q, Greimann JC, Lima CD (2006) Reconstitution, activities, and structure of the eukaryotic RNA exosome. Cell 127: 1223–1237. doi:10.1016/j.cell.2006.10.037. PubMed: 17174896.
18. Bonneau F, Basquin J, Ebert J, Lorentzen E, Conti E (2009) The Yeast exosome functions as a macromolecular cage to channel RNA substrates for degradation. Cell 139: 547–559. doi:10.1016/j.cell.2009.08.042. PubMed: 19879841.
19. Makino DL, Baumgärtner M, Conti E (2013) Crystal structure of an RNA-bound 11-subunit eukaryotic exosome complex. Nature 495: 70–75. doi:10.1038/nature11870. PubMed: 23376952.
20. Moser MJ, Holley WR, Chatterjee A, Mian IS (1997) The proofreading domain of *Escherichia coli* DNA polymerase I and other DNA and/or RNA exonuclease domains. Nucleic Acids Res 25: 5110–5118. doi:10.1093/nar/25.24.5110. PubMed: 9396823.
21. Midtgaard SF, Assenholt J, Jonstrup AT, Van LB, Jensen TH et al. (2006) Structure of the nuclear exosome component Rrp6p reveals an interplay between the active site and the HRDC domain. Proc Natl Acad Sci U S A 103: 11898–11903. doi:10.1073/pnas.0604731103. PubMed: 16882719.
22. Steitz TA, Steitz JA (1993) A general two-metal-ion mechanism for catalytic RNA. Proc Natl Acad Sci U S A 90: 6498–6502. doi:10.1073/pnas.90.14.6498. PubMed: 8341661.
23. Briggs MW, Burkard KT, Butler JS (1998) Rrp6p, the yeast homologue of the human PM-Scl 100-kDa autoantigen, is essential for efficient 5.8 S rRNA 3' end formation. J Biol Chem 273: 13255–13263. doi:10.1074/jbc.273.21.13255. PubMed: 9582370.
24. Burkard KT, Butler JS (2000) A nuclear 3'-5' exonuclease involved in mRNA degradation interacts with poly(A) polymerase and the hnRNA protein Npl3p. Mol Cell Biol 20: 604–616. doi:10.1128/MCB.20.2.604-616.2000. PubMed: 10611239.
25. Callahan KP, Butler JS (2008) Evidence for core exosome independent function of the nuclear exoribonuclease Rrp6p. Nucleic Acids Res 36: 6645–6655. doi:10.1093/nar/gkn743. PubMed: 18940861.
26. Wasmuth EV, Lima CD (2012) Exo- and endoribonucleolytic activities of yeast cytoplasmic and nuclear RNA exosomes are dependent on the noncatalytic core and central channel. Mol Cell 48: 133–144. doi:10.1016/j.molcel.2012.07.012. PubMed: 22902556.
27. Stead JA, Costello JL, Livingstone MJ, Mitchell P (2007) The PMC2NT domain of the catalytic exosome subunit Rrp6p provides the interface for binding with its cofactor Rrp47p, a nucleic acid-binding protein. Nucleic Acids Res 35: 5556–5567. doi:10.1093/nar/gkm614. PubMed: 17704127.
28. Costello JL, Stead JA, Feigenbutz M, Jones RM, Mitchell P (2011) The C-terminal region of the exosome-associated protein Rrp47 is specifically required for box C/D small nucleolar RNA 3'-maturation. J Biol Chem 286: 4535–4543. doi:10.1074/jbc.M110.162826. PubMed: 21135092.
29. Milligan L, Decourty L, Saveanu C, Rappsilber J, Ceulemans H et al. (2008) A yeast exosome cofactor, Mpp6, functions in RNA surveillance and in the degradation of noncoding RNA transcripts. Mol Cell Biol 28: 5446–5457. doi:10.1128/MCB.00463-08. PubMed: 18591258.
30. Butler JS, Mitchell P (2011) Rrp6, Rrp47 and cofactors of the nuclear exosome. Adv Exp Med Biol 702: 91–104. PubMed: 21713680.
31. Schneider C, Kudla G, Wlotzka W, Tuck A, Tollervey D (2012) Transcriptome-wide analysis of exosome targets. Mol Cell 48: 422–433. doi:10.1016/j.molcel.2012.08.013. PubMed: 23000172.
32. van Hoof A, Lennertz P, Parker R (2000) Three conserved members of the RNase D family have unique and overlapping functions in the processing of 5S, 5.8S, U4, U5, RNase MRP and RNase P RNAs in yeast. EMBO J 19: 1357–1365. doi:10.1093/emboj/19.6.1357. PubMed: 10716935.
33. Peng WT, Robinson MD, Mnaimneh S, Krogan NJ, Cagney G et al. (2003) A panoramic view of yeast noncoding RNA processing. Cell 113: 919–933. doi:10.1016/S0092-8674(03)00466-5. PubMed: 12837249.
34. Lardenois A, Liu Y, Walther T, Chalmel F, Evrard B et al. (2011) Execution of the meiotic noncoding RNA expression program and the onset of gametogenesis in yeast require the conserved exosome subunit Rrp6. Proc Natl Acad Sci U S A 108: 1058–1063. doi:10.1073/pnas.1016459108. PubMed: 21149693.
35. Lee TI, Rinaldi NJ, Robert F, Odom DT, Bar-Joseph Z et al. (2002) Transcriptional regulatory networks in *Saccharomyces cerevisiae*. Science 298: 799–804. doi:10.1126/science.1075090. PubMed: 12399584.
36. Harbison CT, Gordon DB, Lee TI, Rinaldi NJ, Macisaac KD et al. (2004) Transcriptional regulatory code of a eukaryotic genome. Nature 431: 99–104. doi:10.1038/nature02800. PubMed: 15343339.
37. Nishizawa M, Komai T, Katou Y, Shirahige K, Ito T et al. (2008) Nutrient-regulated antisense and intragenic RNAs modulate a signal transduction pathway in yeast. PLOS Biol 6: 2817–2830. PubMed: 19108609.
38. Cairrão F, Chora A, Zilhão R, Carpousis AJ, Arraiano CM (2001) RNase II levels change according to the growth conditions: characterization of *gmr*, a new *Escherichia coli* gene involved in the modulation of RNase II. Mol Microbiol 39: 1550–1561. doi:10.1046/j.1365-2958.2001.02342.x. PubMed: 11260472.
39. Chen C, Deutscher MP (2010) RNase R is a highly unstable protein regulated by growth phase and stress. RNA 16: 667–672. doi:10.1261/rna.1981010. PubMed: 20185542.
40. Liang W, Malhotra A, Deutscher MP (2011) Acetylation regulates the stability of a bacterial protein: growth stage-dependent modification of RNase R. Mol Cell 44: 160–166. doi:10.1016/j.molcel.2011.06.037. PubMed: 21981926.
41. Liang W, Deutscher MP (2012) Transfer-messenger RNA-SmpB protein regulates ribonuclease R turnover by promoting binding of

HslUV and Lon proteases. J Biol Chem 287: 33472–33479. doi: 10.1074/jbc.M112.375287. PubMed: 22879590.
42. Moreira RN, Domingues S, Viegas SC, Amblar M, Arraiano CM (2012) Synergies between RNA degradation and trans-translation in *Streptococcus pneumoniae*: cross regulation and co-transcription of RNase R and SmpB. BMC Microbiol 12: 268. doi: 10.1186/1471-2180-12-268. PubMed: 23167513.
43. Feigenbutz M, Jones R, Besong TMD, Harding SE, Mitchell P (2013) Assembly of the yeast exoribonuclease Rrp6 with its associated cofactor Rrp47 occurs in the nucleus and is critical for the controlled expression of Rrp47. J Biol Chem 288: 15959–15970. doi:10.1074/jbc.M112.445759. PubMed: 23580640.
44. Garland W, Feigenbutz M, Turner M, Mitchell P (2013) Rrp47 functions in RNA surveillance and stable RNA processing when divorced from the exoribonuclease and exosome-binding domains of Rrp6. RNA (. (2013)) PubMed: 24106327.
45. Allmang C, Petfalski E, Podtelejnikov A, Mann M, Tollervey D et al. (1999) The yeast exosome and human PM-Scl are related complexes of 3'5' exonucleases. Genes Dev 13: 2148–2158. doi:10.1101/gad.13.16.2148. PubMed: 10465791.
46. Sikorski RS, Hieter P (1989) A system of shuttle vectors and yeast host strains designed for efficient manipulation of DNA in *Saccharomyces cerevisiae*. Genetics 122: 19–27. PubMed: 2659436.
47. Christianson TW, Sikorski RS, Dante M, Shero JH, Hieter P (1992) Multifunctional yeast high-copy-number shuttle vectors. Gene 110: 119–122. doi:10.1016/0378-1119(92)90454-W. PubMed: 1544568.
48. Goldstein AL, McCusker JH (1999) Three new dominant drug resistance cassettes for gene disruption in *Saccharomyces cerevisiae*. Yeast 15: 1541–1553. doi:10.1002/(SICI)1097-0061(199910)15:14. PubMed: 10514571.
49. Motley AM, Nuttall JM, Hettema EH (2012) Pex3-anchored Atg36 tags peroxisomes for degradation in *Saccharomyces cerevisiae*. EMBO J 31: 2852–2868. doi:10.1038/emboj.2012.151. PubMed: 22643220.
50. Tollervey D, Mattaj IW (1987) Fungal small nuclear ribonucleoproteins share properties with plant and vertebrate U-snRNPs. EMBO J 6: 469–476. PubMed: 2953599.
51. Untergasser A, Nijveen H, Rao X, Bisseling T, Geurts R et al. (2007) Primer3Plus, an enhanced web interface to Primer3. Nucleic Acids Res 35: W71–W74. doi:10.1093/nar/gkm093. PubMed: 17485472.
52. Schmittgen TD, Livak KJ (2008) Analyzing real-time PCR data by the comparative CT method. Nat Protoc 3: 1101–1108. doi:10.1038/nprot.2008.73. PubMed: 18546601.
53. van Hoof A, Lennertz P, Parker R (2000) Yeast exosome mutants accumulate 3'-extended polyadenylated forms of U4 small nuclear RNA and small nucleolar RNAs. Mol Cell Biol 20: 441–452. doi:10.1128/MCB.20.2.441-452.2000. PubMed: 10611222.
54. Grzechnik P, Kufel J (2008) Polyadenylation linked to transcription termination directs the processing of snoRNA precursors in yeast. Mol Cell 32: 247–258. doi:10.1016/j.molcel.2008.10.003. PubMed: 18951092.
55. Yeh L-CC, Lee JC (1990) Structural analysis of the internal transcribed spacer 2 of the precursor ribosomal RNA from *Saccharomyces cerevisiae*. J Mol Biol 211: 699–712. doi:10.1016/0022-2836(90)90071-S. PubMed: 2179564.
56. Warner JR (1999) The economics of ribosome biosynthesis in yeast. Trends Biochem Sci 24: 437–440. doi:10.1016/S0968-0004(99)01460-7. PubMed: 10542411.
57. Kadaba S, Wang X, Anderson JT (2006) Nuclear RNA surveillance in *Saccharomyces cerevisiae*: Trf4p-dependent polyadenylation of nascent hypomethylated tRNA and an aberrant form of 5S rRNA. RNA 12: 508–521. doi:10.1261/rna.2305406. PubMed: 16431988.
58. Milligan L, Torchet C, Allmang C, Shipman T, Tollervey D (2005) A nuclear surveillance pathway for mRNAs with defective polyadenylation. Mol Cell Biol 25: 9996–10004. doi:10.1128/MCB.25.22.9996-10004.2005. PubMed: 16260613.
59. Gavin AC, Bösche M, Krause R, Grandi P, Marzioch M et al. (2002) Functional organization of the yeast proteome by systematic analysis of protein complexes. Nature 415: 141–147. doi:10.1038/415141a. PubMed: 11805826.
60. Stuparevic I, Mosrin-Huaman C, Hervouet-Coste N, Remenaric M, Rahmouni AR (2013) Co-transcriptional recruitment of the RNA exosome cofactors Rrp47p, Mpp6p and two distinct TRAMP complexes assists the exonuclease Rrp6p in the targeting and degradation of an aberrant mRNP in yeast. J Biol Chem (. (2013)) PubMed: 24047896.
61. Ozanick SG, Wang X, Costanzo M, Brost RL, Boone C et al. (2009) Rex1p deficiency leads to accumulation of precursor initiator $tRNA^{Met}$ and polyadenylation of substrate RNAs in *Saccharomyces cerevisiae*. Nucleic Acids Res 37: 298–308. doi:10.1093/nar/gkn925. PubMed: 19042972.
62. Schilders G, van Dijk E, Pruijn GJM (2007) C1D and hMtr4p associate with the human exosome subunit PM/Scl-100 and are involved in pre-rRNA processing. Nucleic Acids Res 35: 2564–2572. doi:10.1093/nar/gkm082. PubMed: 17412707.
63. Chen CY, Gherzi R, Ong SE, Chan EL, Raijmakers R et al. (2001) AU binding proteins recruit the exosome to degrade ARE-containing mRNAs. Cell 107: 451–464. doi:10.1016/S0092-8674(01)00578-5. PubMed: 11719186.
64. Wilmes GM, Bergkessel M, Bandyopadhyay S, Shales M, Braberg H et al. (2008) A genetic interaction map of RNA-processing factors reveals links between Sem1/Dss1-containing complexes and mRNA export and splicing. Mol Cell 32: 735–746. doi:10.1016/j.molcel.2008.11.012. PubMed: 19061648.